



**HAL**  
open science

# Oméga 3 et troubles de l'humeur : mécanismes d'actions neuroprotecteurs

Maud Martinat

► **To cite this version:**

Maud Martinat. Oméga 3 et troubles de l'humeur : mécanismes d'actions neuroprotecteurs. Neurosciences. Université de Bordeaux, 2022. Français. NNT : 2022BORD0427 . tel-04047465

**HAL Id: tel-04047465**

**<https://theses.hal.science/tel-04047465v1>**

Submitted on 27 Mar 2023

**HAL** is a multi-disciplinary open access archive for the deposit and dissemination of scientific research documents, whether they are published or not. The documents may come from teaching and research institutions in France or abroad, or from public or private research centers.

L'archive ouverte pluridisciplinaire **HAL**, est destinée au dépôt et à la diffusion de documents scientifiques de niveau recherche, publiés ou non, émanant des établissements d'enseignement et de recherche français ou étrangers, des laboratoires publics ou privés.

**Université de Bordeaux**

Ecole Doctorale Sciences de la Vie et de la Santé

**Thèse de doctorat**

Pour l'obtention du grade de :

Docteur de l'Université de Bordeaux

Spécialité : Neurosciences

---

## **OMÉGA 3 ET TROUBLES DE L'HUMEUR : MÉCANISMES D'ACTION NEUROPROTECTEURS**

---

Maud Martinat

Thèse réalisée en codirection avec l'Université de Toronto sous la direction de :

Sophie Layé

Richard Bazinet

Présentée et soutenue publiquement le 16 décembre 2022

Membres du jury :

<b>Pr Mélanie Plourde</b> , Professeure, Université de Sherbrooke, Québec, Canada,	<b>Rapportrice</b>
<b>Dr Pascale Chavis</b> , Directrice de Recherche, Inmed, Marseille, France,	<b>Rapportrice</b>
<b>Dr Niyazi Acar</b> , Directeur de Recherche, INRAE, Dijon, France,	<b>Examineur</b>
<b>Pr Frédéric Calon</b> , Professeur, Université de Laval, Canada,	<b>Président, Examineur</b>
<b>Pr Richard Bazinet</b> , Professeur Associé, Université de Toronto, Canada,	<b>Co-directeur de thèse</b>
<b>Dr Sophie Layé</b> , Directrice de Recherche, INRAE, Bordeaux, France,	<b>Directrice de thèse</b>



### **Oméga 3 et troubles de l'humeur : mécanismes d'action neuroprotecteurs**

Le cerveau est riche en acides gras polyinsaturés (AGPI) dont les chaînes longues, comme l'acide docosahexaénoïque (DHA) et l'acide ecosapentaénoïque (EPA) issus des oméga 3 (n-3), s'accumulent au cours du développement. Leurs précurseurs ne sont pas synthétisés *de novo* par les mammifères et doivent être apportés par la nourriture. Or, il a été démontré qu'un apport nutritionnel maternel déséquilibré et carencé en AGPI n-3 induit des altérations cognitives et électrophysiologiques chez le nourrisson et dans des modèles murins de carence nutritionnelle.

Nous nous intéressons à l'impact d'une intervention nutritionnelle au cours du développement et comment un régime déséquilibré en AGPI n-3 altère les réseaux neuronaux et la cognition, en étudiant les mécanismes moléculaires et en prenant en compte le sexe. Pour cela différents modèles sont utilisés 1) les souriceaux sont carencés en AGPI pendant le développement puis exposés à une diète riche en AGPI n-3 au sevrage ; 2) développer un modèle de carence locale par injection virale bloquant l'expression de l'élongase ELOVL2 (impliquée dans la synthèse des AGPI à longues chaînes) dans les astrocytes pour évaluer l'impact sur les propriétés des neurones environnants.

Nos résultats suggèrent qu'un changement de statut nutritionnel d'une carence vers un régime riche en AGPI n-3 au sevrage restaure 1) la plasticité synaptique à long terme dans l'hippocampe chez les mâles et les femelles, 2) la cognition ainsi que les taux d'acides gras dans le cerveau mais de manière différentielle entre les deux sexes. Dans la seconde partie des résultats, une variation locale de la synthèse des AGPI dans l'astrocyte modifie l'excitabilité des neurones sans modifier les taux d'acides gras dans la structure cérébrale tout en modifiant certains critères de comportement émotionnel.

**Mots clés :** AGPI, développement, cognition, neuroprotection



## SUMMARY

---

### **Omega 3 and mood disorders: neuroprotective mechanisms**

The brain is rich in polyunsaturated fatty acids (PUFA) whose long chains, such as docosahexaenoic acid (DHA) and eicosapentaenoic acid (EPA) from omega 3 (n-3), accumulate during development. Their precursors are not synthesized de novo by mammals and must be provided by food. However, it has been shown that an unbalanced and deficient maternal dietary intake of n-3 PUFAs induces cognitive and electrophysiological alterations in infants and in mouse models of nutritional deficiency.

We are interested in the impact of a nutritional intervention during development and how a diet unbalanced in n-3 PUFA alters neural networks and cognition, by studying the molecular mechanisms and taking into account the gender. To this end, different models are used: 1) mice are deficient in PUFAs during development and then exposed to a diet rich in n-3 PUFAs at weaning; 2) to develop a local deficiency model by viral injection blocking the expression of the elongase ELOVL2 (involved in the synthesis of long-chain PUFAs) in astrocytes to assess the impact on the properties of the surrounding neurons.

Our results suggest that a change in nutritional status from deficiency to a diet rich in n-3 PUFA at weaning restores 1) long-term synaptic plasticity in the hippocampus in males and females, 2) cognition as well as fatty acid levels in the brain but in a differential manner between the two sexes. In the second part of the results, a local variation of PUFA synthesis in the astrocyte modifies the excitability of neurons without modifying the levels of fatty acids in the brain structure while modifying some criteria of emotional behavior.

**Key words** : PUFA, development, cognition, neuroprotection



## REMERCIEMENTS

---

Avant tout, je tenais à remercier Sophie Layé pour m'avoir donné l'opportunité de réaliser ma thèse au sein du laboratoire NutriNeuro. Merci pour tout, pour la confiance que tu m'as accordé et surtout ton écoute. Ce fut un réel plaisir de travailler à tes côtés, j'ai énormément appris, tant scientifiquement que personnellement. Merci pour ces 5 belles années (déjà ?) remplies d'échanges, de congrès et de « mais quelle est la question ? ».

Merci au professeur Richard Bazinet pour avoir accepté de co-diriger cette thèse, pour ses retours, et pour le joli projet qui a ainsi pu être accompli, sans voyage à Toronto malheureusement !

Merci aux membres du jury, Mélanie Plourde, Pascale Chavis, Frédéric Calon et Niyazi Acar d'avoir accepté d'évaluer l'ensemble de ces travaux de thèse.

Au professeur Miriam Melis pour m'avoir accueillie dans son laboratoire en Sardaigne et donné l'opportunité d'étudier d'autres techniques d'électrophysiologie et de rencontrer des gens formidables.

Je tiens à remercier très chaleureusement l'ensemble du laboratoire Nutrineuro UMR1286 et le personnel présent au sein du Neurocampus de Bordeaux pour leur aide et la bonne ambiance transmise au laboratoire. En particulier, merci à Marie-Pierre Manain, Alexandra Séré, et Gregory Artaxet pour leur aide au quotidien. Un grand merci à tous ceux qui de près ou de loin ont participé à ce projet.

Mathieu, un immense merci pour tout ce que tu m'as appris autant sur le plan technique que sur la réflexion scientifique et personnelle. Je souhaite à tout le monde d'avoir un labmate comme toi, ou comme Moïra et Flore, des partenaires de manip en or, merci pour tout les filles !

Merci aux électrophysiologistes pour le partage et l'entraide, Xavier, Pierre, Clem, David

Petite dédicace à notre allemand refoulé parti s'exiler aux States, merci Hugo pour les heures passées en électrophy à refaire le monde, mention spéciale pour les chants avec Math. Merci aux boys du bureau/labo d'à côté, Andrea l'italiano, les acolytes Pierre et Steph, Roman (ça fait longtemps qu'on a pas lâché les chiens dis !), merci pour l'entraide et la bonne humeur au quotidien. Merci à toi Johny Boy, hâte de venir danser le Sirtaki à Berlin ! Et enfin, merci aux super nanas du labo : aux reines de la fiesta Mathou et Camille, aux bêtises et plans foireux de Fanny, à la bonne bouffe avec Nana et aux râleries d'Anaïs, grand-mère et coloc éphémère (mais de qualité). Merci pour la vie *in labo* et *ex labo* !

Merci à mes petites Gambas, pour ces années universitaires, la coloc, les vacances, le ski, la vida loca... une belle bande de joyeux lurons dont 4 talentueux docteurs, 4 fabuleux « essais cliniciens » et notre petite douceur sucrée, Raphou. A tous les amis de longue et très longue date et ma team de médecins préférés Constance, Claire, Aude et PE, merci ! Et un grand merci à ma Jo qui a toujours eu les mots qui font du bien au moral.

Max, tu auras vécu les montagnes russes de la thèse par procuration, merci pour ta patience et ton soutien sans faille chaque jour depuis le début de cette aventure et surtout au cours de ces derniers mois et derniers jours.

Pour ma maman, et la fratrie : Balou et Rayman, mes piliers et ma force dans la vie, merci pour tout.



## Table des matières

LISTE DES FIGURES.....	1
LISTE DES TABLEAUX .....	1
LISTE DES ABREVIATIONS .....	2
PREAMBULE.....	5
INTRODUCTION .....	9
1. Acides gras polyinsaturés (AGPI), sources alimentaires et digestion.....	10
1.1. Nomenclature et classification des AGPI.....	10
1.2. Sources alimentaires des AGPI n-3 et n-6 .....	11
1.3. Digestion des AGPI alimentaires .....	12
2. Métabolisme des AGPI .....	15
2.1. Les désaturases .....	16
2.2. Les élongases.....	18
3. AGPI et cerveau .....	20
3.1. Incorporation des AGPI dans le cerveau .....	21
3.2. Différences de composition d'AGPI des types cellulaires du cerveau .....	23
3.3. Influence du sexe sur la composition en AGPI du cerveau. ....	24
3.4. Transport des AGPI dans le cerveau.....	25
3.5. Influence des SNPs des gènes du métabolisme des AGPI sur la biodisponibilité du DHA et les pathologies du cerveau.....	28
4. Métabolisme des AGPI en dérivés bioactifs.....	30
4.1. Qu'est-ce que la neuroinflammation ?.....	30
4.2. Métabolisme des AGPI en oxylipines .....	31
4.3. Endocannabinoïdome.....	41
5. Rôle des AGPI dans le cerveau et le comportement.....	44
5.1. AGPI n-3 et période développementale.....	44
5.2. AGPI n-3 et cognition chez l'enfant.....	45
5.3. AGPI, cognition et intégrité structurelle et fonctionnelle du cerveau des sujets adultes et âgés	47
5.4. Modèles animaux pour étudier les mécanismes impliqués dans les effets des AGPI sur la cognition.....	49
5.4.1. AGPI alimentaires et cognition chez l'animal.....	51
5.4.2. AGPI et troubles anxio-dépressifs .....	52
6. Rôle des AGPI dans la plasticité neuronale .....	54
6.1. Généralités sur la plasticité synaptique .....	54
6.2. Plasticité synaptique de l'hippocampe et dans le striatum .....	55

6.2.1.	Hippocampe et noyau accumbens .....	55
6.2.2.	Neurotransmission glutamatergique .....	56
6.3.	Rôle des astrocytes dans la neurotransmission .....	58
6.3.1.	Astrocyte et synapse tripartite .....	58
6.4.	Modulation de la plasticité neuronale par les AGPI .....	61
6.4.1.	Impact des AGPI sur la transmission neuronale .....	62
6.4.2.	Impact des AGPI sur les fonctions astrocytaires à la synapse .....	64
OBJECTIFS .....		66
RESULTATS .....		68
CHAPITRE 01 : Conséquences de l'exposition à partir de la période de sevrage à une diète équilibrée en ALA sur les AGPI et leurs métabolites (oxylipines) dans le cerveau, la plasticité synaptique hippocampique et la cognition à l'âge adulte .....		70
CHAPITRE 02 : Etat des connaissances des effets des AGPI nutritionnels sur le développement cérébral .....		105
CHAPITRE 03 : Utilisation d'un modèle murin génétique pour modifier l'expression d'Elovl2 dans les astrocytes .....		148
CHAPITRE 04 : Effet d'une supplémentation en AGPI n-3 sur le comportement émotionnel et la plasticité synaptique dans un modèle de stress .....		168
DISCUSSION .....		190
1.	Synthèse des résultats obtenus .....	191
2.	Modèles animaux utilisés .....	192
2.1.	Modèle nutritionnel (modification globale dans le cerveau) .....	192
2.2.	Modèle transgénique (modification locale par modification du métabolisme des AGPI au niveau astrocytaire) .....	197
3.	Les effets neurobiologiques de la carence maternelle sont partiellement réversibles chez la descendance à l'âge adulte grâce à une intervention nutritionnelle : différences liées au sexe .....	201
3.1.	Les altérations du profil lipidique et dérivés sont restaurées par le régime équilibré ...	201
3.2.	Récupération comportementale et de la plasticité synaptique en fonction du sexe .....	202
3.3.	L'hypothèse du 18-HEPE dans la récupération synaptique .....	206
4.	L'inhibition de la synthèse d'elovl2 astrocytaire altère les propriétés électrophysiologiques des MSNs dans le NAc des souris mâle et femelle .....	208
5.	La supplémentation en AGPI n-3 à longue chaîne modifie les propriétés électrophysiologiques du NAc et le comportement émotionnel de souris naïves et stressées chroniquement .....	210
REFERENCES .....		214
LISTE DES PUBLICATIONS .....		266
PUBLICATIONS ANNEXES .....		268



## LISTE DES FIGURES

---

<b>Figure 1</b> : Schéma des deux familles d'acide gras oméga 6 (n-6) et oméga 3 (n-3).....	10
<b>Figure 2</b> : Représentation schématique de la digestion des lipides et de leur absorption dans l'intestin grêle.....	13
<b>Figure 3</b> : Voies de synthèse des acides gras polyinsaturés à chaîne longue (adapté de (Joffre, 2019)) .....	20
<b>Figure 4</b> : Mécanismes de transport des AGPI dans le cerveau (Adapté de Bazinet et Layé, 2014).....	27
<b>Figure 5</b> : Les AGPI n-3 et n-6 sont métabolisés en oxylipines par les voies COX, LOX et CYP450. (Adapté de Michael-Titus and Priestley, 2014) .....	36
<b>Figure 6</b> Effets membranaires des différents médiateurs lipidiques issus des AG n-3 et n-6 et agissant au sein de l'endocannabinoidome (extrait de Cristoni et al., 2019) .....	43
<b>Figure 7</b> : Voies hippocampales glutamatergiques. ....	56
<b>Figure 8</b> : Communication bidirectionnelle neurone-astrocyte.....	61
<b>Figure 9</b> : Représentation des mécanismes d'action des AGPI au niveau de la synapse (adapté de Di Miceli et al., 2018).....	64
<b>Figure 10</b> : Biosynthèse des Acide Gras à Longue et très Longue Chaîne chez les mammifères.....	197
<b>Figure 11</b> : Composition en AGPI n-6 et n-3 du cerveau d'animaux WT et KO pour Elov12 sous régime équilibré en AGPI n-3 (extrait de Talamonti et al., 2019) .....	198
<b>Figure 12</b> : Corrélations des taux d'AG avec le paramètre bras nouveaux du Ymaze (mâles) .....	204
<b>Figure 13</b> : Corrélations des taux d'AG avec le paramètre bras nouveaux du Ymaze (femelles) .....	205
<b>Figure 14</b> : Enregistrement de la plasticité synaptique à long terme dans l'hippocampe d'animaux carencés en AGPI n-3 en présence de 18-HEPE (1µM) mâles et femelles. ....	208

## LISTE DES TABLEAUX

---

<b>Tableau 1</b> Exemples de sources d'acides gras (issus de la table ciqual ANSES).....	12
<b>Tableau 2</b> Enzymes de synthèse des oxylipines et localisation cérébrale et cellulaire des enzymes...	34
<b>Tableau 3</b> : Apports Nutritionnels Conseillés pour un adulte selon l'ANSES et apports moyen selon l'INCA2 Données en % de l'apport énergétique ou en mg/jour.....	44
<b>Tableau 4</b> : Références utilisant différents régimes et impact sur la composition cérébrale en DHA	193
<b>Tableau 5</b> : composition des régimes équilibrés et carencés en AGPI n-3 utilisés .....	195
<b>Tableau 6</b> Composition lipidiques des régimes, extrait de (Labrousse et al., 2012).....	199

## LISTE DES ABREVIATIONS

---

**2-AG** : 2-arachidonylglycerol  
**AA** : acide arachidonique  
**ACSL** : long chain acyl-coA synthetases  
**AE** : apport énergétique  
**AEA** : anandamide  
**AG** : acide gras

autistique  
**BDNF** : brain-derived neurotrophic factor  
**BHCR** : barrière hémato-céphalo-rachidienne  
**BHE** : barrière hémato-encéphalique  
**BHE** : Barrière Hémato-Encéphalique  
**CD36** : cluster of differentiation 36  
**COX** : cyclooxygenase  
**COX** : cyclooxygénase  
**cPLA2** : phospholipase A2 cytosolique dépendante du calcium  
**D5D** : désaturase Delta-5  
**D6D** : désaturase Delta-6  
**DAGL** : (diacylglycérol lipase  
**DGLA** : acide dihomo- $\gamma$ -linolénique  
**DHA** : acide docosahexaénoïque  
**eCB** : endocannabinoïde  
**Egr-1** : early growth response protein 1  
**Elovl** : elongation of very long chain-fatty acids  
**Elovl2** : elongase 2  
**Elovl5** : elongase 5  
**EPA** : acide eicosapentaénoïque  
**FABP** : fatty acid binding protein  
**Fads** : fatty acid desaturase  
**fads1** : *fatty acid desaturase 1*  
**fads2** : *fatty acid desaturase 2*  
**FAS** : fatty acid synthase

**AGMI** : acides gras monoinsaturés  
**AGPI** : acides gras polyinsaturés  
**AGPI-LC** : acides gras polyinsaturés à longues chaînes  
**AGS** : acides gras saturés  
**FAT (CD36)** : fatty acid translocase  
**FATP** : fatty acid transport protein  
**FATP4** : fatty acid transport protein 4  
**FST** : forced swim test = Test de nage forcée  
**iPLA2** : phospholipase A2 indépendante du calcium  
**KO** : Knock-out  
**LA** : acide linoléique  
**LCR** : liquide céphalo-rachidien  
**LDL** : lipoprotéine de basse densité  
**LDLR** :  
**LNA** : acide  $\alpha$ -linolénique  
**LOX** : lipooxygénase  
**LOX** : lipoxygénase  
**LPS** : lipopolysaccharides  
**LPS** : lipopolysaccharides  
**LRP1** :  
**LT** : leukotriènes  
**LysoPC** : lysophosphatidylcholine  
**MA** : maladie d'Alzheimer  
**MALDI** : matrix-assisted laser desorption ionization as a mass spectrometry imaging  
**MDD** : trouble dépressif majeur  
**MFSD2A** : major facilitator superfamily domain-containing protein 2A  
**NAPE-PLD** : N-acylphosphatidyléthanolami

**ANSES** : agence nationale de sécurité sanitaire alimentaire  
**APOE** : apolipoprotéine E  
**Arc1** : activity-regulated cytoskeleton-associated protein 1  
**ASD** : désordres du spectre  
ne-phospholipase D-like hydrolase  
**NF- $\kappa$ B** : facteur nucléaire kappa B  
**NMDA** : récepteur N-méthyl-D-aspartate  
**NPC1L1** : niemann pick C1 like 1  
**NRI** : Indice de risque nutritionnel  
**OA** : acide oléique  
**PA** : acide palmitique  
**PC** : phosphatidylcholine  
**PE** : phosphatidylethanolamine  
**PG** : prostaglandines  
**PI** : phosphatidylinositol  
**PL** : phospholipide  
**PLA** : phospholipase A  
**PLA2** : phospholipase A2  
**PLA2** : phospholipase A2  
**PPAR** : peroxysomeproliferator-activated receptor  
**PPAR- $\gamma$**  : récepteur activé par les proliférateurs de peroxysomes  
**PS** : phosphatidylserine  
**RCT** : essai clinique randomisé  
**RE** : réticulum endoplasmique  
**ROS** : retina rod outer segment = segment externe de tige de la rétine  
**SA** : acide stéarique  
**SM** : sphingomyéline

**SNP** : single nucleotide polymorphism = polymorphisme d'un nucléotide unique  
**sPLA2** : phospholipase A2 sécrétoire **dépendante du calcium**

**SPM** : médiateur lipidique spécialisé pro-résolvant  
**SR-BI** : scavenger receptor de type BI  
**SREBP-1** : sterol regulatory element-binding protein1  
**TG** : triglycérides

**TLR4** : récepteurs Toll-like 4  
**VLCFA** : very long fatty acid  
**VLDL** : lipoprotéine de très faible densité



## PREAMBULE

---

Les lipides font partie des sept constituants principaux de notre alimentation avec les glucides, les protéines, les vitamines, les oligo-éléments et minéraux et l'eau. On distingue plusieurs classes de lipides, toutes constituées en majeure partie d'**acides gras** : les triglycérides, les phospholipides, les sphingolipides et les ester de cholestérol (minoritaires). Les acides gras (AG) sont classés selon leurs structures (chaîne carbonée et degré d'insaturation) en acides gras saturés (AGS), monoinsaturés (AGMI) (une double liaison) et polyinsaturés (AGPI) (plusieurs doubles liaisons).

Les AGS et AGMI proviennent d'une synthèse endogène chez l'Homme dans le foie, le cerveau et le tissu adipeux et sont également apportés par l'alimentation. Ils ont un rôle dans l'apport énergétique via les triglycérides de réserve (pour les AGS) et également dans la constitution des phospholipides membranaires. Ils participent également à la modulation de l'activité des enzymes, des transporteurs et des récepteurs (Beauchamp et al., 2009).

Les AGPI, à la différence des AGS et AGMI, sont des molécules dites « **indispensables** » car nécessaires à la croissance normale et aux fonctions physiologiques des cellules. Les AGPI les plus répandus et importants sont l'acide linoléique (LA, C18 :2) et l'acide  $\alpha$ -linoléique (ALA, C18 :3) qui appartiennent à la famille n-6 (ou omega 6) et n-3 (ou omega 3) respectivement. Ces précurseurs d'AGPI ne sont pas synthétisés *de novo* par les mammifères qui doivent les trouver dans des sources nutritionnelles (Bazinet and Layé, 2014). Une fois consommés, LA et ALA (qui sont d'origine végétale) sont métabolisés en AGPI dérivés à chaînes carbonées allongées avec plusieurs insaturations (AGPI-LC), majoritairement au niveau du foie. Ces formes (principalement acide eicosapentaénoïque, EPA 20:5 et acide docosahexaénoïque, DHA C22 :6 à partir de ALA et acide arachidonique AA C20 :4 à partir du LA) sont dites « **conditionnellement indispensables** » car elles sont nécessaires aux fonctions physiologiques. Cependant, comme le taux de biosynthèse des AGPI-LC à partir de leurs précurseurs est faible et insuffisant pour répondre aux besoins nutritionnels et physiologiques, la consommation d'AGPI-LC préformés, à partir de ressources animales, est recommandée. Ainsi, les AGPI-LC n-3 et n-6 sont également fournis aux organismes directement dans l'alimentation à partir de sources alimentaires distinctes, tout comme leurs précurseurs. Les précurseurs des AGPI et leurs produits de métabolisation sont des AG « **essentiels** ».

Au début des années 1990, les graisses alimentaires étaient considérées comme des contributeurs caloriques pour les organismes qui les consommaient. En effet, le catabolisme des AG alimentaires, notamment par la  $\beta$ -oxydation mitochondriale fournissent de l'énergie. De plus, les AG ont des fonctions structurales et sont des constituants des phospholipides membranaires. En revanche, les



AGPI, qui sont des nutriments indispensables, et leurs dérivés bioactifs, exercent des fonctions apparentées à celles des hormones et régulent de nombreuses fonctions physiologiques. Ainsi, dès les années 30, Mildred et George Burr ont démontré que les acides gras « essentiels » étaient important pour la santé. Des premières expériences menées chez des rats ont ainsi révélé qu'en supprimant les acides gras du régime alimentaire, les rongeurs présentaient un retard de croissance et des troubles fonctionnels avec notamment une sensibilité aux infections bactériennes et une infertilité chez les mâles et les femelles (Burr and Burr, 1930, 1929). Ces premières données suggéraient que les AGPI jouaient un rôle dans la physiologie de la reproduction et le contrôle de l'immunité. Il s'en est suivi la découverte que par leur nature et leur abondance dans l'alimentation, les AGPI contribuent à l'étiologie d'un grand nombre de pathologies en cardiologie, cancer, mais aussi neurobiologiques. Il est important de signaler que les apports alimentaires en AGPI, que ce soit ceux de la famille n-3 ou n-6, impactent directement la métabolisation de ces AGPI et leur accumulation dans les membranes. Ainsi, la consommation de diètes de faible teneur en AGPI n-3 et haute teneur en AGPI n-6 conduit à une diminution de leur teneur dans les membranes cellulaires et à une augmentation de celle en AGPI n-6. Le caractère indispensable des AGPI chez l'homme n'est établi que dans les années 60. Cet aspect concerne essentiellement l'ALA, qui, administré seul suffisait à corriger les altérations fonctionnelles qui se développaient chez des adultes ou des nouveau-nés nourris avec des diètes dépourvues de graisses. Ce n'est que plus tard que l'existence de rôles distincts des AGPI n-3 et n-6 a été reconnue avec, dans les années 70, l'observation chez l'homme d'une prévalence élevée de protection vis-à-vis des pathologies cardiovasculaires dans des populations consommant des graisses de poisson riches en AGPI n-3.

Les AGPI sont des constituants importants des phospholipides membranaires et sont métabolisés en dérivés oxygénés qui régulent de nombreuses voies métaboliques et processus intracellulaires. Ces connaissances ont ouvert une nouvelle voie aux recherches portant sur les mécanismes d'action reliant les taux alimentaires en AGPI, les teneurs membranaires de ces AGPI et les fonctions cellulaires, physiologiques ou pathophysiologiques qui en découlent, notamment dans le cerveau. En effet, la composition en acides gras des phospholipides cérébraux est unique. Elle est particulièrement concentrée en acide palmitique (C16:0 ; PA), en acide stéarique (C18:0 ; SA), en acide oléique (C18:1n-9 ; OA), en acide arachidonique (C20:4n-6 ; AA) et en acide docosahexaénoïque (C22:6n-3 ; DHA). Des niveaux optimaux d'AGPI sont nécessaires dans le cerveau et la rétine pour assurer un fonctionnement cérébral et une acuité visuelle suffisants, surtout chez les enfants (Cunnane et al., 2000). Dans les années 90, des études épidémiologiques ont associé les habitudes alimentaires avec des taux faibles en AGPI n-3, le neurodéveloppement et les performances cognitives des enfants (Al et al., 1995; Gibson and Makrides, 1998; Soto-Moyano et al.,

1995) et des sujets âgés. Ces approches ont également révélé qu'un lien existe entre une carence alimentaire en AGPI n-3 et la prévalence de pathologies neuropsychiatriques, notamment les troubles de l'humeur (Sinclair et al., 2007). Ces observations ont été corroborées par des études cliniques montrant que les taux circulants et cérébraux sont plus bas chez des patients souffrant de dépression ou de troubles anxieux (Lin et al., 2010; McNamara and Liu, 2011), conduisant à de nombreux essais cliniques consistant en la supplémentation alimentaire avec des AGPI n-3 aux résultats mitigés ou contradictoires. En parallèle, des travaux réalisés sur des modèles animaux, du rongeur au singe, soumis à des interventions nutritionnelles avec des diètes carencées ou, au contraire, enrichies en AGPI n-3 se sont développés afin d'étudier les mécanismes neurobiologiques par lesquels ces diètes influencent les comportements émotionnels et la mémoire. La plupart des études utilisaient des diètes carencées en ALA et riche en LA, auxquels les animaux étaient exposés pendant plusieurs générations. L'équipe de recherche NutriMind que j'ai rejointe à Bordeaux étudie les mécanismes d'action des AGPI dans le cerveau. Pour cela, l'équipe a développé au début des années 2000 des approches qui consistaient à exposer les rongeurs sur une seule génération à des diètes carencées en ALA et ce dès la gestation ou après le sevrage afin de limiter les éventuels mécanismes compensatoires de l'exposition multi-générationnelle. Les effets de cette diète sont comparés à celle d'une diète isocalorique équilibrée en LA et ALA (1/5), proche des recommandations émises chez l'homme. Dans ce contexte, une partie des recherches menées lors de ma thèse concernent la compréhension des conséquences biochimiques, comportementales et synaptiques d'une modification de l'apport alimentaire en AGPI n-3 en tenant compte du sexe. J'ai par ailleurs développé de nouvelles approches génétiques pour modifier plus localement les taux d'AGPI dans le cerveau, en agissant sur des enzymes de la conversion des précurseurs en AGPI à chaîne longue qui s'accumulent dans le cerveau. Une autre partie de ces travaux de recherche concernera l'effet neuroprotecteur des AGPI n-3 en particulier dans le cas de la dépression et comment une supplémentation en AGPI n-3 par le régime induit des changements comportementaux et électrophysiologique.

Cette thèse a été réalisée avec les apports du Dr Richard Bazinet (Université de Toronto), spécialiste du métabolisme des lipides dans le cerveau. Je n'ai malheureusement pas pu effectuer un séjour au sein de son laboratoire, comme initialement prévu, pour les raisons sanitaires liées au COVID qui se sont déroulées au cours de mon doctorat.

Dans leur ensemble, mes travaux apportent de nouvelles données 1) sur la réversibilité par des apports nutritionnels riche en ALA sur les effets neurobiologiques et comportementaux d'une carence alimentaire précoce en AGPI n-3 (Martinat et al., soumis), 2) sur l'impact de la manipulation génétique locale d'enzyme impliquées dans le métabolisme des AGPI n-3 sur la plasticité synaptique (Martinat et al., en préparation) et 3) sur les effets de la supplémentation alimentaire d'une diète

riche en EPA et DHA sur les comportements émotionnels et la plasticité synaptique chez des rongeurs soumis à un stress chronique (Di Miceli et al., 2022). J'ai également fortement contribué à plusieurs travaux collaboratifs en lien avec les effets neurobiologiques des AGPI ou des lipides qui seront présentés en annexe (trois papiers). Dans ce manuscrit de thèse sont présentés une introduction générale visant à présenter les AGPI et leur métabolisme dans le cerveau, l'influence exercée par les apports nutritionnels, l'impact des variations alimentaires et métaboliques des AGPI cérébraux sur la cognition et les comportements émotionnels ; les résultats principaux sont présentés sous forme d'articles et cette section est suivie par une discussion de l'ensemble des travaux.

## ***INTRODUCTION***

---

# 1. Acides gras polyinsaturés (AGPI), sources alimentaires et digestion

## 1.1. Nomenclature et classification des AGPI

Comme évoqué dans le préambule, la structure des AG permet de les classer en acides gras saturés (AGS), monoinsaturés (AGMI) (une double liaison) et polyinsaturés (AGPI) (plusieurs doubles liaisons).

On distingue deux familles d'AG parmi les AGPI : les oméga 6 ou n-6 et les oméga 3 ou n-3. Les AGPI de ces familles se différencient par la longueur de la chaîne carbonée ainsi que le nombre, la position et la structure spatiale (*cis*, *trans*) des doubles liaisons. Chacune de ces doubles liaisons est éloignée des autres par 3 atomes de carbone. Généralement, les acides gras sont naturellement présents en position *cis*. Dans le système de nomenclature n-x (ou « oméga x »), la formule générale qui décrit les acides gras est la suivante : C : D n-x avec C=longueur de chaîne carbonée, D= nombre de doubles liaisons et n-x qui indique la position de la première double liaison à partir de l'extrémité méthyle de l'insaturation

Les précurseurs de ces deux familles, qualifiés d'indispensable comme précédemment indiqué, sont l'acide linoléique (C18 :2 n-6 ; LA) et l'acide  $\alpha$ -linoléique (C18 :3 n-3 ; ALA ou LNA). Ces précurseurs sont ensuite métabolisés en AGPI à longue chaîne (AGPI-LC) avec une chaîne carbonée entre 20 et 24 carbones, via l'action de désaturases et d'élongases, constitutives de toutes les membranes cellulaires. Les principaux AGPI-LC sont l'acide arachidonique (C20 :4 n-6 ; AA) pour les oméga 6 et l'acide docosahexaénoïque (C22 :6 n-3 ; DHA) et l'acide eicosapentaénoïque (C20 :5 n-3 ; EPA) pour les oméga 3 (**Figure 1**). Les AGPI à très longue chaîne présentent une longueur de chaîne de plus de 24 carbones et deux ou plusieurs doubles liaisons. Dans le reste du manuscrit, un focus sera fait sur le LA, ALA, DHA, EPA et AA.

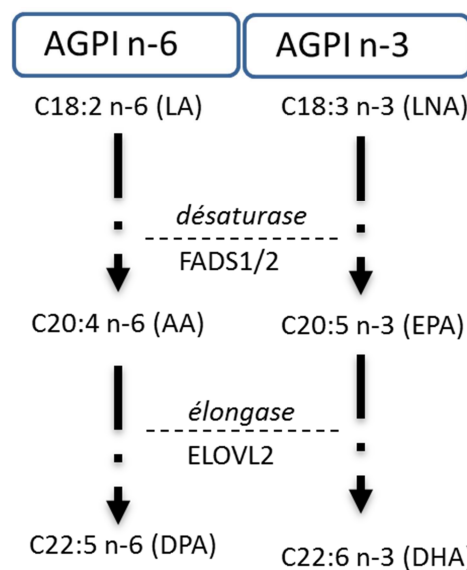


Figure 1 : Schéma des deux familles d'acide gras oméga 6 (n-6) et oméga 3 (n-3).

## 1.2. Sources alimentaires des AGPI n-3 et n-6

Les précurseurs des AGPI n-3 et n-6 sont principalement de source végétale. Le précurseur des oméga 6, LA, est principalement retrouvé dans les graines et huiles végétales issues du tournesol, du maïs, du soja et du blé. L'AA est présent en grande partie dans les sources animales comme la viande et les œufs (dépendant de la quantité de précurseurs présente dans le fourrage des animaux). Pour les AGPI n-3, les principales sources alimentaires du précurseur, ALA, sont le lin, le chia, l'airelle (environ 50% de ALA dans ces huiles au total), la noix et le colza (environ 10%). Le DHA et l'EPA sont massivement obtenus à partir de ressources halieutiques, en particulier les poissons gras comme la sardine, le hareng, le saumon, le thon et les huiles de poisson ou de foie de morue (Bentsen, 2017)

**Tableau 1.** Les recommandations actuelles sont discutées dans un autre chapitre de l'introduction.

Avec l'augmentation de la demande mondiale concernant les huiles riches en EPA et DHA, les sources classiques alimentaires que représentent les poissons gras se tarissent. De plus, la surpêche et l'aquaculture, qui représentent une alternative à la pêche marine, épuisent également les huiles riches en EPA et DHA. Enfin, le changement climatique entraîne le déclin des microalgues marines qui représentent la source principale de DHA et EPA pour les poissons gras. Les microalgues cultivables, qui sont riches en AGPI-LC n-3, représentent une alternative aux huiles de poisson car elles sont facilement cultivables. Une recherche intense, basée sur le développement de technologies de bio-ingénierie permet d'envisager à court terme d'utiliser les microalgues comme sources d'EPA ou de DHA, ce qui évite les processus de séparation et de purification en EPA ou DHA extraits à partir d'huile de poisson (Liu et al., 2022). D'autres alternatives de production d'EPA et de DHA à partir de bactéries marines sont envisagées (Moi et al., 2018).

L'AA se trouve dans les membranes cellulaires, en particulier chez les animaux. Par conséquent, la viande, le poisson, les abats comme le foie, les reins et la cervelle et les œufs sont des sources d'AA. Les apports alimentaires estimés en AA chez les adultes est entre 100 et 350 mg/jour avec ce qui correspond à <0-1 % de l'apport énergétique total (recommandation ANSES).

**Tableau 1** Exemples de sources d'acides gras (issus de la table ciqual ANSES)

AG (% AG totaux, en partie présentés ici)	Source alimentaire									
	Huile de tournesol	Huile de soja	Huile de colza	Noix	Lin	Sardine	Saumon	Boeuf	Oeufs	
<b>C18:2 n-6 linoléique</b>	56.3	52	19.4	19.5	4.31	0.21	/	0.14	1.25	
<b>C18:3 n-3 α-linolénique</b>	0.05	6.89	7.54	3.77	16.7	0.77	/	0.05	0.056	
<b>AA</b>	<0.01	0	0	<0.01	0	0	0	0.017	0.13	
<b>EPA</b>	<0.01	0	0	<0.01	0	1.09	0.32	0.0017	0	
<b>DHA</b>	<0.01	0	0	<0.01	0	1.58	1.12	Traces	0.069	
<b>AGS</b>	11.1	14.7	7.26	2.93	3.17	2.4	1.92	5.94	2.71	
<b>AGMS</b>	27.6	22.1	59.7	4.1	6.51	1.2	2.87	5.11	3.43	
<b>AGPI</b>	56.3	59.1	26.9	23.3	24.9	3.25	2.43	0.27	1.03	

### 1.3. Digestion des AGPI alimentaires

Le processus de digestion des lipides alimentaires commence au niveau buccal, se poursuit au niveau gastrique et implique des lipases. En raison de leur nature lipophile, la digestion intraluminale des lipides, qui se réalise en milieu aqueux, est un processus complexe. Les lipides sont hydrolysés par des lipases pancréatiques et des colipases. Les étapes d'hydrolyse permettent de libérer les AG libres par des enzymes spécifiques : la lipase pancréatique pour les triglycérides, la phospholipase A2 pour les phospholipides et les esters de cholestérol pour le cholestérol. Les produits lipolytiques sont émulsifiés par les sels biliaires issus du foie dans la lumière intestinale. Certains lipides alimentaires, comme ceux issus du lait, sont naturellement émulsifiés, ce qui facilite la digestion par les enfants. Les micelles sont ensuite absorbées par les entérocytes, au niveau de l'intestin grêle. Les triglycérides et diglycérides ne sont pas absorbables car non incorporés dans les micelles. Plusieurs transporteurs ont été identifiés au niveau des entérocytes : la FABPpm (fatty acid binding protein) qui lie les AG et a une forte affinité pour les AG à chaîne longue, le NPC1L1 (Niemann Pick C1 like 1), le SR-BI (scavenger receptor de type BI), l'annexine-2, FATP4 (FA transport protein 4) et la protéine CD36 (cluster of

differentiation 36). La diffusion des acides gras à travers la membrane cellulaire des entérocytes est facilitée. L'absorption des AG libres (non estérifiés) de moins de 12 atomes de carbone par le sang portal se fait par le canal hépatique commun, communément appelé veine porte. Les AG de plus de 12 atomes de carbone sont ré-estérifiés en triglycérides (TG) et phospholipides (PL) et contribuent à la formation de lipoprotéines, les chylomicrons et les VLDL (very low density lipoprotéines), qui sont transportés dans la lymphe puis dans le sang (Favé et al., 2004). La ré-estérification du cholestérol participe aussi à générer la production de chylomicrons. Les lipoprotéines sont alors dirigées vers les tissus utilisateurs (tissu adipeux, muscle, foie). Après un premier passage dans la lymphe, les résidus de chylomicrons se rendent au foie pour être réorganisés et former les VLDL. Les chylomicrons sont maturés par un échange d'apolipoprotéines avec les lipides à haute densité (HDL pour High Density Lipid) pour former des apolipoprotéines E (apoE) et C. Il s'ensuit un processus de synthèse des lipides, et des AG en particulier, appelé lipogénèse.

Dans le sang, les AG sont associés à l'albumine pour être transportés. La concentration en AG libre dans la lumière intestinale est de l'ordre du micromolaire alors qu'elle est de l'ordre du nanomolaire pour les AG c.

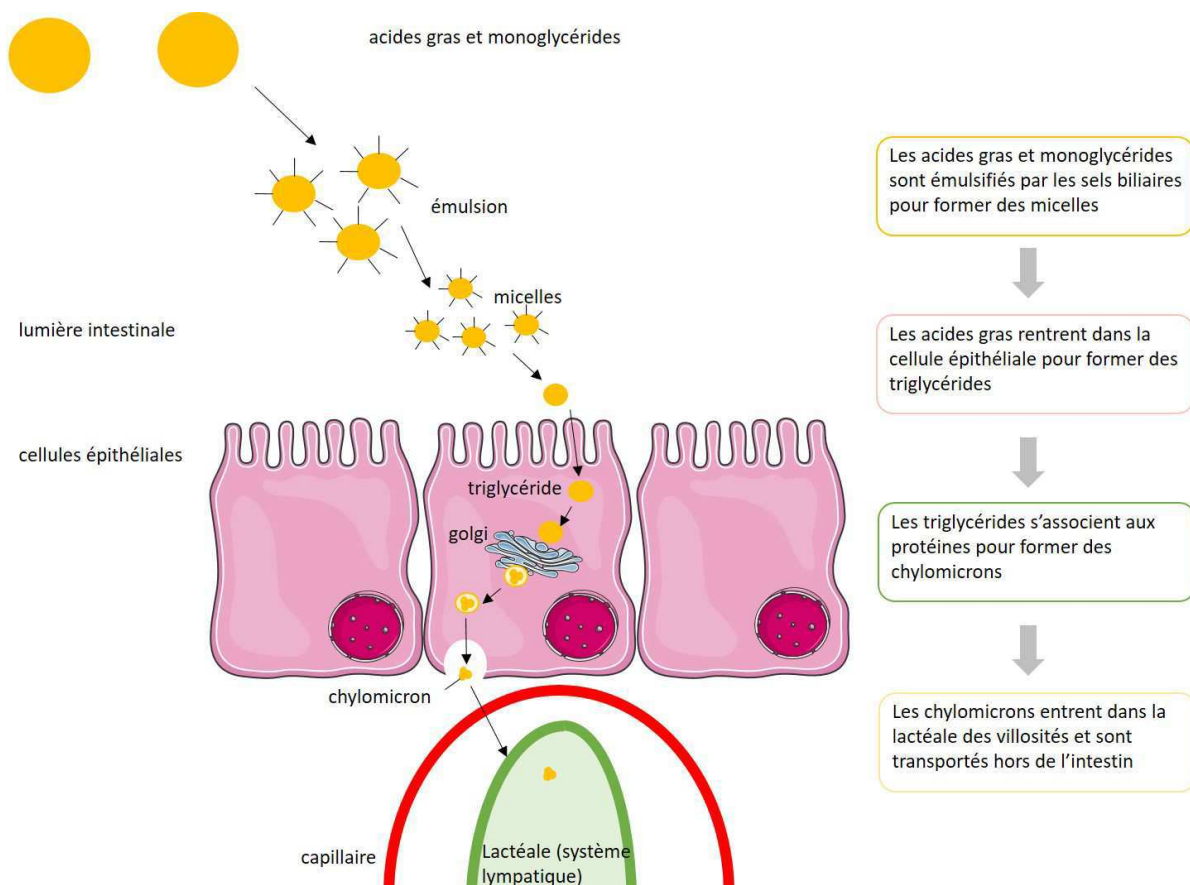


Figure 2 : Représentation schématique de la digestion des lipides et de leur absorption dans l'intestin grêle.



L'émulsification permet la dispersion des lipides grâce aux contractions gastriques et aux sels biliaires. L'hydrolyse lipidique par les enzymes digestives libèrent ensuite les triglycérides qui s'associent aux protéines pour former les chylomicrons ou lipoprotéines qui sont ensuite transportées vers les organes cibles. (*Adapté de « lipid absorption » by OpenStax*)

## 2. Métabolisme des AGPI

La biosynthèse des AG est catalysée par deux systèmes enzymatiques, l'acétyl-CoA carboxylase et le complexe cytosolique de synthèse d'acide gras multienzymatique (FAS pour Fatty Acid Synthase). Le FAS utilise l'acétyl-CoA comme source de carbone pour produire les acides gras saturés (AGS) : principalement l'acide palmitique (C16 :0 ; PA) chez les animaux et l'acide stéarique (C18 :0 ; SA) chez les végétaux (Castro et al., 2016). Chez les végétaux, l'acide linoléique (C18 :2 ; LA) et l'acide  $\alpha$ -linoléique (C18 :3 ; ALA) sont synthétisés à partir de l'acide oléique (C18 :1 n-9), leur première double liaison est située respectivement au niveau du 6<sup>ème</sup> carbone (n-6) ou du 3<sup>ème</sup> carbone (n-3). Ce n'est pas le cas chez les mammifères, qui doivent consommer ces précurseurs indispensables car ils ne peuvent pas les synthétiser. Une fois absorbés, ces précurseurs issus des végétaux sont métabolisés de façon spécifique au niveau du foie en AGPI à longue chaîne (AGPI-LC). Dans un premier temps, LA et ALA subissent une série de désaturations (ajout de doubles liaisons) et d'élongations (ajout d'atomes de carbones) successives à partir de leur extrémité carboxyle dans le réticulum endoplasmique (RE) **Figure 3**. Ces étapes permettent la synthèse de l'acide arachidonique (AA, 20:4 n-6) et de l'acide eicosapentaénoïque (EPA, 20:5 n-3) à partir du LA et du ALA, respectivement. En revanche, la synthèse des acides docosapentaénoïque (DPA, 22:5 n-6) et docosahexaénoïque (DHA, 22:6 n-3) a lieu dans les peroxysomes par une étape de  $\beta$ -oxydation partielle des AGPI à 24 carbones (Burdge and Calder, 2005; Sprecher, 2002). Il est important de noter que les voies de conversion du LA et du ALA sont indépendantes et qu'aucune conversion n'est possible entre les n-6 et les n-3 chez les mammifères (Burdge and Calder, 2005). En l'occurrence, les enzymes impliquées dans la conversion des AGPI précurseurs en AGPI-LC sont des enzymes limitantes car elles sont partagées par les deux familles d'AGPI n-6 et n-3 et sont donc en compétition (Simopoulos, 2011). Les enzymes impliquées dans la conversion ont généralement une préférence pour les AGPI n-3 (Tocher et al., 1998). De plus, lorsque les apports LA/ALA sont équilibrés, la conversion du LA s'arrête au niveau de l'AA. Néanmoins, en condition de déficience alimentaire en AGPI n-3, la conversion des AGPI n-6 se poursuit jusqu'à la production de DPA n-6. Ce dernier, qui a des analogies moléculaires avec le DHA, compense la diminution de ce dernier. La présence de DPA n-6 est ainsi un marqueur de carence alimentaire en AGPI n-3. Comme indiqué précédemment, les voies de conversion de LA et ALA sont communes, entraînant une compétition métabolique pour ces deux familles. Ainsi, la quantité d'AGPI-LC est fortement influencée par les apports alimentaires et le rapport en LA et ALA. Cette compétition concerne également la métabolisation des AGPI-LC de la famille des n-3 et n-6, lors de leur métabolisation en oxylipines, ou en endocannabinoïdes, qui implique également des enzymes communes. Ce point sera discuté dans un autre chapitre. Les AGPI-LC peuvent également être apportés directement par l'alimentation sous

forme d'AA, de DHA et d'EPA issus des produits animaux. En effet, la synthèse d'AGPI-LC à partir des précurseurs est inférieure à 5% car LA et ALA sont majoritairement dégradés par  $\beta$ -oxydation pour fournir de l'énergie d'une part et fournir de l'acétate pour la synthèse des AGS et AGMI d'autre part (Brenna, 2002; Brenna and Diau, 2007; Plourde and Cunnane, 2007). Chez l'homme, de 1 à 2 % du LA est converti en AGPI n-6 dont 0-5 % en AA (Emken, 1994). Cependant, l'efficacité de la conversion est plus importante chez la femme que chez l'homme, avec une régulation accrue des désaturases (Burdge and Calder, 2005)

## 2.1. Les désaturases

### 2.1.1. Présentation générale des désaturases

Les désaturases (D) introduisent des doubles liaisons éthyléniques à l'extrémité carboxyle de la chaîne carbonée des AGPI. Les désaturases sont classées selon leur localisation subcellulaire, avec les désaturases solubles et celles qui sont liées à la membrane. La seule désaturase soluble est la protéine porteuse d'acyl-acyl ou stéaroyl-ACP désaturase principalement retrouvée dans le stroma des plantes et qui induit la production d'acide oléique (C18 :1 n-9) à partir de l'acide stéarique (C18 :0) (Castro et al., 2016). Les désaturases liées à la membrane sont quant à elles omniprésentes chez les bactéries et les eucaryotes (Hashimoto et al., 2006). Les désaturases acyl-lipides et les désaturases acyl-coA se distinguent selon la nature du substrat lipidique auquel sont rattachés les acides gras, respectivement, AG estérifié à des glycérolipides ou à une coenzyme A (CoA) (Tocher et al., 1998).

Le cluster de gènes de désaturase (*fads*) est une famille de trois gènes (*fads* 1, 2, 3) localisés sur le chromosome humain 11 et assurant une activité enzymatique qui catalyse l'insertion d'une double liaison à partir du groupe carboxyle des AGS et AGPI et d'au moins un AGS, l'acide palmitique (C16 :0) (Nakamura and Nara, 2004). On distingue la désaturase delta-5 (D5D) (la double liaison est insérée à 5 carbones du groupe carboxyle), impliquée dans la synthèse de l'AA et de l'EPA à partir des précurseurs n-6 (LA) et n-3 (ALA), et la désaturase delta-6 (D6D). D5D et D6D sont respectivement codées par la *désaturase d'acides gras 1* (*fads1*) et la *désaturase d'acides gras 2* (*fads2*) (Marquardt et al., 2000). *Fads2* assure aussi une activité delta-8 (D8D) (Park et al., 2009) et delta-4 (D4D) (Park et al., 2015). Le troisième gène du cluster, *fads3* n'a à ce jour pas de fonction connue.

### 2.1.2. Altérations génétiques des désaturases et conséquences métaboliques et neurobiologiques

L'altération génétique des gènes *fads* a des conséquences sur la biosynthèse d'AGPI-LC, la composition du lait maternel, certaines fonctions physiologiques comme la fertilité mais également le risque de développer des pathologies, notamment neurodéveloppementales. Chez l'homme, des polymorphismes d'un nucléotide unique (SNP, single nucleotide polymorphism) communs aux

clusters de gène *fads* et de gène des élongases sont associés aux niveaux plasmatiques d'AGPI-LC n-6 et n-3 (Tanaka et al., 2009). Des polymorphismes de *fads2* ont été associés à une susceptibilité accrue de développer des désordres du spectre autistique (ASD pour Autism Spectrum disorder) chez des enfants chinois (Sun et al., 2018) ou la dépression (Cribb et al., 2018). De plus, un allèle mineur de *fads2* a été récemment associé à des défauts neurodéveloppementaux chez l'enfant prématuré (Kim et al., 2022), renforçant le lien entre métabolisme lipidique et développement cérébral. Le SNP rs175547 du cluster de gène *fads* altère l'activité désaturase dans des populations caucasiennes et asiatiques (Merino et al., 2011). Une altération de *fads2* dans les globules de matière grasse du lait maternel humain, *fads2AT2*, modifie la synthèse endogène d'AGPI-LC n-3 en supprimant l'activité D6D (Kothapalli et al., 2018). D6D est ainsi, en plus de la source alimentaire, clé dans le pool sanguin de DHA. *Fads2* est exprimé dans le foie et le tissu adipeux, et son expression est régulée par SREBP-1 (sterol regulatory element-binding protein1) et PPAR (peroxysomeproliferator-activated receptor) qui sont de puissants régulateurs du métabolisme lipidique (Dong et al., 2017; Ralston et al., 2015; Revilla et al., 2018). *Fads2* est exprimé dans le cerveau, notamment dans le noyau accumbens et son expression est régulée par le niveau d'EPA et DHA de la diète (Di Miceli et al., 2022). Au niveau cellulaire, *fads2* est exprimé par les astrocytes, avec une expression réduite en présence de DHA, mais pas en ALA, *in vitro* (Bewicz-Binkowska et al., 2019). *Fads1* est également exprimé par les astrocytes (Guttenplan et al., 2021) alors que *fads3* est faiblement exprimé (Zhang et al., 2014). Récemment, le microbiote a été incriminé dans la régulation de l'expression de *fads1* et *fads2* qui varie avec l'âge dans le cerveau (Albouery et al., 2020). Cependant, des études sont nécessaires pour déterminer précisément comment le cluster *fads* contribue à la production *in situ* d'AGPI-LC n-3 dans le cerveau, quels types cellulaires cérébraux expriment précisément ces différents gènes et comment leur expression est régulée et varie en fonction du sexe ou de l'âge. Des modèles murins génétiquement modifiées (KO, knock-out) *fads2* ont été développés pour étudier le rôle de cette enzyme à l'échelle de l'organisme et la contribution des différents AGPI-LC aux fonctions physiologiques (Stroud et al., 2009). Si les souris *fads2*<sup>-/-</sup> ne présentent pas d'altérations du développement et de la durée de vie, elles ont non seulement des altérations des taux d'AGPI-LC mais également de plusieurs grandes fonctions physiologiques comme la reproduction/fertilité (Stoffel et al., 2008), l'immunité (Monk et al., 2016) ou le métabolisme (Hayashi et al., 2021). La supplémentation alimentaire en AA et DHA permet de remodeler le profil en AGPI-LC des souris *fads2*<sup>-/-</sup> et de corriger les défauts de fertilité (Stoffel et al., 2020). Enfin, les variants génétiques du cluster des gènes *fads* 1, 2 et 3 contrôlent non seulement les taux des AGPI libres, mais également des phospholipides, lysophospholipides et les endocannabinoïdes (Reynolds et al., 2020).

## 2.2. Les élongases

### 2.2.1. Présentation générale des élongases

La famille des enzymes d'élongation des AG à très longues chaînes (Elovl pour elongation of very long chain-fatty acids) compte 7 membres qui sont formés d'un complexe multimérique. Elles résident dans le réticulum endoplasmique et sont classées en élongases des AGS et des AGMS (Elovl1, Elovl3, Elovl6 et Elovl7) et élongases des AGPI (Elovl2, Elovl4 et Elovl5) (Guillou et al., 2010; Jakobsson et al., 2006; Naganuma et al., 2011). Les Elovl2, Elovl5 et Elovl4 sont codées par les gènes *elovl2*, *elovl5* et *elovl4* respectivement (Jakobsson et al., 2006).

Elovl2 est particulièrement impliquée dans l'élongation des AGPI de 20 à 22 carbones et les AGS de 18 à 20 carbones (Guillou et al., 2010) et est peu exprimée dans le cerveau (Tvrđik et al., 2000). Un screening épigénétique chez l'homme a montré une augmentation de méthylation du gène *elovl2* qui commence à des stades précoces de la vie ce qui en fait un marqueur prometteur du vieillissement dans tous les tissus (Garagnani et al., 2012). Elovl5 joue un rôle dans l'élongation des AGPI et AGS à longue chaîne d'une longueur entre 18 et 22 carbones (Guillou et al., 2010) et est fortement exprimée dans les cellules de Purkinje du cervelet (Di Gregorio et al., 2014). Elovl4 contribue également à l'élongation des AGPI et AGS à longue chaîne de 24 carbones en AGPI et AGS à très longue chaîne (VLCFA, plus de 26 carbones) (Guillou et al., 2010) avec la particularité d'ensuite allonger ces AGPI et AGS à très longue chaîne jusqu'à 38 carbones. L'expression d'*elovl4* et les VLCFA ont été mis en évidence dans le cerveau, au niveau des neurones et des cellules gliales, et voient leurs niveaux augmentés dans le cerveau de patients atteints de démence fronto-temporale (He et al., 2021).

### 2.2.2. Altérations génétiques des désaturases et conséquences métaboliques et neurobiologiques

Bien que des polymorphismes du gène *elovl2* aient été récemment reportés comme associés à l'ASD, aucune pathologie n'est clairement associée à des mutations de ce gène (Sun et al., 2018). À l'inverse, deux mutations distinctes du gène *elovl5* sont à l'origine de l'ataxie spinocérébelleuse 38 chez l'Homme, caractérisée entre autre par une ataxie de la marche, une anosmie et une atrophie du cervelet (Di Gregorio et al., 2014). Les mutations du gène *elovl4* provoquent également des pathologies spécifiques comme la dystrophie maculaire de type Stargardt, l'ataxie spinocérébelleuse 34 et un syndrome neuro-ichtyotique (Deák et al., 2019). Chez la souris, la perte de fonction d'*elovl4* diminue les taux d'AGPI-LC de plus de 28 carbones et les oméga-O-acylcéramides dans la peau, conduisant à la mort néonatale (Vasireddy et al., 2007). Les souris *elovl2*<sup>-/-</sup>, générées en 2011, sont stériles et les souris mâle *elovl2*<sup>+/-</sup> (avec 50% d'inhibition de l'expression d'*elovl2*) présentent de graves problèmes de reproduction (Zadravec et al., 2011). De plus, les taux de DHA sont diminués dans les testicules des souris *elovl2*<sup>-/-</sup>, qui présentent également une augmentation de C22:4 n-6 et

une diminution de C22:5 n-6 (Zadravec et al., 2011). Le rôle d'Elovl2 dans la synthèse de DHA au niveau du foie chez la souris (Pauter et al., 2017) a été confirmé par l'utilisation d'un modèle de poisson zèbre Elovl2 KO (C. Liu et al., 2020). Lorsque les souris *elovl2* <sup>-/-</sup> sont nourries avec une diète riche en DHA, les déficits en DHA tissulaires sont corrigés, y compris chez les femelles gestantes et leurs petits, qui accumulent le DHA fournis par l'alimentation (Pauter et al., 2017). D'autres fonctions que la fonction reproductive sont altérées par l'ablation génétique d'*elovl2*, comme l'immunité innée (Talamonti et al., 2017), le métabolisme énergétique (Gómez Rodríguez et al., 2022; Pauter et al., 2019) ou les fonctions cérébrales (Talamonti et al., 2019). Ainsi, dans le cortex, l'absence de synthèse d'Elovl2 provoque chez la souris une altération de l'expression de marqueurs impliqués dans la plasticité synaptique ainsi que de l'apprentissage et de la mémoire (Talamonti et al., 2019). Récemment, un profilage épigénétique post-mortem d'hippocampes de patients atteints de la maladie d'Alzheimer a identifié un cluster de gènes associés, notamment *elovl2*, qui est corrélé positivement au niveau de la protéine phosphorylée Tau (Blanco-Luquin et al., 2020). Si le rôle de la méthylation de *elovl2* dans la maladie d'Alzheimer reste à démontrer, de nombreuses données de la littérature lient le DHA à l'incidence de pathologies neurodégénératives (Balakrishnan et al., 2021) suggérant que la dysfonction de cette enzyme pourrait relier les PUFA-LC ou les VLCFA à leur physiopathologie.

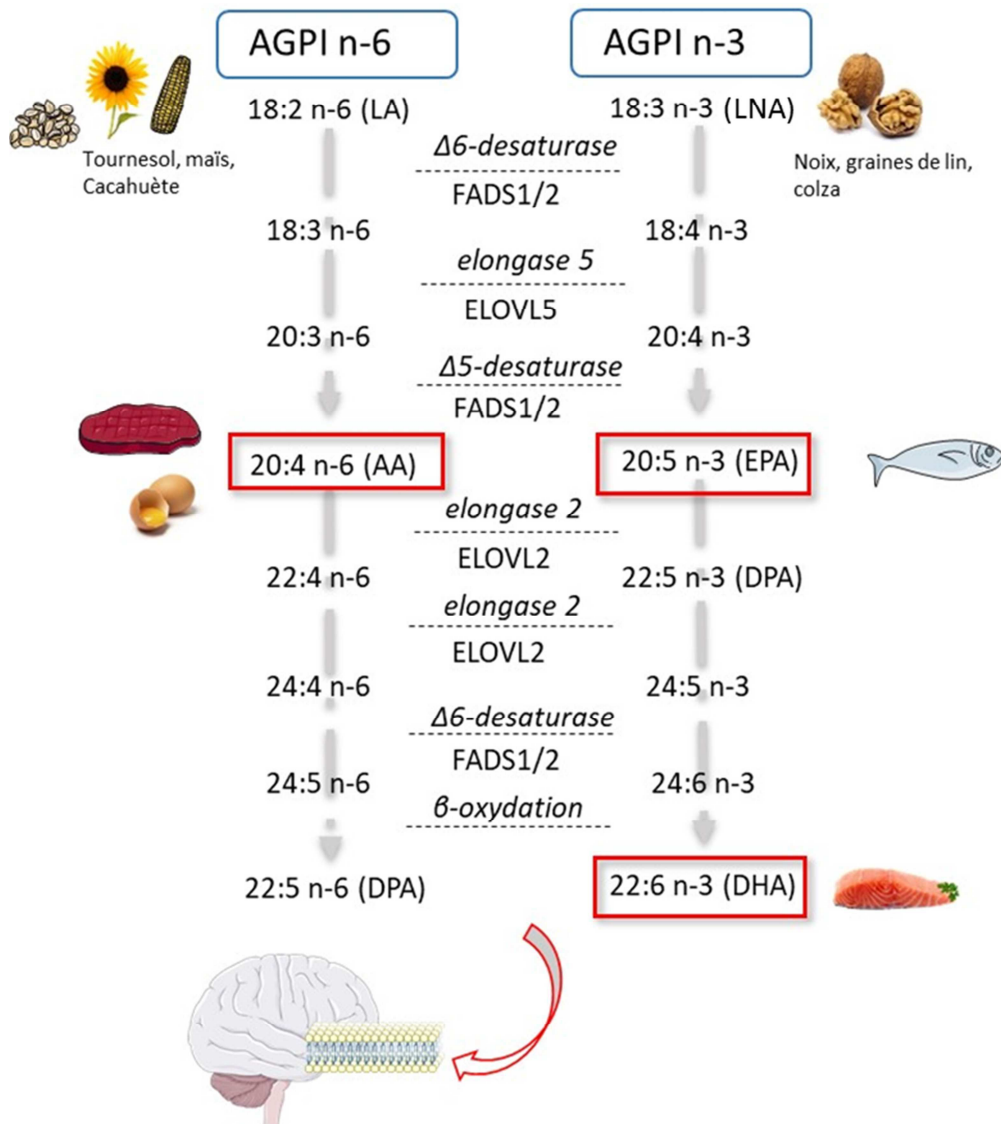


Figure 3 : Voies de synthèse des acides gras polyinsaturés à chaîne longue (adapté de (Joffre, 2019))

### 3. AGPI et cerveau

Le cerveau, avec le tissu adipeux, est l'organe le plus riche en lipides, qui représentent de 50 à 60% de son poids sec. La détermination de la composition lipidique du cerveau, bien que les approches en lipidomique aient beaucoup évoluées dans les dernières années, reste problématique. En effet, le cerveau subit de profondes modifications structurales au cours du développement et du vieillissement, comme la myélinisation, et possède une grande hétérogénéité cellulaire. Par exemple, dans le cerveau humain, la phosphatidylcholine (PC) prédomine à la naissance où elle représente près de 50% des lipides du cerveau pour décliner ensuite. Inversement, la sphingomyéline (SM) augmente de 2 à 15% à l'âge de 3 ans, ce qui correspond à la formation de la gaine de myéline et à la maturation des membranes. De plus, les différents types cellulaires présents (neurones, astrocytes, oligodendrocytes, cellules microgliales) ont une composition lipidique très distincte. Par exemple, les

neurones présentent des gangliosides complexes alors que les oligodendrocytes sont riches en galactosylcéramides. Ainsi, l'échantillonnage des différentes zones du cerveau est critique pour la mesure des lipides. Le développement de nouvelles technologies comme le MALDI (matrix-assisted laser desorption ionization as a mass spectrometry imaging) offre une nouvelle alternative pour obtenir une résolution spatiale des lipides dans le cerveau (Dawson, 2015). Ainsi, l'analyse MALDI de l'accrétion spatiale et temporelle des espèces lipidiques au cours du développement du cerveau a montré que le lipidome cérébral évolue de manière hétérogène au cours du développement du cerveau (Oliveira et al., 2022). Cette approche est utilisée par exemple pour générer des atlas lipidomiques en résolution spatiale de cerveaux post-mortem humains (Hunter et al., 2021).

En ce qui concerne les AG, la composition du cerveau du rongeur comporte de 36 à 46 % d'AGS, de 18 à 33% d'AGMI et de 18 à 28% d'AGPI (en % d'acides totaux) (Joffre et al., 2016). Comme indiqué précédemment, les AGPI n-3 et n-6 sont majoritairement estérifiés dans les phospholipides (PL), qui représentent 50 % des lipides totaux du cerveau. Parmi les phospholipides on distingue : les phosphatidylcholines (PC, 42-44%), les phosphatidyléthanolamines (PE, 36-40%), les phosphatidylsérines (PS, 11-13%) et les phosphatidylinositols (PI, 2-3%) (Sastry, 1985). Ces PL se distinguent par leur richesse en AGPI, qui représentent 33% des acides gras (Alessandri et al., 2004; Yehuda et al., 1999) et plus particulièrement les AGPI-LC tels que l'AA et le DHA. Ainsi, le DHA et l'AA représentent à eux seuls 50% et 30% respectivement des AGPI des PL cérébraux, alors que les précurseurs, LA et ALA, sont pratiquement absents. La substance blanche est moins riche en DHA et AA que la substance grise (Brenna and Diau, 2007). L'EPA est présent à de très faibles concentrations dans le parenchyme (Leyrolle et al., 2019). Bien que l'EPA et le DHA pénètrent dans le cerveau à un rythme similaire, l'EPA a un renouvellement relativement rapide au sein du cerveau, qui inclut la conversion en médiateurs lipidiques ayant des propriétés anti-inflammatoires (Bazinet et al., 2020; Layé et al., 2018). En l'occurrence, l'EPA est rapidement  $\beta$ -oxydé lors de son entrée dans le cerveau et pourrait servir à réguler les niveaux d'AG du cerveau en l'absence de transport sélectif (Chen and Bazinet, 2015). Récemment, il a été montré que l'EPA est rapidement estérifié dans les phospholipides des cellules microgliales murines et humaines, sans différence liée au sexe (Cisbani et al., 2021; Madore et al., 2020; Rey et al., 2018)

### *3.1. Incorporation des AGPI dans le cerveau*

Le développement pré- et post natal du cerveau ainsi que le vieillissement représentent des périodes critiques pour la composition lipidique du cerveau. L'accumulation d'AGPI n-3 et n-6 dans le cerveau, aussi appelée accrétion, débute pendant la gestation, période au cours de laquelle l'apport nutritionnel du fœtus dépend de l'apport alimentaire de la mère (Haggarty, 2010). Cette accrétion a



lieu plus particulièrement pendant la période périnatale entre le 3<sup>ème</sup> trimestre et 2 ans chez l'Homme (Martinez, 1992) et entre le 7<sup>ème</sup> et le 21<sup>ème</sup> jour post-natal chez les rongeurs (Lauritzen, 2001). Bien que les enzymes de synthèse des acides gras soient présentes dans le cerveau, le taux de synthèse du DHA et de l'AA est bas dans le cerveau et les apports pour le cerveau en développement dépendent essentiellement des apports maternels (Gibson and Makrides, 1998) .

Au cours du dernier trimestre de grossesse, le taux d'incorporation du DHA est de 3 mg/jour dans les membranes des cellules du cerveau puis de 5 mg/jour au cours des premiers mois du nourrisson (Cunnane et al., 2000). Les 6 premiers mois de la vie postnatale représentent le moment où le cerveau accumule près de 50 % du DHA corporel total incorporé soit 900 mg. Le DHA est apporté *via* le placenta puis le lait maternel et dépend donc des apports nutritionnels de la mère (Innis, 2005, 2004). Les teneurs en DHA chez le rat à la naissance augmentent en fonction de la teneur en ALA du régime maternel. Ainsi, les auteurs ont déterminé qu'un apport de 400mg/100g de ALA pendant la gestation puis de 200mg/100g pendant la lactation était optimal pour atteindre les teneurs cérébrales de DHA nécessaires à un bon développement (Guesnet et al., 2005).

Dans le cerveau adulte, l'AA et le DHA ne sont plus agrégés et les taux plasmatiques servent à remplacer ce qui est consommé par le cerveau (Carver, 2001). Dans le cerveau de rongeur mâle adulte, le DHA est présent en concentration plus importante dans le cortex préfrontal et dans l'hippocampe (respectivement 14,3% et 13,7% des acides gras totaux) (Carrié et al., 2000a; Delion et al., 1997; Joffre et al., 2016; McNamara and Carlson, 2006) que dans l'hypothalamus, le cortex ou le cervelet. L'AA est lui aussi présent majoritairement dans l'hippocampe (10,2 % des acides gras totaux) et dans le cortex préfrontal (9,7%) (Joffre et al., 2016).

Chez l'homme, les niveaux de DHA et d'AA sont plus élevés dans le cortex préfrontal et l'hippocampe (entre 16 et 22% des acides gras totaux) que dans le striatum (environ 14% des acides gras totaux) d'après des études réalisées *post-mortem* sur des cerveaux humains adultes (McNamara and Carlson, 2006). Les concentrations d'EPA sont très faibles dans le cerveau comme indiqué précédemment (Chen et al., 2009). Dans le cerveau humain, les formes de DHA et d'AA détectées sont celles estérifiées dans les membranes (Green et al., 2010). Le pourcentage d'AGPI n-3 est généralement mesuré dans les pools de lipides (lipides totaux, phospholipides) du plasma, qui reflètent la consommation régulière et les taux incorporés dans le cerveau (Hu et al., 2017; Létondor et al., 2014).

Par détection du C<sup>13</sup> des AG du cerveau, des études récentes montrent que dans le cerveau humain, les AG les plus abondants sont (par ordre décroissant) l'acide oléique (AGM), l'acide stéarique (AGS), l'acide palmitique (AGS), le DHA et l'AA. Le cholestérol et les AGS cérébraux sont issus de la métabolisation endogène du sucre (riche en C<sup>13</sup>), alors que DHA et AA sont essentiellement de source alimentaire animale marine et terrestre (pauvre en C<sup>13</sup>) (Lacombe et al., 2022). Comme

précédemment indiqué, l'origine du DHA cérébral est issue essentiellement de source alimentaire animale marine (Strobel et al., 2012) car le taux de conversion de l'ALA en DHA par le foie est faible (Plourde and Cunnane, 2007). De plus, l'accrétion de l'AA et du DHA est plus efficace lorsqu'ils sont apportés sous forme de PL que de TG (Werner et al., 2004).

Les variations d'AGPI-LC n-3 dans le cerveau des rongeurs au cours du vieillissement sont variables d'une étude à l'autre avec soit une diminution des niveaux de DHA, en particulier dans l'hippocampe, le cortex, le striatum et l'hypothalamus (Favrelière et al., 2003) ou, au contraire un maintien ou une augmentation (Moranis et al., 2012). Des modifications de composition lipidique globale ont été mises en évidence dans le cerveau de sujets âgés et atteints de pathologies neurodégénératives comme la Maladie d'Alzheimer (Naudí et al., 2015). Une diminution de l'activité D6D avec l'âge impacte l'efficacité de conversion des précurseurs en chaînes longues (Bourre and Piciotti, 1992). Le taux de conversion de l'ALA en DHA est faible dans le cerveau humain et devient encore moins efficace avec l'âge (Burdge and Calder, 2005).

### *3.2. Différences de composition d'AGPI des types cellulaires du cerveau*

Quelques données de la littérature montrent que les AGPI-LC s'accumulent dans les synaptosomes (Cao et al., 2009) ainsi que dans les membranes des astrocytes, de la microglie (Rey et al., 2018) et des oligodendrocytes (Brand et al., 2008; Yeh et al., 1998). De plus, les apports alimentaires en AGPI impactent de façon différentielle les teneurs en AGPI des cellules gliales et neuronales. Un régime déficient en AGPI n-3 (ALA 0,2% vs 6,5%) administré depuis la gestation jusqu'à l'âge de 2 semaines post-natale chez le rat provoque la diminution des taux en DHA des neurones, des astrocytes et des oligodendrocytes (Bourre et al., 1984). Cette diminution est compensée par une augmentation des taux de DPA n-6 (Bourre et al., 1984). La déficience nutritionnelle multigénérationnelle en AGPI n-3 diminue de moitié les taux de DHA dans les cellules du cerveau, neurones, astrocytes et oligodendrocytes (Bourre et al., 1989). Des rats carencés en AGPI n-3 puis nourris avec une diète enrichie en ALA (7,4% vs 0,4%) voient un recouvrement de 75% des taux de DHA dans les neurones et les astrocytes et de 50% dans les oligodendrocytes après 4 mois d'exposition (Bourre et al., 1989), suggérant que la correction des niveaux d'AGPI est cellule dépendante. Chez le rongeur, la consommation de diètes enrichies en DHA ou en DHA+EPA au cours de la gestation et de la lactation, augmente les taux de PE-DHA et PS-DHA dans les cellules gliales (Bowen and Clandinin, 2005; Destailats et al., 2010). Une supplémentation en DHA+EPA provoque également la diminution des taux d'AA et de DPA n-6 tandis qu'une supplémentation en DHA seul conduit seulement à une réduction du taux de DPA n-6 (Bowen and Clandinin, 2005; Destailats et al., 2010). L'AA s'accumule

dans les membranes des cellules vasculaires du cerveau qui pourraient jouer un rôle de stockage de l'AA (Brenna and Diau, 2007)

### *3.3. Influence du sexe sur la composition en AGPI du cerveau.*

Les taux d'AGPI varient dans le cerveau en fonction de facteurs extrinsèques et intrinsèques. Comme indiqué précédemment, les apports alimentaires en AGPI et les polymorphismes des gènes impliqués dans le métabolisme des AGPI-LC sont des déterminants clés de la teneur en AGPI du cerveau. Cependant, si toutes les structures cérébrales sont affectées, certaines sont plus affectées que d'autres comme le cortex préfrontal et l'hippocampe (Calder et al., 2007; Joffre et al., 2016). Plus récemment, des études menées chez l'homme et chez les rongeurs ont révélé que le genre influence les niveaux d'AGPI-LC, notamment dans le cerveau. En effet, chez les rongeurs, les femelles ont des taux de DHA plus élevés que les mâles, et ce indépendamment des teneurs alimentaires en AGPI de la diète (Lin et al., 2016). L'augmentation du DHA est associée aux niveaux d'hormones femelles, les oestrogènes (Giltay et al., 2004) qui influencent l'expression de *fads2* et de la D6D dans des cultures primaires d'hépatocytes humains (Sibbons et al., 2014) et le foie des rats (Extier et al., 2010). Chez l'homme, les niveaux érythrocytaires de DHA sont plus élevés chez les femmes en âge de procréer ainsi que chez les femmes ménopausées sous traitement hormonal substitutif (Magnusardottir et al., 2009). Ceci a été également observé chez les rats femelles adultes où le DHA est plus élevé dans les phospholipides hépatiques, mais pas dans les triglycérols (Burdge et al., 2008). Dans cette étude, il a également été révélé que l'expression de la D5D est plus élevée chez les femelles (Burdge et al., 2008). A l'inverse du DHA, l'AA est moins présent dans le plasma de rat femelle lorsque l'ALA est plus élevé dans le régime. Cependant, les taux d'AA sont équivalents pour les mâles et les femelles si l'apport alimentaire est faible en ALA. Dans le cas d'une carence alimentaire prolongée en ALA, les femelles accumulent plus d'AA par rapport aux femelles nourries avec une diète riche en ALA. Cette surproduction d'AA pourrait permettre de répondre à des besoins physiologiques qui seraient plus élevés chez les femelles que chez les mâles (Lin et al., 2016). Ces données renforcent l'idée que les besoins alimentaires en AGPI-LC n-3 sont différents chez les mâles et les femelles, cependant plus d'études sont nécessaires pour comprendre quels sont ces besoins (de Groot and Meyer, 2020). Au final, au-delà de l'apport alimentaire en AGPI, le sexe, les polymorphismes des gènes d'élongation et de désaturation des précurseurs des AGPI n-3 et n-6, l'âge et le statut métabolique influencent la biodisponibilité des AGPI-LC, notamment dans le cerveau. Une meilleure compréhension de ces interactions est nécessaire pour établir les besoins précis à l'échelle de l'individu en AGPI.

### 3.4. Transport des AGPI dans le cerveau

Le cerveau est à l'interface du sang par l'intermédiaire de plusieurs structures : la barrière hémato-encéphalique (BHE au niveau de l'endothélium des micro-vaisseaux cérébraux), la barrière hémato-céphalo-rachidienne (BHCR) et les plexus choroïdes (Strazielle and Ghersi-Egea, 2013). La BHE est composée de cellules endothéliales jointes par des jonctions serrées et étendues à l'unité neurovasculaire qui est formée par les cellules environnantes (péricytes, astrocytes, neurones et microglie) (Iadecola, 2017). Les AGPI sont transportés vers le cerveau par des lipoprotéines comme les LDL et les VLDL ou sous forme de complexe avec l'albumine, principalement depuis le foie *via* la circulation sanguine sous forme estérifiée ou non (Liu et al., 2015). Différents travaux réalisés chez le rongeur ont mis en évidence que les AGPI peuvent traverser la BHE. Cette dernière représente une barrière protectrice entre les vaisseaux sanguins du cerveau et l'environnement extracellulaire. Des études ont notamment utilisés des AGPI non-estérifiés radioactifs injectés dans le plasma qui ont ensuite été détectés dans le cerveau (Rapoport et al., 2001). Le transport des AGPI à travers la BHE et la BHCR se fait par diffusion passive ou par des protéines de transport et pour la BHCR, implique les plexus choroïdes (Pifferi et al., 2021). L'activité métabolique des plexus choroïdes mesurée *in vivo* et *in vitro* chez le lapin adulte a révélé que l'incorporation des traceurs radiomarqués en TG ou en PL était différente selon le plexus choroïde (gauche, droite, 3<sup>ème</sup> et 4<sup>ème</sup>) (Marinetti et al., 1971).

#### Diffusion passive

Le mécanisme de diffusion passive nécessite que les AGPI non-estérifiés se dissocient de l'albumine, pour se lier à la surface des cellules endothéliales et intégrer la bicouche lipidique en se transloquant dans le feuillet interne de la membrane par un mouvement transmembranaire ou « fli-flop » (Hamilton and Brunaldi, 2007; Lacombe et al., 2018). L'utilisation d'approches de perfusion de DHA et d'EPA radioactif *in situ* dans la carotide de souris adultes a permis de montrer que le DHA et l'EPA passent la BBB par diffusion car le coefficient de transport ne sature pas (Ouellet et al., 2009). Il a également été montré que l'albumine réduit le coefficient de transport du DHA (Ouellet et al., 2009).

#### Protéines de transport

Lorsqu'ils sont estérifiés à une lysophosphatidylcholine (lysoPC), les AGPI passent plus facilement la BHE (Lacombe et al., 2018), notamment *via* différentes protéines de transport d'AG. Le transporteur MFSD2A (major facilitator superfamily domain-containing protein 2A) est un des transporteurs majeurs de lysoPC contenant du DHA, qui est exprimé par les cellules endothéliales de la BHE (Nguyen et al., 2014). En effet, la délétion induite de *Mfsd2a* dans l'endothélium vasculaire de souris provoque la diminution du DHA dans le cerveau, révélant l'importance de MFSD2A dans l'assimilation cérébrale des lysoPC (Nguyen et al., 2014). De plus, la délétion de MFSD2A a des

conséquences majeures sur le développement de la BHE, le métabolisme des lipides et provoque une microencéphalie (Andreone et al., 2017; Ben-Zvi et al., 2014), renforçant l'importance de ce transporteur dans le développement postnatal du cerveau (Chan et al., 2018).

Les protéines de liaison aux acides gras (FABP, Fatty Acid binding Protein) permettent la dissociation des AG de l'albumine pour pouvoir traverser la bicouche lipidique membranaire (Zhang et al., 2017). Parmi les différentes FABP qui existent, seules FABP5 et FABP7 jouent un rôle dans l'utilisation du DHA (Pélerin et al., 2014). Leur expression est plus élevée au cours du développement pré-natal, puis elle décline après la naissance (Pélerin et al., 2014). Des expériences *in vitro* menées sur des cultures de neurones et de cellules gliales de rongeurs ont montré une corrélation de FABP7 avec la différenciation neuronale et une implication dans la signalisation dépendante du récepteur N-méthyl-D-aspartate (NMDA) (Owada et al., 2006). La FABP-7 a une forte affinité pour les AGPI n-3 et plus spécifiquement pour le DHA. Elle est abondamment exprimée dans les zones où la neurogénèse est prédominante comme l'hippocampe et les cellules gliales. A l'inverse, la FABP-3 a une affinité préférentielle pour les AGPI n-6 et est fortement exprimée par les neurones présents dans l'hippocampe et les couches corticales.

Les protéines de transport des AG (FATP pour Fatty Acid Transport Protein) permettent un transport sélectif des AG-LC à travers la BHE (Mitchell et al., 2011). FATP-1 et FATP-4 sont les principales protéines de transport des AG qui sont exprimées à la BHE, contrairement à la translocase d'acides gras (FA translocase/CD36) qui transporte les AG à travers les cellules endothéliales du cerveau (Mitchell et al., 2011). L'expression de FATP-1 est régulée par des facteurs comme PPAR ou RXR (Zhang et al., 2017).

Les cavéoles qui sont de petites invaginations intracellulaires des membranes plasmiques formées à partir des rafts lipidiques, transportent également les AG (Mitchell and Hatch, 2011). La calvéoline-1 est retrouvée dans les cellules endothéliales et les astrocytes et peut agir indirectement en contrôlant la localisation de CD36 (Kagawa et al., 2015).

Les ACSL (long chain acyl-coA synthetases) sont des protéines membranaires qui convertissent les formes libres d'AG en acyl-coA et sont, comme les FATPs, impliquées dans leur absorption cellulaire (Hall et al., 2005). Leurs activités semblent d'ailleurs liées à celle des FATP. Ainsi, dans des cultures d'adipocytes, FATP1 et ACSL1 sont colocalisés et agissent ensemble pour augmenter l'absorption d'AG (Richards et al., 2006). Dans le cerveau, ACSL4 est impliquée dans la régulation du signal de l'AA (recyclé en phospholipides) et ACSL6, quant à elle, peut moduler la différenciation neuronale en favorisant l'estérification du DHA dans les phospholipides (Marszalek et al., 2005, 2004).

Certaines protéines facilitent l'utilisation des AGPI. C'est le cas notamment des FATP qui possèdent une activité acyl CoA synthétase qui facilite le métabolisme des AGPI et augmente leur métabolisation mais pas leur transport (DiRusso et al., 2005). En effet, dans un modèle murin de

knock-out pour CD36, les niveaux cérébraux d'AGPI ne sont pas altérés, ce qui suggère qu'un autre mécanisme de transport des AGPI vers le cerveau existe (Song et al., 2010).

Enfin, l'apolipoprotéine E (APOE), synthétisée par les cellules gliales et les plexus choroïdes, s'associe aux lipides pour former des particules de transport de ces derniers dans le LCR (Koch et al., 2001). La majeure partie de l'APOE circulante est produite par le foie (Yu et al., 2014) et de façon moins importante par les macrophages (Kockx et al., 2008). D'autres cellules sont capables de synthétiser APOE comme les cellules endocriniennes telles que les cellules ovariennes et surrénales (Huang et al., 2015). Dans le cerveau, les astrocytes, les oligodendrocytes, les péricytes, le plexus choroïde et les neurones synthétisent APOE (Flowers and Rebeck, 2020; Kang et al., 2018). Les lipoprotéines APOE produites par le plexus choroïde sont directement sécrétées dans le LCR (Achariyar et al., 2016). APOE est un ligand des récepteurs des lipoprotéines de surface cellulaire appartenant à la famille des récepteurs des lipoprotéines de basse densité (LDLR) (Holtzman et al., 2012). Il existe 3 isoformes du gène *APOE* : *apoE2*, *apoE3* et *apoE4*. Les isoformes APOE3 et APOE4 se lient avec une haute affinité au LDLR et au récepteur 1 lié au LDLR (LRP1). LDLR est exprimé dans les neurones et les hépatocytes et LRP1 est présent dans les membranes plasmiques de nombreuses cellules y compris de la microglie, des astrocytes et des neurones (Goldstein and Brown, 2009).

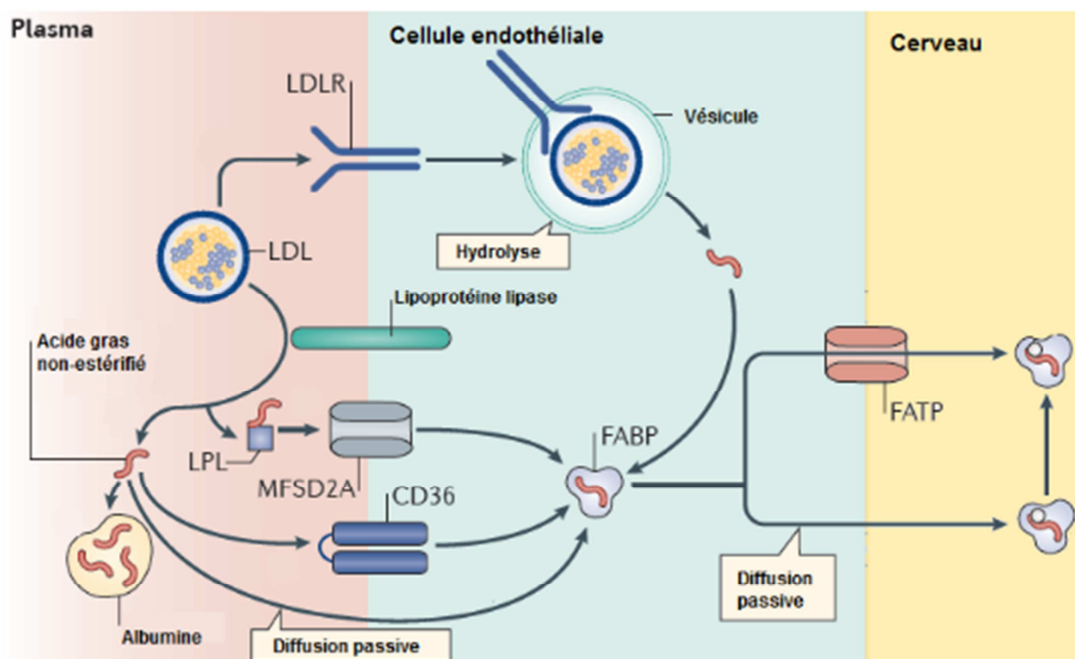


Figure 4 : Mécanismes de transport des AGPI dans le cerveau (Adapté de Bazinet et Layé, 2014)

### 3.5. Influence des SNPs des gènes du métabolisme des AGPI sur la biodisponibilité du DHA et les pathologies du cerveau

Des variations génétiques des gènes *fads* et *elovl* peuvent être à l'origine d'une altération des niveaux d'AGPI dans le plasma, indépendamment d'une variation nutritionnelle. On parle de polymorphismes de nucléotide unique (SNPs pour Single Nucléotide Polymorphisms). Ces SNPs peuvent causer des problèmes de santé (syndrome métabolique) et des modifications des profils lipidiques plasmatiques, c'est le cas de certains SNPs de *fads* par exemple (Muc et al., 2015). Les travaux de Muc et al., ont également démontré que les enfants touchés par des polymorphismes de *fads* avaient une expression de cytokines inflammatoires plus élevée (Muc et al., 2015).

D'autres SNPs dans le cluster de gène *fads1-fads2* (rs174537, rs174761 et rs383458) induisent une modification de l'activité désaturase et par conséquent des niveaux d'AGPI-LC. Le génotype rs174537 a notamment été associé à une modulation de l'activité de la D5D (Al-Hilal et al., 2013). Une méta-analyse conduite par Lemaître et al., sur les locus génétiques associés aux phospholipides plasmatiques a mis en avant le rôle des SNPs de *Fads1/2* dans l'augmentation des niveaux d'ALA et la diminution des niveaux d'EPA. Tandis que les SNPs sur *elovl2* sont plus susceptibles d'induire une augmentation d'EPA et une diminution des taux sanguins de DHA (Lemaitre et al., 2011).

Des mutations d'*elovl4* ou *elovl5* provoquent des pathologies neurologiques chez l'homme (Deák et al., 2019). Au début de l'embryogenèse du poisson zèbre, l'expression des gènes de désaturase et d'élongation, mesurée par qRT-PCR et l'hybridation in situ, est restreinte dans le temps et dans l'espace (Monroig et al., 2009). Les trois transcrits *FADS*, *ELOVL2* et *ELOVL5* sont fortement exprimés dans la région de la tête dès le début de l'embryogenèse, ce qui a également été confirmé par une autre étude (Tan et al., 2010). La détection précoce de ces gènes dans le cerveau au cours du développement embryonnaire peut suggérer que la production in situ d'AGPI LC pourrait avoir lieu. Cependant, la contribution de ces gènes par rapport à l'apport maternel en AGPI a été peu étudiée au cours du développement cérébral.

Certains génotypes sont responsables d'une modification de la biodisponibilité du DHA. C'est le cas notamment de l'APOE4. APOE régule l'homéostasie des lipides en modulant le transport des lipides d'un tissu ou d'un type cellulaire à un autre (Holtzman et al., 2012). L'APOE, présente dans le SNC et la périphérie, représente un lien critique entre ces deux compartiments. De plus, la présence de l'allèle epsilon 4 de l'APOE, est associé à un risque accru de développer la maladie d'Alzheimer (MA) (Corder et al., 1993) en perturbant notamment l'intégrité de la barrière hémato-encéphalique (BHE) (Chernick et al., 2019). Le gène *APOE* a trois variantes d'allèles *apoe2*, *apoe3* et *apoe4* qui sont déterminées par deux SNPs rs429358 et rs7412. La fréquence de l'allèle epsilon 4 d'*APOE* est plus que doublée chez les patients atteints d'Alzheimer (de 13,6 % à 36,7 %) (Farrer et al., 1997).

Certaines études chez l'homme et l'animal montrent une corrélation positive entre un régime enrichi en AGPI n-3 et une prévalence diminuée de la pathologie d'Alzheimer (Calon et al., 2004; Morris et al., 2003). Ce n'est pas le cas pour les porteurs d'*APOE4* (Samieri et al., 2011). L'essai clinique conduit par Quinn et al., en 2010 confirme ces observations : des patients Alzheimer consommant 2g de DHA par jour ont un score de démence amélioré, s'ils ne sont pas porteurs d'*APOE4* (Quinn et al., 2010). Les travaux de Vandal et al., montrent que les taux de DHA dans le plasma et dans le cerveau ainsi que le transport à travers la BHE sont modulés par le génotype *APOE*. Et plus particulièrement, l'expression de *APOE4* humain chez la souris provoque la diminution des niveaux de DHA dans le cerveau en comparaison avec l'expression de *APOE2* (Vandal et al., 2014).



## 4. Métabolisme des AGPI en dérivés bioactifs

L'AA, l'EPA et le DHA sont convertis en métabolites bioactifs qui exercent des effets neurobiologiques souvent opposés dans l'inflammation et, comme étudié plus récemment, dans la neuroinflammation. Ainsi, les dérivés de l'EPA et du DHA sont les intermédiaires des actions neuroprotectrices, neurotrophiques et anti-inflammatoires, alors que ceux issus de l'AA ont des effets majoritairement pro-inflammatoires et, seulement pour quelques espèces moléculaires, anti-inflammatoires. Dans ce chapitre, les principaux dérivés de l'AA, l'EPA et le DHA seront présentés ainsi que leurs effets potentiels dans la régulation de la neuroinflammation, car les dérivés ont été découverts et surtout étudiés dans ce contexte. Un focus sera fait sur les oxylipines et les endocannabinoïdes issus des AGPI n-3

### 4.1. Qu'est-ce que la neuroinflammation ?

L'inflammation est un processus autolimité et protecteur qui se résout généralement de lui-même, notamment par l'action de molécules aux activités pro-résolutives et anti-inflammatoires et rétablit l'homéostasie des tissus lésés. Le cerveau n'est pas un organe immuno-privilégié comme il a été prôné au siècle dernier. Ainsi, des événements neuro-inflammatoires se produisent dans le parenchyme cérébral et entraînent l'activation des cellules gliales, particulièrement les cellules microgliales et les astrocytes, et le recrutement de leucocytes périphériques (Harry and Kraft, 2008). La neuroinflammation, ainsi définie par la production de facteurs inflammatoires, dans le cerveau a également des vertus neuroprotectrices si elle est résolue. Cependant, si elle est persistante ou non résolue, elle altère de nombreuses fonctions neurologiques, entraîne des modifications comportementales, notamment de la mémoire, et contribue à la physiopathologie de pathologies neurovégétatives ou neuropsychiatriques (Dantzer, 2001). De plus, la neuroinflammation est une caractéristique commune à de nombreuses pathologies du cerveau et si les mécanismes ne sont pas encore complètement compris, les interactions entre les cellules immunitaires circulantes et résidentes du cerveau font l'objet d'intense recherche pour mieux comprendre leur rôle dans l'immunosurveillance et les pathologies du cerveau afin d'empêcher le basculement vers une neuroinflammation délétère pour le cerveau (Da Mesquita et al., 2018; Rustenhoven et al., 2021). Ainsi, l'immunosurveillance est un mécanisme physiologique essentiel pour la protection, la réparation et le maintien du cerveau, tant en situation de santé que pathologique (Schwartz et al., 1999), mais repose sur la résolution de l'inflammation. Les médiateurs lipidiques de la résolution de l'inflammation jouent un rôle crucial dans l'homéostasie cérébrale et la protection vis-à-vis des processus neurodégénératifs (Joffre et al., 2020; Layé et al., 2018; Rey et al., 2019). En effet, au cours

de la résolution de l'inflammation, les mêmes cellules qui sont impliquées dans les premières étapes de l'inflammation aiguë (*cie*, les cellules endothéliales vasculaires et les cellules immunitaires innées comme les cellules microgliales dans le cerveau) cessent progressivement de produire les eicosanoïdes classiques aux activités pro-inflammatoires (prostaglandines, leucotriènes, thromboxanes générés à partir de AA) et commencent à utiliser l'EPA et le DHA pour générer plus de 30 SPMs (Specialized Proresolving lipid Mediator) différents, y compris dans le cerveau (Basil and Levy, 2016; Chiurchiù et al., 2018; Layé et al., 2018; Serhan, 2014). Celles-ci incluent différentes familles telles que les résolvines, les protectines et les marésines et, bien qu'issues de voie enzymatiques distinctes et ayant des structures biochimiques différentes, partagent toutes la caractéristique d'activer la résolution de l'inflammation (élimination des cellules immunitaires extravasées dans les tissus, restauration, régénération et rémission) (Basil and Levy, 2016; Serhan, 2014; Serhan et al., 2020). Plus récemment, le rôle des SPMs a été questionné dans le cerveau, notamment dans la résolution de la neuroinflammation ainsi que l'impact que peut avoir la teneur alimentaire en AGPI-LC n-3 et n-6 dans la production et l'action des SPMs dans le cerveau (Layé et al., 2018). Des travaux récents ont mis en évidence que les SPMs et leurs récepteurs sont exprimés par les cellules du cerveau, notamment les cellules microgliales et que leur production et action sont régulées par les apports nutritionnels en AGPI (Calder, 2001; Joffre et al., 2020; Madore et al., 2020; Rey et al., 2019). Ces données suggèrent que l'activation des voies pro-résolutives se produit dans le cerveau. De plus, les SPMs pourraient être critiques dans la modulation de la diaphonie entre les cellules gliales et les neurones et ainsi affecter l'initiation et la progression de plusieurs neuropathologies.

## 4.2. Métabolisme des AGPI en oxylipines

### 4.2.1. Les phospholipases

Les phospholipases (PLA)<sub>1</sub> et <sub>2</sub> hydrolysent les liaisons des AG en position sn-1 et sn-2 pour libérer les AG et les lysophospholipides 2-acyl ou 1-acyl, respectivement. A l'inverse, la phospholipase B hydrolyse les AG en position sn-1 et sn-2 (Bornscheuer and Kazlauskas, 2004). PLA<sub>1</sub> et PLA<sub>2</sub> jouent un rôle important dans le remodelage de la structure membranaire cellulaire et de l'homéostasie et contribuent également à plusieurs aspects du métabolisme cellulaire par le biais de voies de signalisation spécifiques (Kita et al., 2019). Un intérêt tout particulier a été porté à la PLA<sub>2</sub> en raison de son implication dans la libération des AGPI des phospholipides membranaires. L'AA et le DHA sont présents en grandes quantités sur la position (sn)-2 des phospholipides membranaires dont ils sont libérés *via* l'action des PLA<sub>2</sub>, qui constituent une superfamille d'enzymes spécialisées dans l'hydrolyse en sn-2 des glycérophospholipides (Rapoport, 2003). Les PLA<sub>2</sub> sont soit associées à la membrane, soit cytosolique ou encore sécrétées. La localisation subcellulaire et leur substrat

confèrent aux PLA2 des spécificités en terme d'activités. Elles hydrolysent les phospholipides au niveau des liaisons ester. Les AGPI sont libérés des phospholipides de la membrane via les activités de trois principaux types de PLA2 : la PLA2 cytosolique dépendante du calcium (cPLA2), la PLA2 indépendante du calcium (iPLA2) et la PLA2 sécrétoire dépendante du calcium (sPLA2). Chaque PLA2 a une structure moléculaire et des modes d'actions distincts ainsi que des besoins en calcium différents selon les types de cellules. Parmi les nombreux isoformes de cPLA2, cPLA2 $\alpha$  est la plus courante chez les mammifères. Son activité dépend des taux de calcium intracellulaire (Leslie et al., 2010). Lorsque ces derniers augmentent, cPLA2 $\alpha$  est transloquée du cytosol jusqu'au noyau. De plus, la liaison au calcium augmente l'hydrophobicité de la membrane pour faciliter l'insertion des enzymes dans la bicouche lipidique (Hirabayashi et al., 2004). Le substrat préférentiel de la cPLA2 est la phosphatidylcholine qui porte l'AA en sn-2. Son action enzymatique libère la lysophosphatidylcholine (lysoLPC) et l'AA, ce dernier étant ensuite disponible pour une métabolisation ultérieure en dérivés bioactifs (Leslie, 2004; Riendeau et al., 1994). La sPLA2 est également spécifique de l'AA. La iPLA2, qui est indépendante du calcium, est soupçonnée d'hydrolyser les phospholipides cérébraux pour libérer le DHA (Green et al., 2008). En ce qui concerne le cerveau, des différences de localisation cellulaire des PLA2 ont été observées. La cPLA2 est exprimée notamment par les neurones, les astrocytes et la microglie (Sun et al., 2014). De plus, dans le cerveau, le DHA est estérifié majoritairement dans les phosphatidyléthanolamine (PE) et les phosphatidylcholine (PC). 90% du DHA libre après hydrolyse des PE et PC est re-ésterifié et 10% métabolisés en dérivés. Il existe 2 isoformes de iPLA2, VIA et VIB, qui présentent des homologies dans leurs parties C terminale. Le bromoenolactone, un inhibiteur spécifique des PLA2 non dépendante du calcium, et l'inhibition de la synthèse de iPLA2 inhibe la libération de DHA par les astrocytes, renforçant son rôle dans la genèse des formes libres de DHA (Strokin et al., 2007). Chez l'homme, la cPLA2 a une préférence pour l'AA, la iPLA2 pour l'EPA et la sPLA2 pour le DHA (Hayashi et al., 2021). Il est important de souligner que chez les souris des souches C57bl6, 129Sv et B10.RIII une mutation non-sens naturelle existe dans le gène de la sPLA2 (Bosetti, 2007).

L'AA, l'EPA et le DHA libres sont rapidement et majoritairement réincorporés dans les membranes *via* l'action de l'acyl-CoA synthétase (autour de 90%). Cependant, une petite partie de ces AGPI-LC non estérifiés (autour de 10%) va rentrer dans des voies cataboliques de conversion en oxylipines comme les eicosanoïdes ou les docosanoïdes par l'action des cyclooxygénases (COXs), des lipoxygénases (LOXs) ou cytochrome P450 (Cyp450) (Farooqui et al., 2007). Les dérivés bioactifs oxygénés, comme les oxylipines, ou les endocannabinoïdes ont un rôle primordial dans la régulation des fonctions immunitaires, l'inflammation et les fonctions synaptiques (Buckley et al., 2014; Rey et al., 2019; Serhan et al., 2015; Yang and Chen, 2008)

#### 4.2.2. Biosynthèse des oxylipines

Comme indiqué précédemment, une partie des AGPI-LC AA, EPA et DHA libérés des phospholipides membranaires est métabolisée en dérivés oxygénés, les oxylipines, par des enzymes spécifiques lipoxygénase (LOX), cyclooxygénase (COX) et cytochrome P450 (CYP450) (Smith and Murphy, 2016). Les oxylipines issues de l'AA sont des eicosanoïdes et regroupent les prostanoïdes, les leucotriènes, et les thromboxanes; celles issues de l'EPA et du DHA sont des médiateurs de résolution de l'inflammation (résolvines, marésines et protectines), des acides dihydroxy-eicosatriénoïque (diHEtrE), epoxy-eicosatriénoïque (EET), hydroxy-eicosapentaénoïque (HEPE), hydroxy-eicosatétraénoïque (HETE), hydroxydocosahexaénoïque (HpDHA) et oxo-eicosatétraénoïque (oxo-ETE) (Gabbs et al., 2015).

**Tableau 2** Enzymes de synthèse des oxylipines et localisation cérébrale et cellulaire des enzymes.

(AA : acide arachidonique, COX : cyclooxygénase, CYP : cytochrome P450, DHA : acide docosahexaénoïque, EET : acide epoxy-eicosatriénoïque, EPA : acide eicosapentaénoïque, HEPE : acide hydroxy-eicosapentaénoïque, HETE : acide eicosatétraénoïque, HpDHA : acide hydroxy-docosahexaénoïque, LOX : lipoxygénase, LT : leucotriène, LX : lipoxine, oxoETE : acide oxo-eicosatétraénoïque, PG : prostaglandine, RV : résolvine, TX : thromboxane)

<i>Enzyme</i>	<i>AG ou dérivé impliqué</i>	<i>Métabolite formé</i>	<i>Localisation</i>	<i>Référence</i>
COX-2	AA	PG et TX série 2	Cellules endothéliales, neurones, microglie	(Breder, 1997; Font-Nieves et al., 2012; Harris, 2003; Hoozemans et al., 2001; Kaufmann et al., 1996; Li et al., 2018; Yamagata et al., 1993; Yang and Chen, 2008)
	EPA	PG et TX série 2	Hippocampe, cortex, amygdale	
LOX-15	AA	15-HETE, 12-HETE	Neurones, cellules	(Calder, 2001; Gabbs et al., 2015; Guo et al., 2011; Huang et al., 1999; Sun et al., 2015)
	DHA	17-HpDHA	gliales	
	EPA	15-HEPE	Cortex préfrontal, Hippocampe	
LOX-5	AA	5-HEPE	Neurones, cellules gliales Cortex, hippocampe, cervelet	(Samuelson et al, 1999 ; Fredman et al., 2014 ; Jatan et al., 2006 ; Chinnici et al., 2007)
	15-HETE	LX série 4		
	EPA	5-HEPE		
	5-HEPE	LT série 5		
	15-HEPE	LX série 5		
	17-HpDHA	RV série D		
	18-HEPE	RV série E		
CYP450	AA	EET et 16-20 HETE	Neurones, astrocytes,	(Gabbs et al., 2015; Huang et al., 2016) Bystrom et al., 2011, Fleming, 2011, Nebert et al., 2013, Gilroy et al., 2016
	EPA	18-HEPE	vaisseaux sanguins	

#### 4.2.3. Enzymes de conversion impliquées dans la métabolisation des AGPI-LC en oxylipines

Les cyclooxygénases (COX) sont un groupe d'enzymes qui catalysent la conversion de l'AA en prostaglandines (PG) bioactives grâce à l'ajout d'oxygène (Choi et al., 2009). Il existe deux isoformes principaux de COX, COX-1, dont l'expression est constitutive et COX-2, dont l'expression est inductible notamment par des stimuli inflammatoires (Breder, 1997; Harris, 2003). Cependant, dans le cerveau COX-2 est constitutive dans les neurones où elle joue un rôle dans la physiologie neuronale (Hoozemans et al., 2001)(Breder et al., 1995; Li et al., 2018; Yamagata et al., 1993). La COX-2 neuronale est concentrée dans les dendrites post-synaptiques et les terminaisons excitatrices

du cortex, de l'hippocampe, de l'amygdale et de la moelle épinière (Kaufmann et al., 1996; Yamagata et al., 1993; Yang and Chen, 2008).

Au niveau cérébral, dans la réponse neuroinflammatoire induite par des cytokines ou des inducteurs de cytokines comme le lipopolysaccharide (LPS, une endotoxine des bactéries gram+), la COX-2 contribue à la production des prostaglandines et des thromboxanes (Davidson et al., 2001; Salinas et al., 2007) et son expression augmente dans les astrocytes et les microglies (Font-Nieves et al., 2012). COX-2 interagit avec le système endocannabinoïde et plus particulièrement le l'arachidonoyl-glycérol (2-AG). Par exemple, en culture de neurones hippocampique murins, le 2-AG endogène inhibe l'expression de COX-2 et les courants excitateurs postsynaptiques en réponse à un stimuli inflammatoire (Du et al., 2011). Finalement, COX peut, en plus des prostaglandines, produire des acides gras hydroxylés comme le 11-hydroxy-eicosatétraénoïque (11-HETE) à partir de l'AA, le 13-hydroxy-docosahexaénoïque acide (13-HDoHE) à partir du DHA et 9-hydroxy-octadécadiénoïque (9-HODE) à partir du précurseur LA (Serhan et al., 2002).

Les lipoxigénases exprimées dans le cerveau sont LOX-15 et LOX-5. Elles catalysent la formation d'acides gras hydroxylés et de leur métabolites (ou oxylipines) dont les leucotriènes, les lipoxines, les résolvines, les protectines, les marésines, les hepoxilines et les éoxines. La LOX-5, activée par la protéine activatrice de la 5-lipoxigénase (FLAP) produit les leucotriènes dont les leucotriène B4 (Samuelsson et al., 1987). Les activités LOX (et parfois y compris les activités époxygénase et hydrolase) entraînent la formation de di- et tri-hydroxy AG, comprenant les lipoxines, les résolvines, les protectines et les marésines (Buckley et al., 2014; Serhan et al., 2015). Les hepoxilines peuvent également être formées à partir du 12-HETE (Pace-Asciak, 2015). Comme pour les prostanoïdes, les oxylipines dérivées de LOX se lient à des récepteurs couplés aux protéines G, bien que les récepteurs de toutes ces oxylipines n'aient pas été identifiés. Chez l'homme et l'animal, la LOX-15, qui réside dans le cytosol des cellules mais qui est également liée aux membranes intracellulaires, catalyse l'AA pour donner les oxylipines 12-HETE et 15-HETE qui induisent des cascades de signalisation pro- et anti-inflammatoires. S'ils se lient à PPAR, ces dérivés ont un effet neuroprotecteur (Sun et al., 2015) et à l'inverse, en se liant au récepteur GPR31, les voies de signalisation activent la production de cytokines pro-inflammatoires (Interleukine 6 IL-6 et 12 IL-12) (Guo et al., 2011; Huang et al., 1999). L'AA est le substrat majoritaire de la 15-LOX par rapport à DHA et EPA (Calder, 2001). Lorsque LOX-15 utilise le DHA comme substrat, il y a une production de 17-HDHA et de 14-HDHA (Kutzner et al., 2017).

Comme la LOX-15, la LOX-5 peut générer des oxylipines aux fonctions pro- ou anti-inflammatoires, en fonction de sa localisation cellulaire et du substrat oxydé. Ainsi, à partir de l'AA, la LOX-5 favorise la synthèse de leucotriènes pro-inflammatoires lorsqu'elle se trouve dans le noyau tandis qu'elle facilite la production de LxA4 anti-inflammatoire lorsqu'elle est dans le cytoplasme (Fredman et al., 2014).

Dans le cerveau, l'inhibition de la LOX-5 est protectrice car elle entraîne une inhibition de la voie pro-inflammatoire NFκB ce qui limite les dommages cérébraux associés (Jatana et al., 2006). Avec l'âge, l'expression de la LOX-5 augmente dans l'hippocampe (Chinnici et al., 2007).

La dernière voie du métabolisme des oxylipines est celle du cytochrome P450 (CYP) qui forme un large éventail d'enzymes liées à la membrane et nommées ainsi car elles ont une absorbance unique à 450 nm lorsqu'elles sont réduites et liées par le monoxyde de carbone. Chez les mammifères, il existe une cinquantaine de CYP différentes divisées en 4 familles (CYP1 à 4) et sous-familles (Christmas, 2015). Les enzymes CYP peuvent avoir une activité époxygénase ou hydroxylase. Le rôle des CYP450 est large et complexe. Les epoxydes (EET) générés par les familles enzymatiques CYP2C et CYP2J à partir de l'AA ont des propriétés anti-inflammatoires dans les monocytes et les macrophages (Bystrom et al., 2011; Fleming, 2011; Gilroy et al., 2016; Nebert et al., 2013). Les CYP peuvent convertir l'AA, l'EPA et le DHA en acide époxyeicosatriénoïque (EpETrE), en acide époxyeicosatétraénoïque (EpETE) et en acide époxydocosapentaénoïque (EpDPE) respectivement, *via* leur activité époxygénase. Mais elles peuvent aussi convertir l'AA, l'EPA et le DHA en HETE, acide hydroxyeicosapentaénoïque (HEPE) et HDoHE, respectivement *via* leur activité hydroxylase. Les produits issus de l'activité époxygénase sont rapidement métabolisés *via* l'hydrolase époxyde soluble (sEH) pour former les acides gras dihydroxyles comme les métabolites de l'AA, de l'EPA et du DHA : l'acide dihydroxyeicosatriénoïque (DiHETrE), le DiHETE et l'acide dihydroxydocosapentaénoïque respectivement. De la même façon que pour les autres voies de formation des oxylipines, les métabolites issus de la voie CYP vont se lier à des récepteurs spécifiques ou avec des récepteurs communs à d'autres oxylipines.

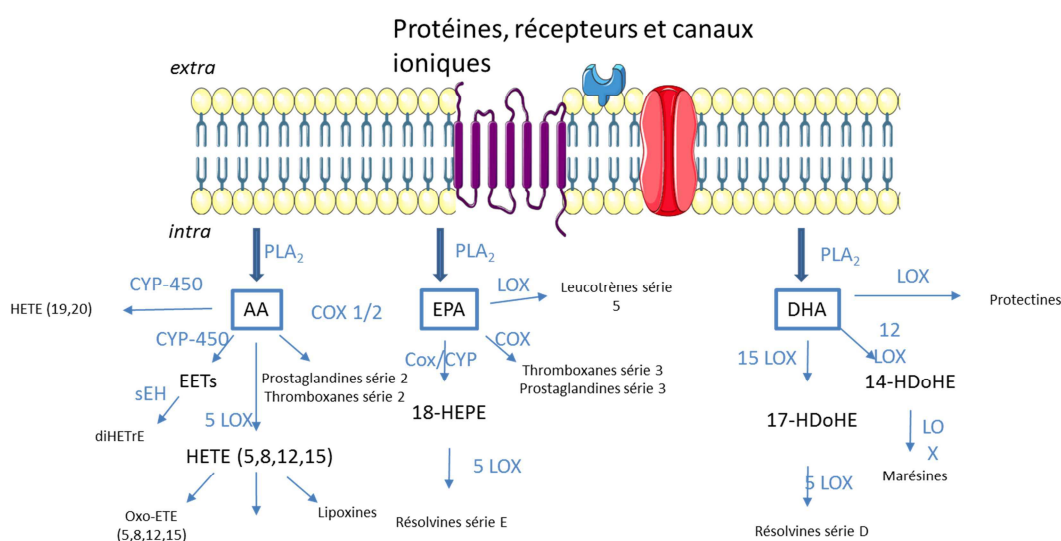


Figure 5 : Les AGPI n-3 et n-6 sont métabolisés en oxylipines par les voies COX, LOX et CYP450. (Adapté de Michael-Titus and Priestley, 2014)

#### 4.2.4. SPMs et leurs récepteurs dans le cerveau

Les SPMs (Specialized pro-resolving lipid mediators) font partie d'une grande famille de molécules pro-résolutive (Serhan, 2017). Les SPMs sont retrouvés dans le sang, le liquide céphalo-rachidien, le placenta, les fluides synoviaux, l'urine mais aussi dans les tissus, dont le cerveau (Layé et al., 2018). Parmi ces molécules on compte les lipoxines issues de l'AA (LxA4 et LxB4), les résolvines de la série E issues de l'EPA (RvE1-RvE3), les Rv de la série D issues du DHA (RvD1-RvD6), les protectines, les neuroprotectines (PD1/NPD1 et PDX), les maresines (MaR1 et MaR2) et les dérivés du docosapentaénoic (DPA) de la série 13 (RvT1-RvT4) ainsi que leurs formes épimériques induites par l'aspirine (AT-RvD1-AT-RvD6) (Joffre et al., 2020; Layé et al., 2018; Serhan et al., 2015). Les activités pro-résolutives et anti-inflammatoires des SPMs sont principalement produites par leur effet sur des récepteurs à protéine G (GPR) dont certains ont été identifiés dans le cerveau (Joffre et al., 2020)

##### ***Lipoxines dérivées de l'AA***

Les Lx sont catalysées par plusieurs voies enzymatiques : la voie 15-LOX dans les cellules endothéliales, les monocytes ou les éosinophiles, qui génère l'intermédiaire 15-S-HpETE, ensuite converti en 5,6-époxytétraène par la 5-LOX avant d'être finalement hydrolysé en LxA4 ou LxB4 (Bennett and Gilroy, 2017) ; l'oxygénation de l'AA en leucotriène A4 (LTA4) ensuite converti en LxA4 et LxB4 via la 12-LOX (Freire et Van Dyke, 2013) ; une troisième voie de biosynthèse qui implique l'administration d'aspirine, un anti-inflammatoire non stéroïdien couramment utilisé, qui déclenche l'acétylation irréversible de la COX-2. Le blocage de l'activité de la COX-2 permet la formation de l'intermédiaire 15-R-HETE qui est rapidement libéré et capturé par les leucocytes adhérents ou les cellules endothéliales vasculaires, puis métabolisé par la 5-LOX pour former des Lx 15-épimères ou des Lx déclenchés par l'aspirine (AT- Lx) (Serhan, 2005). Les effets pro-résolutifs des Lx est exercé par le récepteur ALX/FRP2 (lipoxinA4 receptor/formyl peptide receptor 2) qui est partagé par d'autres SPMs (Chiang et al., 2005). Les Lx, qui ont été les premiers SPMs identifiés sont considérés comme les initiateurs de ce processus biologique et le déclencheur du changement métabolique (Serhan and Oliw, 2001). À ce jour, aucun récepteur spécifique pour LxB4 n'a encore été identifié. Dans le cerveau, les récepteurs ALX/FRP2 sont exprimés notamment par les astrocytes, les cellules microgliales et les neurones, suggérant l'interaction de ces types cellulaires dans la régulation de la neuroinflammation (Krashia et al., 2019). L'activation de ces récepteurs par des agonistes spécifiques, la LxA4 ou l'AT-Lx conduit à la réduction de la production des cytokines inflammatoires par les cellules microgliales (Futokoro et al., 2022; X.-J. Wang et al., 2011), la neuroinflammation (Derada Troletti et al., 2019) y compris en situation neurodégénérative (Pamplona et al., 2022). Les neurones et cellules microgliales produisent de grande quantité de LxA4 qui a un effet protecteur vis-



à-vis du déclin cognitif lié à l'âge chez le rongeur et les sujets atteints de démence présentent des taux réduits de LxA4 dans le LCR (Pamplona et al., 2022).

### ***Résolvines dérivées de l'EPA***

Comme indiqué précédemment, les RvE sont issues du catabolisme de l'EPA par aspirin-COX2, 5-LOX et CYP450, notamment en situation inflammatoire. Au cours de l'inflammation, les mêmes cellules qui ont généré les eicosanoïdes commencent à utiliser l'EPA comme substrat au lieu de l'AA. La biosynthèse des RvE est initiée par les cellules endothéliales vasculaires qui convertissent l'EPA en 18-HEPE et procède par une biosynthèse transcellulaire via la COX-2 acétylée et le CYP450. Ensuite, les leucocytes, par le biais de la 5-LOX et d'une série d'époxydations et d'hydrolyses enzymatiques, génèrent RvE1 (Serhan et al., 2002) et, RvE2 (Tjonahen et al., 2006). La 18-HEPE peut être directement transformée en RvE3 par la 12/15-LOX dans les leucocytes (Isobe et al., 2012). La RvE4, récemment découverte, est synthétisée par les neutrophiles et les macrophages humains par la 5-LOX (Libreros et al., 2021). Les RvE1-E4 augmentent l'efferocytose des cellules apoptotiques par les macrophages et bloquent le recrutement des leucocytes dans les tissus inflammés (Vik and Hansen, 2021). Les actions pro-résolutives de RvE1 et RvE2 sont dues à leur capacité à activer ChemR23 et à antagoniser BLT1, qui est impliqué dans les effets pro-inflammatoires de LTB4 (Chiang and Serhan, 2017). Ces deux récepteurs sont des récepteurs largement exprimés dans plusieurs cellules de la périphérie et le cerveau. À ce jour, les récepteurs de RvE3 et RvE4 restent à identifier. ChemR23, qui est aussi le récepteur de la chemerine, une adipocytokine anti-inflammatoire (Wittamer et al., 2003), est exprimé par les neurones et les cellules microgliales (Wang et al., 2015) et est impliqué dans les effets anti-inflammatoire de la RvE1 (Arita et al., 2005). BLT1 et ChemR23 ont été détectés dans les neurones et les cellules gliales de toutes les régions examinées du cerveau humain, avec des niveaux nettement plus élevés dans ceux de patients atteints de la maladie d'Alzheimer que dans les cerveaux contrôles (Emre et al., 2020). Ces données sont cohérentes avec l'observation que les voies de résolution sont perturbées dans la maladie d'Alzheimer (Wang et al., 2015; Zhu et al., 2021). Chez le rongeur, l'administration intracérébroventriculaire de RvE1/E2 protège des effets anxiogènes de l'inflammation par leur action via ChemR23 (Deyama et al., 2018). De plus, l'administration chronique de RvE1 à un modèle murin de Down Syndrome améliore les altérations mnésiques et diminue la neuroinflammation, notamment l'activation microgliale dans l'hippocampe (Hamlett et al., 2020). Les effets bénéfiques de la RvD1 sur la mémoire et la neuroinflammation ont également été décrits dans un modèle murin de maladie d'Alzheimer (Kantarci et al., 2018) ou, de lésion focale cérébrale (Harrison et al., 2015). La RvE1 a un effet direct sur les cellules microgliales, par son action sur ChemR23/ALX et les voies inflammatoires (Rey et al., 2016). Dans un modèle de douleur inflammatoire, RvE1 abolit les augmentations du courant postsynaptique exciteur et l'hyperactivité

des récepteurs de l'acide N-méthyl-D-aspartique (NMDA) provoquées par l'inflammation dans les neurones de la corne dorsale de la moelle épinière (Xu et al., 2010).

### ***Résolvines, maresins et protectines dérivées du DHA***

Le DHA est converti en résolvines (RvD), en protectines (PD) et en marésines (MaR) de la série D. Ces 3 classes de SPMs dérivés du DHA sont clés dans la résolution de l'inflammation en réduisant l'infiltration des leucocytes, en éliminant les pathogènes, les débris, les cellules mortes par efferocytose et en réduisant la production des médiateurs pro-inflammatoires et augmentant celle des médiateurs anti-inflammatoires. Chaque groupe est constitué de plusieurs molécules comprenant au total plus de 20 SPMs biologiquement actifs.

La synthèse des RvD commence par la conversion du DHA par la 15-LOX en 17(S)-HpDHA (hydroperoxyDHA) qui est à son tour converti par la 5-LOX en RvD1, RvD2 et RvD5 ou RvD3, RvD4 et RvD6 ou en PD1 (ou NPD1 lorsqu'elle est produite dans les tissus cérébraux) et en PDX. La COX-2 acétylée par l'aspirine peut aussi métaboliser le DHA en 17(R)-HpDHA, qui est ensuite transformée par la 5-LOX en AT-D-résolvines ou AT-protectines (Serhan, 2014, p. 201; Serhan et al., 2015). L'activité des RvD1, 3 et 5 et AT-RvD se fait par ALX/FPR2 (lipoxinA4 receptor/formyl peptide receptor 2) chez les rongeurs et GPR32/DRV1 chez l'homme qui sont tous deux exprimés par les cellules T (Chiurchiù et al., 2019). GPR32 qui appartient à la famille des rhodopsines, est exprimé majoritairement par les macrophages. Dans les macrophages humains, l'activation de GPR32 par la RvD1 active la phagocytose et l'élimination des débris cellulaires (Krishnamoorthy et al., 2010). *In vitro*, RvD1 réduit l'activation des cellules microgliales par ses effets sur ALX (Rey et al., 2016). Notamment, RvD1 module l'expression des miR-155, miR-146, miR-21 et miR-219 par les cellules microgliales (Rey et al., 2016). Ces miRs ont différents rôles biologiques: miR-21 est essentiel à la production de la cytokine anti-inflammatoire IL-10, miR-146 régule la transcription des cytokines, des chimiokines et de leur récepteur, miR-219 diminue la transcription du TNF- $\alpha$  et miR-208a régule l'activation de NF $\kappa$ B (Recchiuti et al., 2011). Chez l'homme, une diminution de RvD1 a été trouvée dans le sang de patients atteints de pathologies neurodégénératives ou neuropsychiatriques (revue récente de (Roohbakhsh et al., 2022)). De nombreux travaux menés chez l'animal montrent que l'administration de RvD1 réduit la neuroinflammation dans des modèles de lésions cérébrales, d'anxiété/dépression ou de maladies neurodégénératives (Layé et al., 2018; Tomaszewski et al., 2020; Wang et al., 2015). RvD2 engage le récepteur GPR18/DRV2 (Chiang and Serhan, 2017) pour provoquer la phagocytose des cellules apoptotiques et des microbes et la résolution de l'inflammation (Chiang et al., 2015). GPR18 est exprimé dans le cerveau notamment par la microglie (Chiang et al., 2015). Récemment, RvD2 a été montré comme ayant un effet neuroprotecteur vis-à-vis de la neuroinflammation et les lésions cérébrales *via* son action sur GPR18 (Zhang et al., 2022). Il

est important de souligner que les RvD agissent à des concentrations proches du nM, alors que les AT-RvD ont des activités lorsqu'elles sont de l'ordre du mM.

Dans le cerveau, le DHA est métabolisé par la LOX-15 en NPD1 (Calandria et al., 2009). NPD1 possède une activité neuroprotectrice par la modulation de l'inflammation et une fonction anti-apoptotique qui contribue au maintien de l'homéostasie cérébrale (Mukherjee et al., 2004). En effet, l'activation des voies de signalisation en aval de NPD1 entraîne l'activation de gènes pro-survie et la suppression de gènes pro-apoptotiques (Asatryan and Bazan, 2017). De plus, des niveaux réduits de NPD1 et de son précurseur DHA ont été mis en évidence dans le tissu cérébral post-mortem de la maladie d'Alzheimer tout comme ceux du LXA4, de MaR1 et de RvD5. PD1 se lie aux récepteurs GPR37 (Bang et al., 2018). Dans le cerveau, les macrophages, les neurones, les astrocytes et les oligodendrocytes expriment très fortement GPR37 qui joue un rôle neuroprotecteur en interagissant avec la prosaposin et la prosaptide qui sont des neuropeptides. Cette interaction protège du stress oxydatif et permet la survie cellulaire (Meyer et al., 2013).

Les marésines MaR1 et MaR2 sont générées à partir du DHA par la voie 12-LOX dans les macrophages humains et 12/15-LOX dans les macrophages murins (Deng et al., 2014; Serhan et al., 2008). La présence de l'intermédiaire 14(S)-HDHA est un marqueur des MaR (Deng et al., 2014; Serhan et al., 2008). Le profilage d'oxylipines d'exsudats murins montre que les niveaux de 14-HDHA forment un pic tard dans la phase de résolution, suggérant un rôle pour ces médiateurs dans le rétablissement de l'homéostasie tissulaire (Serhan et al., 2008). Mar1 interagit avec BLT1, qui est fortement exprimé par les leucocytes, les macrophages, les neurones et les cellules gliales (Tager et al., 2003), où il exerce une activité d'agoniste partiel et antagonise l'activation de LTB<sub>4</sub> (Colas et al., 2016). LGR6 est un récepteur de Mar1 qui est exprimé dans les macrophages, mais aussi les neurones et les astrocytes (Chiang et al., 2019). Très récemment Mar2 a été identifié comme le médiateur de la résolution de l'inflammation induite par l'obésité au sein du tissu adipeux brun (Sugimoto et al., 2022). L'administration intrathécale de MaR améliore l'inflammation et les troubles cognitifs induits par une hypoperfusion cérébrale chez le rat (Li et al., 2022). Le niveau de MaR est diminué dans le cerveau de patients atteints de la maladie d'Alzheimer (Zhu et al., 2016) et MaR1 augmente l'activité phagocytaire des cellules microgliales vis-à-vis de la protéine Aβ (Zhu et al., 2016). Enfin, il est important de noter parmi les dérivés bioactifs du DHA les élovanoïdes (ELV), qui sont des métabolites oxydés synthétisés à partir des produits d'élongation du DHA contenant 32- ou 34-carbones (Jun et al., 2017). Les composés formés ELV-N32 et ELV-N34, qui sont des produits d'élongation par ELOVL4 dans l'épithélium pigmentaire rétinien ont des propriétés antioxydantes et préviennent la dégénérescence rétinienne.

Enfin, le DPA n-3 peut également être converti en résolvines, protectines et marésines de la série n-3 DPA (Dalli et al., 2013) et est également le précurseur de résolvines de la série 13 ou T (RvT1-4) (Dalli

et al., 2015). Le rôle de ces dérivés n'est pas encore élucidé, même si des données indiquent que l'action de RvD5 n-3 DPA sur son récepteur GPR101 permet la résolution de l'arthrite inflammatoire (Flak et al., 2020). Bien que l'expression de GPR101 ait été mise en évidence dans l'hypophyse et certaines régions cérébrales du fœtus humain et que DPA n-3, le précurseur de RvD5 n-3 DPA, soit présent dans le cerveau (Drouin et al., 2019; Trivellin et al., 2020), aucune étude n'a été menée sur les effets de ce dérivé sur les fonctions cérébrales.

#### 4.3. Endocannabinoïdome

Le système endocannabinoïde (eCB) est composé de l'arachidonylethanolamide (anandamide, AEA), du 2-arachidonyleglycerol (2-AG) qui sont des dérivés métaboliques de l'AA, des récepteurs canoniques CB1R et CB2R et des enzymes de synthèse et de dégradation des eCBs. La NAPE-PLD (N-acylphosphatidyléthanolamine-phospholipase D-like hydrolase) catalyse la synthèse de l'AEA et la FAAH (fatty acid amide hydrolase) catalyse son hydrolyse. La DAGL (diacylglycérol lipase) catalyse la synthèse du 2-AG et la monoacylglycérol lipase (MAGL) catalyse son hydrolyse. Les récepteurs CB1R et CB2R sont des GPR. CB1R a une expression pléiotropique et est très exprimé dans le cerveau, surtout dans les neurones, mais également à plus faible niveau dans les astrocytes, où ils jouent un rôle dans les processus mnésiques (Covelo et al., 2021) et les cellules microgliales, où ils contribuent à la réponse neuroinflammatoire (De Meij et al., 2021a). L'activation des CB1R est associée à une pléthore de fonctions physiologiques (Scheen et al., 2008) et neurobiologiques, y compris de la plasticité synaptique (Puente et al., 2010). A l'inverse, l'expression de CB2R est plus restreinte et son activation est limitée, notamment à la régulation de l'immunité (Ashton et al., 2006). En raison de sa faible expression dans le cerveau, les effets du CB2R dans les fonctions cérébrales a été peu étudié, et ce n'est que récemment que son rôle dans les pathologies psychiatriques a été évoqué (Kibret et al., 2022). De nombreuses études soulignent l'importance des eCB dans la modulation de l'inflammation. En situation inflammatoire, les cellules immunitaires produisent des eCBs et leur produit de dégradation qui exercent des effets anti-inflammatoires *via* l'activation des récepteurs CB2 (Facchinetti et al., 2003; Pacher et al., 2006). De plus, les cellules microgliales, qui régulent la production de cytokines inflammatoires lorsqu'elles sont activées expriment le récepteur CB2 (Stella, 2022).

Le système eCB a été récemment enrichi de nouveaux médiateurs lipidiques, enzymes et récepteurs, pour devenir l'endocannabinoïdome (eCBome) (Di Marzo, 2020) **Figure 6**. Ainsi les récepteurs GPR55, TRPV1, PPAR, GPR18, GPR110, GPR119 et leurs ligands, N-acylated amino acids (lipoamino acids), N-acylethanolamines (NAEs comme PEA, OEA, LEA, DHEA) et 2-AcGs (2-OG, 2-LG), N-acyl-neurotransmitters (N-acyl-dopamines and N-acyl-serotonins) sont de nouveaux acteurs de l'eCBome

**Figure 6.** Les AGPI-LC n-3 sont également métabolisés en molécules de type eCB, les NAEs : le docosahexaénoylethanolamide (DHEA) ou synaptamide qui est dérivé du DHA et l'eicosapentaénoylethanolamide (EPEA) est dérivé de l'EPA. Le DHEA est fortement exprimé dans le cerveau, notamment l'hippocampe, où il est exprimé par les neurones embryonnaires (Kim et al., 2022). La synthèse de DHEA utilise les mêmes voies biochimiques que celles utilisées pour générer l'AEA, notamment la N-Acylphosphatidyléthanolamine(NAPE)-phospholipase D (NAPLD) à l'activité de N-acylation phosphodiesterase. Le DHEA est hydrolysé en DHA et éthanolamine par la FAAH, suggérant qu'une grande partie de cet analogue eCB est rapidement hydrolysé après sa formation dans le cerveau (Kim and Spector, 2018). Enfin, le DHEA peut être converti en métabolites oxydés qui sont des ligands du CB2 et ont des effets anti-inflammatoires (McDougle et al., 2017). Des données récentes ont mis en évidence que le DHEA est l'intermédiaire des effets neurodéveloppementaux du DHA comme la croissance des neurites et la synaptogenèse via le récepteur GPR110 (Kharebava et al., 2015).

La production endogène de DHEA dans le cerveau est influencée par l'apport alimentaire en AGPI n-3 (Berger et al., 2001). L'augmentation de DHEA s'accompagne d'une diminution de 2-AG et d'AEA lorsque les animaux sont nourris avec une diète riche en DHA (Watanabe et al., 2003). Inversement, un régime maternel déficient en AGPI n-3 altère la plasticité synaptique, notamment la potentialisation à long terme (LTP) dans l'hippocampe et la dépression à long terme (LTD) médiées par les endocannabinoïdes dans le noyau accumbens (NAC) et le cortex préfrontal (PFC), ainsi que les voies de signalisation du CB1R dans la progéniture (Lafourcade et al., 2011; Larrieu et al., 2012; Thomazeau et al., 2016). Cependant, alors que l'AA augmente, les taux de 2-AG et AEA ne varient pas dans le cerveau. La consommation de diète appauvrie en AGPI n-3 augmente l'expression de CB2R dans le cerveau de la progéniture adulte et ce dès la naissance (Isaac et al., 2021). Inversement, la consommation de diète riche en DHA augmente le DHEA et l'EPEA et diminue le 2-AG dans le cerveau des nouveaux-nés (Isaac et al., 2021). Ces modifications de l'endocannabinoïdome du nouveau-né s'accompagnent de la variation de protéines synaptiques, mais pas du nombre de cellules microgliales, comme précédemment décrit (Madore et al., 2020, 2014). Ainsi, les taux et type d'AGPI n-3 dans la diète influencent l'endocannabinoïdome qui pourrait contribuer aux effets de la diète sur les systèmes synaptiques et de plasticité neuronale et/ou la plasticité synaptique et/ou la neuroinflammation. Cependant, des études supplémentaires sont nécessaires pour déterminer le rôle précis de l'endocannabinoïdome dans ces effets. D'autre part, étant donné que les eCBs et les oxylipines sont en étroite relation, de par leurs origines communes, il serait intéressant de mieux décrypter si ces deux systèmes interagissent dans les effets de la diète enrichie en DHA et EPA sur le cerveau.

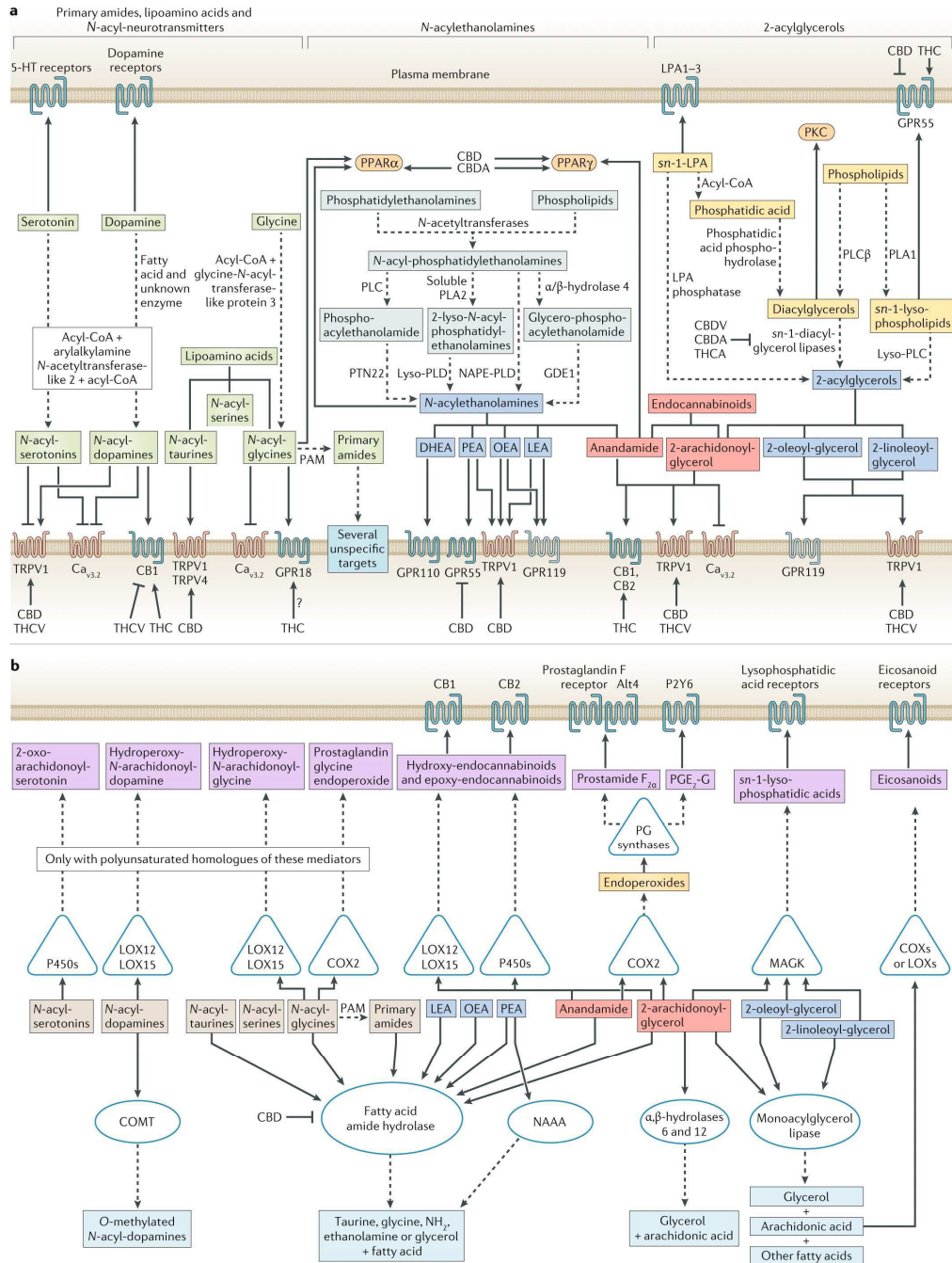


**Figure 6** Effets membranaires des différents médiateurs lipidiques issus des AG n-3 et n-6 et agissant au sein de l'endocannabinoïdome (extrait de Cristoni et al., 2019)

## 5. Rôle des AGPI dans le cerveau et le comportement

### 5.1. AGPI n-3 et période développementale

Le dernier rapport de l'Agence Nationale de Sécurité Sanitaire de l'alimentation, de l'environnement et du travail (ANSES, 2011) définit un besoin physiologique minimal (apport nutritionnel conseillé ANC) en lipides totaux de 30% de l'apport énergétique (AE) chez un adulte homme ou femme en bonne santé avec un AE proche de 2000 kcal. En ce qui concerne les AGPI, la recommandation porte d'une part sur le rapport LA/ALA qui doit être autour de  $\frac{1}{4}$ , puis sur la consommation des AGPI-LC n-3 avec une dose minimale journalière de 250 mg pour l'EPA et 250 mg pour le DHA. Pour les populations particulières comme les nourrissons, enfants, femmes allaitantes ou enceintes et les personnes âgées, ces besoins peuvent varier. En France, l'étude individuelle de consommation alimentaire (INCA2) réalisée entre 2006-2007 a permis de créer une base de données reflétant la consommation alimentaire de la population. L'apport moyen en AGPI n-3 est près de deux fois plus faible que les ANC (tableau 3).

L'ISSFAL recommande de consommer au moins 200mg par jour de DHA pour une femme enceinte (Koletzko et al., 2007), cependant ces valeurs ne prennent pas en compte les effets des AGPI n-3 sur la prématurité. Aux Etats-Unis, une étude récente financée par les instituts nationaux de la santé, de la santé infantile et du développement humain (NICHD) a conduit à conseiller aux cliniciens de prescrire 1000 mg de DHA par jour pour réduire le risque de prématurité précoce (moins de 34 semaines avant terme) (Best et al., 2022; Carlson et al., 2021). Très récemment, une synthèse a été réalisée par un groupe d'experts (ISSFAL) et conclut que le DHA et l'EPA ont un rôle crucial dans la durée des grossesses à un seul enfant. L'apport adéquat d'AGPI-LC n-3 en début de grossesse, conformément aux recommandations nutritionnelles existantes, diminue le risque de naissances prématurées. Par ailleurs, les femmes ayant de faibles apports en AGPI sont celles qui bénéficient le plus d'une supplémentation en EPA/DHA telle que recommandée (autour de 1000 mg DHA+EPA en débutant avant 20 semaines de gestation) (Best et al., 2022).

**Tableau 3 :** Apports Nutritionnels Conseillés pour un adulte selon l'ANSES et apports moyen selon l'INCA2  
Données en % de l'apport énergétique ou en mg/jour.

	ANC 2011	Apport moyen quotidien en France
LA C18 :2 n-6	4%	3,9%
ALA C18 :3 n-3	1%	0,4%
DHA C22 :6 n-3	250 mg	137 mg
EPA C20 :5 n-3	250 mg	102 mg

## 5.2. AGPI n-3 et cognition chez l'enfant

Chez l'Homme, l'accrétion des AGPI et plus particulièrement du DHA et de l'AA commence lors du troisième trimestre de grossesse (Clandinin et al., 1980). On observe donc une accrétion exponentielle des AGPI LC n-3 et n-6 entre les 26<sup>ème</sup> et 43<sup>ème</sup> semaines de grossesse tandis que l'accrétion postnatale des AGPI-LC est plutôt stable (Martinez, 1992). La forte demande en DHA du cerveau fœtal est soutenue par les apports fournis par la mère, grâce à la synthèse accrue de DHA à partir de l'ALA et à la mobilisation des réserves maternelles de DHA à partir du tissu adipeux (Metherel et al., 2017). L'apport en AGPI-LC n-3 et n-6 du fœtus et du nouveau-né dépend donc des apports maternels pendant la gestation et la lactation. Cette contribution résulte de l'apport alimentaire maternel, qui est transféré par le placenta pendant la gestation (Larqué et al., 2006), puis par le lait pendant la lactation (Innis, 2004). La teneur du lait maternel en AGPI-LC n'est pas régulée par la glande mammaire mais reflète les concentrations d'AGPI-LC dans le plasma de la mère qui, à leur tour, dépendent des teneurs en AGPI n-3 de son régime alimentaire et des activités de ses désaturases et élongases, impliquées dans la conversion de LA et ALA alimentaires en AGPI-LC (Heird, 2001). Malgré les avantages connus, de nombreuses familles ont du mal à atteindre leurs objectifs en matière d'allaitement, et seulement 25 % des mères américaines respectent les recommandations de lactation exclusive pendant 6 mois et de poursuite de l'allaitement jusqu'à l'âge de 1 ou 2 ans (CDC 2022).

Il est important de noter que des travaux récents ont montré la présence d'AGPI-LC libres ou estérifiés ainsi que des oxylipines dérivées du DHA dans le lait humain (Gan et al., 2020; Pitino et al., 2019; Robinson et al., 2017). Les formes d'oxylipines les plus représentées dans le lait maternel sont celles dérivées du LA (Gan et al., 2020), qui jouent un rôle essentiel dans le développement du cerveau du rat (Hennebelle et al., 2020). Dans le lait maternel lié à la prématurité, des associations positives existent entre l'AA et le TxB2, l'EPA et la 18-HEPE et entre le DHA, le PDX et 14- et 17-HDHA. De plus, les concentrations de DHA sont 1,5 fois plus élevées et celles de 14-HDHA 1,7 fois plus élevées dans le lait des femmes prenant des suppléments de DHA (Robinson et al., 2017). LTB<sub>4</sub>, Lx et RVDs sont détectés dans le lait humain au début de la lactation (Weiss et al., 2013). En outre, le DHA et son produit hydroxylé non estérifié, le 17-HDoHE, diminuent avec le temps au cours de la lactation. Les taux d'oxylipines du lait maternel de donneur ne sont pas affectés par la pasteurisation (Pitino et al., 2019). Les oxylipines du lait pourraient, avec les taux d'acides aminés être des biomarqueurs des liens entre le statut métabolique et nutritionnel de la mère et le développement corporel du nourrisson (Riederer et al., 2020). La présence de SPMs en particulier dans le lait maternel représente un potentiel pour réduire la gravité des maladies à composantes inflammatoires, et pourquoi pas neuroinflammatoires, chez les nourrissons (Arnardottir et al., 2016).



Cependant, le rôle des oxylipines du lait dans les processus neurodéveloppementaux n'est pas connu et reste peu étudié. La question de la biodisponibilité des oxylipines du lait maternel vers l'enfant allaité est posée. Bien que les oxylipines non estérifiées soient les principales molécules bioactives, celles estérifiées dans les TG et les PL peuvent être rendues biodisponibles par l'activité des lipases, notamment celles activées dans l'intestin du nourrisson par les sels biliaires du lait maternel (Gan et al., 2020; Walker, 2022). En ce qui concerne les mères, une supplémentation en EPA+DHA au cours de la grossesse atténue le déclin de DHA, de 7-HDHA et 4-HDHA et du 14-HDHA, mais pas de l'EPA et des oxylipines associées pendant la gestation. Cependant, ces variations sanguines dépendent du statut en DHA des femmes au début de la supplémentation (Best et al., 2022).

Les enfants nés avant terme (<37 semaines de gestation), en particulier ceux nés <29 semaines de gestation, présentent un risque accru de développer des troubles du neurodéveloppement (Pravia and Benny, 2020; Soleimani et al., 2014). La période d'accrétion in utero du DHA est perturbée par la prématurité et, bien que ces enfants reçoivent du DHA via le lait maternel et/ou les préparations pour nourrissons prématurés, cette quantité est insuffisante pour atteindre les taux nécessaires (Hewawasam et al., 2021). Ainsi, les enfants nés prématurément ont des niveaux de DHA cérébral inférieurs à ceux retrouvés chez des enfants nés à terme (Lapillonne and Jensen, 2009). De plus, les taux de DHA sont inférieurs dans le plasma, les érythrocytes et le cerveau d'enfants nourris par du lait maternisé par rapport à ceux allaités (Carlson and Neuringer, 1999). Enfin, un taux de DHA bas est un facteur de risque de prématurité (Brantsæter et al., 2017), et augmente le risque de complications et de mortalité des enfants prématurés (Fares et al., 2017). Afin de réduire le risque de gestation courte et de palier au défaut d'accrétion de DHA dans le cerveau des enfants prématurés, plusieurs cohortes ont été créées pour compléter des femmes au cours de la grossesse avec du DHA. Cependant, les supplémentations en DHA ont donné des résultats mitigés, notamment sur l'amélioration des fonctions cognitives des enfants prématurés avec des améliorations de l'attention (Jasani et al., 2017; Westerberg et al., 2011) ou sans effet (Hewawasam et al., 2021). Ces différences pourraient être liées aux doses et composition en AGPI-LC n-3, le niveau d'éducation des familles et l'âge auquel les évaluations cognitives ont été réalisées. Un autre paramètre concerne la santé mentale des mères. En effet, de faibles taux de DHA ont été associés à un risque accru de dépression post-partum chez la mère (Hamazaki et al., 2016).

La période de la conception au deuxième anniversaire de l'enfant, communément appelée "les 1000 premiers jours", est une période cruciale pour la nutrition de la dyade mère-enfant. Comme indiqué précédemment, le DHA joue un rôle important dans la construction du cerveau pendant les périodes périnatales. L'ajout de DHA dans les formules de lait maternisé améliore le développement visuel, mental et moteur chez des enfants prématurés (Fewtrell, 2006). Les taux sanguins élevés de DHA ou une consommation plus importante en AGPI n-3 de la mère sont associés à de meilleures capacités

cognitives chez leurs enfants (Braarud et al., 2018). Par exemple, des taux sanguins élevés en AGPI n-3 pendant la grossesse ont été corrélés avec de meilleures réponses émotionnelles mais également avec une meilleure concentration chez les enfants à l'âge de 5 ans (Loomans et al., 2014).

L'étude clinique COGNIS a étudié les effets à long terme d'une formule enrichie en AGPI-LC comparé à une formule standard, le groupe de référence étant représenté par des enfants ayant été allaités jusqu'à l'âge de 18 mois. Les résultats montrent que la formule supplémentée est associée à des effets à long terme sur le développement cognitif des enfants ainsi que sur la structure cérébrale. Les enfants présentent, suite aux tests neurocognitifs et aux IRM réalisés à 6 ans, des volumes plus importants dans le cortex orbital, un meilleur score de QI et une meilleure attention que les enfants allaités. Des analyses corrélatives suggèrent que de plus grand volumes et une épaisseur corticale des régions frontales et pariétales sont associés au développement cognitif (langage et fonctions exécutives) (Nieto-Ruiz et al., 2022). Des nourrissons nés avant 29 semaines de gestation et supplémentés en DHA par voie d'administration entérale jusqu'à 36 semaines ont des scores cognitifs améliorés à l'âge de 5 ans (Gould et al., 2022). Cependant, d'autres études indiquent que l'hyperactivité/inattention et les problèmes relationnels avec des pairs ne sont pas améliorés, voire altérés par la supplémentation prénatale en DHA d'enfants nés à terme (Gould et al., 2022). Enfin, une meta-analyse des données de supplémentation en DHA administrée à des femmes enceintes ou à des nourrissons au cours des 1000 premiers jours n'a pas révélé d'effets sur le développement comportemental. Ainsi, l'effet des suppléments en DHA pendant le neurodéveloppement ne fait pas consensus en terme d'impact sur la cognition de l'enfant (Gould et al., 2022).

### *5.3. AGPI, cognition et intégrité structurelle et fonctionnelle du cerveau des sujets adultes et âgés*

#### *5.3.1. Données épidémiologiques et cliniques*

L'adhésion à des régimes alimentaires dit « prudents » tels que le régime méditerranéen (MeDI), DASH et MIND (Mediterranean-DASH Intervention for Neurodegenerative Delay) est associée à une préservation de la santé cognitive avec l'âge et une réduction du risque de développer des démences (Samieri et al., 2013). Chez l'adulte sain, l'adhésion à un régime MeDI ou MIND est également positivement associée aux performances de mémoire de travail et des fonctions exécutives (Reddan et al., 2019; Thomas et al., 2022). Les effets protecteurs de ces diètes pourraient être liés entre-autre aux AGPI n-3 dont les teneurs sont élevées. Ainsi, des études observationnelles ont révélé des associations entre le statut en AGPI n-3, les fonctions cognitives et l'intégrité structurelle du cerveau. Chez les individus âgés et cognitivement sains, une consommation élevée en poisson gras est corrélée à un plus grand volume de matière grise dans le cortex orbitofrontal, le cingulaire postérieur, le précuneus et l'hippocampe (Raji et al., 2014). La consommation élevée de poisson

prédit également l'intégrité macrostructurale de la matière blanche (Virtanen et al., 2008) et la santé cérébrovasculaire (Thomas et al., 2021). Des associations identiques ont été trouvées avec le statut en AGPI-LC n-3 (McNamara and Almeida, 2019). Des niveaux plus élevés d'EPA+DHA plasmatiques ont été systématiquement associés à un risque plus faible de démence, d'accumulation de la protéine Ab, à un déclin plus faible de la cognition globale, de la mémoire et du volume du lobe temporal médian (Rouch et al., 2022; Thomas et al., 2020). De plus, la mémoire verbale épisodique est associée à l'EPA alors que les fonctions exécutives ne sont pas associées aux AGPI circulants (Duchaine et al., 2022). De plus, les associations entre AGPI n-3 et mémoire dépendent du sexe (Duchaine et al., 2022). Le lien entre AGPI-LC n-3 et déclin cognitif a été corroboré récemment par la mise en évidence que le DHA est parmi les 15 métabolites sanguins (sur 299 mesurés) associés au déclin cognitif (van der Lee et al., 2018). Cependant, une signature lipidique sanguine associée au déclin cognitif corrèle la PE (18:1 ;20:4), riche en AA, au déclin cognitif (Lefèvre-Arbogast et al., 2021). Un indice de risque nutritionnel (NRI) basé sur les dosages sanguins de DHA, DPA n-3, vitamine D et homocystéine permet de lier le NRI au déclin cognitif (Bowman et al., 2019). Au final, le lien entre les taux faibles de DHA et EPA sanguins et le déclin cognitif lié à l'âge et/ou la démence est clairement établie. Cependant, les essais contrôlés randomisés (RCT) avec des suppléments en DHA+EPA pour limiter le déclin cognitif ont donné des résultats mitigés avec, au mieux, des effets modestes et le plus souvent pas d'effets (Burckhardt et al., 2016; Yassine et al., 2022). Plusieurs raisons peuvent être à l'origine de cette absence d'effet 1) le niveau d'AGPI-LC n-3 des sujets supplémentés qui, s'il est faible avant la supplémentation, permet le maintien des fonctions exécutives par la supplémentation en DHA+EPA (Hooper et al., 2017). Des études récentes ont établi un seuil d'index omega-3 (EPA+DHA des erythrocytes) < à 5% (Coley et al., 2018); 2) L'âge, le sexe et le génotype APOE4, qui influencent l'absorption des AGPI n-3 par le cerveau (Maltais et al., 2022) : chez les sujets âgés, l'augmentation des concentrations circulantes en AGPI-LC n-3 rend le DHA plus disponible pour la  $\beta$ -oxydation (Plourde et al., 2014). De plus, la supplémentation en DHA améliore la cognition et le niveau de DHA dans le LCR et le sang chez les sujets âgés non porteur d'APOE4 (Quinn et al., 2010; Tomaszewski et al., 2020) ; 3) le type, la durée d'exposition et la dose d'AGPI-LC n-3. En l'occurrence, beaucoup de RCTs ont utilisé des suppléments riches en DHA, alors que des données récentes indiquent que l'EPA pourrait avoir des effets plus efficaces (Fairbairn et al., 2020; Martins, 2009; Rogers et al., 2008; Sublette et al., 2011). Ainsi, identifier le seuil optimal de l'indice d'AGPI-LC n-3 qui permet de prédire le déclin cognitif et/ou la réponse au traitement par les AGPI-LC n-3, permettra de définir la population cible pour prévenir le déclin cognitif et/ou la démence. En l'occurrence, des travaux récents indiquent que les profils en oxylipines sont des pistes prometteuses de détermination d'indicateurs de réponses aux AGPI n-3 vis-à-vis de l'inflammation cérébrale chez les sujets à risque de démence et porteurs de l'allèle APOE4 (Ebright et al., 2022).

Si les données sont nombreuses chez les sujets âgés et les enfants prématurés, le lien entre statut en AGPI, structure du cerveau et cognition est plus tenu chez les adultes et les adolescents. Comme pour les enfants, les métaanalyses des effets d'une supplémentation en AGPI n-3 sur la cognition chez les personnes en bonne santé ne sont pas concluantes (Stonehouse, 2014), même si quelques données indiquent une amélioration de la mémoire par le DHA chez des adultes sains (Stonehouse et al., 2013). Plus récemment, des RCTs conduits avec de l'EPA chez des adultes en bonne santé ont révélé que cette espèce d'AGPI-LC n-3 a une incidence bénéfique sur les fonctions cognitives et le traitement des informations visuelles par le cortex (Bauer et al., 2014, 2011). Des individus âgés de 25 à 49 ans sains et non consommateur de suppléments alimentaires riche en AGPI n-3 ont reçu des suppléments en EPA+DHA enrichi en DHA (900+270 mg/j) ou enrichi en EPA (360+900 mg/j) micro-émulsifiés, ce qui augmente sa biodisponibilité, pendant 26 semaines et les fonctions cognitives, la consolidation de la mémoire et la fatigue perçue ont été mesurées (Patan et al., 2021). La formule enrichie en EPA améliore les fonctions cognitives globales et la précision de l'exécution des tâches de mémoire en comparaison à la formule DHA et le placebo (Patan et al., 2021). Ce travail suggère que l'EPA est plus efficace que le DHA, cependant les mécanismes d'action ne sont pas connus.

#### *5.4. Modèles animaux pour étudier les mécanismes impliqués dans les effets des AGPI sur la cognition*

Comme précédemment discuté, le lien entre le statut nutritionnel et la cognition a largement été établi par de nombreuses études épidémiologiques chez l'homme et ce tout au long de la vie. En l'occurrence, le statut cérébral en AGPI relie les apports nutritionnels, leur métabolisation et les capacités cognitives (Bazinet and Layé, 2014; Joffre, 2019; Makrides, 2013). Afin de comprendre les mécanismes neurobiologiques impliqués, des modèles animaux ont été développés. En l'occurrence, l'utilisation de diètes isocaloriques qui diffèrent sur les proportions de précurseurs LA et ALA, apportés par des huiles végétales, et/ou en formes longues EPA, DHA, DPA n-3 ou AA, apportés par des produits animaux, ont été développées, notamment sur des rongeurs, mais également chez le singe (Fedorova and Salem, 2006). Des diètes équilibrées en ALA/LA (1/4) sont utilisées comme contrôle des diètes carencées en ALA et en AGPI-LC n-3 et riches en LA, qui provoquent des modifications drastiques des taux de DHA dans le cerveau (Joffre et al., 2016). Cependant, les diètes carencées en AGPI n-3 sont parfois utilisées comme contrôle de l'effet des diètes supplémentées en AGPI-LC n-3. Il est important de noter que la carence alimentaire en AGPI n-3 est bien plus sévère que ce que l'on peut trouver dans les populations humaines (Innis, 2000). Certaines études ont aussi utilisé des modèles multigénérationnels en mesurant les effets du régime sur la 2<sup>ème</sup> ou 3<sup>ème</sup> génération d'animaux déficients en AGPI n-3 (Chalon, 2006). Des modèles transgéniques ont également été développées pour diminuer les taux de DHA, y compris dans le cerveau : les souris KO

pour *elovl2* nourries avec des diètes avec ou sans DHA pour assurer leur reproduction (Pauter et al., 2014; Zadavec et al., 2011). Des souris avec une déficience du gène *fads2* ont également été générées pour modifier les AGPI n-3 accumulés dans l'organisme (Stoffel et al., 2008). Tout comme les *elovl2* KO, elles sont stériles et doivent être nourries avec des diètes riches en DHA pour se reproduire. La diminution de DHA est drastique dans le foie des souris KO *fads2*, mais modeste dans le cerveau (Stroud et al., 2009). Aucune production de AA n'est mesurée lorsque ces animaux sont nourris avec du LA. A noter, la découverte récente de l'importance de l'*acsl6* dans la teneur de DHA dans le cerveau fait des souris KO *acsl6* un modèle potentiel pour étudier l'impact de la diminution de DHA dans les neurones et les fonctions cérébrales (Fernandez et al., 2021, 2018).

Les huiles de poisson gras ou de krill, aux teneurs variables en DHA et EPA, sont classiquement utilisées pour apporter les AGPI-LC n-3 sous forme de triglycérides (Moffat et al., 1993), mais elles contiennent aussi des SFA et des MUFA ainsi que de l'iode, de l' $\alpha$ -tocopherol ou de la vitamine K. Les petits peptides issus du poisson gras, qui ont des vertus protectrices vis-à-vis de la neuroinflammation et du stress, ne sont pas présents dans les huiles de poisson (Chataigner et al., 2021). Certaines microalgues, comme *Schizochytrium* sp, sont aussi utilisées comme source de DHA sous forme de phospholipide (Hadley et al., 2017; Harel et al., 2002). L'application de ces diètes est réalisée soit en amont de la mise en accouplement, soit au début de la gestation, soit plus tard dans la vie, dans les périodes périnatales, à l'âge adulte ou pendant le vieillissement. Certaines études consistent aussi à administrer les AGPI d'intérêt par voie intraveineuse ou intrapéritonéale (Fourrier et al., 2017; Sun and Zhang, 2022), intra-cérébroventriculaire ou intrathécale pour des études d'effets de court terme. Enfin, l'administration par voie entérale ou gavage ou par pompe mini-Alzet est aussi pratiquée (Manual Kollareth et al., 2020). Enfin, des modèles transgéniques ont été développés pour augmenter les AGPI n-3 sans modifier les apports alimentaires. En l'occurrence, les souris *Fat-1*, qui expriment le gène *fat-1*, une AGPI n-3 desaturase exprimée par *C. Elegans*, convertissent les AGPI n-6 en AGPI n-3 de la même longueur de chaîne carbonée (Kang, 2007). Nourries avec une diète carencée en AGPI n-3, elles convertissent les AGPI n-6 accumulés dans les tissus en AGPI n-3, y compris dans le cerveau où les niveaux de DHA augmentent. Nourries avec une diète A04, les souris *Fat1* n'ont pas plus de DHA, mais plus d'EPA dans le cerveau par rapport aux souris contrôle (Delpech et al., 2015). L'expression spécifique du gène cre-inductible *fat1* (Clarke et al., 2014) dans des sous types neuronaux permet d'étudier dans un contexte carencé en AGPI n-3, l'impact du maintien du statut en AGPI n-3 dans ces cellules spécifiques (Ducrocq et al., 2020). L'utilisation de ces différents modèles a permis d'étudier les mécanismes d'action des AGPI dans le cerveau et le comportement.

#### 5.4.1. AGPI alimentaires et cognition chez l'animal

L'utilisation des modèles animaux décrits ci-dessus ont permis de mettre en évidence le lien entre une déficience alimentaire en AGPI n-3 dès la période périnatale et les altérations de mémoire à l'âge adulte (Joffre et al., 2014; Luchtman, 2013). Ainsi, chez le rat, l'exposition multigénérationnelle, où la déficience en AGPI n-3 s'aggrave à chaque génération, provoque de profondes altérations comportementales, émotionnel et cognitif, qui s'aggravent avec l'augmentation du déséquilibre entre AGPI n-3 et n-6 dans le cerveau (Chalon, 2006; Moriguchi et al., 2000). L'exposition unigénérationnelle au régime déficient en AGPI n-3 provoque également une altération de la mémoire spatiale si cette carence commence dès la gestation, mais pas après le sevrage (Labrousse et al., 2018; Lépinay et al., 2015; Moranis et al., 2012). Les altérations mnésiques et de comportement spontanés apparaissent dès le sevrage (Leyrolle et al., 2022; Madore et al., 2020). Dans ces études, les mesures cognitives utilisées sont des « maze-tests » comme le labyrinthe d'eau de Morris (Morris water maze), le labyrinthe circulaire de Barne, le labyrinthe radiaire (Fedorova and Salem, 2006) ou le labyrinthe en Y (Labrousse et al., 2009). Ce sont des tests hippocampo-dépendants de mémoire spatiale. Le test de reconnaissance d'objet est également utilisé comme tâche hippocampo-indépendante (Dere et al., 2007). Les altérations des capacités mnésiques des rongeurs provoquées par la carence en AGPI n-3 gestationnelle (Fedorova et al., 2009, 2007; Lim et al., 2005; Moriguchi et al., 2000; Xiao et al., 2006) sont partiellement ou totalement restaurées à l'âge adulte par un apport en AGPI n-3 (ALA ou DHA+EPA) s'il a lieu à la naissance ou au sevrage (Lozada et al., 2017; Moriguchi and Salem Jr, 2003). Administré après le sevrage, la diète carencée en AGPI n-3 sensibilise aux effets néfastes de stimuli inflammatoire ou de stress sur la mémoire (Delpech et al., 2015; Leyrolle et al., 2022). Inversement, les diètes riches en EPA+DHA protègent vis-à-vis du développement d'altérations de mémoire et de comportements émotionnels provoquées par le vieillissement (Chataigner et al., 2021; Labrousse et al., 2012; Taoro-González et al., 2022), le stress chronique (Chataigner et al., 2021; Costa et al., 2022; Di Miceli et al., 2022; Larrieu et al., 2014) ou l'obésité (Demers et al., 2020; Fourrier et al., 2020). Des résultats identiques ont été observés chez le lémurien et le singe (Languille et al., 2012). De plus, les diètes riches en AGPI n-3 restaurent les altérations de la sphère sociale, émotionnelles ou cognitives dans des modèles de pathologies neurodéveloppementales (Dinel et al., 2016; Leyrolle et al., 2022; Pietropaolo et al., 2014; Reemst et al., 2022). Très récemment, des travaux conduits dans des modèles murins de la maladie d'Alzheimer ont montré que l'administration intranasale de DHA nanovectorisé améliore les déficits des fonctions cognitives et la pathogénèse (Zussy et al., 2022). Cependant, la carence en ALA et la supplémentation en PUFA-LC n-3 périnatale provoquent des altérations des interactions mère-enfant (comportement maternel, vocalisations) et des troubles comportementaux précoces chez la progéniture (Colucci et

al., 2020). Enfin, un rapport récent indique que l'administration aiguë d'EPA altère l'apprentissage et la mémoire ainsi que la LTP hippocampique chez les souris adultes et prépubères (Liu et al., 2020). Des déficits similaires sont reproduits par une augmentation endogène de l'EPA dans l'hippocampe de la souris transgénique fat-1. En conclusion, de nombreuses études montrent que la teneur en AGPI n-3 de la diète est un déterminant alimentaire de la trajectoire comportementale émotionnelle et cognitive. Les mécanismes par lesquels les AGPI n-3 contribuent au développement et le maintien des capacités d'apprentissage et de mémorisation font l'objet d'intenses recherches. La façon dont ils régulent les phénomènes de plasticité synaptique fait l'objet du paragraphe suivant (Su, 2010).

#### *5.4.2. AGPI et troubles anxio-dépressifs*

Les animaux soumis à la carence en AGPI n-3 développent non seulement des altérations cognitives, mais aussi des comportements de type anxiodépressifs (Lafourcade et al., 2011; Larrieu et al., 2012). Ainsi, chez les rongeurs, un déficit d'accumulation de DHA dans le cerveau au cours du développement périnatal est associé à des altérations de la neurogenèse (Beltz et al., 2007), de la synaptogenèse (Cao et al., 2009) et également d'une augmentation des comportements de types anxieux et dépressifs (DeMar et al., 2006; Lafourcade et al., 2011; Larrieu et al., 2014, 2012; Weiser et al., 2015). Ces données expérimentales corroborent les données cliniques et épidémiologiques. En effet, il existe une association inversée entre la consommation de poissons gras (riches en EPA et DHA) et la prévalence de développer une dépression majeure (MDD pour Major Depressive Disorder) (Luo et al., 2020). De plus, les taux de DHA périphériques et dans diverses structures cérébrales impliquées dans la dépression sont diminués chez les patients diagnostiqués pour une dépression.

De plus, Les AGPI-LC n-3 sont considérés comme des stratégies thérapeutiques de prévention et de traitement du MDD (Bazinet et al., 2020; Bazinet and Layé, 2014). Citer travaux diminution dha dans le cerveau. Des analyses transnationales ont suggéré qu'une consommation plus élevée de poisson et de fruits de mer par personne de poissons et de fruits de mer par habitant est associée à des taux de prévalence plus faibles de TDM (Tanskanen et al., 2001), de dépression post-partum et de troubles bipolaires post-partum (Hibbeln, 2002).

Cependant, les effets d'une supplémentation alimentaire en AGPI-LC n-3 sur la symptomatologie dépressive sont très mitigés. Des études cliniques portant sur l'efficacité de l'EPA, du DHA ou d'une combinaison EPA + DHA suggèrent que la supplémentation en EPA couplée à des médicaments antidépresseurs est la plus efficace vis-à-vis des symptômes et pas d'effets des mono-thérapies (Gertsik et al., 2012; Lespérance et al., 2010). En 2014, un essai randomisé portant sur les effets de monothérapies EPA ou DHA sur la dépression majeure met en évidence l'effet correcteur de l'EPA (Mischoulon et al., 2014). Ce résultat concorde avec les méta-analyses qui suggèrent que l'EPA ou

l'EPA + DHA (mais pas le DHA seul) présentent un léger avantage en terme d'efficacité pour le traitement des dépressions (Bloch and Hannestad, 2012; Martins, 2009). Seuls les patients atteints de dépression présentant une inflammation bénéficient du traitement en EPA (Rapaport et al., 2016), ce qui est cohérent avec les effets pro-résolutifs de l'EPA (Layé et al., 2018). Très récemment, un essai clinique montre que des patients atteints de dépression majeure supplémentés avec de l'EPA à raison de 4 g/j pendant 12 semaines ont une amélioration modeste de leurs symptômes. Cependant, les symptômes sont améliorés chez les patients en surpoids avec une inflammation élevée, qui se voit également améliorée (Mischoulon et al., 2022). De plus, chez ces sujets, la supplémentation en EPA augmente drastiquement les taux plasmatiques d'EPA et de 18-HEPE, associée à une meilleure conversion en RvE2-3, et des taux de LXB4 (Lamon-Fava et al., 2021).

Récemment, par une approche d'IRM, la mise en évidence que les patients dépressifs qui ont les taux érythrocytaires d'EPA+DHA les plus faibles ont des regroupements de réseau neuronaux, une efficacité globale et une connectivité plus faibles dans les régions frontales-limbiques (Lei et al., 2021; McNamara, 2016). De plus, une supplémentation en EPA+DHA de 12 semaines augmente ces paramètres dans les régions temporales. L'expression de cPLA2 est induite par l'EPA, mais pas par le DHA chez les patients dépressifs supplémentés (Su et al., 2018). L'ensemble de ces données suggèrent que les AGPI-LC n-3 pourrait non seulement limiter le développement de symptômes dépressifs chez les patients avec inflammation, mais également que les AGPI-LC n-3 pourrait prévenir la survenue de ces symptômes (Guu et al., 2020). Cependant une étude récente de grand envergure (18 353 participants) incluant des adultes âgés de 50 ans ou plus sans symptômes dépressifs voit une augmentation faible, mais significative, du risque de dépression ou de symptômes dépressifs après supplémentation (huile de poisson, 1 g/j contenant 465 mg d'EPA et 375 mg de DHA) avec un suivi de 5 ans (Okereke et al., 2021). Des études supplémentaires sont nécessaires pour mieux comprendre la quantité et le type d'AGPI-LC n-3 nécessaires pour prévenir les troubles de l'humeur, en tenant compte des facteurs de risque, notamment ceux liés au taux d'AGPI n-6 et n-3, le sexe, l'âge ou le stress. Ainsi, des études montrent que les sujets qui développent une dépression lors d'un traitement par interféron- $\gamma$ , une cytokine inflammatoire, ont des taux élevés d'AA (Lotrich et al., 2013). D'un point de vue des mécanismes, les études chez l'animal montrent que des diètes riches en EPA+DHA ou EPA seul protègent vis-à-vis du développement de comportement de type dépressif dans plusieurs modèles de stress chronique ou de bulbectomie (Di Miceli et al., 2022; Larrieu et al., 2014). Dans les modèles de stress chronique, les AGPI-LC promeuvent la plasticité synaptique au sein du NAc, préserve l'intégrité dendritique des neurones du PFC, la neurogénèse au niveau hippocampique et limite la neuroinflammation (Di Miceli et al., 2022; Larrieu et al., 2014; Larrieu and Layé, 2018). Ces effets pourraient être dus aux oxylipines dérivées de EPA/DHA, notamment celles de la voie LOX, qui protègent des altérations de la neurogénèse dans un modèle humain (Borsini et al., 2021). Enfin, la



sEH pourrait être impliquée dans la pathogenèse de la dépression majeure. Son inhibition pharmacologique ou génétique réduit la genèse d'oxylipines-epoxydes pro-inflammatoires et l'apparition de comportements de type dépressif après une inflammation ou un stress de défaite sociale répété, renforçant l'importance des dérivés des AGPI dans la physiopathologie de la dépression (Ren et al., 2016).

## **6. Rôle des AGPI dans la plasticité neuronale**

La plasticité neuronale fait référence à la capacité du système nerveux à se modifier fonctionnellement et structurellement suite à une expérience ou une blessure. Pendant le développement embryonnaire, la plasticité neuronale est très active et assure la mise en place des connexions neuronales (Hensch and Stryker, 2004). C'est non seulement un processus clé du neurodéveloppement mais également de la réponse adaptative du cerveau face aux modifications environnementales, comme le stress, le vieillissement ou les processus pathologiques. La plasticité neuronale s'exprime à différentes échelles cellulaire et moléculaire, synaptique et non synaptique. La plasticité moléculaire désigne les cascades de signalisation moléculaires qui, lorsqu'elles sont activées, entraînent une modification du fonctionnement de protéines clés dans la plasticité synaptique. C'est le cas des récepteurs glutamatergiques AMPA et NMDA qui peuvent être phosphorylés et changer leur perméabilité pour modifier la transmission neuronale (Lisman and McIntyre, 2001). La plasticité synaptique correspond à une transmission entre deux neurones qui induit des courants post-synaptiques dont l'amplitude peut être modulée par des phénomènes de plasticité. La dynamique calcique est un acteur important à la fois pour la potentialisation et pour la dépression des courants synaptiques même si d'autres mécanismes avant et après la libération de calcium peuvent aussi générer différentes plasticités. La plasticité non-synaptique, quant à elle, fait référence à des changements électrophysiologiques non-synaptique au niveau des canaux voltages-dépendants qui peuvent modifier l'excitabilité des neurones (Daoudal and Debanne, 2003). L'excitabilité neuronale est la capacité du neurone à émettre un potentiel d'action selon les entrées synaptiques qu'il reçoit.

### **6.1. Généralités sur la plasticité synaptique**

La découverte par Cajal de la discontinuité entre les cellules neuronales a été suivie de la démonstration que les cellules nerveuses communiquent au travers de jonctions spécifiques appelées synapses (Tansey, 1997), les premières dynamiques de composants synaptiques. La transmission d'information entre les neurones se propage le long de l'axone sous la forme d'un signal électrique : le potentiel d'action. Au sein de la synapse on distingue les structures pré-synaptiques ou

boutons axonaux et les structures post-synaptiques ou épines dendritiques. La plasticité synaptique désigne la capacité du système nerveux à former des connexions, notamment lors de l'apprentissage et de la mise en place de la mémoire qui impliquent les synapses glutamatergiques. On distingue 2 grands types de plasticité, la LTP (Potentialisation à long terme) et la LTD (Dépression à long terme) (Citri and Malenka, 2008). La LTP désigne une augmentation à long terme de la transmission synaptique à la suite d'une stimulation courte à haute fréquence (Bennett, 2000).

## 6.2. Plasticité synaptique de l'hippocampe et dans le striatum

### 6.2.1. Hippocampe et noyau accumbens

L'hippocampe des mammifères est une structure sous-corticale enroulée sur elle-même. On distingue le gyrus denté (GD) et la corne d'Ammon (divisée en 3 zones : CA1, CA2 et CA3) qui est composée de neurones pyramidaux. L'hippocampe forme un réseau uni-directionnel dans lequel les fibres qui proviennent du cortex entorhinal (CE) projettent vers le gyrus denté (GD) par les voies perforantes médiales et latérales. Les cellules granuleuses du gyrus émettent des fibres moussues vers les cellules apicales de la zone CA3. Les cellules de la zone CA3 émettent des axones vers les cellules pyramidales de la zone CA1 *via* les voies des collatérales de Schaeffer (SC) et des fibres commissurales. Les neurones de la zone CA1 envoient des axones vers le subiculum (Sb), qui à leur tour, vont renvoyer un signal vers le cortex entorhinal **Figure 7**. Dans l'hippocampe, qui est le siège de l'apprentissage et de la mémoire, la LTP est induite par une stimulation des collatérales de Schaeffer (afférences glutamatergiques) dans la région du CA1 (Lynch, 2004). Cette forme de plasticité synaptique dépend des récepteurs glutamatergiques NMDA et est médiée par les endocannabinoïdes (eCBs) agissant à la synapse inhibitrice. On parle de dépression à long terme inhibiteur hétérosynaptique (iLTD) (Carlson et al., 2002) (Castillo et al., 2012). L'iLTD hétérosynaptique repose sur l'activation de récepteurs CB1 couplé à une protéine G qui vont réduire la libération de GABA à la synapse inhibitrice. La LTP à la synapse des collatérales de Schaeffer du CA1 est donc médiée par la iLTD hétérosynaptique des interneurons GABAergiques, qui est dépendante de la production d'eCB et de l'activation des récepteurs CB1 (Castillo et al., 2012).

Le striatum a été décrit comme une structure capable de détecter et intégrer les informations corticales (Graybiel, 1995). Cette structure est composée à 95% de neurones de projections GABAergiques et à 5% d'interneurones GABAergiques, cholinergiques et à NO-synthase (Kawaguchi and Kubota, 1993). Chez le rongeur, on distingue le striatum dorsal et le striatum ventral aussi appelé nucleus accumbens (NAc). Nous focaliserons ici sur le NAc. Le NAc est une structure méso-corticale divisée en deux sous-régions : une région « shell » plus médiale et une région « core » plus latérale (Zahm and Brog, 1992). Les types cellulaires les plus représentés dans le NAc sont les neurones

épineux moyens (MSN pour Medium Spiny Neuron) à projection GABAergique qui vont exprimer des récepteurs à la dopamine de type D1 ou D2 (Francis et al., 2015) Les neurones MSN du Nac reçoivent et intègrent des inputs glutamatergiques provenant du cortex préfrontal (PFC), de l'hippocampe ventral (vHipp) et de l'amygdale baso-latérale (BLA) (Groenewegen et al., 1999) (Britt et al., 2012) mais également de l'hippocampe dorsal (dHipp) (Qi et al., 2016). Toutes ces régions communiquent entre elles et traitent différents types d'information et l'activation spécifique de ces voies peut susciter des fonctions comportementales différentes selon les interactions avec le NAc (Sesack and Grace, 2010). En particulier, l'axe vHipp-NAc est nécessaire pour la navigation spatiale (Compton, 2004; Mannella et al., 2013; Miyoshi et al., 2012) et encodant la dynamique temporelle de la prise de décision (Abela et al., 2015). Les MSN sont particuliers car silencieux au repos, grâce à des conductances potassiques fortes qui les maintiennent très hyperpolarisés (Wilson and Kawaguchi, 1996). Les interneurones GABAergiques inhibent fortement les MSN car ils sont plus facilement excitables par les entrées glutamatergiques corticales et thalamiques. Les MSN ne répondent à l'émission d'un potentiel d'action que lorsque les afférences excitatrices sont fortes (Mahon et al., 2006). Le striatum reçoit des afférences glutamatergiques de l'ensemble des aires corticales et de certains noyaux thalamiques (McFarland and Haber, 2000).

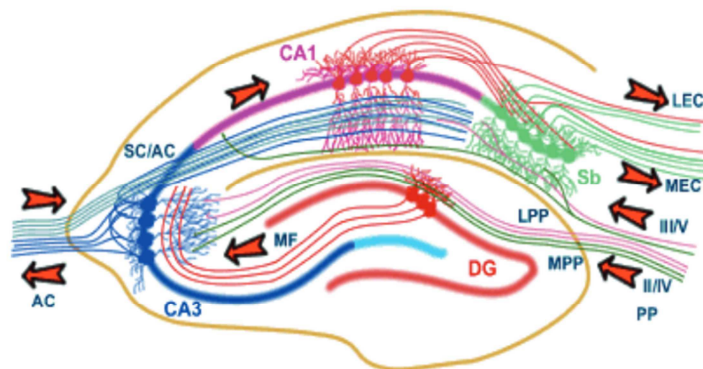


**Figure 7 :** Voies hippocampales glutamatergiques.

Les fibres provenant du cortex entorhinal (EC) se projettent vers le gyrus denté (DG) via les voies perforantes médiales (MPP) et latérales (LPP). Les cellules granuleuses du gyrus vont émettre des fibres moussues (MF) vers les cellules apicales de la zone CA3. Les cellules de la zone CA3 vont émettre des axones vers les cellules pyramidales de la zone CA1 via les voies des collatérales de Schaeffer (SC) et des fibres commissurales (AC). Les neurones de la zone CA1 envoient des axones vers le subiculum (Sb), qui à leur tour, vont renvoyer un signal vers le cortex entorhinal. (Adapté de la thèse de Hennebelle Marie)

### 6.2.2. Neurotransmission glutamatergique

Le glutamate est le principal neurotransmetteur exciteur dans le cerveau et est impliqué dans la plupart des fonctions cérébrale y compris la cognition et les émotions. Chez les mammifères, il

représente 80 à 90 % des synapses cérébrales (Watkins, 2000). Afin d'assurer la neurotransmission, les terminaisons synaptiques des neurones sont enrichies en mitochondries, principal siège du métabolisme énergétique. C'est au niveau de ces mitochondries présynaptiques qu'est formé le L-glutamate. Le glutamate est synthétisé principalement à partir de 3 voies métaboliques : la dégradation des protéines, la conversion de la glutamine sous l'action de la glutaminase (Kvamme et al., 2000) (Bak et al., 2006), et enfin la transamination de l'acide  $\alpha$ -cétooglutarate issu du cycle de Krebs (Bak et al., 2006). Une fois dans le cytosol de la cellule, le glutamate va être chargé dans des vésicules sous l'action de transporteurs vésiculaires spécifiques. Actuellement, trois types de transporteurs ont été identifiés : V-Glut 1, 2 et 3. Contrairement aux transporteurs V-Glut-1 et 2, le transporteur V-Glut 3 est exprimé principalement par des neurones non glutamatergiques tels que les neurones cholinergiques ou sérotoninergiques (Omote et al., 2011) (Gras et al., 2002). Lorsqu'une dépolarisation présynaptique survient, les vésicules chargées de glutamate déversent leur contenu dans la fente synaptique via un processus  $\text{Ca}^{2+}$ -dépendant -l'exocytose-, provoquant une augmentation de la concentration extracellulaire de glutamate pouvant atteindre 1000 fois celle de repos.

Les cellules du SNC possèdent au niveau de leurs membranes des transporteurs spécifiques du glutamate. Cinq types de transporteurs ont été identifiés. Au niveau des astrocytes, la capture du glutamate s'effectue principalement via les transporteurs GLAST/EATT1 et GLT1/EAAT2. Les neurones possèdent également leurs propres récepteurs, EAAC1/EAAT3, qui sont exprimés en moindres proportions comparées à ceux des cellules gliales (Nieoullon et al., 2006). Enfin, les transporteurs EAAT4 et EAAT5, contrairement aux autres qui sont ubiquitaires, sont exprimés exclusivement au niveau du cervelet et de la rétine.

Dans le SNC, 90% de la capture du glutamate est effectuée par les astrocytes (Rothstein et al., 1996), ce qui traduit l'importance de leur rôle dans le maintien de l'homéostasie au niveau de la fente synaptique en captant le glutamate en excès. Lors de la neurotransmission, la concentration de glutamate dans la fente s'élève de manière dramatique d'un niveau de base (ou de repos d'environ 25nM) à des niveaux pouvant être toxiques s'ils ne sont pas atténués rapidement (proche de 100  $\mu\text{M}$  à 1mM) (Danbolt, 2001). Une fois capté dans les astrocytes, le glutamate peut suivre différentes voies métaboliques, dont les principales sont son entrée dans le cycle de Krebs, fournissant de l'énergie à l'organisme, sa conversion en glutathion pour prévenir du stress oxydatif et son recyclage en glutamine, qui va pouvoir être redistribuée au niveau du neurone présynaptique et alimenter un nouveau pool de neurotransmetteur (Kvamme et al., 2000). Le glutamate est converti en association avec de l'ammonium en glutamine sous l'action de la glutamine synthetase (GS), enzyme spécifique des astrocytes dans le SNC (Walton and Dodd, 2007). Cette glutamine est ensuite transférée aux

neurones par des systèmes de transports spécifiques (Chaudhry et al., 2002) pour être recyclée en glutamate sous l'action de la glutaminase phosphate-dépendante.

### 6.3. Rôle des astrocytes dans la neurotransmission

Historiquement, les cellules gliales ont souvent été considérées comme de simples supports physiques aux neurones. Or, on sait désormais que les cellules gliales jouent un rôle important dans le fonctionnement cérébral et sont des partenaires essentiels des neurones. On distingue différents types de cellules gliales. Les oligodendrocytes qui ont un rôle de synthèse de la myéline qui entoure les axones. Les cellules microgliales qui sont les cellules immunitaires résidentes du SNC ayant un rôle neuroprotecteur. Les cellules NG2+ dont le rôle serait de constituer les cellules souches multipotentes (Richardson et al., 2011). Et enfin les astrocytes qui sont les cellules gliales présentes en plus grand nombre dans le cerveau et qui seront décrit plus précisément dans les paragraphes suivants. Le concept de la synapse tripartite a émergé en 1999 grâce à la considération des astrocytes comme éléments fonctionnels de la synapse. Ce concept fait donc référence à l'association fonctionnelle des neurones pré et post-synaptiques et les astrocytes.

#### 6.3.1. Astrocyte et synapse tripartite

Les astrocytes se présentent sous forme étoilée et ont la particularité de n'avoir que peu de zones de recouvrements entre eux (Bushong et al., 2004). Leur corps cellulaire est enrichi en protéine des filaments intermédiaires (GFAP pour Glial Fibrillary Acidic Protein) (Bignami et al., 1972). En immunohistochimie, le marqueur GFAP est donc utilisé pour la caractérisation des astrocytes. Cependant tous les astrocytes ne sont pas GFAP-positifs et la GFAP peut être présente dans d'autres cellules (Liu et al., 2006). D'autres marqueurs que la GFAP peuvent être utilisés, comme ceux des transporteurs astrocytaires du glutamate (GLAST et GLT-1), la vimentine ou la glutamine synthase capable de convertir le glutamate en glutamine (Sofroniew and Vinters, 2010). Les astrocytes, à l'inverse des neurones, sont électriquement silencieux. Ils n'émettent pas de potentiel d'action. Des enregistrements électriques ont montré qu'ils avaient un potentiel de repos très négatif, un input de résistance faible et une conductance sensible aux ions potassiques. L'imagerie calcique a permis, tout d'abord en culture cellulaire puis in situ et enfin in vivo, de voir que les astrocytes répondent à une application de transporteurs chimiques avec une élévation de leurs niveaux de calcium intracellulaire.

Les astrocytes capturent le glutamate extracellulaire prévenant ainsi son accumulation ce qui protège les neurones de sa excitotoxicité. Cette recapture de glutamate va aussi réguler l'efficacité des synapses glutamatergiques (Danbolt, 2001). La régulation des transporteurs de glutamate

astrogliaux GLAST et GLT-1 est d'autant plus importante pour la neuroprotection et la neurotransmission (Sattler and Rothstein, 2006). Une altération dans la diffusion du transporteur GLT-1 à la surface des astrocytes à la fois *in vitro* et *ex vivo* sur des tranches d'hippocampe a un effet direct sur les cinétiques des courants postsynaptiques excitateurs associé avec une altération de l'élimination du glutamate à la synapse (Murphy-Royal et al., 2015).

Au-delà d'un soutien structurel et métabolique des neurones, les astrocytes jouent un rôle dans les fonctions synaptiques des neurones (Haydon, 2001). De nombreuses études ont mis en évidence une régulation dynamique et bidirectionnelle de la communication neuronale par les astrocytes. La plupart des études ont été menées sur des cellules uniques en patchant un astrocyte isolé pour moduler son activité (Panatier et al., 2011). Les astrocytes présentent à leur surface des récepteurs ionotropiques et métabotropiques de neurotransmetteurs pouvant détecter l'activité neuronale périphérique. Lorsque ces récepteurs sont activés, ils traduisent l'activité neuronale par une augmentation intracellulaire de la concentration de  $Ca^{2+}$  (Perea et al., 2009; H.-L. Wang et al., 2011). Ce signal calcique va provoquer la libération de gliotransmetteurs tels que le glutamate, la D-sérine ou l'ATP (stimulateurs de l'activité synaptique) (Bezzi and Volterra, 2011). On parle alors de gliotransmission (Adamsky et al., 2018; Perea et al., 2009). Ces gliotransmetteurs vont ensuite activer les récepteurs neuronaux et induire une neuromodulation de la transmission synaptique et de la plasticité médiée par les astrocytes dans différentes régions du cerveau. Les actions des différents gliotransmetteurs dans les régions cérébrales ont été reviewé par Araque et al., 2014 (Araque et al., 2014). Les astrocytes expriment mGluR5 qui une fois activé va induire la gliotransmission (Fellin et al., 2004). Par exemple, il a été montré *ex vivo*, dans le NAc de souris, que l'activation de mGluR5 a induit des oscillations calciques astrocytaires aboutissant à une libération de glutamate par l'astrocyte. Cette gliotransmission a activé les récepteurs NMDA des MSNs, mettant en avant l'implication de la gliotransmission dans la modification de l'excitabilité neuronale (D'Ascenzo et al., 2007). La D-sérine participe à l'activation des récepteurs NMDA (Oliet and Mothet, 2009). Comme les astrocytes peuvent contacter plus de 100 000 synapses, le contrôle de la diffusion du signal calcique pourrait jouer un rôle déterminant dans la physiologie du système nerveux (Halassa et al., 2007).

Il a également été montré que les astrocytes répondent au signal donné par le glutamate en libérant de l'ATP/Adénosine (Araque et al., 2014; Illes et al., 2019). Les astrocytes sont également impliqués dans la régulation synaptique induite par la dopamine dans le Nucleus Accumbens. En effet, les astrocytes du NAc répondent à la libération synaptique de dopamine *in vivo* et sur tranches, avec une augmentation du calcium via l'activation du récepteur D1, exprimé par les astrocytes (Corkrum and Araque, 2021). De plus, l'activation de ces astrocytes par la dopamine, l'amphétamine ou DREADD stimule la libération d'ATP/Adénosine qui active les récepteurs A1 neuronaux postsynaptiques et diminue la transmission synaptique excitatrice (Corkrum and Araque, 2021).

Il est mentionné un peu plus haut que les astrocytes régulent de façon bidirectionnelle la communication neuronale. En effet, bien que les astrocytes soient proches des neurones pre- et post-synaptiques, ils sont relativement distants de la fente synaptique et des systèmes de recapture des neurotransmetteurs ce qui représente des limitations structurales et fonctionnelle de la signalisation neurone-astrocyte. Or, la présence de récepteurs à haute affinité et faible désensibilisation va permettre une communication bidirectionnelle. Lors de la libération de neurotransmetteurs à la fente synaptique, ils atteignent rapidement l'élément postsynaptique puis diffusent jusqu'à l'astrocyte avec une diminution rapide de leur concentration (**Figure 8 A et B**). Plusieurs récepteurs impliqués dans la capacité de l'astrocyte à détecter l'activité synaptique, tels que les récepteurs métabotropiques au glutamate, muscariniques, CB1, P2Y et GABA<sub>B</sub>, ont été caractérisé comme des récepteurs à haute affinité et faible désensibilisation et donc activités même avec de faibles concentrations de neurotransmetteurs (Araque et al., 2014). A l'inverse, les actions des gliotransmetteurs sont possibles grâce à la présence de récepteurs à la fente synaptique plus sensible à la libération de gliotransmetteurs (**Figure 8 C**).

De plus, les astrocytes du cerveau sain sont très diversifiés et spécialisés afin de jouer des rôles différents dans des circuits distincts du SNC (Chai et al., 2017). Cette diversité de phénotypes astrocytaires repose non seulement sur la programmation embryonnaire, mais aussi sur les signaux neuronaux locaux (Haim and Rowitch, 2017). En situation pathologiques, lésionnelle et neuroinflammatoires, les astrocytes dits « réactifs » sont également très diversifiés, comme montrés par la diversité de leurs profils transcriptomiques (Escartin et al., 2021). De plus, les changements fonctionnels complexes des astrocytes réactifs leur confèrent de nouvelles fonctions, notamment neuroprotectrices ou, au contraire, neurotoxiques. Ainsi, au-delà de leur rôle crucial dans la plasticité synaptique (Oliveira and Araque, 2022), les astrocytes contribuent de façon très importante au maintien de l'homéostasie du cerveau (Escartin et al., 2021) en régulant entre autres la neuroinflammation et les neurotrophines (De Keyser et al., 2008).

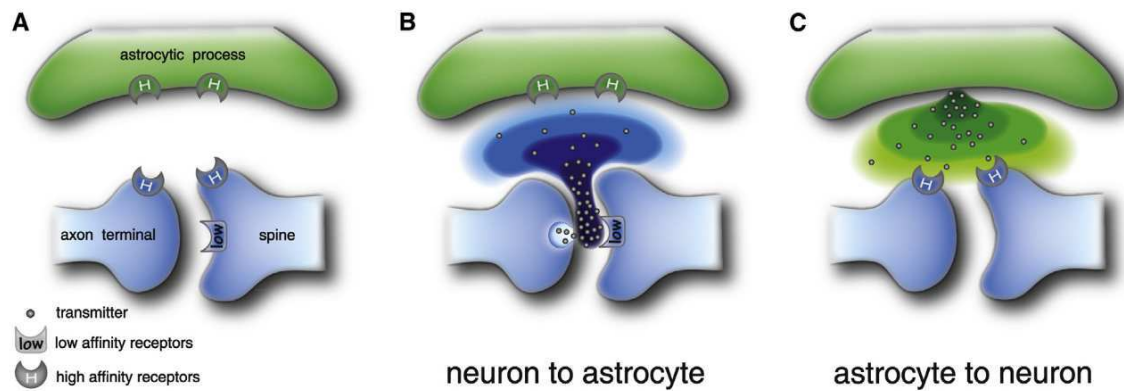


**Figure 8 :** Communication bidirectionnelle neurone-astrocyte

Cette communication est médiée par des récepteurs à haute et à faible affinité. A – synapse tripartite illustrant la localisation des récepteurs à haute et faible affinité. B – les neurotransmetteurs activent rapidement les récepteurs à faible affinité de l'élément postsynaptique et diffusent hors de la fente synaptique pour activer les récepteurs à haute affinité de la membrane de l'astrocyte. C – les gliotransmetteurs activent les récepteurs à haute affinité situés sur les membranes neuronales. La diminution des concentrations de neurotransmetteurs ou de gliotransmetteurs avec la distance est symbolisée par les différentes intensités de couleurs (B et C). D'après (Araque et al., 2014).

#### 6.4. Modulation de la plasticité neuronale par les AGPI

Les mécanismes par lesquels les AGPI agissent dans le cerveau font l'objet d'intenses recherches. In vivo, une carence alimentaire en AGPI n-3 altère sur la neuritogénèse, la synaptogénèse et les fonctions synaptiques (Ahmad et al., 2002; Calderon and Kim, 2004; Cao et al., 2009; Sidhu et al., 2011). De plus, elle modifie les phénotypes microgliaux et diminue leur motilité dans le cerveau en développement, et plus particulièrement dans l'hippocampe (Madore et al., 2014). L'exposition de la mère à un régime carencé en AGPI n-3 altère les fonctions microgliales de la progéniture (homéostasie et activité phagocytaire) aboutissant à un élagage synaptique excessif et des conséquences sur la formation des réseaux neuronaux hippocampiques, la LTP et la mémoire (Madore et al., 2020). Les AGPI n-3 régulent les fonctions cérébrales en favorisant la capture et le métabolisme du glucose ce qui a été corrélé avec de meilleure performance cognitive (Pifferi et al., 2015; Ximenes da Silva et al., 2002). Enfin, l'association entre la carence en AGPI n-3 et les symptômes anxieux et dépressifs pourraient, au moins en partie, reposer sur une altération de l'axe corticotrope (ou axe du stress) (Larrieu et al., 2014, 2012). Des études récentes ont révélé l'implication des AGPI n-3 dans les capacités de neurogénèse du cerveau (Borsini et al., 2020; Tang et al., 2018). Dans les chapitres suivants un accent est mis sur les effets des AGPI sur la neurotransmission. En effet, des modèles de déficience en AGPI n-3 ont mis en avant l'impact des AGPI n-3 sur la neurotransmission. Il a notamment été observé une diminution des taux de sérotonine dans le cortex préfrontal accompagnée d'une diminution de la synthèse ou de la transmission (récepteurs, voies de signalisations) dans les systèmes GABAergiques, dopaminergiques et cholinergiques (Aïd et al., 2003; Chalon, 2006; Innis and de la Presa Owens, 2001; Owens and Innis,



1999; Takeuchi et al., 2003). Par ailleurs, les AGPI sont des précurseurs des endocannabinoïdes, connus pour leur rôle régulateur de la neurotransmission (Lafourcade et al., 2007; Marzo et al., 2004). La carence en AGPI n-3 déséquilibre ce système et diminue ses capacités de modulation de la transmission synaptique et induit donc des déficits comportementaux (Bosch-Bouju et al., 2016; Lafourcade et al., 2011; Larrieu et al., 2012; Thomazeau et al., 2016).

#### 6.4.1. Impact des AGPI sur la transmission neuronale

Des données *in vitro* ont permis d'étudier l'effet de l'administration *ex vivo* d'AGPI sur la plasticité synaptique. Pour cela, des tranches de cerveau, qui maintiennent un certain niveau d'intégration neuronale, ont été utilisées pour étudier l'effet synaptique du DHA par des approches de patch-clamp. Le DHA libre bloque l'induction de la LTD sur des tranches d'hippocampe (Itokazu et al., 2000). Une dose plus élevée de DHA entraîne l'altération de la plasticité synaptique dans des tranches cortico-striatales, avec une facilitation de la LTP, sans effet sur la LTD (Mazzocchi-Jones, 2015). La perfusion d'AA à de faible concentration active la LTP, tandis que le DHA et l'EPA désactivent la LTP dans l'hippocampe (Mirnikjoo et al., 2001). Ces données suggèrent que les effets synaptiques des AGPI-LC sont dépendants de la dose, ou que le DHA a une activité bidirectionnelle dans l'hippocampe (Itokazu et al., 2000). De façon très intéressante, le DHA, mais pas l'ALA, reverse les effets délétères du bromoenol lactone (un inhibiteur de la libération du DHA) sur la LTP (Fujita et al., 2001). Les effets des AGPI-LC sur la neuroplasticité pourraient être médiés par leurs dérivés, notamment les oxylipines et/ou les endocannabinoïdes (Di Miceli et al., 2022). Ainsi, l'acide époxyeicosatriénoïque, un eicosanoïde dérivé de l'ARA, diminue la libération de glutamate dans des tranches d'hippocampe par ses effets sur les canaux potassiques à rectification interne couplés à la protéine G (Mule, Orjuela Leon et Falck). De plus, la N-palmitoyléthanolamine (PEA), un composé endogène de la famille des eCB qui dérive de l'acide hexadécanoïque, augmente les fréquences des courants post-synaptiques inhibiteurs GABAergiques spontanés, par l'intermédiaire de son effet sur le récepteur GPR55 (Musella et al., 2017). Très récemment, l'EPA a été montré comme un activateur de la transmission GABAergique via le 5-HT6R (J.-H. Liu et al., 2020).

La modulation des capacités d'apprentissage des individus par le statut nutritionnel en AGPI n-3 est associée à des modifications des propriétés de plasticité synaptique (Su, 2010). Ainsi, une déficience chronique en DHA se traduit par l'inhibition de l'induction de LTP au niveau de l'hippocampe chez des souris, associée à une réduction de l'expression des protéines synapsines et des sous-unités des récepteurs NMDA (Cao et al., 2009) et à un retard de l'apparition de ces protéines au cours du neurodéveloppement (Moreira et al., 2010). La déficience alimentaire en AGPI n-3 modifie également les fonctions des récepteurs au cannabinoïdes CB1R et la LTD dans le NAC et le cortex

préfrontal, sans modifications de niveau des eCBs (Lafourcade et al., 2011). Dans l'hippocampe, la LTP dépend des récepteurs NMDA et des eCBs. Ces eCBs sont des signaux lipidiques produits par les AGPI-LC présents dans les phospholipides des membranes neuronales suite à une activité neuronale. Dans l'hippocampe de souriceaux au sevrage, cette LTP NMDA-dépendante est altérée par la déficience alimentaire en AGPI n-3 et ceci est dû à l'ablation de la iLTD CB1-dépendante (Thomazeau et al., 2016). Une déficience alimentaire en AGPI n-3 commencée après le sevrage provoque également une altération de la LTD eCB dépendante dans le cortex préfrontal, qui est restaurée lorsque ces derniers sont stimulés (Manduca et al., 2015). Enfin, la carence post-natale, si elle n'altère pas la LTP et la LTD au niveau de l'hippocampe de souris adulte, sensibilise ces dernières aux altérations provoquées par un stimulus inflammatoire (Delpech et al., 2015)

A l'inverse, une supplémentation en AGPI-LC n-3, qui augmente les capacités cognitives chez le rongeur, augmente également l'expression de protéines synaptiques ou impliquées dans la plasticité synaptique, telles que la synapsine I, la syntaxine, CamKII, CREB ou encore des sous-unités des récepteurs NMDA. Cet effet est d'autant plus marqué lorsque le régime alimentaire est associé à une activité physique (Chytrova et al., 2010; Wu et al., 2012). Les AGPI n-3 participeraient ainsi à l'induction et au maintien de la LTP (Fujita et al., 2001; Kawashima et al., 2010). Au cours du vieillissement, la diminution des capacités cognitives des individus est associée à une réduction de la proportion cérébrale du DHA et de l'activité cérébrale (Delion et al., 1997; Whelan, 2008). Le vieillissement physiologique ou pathologique (comme la maladie d'Alzheimer ou de Parkinson) constitue un champ d'étude souvent exploité pour apprécier l'impact des AGPI n-3 sur les fonctions cognitives et sur la plasticité synaptique. La supplémentation en AGPI-LC n-3 restaure, partiellement ou totalement, les capacités cognitives, ainsi que l'expression de marqueurs de la plasticité synaptique, tels que la CamKII, les sous-unités des récepteurs AMPA et NMDA, aussi bien en condition de vieillissement physiologique (Dyall et al., 2007; Martin and Kosik, 2002), que pathologique (Boudrault et al., 2009; Calon et al., 2004; Hashimoto, 2009; Kotani et al., 2006). Cependant, les résultats restent assez disparates et certaines études n'ont pas permis de confirmer l'effet bénéfique des AGPI n-3 sur le déclin cognitif et le développement de maladies neurodégénératives (Arendash et al., 2007; Fotuhi et al., 2009; van de Rest et al., 2008). Le rôle des AGPI n-3 reste complexe et dépend fortement du modèle utilisé, du stade d'avancement du déclin cognitif et/ou de la pathologie, ainsi que du type de supplémentation.

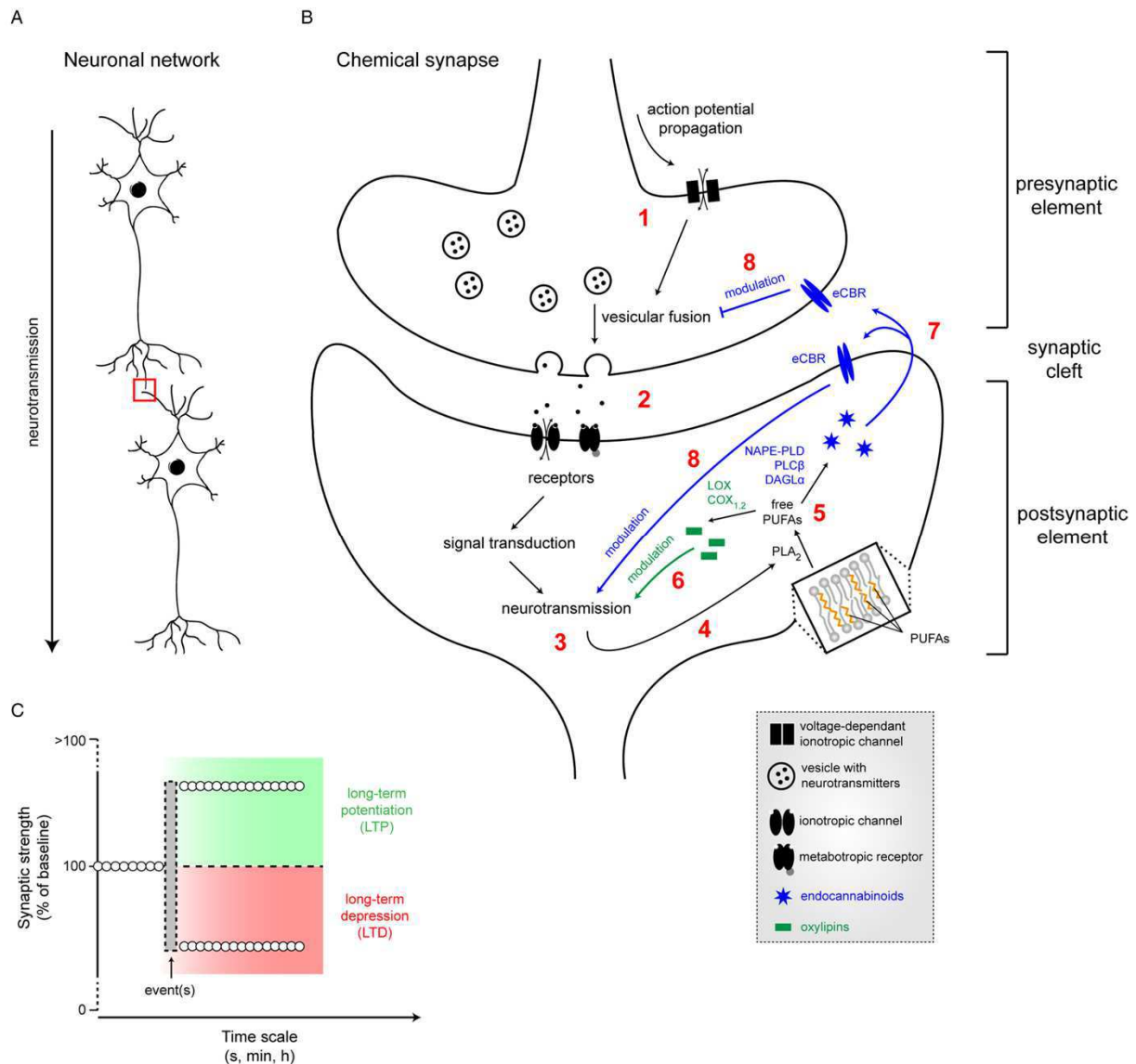


**Figure 9 :** Représentation des mécanismes d'action des AGPI au niveau de la synapse (adapté de Di Miceli et al., 2018)

#### 6.4.2. Impact des AGPI sur les fonctions astrocytaires à la synapse

De nombreux articles ont révélé que l'inhibition des transporteurs de glutamate GLAST et GLT-1 par les AGPI participe aux altérations dues à l'excitotoxicité du glutamate, lorsqu'une grande quantité d'AGPI est libérée dans le milieu extracellulaire suite à une destruction des cellules membranaires (Lau and Tymianski, 2010). Le DHA et l'AA étant abondants dans les neurones et les astrocytes, ils représentent d'excellents candidats en tant que régulateurs de la concentration glutamatergique dans la fente synaptique (Barbour et al., 1989; Green et al., 2008; Lundy and McBean, 1995; Manzoni and Mennini, 1997). En effet, comme indiqué précédemment, le DHA et l'AA sont libérés grâce à l'action de l'enzyme PLA2 et celle-ci est activée par la liaison du glutamate sur des récepteurs postsynaptiques et astrogliaux (Bazan, 2003). L'AA inhibe la recapture du glutamate par les synaptosomes issus de cerveau de rat (Lundy and McBean, 1995; Manzoni and Mennini, 1997), mais également les

cellules rétinales de Müller (Barbour et al., 1989) et les astrocytes corticaux (Volterra et al., 1994). Cependant cet effet inhibiteur de l'AA semble être un effet non spécifique d'AG qui pourrait être lié à l'action peroxydative des AGPI. D'autres résultats indiquent que le DHA (Berry et al., 2005) et l'AA (Zerangue et al., 1995) inhibent la recapture de glutamate par GLAST et stimulent la recapture de glutamate par GLT-1. Cependant il est important de noter que ces deux études ont été réalisées sur des cellules rénales transfectées. En 2009, Grintal et al., ont confirmé l'inhibition de la recapture du glutamate par les astrocytes dans des cultures primaires d'astrocytes (isolés de cortex de rats) par le DHA, sans observer d'effet significatif de l'AA (Grintal et al., 2009). L'équilibre membranaire astrocytaires en DHA et en AA serait donc impliqué dans le couplage entre les cellules, notamment via les Connexines 43 (Champeil-Potokar et al., 2006), ainsi qu'à la maturation et à la différenciation des astrocytes en culture (Joardar et al., 2006; Joardar and Das, 2007)

Il est important de souligner que la carence maternelle en AGPI n-3 inhibe la maturation des astrocytes ce qui entrave le développement des cellules gliales et de leurs fonctions (Yamamoto et al., 2021).

Bien que les études sur l'impact des AGPI n-3 sur le fonctionnement astrocytaire soient peu nombreuses, elles semblent souligner néanmoins un rôle complexe de ces AGPI dans la régulation de la fonction astrocytaire et, en conséquence, de la plasticité synaptique (Di Miceli et al., 2020)

## OBJECTIFS

---

De nombreuses données épidémiologiques indiquent que la consommation de diètes riches en AGPI, comme les diètes de type méditerranéen, la diète DASH ou la diète MIND sont associées à un moindre risque de développer des pathologies du cerveau, que ce soit des pathologies neuropsychiatriques, comme la dépression, ou des pathologies neurodégénératives (Bazinet and Layé, 2014; Feart and Barberger-Gateau, 2015). De plus, des études cliniques et expérimentales montrent qu'il existe des liens entre les niveaux d'AGPI n-3 de la diète, le statut du cerveau en AGPI n-3, les performances cognitives et les comportements émotionnels. En particulier, des données chez l'animal ont mis en valeur l'importance de l'exposition périnatale à des diètes carencées en AGPI n-3, notamment en ALA, sur le métabolisme et les teneurs cérébrales en AGPI n-3 et les conséquences morphofonctionnelles et comportementales précoces de cette exposition, ainsi que leur persistance à long terme. Cependant, très peu d'études ont abordé la question de la réversibilité des effets de l'exposition précoce à ces diètes carencées en AGPI n-3 et de nombreuses questions restent en suspens. Or, cette question est d'une très haute importance quand on considère les données récentes qui indiquent qu'une proportion élevée de la population infantile mondiale est à risque de carence en AGPI n-3 LC au début de la vie (Forsyth et al., 2016). Ainsi, il est important de répondre aux questions suivantes : est-ce que le rééquilibrage alimentaire en AGPI n-3 du jeune peut restaurer les niveaux d'AGPI n-3 et notamment ceux des AGPI-LC DHA et EPA ? Est-ce que la restauration en AGPI n-3 du cerveau est associée à une restauration des métabolites bioactifs associés aux AGPI ? Les altérations morphofonctionnelles cérébrales et de la cognition sont-elles restaurées ? Est-ce que les effets restaurateurs de la diète sont identiques chez les mâles et les femelles ? Peut-on identifier les acteurs moléculaires des effets restaurateurs de la diète administrée après le sevrage ? Le **premier objectif** de cette thèse a donc été d'étudier, dans des souris mâles et femelles carencées en ALA dans les périodes périnatales, les conséquences de l'exposition à partir de la période de sevrage à une diète équilibrée en ALA sur les AGPI et leurs métabolites (oxylipines) dans le cerveau, la plasticité synaptique hippocampique et la cognition à l'âge adulte (**Publication 1**). Une revue faisant état des connaissances des effets des AGPI nutritionnels sur le développement cérébral s'en est suivi (**Publication 2**).

D'autre part, les AGPI présents dans le cerveau sont principalement fournis par l'alimentation, pourtant les enzymes impliquées dans l'élongation et la désaturation des AGPI sont exprimées dans le cerveau, notamment par les astrocytes, dont le rôle dans les fonctions synaptiques est très important. De plus, les AGPI sont de puissants régulateurs de la plasticité synaptique (Di Miceli et al., 2020), cependant peu de données existent sur le rôle de ces enzymes dans la production locale d'AGPI et la régulation de l'activité neuronale. Pourtant, l'inhibition génétique d'Acsl6 dans les

astrocytes provoque une diminution de DHA dans le cerveau et une diminution des épines dendritiques dans le cervelet (Fernandez et al., 2018), suggérant que la production locale d'AGPI n-3 par les astrocytes ont un impact sur les neurones. Le NAc est une structure sensible aux modifications en lipides, et en particulier en AGPI n-3 ou de leurs dérivés (Berland et al., 2020; Ducrocq et al., 2020; Lafourcade et al., 2011; Manduca et al., 2015; Takeuchi et al., 2020). Le **deuxième objectif** a été de comprendre si *elovl2*, qui est impliquée dans l'élongation des AGPI-LC, joue un rôle dans l'activité neuronale des MSNs. Pour cela, nous avons généré un modèle de souris génétiquement modifiée pour l'expression d'*elovl2* dans les astrocytes et étudié l'impact de cette inactivation sur les propriétés électrophysiologiques des MSNs, le statut en AGPI n-3 du NAc et les comportements émotionnels (**Manuscrit 3**).

Enfin, dans un troisième objectif, nous avons étudié comment une diète enrichie en EPA et DHA protège du développement de comportements émotionnels altérés après un stress chronique (Larrieu et al., 2014). En l'occurrence, nos travaux précédents ont établi qu'après un protocole de stress chronique social (CSDS), les souris développent des altérations des comportements sociaux et anxieux qui sont sous la dépendance de l'altération de la plasticité synaptique du noyau accumbens (Bosch-Bouju et al., 2016). De plus, la carence alimentaire en AGPI n-3 qui altère les niveaux de DHA dans le NAc, le PFC et l'hippocampe provoque également une augmentation des comportements de type anxieux et une diminution des comportements d'interaction sociale, une altération de la plasticité synaptique LTD endocannabinoïde dépendante dans le NAc et le PFC et une altération de l'intégrité dendritique des neurones de ces structures (Lafourcade et al., 2011; Larrieu et al., 2014, 2012; Manduca et al., 2015). Nous avons recherché si la consommation de diètes riches en EPA+DHA modifie les profils en AGPI du NAc et la signature moléculaire lipidique associée et promeut la LTD-dépendante des ECBs et limite les altérations comportementales associées au stress chronique (**Manuscrit 4**).

## **RESULTATS**

---





***CHAPITRE 01 : Conséquences de l'exposition à partir de la période de sevrage à une diète équilibrée en ALA sur les AGPI et leurs métabolites (oxylipines) dans le cerveau, la plasticité synaptique hippocampique et la cognition à l'âge adulte***

---

# **Post-natal exposure to a n-3 PUFA containing diet differentially reverses brain PUFAs and oxylipins, synaptic plasticity and memory alterations triggered by early-life exposure to a diet deficient in n-3 PUFA according to sex**

**Martinat M<sup>1</sup>, Rossito M<sup>1</sup>, Di Miceli M<sup>1</sup>, Morel L<sup>1</sup>, Graland M<sup>1</sup>, Durand E<sup>1</sup>, Marchaland Flore<sup>1</sup>, Séré A<sup>1</sup>, Grégoire S<sup>3</sup>, Aubert A<sup>1</sup>, Bosch-Bouju C<sup>1</sup>, Ferreira G<sup>1</sup>, Capuron L<sup>1</sup>, Acar N<sup>4</sup>, Fioramonti X<sup>1</sup>, Madore C<sup>1</sup>, Delpech JC<sup>1</sup>, Bazinet RP<sup>4</sup>, Joffre C<sup>1</sup> and Layé S<sup>1\*</sup>.**

<sup>1</sup> Univ. Bordeaux, INRAE, Bordeaux INP, NutriNeuro, UMR 1286, F-33000 Bordeaux, France

<sup>2</sup> Worcester Biomedical Research Group, School of Science and the Environment, University of Worcester, Worcester WR2 6AJ, UK

<sup>3</sup> Eye and Nutrition Research Group, Centre des Sciences du Goût et de l'Alimentation, AgroSup Dijon, CNRS, INRAE, Université Bourgogne Franche-Comté, Dijon, France

<sup>4</sup>Department of Nutritional Sciences, Faculty of Medicine, University of Toronto, Toronto, ON M5S 1A1, Canada

This work has been conducted in the frame of the International Research Network Food4BrainHealth

\* Corresponding author Sophie Layé

## **ABSTRACT**

The brain is highly enriched in n-6 and n-3 long chain polyunsaturated fatty acids (LC-PUFAs) that are crucial to brain development. In humans, the link between low n-3 PUFA dietary intake during development and the risk to higher cognitive alteration has been established. In rodents, perinatal dietary n-3 PUFA deficiency alters brain n-3 LC-PUFA levels, synaptic plasticity and memory. However, most of the studies have been conducted in male, and not in female rodents. In addition, whether these neuronal and cognitive alterations triggered by an early-life n3 PUFA deficiency are reversible has been poorly addressed. In this work, we sought to determine how a diet balanced in n-3 PUFAs given at weaning can correct the alteration of the long-term potentiation (LTP) measured in the hippocampus and spatial memory triggered by exposure at the beginning of life to a diet low in PUFA n-3, taking sex into account. Female mice were fed either with a diet deficient in n-3 PUFA or to a diet balanced in n-3 PUFA throughout pregnancy and lactation and, at weaning, the male and female offspring were maintained until adulthood under the same diets as their mothers. In a third cohort, male and female offspring from the n-3 PUFA-deficient diet were exposed to the n-3 PUFA balanced diet from weaning to adulthood. In adulthood, behaviour and spatial memory, hippocampal PUFAs and their metabolites (oxylipins), hippocampal LTP and spine density were measured. Our results revealed that early exposure to an n-3 PUFA-deficient diet impairs memory and hippocampal synaptic plasticity, but not spine density in male and female adult offspring. Importantly, exposure of n-3 PUFA-deficient offspring to a balanced diet at weaning differentially reverses spatial memory and hippocampal PUFA differently according to females based on our results. Interestingly, oxylipins and synaptic plasticity is restored in both male and female. Overall, our results indicate for the first time that impairments in memory, hippocampal PUFA metabolism, and synaptic plasticity induced by dietary n-3 PUFA deficiency in early life are more easily corrected by dietary correction with n-3 PUFA in early life in females than in males.

## INTRODUCTION

The brain contains high amounts of n-3 and n-6 long chain polyunsaturated fatty acids (LCPUFAs) and more precisely of docosahexaenoic acid (DHA, n-3) and arachidonic acid (AA, n-6) (Bazinet and Layé, 2014; Joffre et al., 2016). In addition, eicosapentaenoic acid (EPA, n-3), which is poorly found in neurons, accumulates in microglia cells (Cisbani et al., 2021; Rey et al., 2018). N-6 and n-3 LCPUFAs are metabolically derived from their respective precursors, alpha-linolenic acid (ALA, n-3) and linoleic acid (LA, n-6) which are not synthesized *de novo* by mammals and have to be provided through the diet (Bazinet and Layé, 2014). A substantial amount of DHA is accreted in the brain during the perinatal period (Lauritzen, 2001). Indeed, n-3 PUFA maternal dietary supply is a critical component of DHA composition of the offspring brain (recently reviewed in (Martinat et al., 2021)). We and others have previously reported that early-life exposure to diet deficient in ALA and rich in LA decreases brain DHA and increases emotional behavior and memory alteration at weaning (Madore et al., 2020, 2014) and at adulthood (Fedorova et al., 2009, 2007; Lafourcade et al., 2011; Larrieu et al., 2012; Leyrolle et al., 2022, 2021; Moranis et al., 2012). As the neuronal content of DHA decreases, synaptic plasticity (long-term potentiation, LTP) is altered in the hippocampus of male offspring at weaning and adulthood (Di Miceli et al., 2020; Madore et al., 2020; Thomazeau et al., 2016). Interestingly, dendritic arborization and spine density is altered in the hippocampus of n-3 PUFA deficient mice at weaning (Madore et al., 2020), but not at adulthood (Larrieu et al., 2014). Endocannabinoid-dependent long-term depression (eLTD) is also altered in the nucleus accumbens and the prefrontal cortex of n-3 PUFA deficient male adult mice (Lafourcade et al., 2011; Manduca et al., 2015). Transcriptional profiles are altered in the hippocampus and prefrontal cortex of n-3 PUFA deficient male mice, with a majority of genes belonging to cell communication defined as synaptic transmission or neurotransmitter release, immune system or brain development (Leyrolle et al., 2022). Importantly, altered hippocampal structure and function, together with memory impairment observed at adulthood, is dependent on early life dietary exposure to n-3 PUFA deficiency as such alterations are not observed in adult mice submitted to the deficient diet starting at weaning (Delpech et al., 2015; Labrousse et al., 2018; Leyrolle et al., 2022; Rey et al., 2018). Indeed, developmental deprivation of brain DHA could be a determinant of long lasting memory and neuronal alterations associated to low dietary intake of n-3 PUFA. This is consistent with the previously reported activity of DHA on neurodevelopment (Lozada et al., 2017) and the highest risk of developing cognitive alteration in infants fed with diets poor in n-3 PUFA (recently reviewed in (Martinat et al., 2021) ; Basak et al., 2020; Madore et al., 2020; Makrides et al., 2019). The mechanisms underlying the effect of decreased DHA on synaptic plasticity and behavior are still poorly understood. In the hippocampus, decreased brain DHA is associated with increased arachidonic acid (AA, n-6) (Delpech et al., 2015; Joffre et al., 2016). AA is metabolized by cyclooxygenases (COX), lipoxygenases (LOX), or cytochrome P450 monooxygenases (CYP) to several eicosanoids (prostaglandins, leukotrienes, HETE, etc) which have pro-inflammatory activities (Calder, 2001). The same enzymes convert DHA and EPA

to metabolites (maresin, neuroprotectin, resolving) which are considered to exhibit pro-resolutive and anti-inflammatory activities (Serhan et al., 2015, 2002). As AA and DHA compete with the same enzymes, diet-induced changes in AA/DHA alters the synthesis of their respective oxidized products called oxylipins, including in the brain (Joffre et al., 2016; Layé et al., 2018; Reemst et al., 2022; Rey et al., 2019). Recently, we revealed that 12-HETE, a AA-derived oxylipin increased in microglia by dietary n-3 PUFA deficiency, is crucial to hippocampal spine and spatial memory alterations triggered by early-life exposure to a diet deficient in n-3 PUFA at weaning (Madore et al., 2020). However, whether the deleterious effect of early-life brain DHA decrease can be reversed by a later-life exposure to a diet balanced with n-3 PUFA has been poorly addressed and never addressed in female mice. In this work, we aimed to determine whether and how a diet balanced in n-3 PUFA given at weaning can correct hippocampal and memory alteration triggered by early-life exposure to a diet poor in n-3 PUFA, taking into account sex. To do so, female mice were fed either to a n-3 PUFA deficient diet or to a n-3 PUFA balanced diet (Joffre et al., 2016) and at weaning, male and female offspring were maintained until adulthood under the same diets than their mothers. In a third cohort, male and female offspring from the n-3 PUFA deficient diet were exposed to the balanced diet from weaning until adulthood. At adulthood, emotional behavior and spatial memory, hippocampal PUFAs and their metabolites (oxylipins), hippocampal synaptic plasticity (long-term potentiation, LTP) and spine density were measured. Our findings reveal that early-life exposition to a diet deficient in n-3 PUFA alters memory and hippocampal synaptic plasticity, but not spine density in adult male and female. Importantly, the exposure of n-3 PUFA deficient offspring to a balanced diet at weaning differentially reverses spatial memory and PUFA in the hippocampus according to to females based on our results. Interestingly, synaptic plasticity were restored in both male and female. Altogether, our results pinpoint for the first time that early-life dietary n-3 PUFA deficiency-induced memory, PUFA metabolism and synaptic plasticity alterations are more easily rescued by an early life n-3 PUFA dietary correction in female than in male mice.

## MATERIAL AND METHODS

### ANIMALS AND DIETS

All experiments were performed according to criteria of the European Communities Council Directive 2010/63/EU for animal experiments and were approved by the national ethical committee for the care and use of animals (N°APAFIS 2018061514419181 #15533).

In this study, male and female CD1 mice were used. Male and female CD1 breeders were purchased from Janvier Labs (le Genest-Saint-Isle, France). They were placed on n-3 PUFA balanced (n-3 bal) or n-3 PUFA deficient diet (n-3 def) (INRAE Jouy-en-Josas (Mingam et al., 2008), see Table 1 for fatty acid composition of the n-3 PUFA balanced and deficient diets) since the first day of mating (**Figure 1**). At weaning (21 days post-natal), offspring were separated by sex and housed in group of 6-9 in polycarbonate cages in an air-conditioned (22 +/- 1°C) colony room with a 12: 12 light/dark cycle with *ad libitum* access to food and water. Half of the n-3 def animals were fed with a n-3 bal diet (n-3 rev for reverse) while the rest of the animals were maintained under the same diets than their mothers. All groups of mice were fed for 8 weeks with their respective diet. In total, 325 offspring were used for experiments; n-3 bal: 66 males and 71 females; n-3 def: 43 males and 49 females; n-3 rev 49 males and 47 females. The first cohort was used for behavioral and electrophysiological or fatty acids or oxylipins or enzyme or arborization measurement and the second cohort was used for oxylipin or electrophysiological assessment (**Figure 1**) and weighed once a week.

### BEHAVIORAL TEST

Behavioural tests were all performed during the light phase (between 8:00 AM and 11:00 AM) as previously described (Delpech et al., 2015; Labrousse et al., 2018; Lafourcade et al., 2011). Mice were handled 5 min every day for 2 weeks before the behavioral measurements. Spatial recognition memory was evaluated using the Y-maze test (Delpech et al., 2015). The apparatus is a Y-shaped maze with 3 arms (35cm long and 10cm deep), illuminated at 15 Lux and placed in a room with visual cues. Briefly, in a first trial, mice explored two arms for 5 min and after a 1h inter-trial interval (ITI) they explored three arms for 5 minutes. Initial and new arms were randomly assigned for each mouse. A tracking system was used (SMART system; San Diego Instruments) to analyse the time spent in the different arms, data are expressed as second or cm. Anxiety-like behavior was assessed in the Open Field test as described elsewhere (Seibenhener and Wooten, 2015). Mice were placed in an open area of 40x40 cm and 20cm deep illuminated at 30 Lux for 5 min. The time spent in the peripheral zone and the central zone was analyzed using with the SMART system (San Diego Instruments).

## **ELECTROPHYSIOLOGY**

Coronal hippocampal slices (350  $\mu\text{m}$ ) were prepared from adult mice. Brain slices were obtained with a vibrating blade microtome (VT1000S, Leica Microsystems, Germany) in an ice cold oxygenated artificial cerebrospinal fluid (ACSF) containing in (mM): 23  $\text{NaHCO}_3$ , 87  $\text{NaCl}$ , 75 Sucrose, 25 Glucose, 4  $\text{MgCl}_2$ , 2.5  $\text{KCl}$ , 0.5  $\text{CaCl}_2$ , 1.25  $\text{NaH}_2\text{PO}_4$ . Slices were placed 20 minutes in ACSF at 32°C, then 40 minutes at room temperature and recordings were started after. ACSF solution for storage contained (in mM): 23  $\text{NaHCO}_3$ , 130  $\text{NaCl}$ , 11 Glucose, 2.4  $\text{MgCl}_2$ , 2.5  $\text{KCl}$ , 1.2  $\text{CaCl}_2$ , 1.2  $\text{NaH}_2\text{PO}_4$ . ACSF solution for recordings contained (in mM): 23  $\text{NaHCO}_3$ , 130  $\text{NaCl}$ , 11 Glucose, 1.2  $\text{MgCl}_2$ , 2.5  $\text{KCl}$ , 2.4  $\text{CaCl}_2$ , 1.2  $\text{NaH}_2\text{PO}_4$ . Extracellular field excitatory post-synaptic potentials (fEPSPs) were evoked by stimulation (150  $\mu\text{s}$ , 0.1 Hz) of the Schaeffer collateral pathway afferents of the CA3 area using a bipolar concentric electrode (Phymep, Paris, France and stimulator A365, WPI, Sarasota FL, USA). Recordings in the CA1 *stratum radiatum* with borosilicate glass pipettes of 4 to 8  $\text{M}\Omega$  resistance filled with recording ACSF. Recordings were performed at 28°C using a temperature control system (TC-344B, Warner Instrument Corporation) and slices were continuously superfused at 3-4 ml/min with ACSF. Signals were amplified using Multiclamp 700B amplifier (Molecular Devices, Sunnyvale, CA, USA) controlled with pClamp 10.3 software *via* a Digidata 1440A interface (Molecular Devices). Baseline was obtained with stable fEPSPs recorded for 10 min at 0.1 Hz with a stimulus intensity of 40-50% of the maximum fEPSP. Long Term Potentiation (LTP) was induced using the high frequency stimulation (HFS) consisting in 3 stimulations trains at 100 Hz for 1 sec with 20 sec interval. After HFS protocol, fEPSPs were recorded for 45 min at 0.1 Hz. For each experiment, fEPSP amplitudes were measured 10 min before the induction of plasticity and up to 45 min after the protocol using Clampfit 10.3. All products for ACSF were provided by Sigma (Saint Quentin Fallavier, France).

## **FATTY ACID PROFILE**

Briefly, fatty acids from the hippocampus were analysed as previously described (Delpech et al., 2015; Labrousse et al., 2012; Madore et al., 2014). Fatty acids composition of the hippocampus is expressed as the percentage of total fatty acids.

## **OXYLIPINS**

The different metabolites derived from n-3 and n-6 PUFA families were extracted and analysed by mass spectrometry (LC-MS/MS) at METATOUL-lipidomic platform (MetaboHUB, INSERM UMR 1048, I2MC, Toulouse, France) as previously described (Rey et al., 2018).

## **DENDRITIC SPINE LABELLING AND COUNTING**

After anaesthesia by isoflurane, brains were removed, washed in phosphate-buffered saline and processed for staining of individual neurons following the manufacturer's instructions for the rapid

Golgi kit (FD Neurotech, Columbia, MD, USA) (Madore et al., 2020). After 24h hours, the solution was renewed and the impregnation continued for 4 days. Tissues were then immersed into a protective solution (phosphate buffer with sucrose and ethylene glycol). Brains were frozen and then sliced at 100  $\mu\text{m}$  with cryostat. Slices containing the dorsal hippocampus were used for morphological analysis. Images were acquired by a trained experimenter blind to the conditions using motorized Leica DM5000 microscope at a 63X magnification. Images were acquired using a CCD Coolsnap camera and Metamorph software (Madore et al., 2014).

For analysis, we randomly selected pyramidal neurons from the CA1 region of the dorsal hippocampus that were fully penetrated by the Golgi coloration and clearly distinguishable from other neurons. Neuron reconstruction was performed using the Fiji platform (Schindelin et al., 2012). Between 3 and 5 neurons were selected from each animal. Spine density in these neurons was determined by counting the number of spines on at least 3 basal and 3 apical dendritic segments of 10  $\mu\text{m}$  in length. Segments from dendrites situated as far from the cell body as possible, with no overlap with other dendrites were randomly selected. Primary dendrites were never used for analysis as their thickness hampers detection of spines. Spine density was calculated per 10  $\mu\text{m}$  and averaged across the different segments in the same neuron. A dendritic complex index (DCI) was used based on the number of dendrites from N order divided by the total number of dendrites.

## **NUCLEAR MAGNETIC RESONANCE**

Body composition of animals (fat mass, lean mass, fluids) was measured by nuclear magnetic resonance, a non-invasive method assessed on awake animals by pulsed frequency radiation of 6.5 MHz during 2 minutes (LF minispec, Bruker Corporation). Results are expressed in % of total weight.

## **STATISTICAL ANALYSES**

Statistical analyses were performed using GraphPad 7, 9 and Statistica softwares. All parameters were analyzed using Kruskal-Wallis one-way ANOVA between independent groups, with an exception for Y-maze that was analyzed using two-way repeated measures ANOVA with diet as between-subject factors and arm (novel vs. familiar) as the within-subjects factor was performed. All post hoc comparisons were made using Bonferroni test, with an exception for Y-maze where specific comparisons between novel and familiar arms were assessed by paired Student's t-tests.. The threshold for statistical significance was set at  $p < 0.05$ .

For electrophysiological recordings, fEPSPs were normalized to 10 min baseline prior to plasticity induction. Strength of synaptic plasticity was tested for each condition using a paired t-test between normalized baseline value and normalized fEPSP value at 45 min after plasticity induction (mean of the last 5 minutes of recording). To compare plasticity between n-3 PUFA balanced and n-3 PUFA deficient animals, we used a Mann-Whitney test. To compare time courses of synaptic plasticity for



each diet, a two-way ANOVA with time and diet (n-3 bal vs n-3 def vs n-3 rev) as factors was performed and when a significant interaction was reported, ANOVAs were followed by *post hoc* Bonferroni test comparisons.

The oxylipins pattern was assessed by using the Principal Components Analysis (PCA) for the three different diet groups for each sex group. This dimension-reduction technique summarizes data into principal components (PC) that maximize the variance of the data considered. These PCs are uncorrelated linear combinations of the initial variables which can be interpreted as patterns. PCA generates factor loadings that reflect the correlation of each variable with the PC and a PC score for each individuals. We selected the number of components using the Cattell criterion. Multivariate analysis was used with correlation matrix and heat map representation performed with GraphPad software. For those analyses, a zscore was calculated for each sample, based on the mean of group condition results and standard deviation. It is the proportion of the number of standard deviation above and below the population represented by raw datas :  $Z = (x-\mu)/\sigma$  (with x the data,  $\mu$  the mean and  $\sigma$  :the standard deviation).

## RESULTS

### **N-3 PUFA balanced diet given at weaning differentially rescues the deleterious effect of n-3 PUFA dietary deficiency on PUFA levels in the male and female hippocampus**

First, we investigated the impact of the different diets under study n-3 bal, n-3 def and n-3 rev on brain fatty acid composition in the hippocampus of male and female adult mice (**Fig. 2**). Statistical analysis revealed no significant effect of the diets on the total amount of saturated fatty acid (SFA), monounsaturated fatty acid (MUFA) and PUFA (Table 4) with a significant effect of the diets on total n-6 and n-3 PUFAs and their ratio (Table 4) in the hippocampus of male mice. In particular, the PUFAs belonging to the n-6 PUFA family (18:2, 20:3, 20:4, 22:4 and 22:5) were significantly altered by the n-3 def as compared to the n-3 bal diet (**Fig. 2.C, Table 4**). Importantly, the exposure to the n-3 PUFA balanced diet at weaning lead to a significant change of the level of these species, except for AA (20:4), which is not restored (**Fig. 2.C**). Concerning the n-3 PUFA family, a significant decrease of 20:5, 22:5 and 22:6 species was triggered by the exposure to the n-3 PUFA deficient diet, which was reversed by the n-3 PUFA balanced diet given at weaning (**Table 4, Fig. 2.D**). The results were different in the hippocampus of adult female mice with a significant effect of the diets on MUFA and PUFA, but not SFA (**Table 5**). Concerning the total level of n-6 and n-3 PUFA and their ratio, the exposure to a n-3 PUFA deficient diet significantly decreased their levels which were restored by the exposure to a n-3 PUFA balanced diet since weaning (**Fig. 2.E-F**). These significant changes were also observed for the individual species EPA (22:5), DPA (22:5) and DHA (22:6) (**Table 5, Fig. 2**).

### **Different effect of diets on oxylipin level in male and female hippocampus**

As PUFA levels were differentially affected by the early-life exposure to the diets according to sex and that we previously reported that dietary n-3 PUFA strongly influence brain oxylipins levels (Rey et al., 2018), we then measured oxylipin in the hippocampus of male and female mice exposed to the diets under study (Fig 3.A, heat map representation). 5 out of 24 measured oxylipins were significantly altered by the diets in the male hippocampus (**Table 1**). In particular, 13-HODE and 9-HODE, derived from LA and 8isoPGA2, derived from AA, were significantly decreased in n-3 rev as compared to n-3 def or n-3 bal (**Table 1**). On the opposite, 18-HEPE and 14-HDoHE, which are respectively EPA and DHA-derived oxylipins, were significantly decreased in the hippocampus of n-3 def as compared to n-3 bal or n-3 rev ( $p < 0,001$ ). In female, 15 out of 24 oxylipins detected were significantly altered by dietary intervention (**Table 2**). Overall, LA and AA-derived oxylipins were significantly increased in the hippocampus of n-3 def as compared to n-3 bal (13-HODE, 9-HODE, 14,15 EET, 8-HETE, 5-HETE, 5oxoHETE, LXB4), while decreased as compared to n-3rev (13-HODE, 9-HODE, 14,15 EET, 12,11-EET, 5,6-EET, 5-HETE, 5oxoHETE, 8isoPGA2, 15dPGJ2). On the opposite, EPA and DHA-derived oxylipins in female hippocampus were significantly decreased in n-3 def as compared to n-3 bal (18-HEPE, 17HDoHE) and increased in n-3 rev as compared to n-3d ef (18-HEPE, 14-HDoHDE, 17-HDoHDE). All statistical analysis are presented in Table 2 and 3. Multivariate data analysis of oxylipins in male and female hippocampi further revealed the separation of oxylipin pattern according to diet (**Fig. 3.A-B**). A correlation matrix revealed that LA-derivatives (13-HODE and 9-HODE) were inversely correlated to EPA- and DHA-derivatives (18-HEPE, 14-HDoHE and 17-HDoHE) and positively correlated to most of the AA-derivatives in male hippocampus. In addition, oxylipins derived from AA were positively correlated together and DHA and EPA-derived oxylipins were negatively correlated to EETs (14,15-EET and 11,12-EET) and positively correlated to prostaglandins (PGE2 and PGD2). In the hippocampus of female mice, LA-derived oxylipins were negatively correlated to 5,6-EET, 18-HEPE, 14-HDoHE and 17-HDoHE while positively correlated to AA-derived oxylipins. AA-derived oxylipins were positively correlated together and to 5,6-EET while EPA and DHA-derived oxylipins were negatively correlated to LA- and some AA-derived oxylipins (14,15-EET, 11,12-EET, 5oxoETE, 8isoPGA2 and 15dPGJ2). To further gain insight in which oxylipin pattern was responsible of the differences between groups and in the visualization of their individual repartition, we performed PCA (principal component analysis) (**Fig. 3.E-F**). PC1 explained 49,10% of the total variance and reported a positive score for all LA, AA, EPA and DHA metabolites except for 11,12-EET and 14,15EET in male hippocampus. In addition, PC2 explained 20,93% of the total variance with a positive score for AA, EPA and DHA metabolites (5,6-EET, 12-HETE, 6kPGF1a, TXB2, PGE2, PGF2a, PGD2, 18-HEPE, 14-HDoHE and 17-HDoHE) (**Fig. 3.E**). In female, PC1 explained 41,05% of the total variance with a positive score for all LA, AA, EPA and DHA metabolites except for 5,6-EET, 18-HEPE and 17-HDoHE. In addition, PC2 explained 25,19% of the total variance with a positive score for AA, EPA and DHA metabolites (5,6-EET, 15-HETE, 8-HETE, 12-HETE, LXA4, 6kPGF1a, TXB2, PGE2, PGF2a, PGD2, 18-HEPE, 14-HDoHE and 17-HDoHE)

and a negative score for some AA metabolites (14,15-EET, 11,12-EET, 8,9-EET, -HETE, 8-HETE, 5oxoETE, 6kPGF1a, 8isoPGA2 and 15dPGJ2) (**Fig. 3.F**). The study of individual repartition revealed a clear separation on n-3 bal and n-3 def male (**Fig. 3.E**) and female (**Fig. 3.F**). N-3 reversed males animals were not totally fitting n-3 deficient or n-3 balanced groups while n-3 reversed females showed a repartition close to the n-3 balanced group.

### **N-3 PUFA balanced diet given at weaning differentially rescues the deleterious effect of n-3 PUFA dietary deficiency on memory in male and female**

N-3 PUFA dietary deficiency-altered DHA levels in the hippocampus has been reported to alter spatial memory (Delpech et al., 2015) in male, but not in female mice. To further get insight into the consequences of early-life exposure on memory at adulthood in both sexes and determine whether switching to a n-3 PUFA balanced diet at weaning can protect from these deficits, spatial memory was measured in adult mice submitted to the 3 diets under study using a Y-maze test with a 1-h ITI (Labrousse et al., 2012) (**Fig. 4**). No significant effect of the diets was revealed on the total time and distance travelled in both male and female. In male, a two-way ANOVA analysis revealed a significant effect of arm ( $F(1,72) = 14,5$ ,  $p < 0,001$ ) and diet by arm interaction ( $F(2,72) = 3,24$   $p < 0,05$ ) on the time spent in the arms (**Fig. 4.A**). The post-hoc analysis further revealed that n-3 bal mice spent more time exploring the novel arm as compared to the familiar arm ( $p < 0,05$ ) which was not the case for n-3 def and n-3 rev male mice. In female, a two-way ANOVA analysis revealed a significant effect of arm ( $F(1,82) = 17,12$ ,  $p < 0,001$ ) and dietxarm interaction ( $F(2,82) = 3,3$ ,  $p < 0,05$ ) on the time spent in the arms (**Fig. 4.A**). A post hoc analysis further revealed that n-3 bal and n-3 rev female mice spent significantly more time in the novel arm as compared to the familiar arm ( $p < 0,01$ ) and this was not the case for n-3 def mice. In the open-field test, used to measure anxiety-like behavior, a significant effect of the diets were observed on the total distance travelled (**Fig. 8.B**) and the time in the center ( $F(2,87) = 6,3$ ,  $p < 0,01$ ) (**Fig. 8.A**) in male, but not in female. Post-hoc analysis further revealed that n-3 bal male spent significantly more time in the center and travel more distance in the open-field as compared to n-3def ( $p < 0,001$ ) and n-3 rev ( $p < 0,05$ ) mice.

### **N-3 PUFA balanced diet given at weaning rescues the deleterious effect of n-3 PUFA dietary deficiency on long term potentiation in both male and female hippocampus**

As early-life exposure to a n-3 PUFA deficient diet alters LTP in the hippocampus of male mice at weaning and adulthood (Madore et al., 2014; Thomazeau et al., 2016) which is a hallmark of spatial memory (Lafourcade et al., 2011) which is differentially restored in male and female fed with a balanced n-3 diet until weaning. We therefore analyzed LTP until 45 minutes after stimulation in the hippocampus of male and female mice with the different diets under study using a presynaptic stimulation of 3 pairings at 100 Hz (high frequency stimulation protocol HFS) (**Fig. 5.A-5.B**). Using this protocol, LTP was displayed in n-3 bal and n-3 rev male and female, but not in n-3 def.

### **N-3 PUFA deficient diet does not alter dendritic arborization and spine number of neurons in the CA1 zone of the hippocampus of male and female.**

We previously found that cornus amniosis (CA1) neurons, which are crucial in the processing of hippocampus-dependent memory and LTP (Thomazeau et al., 2016) have altered spine and dendritic morphology and number at weaning (Madore et al., 2014), but not adulthood (Larrieu et al., 2014) of n-3 def male mice. We therefore explored the effect of the different dietary exposure on neuronal morphology in male and female adult hippocampus CA1 using Golgi staining (**Fig. 6**). No significant effect of diets under study were measured on dendritic basal and apical length of neurons in the CA1 zone of adult male and female mice (**Fig. 6A-C**). Consequently, dendritic complex index (DCI) was not significantly altered by the diet (**Fig. 6E-F**). However, diet significantly alters spine density of female ( $F(2,17)=9,58$ ,  $p<0,01$ ), but not male CA1 neurons (**Fig. 6G**). In particular, spine density was higher in CA1 neurons of n-3 rev female as compared to n-3 def ( $p<0.01$ ) and n-3 bal ( $p<0.05$ ) mice.

## **DISCUSSION**

Our results revealed for the first time that a dietary intervention with a n-3 PUFA balanced diet starting at weaning reverses the deleterious effect of early-life n-3 PUFA deficient diet on spatial memory and hippocampal PUFA profile in female, but not in male. However, the dietary intervention was sufficient to improve early-life n-3 PUFA deficient diet-induced LTP alteration in both sex. Importantly, we identified specific oxylipin signature in the hippocampus of mice under the 3 diets which are specific to sex, opening new insights into mechanistic activity of dietary n-3 PUFA level on memory function.

Exposure to a diet deficient in n-3 PUFA since pregnancy has been previously shown by us and others to alter spatial memory, emotional behavior and synaptic plasticity and DHA level in the hippocampus, prefrontal cortex and nucleus accumbens of offspring at adulthood (Labrousse et al., 2018; Lafourcade et al., 2011; Larrieu et al., 2012; Moranis et al., 2012). While most of the previous studies have been conducted in males, our current work further revealed that females are overall similarly impacted by the exposure to the n-3 deficient diet with decreased hippocampal DHA, altered spatial memory and impaired LTP. Previous work reported that female rodents fed with a diet poor in n-3 PUFA develop depressive-like behavior and display neurochemical alteration in the hippocampus (Morgese et al., 2020) but, to our knowledge this is the first report on the memory and LTP defect reported in female. Interestingly, maternal dietary n-3 PUFA deficiency alters fatty acid levels in the liver and induces neurogenesis and neurochemical alterations in the hippocampus of females rat at weaning (Tang et al., 2018), suggesting that maternal dietary n-3 PUFA deficiency impairs female brain development, like we previously reported in male (Madore et al., 2020, 2014). At adulthood, n-3 and n-6 PUFA level were similar in the hippocampus of both male and female fed with a n-3 PUFA

deficient diet with decreased EPA and DHA and increased AA and DPA n-6, as expected (Joffre et al., 2016). However, a dietary intervention with a n-3 PUFA balanced diet starting at weaning differentially restores the level of AA, but not of EPA and DHA, in the hippocampus of male and female. Overall, our results suggest that long-life dietary intervention alters differentially LA and ALA metabolism and/or brain n-3 and n-6 LC-PUFA accretion in male and female. This is a matter of debate as some differences have been previously reported in humans, with DHA level in the PFC of patients diagnosed with major depression being significantly reduced in female, but not male (McNamara et al., 2007). These differences in DHA level in men and women could be linked to the effect of ovarian hormones on the biosynthesis of DHA from its dietary precursor ALA (Childs et al., 2008; McNamara et al., 2009). Whether hormonal changes were associated to the restoration of PUFA in the hippocampus of female, but not male, remains to be studied. However, a recent study reported no variation of AA level in the cortex of ovariectomized female mice treated or not with estradiol (Herrera et al., 2018).

We further determined whether the differences in PUFA accretion in the brain were also associated to differences in PUFA-derived oxylipins in male and female. First, the oxylipin profile was differently altered in the hippocampus of male and female by the diets under study with only 5 species altered in male as compared to 15 in female, showing a specific brain oxylipin signature according to sex. Interestingly, LA- and EPA- derived oxylipins were altered by diets in the hippocampus of male and female, while strong differences were observed for AA-derived oxylipins. As a result, only 8iso-PGA2 was differed according to dietary intervention in male, while 10 species, including 8iso-PGA2, were altered in the hippocampus of female. Importantly, AA increase triggered by the n-3 PUFA deficient diet was accompanied by a decrease in 8iso-PGA2. AA and 8iso-PGA2 profile remains identical after the dietary switch to a n-3 PUFA balanced diet. PGA2 is a cyclopentenone prostaglandin from PGE2 (Straus and Glass, 2001), which level were not found to be significantly affected by dietary intervention in our study. 8-iso-PGA2 was previously reported to activate neuronal nociceptors and pain through its interaction with TRPA1 (transient receptor potential A1) (Materazzi et al., 2008), however to our knowledge, its effect in the brain has not been reported. Agonism of TRPA1 activates glutamate release by neurons (Sun et al., 2009), however whether 8iso-PGA2 activates glutamate in the hippocampus remains to be investigated. Of note, 8-HETE, 12-HETE and LxB4, which are AA-derived oxylipins were not restored in the hippocampus of female fed with the n-3 PUFA balanced diet from weaning. In addition, 18-HEPE and 14-HDoHE, which are EPA- and DHA-derived and markers of resolvin E and D respectively (Layé et al., 2018; Serhan et al., 2002), are equally altered by the dietary interventions in the hippocampus of male and female. Increased level of these species in the brain by dietary intervention high in n-3 PUFA has been previously reported by us and others (Rey et al., 2019; Wang et al., 2022). EPA and DHA-derived oxylipins have been reported to be neuroprotective towards inflammatory stimuli (Layé et al., 2018; Rey et al., 2019, 2018), including on

human neurogenesis *in vitro* (Borsini et al., 2021). In addition, 18-HEPE activates BDNF synthesis in the retina (Suzumura et al., 2020) and was associated to remyelination and resolution to neuroinflammation (Rey et al., 2019; Siegert et al., 2017). These compounds have also been reported in the human cerebrospinal fluid (Terrando et al., 2021). However, whether 18-HEPE and 14-HDoHE mediates LC n-3 PUFA effect in the brain remains to be determined. Importantly to the question addressed in our work, switching male and female n-3 PUFA deficient mice to a diet balanced in LA/ALA at weaning until adulthood displays differential effect on memory, but not on LTP according to sex. EPA, DHA and AA levels were restored by the balanced n-3 PUFA diet given at weaning in female hippocampus, while AA level was not restored in the male hippocampus. The deleterious impact of early-life n-3 PUFA deficient diet on working memory at adulthood has been previously reported by us and others in male (Lafourcade et al., 2011; Lozada et al., 2017; Madore et al., 2014; Thomazeau et al., 2016) but not in female mice. Interestingly, previous work reported that an early correction of the brain DHA deficit is critical for preventing cognitive impairments in adult mice fed an early-life n-3 PUFA deficient diet, while later-life dietary supplementation restores brain DHA, but not memory impairment (Lozada et al., 2017). However, the length of dietary supplementation is also critical as longer time of exposure to diets rich in n-3 PUFA can reverse the deleterious effect of n-3 PUFA dietary deficiency on memory (Gao et al., 2016; Moriguchi and Salem Jr, 2003). Together with our results, this suggests that the normalization of brain DHA is not sufficient to improve memory function. Indeed, our results suggest that AA restoration and metabolization in the brain is critical for memory. This is in accordance with recent work showing that phospholipid metabolite landscape is modulated in response to memory acquisition (Wallis et al., 2021) and the role of cyclooxygenase(COX)-2, which metabolizes AA into prostanoids, in memory process in physiological conditions (López and Ballaz, 2020a). Furthermore, spatial memory impairment observed in early-life n-3 PUFA deficient diet mice in Y-maze test was not reproduced when the deficiency starts after weaning (Delpech et al., 2015), suggesting that impairment promoted by the n-3 PUFA deficient diet is probably triggered in during CNS development (Madore et al., 2020, 2014). Indeed, we previously reported that AA and its derivative 12-HETE are critical in mediating altered memory and synaptic function at weaning (Madore et al., 2020). Indeed, the role of AA and 12-HETE in early-life memory processes have been proposed, but how AA and 12-HETE interferes with memory at adulthood remains to be solved. We further report for the first time that hippocampal LTP is altered by n-3 PUFA deficient in both male and female mice. We and others previously reported this effect in male and identified starting at weaning (Cao et al., 2009; Di Miceli et al., 2020; Thomazeau et al., 2016). LTP alteration was not associated to changes in dendritic arborization or spine number. Previous work reported that n-3 PUFA deficiency-induced LTP impairment in male is mediated by the AMPA/NMDA ratio increase in the hippocampus and the decrease in the expression of NMDA receptor subunit (Cao et al., 2009; Thomazeau et al., 2016). Importantly, LTP deficits were fully

restored in both male and female by the n-3 PUFA balanced diet. However, the mechanisms underlying this restoration remain to be determined.

In conclusion, this study demonstrates that an adequate supply of n-3 PUFA in form of LNA starting at weaning in mice is sufficient to support cognitive function and hippocampal synaptic plasticity in early-life n-3 PUFA deficient female, but not male mice. Our finding identifies specific and distinct oxylipin signature in the hippocampus of male and female and pinpoint that these profile are differently affected by dietary intervention with n-3 PUFA. Our results reinforce the idea that a particular attention should be given to early-life n-3 PUFA in high-risk populations such as preterm infants in the immediate perinatal period and take account of sex.

### **Author Contributions**

S.L. and M.M. designed the study; M.M., M.R., AS., A.A., MG., ED., NA., GS., and S.A. conducted the experiments; analyzed the data MM, MR, M.D.M., NA., GS., CM, JCD, CJ, RB; MM and SL wrote the draft; MM, SL, XF, JCD, CM, CJ performed literature search and participated in data interpretation. All authors have read and agreed to the published version of the manuscript.

### **Funding**

This work was financially supported by the Fondation pour la Recherche Médicale (FRM PRINSS DEQ 20170336724, to SL ; FRM fin de thèse 202204014903, to MM), Région Nouvelle Aquitaine (00070700, 2017-1R30237-00013179, 2019-1R3M08, to SL), Chaire d'excellence Région Nouvelle Aquitaine ExoMarquAge (13059720-13062120, to SL and JCD), JPI HDHL (Ambrosiac ANR-15-HDHL-0001-03 to LC) and Food4BrainHealth, INRAE.

### **Institutional Review Board Statement**

Ethics Committee of the University of Bordeaux (CEEA50). French Ministry of Education and Research (Ministère de l'Éducation Nationale, de l'Enseignement Supérieur et de la Recherche), agreement number N°APAFIS 2018061514419181 #15533

### **Acknowledgments**

The authors wish to thank Grégory Artaxet, Elona Lalaj, and Eva Bruchet for taking care of the animals.

### **Conflicts of Interest**

The authors declare no conflict of interest

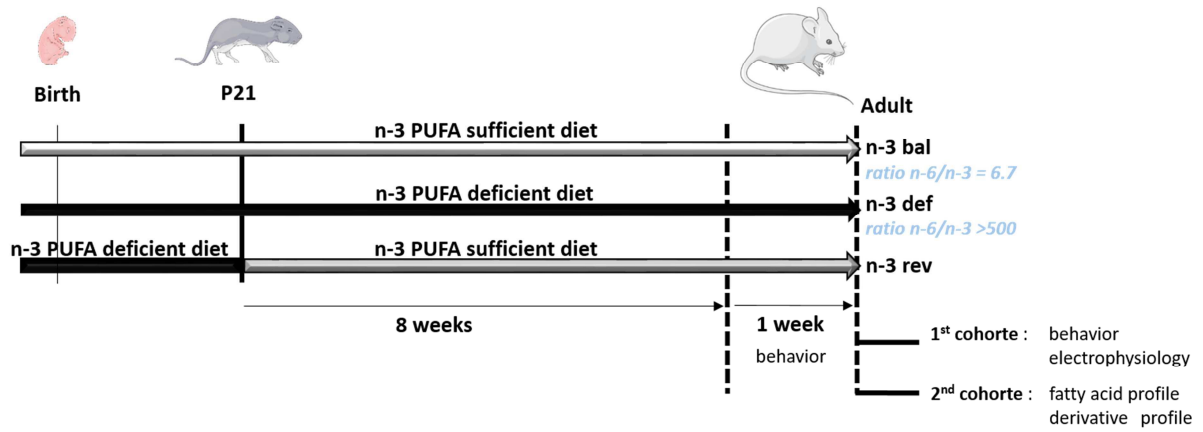


**Figure 1.** Scheme of the experimental design.



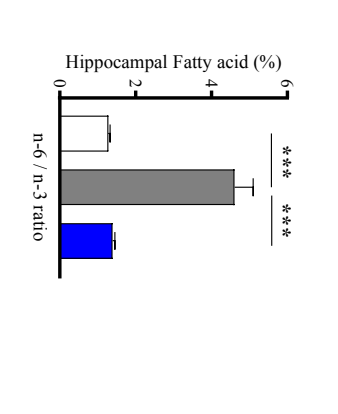
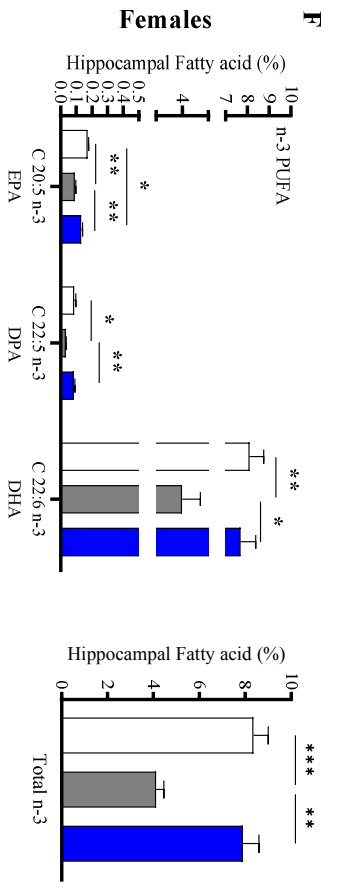
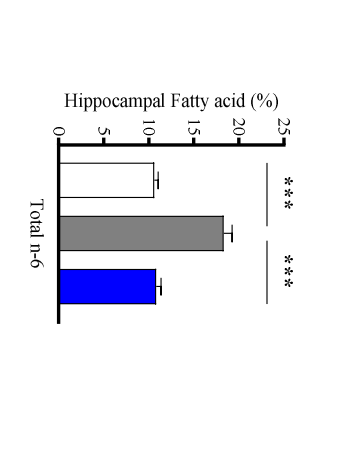
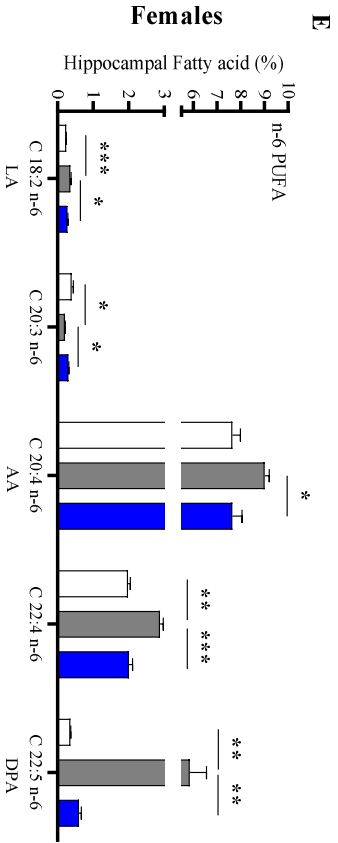
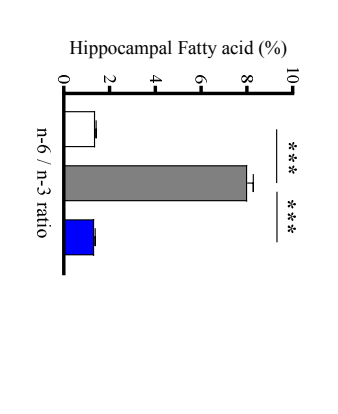
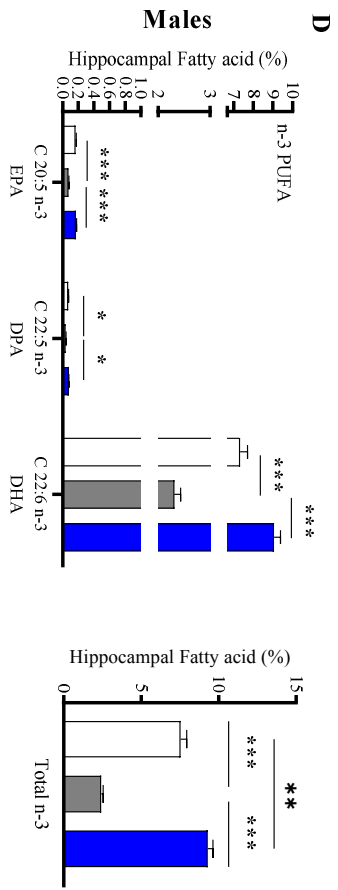
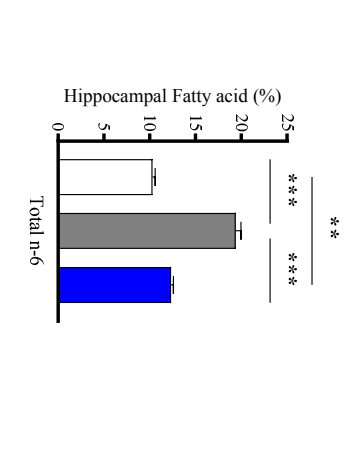
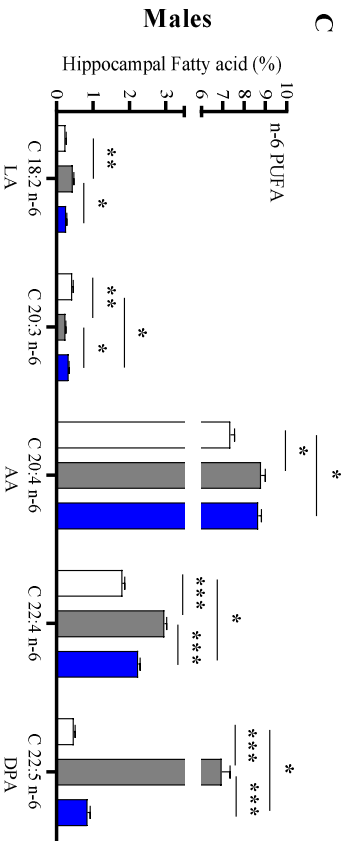
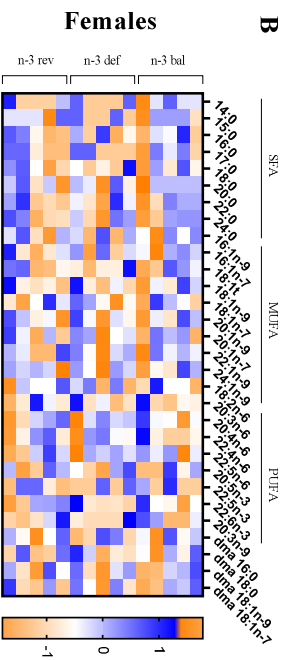
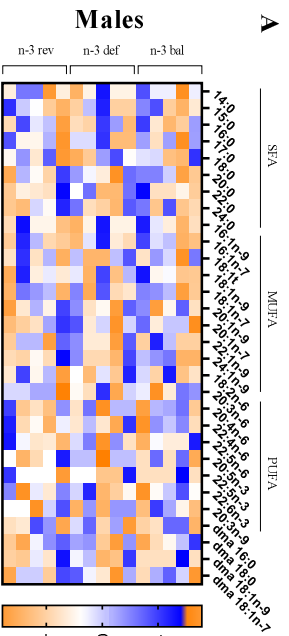


**Figure 2** Fatty acid profile in the hippocampus of n-3 bal, n-3 def and n-3 rev male and female mice. (A-B) Heatmap representation of the PUFA levels for each individual. (C) n-6 PUFA species and total n-6 PUFA in male hippocampus. (D) n-3 PUFA species, total n-3 PUFA and n-6/n-3 PUFA ratio in male hippocampus. (E) n-6 PUFA species and total n-6 PUFA in female hippocampus. (F) n-3 PUFA species, total n-3 PUFA and n-6/n-3 PUFA ratio in male hippocampus. Results of C-D-E and F are expressed in % of total fatty acids. Box and whiskers represent min to max values. \* p<0.05, \*\* p<0.01, \*\*\* p<0.001.

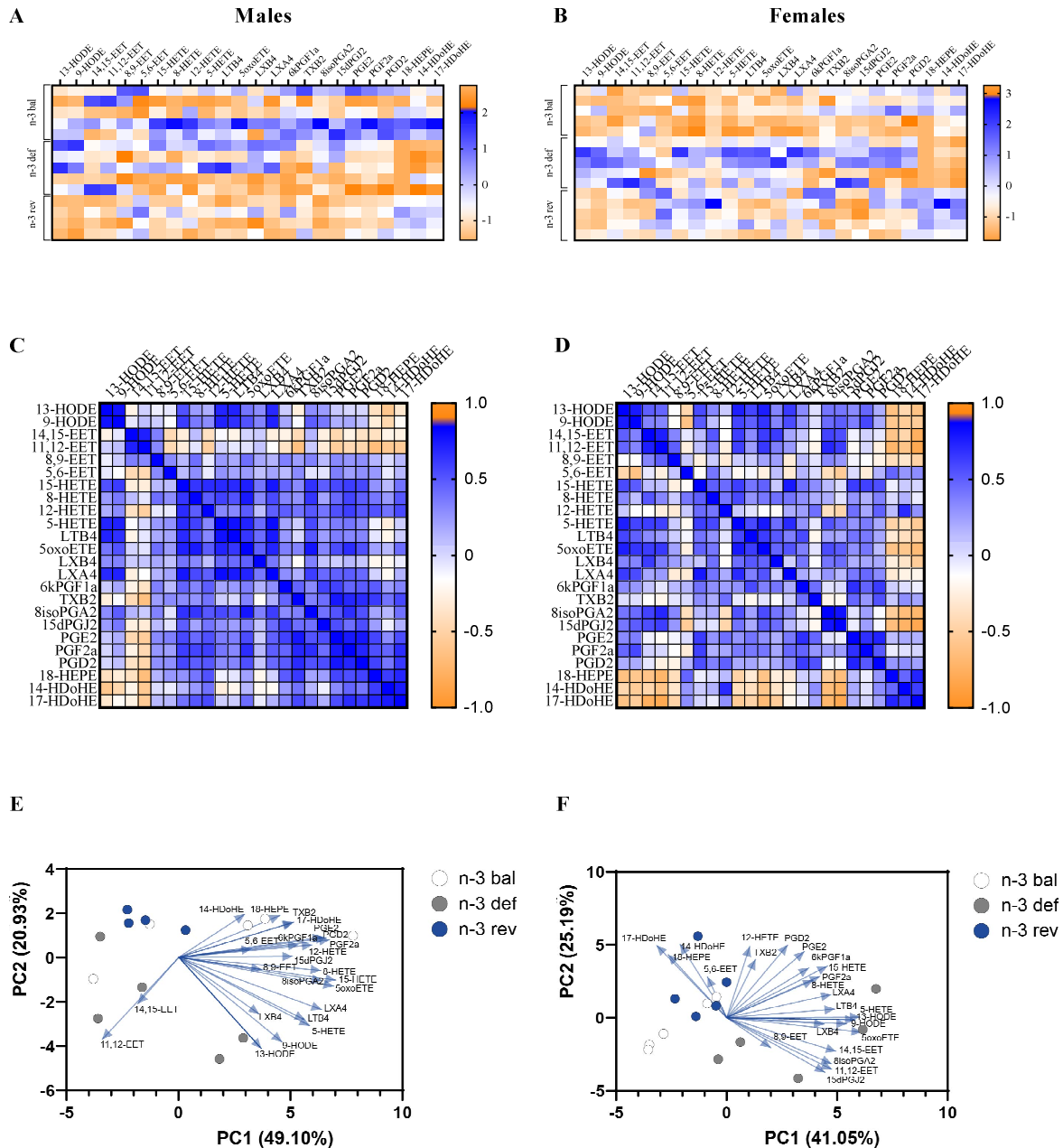


**Figure 3** Multivariate analysis of oxylipins measured in the hippocampus of n-3 bal, n-3 def n-and 3 rev male and female mice. (A-B) Heat map of all AA-, EPA-, and DHA-derived oxylipins in the hippocampus of mice under all diets studied. (C-D) Correlation matrix of the 24 oxylipins measured (blue: positive correlation, orange: negative correlation, white: no significant correlation). (E-F) Correlation of variable and individuals from the n-3 bal, n-3 def and n-3 rev oxylipins measured in the hippocampus of n3 bal, n-3 def and n-3 rev mice based on the principal component score from PCA. The two pattern PC1 and PC2 (Principal Component) represent 70.03% of the variance. The length of each arrow is proportional to the weight of the corresponding factor in defining the pattern. Two arrows with opposite directions are anti-correlated variables. Circles represent individual mice of the n-3 bal, n-3 def and n-3 rev groups.

**Table 1** Oxylipins measured in the hippocampus of n-3 bal, n-3 def and n-3 rev male mice. Data are presented as mean  $\pm$  SEM (n=5) and are expressed in pg/mg protein. Data were analysed by a One-Way ANOVA followed, if a significant effect is revealed ( $p < 0.05$ ), by a Bonferroni multiple comparison test.

	Fatty acids derivatives (pg/mg protein)	Males			Statistical effects (One- Way ANOVA)		
		n-3 Bal (a)	n-3 Def (b)	n-3 Rev (c)	ANOVA	Multiple comparison	
<i>n-6 derivatives</i>	<b>LA</b>	13-HODE	7765.6 $\pm$ 2578.7	8005.3 $\pm$ 6375.1	3581.8 $\pm$ 849.0	p<0.05	b-c p<0.05
		9-HODE	4102.3 $\pm$ 1363.0	3405.4 $\pm$ 2328.7	1599.3 $\pm$ 371.9	p<0.05	b-c p<0.05
	<b>AA</b>	14,15-EET	803.0 $\pm$ 640.7	721.5 $\pm$ 684.4	1139.5 $\pm$ 705.9	ns	ns
		11,12-EET	1131.4 $\pm$ 1189.3	1132.6 $\pm$ 1041.0	1172.1 $\pm$ 961.6	ns	ns
		8,9-EET	6382.7 $\pm$ 1082.4	3447.5 $\pm$ 1189.2	4686.0 $\pm$ 2326.4	ns	ns
		5,6-EET	2483.6 $\pm$ 2192.7	1596.3 $\pm$ 1128.1	2965.6 $\pm$ 767.0	ns	ns
		15-HETE	91845.0 $\pm$ 47238.0	56101.7 $\pm$ 47142.1	48643.0 $\pm$ 7514.8	ns	ns
		8-HETE	4831.4 $\pm$ 2712.4	3098.4 $\pm$ 1380.9	3633.7 $\pm$ 1052.3	ns	ns
		12-HETE	43595.5 $\pm$ 26775.5	23936.2 $\pm$ 18402.1	25671.2 $\pm$ 8161.8	ns	ns
		5-HETE	48271.9 $\pm$ 25127.4	39352.5 $\pm$ 29710.7	30944.0 $\pm$ 16417.8	ns	ns
		LTB4	134.2 $\pm$ 38.6	98.7 $\pm$ 86.5	95.0 $\pm$ 73.8	ns	ns
		5oxoETE	68713.8 $\pm$ 44498.7	43790.4 $\pm$ 24670.9	40305.9 $\pm$ 16790.6	ns	ns
		LXB4	1754.8 $\pm$ 450.0	1379.1 $\pm$ 566.4	1553.4 $\pm$ 323.7	ns	ns
		LXA4	3090.2 $\pm$ 1686.4	2240.2 $\pm$ 2097.2	1385.0 $\pm$ 274.1	ns	ns
		6kPGF1a	2196.9 $\pm$ 785.6	1000.8 $\pm$ 1055.9	1202.3 $\pm$ 375.4	ns	ns
		TXB2	7144.9 $\pm$ 2787.7	2284.9 $\pm$ 1231.1	4371.0 $\pm$ 1649.8	ns	ns
		8isoPGA2	2647.2 $\pm$ 1552.4	1500.4 $\pm$ 446.6	1131.4 $\pm$ 449.0	p<0.05	a-c p<0.05
		15dPGJ2	122.4 $\pm$ 73.0	66.0 $\pm$ 63.9	65.8 $\pm$ 63.9	ns	ns
		PGE2	13314.0 $\pm$ 4661.7	5325.7 $\pm$ 2667.6	6590.5 $\pm$ 1577.3	ns	ns
		PGF2a	46290.2 $\pm$ 30034.7	21091.2 $\pm$ 5186.7	23162.3 $\pm$ 3510.6	ns	ns
PGD2	20961.6 $\pm$ 12533.2	9000.0 $\pm$ 3074.3	12272.4 $\pm$ 4094.5	ns	ns		
<i>n-3 derivatives</i>	<b>EPA</b>	18-HEPE	131.6 $\pm$ 64.5	0 $\pm$ 0.0	59.4 $\pm$ 69.2	p<0.001	a-b / b-c p<0.001
		<b>DHA</b>	14-HDoHE	5073.8 $\pm$ 2910.5	1503.6 $\pm$ 1337.7	4161.4 $\pm$ 746.9	p<0.05
	17-HDoHE		14837.6 $\pm$ 11321.8	3653.0 $\pm$ 2169.0	9305.8 $\pm$ 2597.7	ns	ns

**Table 2** Oxylipins measured in the hippocampus of n-3 bal, n-3 def and n-3 rev female mice. Data are presented as mean  $\pm$  SEM (n=5) and are expressed in pg/mg protein. Data were analysed by a One-Way ANOVA followed, if a significant effect is revealed ( $p < 0.05$ ), by a Bonferroni multiple comparison test.

	Fatty acids derivatives (pg/mg protein)	Females			Statistical effects (One Way ANOVA)		
		n-3 Bal (a)	n-3 Def (b)	n-3 Rev (c)	ANOVA	Multiple comparison	
<i>n-6 derivatives</i>	<i>LA</i>	13-HODE	3165.6 $\pm$ 1398.7	6362.6 $\pm$ 3198.4	3374.3 $\pm$ 617.7	$p < 0.01$	a-b / b-c $p < 0.01$
		9-HODE	1751.7 $\pm$ 927.8	2490.5 $\pm$ 1183.1	1455.7 $\pm$ 130.6	$p < 0.05$	b-c $p < 0.05$
	<i>AA</i>	14,15-EET	278.0 $\pm$ 98.2	637.9 $\pm$ 236.9	437.4 $\pm$ 76.6	$p < 0.001$	a-b $p < 0.001$ / b-c / a-c $p < 0.05$
		11,12-EET	406.7 $\pm$ 194.7	1000.0 $\pm$ 741.8	480.0 $\pm$ 130.6	$p < 0.01$	a-b $p < 0.01$ / b-c $p < 0.05$
		8,9-EET	2511.8 $\pm$ 558.5	2639.8 $\pm$ 699.3	2576.3 $\pm$ 675.1	ns	ns
		5,6-EET	1064.4 $\pm$ 244.8	1145.4 $\pm$ 210.7	1786.4 $\pm$ 497.7	$p < 0.001$	a-c / b-c $p < 0.001$
		15-HETE	34452.4 $\pm$ 17629.4	43856.3 $\pm$ 21722.9	39954.5 $\pm$ 10059.2	ns	ns
		8-HETE	1552.6 $\pm$ 430.8	2630.0 $\pm$ 546.7	2758.1 $\pm$ 422.7	$p < 0.001$	a-b / a-c $p < 0.001$
		12-HETE	14503.4 $\pm$ 6033.9	16287.9 $\pm$ 10125.2	24890.9 $\pm$ 12662.1	$p < 0.05$	a-c $p < 0.05$
		5-HETE	16646.5 $\pm$ 5641.3	30880.2 $\pm$ 11024.4	21591.3 $\pm$ 3341.3	$p < 0.001$	a-b $p < 0.001$ / b-c $p < 0.05$
		LTB4	58.5 $\pm$ 10.6	84.6 $\pm$ 45.0	65.4 $\pm$ 42.6	ns	ns
		5oxoETE	26020.2 $\pm$ 4205.6	37283.2 $\pm$ 9742.2	27679.1 $\pm$ 5902.8	$p < 0.01$	a-b $p < 0.01$ / b-c $p < 0.01$
		LXB4	818.2 $\pm$ 223.0	1307.6 $\pm$ 617.4	1139.6 $\pm$ 333.3	$p < 0.05$	a-b $p < 0.05$
		LXA4	1056.1 $\pm$ 734.1	1602.1 $\pm$ 981.2	1162.0 $\pm$ 373.9	ns	ns
		6kPGF1a	863.9 $\pm$ 488.3	1238.0 $\pm$ 1178.2	1370.5 $\pm$ 353.4	ns	ns
		TXB2	2746.8 $\pm$ 960.8	2723.8 $\pm$ 796.4	3168.4 $\pm$ 1442.0	ns	ns
		8isoPGA2	1091.7 $\pm$ 960.8	1531.5 $\pm$ 641.4	962.2 $\pm$ 197.3	$p < 0.05$	b-c $p < 0.05$
		15dPGJ2	70.0 $\pm$ 23.6	99.3 $\pm$ 28.3	51.0 $\pm$ 29.1	$p < 0.05$	b-c $p < 0.01$
		PGE2	5093.2 $\pm$ 2022.8	5436.9 $\pm$ 3780.3	5555.1 $\pm$ 2212.9	ns	ns
PGF2a	19092.3 $\pm$ 8880.6	20526.4 $\pm$ 10873.6	18103.7 $\pm$ 2931.7	ns	ns		
PGD2	7932.3 $\pm$ 3181.1	8801. $\pm$ 5172.8	10120.0 $\pm$ 3327.2	ns	ns		
<i>n-3 derivatives</i>	<i>EPA</i>	18-HEPE	48.9 $\pm$ 69.2	0 $\pm$ 0.0	91.1 $\pm$ 27.9	$p < 0.001$	a-b $p < 0.05$ / b-c $p < 0.001$
		<i>DHA</i>	14-HDoHE	2737.1 $\pm$ 879.0	1507.2 $\pm$ 736.5	3657.0 $\pm$ 972.3	$p < 0.05$
	17-HDoHE		6386.7 $\pm$ 2807.0	3248.3 $\pm$ 1240.7	7742.6 $\pm$ 2466.9	$p < 0.001$	a-b $p < 0.01$ / b-c $p < 0.001$

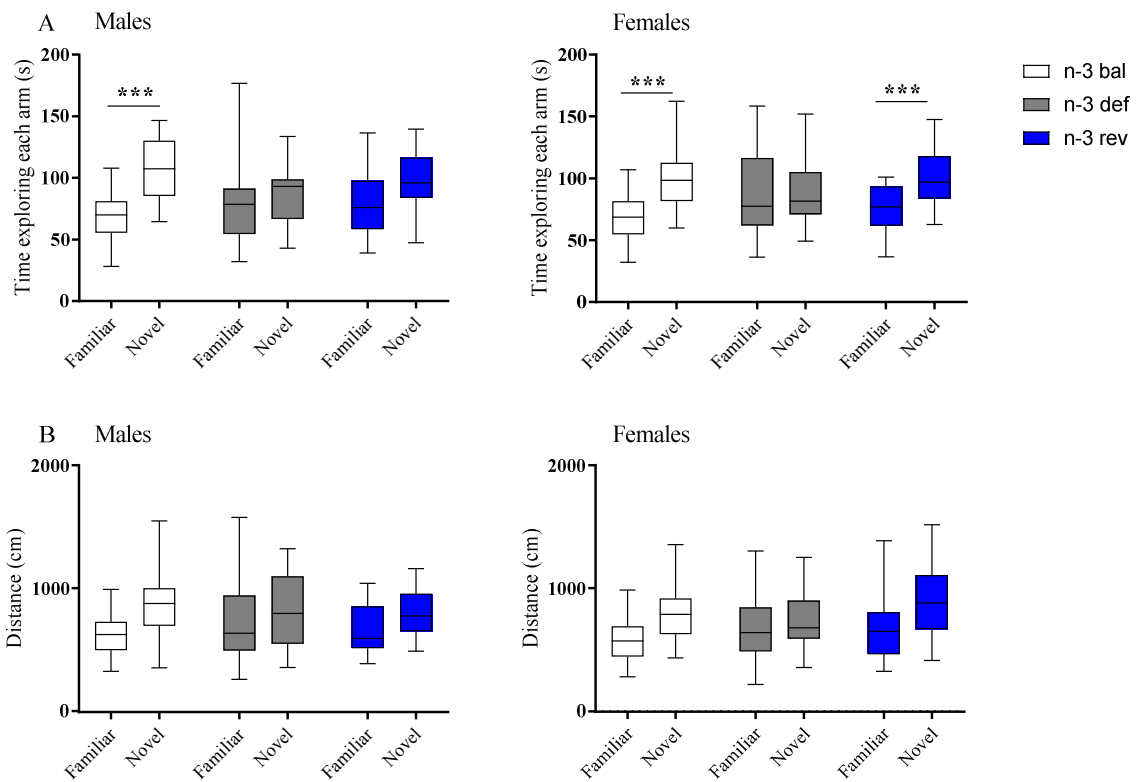


**Figure 4** Spatial memory of n-3 bal, n-3 def and n-3 rev male and female mice. **(A)** Time spent (in sec) exploring the familiar and the new arm of the Y-maze by n-3 bal, n-3 def and n-3 rev male and female mice (n=[20-33]). Paired t-test \*  $p < 0.05$ , \*\* $p < 0.01$ , \*\*\*  $p < 0.001$ . **(B)** Distance travelled (in cm) in the arms of the Y-maze by n-3 bal, n-3 def and n-3 rev male and female mice (n=[20-33]). Paired t-test.

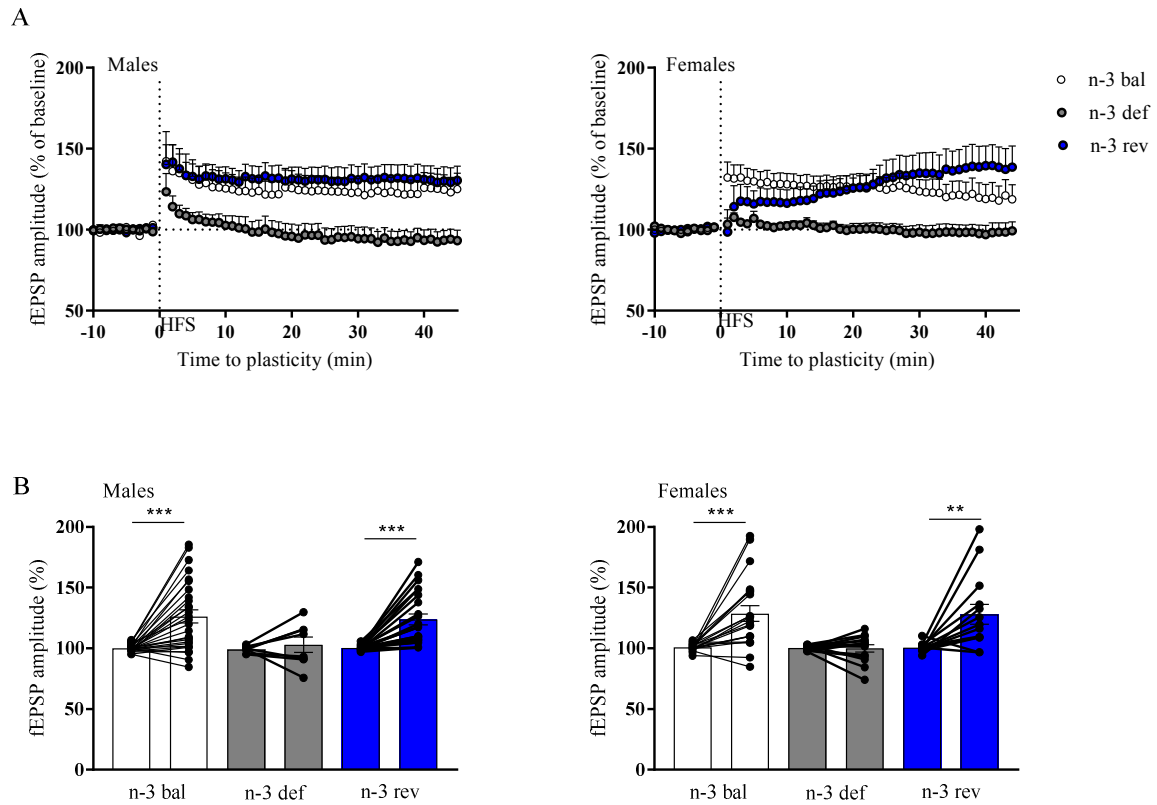


**Figure 5** Field recordings in the hippocampus of n-3 bal, n-3 def and n-3 rev male and female mice. (A) Field excitatory post synaptic potential (fEPSP) amplitudes were measured after high frequency stimulation (HFS) protocol of 3x100 Hz. (B) Pre and post (Last 5 minutes of fEPSP amplitude recordings) comparison. Paired t-test \*\*  $p < 0.01$  \*\*\*  $p < 0.001$ .

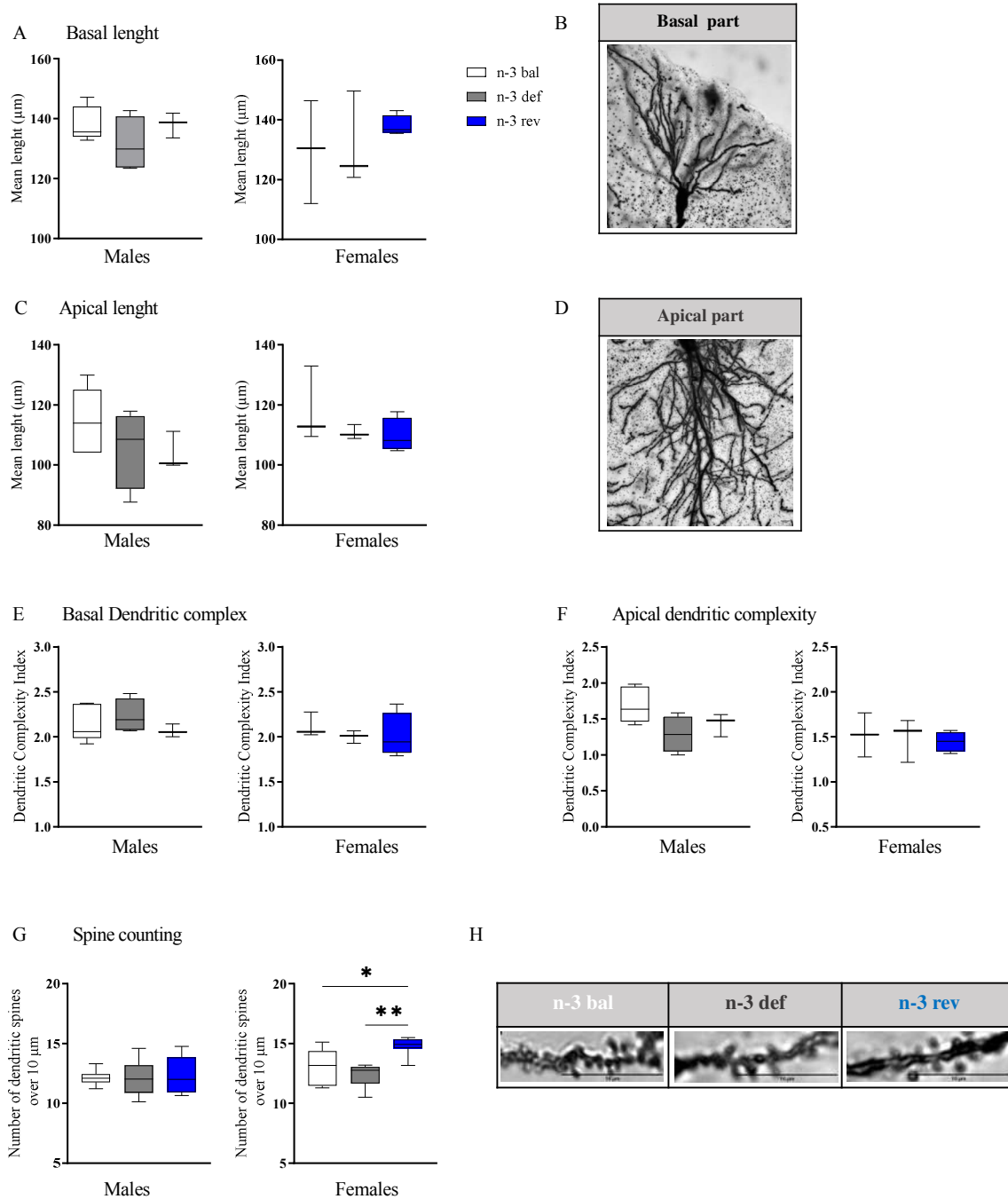


**Figure 6** Basal and apical dendrite length of hippocampal CA1 pyramidal neurons from n-3 bal, n-3 def and n-3 rev male and female mice. **(A)** Basal length of hippocampal CA1 pyramidal neurons. **(B)** Representative images of basal part of dendrites **(C)** Apical length of hippocampal CA1 pyramidal neurons. **(D)** Representative images of apical part of dendrites. **(A-C)** results are expressed as the mean length (nm). **(E)** and **(F)** Dendritic complexity index in apical **(E)** and basal **(F)** hippocampal CA1 pyramidal neurons. **(G)** Dendritic spine density over 10 $\mu\text{m}$  (n=5) of hippocampal CA1 pyramidal neurons. **(H)** Representative image of spines of hippocampal CA1 pyramidal neurons from n-3 bal, n-3 def and n-3 rev male and female mice. Datas are represented by violin plot. One way ANOVA followed by Bonferroni test \* p<0.05, \*\* p<0.01, \*\*\* p<0.001.



## SUPPLEMENTARY DATA

**Table 3.** Fatty acid composition of the diets used for the experiments (in % weight of total fatty acids). FA : fatty acids; LA : linoleic acid; AA : arachidonic acid; ALA : alpha-linolenic acid; DHA : docosahexaenoic acid; EPA : eicosapentaenoic acid; DPA : docosapentaenoic acid; ND : not detected.

	<b>n-3 PUFA balanced diet</b>	<b>n-3 PUFA deficient diet</b>
16:0	22.6	6.2
18:0	3.3	4.4
Others saturated FA	1.8	1.6
Total saturated FA	27.7	12.2
16:1 n-7	0.2	0.1
18:1 n-9	57.9	26.0
18:1 n-7	1.5	0.9
Other monosaturated FA	0.4	0.2
Total monosaturated FA	60.0	27.2
18:2 n-6 (LA)	10.6	60.5
20:4 n-6 (AA)	ND	ND
Total n-6 PUFA	10.7	60.5
18:3 n-3 (ALA)	1.6	0.1
18:4 n-3	ND	ND
20:5 n-3	ND	ND
22:5 n-3	ND	ND
22:6 n-3 (DHA)	ND	ND
Total n-3 PUFA	1.6	0.1
Total PUFA	12.3	60.6
Ratio n-6 / n-3	6.7	>500

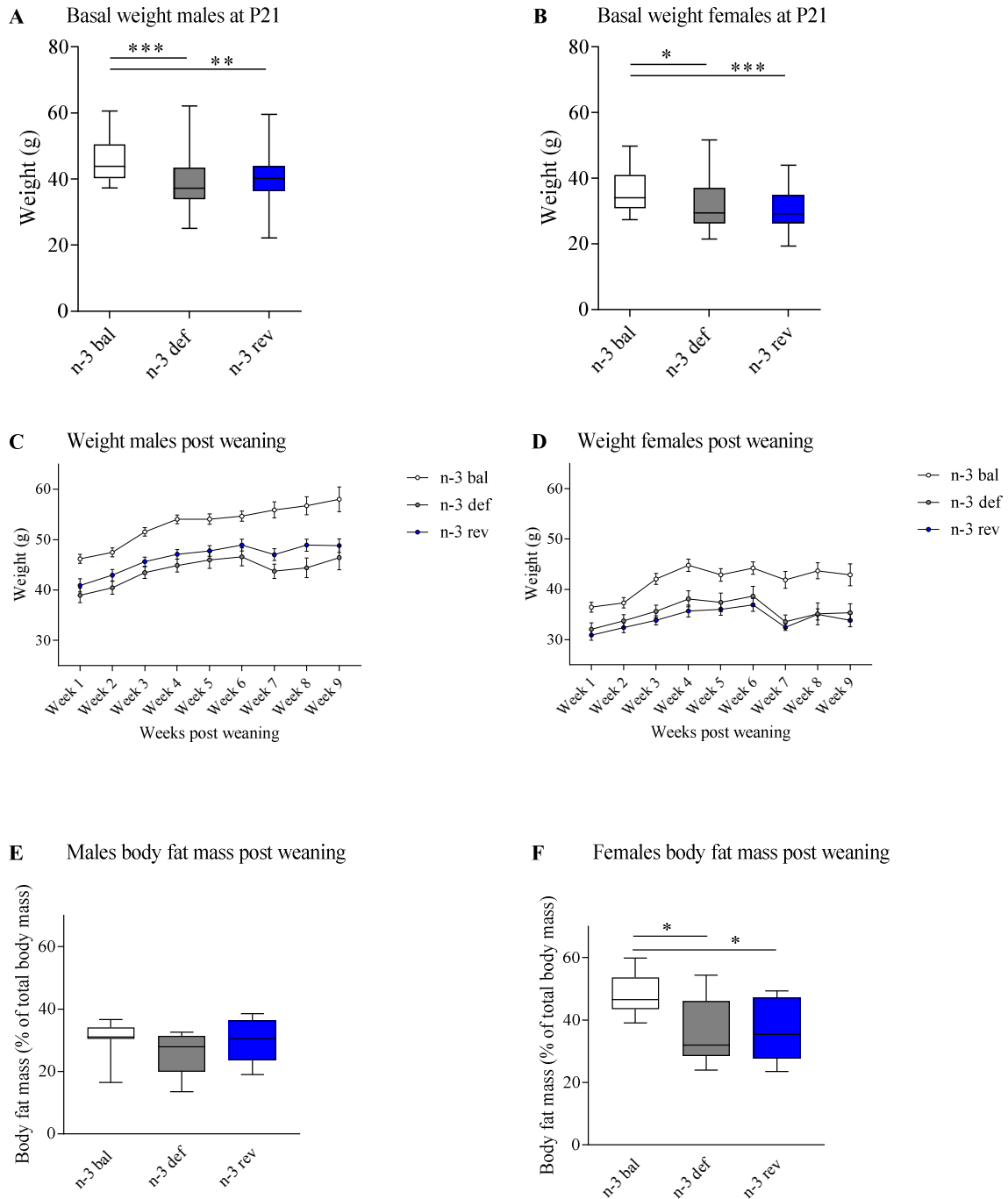


**Figure 7** Weight of n-3 bal, n-3 def and n-3 rev male and female mice. **(A-B)** Mice weight of n-3 bal and n-3 def male and female mice at weaning (expressed in g). Box and Whiskers (5-95 percentile). One way ANOVA males  $F(2,158) = 10.24$ ;  $p < 0.001$  and females  $F(2,153) = 7.793$  followed by Bonferroni multiple comparison test \*  $p < 0.05$ , \*\*  $p < 0.01$ , \*\*\*  $p < 0.001$ . **(C-D)** Weight of male and female mice during the 8 weeks exposure of diets after weaning (expressed in g). Two-Way ANOVA male Diet effect  $F(2, 915) = 92.08$   $p < 0.001$ , Time effect  $F(8,915) = 19.15$   $p < 0.001$  and female Diet effect  $F(2,876) = 59.86$   $p < 0.001$ , Time effect  $F(8,876) = 10.80$   $p < 0.001$ . **(E-F)** Body fat mass proportion (in % of total body mass) in male and female. One way ANOVA male  $F(2,29) = 2.345$   $p = 0.12$  and female  $F(2,22) = 6.061$   $p < 0.01$  followed by Tukey's multiple comparison test \*  $p < 0.05$ .

**Table 4.** Hippocampal fatty acid composition of n-3 bal, n-3 def and n-3 rev male mice (expressed as % of total fatty acids, except n-6/n-3 ratio). Values are expressed as means  $\pm$  SEM. AA : arachidonic acids; DHA : docosahexaenoic acid; DPA : docosapentaenoic acid; DMA : dimethylacetal; LA : linoleic acid; MUFA : monosaturated fatty acids; PUFA : polyunsaturated fatty acids; SFA : saturated fatty acids.

Fatty acids (% of total fatty acids)	Males			Statistical effects (One Way ANOVA)	
	n-3 Bal (a)	n-3 Def (b)	n-3 Rev (c)	ANOVA	Bonferroni Multiple comparison
14:0	0.13 $\pm$ 0.02	0.11 $\pm$ 0.01	0.11 $\pm$ 0.01	ns	ns
15:0	0.08 $\pm$ 0.03	0.07 $\pm$ 0.01	0.07 $\pm$ 0.03	ns	ns
16:0	24.98 $\pm$ 0.79	24.92 $\pm$ 0.95	23.11 $\pm$ 0.64	p<0.01	a-c p<0.01 / b-c p<0.05
17:0	0.16 $\pm$ 0.01	0.17 $\pm$ 0.01	0.14 $\pm$ 0.01	p<0.01	a-c p<0.05 / b-c p<0.01
18:0	22.53 $\pm$ 0.34	22.21 $\pm$ 0.24	21.95 $\pm$ 0.34	p<0.05	a-c p<0.05
20:0	0.20 $\pm$ 0.02	0.27 $\pm$ 0.03	0.31 $\pm$ 0.03	ns	ns
22:0	0.39 $\pm$ 0.04	0.27 $\pm$ 0.04	0.42 $\pm$ 0.09	p<0.01	a-b p<0.05 / b-c p<0.01
24:0	0.53 $\pm$ 0.07	0.29 $\pm$ 0.06	0.52 $\pm$ 0.0-	p<0.001	a-b p / b-c p<0.001
<b>Total SFA</b>	<b>49.09 <math>\pm</math> 1.12</b>	<b>48.30 <math>\pm</math> 1.05</b>	<b>46.65 <math>\pm</math> 0.85</b>	<b>p&lt;0.01</b>	<b>a-c p&lt;0.01</b>
16:1n-9	0.27 $\pm$ 0.05	0.21 $\pm$ 0.03	0.25 $\pm$ 0.03	p<0.05	a-b p<0.05
16:1n-7	0.57 $\pm$ 0.09	0.49 $\pm$ 0.04	0.50 $\pm$ 0.06	ns	ns
18:1n-9	16.72 $\pm$ 0.49	14.98 $\pm$ 0.60	15.55 $\pm$ 0.29	p<0.001	a-b p<0.001 / a-c p<0.01
18:1n-7	3.72 $\pm$ 0.10	3.90 $\pm$ 0.18	3.43 $\pm$ 0.08	p<0.001	a-c p<0.01 / b-c p<0.001
20:1n-9	1.25 $\pm$ 0.06	1.13 $\pm$ 0.12	1.17 $\pm$ 0.13	ns	ns
20:1n-7	0.27 $\pm$ 0.02	0.28 $\pm$ 0.03	0.26 $\pm$ 0.04	ns	ns
22:1n-9	0.21 $\pm$ 0.03	0.19 $\pm$ 0.03	0.23 $\pm$ 0.02	p<0.05	b-c p<0.05
24:1n-9	0.53 $\pm$ 0.10	0.41 $\pm$ 0.08	0.48 $\pm$ 0.09	ns	ns
<b>Total MUFA</b>	<b>23.93 <math>\pm</math> 0.80</b>	<b>21.80 <math>\pm</math> 0.94</b>	<b>22.20 <math>\pm</math> 0.49</b>	<b>p&lt;0.01</b>	<b>a-b p&lt;0.01 / a-c p&lt;0.05</b>
18:2n-6 (LA)	0.25 $\pm$ 0.04	0.45 $\pm$ 0.05	0.27 $\pm$ 0.05	p<0.001	a-b / b-c p<0.001
20:3n-6	0.43 $\pm$ 0.05	0.24 $\pm$ 0.03	0.33 $\pm$ 0.03	p<0.001	a-b p<0.001 / b-c / a-c p<0.01
20:4n-6 (AA)	7.35 $\pm$ 0.47	8.80 $\pm$ 0.45	8.67 $\pm$ 0.34	p<0.001	a-b / a-c p<0.001
22:4n-6	1.81 $\pm$ 0.14	2.96 $\pm$ 0.12	2.24 $\pm$ 0.11	p<0.001	a-b / b-c / a-c p<0.001
22:5n-6 (n-3 DPA)	0.48 $\pm$ 0.07	6.95 $\pm$ 0.87	0.85 $\pm$ 0.16	p<0.001	a-b / b-c p<0.001
<b>Total n-6</b>	<b>10.32 <math>\pm</math> 0.60</b>	<b>19.41 <math>\pm</math> 1.23</b>	<b>12.35 <math>\pm</math> 0.52</b>	<b>p&lt;0.001</b>	<b>a-b / a-c p&lt;0.001 / b-c p&lt;0.01</b>
20:5n-3 (EPA)	0.17 $\pm$ 0.01	0.08 $\pm$ 0.00	0.17 $\pm$ 0.02	p<0.001	a-b / b-c p<0.001
22:5n-3 (n-3 DPA)	0.07 $\pm$ 0.00	0.04 $\pm$ 0.01	0.08 $\pm$ 0.01	p<0.001	a-b / b-c p<0.001
22:6n-3 (DHA)	7.32 $\pm$ 0.85	2.32 $\pm$ 0.26	9.05 $\pm$ 0.74	p<0.001	a-b / b-c p<0.001 / a-c p<0.01
<b>Total n-3</b>	<b>7.56 <math>\pm</math> 0.86</b>	<b>2.43 <math>\pm</math> 0.26</b>	<b>9.30 <math>\pm</math> 0.74</b>	<b>p&lt;0.001</b>	<b>a-b / b-c p&lt;0.001 / a-c p&lt;0.01</b>
20:3n-9	0.21 $\pm$ 0.01	0.07 $\pm$ 0.01	0.21 $\pm$ 0.03	p<0.001	a-b / b-c p<0.001
<b>Total PUFA</b>	<b>18.09 <math>\pm</math> 1.44</b>	<b>21.91 <math>\pm</math> 1.43</b>	<b>21.87 <math>\pm</math> 1.15</b>	<b>ns</b>	<b>ns</b>
DMA 16:0	2.03 $\pm$ 0.05	1.99 $\pm$ 0.02	2.12 $\pm$ 0.08	p<0.01	a-c p<0.05 / b-c p<0.01
DMA 18:0	3.91 $\pm$ 0.20	3.49 $\pm$ 0.09	4.12 $\pm$ 0.14	p<0.001	a-b p<0.05 / b-c p<0.001
DMA 18:1n-9	1.33 $\pm$ 0.03	1.08 $\pm$ 0.05	1.39 $\pm$ 0.10	p<0.001	a-b / b-c p<0.001
DMA 18:1n-7	1.62 $\pm$ 0.07	1.43 $\pm$ 0.12	1.65 $\pm$ 0.07	p<0.01	a-b p<0.05 / b-c p<0.01
<b>Total DMA</b>	<b>8.89 <math>\pm</math> 0.22</b>	<b>7.99 <math>\pm</math> 0.25</b>	<b>9.28 <math>\pm</math> 0.27</b>	<b>p&lt;0.001</b>	<b>a-b / b-c p&lt;0.001</b>
n-6/n-3 ratio	1.37 $\pm$ 0.09	8.01 $\pm$ 0.60	1.33 $\pm$ 0.09	p<0.001	a-b / b-c p<0.001

**Table 5.** Hippocampal fatty acid composition of n-3 bal, n-3 def and n-3 rev female mice (expressed as % of total fatty acids, except n-6/n-3 ratio). Values are expressed as means  $\pm$  SEM. AA : arachidonic acids; DHA : docosahexaenoic acid; DPA : docosapentaenoic acid; DMA : dimethylacetal; LA : linoleic acid; MUFA : monosaturated fatty acids; PUFA : polyunsaturated fatty acids; SFA : saturated fatty acids.

Fatty acids (% of total fatty acids)	Females			Statistical effects (One Way ANOVA)	
	n-3 Bal (a)	n-3 Def (b)	n-3 Rev (c)	ANOVA	Bonferroni Multiple comparison
14:0	0.12 $\pm$ 0.01	0.11 $\pm$ 0.01	0.12 $\pm$ 0.01	ns	ns
15:0	0.06 $\pm$ 0.01	0.06 $\pm$ 0.01	0.08 $\pm$ 0.01	ns	ns
16:0	24.64 $\pm$ 0.82	24.21 $\pm$ 0.66	24.92 $\pm$ 0.93	ns	ns
17:0	0.17 $\pm$ 0.01	0.16 $\pm$ 0.01	0.17 $\pm$ 0.02	ns	ns
18:0	22.36 $\pm$ 0.45	22.25 $\pm$ 0.28	22.74 $\pm$ 0.60	ns	ns
20:0	0.27 $\pm$ 0.03	0.26 $\pm$ 0.03	0.30 $\pm$ 0.04	ns	ns
22:0	0.32 $\pm$ 0.07	0.28 $\pm$ 0.02	0.37 $\pm$ 0.08	ns	ns
24:0	0.41 $\pm$ 0.11	0.29 $\pm$ 0.03	0.45 $\pm$ 0.14	ns	ns
<b>Total SFA</b>	<b>48.35 <math>\pm</math> 1.38</b>	<b>47.62 <math>\pm</math> 0.73</b>	<b>49.14 <math>\pm</math> 1.74</b>	<b>ns</b>	<b>ns</b>
16:1n-9	0.23 $\pm$ 0.01	0.18 $\pm$ 0.03	0.23 $\pm$ 0.03	p<0.05	a-b / b-c p<0.05
16:1n-7	0.49 $\pm$ 0.04	0.48 $\pm$ 0.06	0.48 $\pm$ 0.04	ns	ns
18:1n-9	16.67 $\pm$ 0.62	14.93 $\pm$ 0.76	16.42 $\pm$ 0.93	p<0.01	a-b / b-c p<0.05
18:1n-7	3.74 $\pm$ 0.24	3.84 $\pm$ 0.14	3.66 $\pm$ 0.06	ns	ns
20:1n-9	1.36 $\pm$ 0.12	1.17 $\pm$ 0.17	1.28 $\pm$ 0.19	ns	ns
20:1n-7	0.29 $\pm$ 0.04	0.28 $\pm$ 0.05	0.28 $\pm$ 0.02	ns	ns
22:1n-9	0.20 $\pm$ 0.02	0.18 $\pm$ 0.03	0.21 $\pm$ 0.03	ns	ns
24:1n-9	0.50 $\pm$ 0.08	0.44 $\pm$ 0.07	0.47 $\pm$ 0.09	ns	ns
<b>Total MUFA</b>	<b>23.78 <math>\pm</math> 1.01</b>	<b>21.71 <math>\pm</math> 1.08</b>	<b>23.38 <math>\pm</math> 1.25</b>	<b>p&lt;0.05</b>	<b>a-b p&lt;0.05</b>
18:2n-6 (LA)	0.24 $\pm$ 0.02	0.36 $\pm$ 0.03	0.28 $\pm$ 0.03	p<0.001	a-b / b-c p<0.001
20:3n-6	0.39 $\pm$ 0.11	0.21 $\pm$ 0.02	0.30 $\pm$ 0.03	p<0.01	a-b p<0.01
20:4n-6 (AA)	7.65 $\pm$ 0.75	9.01 $\pm$ 0.44	7.65 $\pm$ 0.90	p<0.05	a-b / b-c p<0.05
22:4n-6	1.98 $\pm$ 0.14	2.89 $\pm$ 0.18	2.00 $\pm$ 0.23	p<0.001	a-b / b-c p<0.001
22:5n-6 (n-6 DPA)	0.36 $\pm$ 0.02	5.85 $\pm$ 1.60	0.60 $\pm$ 0.15	p<0.001	a-b / b-c p<0.001
<b>Total n-6</b>	<b>10.62 <math>\pm</math> 0.97</b>	<b>18.32 <math>\pm</math> 2.17</b>	<b>10.83 <math>\pm</math> 1.25</b>	<b>p&lt;0.001</b>	<b>a-b / b-c p&lt;0.001</b>
20:5n-3 (EPA)	0.17 $\pm$ 0.01	0.09 $\pm$ 0.02	0.13 $\pm$ 0.02	p<0.001	a-b p<0.001 / b-c / a-c p<0.01
22:5n-3 (n-3 DPA)	0.09 $\pm$ 0.02	0.03 $\pm$ 0.01	0.08 $\pm$ 0.02	p<0.001	a-b p<0.001 / b-c p<0.01
22:6n-3 (DHA)	8.11 $\pm$ 1.44	4.00 $\pm$ 0.77	7.69 $\pm$ 1.56	p<0.001	a-b / b-c p<0.001 / a-c p<0.05
<b>Total n-3</b>	<b>8.36 <math>\pm</math> 1.45</b>	<b>4.12 <math>\pm</math> 0.77</b>	<b>7.90 <math>\pm</math> 1.57</b>	<b>p&lt;0.001</b>	<b>a-b p&lt;0.001 / b-c p&lt;0.01</b>
20:3n-9	0.22 $\pm$ 0.02	0.08 $\pm$ 0.04	0.18 $\pm$ 0.04	p<0.001	a-b p<0.001 / b-c p<0.01
<b>Total PUFA</b>	<b>19.21 <math>\pm</math> 2.43</b>	<b>22.52 <math>\pm</math> 1.43</b>	<b>18.91 <math>\pm</math> 2.83</b>	<b>p&lt;0.05</b>	<b>b-c p&lt;0.05</b>
DMA 16:0	1.98 $\pm$ 0.15	1.99 $\pm$ 0.09	1.99 $\pm$ 0.13	ns	ns
DMA 18:0	3.84 $\pm$ 0.16	3.58 $\pm$ 0.12	3.81 $\pm$ 0.13	p<0.05	a-b p<0.05
DMA 18:1n-9	1.28 $\pm$ 0.09	1.11 $\pm$ 0.06	1.23 $\pm$ 0.08	p<0.05	a-b p<0.05
DMA 18:1n-7	1.57 $\pm$ 0.09	1.48 $\pm$ 0.11	1.53 $\pm$ 0.07	ns	ns
<b>Total DMA</b>	<b>8.68 <math>\pm</math> 0.45</b>	<b>8.17 <math>\pm</math> 0.21</b>	<b>8.56 <math>\pm</math> 0.28</b>	<b>ns</b>	<b>ns</b>
<b>n-6/n-3 ratio</b>	<b>1.29 <math>\pm</math> 0.11</b>	<b>4.61 <math>\pm</math> 1.10</b>	<b>1.39 <math>\pm</math> 0.14</b>	<b>p&lt;0.001</b>	<b>a-b / b-c p&lt;0.001</b>

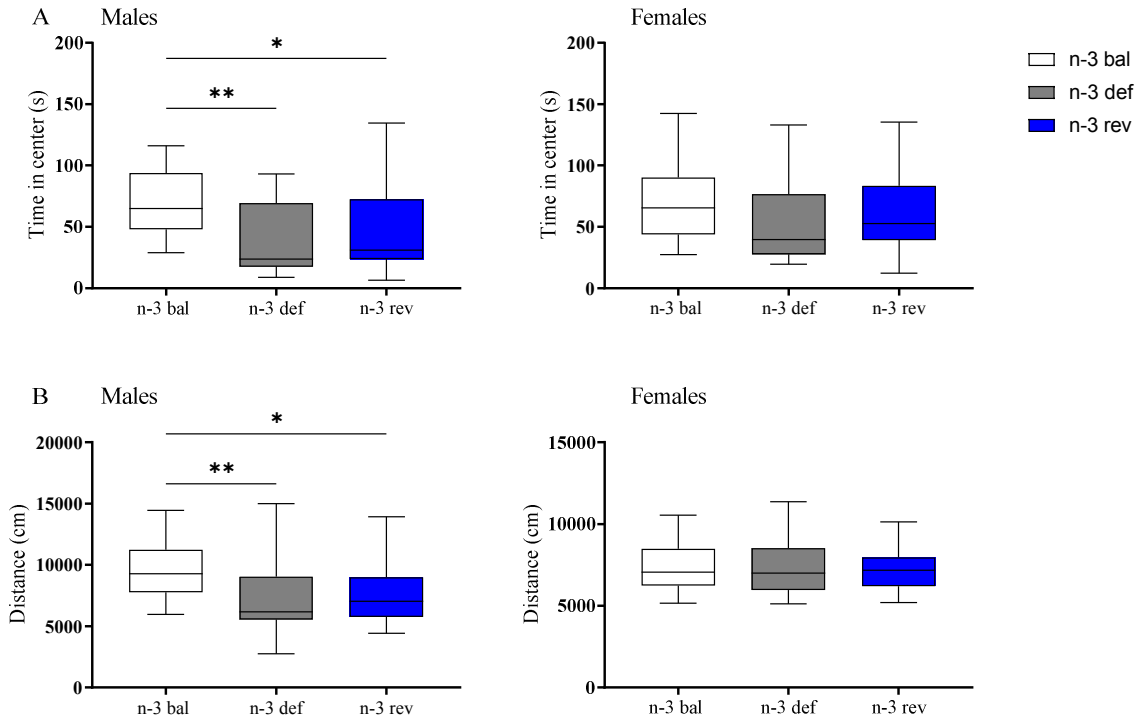


**Figure 8** Emotional behavior of n-3bal, n-3 def and n-3 rev male and female mice. **(A)** Time spent in the center area (in sec) of the open-field by n-3 bal, n-3 def and n-3 rev male and female mice (n=[23-38]). Box and whiskers. One-way ANOVA males  $F(2,87) = 6.219$   $p < 0.01$  followed by Bonferroni multiple comparison \*  $p < 0.05$ , \*\*  $p < 0.01$  and females  $F(2,87) = 1.507$   $p = 0.23$ . **(B)** Distance travelled (in cm) in the open field by n-3 bal, n-3 def and n-3 rev male and female mice (n=[23-38]). One way ANOVA males  $F(2,87) = 6.5$   $p < 0.01$  followed by a Bonferroni multiple comparison test \*  $p < 0.05$ , \*\*  $p < 0.01$  and females  $F(2,87) = 0.15$   $p = 0.9$ .

## REFERENCES

- Basak, S., Mallick, R., Duttaroy, A.K., 2020. Maternal Docosahexaenoic Acid Status during Pregnancy and Its Impact on Infant Neurodevelopment. *Nutrients* 12, 3615. <https://doi.org/10.3390/nu12123615>
- Bazinet, R.P., Layé, S., 2014. Polyunsaturated fatty acids and their metabolites in brain function and disease. *Nature Reviews Neuroscience* 15, 771–785. <https://doi.org/10.1038/nrn3820>
- Borsini, A., Nicolaou, A., Camacho-Muñoz, D., Kendall, A.C., Di Benedetto, M.G., Giacobbe, J., Su, K.-P., Pariante, C.M., 2021. Omega-3 polyunsaturated fatty acids protect against inflammation through production of LOX and CYP450 lipid mediators: relevance for major depression and for human hippocampal neurogenesis. *Mol Psychiatry* 26, 6773–6788. <https://doi.org/10.1038/s41380-021-01160-8>
- Calder, P.C., 2001. Polyunsaturated fatty acids, inflammation, and immunity. *FATTY ACIDS* 36, 18.
- Cao, D., Kevala, K., Kim, J., Moon, H.-S., Jun, S.B., Lovinger, D., Kim, H.-Y., 2009. Docosahexaenoic acid promotes hippocampal neuronal development and synaptic function. *Journal of Neurochemistry* 111, 510–521. <https://doi.org/10.1111/j.1471-4159.2009.06335.x>
- Childs, S., Lynch, C.O., Hennessy, A.A., Stanton, C., Wathes, D.C., Sreenan, J.M., Diskin, M.G., Kenny, D.A., 2008. Effect of dietary enrichment with either n-3 or n-6 fatty acids on systemic metabolite and hormone concentration and ovarian function in heifers. *Animal* 2, 883–893. <https://doi.org/10.1017/S1751731108002115>
- Cisbani, G., Metherel, A.H., Smith, M.E., Bazinet, R.P., 2021. Murine and human microglial cells are relatively enriched with eicosapentaenoic acid compared to the whole brain. *Neurochemistry International* 150, 105154. <https://doi.org/10.1016/j.neuint.2021.105154>
- Delpech, J.-C., Thomazeau, A., Madore, C., Bosch-Bouju, C., Larrieu, T., Lacabanne, C., Remus-Borel, J., Aubert, A., Joffre, C., Nadjar, A., Layé, S., 2015. Dietary n-3 PUFAs Deficiency Increases Vulnerability to Inflammation-Induced Spatial Memory Impairment. *Neuropsychopharmacol* 40, 2774–2787. <https://doi.org/10.1038/npp.2015.127>
- Di Miceli, M., Martinat, M., Bosch-Bouju, C., Layé, S., 2020. Régulation de l'excitabilité neuronale et de la plasticité synaptique dans le striatum ventral par le contenu alimentaire en omega-3. *Nutrition Clinique et Métabolisme* 34, 36. <https://doi.org/10.1016/j.nupar.2020.02.236>
- Gao, H., Yan, P., Zhang, S., Huang, H., Huang, F., Sun, T., Deng, Q., Huang, Q., Chen, S., Ye, K., Xu, J., Liu, L., 2016. Long-Term Dietary Alpha-Linolenic Acid Supplement Alleviates Cognitive Impairment Correlate with Activating Hippocampal CREB Signaling in Natural Aging Rats. *Mol Neurobiol* 53, 4772–4786. <https://doi.org/10.1007/s12035-015-9393-x>
- Herrera, J.L., Ordoñez-Gutierrez, L., Fabrias, G., Casas, J., Morales, A., Hernandez, G., Acosta, N.G., Rodriguez, C., Prieto-Valiente, L., Garcia-Segura, L.M., Alonso, R., Wandosell, F.G., 2018. Ovarian Function Modulates the Effects of Long-Chain Polyunsaturated Fatty Acids on the Mouse Cerebral Cortex. *Front. Cell. Neurosci.* 12, 103. <https://doi.org/10.3389/fncel.2018.00103>
- Joffre, C., Grégoire, S., De Smedt, V., Acar, N., Bretillon, L., Nadjar, A., Layé, S., 2016. Modulation of brain PUFA content in different experimental models of mice. *Prostaglandins, Leukotrienes and Essential Fatty Acids (PLEFA)* 114, 1–10. <https://doi.org/10.1016/j.plefa.2016.09.003>

- Labrousse, V.F., Leyrolle, Q., Amadiou, C., Aubert, A., Sere, A., Coutureau, E., Grégoire, S., Bretillon, L., Pallet, V., Gressens, P., Joffre, C., Nadjar, A., Layé, S., 2018. Dietary omega-3 deficiency exacerbates inflammation and reveals spatial memory deficits in mice exposed to lipopolysaccharide during gestation. *Brain, Behavior, and Immunity* 73, 427–440. <https://doi.org/10.1016/j.bbi.2018.06.004>
- Labrousse, V.F., Nadjar, A., Joffre, C., Costes, L., Aubert, A., Grégoire, S., Bretillon, L., Layé, S., 2012. Short-Term Long Chain Omega3 Diet Protects from Neuroinflammatory Processes and Memory Impairment in Aged Mice. *PLoS ONE* 7, e36861. <https://doi.org/10.1371/journal.pone.0036861>
- Lafourcade, M., Larrieu, T., Mato, S., Duffaud, A., Sepers, M., Matias, I., De Smedt-Peyrusse, V., Labrousse, V.F., Bretillon, L., Matute, C., Rodríguez-Puertas, R., Layé, S., Manzoni, O.J., 2011. Nutritional omega-3 deficiency abolishes endocannabinoid-mediated neuronal functions. *Nature Neuroscience* 14, 345–350. <https://doi.org/10.1038/nn.2736>
- Larrieu, T., Hilal, L.M., Fourrier, C., De Smedt-Peyrusse, V., Sans N, Capuron, L., Layé, S., 2014. Nutritional omega-3 modulates neuronal morphology in the prefrontal cortex along with depression-related behaviour through corticosterone secretion. *Translational Psychiatry* 4, e437–e437. <https://doi.org/10.1038/tp.2014.77>
- Larrieu, T., Madore, C., Joffre, C., Layé, S., 2012. Nutritional n-3 polyunsaturated fatty acids deficiency alters cannabinoid receptor signaling pathway in the brain and associated anxiety-like behavior in mice. *Journal of Physiology and Biochemistry* 68, 671–681. <https://doi.org/10.1007/s13105-012-0179-6>
- Lauritzen, L., 2001. The essentiality of long chain n-3 fatty acids in relation to development and function of the brain and retina. *Progress in Lipid Research* 40, 1–94. [https://doi.org/10.1016/S0163-7827\(00\)00017-5](https://doi.org/10.1016/S0163-7827(00)00017-5)
- Layé, S., Nadjar, A., Joffre, C., Bazinet, R.P., 2018. Anti-Inflammatory Effects of Omega-3 Fatty Acids in the Brain: Physiological Mechanisms and Relevance to Pharmacology. *Pharmacol Rev* 70, 12–38. <https://doi.org/10.1124/pr.117.014092>
- Leyrolle, Q., Decoeur, F., Briere, G., Amadiou, C., Quadros, A.R.A.A., Voytyuk, I., Lacabanne, C., Benmamar-Badel, A., Bourel, J., Aubert, A., Sere, A., Chain, F., Schwendimann, L., Matrot, B., Bourgeois, T., Grégoire, S., Leblanc, J.G., De Moreno De Leblanc, A., Langella, P., Fernandes, G.R., Bretillon, L., Joffre, C., Uricaru, R., Thebault, P., Gressens, P., Chatel, J.M., Layé, S., Nadjar, A., 2021. Maternal dietary omega-3 deficiency worsens the deleterious effects of prenatal inflammation on the gut-brain axis in the offspring across lifetime. *Neuropsychopharmacol.* 46, 579–602. <https://doi.org/10.1038/s41386-020-00793-7>
- Leyrolle, Q., Decoeur, F., Dejean, C., Brière, G., Leon, S., Bakoyiannis, I., Baroux, E., Sterley, T.-L., Bosch-Bouju, C., Morel, L., Amadiou, C., Lecours, C., St-Pierre, M.-K., Bordeleau, M., De Smedt-Peyrusse, V., Séré, A., Schwendimann, L., Grégoire, S., Bretillon, L., Acar, N., Joffre, C., Ferreira, G., Uricaru, R., Thebault, P., Gressens, P., Tremblay, M.-E., Layé, S., Nadjar, A., 2022. N-3 PUFA deficiency disrupts oligodendrocyte maturation and myelin integrity during brain development. *Glia* 70, 50–70. <https://doi.org/10.1002/glia.24088>
- López, D.E., Ballaz, S.J., 2020. The Role of Brain Cyclooxygenase-2 (Cox-2) Beyond Neuroinflammation: Neuronal Homeostasis in Memory and Anxiety. *Mol Neurobiol* 57, 5167–5176. <https://doi.org/10.1007/s12035-020-02087-x>
- Lozada, L.E., Desai, A., Kevala, K., Lee, J.-W., Kim, H.-Y., 2017. Perinatal Brain Docosahexaenoic Acid Concentration Has a Lasting Impact on Cognition in Mice. *J Nutr* 147, 1624–1630. <https://doi.org/10.3945/jn.117.254607>

- Madore, C., Leyrolle, Q., Morel, L., Rossitto, M., Greenhalgh, A.D., Delpech, J.C., Martinat, M., Bosch-Bouju, C., Bourel, J., Rani, B., Lacabanne, C., Thomazeau, A., Hopperton, K.E., Beccari, S., Sere, A., Aubert, A., De Smedt-Peyrusse, V., Lecours, C., Bisht, K., Fourgeaud, L., Gregoire, S., Bretillon, L., Acar, N., Grant, N.J., Badaut, J., Gressens, P., Sierra, A., Butovsky, O., Tremblay, M.E., Bazinet, R.P., Joffre, C., Nadjar, A., Layé, S., 2020. Essential omega-3 fatty acids tune microglial phagocytosis of synaptic elements in the mouse developing brain. *Nature Communications* 11, 6133. <https://doi.org/10.1038/s41467-020-19861-z>
- Madore, C., Nadjar, A., Delpech, J.-C., Sere, A., Aubert, A., Portal, C., Joffre, C., Layé, S., 2014. Nutritional n-3 PUFAs deficiency during perinatal periods alters brain innate immune system and neuronal plasticity-associated genes. *Brain, Behavior, and Immunity* 41, 22–31. <https://doi.org/10.1016/j.bbi.2014.03.021>
- Makrides, M., Best, K., Yelland, L., McPhee, A., Zhou, S., Quinlivan, J., Dodd, J., Atkinson, E., Safa, H., van Dam, J., Khot, N., Dekker, G., Skubisz, M., Anderson, A., Kean, B., Bowman, A., McCallum, C., Cashman, K., Gibson, R., 2019. A Randomized Trial of Prenatal n–3 Fatty Acid Supplementation and Preterm Delivery. *N Engl J Med* 381, 1035–1045. <https://doi.org/10.1056/NEJMoa1816832>
- Manduca, A., Morena, M., Campolongo, P., Servadio, M., Palmery, M., Trabace, L., Hill, M.N., Vanderschuren, L.J.M.J., Cuomo, V., Trezza, V., 2015. Distinct roles of the endocannabinoids anandamide and 2-arachidonoylglycerol in social behavior and emotionality at different developmental ages in rats. *European Neuropsychopharmacology* 25, 1362–1374. <https://doi.org/10.1016/j.euroneuro.2015.04.005>
- Martinat, M., Rossitto, M., Di Miceli, M., Layé, S., 2021a. Perinatal Dietary Polyunsaturated Fatty Acids in Brain Development, Role in Neurodevelopmental Disorders. *Nutrients* 13, 1185. <https://doi.org/10.3390/nu13041185>
- Martinat, M., Rossitto, M., Di Miceli, M., Layé, S., 2021b. Perinatal Dietary Polyunsaturated Fatty Acids in Brain Development, Role in Neurodevelopmental Disorders. *Nutrients* 13, 1185. <https://doi.org/10.3390/nu13041185>
- Materazzi, S., Nassini, R., Andrè, E., Campi, B., Amadesi, S., Trevisani, M., Bunnett, N.W., Patacchini, R., Geppetti, P., 2008. Cox-dependent fatty acid metabolites cause pain through activation of the irritant receptor TRPA1. *Proceedings of the National Academy of Sciences* 105, 12045–12050. <https://doi.org/10.1073/pnas.0802354105>
- McNamara, R.K., Able, J., Jandacek, R., Rider, T., Tso, P., 2009. Gender differences in rat erythrocyte and brain docosahexaenoic acid composition: Role of ovarian hormones and dietary omega-3 fatty acid composition. *Psychoneuroendocrinology* 34, 532–539. <https://doi.org/10.1016/j.psyneuen.2008.10.013>
- McNamara, R.K., Hahn, C.-G., Jandacek, R., Rider, T., Tso, P., Stanford, K.E., Richtand, N.M., 2007. Selective deficits in the omega-3 fatty acid docosahexaenoic acid in the postmortem orbitofrontal cortex of patients with major depressive disorder. *Biol Psychiatry* 62, 17–24. <https://doi.org/10.1016/j.biopsych.2006.08.026>
- Moranis, A., Delpech, J.-C., De Smedt-Peyrusse, V., Aubert, A., Guesnet, P., Laviolle, M., Joffre, C., Layé, S., 2012. Long term adequate n-3 polyunsaturated fatty acid diet protects from depressive-like behavior but not from working memory disruption and brain cytokine expression in aged mice. *Brain, Behavior, and Immunity* 26, 721–731. <https://doi.org/10.1016/j.bbi.2011.11.001>
- Morgese, M.G., Schiavone, S., Maffione, A.B., Tucci, P., Trabace, L., 2020. Depressive-like phenotype evoked by lifelong nutritional omega-3 deficiency in female rats: Crosstalk among kynurenine, Toll-like receptors and amyloid beta oligomers. *Brain Behav Immun* 87, 444–454. <https://doi.org/10.1016/j.bbi.2020.01.015>



- Moriguchi, T., Salem Jr, N., 2003. Recovery of brain docosahexaenoate leads to recovery of spatial task performance. *Journal of Neurochemistry* 87, 297–309. <https://doi.org/10.1046/j.1471-4159.2003.01966.x>
- Reemst, K., Broos, J.Y., Abbink, M.R., Cimetti, C., Giera, M., Kooij, G., Korosi, A., 2022. Early-life stress and dietary fatty acids impact the brain lipid/oxylin profile into adulthood, basally and in response to LPS (preprint). In Review. <https://doi.org/10.21203/rs.3.rs-1663016/v1>
- Rey, C., Delpech, J.C., Madore, C., Nadjar, A., Greenhalgh, A.D., Amadiou, C., Aubert, A., Pallet, V., Vaysse, C., Layé, S., Joffre, C., 2019. Dietary n-3 long chain PUFA supplementation promotes a pro-resolving oxylin profile in the brain. *Brain, Behavior, and Immunity* 76, 17–27. <https://doi.org/10.1016/j.bbi.2018.07.025>
- Rey, C., Nadjar, A., Joffre, F., Amadiou, C., Aubert, A., Vaysse, C., Pallet, V., Layé, S., Joffre, C., 2018. Maternal n-3 polyunsaturated fatty acid dietary supply modulates microglia lipid content in the offspring. *Prostaglandins, Leukotrienes and Essential Fatty Acids* 133, 1–7. <https://doi.org/10.1016/j.plefa.2018.04.003>
- Schindelin, J., Arganda-Carreras, I., Frise, E., Kaynig, V., Longair, M., Pietzsch, T., Preibisch, S., Rueden, C., Saalfeld, S., Schmid, B., Tinevez, J.-Y., White, D.J., Hartenstein, V., Eliceiri, K., Tomancak, P., Cardona, A., 2012. Fiji: an open-source platform for biological-image analysis. *Nat Methods* 9, 676–682. <https://doi.org/10.1038/nmeth.2019>
- Serhan, C.N., Dalli, J., Colas, R.A., Winkler, J.W., Chiang, N., 2015. Protectins and maresins: New pro-resolving families of mediators in acute inflammation and resolution bioactive metabolome. *Biochimica et Biophysica Acta (BBA) - Molecular and Cell Biology of Lipids, Oxygenated metabolism of PUFA: analysis and biological relevance* 1851, 397–413. <https://doi.org/10.1016/j.bbalip.2014.08.006>
- Serhan, C.N., Hong, S., Gronert, K., Colgan, S.P., Devchand, P.R., Mirick, G., Moussignac, R.-L., 2002. Resolvins : A Family of Bioactive Products of Omega-3 Fatty Acid Transformation Circuits Initiated by Aspirin Treatment that Counter Proinflammation Signals. *Journal of Experimental Medicine* 196, 1025–1037. <https://doi.org/10.1084/jem.20020760>
- Siebert, E., Paul, F., Rothe, M., Weylandt, K.H., 2017. The effect of omega-3 fatty acids on central nervous system remyelination in fat-1 mice. *BMC Neurosci* 18, 19. <https://doi.org/10.1186/s12868-016-0312-5>
- Straus, D.S., Glass, C.K., 2001. Cyclopentenone prostaglandins: New insights on biological activities and cellular targets. *Medicinal Research Reviews* 21, 185–210. <https://doi.org/10.1002/med.1006>
- Sun, B., Bang, S.-I., Jin, Y.-H., 2009. Transient receptor potential A1 increase glutamate release on brain stem neurons. *NeuroReport* 20, 1002–1006. <https://doi.org/10.1097/WNR.0b013e32832d2219>
- Suzumura, A., Kaneko, H., Funahashi, Y., Takayama, K., Nagaya, M., Ito, S., Okuno, T., Hirakata, T., Nonobe, N., Kataoka, K., Shimizu, H., Namba, R., Yamada, K., Ye, F., Ozawa, Y., Yokomizo, T., Terasaki, H., 2020. n-3 Fatty Acid and Its Metabolite 18-HEPE Ameliorate Retinal Neuronal Cell Dysfunction by Enhancing Müller BDNF in Diabetic Retinopathy. *Diabetes* 69, 724–735. <https://doi.org/10.2337/db19-0550>
- Tang, M., Zhang, M., Wang, L., Li, H., Cai, H., Dang, R., Jiang, P., Liu, Y., Xue, Y., Wu, Y., 2018. Maternal dietary of n-3 polyunsaturated fatty acids affects the neurogenesis and neurochemical in female rat at weaning. *Prostaglandins, Leukotrienes and Essential Fatty Acids* 128, 11–20. <https://doi.org/10.1016/j.plefa.2017.11.001>
- Terrando, N., Park, J.J., Devinney, M., Chan, C., Cooter, M., Avasarala, P., Mathew, J.P., Quinones, Q.J., Maddipati, K.R., Berger, M., 2021. Immunomodulatory lipid mediator

- profiling of cerebrospinal fluid following surgery in older adults. *Sci Rep* 11, 3047. <https://doi.org/10.1038/s41598-021-82606-5>
- Thomazeau, A., Bosch-Bouju, C., Manzoni, O., Layé, S., 2016. Nutritional n-3 PUFA Deficiency Abolishes Endocannabinoid Gating of Hippocampal Long-Term Potentiation. *Cerebral Cortex* bhw052. <https://doi.org/10.1093/cercor/bhw052>
- Wallis, T.P., Venkatesh, B.G., Narayana, V.K., Kvaskoff, D., Ho, A., Sullivan, R.K., Windels, F., Sah, P., Meunier, F.A., 2021. Saturated free fatty acids and association with memory formation. *Nat Commun* 12, 3443. <https://doi.org/10.1038/s41467-021-23840-3>
- Wang, J., Ossemond, J., Le Gouar, Y., Boissel, F., Dupont, D., Pédrone, F., 2022. Encapsulation of Docosahexaenoic Acid Oil Substantially Improves the Oxylipin Profile of Rat Tissues. *Frontiers in Nutrition* 8.



***CHAPITRE 02 : Etat des connaissances des effets des AGPI nutritionnels sur le développement cérébral***

---

Review

# Perinatal Dietary Polyunsaturated Fatty Acids in Brain Development, Role in Neurodevelopmental Disorders

Maud Martinat <sup>†,‡</sup>, Moira Rossitto <sup>†,‡</sup>, Mathieu Di Miceli <sup>†,‡</sup> and Sophie Layé <sup>\*,†</sup>

Laboratoire NutriNeuro, UMR INRAE 1286, Bordeaux INP, Université de Bordeaux, 146 Rue Léo Saigat, CEDEX, 33076 Bordeaux, France; maud.martinat@inrae.fr (M.M.); moira.rossitto@inrae.fr (M.R.); mathieu.di-miceli@inrae.fr (M.D.M.)

\* Correspondence: sophie.laye@inrae.fr

† International Research Network Food4BrainHealth.

‡ These authors contributed equally to this work.

**Abstract:** n-3 and n-6 polyunsaturated fatty acids (PUFAs) are essential fatty acids that are provided by dietary intake. Growing evidence suggests that n-3 and n-6 PUFAs are paramount for brain functions. They constitute crucial elements of cellular membranes, especially in the brain. They are the precursors of several metabolites with different effects on inflammation and neuron outgrowth. Overall, long-chain PUFAs accumulate in the offspring brain during the embryonic and post-natal periods. In this review, we discuss how they accumulate in the developing brain, considering the maternal dietary supply, the polymorphisms of genes involved in their metabolism, and the differences linked to gender. We also report the mechanisms linking their bioavailability in the developing brain, their transfer from the mother to the embryo through the placenta, and their role in brain development. In addition, data on the potential role of altered bioavailability of long-chain n-3 PUFAs in the etiologies of neurodevelopmental diseases, such as autism, attention deficit and hyperactivity disorder, and schizophrenia, are reviewed.

**Keywords:** n-3 PUFAs; n-6 PUFAs; neurodevelopment; neuroinflammation; ASD; ADHD; schizophrenia; DHA; EPA; FADS; ELOVL; polymorphism; microglia; sex differences; placenta



**Citation:** Martinat, M.; Rossitto, M.; Di Miceli, M.; Layé, S. Perinatal Dietary Polyunsaturated Fatty Acids in Brain Development, Role in Neurodevelopmental Disorders. *Nutrients* **2021**, *13*, 1185. <https://doi.org/10.3390/nu13041185>

Academic Editor: Paolo Brambilla

Received: 7 February 2021

Accepted: 30 March 2021

Published: 2 April 2021

**Publisher's Note:** MDPI stays neutral with regard to jurisdictional claims in published maps and institutional affiliations.



**Copyright:** © 2021 by the authors. Licensee MDPI, Basel, Switzerland. This article is an open access article distributed under the terms and conditions of the Creative Commons Attribution (CC BY) license (<https://creativecommons.org/licenses/by/4.0/>).

## 1. Introduction

Lipids are critical biochemical components of the brain and are essential for proper brain functions. The lipid composition of the brain is unique and exceedingly diverse. Aberrant brain lipid composition, metabolism, and signaling are associated with neurodevelopmental, neuropsychiatric, and neurodegenerative diseases [1]. Polyunsaturated fatty acids (PUFAs) from the n-6 and n-3 families are lipids that rely on dietary supply and are considered crucial for brain development [1–3]. The PUFAs found in nuts, seeds, and certain vegetables, such as alpha-linolenic acid (ALA, n-3) and linoleic acid (LA, n-6), are essential to humans, and mammals in general, because they cannot synthesize them [4,5]. These PUFAs depend on nutritional intake, with ALA and LA found in very distinct sources. Indeed, ALA is found in flaxseed (linseed), English walnut, hemp seed, and chia, while LA is found in soybean oil, safflower oil, and corn oil. Once consumed, both ALA and LA are metabolized into long-chain (LC) PUFAs; ALA to eicosapentaenoic (EPA, n-3) and docosahexaenoic acid (DHA, n-3), and LA to arachidonic acid (ARA, n-6) [1]. Nutritional sources of EPA and DHA are found in fat fishes, seafood, and marine microalgae or animal products fed with ALA and/or DHA (such as eggs, fish, and livestock).

DHA and ARA are particularly aggregated in the brain during the developmental period, while the accretion of EPA in the brain is negligible [6,7], which is discussed below. Importantly, PUFAs from the mother represent the only source of LC n-3 PUFAs for the fetus [8]. According to international agencies such as the National Health Security Agency (ANSES), the European Scientific Committee on Food (ESCF), and the International Society

for the Study of Fatty Acids and Lipids (ISSFAL), the recommendations for LC n-3 PUFA intake for optimal development is around 500 mg/day of EPA and DHA [9]. Based on clinical studies, the dose for EPA + DHA supplementation generally recommended to pregnant women can range from 200 to 1000 mg/day [10]. Of note, health organizations recommend increased consumption of LC n-3 PUFAs-rich marine products. Nevertheless, there is no consensus on the exact dose of EPA and DHA required during gestation and lactation for optimal brain development. In addition, the origin, safety, and sustainable supply of the marine sources have raised concerns. Alternative sustainable sources, such as microalgae-based LC n-3 PUFAs, are investigated [11]. Overall, there is a need for a better understanding of how EPA and DHA contribute to brain development to define specific recommendations for the fetal and post-natal brain. Conversion of LA and ALA to LC PUFAs, respectively ARA-EPA and DHA, is mediated by successive steps of desaturation and elongation. Importantly, both LA and ALA compete for the same enzymes in their biosynthesis (Figure 1). The enzymes involved in desaturation and elongation are rate-limiting enzymes. Delta-5 desaturase (D5D) and delta-6 desaturase (D6D) are respectively encoded by *fatty acid desaturase 1 (fads1)* and *fatty acid desaturase 2 (fads2)*. Elongase 2 (Elov12) and elongase 5 (Elov15) are respectively encoded by *elov12* and *elov15* [12]. The last step for DHA synthesis involves translocation of 24:6 n-3 from the endoplasmic reticulum to peroxisomes, where two carbons are removed to form LC n-3 PUFAs [13]. Of note, Elov14, an enzyme that mediates elongation of LC PUFAs and saturated fatty acids (SFAs) to form very LC PUFAs and very LC SFAs (28 to 38 carbon chain length), has been detected in the brain [14,15]. EPA is preferred as a substrate for elongation to very LC PUFAs over ARA and DHA [16]. However, the main Elov14-derived products are very LC SFAs, with very LC PUFAs being only present in traces in the brain [17]. More studies are needed for the link between Elov14 and very LC PUFAs in the brain. Desaturases have a higher affinity for n-3 PUFAs; however, due to the general higher consumption of LA, desaturation of n-6 PUFAs is greater. Importantly, genetic variations in *fads* and *elovl* genes affect the status of LC PUFAs independently of dietary effects [18]. Indeed, more attention is now given to polymorphisms in these genes, especially during brain development [19]. Single Nucleotide Polymorphisms (SNPs) within these genes can be associated with variations of LC PUFAs in the plasma (Figure 1), as demonstrated before [20]. SNPs in *fads* have been shown to be associated with various health outcomes (including markers of metabolic syndrome) and the plasma lipid profile in children, as well as neurodevelopmental outcomes in breastfed children [21]. The authors also found that breastmilk PUFAs content was inversely correlated to the production of inflammatory factors such as cytokine in infants [21]. Of note, low dietary intake of LC n-3 PUFAs leads to additional EPA and DHA deficiency in subjects with *fads* and *elovl* gene polymorphisms. As an example, some recent data pinpoint that low DHA status in vegetarian women may adversely affect the development of their children [22]. On the contrary, it is not clear whether consumption of diets rich in LA could be detrimental. Indeed, a clinical study conducted in 2001 on mothers supplemented with cod liver oil (enriched in LC n-3 PUFAs) or corn oil (enriched in LC n-6 PUFAs) showed no significant differences regarding pregnancy outcomes and cognitive development or growth of children [23]. Until recently, the capacity of metabolization of PUFA precursors into LC PUFAs was believed to be uniform in individuals and populations. The discovery that European and African populations carry different forms of *fads* alleles may partially explain the differences between blood levels of LC PUFAs in these populations (reviewed in [24]). The geographical differences in *fads* alleles are probably linked to specific selection in the European and African populations due to different food habits [25]. This knowledge, in combination with dietary evaluation, may help to refine dietary recommendation target more precisely population for personalized dietary supplementation in pregnant/lactating women and children at risk of altered level of LC PUFAs.

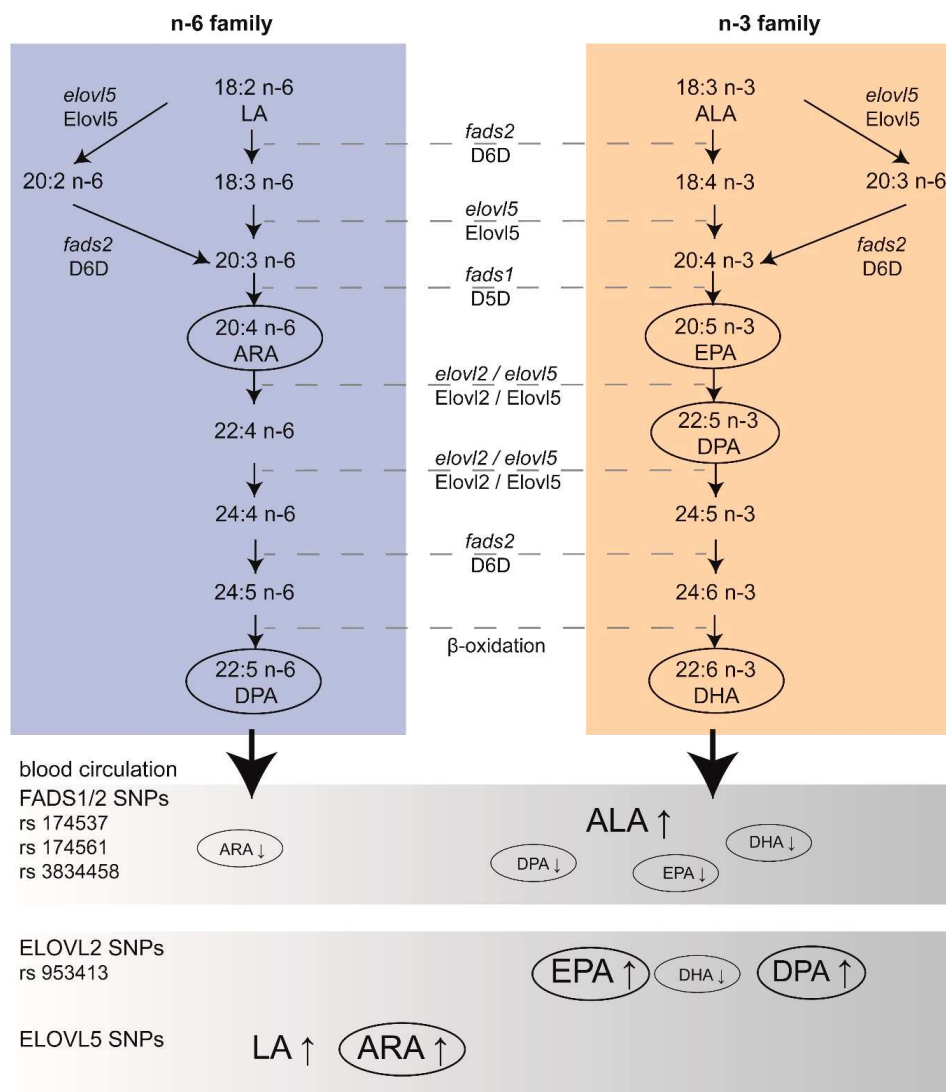


**Figure 1.** Single nucleotide polymorphisms (SNPs) within the metabolic pathways of n-3 and n-6 PUFAs lead to altered circulating levels of PUFAs. Desaturase enzymes (delta-5 desaturase (D5D) and delta-6 desaturase (D6D)) encoded by fatty acid desaturase genes 1 and 2 (*fads1* and *fads2* respectively), as well as elongase enzymes (elongase 2 (Elov12) and elongase 5 (Elov15)) encoded by *elov12* and *elov15* genes (respectively), are involved in desaturation and elongation of PUFAs from the n-6 (cyan) and n-3 (orange) families. Polymorphisms in those genes (SNPs) are associated with variations of plasma (grey) levels of LC PUFAs (represented by circles in the blood circulation). Bold letters represent higher amounts of LC PUFAs in the blood. *fads*: fatty acid desaturase; *elovl*: elongase; EPA: eicosapentaenoic acid; ARA: arachidonic acid; DHA: docosahexaenoic acid; ALA:  $\alpha$ -linolenic acid; LA: linoleic acid; DPA: docosapentaenoic acid; D5D: delta-5 desaturase; D6D: delta-6 desaturase; Elov15: elongase 5; Elov16: elongase 6.

In addition to their crucial role in the structure and function of cell membranes, n-3 and n-6 PUFAs are substrates for the production of several signaling molecules involved in the physiological function of the cells, especially in the brain [1,7]. Indeed, EPA, DHA, and ARA are hydrolyzed by the specific phospholipase A2 (PLA2) and can be further metabolized by cyclooxygenases (COXs), lipoxygenases (LOXs), and the cytochrome P450 system into eicosanoids (prostaglandins, leukotrienes, and hydroxyeicosatetraenoic acids from ARA) or docosanoids (resolvins, protectins, maresins, and neuroprotectin D1 from EPA and DHA), which are named oxylipins. n-3 and n-6 PUFAs-derived oxylipins are crucial to homeostatic functions but often have opposite activities, with ARA-derived eicosanoids being pro-inflammatory and DHA/EPA-derived being anti-inflammatory and pro-resolutive [26–29].

Their role in brain inflammation has been reviewed recently [7]; however, data on the developing brain are rather scarce and are discussed in the present review.

The massive changes in dietary habits from a balanced n-3/n-6 PUFAs ratio to excess n-6 PUFAs in Western societies across the twentieth century raises the question of its impact on brain development and its contribution to neurodevelopmental disorders and later life brain health [2]. Concerning n-3 PUFAs and infant brain development and mental health, the understanding of gene/nutrient interactions may be particularly important for the design of specific nutritional strategies, so-called precision nutrition [24,30].

In this review, we will discuss how maternal and child nutrition and polymorphism of PUFA metabolism genes influence their aggregation and activity in the developing brain, considering the placenta transfer to the in utero developing brain. Specific attention was given to gender. Then, we will discuss the potential role of these PUFAs in neurodevelopmental disorders, focusing on autism spectrum disorders (ASD), attention deficit and hyperactivity disorder (ADHD), and schizophrenia.

## 2. PUFAs and Brain Development

### 2.1. Accretion of PUFAs in the Developing Brain

Brain cell membranes are particularly rich in lipids (50–70%) [31], with LC PUFAs DHA and ARA being the highest species detectable, even if other fatty acids are also detected (such as monounsaturated and saturated fatty acids). As a result, the human prefrontal cortex contains around 30% of PUFAs, with 14% of DHA and 9% of ARA [32]. In rodents, the fatty acid composition of the brain is similar to humans; 12% of DHA and 10% of ARA [33]. Fatty acids are esterified in several type of phospholipids: phosphatidylcholine (PC, 42–44%), phosphatidylethanolamine (PE, 36–40%) phosphatidylserine (PS, 11–13%), and phosphatidylinositol (PI, 2–3%) [31]. DHA is mostly esterified in PE and PS, whereas ARA is esterified in PC and PI [1,34,35]. Striking differences can be found between the white and the grey matter, with DHA and ARA levels being lower in the white matter compared to the grey matter [36]. These differences could be due to the accumulation of DHA in synaptosomes and ARA in vascular cell membranes of the brain, which is suggested to serve as a depot for ARA [36,37]. Besides, the lipidic composition of the myelin sheath could also explain these differences since cholesterol is abundant in myelinated axons, while the grey matter is highly enriched in PUFAs [38,39]. High levels of DHA in synaptosomes are consistent with previous data, demonstrating that DHA promotes neurite outgrowth and synaptogenesis [40,41], which is discussed below.

Brain accumulation of both n-3 and n-6 PUFAs starts during gestation; a process often referred to as “accretion”. As previously noted, the pre and post-natal increase in DHA depends on maternal and infant DHA intake [42,43]. DHA accumulation in the brain is massive, with a nearly 30-fold increase in the first two years of life [44]. In humans, DHA accretion begins during the third trimester of pregnancy [45], while accretion during the first or second trimester is low [46]. In the third trimester, accretion of DHA and ARA is substantial, while accretion of the precursors LA and ALA is minimal [45] and EPA remains poorly aggregated. In humans, exponential accretion of LC n-3 and n-6 PUFAs was observed between gestational weeks 26 and 43, while post-natal LC PUFAs accretion is rather steady [47]. In humans, DHA accretion reaches 40 mg/day in the fetus during the final four weeks of gestation [48]. The high DHA demand for the fetal brain is sustained by the mother, thanks to the increased DHA synthesis from ALA and mobilization of maternal DHA stores from adipose tissue [49,50]. For comparison, in rodents, DHA accumulates in the brain during the first three weeks of neonatal life with a 10-fold increase [51].

There is little data on the rate of accretion of LC PUFAs in different brain cell types (neurons, astrocytes, microglia, and oligodendrocytes) during brain development. This knowledge would be of high interest as neurons and glial cells do not proliferate or mature at the same development stage. In addition, the role of DHA/ARA in the specificity of development is still unknown. As previously mentioned, DHA accumulates in synaptosomes and regulates the functions of synaptic proteins [40,52,53]. DHA is also found in astrocytes [54],



microglia [55], and oligodendrocyte membranes [56,57]. Interestingly, recent data show that DHA in the membrane of glial cells regulates their activity, the formation of syncytium in astrocytes, neuroinflammation in microglia [7], or myelin formation in oligodendrocytes [58]. Of note, EPA is found in microglia [55,59], suggesting that these cells could play an important role in mediating the neuroprotective effect of EPA dietary supplementation in mood disorders [60]. However, the precise role of DHA, EPA, and ARA accretion in these cells during development and the impact of altered accretion on glial cell development remains to be investigated for both term and preterm neonates. Indeed, children born preterm present major alterations of DHA and ARA accretion, as they normally accumulate during the third trimester of gestation, thus exposing preterm neonates to a deficit in LC n-3 PUFAs [61]. Recent data revealed a detrimental role of ARA in the microglia phagocytic activity in the spine, a crucial mechanism of developmental neuronal network wiring [59]. More studies are needed to better understand the type of PUFAs and the dynamic of PUFAs accretion in the different glial cells during development.

Overall, the massive increase in DHA and ARA in the third trimester of the developing brain coincides with the growth spurt characterized by an intensive neuron outgrowth and synaptic wiring [44]. Acquisition of new knowledge is promising for a better understanding of the importance of the optimal nutritional amount of n-3 PUFAs during gestation and lactation and young infants in both humans and rodents.

## 2.2. Needs of LC PUFAs to the Pre and Post-Natal Developing Brain: Transport and Dietary Maternal Supply

### 2.2.1. Pre-Natal Maternal Supply of LC PUFAs to the Developing Brain via the Placenta and the Blood-Brain Barrier

As previously reported, important concentrations of LC PUFAs, particularly ARA and DHA, are accumulated in the brain during early life to support the growth and development of the brain [62]. Numerous studies have demonstrated the importance of LC n-3 and n-6 PUFAs intake by the mother for adequate intake in the fetus and new-born. This contribution is made by maternal dietary intake, which is transferred through the placenta during gestation [63], then by milk during lactation [64]. Particular attention has been paid in the last years to DHA dietary intake in pregnant women to promote optimal brain development of the fetus [65], as the fetus is not able to produce its own DHA and is therefore dependent on maternal supply [66]. According to the World Health Organization, pregnant women should consume at least 200 mg/day of DHA. This amount of DHA intake is poorly met in the general population [67], raising the question of supplementation in DHA of pregnant women, especially the ones at risk for premature birth [68]. An omega-3 Index of 8–10% (DHA plus EPA levels in erythrocytes) is a target range to avoid risks and complications during pregnancy and lactation, such as premature birth [69]. Two major randomized controlled trials conducted in Australia and the United States, respectively DHA to Optimize Mother Infant Outcome (DOMInO) and Kansas DHA Outcomes Study (KUDOS), revealed that supplementation of mothers with 800 and 600 mg of DHA/day significantly reduced the number of preterm births [70] with a poor effect on the neurodevelopment of children [71]. However, a large multicentric trial (ORIP) aiming at studying the effect of prenatal LC n-3 PUFAs supplementation (800 mg of DHA + 100 mg of EPA) on the incidence of preterm birth [72] did not observe a beneficial effect on length of pregnancy [73]. Maternal plasma level of EPA + DHA below 2% in the first trimester of gestation could be a standard evaluation to perform dietary LC n-3 PUFA supplementation [74]. This reinforces the need for monitoring LC PUFAs during pregnancy to design appropriate dietary supplementation and prevent the adverse effects of insufficient supply of these fatty acids to the developing brain.

Maternal lipids are transferred to the fetus across the placenta via free or specific transport of unesterified fatty acids [75]. Indeed, during the third trimester of gestation, PUFAs are transferred from mother to fetus via the placenta, thanks to fatty acid translocase (FAT/CD36) and fatty acid transport protein (FATP), both present at the placental membrane [76]. These transporters are located on both microvillus and basal membranes

(maternal and fetal sides, respectively) of human placental cells and can transport free fatty acids in both directions. The placental membrane fatty acid-binding protein (p-FABP<sub>pm</sub>) is only located on the microvillus membrane and can transport ARA and DHA from maternal plasma to the fetus. The presence of p-FABP<sub>pm</sub> exclusively on the maternal side may favor the unidirectional flow of LC PUFAs from the mother to the fetus. [76–78]. The cytosolic form of FABP is also detected in both primary human trophoblasts and human placental choriocarcinoma (BeWo) cells, two models of in vitro embryonic culture [76,79,80], as well as in murine placenta [81–83].

Regarding DHA, which is crucial for optimal brain development, free DHA is transferred from the mother to the offspring via the placenta [84–87]. Several plasma pools are a major source for free DHA [88]. Indeed, plasma DHA is esterified in several lipids, phospholipids (PL), lysophospholipids, cholesteryl-esters, and triacyl-glycerol (TG). Hydrolysis of chylomicrons rich in TG by lipoprotein lipases (LPL) is an important source of free DHA found in the blood. During gestation, a free DHA maternal pool is a crucial source for placental and fetal DHA uptake and accretion [50,89].

The blood-brain barrier (BBB) limits the entry of blood cells, neurotoxic plasma molecules, pathogens and regulates the delivery of metabolites and essential nutrients to the brain, including LC PUFAs. Several transport systems regulating nutrients entry are expressed by endothelial cells of the BBB, such as glucose, specific amino-acids, vitamins, fatty acids, and DHA transporters [90]. Free DHA and lysophosphatidylcholine (LPC)-DHA are the primary sources of brain DHA [88]. The brain uptake of these forms of DHA relies on several mechanisms, including free passage and specific transporters on the BBB [1]. Recently, the major facilitator superfamily domain-containing protein 2a (Mfsd2a), which is located at the BBB, has been identified as a transporter of LPC-DHA, especially during the post-natal period with an impact on neuronal arborization [91,92]. This transporter is key to the brain amount of DHA [92] and the maintenance of the BBB while also inhibiting the transport of toxic molecules [93,94]. During development, pericytes are necessary to Mfsd2a expression and BBB formation [90]. Indeed, Mfsd2a confers to the endothelial cell of the BBB a specific lipid composition that is crucial to its permeability [94]. In addition, LPC-DHA, through Mfsd2a, represses *de novo* lipogenesis, with a profound effect on brain cell membrane composition in phospholipids during development [92]. Mfsd2a has also been identified in the human placenta, allowing the transport of LPC-DHA from mother to the fetus [95,96]. Very interestingly, deletion or total mutations of *mfsd2a* are responsible in humans of microcephaly and hypomyelination, further reinforcing its importance in brain shaping during development, possibly through DHA brain supply [58,97,98]. Of note, a recent study reports that Zika infection during pregnancy, a flavivirus that triggers fetal brain defect, including hydrocephalus, and alters Mfsd2a and DHA levels in the developing brain [99]. In mice, the genetic deletion of *mfsd2a* reduces DHA brain level and induces microcephaly [91,92]. Thanks to this KO in mice, the authors demonstrated that the expression of Mfsd2a is regulated by sterol regulatory element-binding proteins (Srebps) [92]. Srebp, a transcription factor, exists in three isoforms: Srebp-1a and -1c, both regulating genes required for lipogenesis, and Srebp-2, regulating genes in the metabolism of cholesterol with the two isoforms -1c and -2 being predominant in the brain [100]. A high level of EPA/DHA in the diet in mice induces a decrease in the expression of Srebp-1 in the brain [101]. Srebp-1 expression is significantly reduced in the dysbindin-1 KO mouse model of schizophrenia and post-mortem brain tissue from patients with schizophrenia [102]. Recently, a team showed in mice that KO of Srebp-1c induced an alteration of GABAergic transmission, leading to symptoms similar to schizophrenia: hyperactivity, depression-like symptoms, and social deficits [103]. All these results show that SREBP-1 could play a role in synaptic plasticity and transmission via the regulatory loop with n-3 PUFAs.

#### 2.2.2. Post-Natal Maternal Supply of LC PUFAs to the Developing Brain via Breastmilk or Infant Formula

As already mentioned, endogenous synthesis of LC PUFAs from their precursors (LA and ALA) is limited during infancy [104]. Consequently, post-natal brain uptake of LC

PUFAs relies on maternal milk or formulas [44]. In the maternal circulation, concentrations of LC n-3 and n-6 PUFAs (mostly DHA and ARA) are lower than in the new-born, while concentrations of precursors (ALA and LA) are higher in the maternal circulation [105]. Interestingly, *post-mortem* studies report that breastfed infants have greater amounts of DHA in the cerebral cortex than formula-fed infants without ARA or DHA supplementation [106]. Breastfed infants also present higher *post-mortem* DHA levels in both erythrocytes and the cortex but not in the retina [42]. Here we will focus on post-natal LC PUFAs supply via maternal breastmilk or formulas.

According to the World Health Organization, only 41% of infants under the age of six months are breastfed. Breastfeeding is the most adequate source of nutrients for infants and provides protection against child infections, increases intelligence, and protects against overweight and diabetes due to the presence of antibodies and lipids in maternal milk [107]. Depending on the age of the new-born, three different phases of milk production are distinguished, with three different milk compositions. First, the breast produces the colostrum, beginning on the third trimester of pregnancy until few days after birth. These fluids allow physiological adaptation of the new-born to extra uterine life. After transitional milk (until two weeks after delivery), the breast produces mature milk, which provides high amounts of lipids to the new-born [108]. During the first year of life, breast-milk LC PUFAs concentrations remain rather stable. ARA content is equivalent to 1% of milk total lipids in the colostrum and 0.5% within mature milk, which accounts for 14–15 mg/dL. In parallel, DHA content is equivalent to 0.5% in the colostrum and 0.25% in mature milk, accounting for 7–8 mg/dL [109]. The fatty acid patterns within maternal milk are greatly influenced by maternal lipid intake [110,111]. In fact, lactating mothers with dietary fish oil supplementation (rich in EPA and DHA) displayed increased levels of n-3 PUFAs in breastmilk [112,113]. Levels of DHA and EPA increase in breast milk within two to four days after initiation of supplementation with 10 mL per day of cod liver oil, while no change in the levels of ARA has been observed [111]. Helland et al. also reported that supplementation with cod liver oil increases DHA levels in a dose-response manner [111]. Therefore, nutritional strategies aiming at increasing DHA levels can be effective for replenishing DHA levels in women facing several pregnancies since DHA levels can drop over subsequent pregnancies [114]. Infants need high amounts of DHA for physiological development [115]. The breastmilk content in LC PUFAs is not regulated by the mammary gland but reflects the concentrations of LC PUFAs in maternal plasma that, in turn, are dependent on maternal diet and maternal activities of the desaturases and elongases involved in converting dietary LA and ALA to LC PUFAs [116].

FA from food sources in lactating mothers can be used in three ways: stored in adipose tissues, transferred to the mammary gland for incorporation into milk, or used for energy. However, a study showed that there is no effect of exercise on breastmilk content in LC PUFAs [117]. Different factors can influence the content of LC PUFAs of human breastmilk, such as maternal food intake, gestational age, or smoking. Infants of smoking mothers are present with fewer markers of LC PUFAs synthesis [118]. Concentrations of DHA and ARA in breastmilk presented variations depending on geographical locations, as reviewed earlier [104]. Breastmilk DHA content is linked to dietary intake [119]. Optimum breastmilk DHA concentrations were observed in arctic Canada, Japan, the Dominican Republic, the Philippines, and the Congo (between 1.4% and 0.6%), which mainly contain coastal or insular populations, usually with high marine food intake [104]. Lower breastmilk DHA concentrations were observed in Pakistan, rural South Africa, Canada, the Netherlands, and France (between 0.06% and 0.14%), especially in inland regions or in developed countries, where low marine food consumption is observed [104]. A recent review reports that ARA is detected in animal and human milk, with its content being linked to maternal ARA dietary intake [120]. Interestingly, several recent works report the presence of free and esterified ARA, EPA, and DHA-derived oxylipins in human milk [121–123]. Of note, the most abundant forms of oxylipins are the ones derived from LA [122], which have been recently reported to be key to brain development in rats [124]. However, whether milk

oxylipins play a role as signaling molecules for infant brain development has not been fully investigated.

PUFAs supply to premature infants is a burning question, as these fatty acids are massively incorporated in the developing brain in the last trimester of pregnancy. According to the World Health Organization, around 15 million premature births (before 37 weeks of gestation) occur every year. Prematurity is the main cause of death in children under the age of five [125]. Preterm infants have to face many neurodevelopmental disabilities, including learning, visual and hearing problems [126]. Current treatments consist of magnesium sulfate administration [127], caffeine for treatment of apnoea, and high doses of DHA [128]. To avoid complications in premature infants, different nutritional supports are used, such as enteral or parenteral nutrition, human breast milk, and formula milk [129]. Enteral nutrition is limited in preterm birth because of the immature gastrointestinal motor activity and risks of necrotizing enterocolitis [130]. Premature infants should be fed with human milk, while parenteral nutrition is recommended if *per os* nutrition cannot be achieved to supply adequate amounts of proteins. However, the best alternative to human milk remains preterm formula [131]. In 2008, a study conducted on very preterm infants with human milk supplementation using DHA and ARA brought interesting outcomes regarding improved recognition memory at six months of age [132]. However, the effect on visual, intellectual development, or growth of preterm infants with the addition of LC PUFAs to formula remains unclear [133,134]. Another study showed that supplementation with a 50:50 mixture of DHA:ARA had no negative effect on weight gain or growth [132]. A randomized control trial conducted in 2013 by Gould et al. underlined that preterm infants fed high-dose DHA did not display increased mental development index [135]. This can be explained by the fact that supplementation was conducted on fully- or partially-fed formula infants with fatty acids doses equivalent to the content found in human milk [136]. Assessments of attention had also been conducted by the team of Gould et al. on children from the n-3 Fatty Acids for Improvement in Respiratory Outcomes (N3RO) trial. The authors hypothesized that supplementation in DHA could favor the restoration of normal brain development [137]. Most of the studies carried out do not allow for a clear conclusion on the effect of LC PUFAs supplementation on cognitive development of preterm birth children [132,134,138,139], as also reported in a meta-analysis [140]. A recent review also reports mixed effects of LC PUFAs on cognition in preterm children [141]. A randomized controlled trial conducted on term infants in 2000 revealed that supplementation of formula milk with DHA and AA at an early stage of life improved the Mental Development Index of the Bayley Scales at 18 months of age [142]. Nonetheless, it is important to underline that neurodevelopmental assessment should be performed with neuropsychological tests and procedures adapted to the age of children.

To conclude, maternal dietary supply is crucial for the pre- and post-natal developing brain as the fetus and newborn are not able to produce LC PUFAs. The pre-natal maternal supply is accessed via the placenta and the BBB, thanks to specific transporters. The post-natal supply of LC PUFAs with breastmilk and formulas allows the transfer of nutrients to the developing brain. In the specific case of premature birth, formulas remain the best alternatives to human milk, even though long-term beneficial effects are still unclear.

### 3. Endogenous Production of PUFAs in the Developing Brain

#### 3.1. Expression of Key Enzymes in the Developing Brain

As previously mentioned, maternal PUFAs supply to the infant brain occurs during gestation and lactation, but the developing brain seems to be able to form LC n-6 and n-3 PUFAs from their respective precursors. For a long time, it was assumed that the liver was the main location of elongation and saturation to form LC PUFAs, eventually released in the developing brain, as shown by *in vivo* studies in rats [51,143]. In order to bypass the metabolism of the liver, intra-cranial administration of labeled LA and ALA has been performed in the post-natal rat (11 and 13 days *post-partum*). These results show that the post-natal developing brain is capable of forming LC PUFAs, ARA, and DHA,

respectively [144,145]. Similarly, Sanders et al. have shown that the brains of 21-day-old fetal rats were also capable of forming LC PUFAs, in particular by the presence of D6D, which converts LA and ALA [146,147]. At the end of the 1990s, the human *fads1* [148] and the mammalian *fads2* [148,149] were cloned and characterized, while the *fads1* gene (coding for D5D enzyme) has been shown to be strongly expressed in the human fetal brain [150]. In addition, several members of the Elov1 family (Elov1 1, 3, 4, 5, and 6) have been reported to be expressed in the brain, with strong differences between species. As an example, the expression of Elov12 and Elov17 is very low in the mammalian brain, while Elov12 is expressed in non-mammal species (such as fish). Elov14, which catalyses the synthesis of very LC PUFAs, is expressed in the brain of fish and mammals. Several SNPs in the *fads1-fads2* gene cluster (rs174537, rs174761, and rs383458) are associated with variations in desaturase activity, leading to different LC PUFAs levels, as summarised in Table 1. An increase in EPA and DHA dietary intake is responsible for an increase in D5D and a decrease in D6D activities [151]. In one study, the authors showed that the presence of the rs174537 genotype resulted in dietary EPA and DHA modulation of D5D activity [151]. Besides, a 2011 meta-analysis on genetic loci associated with plasma phospholipids showed that SNPs in *Fads1/2* are responsible for an increase in ALA levels and a decrease in EPA levels, while SNPs on *Elov12* are more likely to induce an increase in EPA (as well as docosapentaenoic acid, DPA) and a decrease in DHA plasma levels [152]. Mutations in either *elov14* or *elov15* cause neurological diseases in humans [153], as explained below. During early embryogenesis in the zebrafish, Monroig et al. were able to detect expression of the desaturase and elongation genes, using qRT-PCR and whole-mount in situ hybridization, respectively showing temporal- and spatially-restricted expression [154]. They showed that the three transcripts *fads*, *elov12*, and *elov15* were highly expressed in the head area from the beginning of embryogenesis, which was also confirmed in another study [155]. Early detection of these genes in the brain during embryonic development may suggest that in situ production of LC PUFAs could be achieved; however, the contribution of these genes as compared to the maternal PUFA supply have been poorly studied during brain development.

**Table 1.** Major SNPs involved in variations of LC PUFAs levels. *fads*: fatty acid desaturase; *elovl*: elongase; LC n-3 PUFA: n-3 long chain polyunsaturated fatty acid; EPA: eicosapentaenoic acid; ARA: arachidonic acid; DHA: docosahexaenoic acid; ALA:  $\alpha$ -linolenic acid; LA: linoleic acid; DPA: docosapentaenoic acid; D5D: delta-5 desaturase; D6D: delta-6 desaturase.

Study (Year)	Ref.	SNPs	Impact on LC PUFAs Levels	Child Development
Morales (2011)	[18]	Mother: <i>fads</i> <i>elov15</i> Children: <i>fads</i> <i>elov15</i> <i>fads1-fads2</i>	Higher colostrum levels of LC n-3 PUFA.	Improved cognition at 14 months. Modification of cognition by breastfeeding.
de Groot et al. (2019)	[19]	(rs174537, rs175461, rs3834458) <i>elov12</i> (rs953413) <i>fads</i>	Decreased levels of EPA and ARA. Reduced DHA levels.	
Tanaka et al. (2009)	[20]	(rs174537) <i>elov12</i> (rs953413)	Higher ALA, LA and lower ARA, EPA, DPA and DHA levels. Lower DHA and higher DPA and ARA levels.	
Al-Hilal et al. (2013)	[151]	<i>fads1-fads2</i> (rs174537)	Interaction of rs174537 genotype with dietary EPA + DHA supplementation influence D5D and D6D activity.	
Lemaitre et al. (2011)	[152]	<i>fads1-fads2</i> <i>elov12</i>	Increase in ALA levels. Decrease in EPA levels. Increase in EPA/DPA levels. Decrease in DHA levels.	

### 3.2. Gender Differences in Brain PUFAs Accretion and Effect of PUFAs on Sex Determination

In humans, it is known that the brain develops differently depending on gender. In a large human cohort, significant gender differences were observed regarding cortical thickness, fiber organization, and total brain volume [156]. These anatomical differences could explain that gender may play a significant role in neurodevelopmental disorders, as observed with autism [157] and attention deficit and hyperactivity disorder [158]. Besides, gender differences are also observed in patients with schizophrenia [159]. However, these differences are sometimes attributed to methodological issues [160,161].

To our knowledge, there are very few studies on differential brain accretion of PUFAs during development according to gender. In addition, previous studies did not focus on whether the dietary status of PUFAs differentially influences brain accretion according to gender. Nevertheless, some studies reported that PUFAs accretion is different in men vs. women. Indeed, in humans, DHA status in serum is reported to be higher in adult women than men. These differences have been associated with a better conversion of ALA to LC n-3 PUFAs in women as compared to men [162,163]. Such metabolic capacity could facilitate maternal supply to their offspring. On the other hand, the proportion of DPA n-3 to EPA is lower in serum of women [162,164]. Studies in rats have shown that D5D and D6D enzymes at both the transcriptional and protein levels are more expressed in the liver of females than males, in contrast to the brain, where similar expressions were found in both genders [165,166]. Different studies suggested that higher serum DHA levels in women than men may be due to the presence of estrogens that positively regulate DHA synthesis from ALA [166,167]. Indeed, it has been shown that taking hormonal contraception induces a significant increase in the level of DHA in women [168]. A recent study in rats has shown that a diet containing low amounts of LA with an estrogen supply induced an increase in the hepatic expression of D6D, Elovl2, and Elovl5, thus inducing an increase in plasma levels of DHA [169]. An in vivo study in rats showed that dietary ALA intake induced a greater proportion of DHA in erythrocytes but lower in the pre-frontal cortex in females compared to males [170]. In this study, the authors showed that ovariectomy, together with a diet rich in ALA, induced a decrease in the amount of DHA in erythrocytes, as well as in the hippocampus, compared to control females fed with a diet rich in ALA. Similarly, another study in rats also showed that ovariectomy-induced an increase on hepatic *fads1* and *fads2* transcripts, but not in the brain, and a decrease in DHA levels in the brain [171]. A study on deficiency or supplementation in n-3 PUFA during the perinatal period and for 16 weeks after weaning in mice, shows that the changes in cerebellar FA were more pronounced in offspring females, with diet having a significant effect [172], due to the presence of estrogen (for a review, see [173]). All these results suggest that ovarian hormones up-regulate DHA content in erythrocytes and brain regions. However, a recent study examining the interaction effects between diet, sex, brain regions, and phospholipid pools in mice demonstrated that DHA concentration was gender independent, while ARA concentration was partially dependent on sex [174].

Gender may influence the preventive effects of n-3 PUFA supplemented diets on neurodevelopmental disorders in animal models. In fact, supplementation with n-3 PUFAs in pregnant spontaneously hypertensive rat dams (SHR) induced a reduction in hyperactivity and impulsivity in the male offspring, but with no effect, or even opposite effects, in the female offspring [175]. A recent study conducted in a two-hit model in mice showed the sex-specific preventive effects of LC n-3 PUFAs [176].

All these studies show that there is a sex effect on the endogenous formation of LC PUFAs. However, further studies are needed to understand the effect of gender, and therefore hormones, on the accretion of PUFAs in the brain.

Trivers and Willard were the first to state that reproductive conditions could affect the sex ratio in the offspring [177]. Numerous in vivo studies have shown an impact of the maternal diet during pregnancy on the offspring sex ratio. Indeed, a low-fat diet (reduced amounts of essential fatty acids, EFA) during pregnancy induces a reduction in the number of males in the litter of mice without changing the total number of females [178].

In opossums, diets rich in LC n-3 PUFAs during gestation induced a greater proportion of males than females in litters [179], whereas a diet rich in n-6 LC PUFAs during gestation induced a greater proportion of females than males, both in mice [180] and rats [181]. Diets rich in n-6 LC PUFAs induced an increase in the production of pro-inflammatory derivatives, in particular prostaglandins, such as PGE<sub>2</sub>, PGF<sub>2α</sub> and its metabolite 13,14-dihydro-15-keto PGF<sub>2α</sub> (PGFM) [182]. This in utero inflammation affects the ovarian cycle, hormone production, and sperm fertilizing ability [183]. Besides, in utero inflammation also affects vaginal pH, inducing more favorable conditions for fertilization with X sperm rather than Y [184], as well as the loss of male embryos [181,182]. Surprisingly, it has been shown that a diet rich in LC n-6 PUFAs induces a higher proportion of males, both in sheep [185] and cows [186]. Various studies carried out in cows have shown that supplementation with n-6 LC PUFAs induced a reduction in the level of progesterone and a delay in oocyte maturation by an increase in the number of dominant follicles [187,188]. In cattle, it has been shown in vitro that the oocytes that mature later are preferentially fertilized by Y than X sperm [189] and that n-6 LC PUFAs supplementation during oocyte maturation and fertilization induced a greater number of male embryos [186]. Additional studies are necessary in order to understand these differences in results, as well as to decipher the different mechanisms that exert PUFAs on hormonal secretions and fertilization. Therefore, it appears that females have higher n-3 PUFAs in the serum, especially DHA, than males, due to the presence of estrogen, which positively regulates its synthesis [167].

#### 4. Mechanisms of Action of PUFAs on Neurodevelopment

##### 4.1. Role of PUFAs in Synaptogenesis and Neuronal Development

As previously mentioned, DHA increases during perinatal development, while the ARA/DHA ratio decreases, which is linked with active periods of synaptogenesis and the establishment of structural connectivity [190,191]. The mechanisms through which LC PUFAs contribute to brain development are still poorly understood. Indeed, several developmental processes have been reported to be regulated by PUFAs from cell migration to proliferation, differentiation, neurogenesis, and myelination to synaptogenesis, which are the most well-described and will be the main focus of the mechanisms described in this section.

Briefly, both DHA and ARA have been reported to influence neural stem cells (NSC) proliferation and differentiation, and neurogenesis. Early-life n-3 PUFAs dietary deficiency induces a delay in migration of neuronal cells in the embryonic brain [192] as well as in new-borns and during post-natal life [193]. Recent data pinpoint that n-3 PUFA deficiency-induced neurodevelopmental defects are linked to an early gliogenic fate shift in NSCs, with ARA and DHA derivatives being key [194]. Indeed, neurogenic transition of NSCs involves the DHA metabolite epoxydocosahexapentaenoic acids (EpDPE), while the gliogenic transition of NSCs is driven by the ARA metabolite epoxyeicosatrienoic acid (EET) [194]. In line with these results, other ARA metabolites such as PGE<sub>2</sub> have been reported to increase the proliferation of NSCs and to promote their differentiation into neuronal-lineage cells [195]. DHA facilitates the differentiation of astrocytes in vitro [196] through its binding to GPR120 and β<sub>2</sub>-AR [197]. Of note, dietary supply in LA promotes ARA-derived endocannabinoids which, in turn, promotes astroglialogenesis from NSCs, reinforcing the idea that ARA metabolites contribute to gliogenesis [198]. Further studies on the exact role of LC PUFAs and their metabolites on NSCs fate (neurogenesis or gliogenesis) should be performed to confirm the importance of LC n-3 and n-6 PUFA dietary supply during brain development.

Regarding the role of LC PUFAs on synaptogenesis, a few lipid metabolism enzymes have been identified at synaptic terminals, where they can locally modulate synaptic transmission [199–201]. Mature synapses, formed during brain growth, require high amounts of ARA and DHA incorporated into the expanding membrane surface [202]. During perinatal rodent brain development, DHA modulates membrane signaling and synaptogenesis [203] by accumulating in the neuronal growth cone [204,205] and mature synaptic

membranes [56,206]. An in vivo model of *Xenopus laevis* embryos from adult female frogs fed with adequate or n-3 PUFA deficient diets and then switched to a fish-oil supplemented diet showed that maternal n-3 PUFA intake impacts the branching and the synaptic connectivity of neurons in the developing brain. This model also revealed that these changes are correlated with a decrease in brain-derived neurotrophic factor (BDNF) in the brain [207]. Moreover, PUFAs-depleted drosophila presented impairments of synaptic transmission at synapses from the visual system [208]. Several in vitro studies have reported that DHA promoted synapse formation [40,209–211]. This effect could be direct, through DHA effect on specific receptors such as retinoid X receptor (RXR) [212] or indirect through specific metabolites such as oxylipins or N-docosahexaenoylethanolamine (DHEA), which have been reported to regulate NSCs differentiation (see below), neurite outgrowth, synaptogenesis and neuroinflammation [7,213,214]. Indeed, an ex vivo study on embryonic neurons from E18 mouse hippocampus' showed that DHEA, a DHA-derived endocannabinoid-like metabolite, was crucial to neuronal development, promotes neurites and synaptogenesis [213]. Synapses enhancement and formation induced by DHA could also be linked to its esterified form via its effect on physical membrane properties [215–218]. As a result, in vivo DHA supplementation specifically promotes neurite growth, synaptogenesis, and raises the levels of pre- and post-synaptic proteins involved in synaptic transmission and long-term potentiation (LTP) [40].

Overall, the mechanistic data brought by animal studies further support the need for LC PUFA for optimal brain development. Concerning post-natal periods, breast milk remains the gold standard, as it provides both ARA and DHA [120]. Concerning infant formulae, the amount of ARA and DHA to be added is still a matter of debate, as recently reviewed [219]. The recent European recommendation does not pinpoint the need for the addition of ARA in infant formulae while adding DHA is mandatory (reviewed in [219]). The lack of recommendation on ARA in formulae has been pinpointed by several experts as being a potential risk for improper brain development [220–222], as a diet poor in ARA causes its decreased bioavailability for the brain [223]. Further studies are therefore needed to better understand the mechanisms underlying ARA and DHA association on brain developmental processes [224].

#### 4.2. Role of PUFAs in the Regulation of Microglia and Neuroinflammation during Brain Development

More recently, specific attention has been given to the role of LC PUFAs on microglia activity and neuroinflammation during brain development [55]. Microglia, the resident macrophage-like brain cells which represent 5% to 15% of the brain cells, are well known to be crucial in neuroinflammatory processes in response to injury or lesions, including through interactions with brain infiltrating immune cells [225–227]. n-6 and n-3 PUFAs regulate neuroinflammation either directly or through their metabolites such as oxylipins or endocannabinoids (for a recent review, see [7]), including during brain development [228]. Of note, SNPs of genes involved in PUFAs metabolism have been reported to influence inflammation and potentially neuroinflammation. Indeed, children of mothers with minor alleles of *fads* rs174556 have been found to have higher ex vivo-stimulated production of IL-10, IL-17, and IL-5 from peripheral blood mononuclear cells [21].

Although microglia are known to contribute to neuroinflammation, accumulating evidence has pinpointed their role in brain wiring during development [229]. Microglia are the first glial cells appearing in the embryonic brain. The developmental origins of microglia have been the subject of intense debate [230]. A mesodermal or monocytic origin of microglia has been first hypothesized until fate-mapping studies showed that microglia derived from erythro-myeloid progenitors from the yolk sac around embryonic day (ED) 7.5 [231]. This primitive hematopoiesis gives rise to pre-macrophages that colonize the whole brain from ED 9.5 and differentiate into microglia from ED 10.5 [232]. Microglia develop according to temporal stages: early, pre, and adult, with the final step being reached during the second post-natal week in mice [233]. Such an early-life origin of microglia confers to these cells a specific life-long history, with gender and perinatal events



potentially influencing their feature later in life [229]. During development, microglia regulate many processes, including the phagocytosis of alive neuronal elements (including synapses), dying and dead cells, and support myelination, neurogenesis, and axon fasciculation [234,235]. Importantly, inflammatory events during pregnancy or early-life influence the microglial developmental trajectory, which may have adverse effects on brain wiring, increasing the risk for neurodevelopmental disorders [236–239]. Indeed, the mechanisms underlying normal and abnormal microglia-mediated synaptic pruning and brain wiring are the subject of intense research [236].

Overall, microglia functioning is largely driven by their microenvironment, with neurons and other glial cells constantly sending signals to which microglia respond. The role of dietary PUFAs in the regulation of microglia developmental features has been poorly addressed, but recent data pinpointed that these cells are influenced by dietary PUFAs. Recently, we reported that maternal n-3 PUFA intake influences the offspring microglial lipid composition (Figure 2) and the oxylipin signature [55,59]. Importantly, at weaning, microglia display a unique fatty acid profile, with an enrichment of EPA, suggesting that these cells could be a source of EPA-derived oxylipins with anti-inflammatory activities [59]. Indeed, resolvin D1 (RvD1) and resolvin E1 (RvE1), which are pro-resolutive oxylipins derived from DHA and EPA, respectively, reduced pro-inflammatory cytokine expression triggered in microglia by LPS *in vitro* [240]. On the other hand, maternal dietary n-3 PUFA deficiency polarizes microglia toward a phagocytic phenotype, which leads to altered brain wiring and memory impairment in the offspring at weaning [59,241]. In line with the importance of n-3 PUFAs in the regulation of microglia-dependant neuroinflammation [55,241–245], a low dietary level of maternal n-3 PUFAs not only promotes a pro-inflammatory microglial profile [241] but also exacerbates inflammatory response in pregnant dams and the embryos after a prenatal LPS treatment [243]. This exaggerated embryonic brain inflammatory response contributes to later-life cognitive, emotional, and neurobiological impairments [243,246]. The mechanisms underlying the deleterious effect of both prenatal dietary n-3 PUFA deficiency and inflammatory stimulus on later-life behavior have started to be understood; for example, the exacerbated production of inflammatory factors in the embryonic brain could disturb brain wiring [247], the microglia phagocytic activity of spines, leading to excessive pruning [248] and/or microbiota disturbance [246], which has been reported to be involved in neurodevelopmental disorders [249,250]. In particular, we recently found that 12-HETE, which is overexpressed in n-3 PUFA deficient microglia, contributes to dendritic spines decrease and memory impairment at weaning [59]. Additional work needs to be conducted to decipher the exact mechanisms underlying n-3 PUFA deficiency and developmental microglia function and whether later-life dietary intervention with n-3 PUFAs can restore the impairment associated with this early-life deleterious developmental effect [251].

To conclude, co-occurring n-3 PUFA deficiency and maternal inflammation can potentiate each other and induce synergistic effects on brain development and a higher risk of developing neurodevelopmental disorders (Figure 2). As a result, women in the age of procreating with low n-3 PUFA bioavailability (linked to diet and/or genetic) could be at risk of higher sensitivity to early-life adverse inflammatory events. Indeed, there is a need to pay attention to n-3 PUFAs bioavailability during pregnancy to limit the risk of impaired brain development and neurodevelopmental disorders.

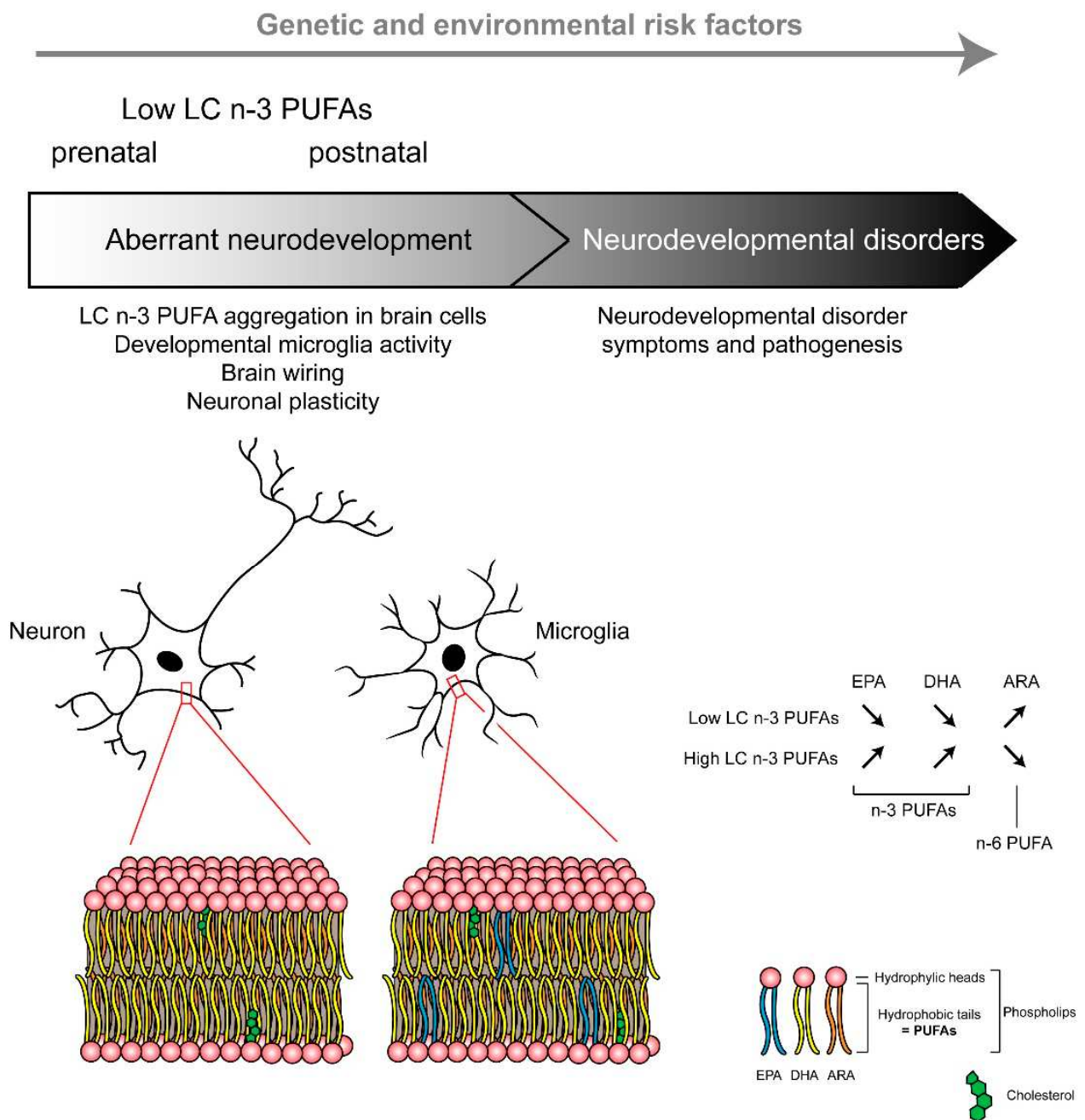


**Figure 2.** Hypothetical summary of events leading to neurodevelopmental disorders. Aberrant neurodevelopment can lead to neurodevelopmental disorders following inadequate levels of LC n-3 PUFAs.

### 5. Role of PUFAs in Neurodevelopmental Diseases

Neurodevelopmental disorders, which affect more than 3% of children worldwide, are characterized by altered or disrupted developmental steps leading to the incapacity to reach cognitive, emotional, communicative, and motor abilities, together with poor adaptation skills (recently reviewed in [252]). Among neurodevelopmental disorders, autism spectrum disorder (ASD), attention deficit hyperactivity disorder (ADHD), and intellectual disability are common, with potential shared neuropathological mechanisms. The factors contributing to neurodevelopmental disorders can be genetic and/or environmental. As an example, clinical and pre-clinical studies show that genetic alterations of genes coding for proteins involved in pre- and post-synapse functions have been found to be implicated in

neurodevelopmental disorders. Schizophrenia, despite not being classified as a neurodevelopmental disorder, is a neuropsychiatric disease with an etiology route of inadequate brain development, with long-lasting consequences. Altogether, these diseases refer to the theory of DOHAD (Developmental Origin of Health and Disease; [253]), with early-life nutritional imbalance playing a key role [254].

Both genetic alteration and inadequate nutrition (amongst others), the latter leading to insufficiency of LC n-3 PUFAs bioavailability, have been reported to be risk factors for neurodevelopmental diseases [228] and schizophrenia [255]. Besides, abnormal features of the placenta (physiological, morphological, and histological abnormalities) have been hypothesized as risk factors for subsequent abnormal neurodevelopment [256,257]. In this section, the potential role of LC PUFAs in neurodevelopmental diseases is discussed, especially the role of the n-3 family. In particular, we focus on the link between perinatal low LC n-3 PUFAs and the risk of compromised brain development and whether dietary supplementation with LC PUFAs could protect and/or correct neurodevelopmental abnormalities.

### *5.1. Early-Life n-3 PUFAs and Cognition in Infants*

In humans, several studies have reported a link between n-3 PUFAs and cognitive capacities. Explanations have been focused on the balance (ratio) between DHA and ARA, as emphasized before [258–260]. Indeed, an association between low levels of DHA and poorer reading abilities and working memory performance was observed in children [261]. Besides, a negative relationship was found between EPA-DHA consumption and overall cognitive function and psychomotor speed in subjects aged 45–70 years old [262]. Moreover, beneficial effects of maternal n-3 PUFA supplementation on child growth and development have been reported [263], suggesting a positive effect on cognitive performance in later life. Due to the observed positive association between n-3 PUFA serum levels and cognitive abilities in infants [261,264], there have been various attempts to enhance cognition through LC n-3 PUFAs supplementation in healthy children and adolescents [71,265–268] as well as in youths from clinical populations, such as patients with autism spectrum disorder (ASD) or attention deficits and hyperactivity disorder (ADHD) [269,270], which will be discussed below.

Different studies have shown that n-3 PUFAs dietary supplementation of the mother or the infant could have beneficial effects on development and cognition in children. In fact, the intelligent quotient (IQ) can be improved at four years of age after LC n-3 PUFA supplementation (1183 mg of DHA and 803 mg of EPA per day) in the mother during pregnancy and lactation [271]. Supplementation of infant formula with DHA (0.36%) and ARA (0.72%) from an early age (four to six months) leads to improved visual function at 12 months [272]. Using the same paradigm, another study found improved visual acuity at six weeks of age [273]. Other studies have also shown that there is a positive correlation between formula rich in ALA and neurodevelopment at one year of age in infants born at full term of pregnancy [274]. It has also been shown that dietary LC PUFAs supplementation (using both DHA and ARA) can improve visual acuity and cognitive development [275]. However, the duration of breastfeeding, without dietary supplementation and the performance score of infants are weakly associated [276]. These studies strongly suggest that supplementation with both DHA and ARA during early life can provide beneficial effects on cognition in infants. However, future studies will need to decipher whether these effects are provided by either n-3 or n-6 LC PUFAs, or the synergy of both.

In parallel, several animal studies have examined the impact of LC PUFAs on cognition. In a model of transgenic mice producing high levels of LC n-3 PUFAs in their milk under dietary n-3 PUFAs deficiency (beta-casein n-3 desaturase transgenic mouse model), pups raised under these conditions had increased brain levels of DHA and faster visual development compared to pups raised by wild type mice [277]. In a review published in 2006, Fedorova and Salem provided an overview of the different animal models used to investigate the cognitive and behavioral effects of LC n-3 PUFAs [278]. Most of these

models use LC n-3 PUFAs dietary deficiency; however, it is important to note that this deficiency is far more severe than what can be found in human populations [136]. In mice, n-3 PUFAs deficient diets during pregnancy and lactation induce spatial memory deficits and behavioral impairment in the adult offspring [243,244,279,280].

## 5.2. Autism Spectrum Disorders (ASD)

Autism Spectrum Disorders (ASD) are neurodevelopmental diseases more frequently diagnosed in males [281]. ASD is characterized by an early-childhood onset (first years of life) with a long-term course and variation in developmental trajectory, a remarkable clinical and biological variability, and a dramatically increased prevalence (0.05% in 1966 and close to 2% in 2019), with a wide symptomatology range in patients [282]. Patients with ASD display a core of symptoms such as impairment in social-communicative skills and restricted/repetitive behaviors/interests, often associated with other symptoms such as intellectual disabilities, impaired language skills, and different medical conditions such as gastrointestinal symptoms.

The substantial heterogeneity which underlies the neurobiology of ASD further supports that the etiology and pathophysiology of these disorders cannot be restricted to a single genetic cause [283]. Indeed, genetic alterations [284], pollution, environmental/gestational stress, including inflammation and nutrition [285,286], as well as neural/anatomical dysfunctions [287–290] are combined risk factors for ASD development. With regard to the link between ASD and PUFAs, polymorphisms in either the *fads* or *elovl* genes have been linked to susceptibility for developing ASD [291].

In rodents, exposure to an n-6-PUFAs-rich diet during gestation and lactation produced social deficits in the adult offspring that resemble autistic features [292]. In a rat model of autism, where pups are exposed to the neurotoxin propionic acid, decreased levels of total n-3 and n-6 PUFAs were observed in the brain [293]. Another study found beneficial effects of LC n-3 PUFAs (200 mg/kg/day for 30 days) in the same model [294]. In another study, in which mice pups were exposed to an immune reaction during intrauterine life (intraperitoneal injection of lipopolysaccharide at E17 in pregnant mice, mimicking bacterial infection), adult animals developed impaired memory if fed with an LC n-3 PUFAs deficient diet [243]. In another model of intrauterine exposure to infection (exposure to PolyI:C on E9, mimicking viral infection), supplementation with LC n-3 PUFAs at weaning (menhaden fish oil at 35 g/kg of diet) dampened the DNA hypo-methylations observed at adulthood [295]. In a mouse model of ASD, in which animals are prenatally exposed to valproic acid, n-3 supplementation with both  $\alpha$ - and  $\gamma$ -linolenic acid protected against the development of autistic-like features [296]. Besides, in an inbred mouse model of ASD (BTBR mouse strain), dietary deficiency in n-3 PUFAs from gestation to early adulthood induced developmental delay and altered sociability [297]. These results were also observed when these animals were fed with dietary n-3 PUFAs supplementation [297], suggesting that LC n-3 PUFAs cannot counterbalance the social deficits induced by such a genetic inbreeding. Finally, in a study of *Frm1* KO mice, another model mimicking ASD-like features, n-3 PUFAs supplementation from weaning to adulthood, led to significant improvements in sociability and emotionality [298], suggesting that n-3 PUFAs supplementation might be used as a therapeutic tool in specific clinical situations.

PUFAs have been investigated for their potential role in alleviating the symptoms of autism since reduced levels of PUFAs have been observed in autistic patients, especially concerning ARA and DHA [299–305], which are believed to be correlated to the symptomatology of ASD [306]. However, one study observed increased levels of PUFAs in high-functioning autistic children [307]. Besides, a decreased risk of ASD in children born from mothers with high total dietary PUFA intake was also observed [308]. Another study found that low dietary PUFAs intake during the second half of pregnancy appears to be a risk factor for ASD [309]. In an open-label study, a six-week supplementation with fish-oil capsules containing EPA + DHA (1.86 g/day) and vitamin E (10 mg/day) failed to improve the behavioral symptoms of young adults with severe autism [310]. In a systematic

review, PUFAs supplementation with either DHA or EPA alone, or in combination, was found to be inefficient in modulating behavioral outcomes in adults and adolescents with autism [311]. However, a recent case report provided evidence that supplementation with EPA + DHA (respectively 2.4 and 1.2 g/day) and vitamin D (25,000 IU per week in a single oral dose) are beneficial to improve the symptoms of a 23 years old autistic patient [312]. Similarly, a meta-analysis performed recently concluded that n-3 PUFAs supplementation could be effective in improving some of the symptoms of autistic patients [305]. A recent randomized clinical trial observed beneficial effects of n-3 PUFAs supplementation (722 mg/day of DHA for 12 months) on irritability and lethargy in 2.5–8 years old autistic children [313], which was also observed in meta-analyses [314]. The beneficial effects of LC PUFAs were also observed in preterm toddlers presenting with ASD symptoms [315,316]. Finally, supplementation with both LA (480 mg/day) and ALA (240 mg/day) for 16 weeks provided therapeutic benefits in 21 patients with ASD [304]. Table 2 summarises the main outcomes of case reports [312,317], open-label clinical trials [304,310,318–320], and randomized clinical trials [313,315,316,321–329] using LC PUFAs in patients diagnosed with ASD. An elegant study has summarised the wide array of possible nutritional interventions for patients with ASD and concluded that dietary interventions have little effect on ASD symptomatology [330]. Recently, a meta-analysis conducted on four randomized clinical trials revealed significant improvements in the symptoms presented by patients with ASD [305].

To conclude, the effects of LC n-3 PUFAs in clinical trials on ASD have led to mitigating effects. As different risk factors can lead to ASD development, it is quite unclear which treatments or dietary interventions could be efficient in preventing symptoms. However, some clinical studies highlight the beneficial effect of dietary supplementation on symptoms in young autistic patients.

**Table 2.** Interventional studies using LC PUFAs in patients with autistic spectrum disorder (ASD) or ASD-like symptoms. ALA:  $\alpha$ -linolenic acid; ARA: arachidonic acid; DHA: docosahexaenoic acid; EPA: eicosapentaenoic acid; GLA:  $\gamma$ -linolenic acid; LA: linoleic acid, n-9: n-9 PUFAs.

Design	Study (Year)	Ref.	Final Sample Size	Duration	Intervention	Main Outcome(s)
Case reports	Johnson (2003)	[317]	One patient	4 weeks	EPA 540 mg/day	Significant improvements in symptoms.
	Infante (2018)	[312]	One patient	24 months	EPA 204 g/day, DHA 1.2 g/day, vitamin D 25,000 IU/week	Beneficial improvements in psychiatric symptoms.
Open-label trials	Politi (2008)	[310]	19 interventions	6 weeks	EPA + DHA 1.86 g/day, vitamin E 10 mg/day	No significant effects.
	Meiri (2009)	[318]	Nine interventions	12 weeks	EPA 380 mg/day, DHA 180 mg/day	Some improvements.
	Johnson (2010)	[320]	10 interventions	3 months	DHA 400 mg/day	No significant effects.
	Ooi (2015)	[319]	41 interventions	12 weeks	DHA 840 mg/day, EPA 192 mg/day, ARA 66 mg/day, GLA 144 mg/day, vitamin E 60 mg/day, thyme oil mg/day	Improved core symptoms.
	Yui (2016)	[304]	21 controls and 21 interventions	16 weeks	LA 480 mg/day, ALA 240 mg/kg	Beneficial effects on aberrant behaviours and social responsiveness.

Table 2. Cont.

Design	Study (Year)	Ref.	Final Sample Size	Duration	Intervention	Main Outcome(s)
Randomised clinical trials	Amminger (2007)	[321]	Five controls and seven interventions	6 weeks	EPA 0.84 g/day, DHA 0.7 g/day	Improved hyperactivity and stereotypy.
	Bent (2011)	[322]	12 controls and 13 interventions	12 weeks	EPA 0.7 g/day, DHA 0.46 g/day	No significant effects.
	Yui (2011 and 2012)	[323,324]	Six controls and seven interventions	16 weeks	DHA 0.24 g/day, ARA 0.24 g/day	Improvements in social withdrawal and stereotypy.
	Bent (2014)	[325]	28 controls and 29 interventions	6 weeks	EPA 0.7 g/day, DHA 0.46 g/day	No significant effects.
	Voigt (2014)	[326]	15 controls and 19 interventions	6 months	DHA 0.2 g/day	No significant effects.
	Mankad (2015)	[327]	19 controls and 18 interventions	6 months	EPA + DHA 1.5 g/day	No significant effects.
	Parellada (2017)	[328]	68 patients	8 weeks	EPA 577.5–693 mg/day, DHA 385–462 mg/day, vitamin E 1.6–2.01 mg/day	Within subject improvements in social motivation and social communication.
	Boone (2017)	[329]	16 controls and 15 interventions	3 months	EPA 338 mg/day, DHA 225 mg/day, GLA 83 mg/day, n-9 306 mg/day	No significant effects.
	Sheppard (2017)	[315]	12 controls and 12 interventions	3 months	EPA 338 mg/day, DHA 225 mg/day, GLA 83 mg/day, n-9 306 mg/day	Improved gesture and word use.
	Keim (2018)	[316]	16 controls and 15 interventions	3 months	EPA 338 mg/day, DHA 225 mg/day, GLA 83 mg/day, n-9 306 mg/day	Improvements in symptoms, but limited to one subscale.
Mazahery (2019)	[313]	16 controls and 23 interventions	12 months	DHA 722 mg/day, vitamin D 2000 IU/day	Improved irritability.	

### 5.3. Attention Deficits and Hyperactivity Disorder (ADHD)

Attention deficits and hyperactivity disorder (ADHD) is classified as a neurodevelopmental disorder. The prevalence of ADHD is around 8% [331] and is diagnosed in children. Some patients may also develop ADHD into adulthood [332]. According to the Diagnostic and Statistical Manual of Mental Disorders (DSM, fifth version), symptoms of ADHD include impulsivity, inattention as well as social and academic difficulties, although a certain fluidity exists [333]. Depending upon the symptoms, three different types of ADHD can be distinguished: predominantly difficulty in concentration, predominantly hyperactivity and impulsiveness, and finally, a combination of all of the above [334]. ADHD can include a wide range of symptoms such as restlessness, fidgeting, anxiety, attention deficit, distractibility, excessive talking, forgetfulness, and frequent interruption of others [335]. In fact, in several studies, low birth weight, premature birth, infections, or traumas could be considered as potential causes of ADHD [336,337]. A few studies have also found an association between several protein-coding genes and ADHD. These include dopamine transporters (DAT<sub>1</sub>), dopamine (D<sub>4</sub>, D<sub>5</sub>), serotonin (5-HT<sub>1B</sub>), and NMDA 2A receptors [338–340]. Finally, morphological abnormalities were found in the brain of ADHD patients [341–343], although this is frequently disputed in the field. The etiology of ADHD needs to be clarified more precisely.

Patients with ADHD present lower levels of PUFAs in the blood [344–348], which appear to correlate to the symptomatology of ADHD [349]. In a recent cohort of children,

lower dietary intakes of fatty fish and seafood were observed in ADHD patients compared to control patients [350]. Thus, strategies aiming at increasing serum levels of PUFAs have been investigated as potential dietary treatments for the management of ADHD symptoms.

Similar to ASD models, ADHD models in rodents are numerous [351]. Since dopaminergic neurotransmission is markedly altered in ADHD [352–356], animal models have focused on genetic alterations of dopaminergic neurotransmission. Indeed, some studies used dopamine D<sub>2</sub> autoreceptor KO mice to investigate ADHD-like symptoms. These mice display spontaneous hyperlocomotion [357] and impulsivity [358], two features frequently observed in ADHD [359]. Other studies used dopamine transporter (DAT) KO rodents, which also present similarities with human symptomatology. In fact, DAT-KO animals present traits of hyperactivity and motor stereotypy [360–364]. Some studies have evaluated the potential effects of PUFAs on spontaneous hypertensive (SHR) rats, a rodent model of ADHD [365]. Indeed, a study showed a significant correlation between a low level of n-3 PUFAs in the prefrontal cortex in rats and locomotor hyperactivity [366]. Interestingly, in the SHR rat, a reduction in hyper-locomotion was observed following dietary enrichment with LC n-3 PUFAs (LA 1.54% and ALA 0.27%) compared to deficiency in LC n-3 PUFAs (LA 1.58% and ALA 0.01%) [367]. An EPA and DHA-enriched diet during pregnancy in SHR dams enhanced reinforcement-controlled attention in males, and reduced hyperactivity and impulsiveness, while there is no change in females [175]. The authors explained this sex-specific effect to be due to increased turnover ratios of dopamine and serotonin for SHR males in the neostriatum, while there was no change for the females SHR.

A double-blind, randomized clinical trial performed in Iran revealed subtle improvements in ADHD symptoms in patients under standard pharmacology (methylphenidate 1 mg/kg/day) combined with n-3 PUFAs supplementation (EPA 180 mg/day and DHA 120 mg/day) after eight weeks, compared to controls (pharmacological treatment alone) patients [368]. Similarly, n-3 PUFAs supplementation with 93 mg/day of EPA and 29 mg/day of DHA during 15 weeks was able to alleviate ADHD-like symptoms in 104 children [369]. Identical results were found by another study, in which 20–25 mg/kg/day of EPA and 8.5–10.5 mg/kg/day of DHA were consumed for 16 weeks [370], while earlier studies revealed mild improvements in such treatment [371,372]. A recent study on ADHD children (6–18 years old) observed improvements in attention and vigilance after 12 weeks of EPA supplementation (1.2 g/day), while attention was worsened by the treatment in patients presenting higher endogenous EPA levels at enrolment [270]. However, one clinical trial in ADHD children (6–12 years old) found no beneficial effects of PUFAs supplementation (241 mg/day of DHA, 33 mg/day of EPA, and 150 mg/day of n-6 PUFAs) after 10 weeks of treatment [373], when combined with the standard pharmacological treatment (methylphenidate 1 mg/kg/day). A meta-analysis performed on 699 children with ADHD from 10 clinical trials revealed a small but significant effect of n-3 PUFAs supplementation on ADHD symptoms [269], while another study failed to find beneficial effects of such a supplementation [374], which might be explained by very different methodologies in all of the clinical trials investigated. Finally, it was recently suggested that the combination of EPA and DHA could be used as an adjuvant therapy, together with the standard pharmacological treatment, using methylphenidate, to improve the clinical symptomatology in ADHD patients [375]. Table 3 summarises the main outcomes of an open-label trial [375] and randomized clinical trials [270,368–373,376–398] using LC PUFAs in patients with ADHD.

**Table 3.** Interventional studies using LC PUFAs in patients with ADHD. ALA:  $\alpha$ -linolenic acid; ARA: arachidonic acid; DHA: docosahexaenoic acid; EPA: eicosapentaenoic acid; GLA:  $\gamma$ -linolenic acid; LA: linoleic acid; n-3: n-3 PUFAs; n-6: n-6 PUFAs.

Design	Study (Year)	Ref.	Final Sample Size	Duration	Intervention	Main Outcome(s)
Open-label trial	Checa-Ros (2019)	[375]	40 patients	1 month	EPA 70 mg/day, DHA 250 mg/day, methylphenidate 1 mg/kg/day	Improved attention, improved core symptoms
	Aman (1987)	[376]	31 patients	4 weeks	LA 2.16 g/day, GLA 270 mg/day	Only minimal effects.
	Voigt (2001)	[377]	27 controls and 27 interventions	4 months	DHA 345 mg/day	No significant effect.
	Richardson (2002)	[371]	14 controls and 15 interventions	12 weeks	EPA 186 mg/day, DHA 450 mg/day, ALA 96 mg/day, LA 864 mg/day, ARA 42 mg/day, vitamin E 60 IU/day, thyme oil 8 mg/day	General behavioral improvements and small effects.
	Stevens (2003)	[372]	22 controls and 25 interventions	4 months	EPA 80 mg/day, DHA 480 mg/day, GLA 96 mg/day, ARA 40 mg/day, vitamin E 24 mg/day	No clear benefit but some improvements.
	Hirayama (2004)	[378]	20 controls, 20 interventions	2 months	DHA 3.6 g/week	Only minimal effects.
	Sinn (2007)	[369]	27 controls and 36 interventions	15 weeks	EPA 558 mg/day, DHA 174 mg/day, GLA 60 mg/day, vitamin E 10.8 mg/day	Improvements in core symptoms.
Randomized clinical trials	Sinn (2008)	[379]	27–38 controls and 72–88 interventions	15–30 weeks	EPA 558 mg/day, DHA 174 mg/day, GLA 60 mg/day	Improved attention.
	Vaisman (2008)	[380]	21 controls and 21 interventions	3 months	Fish oil 799 mg/day	Improved attention.
	Bélanger (2009)	[370]	13 controls and 13 interventions	16 weeks	EPA 20–25 mg/kg/day, DHA 8.5–10.5 mg/kg/day, vitamin E in traces	Improvements in core symptoms.
	Johnson (2009)	[381]	38 controls and 37 interventions	3–6 months	EPA 558 mg/day, DHA 174 mg/day, GLA 60 mg/day, vitamin E 10.8 mg/day	Improved symptoms in a subgroup.
	Raz (2009)	[382]	31 controls and 32 interventions	7 weeks	LA 480 mg/day, ALA 120 mg/day, vitamin E 10 mg/day, mineral oil 190 mg/day	No significant effect.
	Gustafsson (2010)	[383]	42 controls and 40 interventions	15 weeks	EPA 500 mg/day, DHA 2.7 mg/day, vitamin E 10 mg/day	Improved attention.
	Hariri (2012)	[384]	50 controls and 53 interventions	8 weeks	EPA 635 mg/day, DHA 195 mg/day	Improved symptoms.
Manor (2012)	[385]	47 controls and 100 interventions	15–30 weeks	EPA 80 mg/day, DHA 40 mg/day	Improved impulsivity.	



Table 3. Cont.

Design	Study (Year)	Ref.	Final Sample Size	Duration	Intervention	Main Outcome(s)
Randomized clinical trials	Milte (2012)	[386]	90 patients	12 months	EPA 264–1109 mg/day, DHA 108–1032 mg/day, LA 1467 mg/day	Improved symptoms in a subgroup.
	Milte (2015)	[387]	87 patients	12 months	EPA 264–1109 mg/day, DHA 108–1032 mg/day, LA 1467 mg/day	Improved symptoms in a subgroup.
	Perera (2012)	[388]	46 controls and 48 interventions	6 months	n-3 592.7 mg/day, n-6 361.5 mg/day, methylphenidate 0.7–1 mg/kg/day,	Improved symptoms.
	Behdani (2013)	[389]	33 controls and 36 interventions	8 weeks	EPA 720 mg/day, DHA 480 mg/day, methylphenidate 1 mg/kg/day	No significant effect.
	Dashti (2014)	[398]	28 controls and 28 interventions	3 days	n-3 1 g/day, methylphenidate 0.9–3 mg/kg/day	Improved symptoms.
	Dubnov-Raz (2014)	[390]	Nine controls and eight interventions	8 weeks	ALA 1 g/day	No significant effect.
	Widenhorn-Müller (2014)	[391]	44 controls and 49 interventions	16 weeks	EPA 600 mg/day, DHA 120 mg/day	No significant effect
	Bos (2015)	[392]	19 controls and 19 interventions	16 weeks	EPA 650 mg/day, DHA 650 mg/day	Improved attention.
	Matsudaira (2015)	[393]	36 controls and 33 interventions	12 weeks	EPA 558 mg/day, DHA 174 mg/day, GLA 60 mg/day, vitamin E 9.6 mg/day	No significant effect.
	Anand (2016)	[394]	25 controls and 25 interventions	4 months	EPA 180 mg/day, DHA 120 mg/day	Improved symptoms in a subgroup.
	Salehi (2016)	[395]	50 controls and 50 interventions	8 weeks	EPA 100–400 mg/day, methylphenidate 0.5–1 mg/kg/day	Improved symptoms.
	Assareh (2017)	[373]	40 patients	10 weeks	EPA 35 mg/day, DHA 241 mg/day, n-6 LC PUFAs 150 mg/day, methylphenidate 1 mg/kg/day	No significant effect.
	Barragán (2017)	[396]	30 controls and 30 interventions	12 months	EPA 558 mg/day, DHA 174 mg/day, GLA 60 mg/day, methylphenidate 0.5–1 mg/kg/day	Improved symptoms.
	Kean (2017)	[397]	58 controls and 54 interventions	14 weeks	EPA 21.9–29.2 mg/day, DHA 16.5–22 mg/day, vitamin E 0.67–0.9 mg/day	Improved hyperactivity and inattention.
	Moghaddam (2017)	[368]	40 patients	8 weeks	EPA 180 mg/day, DHA 120 mg/day, methylphenidate 1 mg/kg/day	Improvements in symptoms.
Chang (2019)	[270]	44 controls and 48 interventions	12 weeks	EPA 1.2 g/day	Improved attention and vigilance in patients with low levels of EPA only.	

To conclude, the effects of LC n-3 PUFAs supplementation on ADHD patients are ambiguous. While some studies report beneficial effects, others report no significant effects.

Interventions using LC n-3 PUFAs in patients with neurodevelopmental disorders produced mitigated results. Indeed, in patients with ASD, 11 out of 18 interventions produced beneficial effects (Table 2), while 21 out of 31 interventions produced beneficial/minimal effects in patients with ADHD (Table 3).

#### 5.4. Schizophrenia

Schizophrenia is a complex disorder, which affects 1% of the population worldwide. The main symptoms are hallucinations, delusions, disorganized thought, blunted or inappropriate affect, social withdrawal, and cognitive dysfunction [399]. However, the etiology is still unclear.

The possibility that schizophrenia might arise from abnormal neurodevelopment was hypothesized long ago [400–403]. Emerging evidence suggests that a combined neurodevelopment insult, together with another insult, such as inflammation [404], infection [405], psychological trauma [406], consumption of cannabis [407], or malnutrition [408,409], known as the two-hit hypothesis, can lead to schizophrenia. Dysfunction of a variety of neurotransmitter systems (glutamatergic, serotonergic, and GABAergic) has been reported in schizophrenia [410], while the brain dopamine systems seem to play an important role in the disease [411]. Indeed, hyperactivity of the mesolimbic dopamine pathway could mediate the psychotic symptoms of schizophrenia. In addition, hypofunction of the prefrontal cortex, which appears to involve decreased activity of mesocortical dopamine neurons, has been reported in schizophrenic patients [412]. Importantly, effective anti-psychotic drugs are dopamine D2 receptor (D2R) antagonists. A number of clinical studies report a contribution of LC n-3 PUFA to schizophrenia. In fact, psychosis itself is associated with an imbalanced dietary intake of LC PUFAs [413,414]. Not only low levels of PUFAs have been associated with schizophrenia, but also some genetic alterations of genes involved in the transport and the metabolization of PUFAs have been reported in schizophrenic patients. As an example, SNPs in *Fabp7*, a transporter of LC PUFAs, and *ALOX12*, a gene encoding an enzyme, which metabolizes both ARA and DHA into oxylipins, have been linked to schizophrenia [415,416]. *FADS2* and *iPLA2*, which hydrolyzes DHA in the cell membrane, are highly expressed in the brain of schizophrenic patients [417,418]. Importantly, it is well known that genetic or nutritional suboptimal levels of n-3 PUFA influence the dopaminergic system [419], which is highly involved in several neuropsychiatric disorders, including schizophrenia (recently reviewed in [255,420]).

In rodents, prenatal deficiency in LC PUFAs (ARA and DHA) could model the prodromal state of schizophrenia [421]. Dietary PUFA deficiency resulted in schizophrenic-like symptoms, dysregulated expression of genes involved in oligodendrocyte and GABA activity, and epigenetic silencing of the lipid receptors *Rxr* and *Ppar*, which have also been reported in patients [421]. Similarly, LC n-3 PUFAs deficiency during gestation resulted in prepulse inhibition impairments in mice [422], which parallels the abnormal prepulse inhibition responses in patients with schizophrenia [423–425]. Interestingly, *Fabp3* KO mice, which have impaired brain PUFAs access, exhibit D2R dysfunction, impaired glutamate release in the dorsal striatum and the anterior cingulate cortex [426,427] (ACC), which could be hallmarks of schizophrenia and ADHD [428,429]. A causal link between early-life dietary n-3 PUFA deficiency and dopaminergic system impairment has recently been demonstrated in mice, further reinforcing the importance of dietary n-3 PUFA in dopaminergic function [430]. This reinforces the demonstration that striatal D2R neurons are particularly sensitive to fatty acids in rodents [431]. Indeed, both clinical and preclinical studies suggest that inadequate supply of LC n-3 PUFAs during early brain development leads to altered dopaminergic function and schizophrenic symptoms. This corroborates the observation of reduced DHA in the blood and brain of schizophrenic patients. Altogether, these data support the need for adequate n-3 PUFA supply during the perinatal period to promote adequate neurodevelopment, in particular of the dopaminergic system.

As in other neurodevelopmental diseases, the question of correcting schizophrenic symptoms through the use of dietary supply in LC n-3 PUFAs has been questioned in several clinical studies leading to puzzling results. One study observed preventive effects of LC PUFAs (mainly EPA 700 mg/day, DHA 480 mg/day, and vitamin E 7.6 mg/day, during 12 weeks) on the development of psychosis [432], probably via mechanisms implicated in myelination [433,434]. A recent systematic review has summarized all the interventional studies focused on the link between psychosis and LC PUFAs [435]. Patients suffering from schizophrenia present decreased levels of LC PUFAs in the brain [436] and erythrocytes [437–439]. As such, a study investigated the potential therapeutic benefits of LC PUFAs in schizophrenia. Sixteen weeks of supplementation with LC PUFAs (EPA 700 mg/day and DHA 400 mg/day) provided therapeutic improvements in patients [440]. A 2016 review has summarized all previous clinical trials using LC n-3 PUFAs on schizophrenia [441]. While some clinical trials have proven clear beneficial effects of LC n-3 PUFAs, others resulted in no significant effects [441].

## 6. Conclusions and Future Directions

The understanding of the mechanisms underlying perinatal dietary PUFAs to physiological and pathological brain development remains incomplete. However, significant advancements have been made in recent years, with more understanding of how low levels of LC PUFAs (nutritional and/or genetic) during pregnancy and infancy contribute to the etiopathology of neurodevelopmental disorders. This knowledge is essential to design appropriate nutritional intervention with LC PUFAs in mothers and children with low levels of LC PUFAs, children at risk of impaired neurodevelopment, or women facing at-risk pregnancies. A more comprehensive understanding of the genetic, physiological, and behavioral modulators of EPA and DHA status and response to intervention is needed to allow refinement of current dietary LC n-3 PUFA recommendations and stratification of advice to “vulnerable” and responsive subgroups. Overall, PUFA-based gene-diet interactions in humans should provide a solid scientific basis for the development of personalized nutritional intervention early in life.

**Author Contributions:** Writing, M.M., M.R., M.D.M. and S.L.; supervision, S.L., funding acquisition, S.L. All authors have read and agreed to the published version of the manuscript.

**Funding:** M.R. was supported by the Fondation de France (FDF, #00070700) and Région Nouvelle-Aquitaine (Engagement 00070700 and Convention 2017-1R30237-00013179-POST-DOCTORAT, to S.L.). M.M. and M.D.M. were supported by the Fondation pour la Recherche Médicale (équipe FRM PRINSS DEQ20170336724, to S.L.). This work was supported by the Fondation pour la Recherche sur le Cerveau (Connect, to S.L.) and the Région Nouvelle-Aquitaine (2019-1R3M08).

**Institutional Review Board Statement:** Not applicable.

**Informed Consent Statement:** Not applicable.

**Data Availability Statement:** Not applicable.

**Acknowledgments:** The authors would like to thank all of the funding agencies for their financial supports.

**Conflicts of Interest:** The authors have no conflict of interest.

## References

1. Bazinet, R.P.; Layé, S. Polyunsaturated Fatty Acids and Their Metabolites in Brain Function and Disease. *Nat. Rev. Neurosci.* **2014**, *15*, 771–785. [\[CrossRef\]](#)
2. Simopoulos, A.P. Evolutionary Aspects of Diet: The Omega-6/Omega-3 Ratio and the Brain. *Mol. Neurobiol.* **2011**, *44*, 203–215. [\[CrossRef\]](#)
3. Weiser, M.J.; Butt, C.M.; Mohajeri, M.H. Docosahexaenoic Acid and Cognition throughout the Lifespan. *Nutrients* **2016**, *8*, 99. [\[CrossRef\]](#)
4. Rodríguez, M.; G. Rebollar, P.; Mattioli, S.; Castellini, C. N-3 PUFA Sources (Precursor/Products): A Review of Current Knowledge on Rabbit. *Animals* **2019**, *9*, 806. [\[CrossRef\]](#)

5. Smink, W.; Gerrits, W.J.J.; Gloaguen, M.; Ruiter, A.; van Baal, J. Linoleic and  $\alpha$ -Linolenic Acid as Precursor and Inhibitor for the Synthesis of Long-Chain Polyunsaturated Fatty Acids in Liver and Brain of Growing Pigs. *Anim. Int. J. Anim. Biosci.* **2012**, *6*, 262–270. [[CrossRef](#)] [[PubMed](#)]
6. Lauritzen, L.; Brambilla, P.; Mazzocchi, A.; Harsløf, L.B.S.; Ciappolino, V.; Agostoni, C. DHA Effects in Brain Development and Function. *Nutrients* **2016**, *8*, 6. [[CrossRef](#)]
7. Layé, S.; Nadjar, A.; Joffre, C.; Bazinet, R.P. Anti-Inflammatory Effects of Omega-3 Fatty Acids in the Brain: Physiological Mechanisms and Relevance to Pharmacology. *Pharmacol. Rev.* **2018**, *70*, 12–38. [[CrossRef](#)] [[PubMed](#)]
8. De Giuseppe, R.; Roggi, C.; Cena, H. N-3 LC-PUFA Supplementation: Effects on Infant and Maternal Outcomes. *Eur. J. Nutr.* **2014**, *53*, 1147–1154. [[CrossRef](#)] [[PubMed](#)]
9. Medicine, I. *Dietary Reference Intakes for Energy, Carbohydrate, Fiber, Fat, Fatty Acids, Cholesterol, Protein, and Amino Acids*; National Academy Press: Washington, DC, USA, 2002; ISBN 978-0-309-08525-0.
10. Lauterbach, R. EPA+DHA in Prevention of Early Preterm Birth—Do We Know How to Apply It? *EBioMedicine* **2018**, *35*, 16–17. [[CrossRef](#)]
11. Barkia, I.; Saari, N.; Manning, S.R. Microalgae for High-Value Products Towards Human Health and Nutrition. *Mar. Drugs* **2019**, *17*, 304. [[CrossRef](#)]
12. Jakobsson, A.; Westerberg, R.; Jacobsson, A. Fatty Acid Elongases in Mammals: Their Regulation and Roles in Metabolism. *Prog. Lipid Res.* **2006**, *45*, 237–249. [[CrossRef](#)] [[PubMed](#)]
13. Marquardt, A.; Stöhr, H.; White, K.; Weber, B.H. CDNA Cloning, Genomic Structure, and Chromosomal Localization of Three Members of the Human Fatty Acid Desaturase Family. *Genomics* **2000**, *66*, 175–183. [[CrossRef](#)] [[PubMed](#)]
14. Poulos, A.; Sharp, P.; Johnson, D.; Easton, C. The Occurrence of Polyenoic Very Long Chain Fatty Acids with Greater than 32 Carbon Atoms in Molecular Species of Phosphatidylcholine in Normal and Peroxisome-Deficient (Zellweger’s Syndrome) Brain. *Biochem. J.* **1988**, *253*, 645–650. [[CrossRef](#)] [[PubMed](#)]
15. Robinson, B.S.; Johnson, D.W.; Poulos, A. Unique Molecular Species of Phosphatidylcholine Containing Very-Long-Chain (C24–C38) Polyenoic Fatty Acids in Rat Brain. *Biochem. J.* **1990**, *265*, 763–767. [[CrossRef](#)]
16. Yu, M.; Benham, A.; Logan, S.; Brush, R.S.; Mandal, M.N.A.; Anderson, R.E.; Agbaga, M.-P. ELOVL4 Protein Preferentially Elongates 20:5n3 to Very Long Chain PUFAs over 20:4n6 and 22:6n3. *J. Lipid Res.* **2012**, *53*, 494–504. [[CrossRef](#)] [[PubMed](#)]
17. Hopiavuori, B.R.; Deák, F.; Wilkerson, J.L.; Brush, R.S.; Rocha-Hopiavuori, N.A.; Hopiavuori, A.R.; Ozan, K.G.; Sullivan, M.T.; Wren, J.D.; Georgescu, C.; et al. Homozygous Expression of Mutant ELOVL4 Leads to Seizures and Death in a Novel Animal Model of Very Long-Chain Fatty Acid Deficiency. *Mol. Neurobiol.* **2018**, *55*, 1795–1813. [[CrossRef](#)] [[PubMed](#)]
18. Morales, E.; Bustamante, M.; Gonzalez, J.R.; Guxens, M.; Torrent, M.; Mendez, M.; Garcia-Esteban, R.; Julvez, J.; Forn, J.; Vrijheid, M.; et al. Genetic Variants of the FADS Gene Cluster and ELOVL Gene Family, Colostrums LC-PUFA Levels, Breastfeeding, and Child Cognition. *PLoS ONE* **2011**, *6*, e17181. [[CrossRef](#)]
19. de Groot, R.H.M.; Emmett, R.; Meyer, B.J. Non-Dietary Factors Associated with n-3 Long-Chain PUFA Levels in Humans—A Systematic Literature Review. *Br. J. Nutr.* **2019**, *121*, 793–808. [[CrossRef](#)] [[PubMed](#)]
20. Tanaka, T.; Shen, J.; Abecasis, G.R.; Kisiailiou, A.; Ordovas, J.M.; Guralnik, J.M.; Singleton, A.; Bandinelli, S.; Cherubini, A.; Arnett, D.; et al. Genome-Wide Association Study of Plasma Polyunsaturated Fatty Acids in the InCHIANTI Study. *PLoS Genet.* **2009**, *5*, e1000338. [[CrossRef](#)] [[PubMed](#)]
21. Muc, M.; Kreiner-Møller, E.; Larsen, J.M.; Birch, S.; Brix, S.; Bisgaard, H.; Lauritzen, L. Maternal Fatty Acid Desaturase Genotype Correlates with Infant Immune Responses at 6 Months. *Br. J. Nutr.* **2015**, *114*, 891–898. [[CrossRef](#)] [[PubMed](#)]
22. Burdge, G.C.; Tan, S.-Y.; Henry, C.J. Long-Chain n-3 PUFA in Vegetarian Women: A Metabolic Perspective. *J. Nutr. Sci.* **2017**, *6*, e58. [[CrossRef](#)]
23. Helland, I.B.; Saugstad, O.D.; Smith, L.; Saarem, K.; Solvoll, K.; Ganes, T.; Drevon, C.A. Similar Effects on Infants of N-3 and n-6 Fatty Acids Supplementation to Pregnant and Lactating Women. *Pediatrics* **2001**, *108*, E82. [[CrossRef](#)]
24. Chilton, F.H.; Dutta, R.; Reynolds, L.M.; Sergeant, S.; Mathias, R.A.; Seeds, M.C. Precision Nutrition and Omega-3 Polyunsaturated Fatty Acids: A Case for Personalized Supplementation Approaches for the Prevention and Management of Human Diseases. *Nutrients* **2017**, *9*, 1165. [[CrossRef](#)] [[PubMed](#)]
25. Ameer, A.; Enroth, S.; Johansson, A.; Zabolli, G.; Igl, W.; Johansson, A.C.V.; Rivas, M.A.; Daly, M.J.; Schmitz, G.; Hicks, A.A.; et al. Genetic Adaptation of Fatty-Acid Metabolism: A Human-Specific Haplotype Increasing the Biosynthesis of Long-Chain Omega-3 and Omega-6 Fatty Acids. *Am. J. Hum. Genet.* **2012**, *90*, 809–820. [[CrossRef](#)] [[PubMed](#)]
26. Calder, P.C. Omega-3 Polyunsaturated Fatty Acids and Inflammatory Processes: Nutrition or Pharmacology? *Br. J. Clin. Pharmacol.* **2013**, *75*, 645–662. [[CrossRef](#)]
27. Dennis, E.A.; Norris, P.C. Eicosanoid Storm in Infection and Inflammation. *Nat. Rev. Immunol.* **2015**, *15*, 511–523. [[CrossRef](#)]
28. Bazan, N.G. Docosanoids and Elovanooids from Omega-3 Fatty Acids Are pro-Homeostatic Modulators of Inflammatory Responses, Cell Damage and Neuroprotection. *Mol. Aspects Med.* **2018**, *64*, 18–33. [[CrossRef](#)] [[PubMed](#)]
29. Serhan, C.N.; Levy, B.D. Resolvins in Inflammation: Emergence of the pro-Resolving Superfamily of Mediators. *J. Clin. Invest.* **2018**, *128*, 2657–2669. [[CrossRef](#)]
30. Sosa-Castillo, E.; Rodríguez-Cruz, M.; Moltó-Puigmartí, C. Genomics of Lactation: Role of Nutrigenomics and Nutrigenetics in the Fatty Acid Composition of Human Milk. *Br. J. Nutr.* **2017**, *118*, 161–168. [[CrossRef](#)] [[PubMed](#)]
31. Sastry, P.S. Lipids of Nervous Tissue: Composition and Metabolism. *Prog. Lipid Res.* **1985**, *24*, 69–176. [[CrossRef](#)]

32. McNamara, R.K.; Carlson, S.E. Role of Omega-3 Fatty Acids in Brain Development and Function: Potential Implications for the Pathogenesis and Prevention of Psychopathology. *Prostaglandins Leukot. Essent. Fatty Acids* **2006**, *75*, 329–349. [[CrossRef](#)] [[PubMed](#)]
33. Joffre, C.; Dinel, A.L.; Aubert, A.; Fressange-Mazda, C.; Le Ruyet, P.; Layé, S. Impact of Lactobacillus Fermentum and Dairy Lipids in the Maternal Diet on the Fatty Acid Composition of Pups' Brain and Peripheral Tissues. *Prostaglandins Leukot. Essent. Fatty Acids* **2016**, *115*, 24–34. [[CrossRef](#)] [[PubMed](#)]
34. Garcia, M.C.; Ward, G.; Ma, Y.C.; Salem, N.; Kim, H.Y. Effect of Docosahexaenoic Acid on the Synthesis of Phosphatidylserine in Rat Brain in Microsomes and C6 Glioma Cells. *J. Neurochem.* **1998**, *70*, 24–30. [[CrossRef](#)]
35. Bascoul-Colombo, C.; Guschina, I.A.; Maskrey, B.H.; Good, M.; O'Donnell, V.B.; Harwood, J.L. Dietary DHA Supplementation Causes Selective Changes in Phospholipids from Different Brain Regions in Both Wild Type Mice and the Tg2576 Mouse Model of Alzheimer's Disease. *Biochim. Biophys. Acta* **2016**, *1861*, 524–537. [[CrossRef](#)] [[PubMed](#)]
36. Brenna, J.T.; Diau, G.-Y. The Influence of Dietary Docosahexaenoic Acid and Arachidonic Acid on Central Nervous System Polyunsaturated Fatty Acid Composition. *Prostaglandins Leukot. Essent. Fatty Acids* **2007**, *77*, 247–250. [[CrossRef](#)] [[PubMed](#)]
37. Di Miceli, M.; Bosch-Bouju, C.; Layé, S. Polyunsaturated Fatty Acids and Their Derivatives in Neurotransmission and Synapses: A New Hallmark of Synaptopathies. *Proc. Nutr. Soc.* **2020**, *79*, 388–403. [[CrossRef](#)]
38. O'Brien, J.S. Stability Of The Myelin Membrane. *Science* **1965**, *147*, 1099–1107. [[CrossRef](#)] [[PubMed](#)]
39. Poitelon, Y.; Kopec, A.M.; Belin, S. Myelin Fat Facts: An Overview of Lipids and Fatty Acid Metabolism. *Cells* **2020**, *9*, 812. [[CrossRef](#)]
40. Cao, D.; Kevala, K.; Kim, J.; Moon, H.-S.; Jun, S.B.; Lovinger, D.; Kim, H.-Y. Docosahexaenoic Acid Promotes Hippocampal Neuronal Development and Synaptic Function. *J. Neurochem.* **2009**, *111*, 510–521. [[CrossRef](#)]
41. Kim, H.-Y.; Spector, A.A. N-Docosahexaenoylethanolamine: A Neurotrophic and Neuroprotective Metabolite of Docosahexaenoic Acid. *Mol. Aspects Med.* **2018**, *64*, 34–44. [[CrossRef](#)]
42. Makrides, M.; Neumann, M.A.; Byard, R.W.; Simmer, K.; Gibson, R.A. Fatty Acid Composition of Brain, Retina, and Erythrocytes in Breast- and Formula-Fed Infants. *Am. J. Clin. Nutr.* **1994**, *60*, 189–194. [[CrossRef](#)]
43. Haggarty, P. Fatty Acid Supply to the Human Fetus. *Annu. Rev. Nutr.* **2010**, *30*, 237–255. [[CrossRef](#)]
44. Lauritzen, L.; Hansen, H.S.; Jørgensen, M.H.; Michaelsen, K.F. The Essentiality of Long Chain N-3 Fatty Acids in Relation to Development and Function of the Brain and Retina. *Prog. Lipid Res.* **2001**, *40*, 1–94. [[CrossRef](#)]
45. Clandinin, M.T.; Chappell, J.E.; Leong, S.; Heim, T.; Swyer, P.R.; Chance, G.W. Intrauterine Fatty Acid Accretion Rates in Human Brain: Implications for Fatty Acid Requirements. *Early Hum. Dev.* **1980**, *4*, 121–129. [[CrossRef](#)]
46. Percy, P.; Percy, A.; Vilbergsson, G.; Månsson, J.E. Polyunsaturated Fatty Acid Accretion in First- and Second-Trimester Human Fetal Brain: Lack of Correlation with Levels in Paired Placental Samples. *Biochem. Mol. Med.* **1996**, *59*, 38–43. [[CrossRef](#)]
47. Martinez, M. Developmental Profiles of Polyunsaturated Fatty Acids in the Brain of Normal Infants and Patients with Peroxisomal Diseases: Severe Deficiency of Docosahexaenoic Acid in Zellweger's and Pseudo-Zellweger's Syndromes. *World Rev. Nutr. Diet.* **1991**, *66*, 87–102. [[CrossRef](#)] [[PubMed](#)]
48. Kuipers, R.S.; Luxwolda, M.F.; Offringa, P.J.; Boersma, E.R.; Dijck-Brouwer, D.A.J.; Muskiet, F.A.J. Fetal Intrauterine Whole Body Linoleic, Arachidonic and Docosahexaenoic Acid Contents and Accretion Rates. *Prostaglandins Leukot. Essent. Fatty Acids* **2012**, *86*, 13–20. [[CrossRef](#)]
49. Metherel, A.H.; Kitson, A.P.; Domenichiello, A.F.; Lacombe, R.J.S.; Hopperton, K.E.; Trépanier, M.-O.; Alashmali, S.M.; Lin, L.; Bazinet, R.P. Maternal Liver Docosahexaenoic Acid (DHA) Stores Are Increased via Higher Serum Unesterified DHA Uptake in Pregnant Long Evans Rats. *J. Nutr. Biochem.* **2017**, *46*, 143–150. [[CrossRef](#)]
50. Metherel, A.H.; Kitson, A.P.; Domenichiello, A.F.; Lacombe, R.J.S.; Hopperton, K.E.; Trépanier, M.-O.; Alashmali, S.M.; Lin, L.; Bazinet, R.P. Docosahexaenoic Acid (DHA) Accretion in the Placenta but Not the Fetus Is Matched by Plasma Unesterified DHA Uptake Rates in Pregnant Long Evans Rats. *Placenta* **2017**, *58*, 90–97. [[CrossRef](#)] [[PubMed](#)]
51. Sinclair, A.J.; Crawford, M.A. The Incorporation of Linolenic Acid and Docosahexaenoic Acid into Liver and Brain Lipids of Developing Rats. *FEBS Lett.* **1972**, *26*, 127–129. [[CrossRef](#)]
52. Calderon, F.; Kim, H.-Y. Docosahexaenoic Acid Promotes Neurite Growth in Hippocampal Neurons. *J. Neurochem.* **2004**, *90*, 979–988. [[CrossRef](#)]
53. Sidhu, V.K.; Huang, B.X.; Kim, H.-Y. Effects of Docosahexaenoic Acid on Mouse Brain Synaptic Plasma Membrane Proteome Analyzed by Mass Spectrometry and (16)O/(18)O Labeling. *J. Proteome Res.* **2011**, *10*, 5472–5480. [[CrossRef](#)] [[PubMed](#)]
54. Champeil-Potokar, G.; Chaumontet, C.; Guesnet, P.; Lavalie, M.; Denis, I. Docosahexaenoic Acid (22:6n-3) Enrichment of Membrane Phospholipids Increases Gap Junction Coupling Capacity in Cultured Astrocytes. *Eur. J. Neurosci.* **2006**, *24*, 3084–3090. [[CrossRef](#)]
55. Rey, C.; Nadjar, A.; Joffre, F.; Amadiou, C.; Aubert, A.; Vaysse, C.; Pallet, V.; Layé, S.; Joffre, C. Maternal N-3 Polyunsaturated Fatty Acid Dietary Supply Modulates Microglia Lipid Content in the Offspring. *Prostaglandins Leukot. Essent. Fatty Acids* **2018**, *133*, 1–7. [[CrossRef](#)] [[PubMed](#)]
56. Yeh, Y.Y.; Gehman, M.F.; Yeh, S.M. Maternal Dietary Fish Oil Enriches Docosahexaenoate Levels in Brain Subcellular Fractions of Offspring. *J. Neurosci. Res.* **1993**, *35*, 218–226. [[CrossRef](#)]
57. Brand, A.; Schonfeld, E.; Isharel, I.; Yavin, E. Docosahexaenoic Acid-Dependent Iron Accumulation in Oligodendroglia Cells Protects from Hydrogen Peroxide-Induced Damage. *J. Neurochem.* **2008**, *105*, 1325–1335. [[CrossRef](#)] [[PubMed](#)]

58. Harel, T.; Quek, D.Q.Y.; Wong, B.H.; Cazenave-Gassiot, A.; Wenk, M.R.; Fan, H.; Berger, I.; Shmueli, D.; Shaag, A.; Silver, D.L.; et al. Homozygous Mutation in MFSD2A, Encoding a Lysolipid Transporter for Docosahexanoic Acid, Is Associated with Microcephaly and Hypomyelination. *Neurogenetics* **2018**, *19*, 227–235. [[CrossRef](#)] [[PubMed](#)]
59. Madore, C.; Leyrolle, Q.; Morel, L.; Rossitto, M.; Greenhalgh, A.D.; Delpech, J.C.; Martinat, M.; Bosch-Bouju, C.; Bourel, J.; Rani, B.; et al. Essential Omega-3 Fatty Acids Tune Microglial Phagocytosis of Synaptic Elements in the Mouse Developing Brain. *Nat. Commun.* **2020**, *11*, 6133. [[CrossRef](#)] [[PubMed](#)]
60. Bazinet, R.P.; Metherel, A.H.; Chen, C.T.; Shaikh, S.R.; Nadjar, A.; Joffre, C.; Layé, S. Brain Eicosapentaenoic Acid Metabolism as a Lead for Novel Therapeutics in Major Depression. *Brain. Behav. Immun.* **2020**, *85*, 21–28. [[CrossRef](#)]
61. Lapillonne, A.; Moltu, S.J. Long-Chain Polyunsaturated Fatty Acids and Clinical Outcomes of Preterm Infants. *Ann. Nutr. Metab.* **2016**, *69* (Suppl. 1), 35–44. [[CrossRef](#)]
62. Martinez, M. Tissue Levels of Polyunsaturated Fatty Acids during Early Human Development. *J. Pediatr.* **1992**, *120*, S129–S138. [[CrossRef](#)]
63. Larqué, E.; Krauss-Etschmann, S.; Campoy, C.; Hartl, D.; Linde, J.; Klingler, M.; Demmelmair, H.; Caño, A.; Gil, A.; Bondy, B.; et al. Docosahexanoic Acid Supply in Pregnancy Affects Placental Expression of Fatty Acid Transport Proteins. *Am. J. Clin. Nutr.* **2006**, *84*, 853–861. [[CrossRef](#)]
64. Innis, S.M. Polyunsaturated Fatty Acids in Human Milk: An Essential Role in Infant Development. *Adv. Exp. Med. Biol.* **2004**, *554*, 27–43. [[CrossRef](#)] [[PubMed](#)]
65. Innis, S.M.; Friesen, R.W. Essential N-3 Fatty Acids in Pregnant Women and Early Visual Acuity Maturation in Term Infants. *Am. J. Clin. Nutr.* **2008**, *87*, 548–557. [[CrossRef](#)]
66. Gibson, R.A.; Neumann, M.A.; Makrides, M. Effect of Dietary Docosahexanoic Acid on Brain Composition and Neural Function in Term Infants. *Lipids* **1996**, *31*, S177–S181. [[CrossRef](#)] [[PubMed](#)]
67. Wierzejska, R.; Jarosz, M.; Wojda, B.; Siuba-Strzelińska, M. Dietary Intake of DHA during Pregnancy: A Significant Gap between the Actual Intake and Current Nutritional Recommendations. *Rocz. Panstw. Zakl. Hig.* **2018**, *69*, 381–386. [[CrossRef](#)] [[PubMed](#)]
68. Ramsden, C.E.; Makrides, M.; Yuan, Z.-X.; Horowitz, M.S.; Zamora, D.; Yelland, L.N.; Best, K.; Jensen, J.; Taha, A.Y.; Gibson, R.A. Plasma Oxylipins and Unesterified Precursor Fatty Acids Are Altered by DHA Supplementation in Pregnancy: Can They Help Predict Risk of Preterm Birth? *Prostaglandins Leukot. Essent. Fatty Acids* **2020**, *153*, 102041. [[CrossRef](#)]
69. von Schacky, C. Omega-3 Fatty Acids in Pregnancy—The Case for a Target Omega-3 Index. *Nutrients* **2020**, *12*, 898. [[CrossRef](#)]
70. Yelland, L.N.; Gajewski, B.J.; Colombo, J.; Gibson, R.A.; Makrides, M.; Carlson, S.E. Predicting the Effect of Maternal Docosahexanoic Acid (DHA) Supplementation to Reduce Early Preterm Birth in Australia and the United States Using Results of within Country Randomized Controlled Trials. *Prostaglandins Leukot. Essent. Fatty Acids* **2016**, *112*, 44–49. [[CrossRef](#)]
71. Makrides, M.; Gibson, R.A.; McPhee, A.J.; Yelland, L.; Quinlivan, J.; Ryan, P.; DOMInO Investigative Team. Effect of DHA Supplementation during Pregnancy on Maternal Depression and Neurodevelopment of Young Children: A Randomized Controlled Trial. *JAMA* **2010**, *304*, 1675–1683. [[CrossRef](#)]
72. Zhou, S.J.; Best, K.; Gibson, R.; McPhee, A.; Yelland, L.; Quinlivan, J.; Makrides, M. Study Protocol for a Randomised Controlled Trial Evaluating the Effect of Prenatal Omega-3 LCPUFA Supplementation to Reduce the Incidence of Preterm Birth: The ORIP Trial. *BMJ Open* **2017**, *7*, e018360. [[CrossRef](#)] [[PubMed](#)]
73. Makrides, M.; Best, K.; Yelland, L.; McPhee, A.; Zhou, S.; Quinlivan, J.; Dodd, J.; Atkinson, E.; Safa, H.; van Dam, J.; et al. A Randomized Trial of Prenatal N-3 Fatty Acid Supplementation and Preterm Delivery. *N. Engl. J. Med.* **2019**, *381*, 1035–1045. [[CrossRef](#)]
74. Olsen, S.F.; Halldorsson, T.I.; Thorne-Lyman, A.L.; Strøm, M.; Gørtz, S.; Granstrøm, C.; Nielsen, P.H.; Wohlfahrt, J.; Lykke, J.A.; Langhoff-Roos, J.; et al. Plasma Concentrations of Long Chain N-3 Fatty Acids in Early and Mid-Pregnancy and Risk of Early Preterm Birth. *EBioMedicine* **2018**, *35*, 325–333. [[CrossRef](#)]
75. Lorentzen, B.; Drevon, C.A.; Endresen, M.J.; Henriksen, T. Fatty Acid Pattern of Esterified and Free Fatty Acids in Sera of Women with Normal and Pre-Eclamptic Pregnancy. *Br. J. Obstet. Gynaecol.* **1995**, *102*, 530–537. [[CrossRef](#)] [[PubMed](#)]
76. Campbell, F.M.; Bush, P.G.; Veerkamp, J.H.; Dutta-Roy, A.K. Detection and Cellular Localization of Plasma Membrane-Associated and Cytoplasmic Fatty Acid-Binding Proteins in Human Placenta. *Placenta* **1998**, *19*, 409–415. [[CrossRef](#)]
77. Campbell, F.M.; Dutta-Roy, A.K. Plasma Membrane Fatty Acid-Binding Protein (FABPpm) Is Exclusively Located in the Maternal Facing Membranes of the Human Placenta. *FEBS Lett.* **1995**, *375*, 227–230. [[CrossRef](#)]
78. Gil-Sánchez, A.; Larqué, E.; Demmelmair, H.; Acien, M.I.; Faber, F.L.; Parrilla, J.J.; Koletzko, B. Maternal-Fetal in Vivo Transfer of [<sup>13</sup>C]Docosahexanoic and Other Fatty Acids across the Human Placenta 12 h after Maternal Oral Intake. *Am. J. Clin. Nutr.* **2010**, *92*, 115–122. [[CrossRef](#)]
79. Biron-Shental, T.; Schaiff, W.T.; Ratajczak, C.K.; Bildirici, I.; Nelson, D.M.; Sadovsky, Y. Hypoxia Regulates the Expression of Fatty Acid-Binding Proteins in Primary Term Human Trophoblasts. *Am. J. Obstet. Gynecol.* **2007**, *197*, 516.e1–516.e6. [[CrossRef](#)] [[PubMed](#)]
80. Leroy, C.; Tobin, K.A.R.; Basak, S.; Cathrine Staff, A.; Duttaroy, A.K. Fatty Acid-Binding Protein3 Expression in BeWo Cells, a Human Placental Choriocarcinoma Cell Line. *Prostaglandins Leukot. Essent. Fatty Acids* **2017**, *120*, 1–7. [[CrossRef](#)]
81. Islam, A.; Kagawa, Y.; Sharifi, K.; Ebrahimi, M.; Miyazaki, H.; Yasumoto, Y.; Kawamura, S.; Yamamoto, Y.; Sakaguti, S.; Sawada, T.; et al. Fatty Acid Binding Protein 3 Is Involved in N-3 and n-6 PUFA Transport in Mouse Trophoblasts. *J. Nutr.* **2014**, *144*, 1509–1516. [[CrossRef](#)] [[PubMed](#)]

82. Makkar, A.; Mishima, T.; Chang, G.; Scifres, C.; Sadovsky, Y. Fatty Acid Binding Protein-4 Is Expressed in the Mouse Placental Labyrinth, yet Is Dispensable for Placental Triglyceride Accumulation and Fetal Growth. *Placenta* **2014**, *35*, 802–807. [[CrossRef](#)] [[PubMed](#)]
83. Díaz, P.; Harris, J.; Rosario, F.J.; Powell, T.L.; Jansson, T. Increased Placental Fatty Acid Transporter 6 and Binding Protein 3 Expression and Fetal Liver Lipid Accumulation in a Mouse Model of Obesity in Pregnancy. *Am. J. Physiol. Regul. Integr. Comp. Physiol.* **2015**, *309*, R1569–R1577. [[CrossRef](#)] [[PubMed](#)]
84. Lewis, R.M.; Wadsack, C.; Desoye, G. Placental Fatty Acid Transfer. *Curr. Opin. Clin. Nutr. Metab. Care* **2018**, *21*, 78–82. [[CrossRef](#)] [[PubMed](#)]
85. Hanebutt, F.L.; Demmelmair, H.; Schiessl, B.; Larqué, E.; Koletzko, B. Long-Chain Polyunsaturated Fatty Acid (LC-PUFA) Transfer across the Placenta. *Clin. Nutr. Edinb. Scotl.* **2008**, *27*, 685–693. [[CrossRef](#)]
86. Innis, S.M. Essential Fatty Acid Transfer and Fetal Development. *Placenta* **2005**, *26* (Suppl. A), S70–S75. [[CrossRef](#)] [[PubMed](#)]
87. Chen, C.T.; Kitson, A.P.; Hopperton, K.E.; Domenichiello, A.F.; Trépanier, M.-O.; Lin, L.E.; Ermini, L.; Post, M.; Thies, F.; Bazinet, R.P. Plasma Non-Esterified Docosahexaenoic Acid Is the Major Pool Supplying the Brain. *Sci. Rep.* **2015**, *5*. [[CrossRef](#)]
88. Lacombe, R.J.S.; Chouinard-Watkins, R.; Bazinet, R.P. Brain Docosahexaenoic Acid Uptake and Metabolism. *Mol. Aspects Med.* **2018**, *64*, 109–134. [[CrossRef](#)] [[PubMed](#)]
89. Duttaroy, A.K. Transport of Fatty Acids across the Human Placenta: A Review. *Prog. Lipid Res.* **2009**, *48*, 52–61. [[CrossRef](#)]
90. Zhao, Z.; Nelson, A.R.; Betsholtz, C.; Zlokovic, B.V. Establishment and Dysfunction of the Blood-Brain Barrier. *Cell* **2015**, *163*, 1064–1078. [[CrossRef](#)] [[PubMed](#)]
91. Nguyen, L.N.; Ma, D.; Shui, G.; Wong, P.; Cazenave-Gassiot, A.; Zhang, X.; Wenk, M.R.; Goh, E.L.K.; Silver, D.L. Mfsd2a Is a Transporter for the Essential Omega-3 Fatty Acid Docosahexaenoic Acid. *Nature* **2014**, *509*, 503–506. [[CrossRef](#)] [[PubMed](#)]
92. Chan, J.P.; Wong, B.H.; Chin, C.F.; Galam, D.L.A.; Foo, J.C.; Wong, L.C.; Ghosh, S.; Wenk, M.R.; Cazenave-Gassiot, A.; Silver, D.L. The Lysolipid Transporter Mfsd2a Regulates Lipogenesis in the Developing Brain. *PLoS Biol.* **2018**, *16*, e2006443. [[CrossRef](#)] [[PubMed](#)]
93. Ben-Zvi, A.; Lacoste, B.; Kur, E.; Andreone, B.J.; Mayshar, Y.; Yan, H.; Gu, C. Mfsd2a Is Critical for the Formation and Function of the Blood-Brain Barrier. *Nature* **2014**, *509*, 507–511. [[CrossRef](#)] [[PubMed](#)]
94. Andreone, B.J.; Chow, B.W.; Tata, A.; Lacoste, B.; Ben-Zvi, A.; Bullock, K.; Deik, A.A.; Ginty, D.D.; Clish, C.B.; Gu, C. Blood-Brain Barrier Permeability Is Regulated by Lipid Transport-Dependent Suppression of Caveolae-Mediated Transcytosis. *Neuron* **2017**, *94*, 581–594.e5. [[CrossRef](#)] [[PubMed](#)]
95. Prieto-Sánchez, M.T.; Ruiz-Palacios, M.; Blanco-Carnero, J.E.; Pagan, A.; Hellmuth, C.; Uhl, O.; Peissner, W.; Ruiz-Alcaraz, A.J.; Parrilla, J.J.; Koletzko, B.; et al. Placental MFSD2a Transporter Is Related to Decreased DHA in Cord Blood of Women with Treated Gestational Diabetes. *Clin. Nutr. Edinb. Scotl.* **2017**, *36*, 513–521. [[CrossRef](#)]
96. Duttaroy, A.K.; Basak, S. Maternal Dietary Fatty Acids and Their Roles in Human Placental Development. *Prostaglandins Leukot. Essent. Fatty Acids* **2020**, *155*, 102080. [[CrossRef](#)] [[PubMed](#)]
97. Alakbarzade, V.; Hameed, A.; Quek, D.Q.Y.; Chioza, B.A.; Baple, E.L.; Cazenave-Gassiot, A.; Nguyen, L.N.; Wenk, M.R.; Ahmad, A.Q.; Sreekantan-Nair, A.; et al. A Partially Inactivating Mutation in the Sodium-Dependent Lysophosphatidylcholine Transporter MFSD2A Causes a Non-Lethal Microcephaly Syndrome. *Nat. Genet.* **2015**, *47*, 814–817. [[CrossRef](#)]
98. Gumez-Gamboa, A.; Nguyen, L.N.; Yang, H.; Zaki, M.S.; Kara, M.; Ben-Omran, T.; Akizu, N.; Rosti, R.O.; Rosti, B.; Scott, E.; et al. Inactivating Mutations in MFSD2A, Required for Omega-3 Fatty Acid Transport in Brain, Cause a Lethal Microcephaly Syndrome. *Nat. Genet.* **2015**, *47*, 809–813. [[CrossRef](#)]
99. Zhou, J.; Chi, X.; Cheng, M.; Huang, X.; Liu, X.; Fan, J.; Xu, H.; Lin, T.; Shi, L.; Qin, C.; et al. Zika Virus Degrades the  $\omega$ -3 Fatty Acid Transporter Mfsd2a in Brain Microvascular Endothelial Cells and Impairs Lipid Homeostasis. *Sci. Adv.* **2019**, *5*. [[CrossRef](#)]
100. Shimomura, I.; Shimano, H.; Horton, J.D.; Goldstein, J.L.; Brown, M.S. Differential Expression of Exons 1a and 1c in MRNAs for Sterol Regulatory Element Binding Protein-1 in Human and Mouse Organs and Cultured Cells. *J. Clin. Invest.* **1997**, *99*, 838–845. [[CrossRef](#)]
101. Zhu, H.; Fan, C.; Xu, F.; Tian, C.; Zhang, F.; Qi, K. Dietary Fish Oil N-3 Polyunsaturated Fatty Acids and Alpha-Linolenic Acid Differently Affect Brain Accretion of Docosahexaenoic Acid and Expression of Desaturases and Sterol Regulatory Element-Binding Protein 1 in Mice. *J. Nutr. Biochem.* **2010**, *21*, 954–960. [[CrossRef](#)]
102. Chen, Y.; Bang, S.; McMullen, M.F.; Kazi, H.; Talbot, K.; Ho, M.-X.; Carlson, G.; Arnold, S.E.; Ong, W.-Y.; Kim, S.F. Neuronal Activity-Induced Sterol Regulatory Element Binding Protein-1 (SREBP1) Is Disrupted in Dysbindin-Null Mice-Potential Link to Cognitive Impairment in Schizophrenia. *Mol. Neurobiol.* **2017**, *54*, 1699–1709. [[CrossRef](#)] [[PubMed](#)]
103. Lee, S.; Kang, S.; Ang, M.J.; Kim, J.; Kim, J.C.; Kim, S.-H.; Jeon, T.-I.; Jung, C.; Im, S.-S.; Moon, C. Deficiency of Sterol Regulatory Element-Binding Protein-1c Induces Schizophrenia-like Behavior in Mice. *Genes Brain Behav.* **2019**, *18*, e12540. [[CrossRef](#)]
104. Brenna, J.T.; Varamini, B.; Jensen, R.G.; Diersen-Schade, D.A.; Boettcher, J.A.; Arterburn, L.M. Docosahexaenoic and Arachidonic Acid Concentrations in Human Breast Milk Worldwide. *Am. J. Clin. Nutr.* **2007**, *85*, 1457–1464. [[CrossRef](#)]
105. Duttaroy, A.K. Fetal Growth and Development: Roles of Fatty Acid Transport Proteins and Nuclear Transcription Factors in Human Placenta. *Indian J. Exp. Biol.* **2004**, *42*, 747–757.
106. Farquharson, J.; Cockburn, F.; Patrick, W.A.; Jamieson, E.C.; Logan, R.W. Infant Cerebral Cortex Phospholipid Fatty-Acid Composition and Diet. *Lancet Lond. Engl.* **1992**, *340*, 810–813. [[CrossRef](#)]
107. Cacho, N.T.; Lawrence, R.M. Innate Immunity and Breast Milk. *Front. Immunol.* **2017**, *8*, 584. [[CrossRef](#)] [[PubMed](#)]

108. Lawrence, R.A. *La Lactancia Materna. Una Guía Para la Profesiónmédica*, 4th ed.; Mosby/Doyma: Madrid, Spain, 1996.
109. Marangoni, F.; Agostoni, C.; Lammardo, A.M.; Giovannini, M.; Galli, C.; Riva, E. Polyunsaturated Fatty Acid Concentrations in Human Hindmilk Are Stable throughout 12-Months of Lactation and Provide a Sustained Intake to the Infant during Exclusive Breastfeeding: An Italian Study. *Br. J. Nutr.* **2000**, *84*, 103–109. [[CrossRef](#)]
110. Thiemich, M. Ueber Den Einfuss Der Ernährung Und Lebensweise Auf Die Zusammensetzung Der Frauenmilch. *Monatssch Geburtshilfe Gynakol* **1899**, *9*, 504–521.
111. Helland, I.B.; Saarem, K.; Saugstad, O.D.; Drevon, C.A. Fatty Acid Composition in Maternal Milk and Plasma during Supplementation with Cod Liver Oil. *Eur. J. Clin. Nutr.* **1998**, *52*, 839–845. [[CrossRef](#)] [[PubMed](#)]
112. Harris, W.S.; Connor, W.E.; Lindsey, S. Will Dietary Omega-3 Fatty Acids Change the Composition of Human Milk? *Am. J. Clin. Nutr.* **1984**, *40*, 780–785. [[CrossRef](#)]
113. Henderson, R.A.; Jensen, R.G.; Lammi-Keefe, C.J.; Ferris, A.M.; Dardick, K.R. Effect of Fish Oil on the Fatty Acid Composition of Human Milk and Maternal and Infant Erythrocytes. *Lipids* **1992**, *27*, 863–869. [[CrossRef](#)]
114. Al, M.D.; van Houwelingen, A.C.; Hornstra, G. Relation between Birth Order and the Maternal and Neonatal Docosahexaenoic Acid Status. *Eur. J. Clin. Nutr.* **1997**, *51*, 548–553. [[CrossRef](#)] [[PubMed](#)]
115. Makrides, M.; Neumann, M.; Simmer, K.; Pater, J.; Gibson, R. Are Long-Chain Polyunsaturated Fatty Acids Essential Nutrients in Infancy? *Lancet Lond. Engl.* **1995**, *345*, 1463–1468. [[CrossRef](#)]
116. Heird, W.C. The Role of Polyunsaturated Fatty Acids in Term and Preterm Infants and Breastfeeding Mothers. *Pediatr. Clin. N. Am.* **2001**, *48*, 173–188. [[CrossRef](#)]
117. Bopp, M.; Lovelady, C.; Hunter, C.; Kinsella, T. Maternal Diet and Exercise: Effects on Long-Chain Polyunsaturated Fatty Acid Concentrations in Breast Milk. *J. Am. Diet. Assoc.* **2005**, *105*, 1098–1103. [[CrossRef](#)] [[PubMed](#)]
118. Agostoni, C.; Riva, E.; Giovannini, M.; Pinto, F.; Colombo, C.; Risé, P.; Galli, C.; Marangoni, F. Maternal Smoking Habits Are Associated with Differences in Infants' Long-Chain Polyunsaturated Fatty Acids in Whole Blood: A Case-Control Study. *Arch. Dis. Child.* **2008**, *93*, 414–418. [[CrossRef](#)] [[PubMed](#)]
119. Makrides, M.; Neumann, M.A.; Gibson, R.A. Effect of Maternal Docosahexaenoic Acid (DHA) Supplementation on Breast Milk Composition. *Eur. J. Clin. Nutr.* **1996**, *50*, 352–357. [[PubMed](#)]
120. Salem, N.; Van Dael, P. Arachidonic Acid in Human Milk. *Nutrients* **2020**, *12*, 626. [[CrossRef](#)] [[PubMed](#)]
121. Robinson, D.T.; Palac, H.L.; Baillif, V.; Van Goethem, E.; Dubourdeau, M.; Van Horn, L.; Martin, C.R. Long Chain Fatty Acids and Related Pro-Inflammatory, Specialized pro-Resolving Lipid Mediators and Their Intermediates in Preterm Human Milk during the First Month of Lactation. *Prostaglandins Leukot. Essent. Fatty Acids* **2017**, *121*, 1–6. [[CrossRef](#)]
122. Gan, J.; Zhang, Z.; Kurudimov, K.; German, J.B.; Taha, A.Y. Distribution of Free and Esterified Oxylipins in Cream, Cell, and Skim Fractions of Human Milk. *Lipids* **2020**, *55*, 661–670. [[CrossRef](#)] [[PubMed](#)]
123. Pitino, M.A.; Alashmali, S.M.; Hopperton, K.E.; Unger, S.; Pouliot, Y.; Doyen, A.; O'Connor, D.L.; Bazinet, R.P. Oxylipin Concentration, but Not Fatty Acid Composition, Is Altered in Human Donor Milk Pasteurised Using Both Thermal and Non-Thermal Techniques. *Br. J. Nutr.* **2019**, *122*, 47–55. [[CrossRef](#)] [[PubMed](#)]
124. Hennebelle, M.; Morgan, R.K.; Sethi, S.; Zhang, Z.; Chen, H.; Grodzki, A.C.; Lein, P.J.; Taha, A.Y. Linoleic Acid-Derived Metabolites Constitute the Majority of Oxylipins in the Rat Pup Brain and Stimulate Axonal Growth in Primary Rat Cortical Neuron-Glia Co-Cultures in a Sex-Dependent Manner. *J. Neurochem.* **2020**, *152*, 195–207. [[CrossRef](#)]
125. Liu, L.; Oza, S.; Hogan, D.; Chu, Y.; Perin, J.; Zhu, J.; Lawn, J.E.; Cousens, S.; Mathers, C.; Black, R.E. Global, Regional, and National Causes of under-5 Mortality in 2000–15: An Updated Systematic Analysis with Implications for the Sustainable Development Goals. *Lancet Lond. Engl.* **2016**, *388*, 3027–3035. [[CrossRef](#)]
126. Hutchinson, E.A.; De Luca, C.R.; Doyle, L.W.; Roberts, G.; Anderson, P.J.; Victorian Infant Collaborative Study Group. School-Age Outcomes of Extremely Preterm or Extremely Low Birth Weight Children. *Pediatrics* **2013**, *131*, e1053–e1061. [[CrossRef](#)] [[PubMed](#)]
127. Crowther, C.A.; Hiller, J.E.; Doyle, L.W.; Haslam, R.R.; Australasian Collaborative Trial of Magnesium Sulphate (ACTOMg SO4) Collaborative Group. Effect of Magnesium Sulfate given for Neuroprotection before Preterm Birth: A Randomized Controlled Trial. *JAMA* **2003**, *290*, 2669–2676. [[CrossRef](#)]
128. Schmidt, B.; Roberts, R.S.; Davis, P.; Doyle, L.W.; Barrington, K.J.; Ohlsson, A.; Solimano, A.; Tin, W.; Caffeine for Apnea of Prematurity Trial Group. Long-Term Effects of Caffeine Therapy for Apnea of Prematurity. *N. Engl. J. Med.* **2007**, *357*, 1893–1902. [[CrossRef](#)]
129. Puntis, J.W.L. Nutritional Support in the Premature Newborn. *Postgrad. Med. J.* **2006**, *82*, 192–198. [[CrossRef](#)] [[PubMed](#)]
130. Dorling, J.; Kempley, S.; Leaf, A. Feeding Growth Restricted Preterm Infants with Abnormal Antenatal Doppler Results. *Arch. Dis. Child. Fetal Neonatal Ed.* **2005**, *90*, F359–F363. [[CrossRef](#)]
131. Schanler, R.J.; Shulman, R.J.; Lau, C. Feeding Strategies for Premature Infants: Beneficial Outcomes of Feeding Fortified Human Milk versus Preterm Formula. *Pediatrics* **1999**, *103*, 1150–1157. [[CrossRef](#)]
132. Henriksen, C.; Haugholt, K.; Lindgren, M.; Aurvåg, A.K.; Rønnestad, A.; Grønn, M.; Solberg, R.; Moen, A.; Nakstad, B.; Berge, R.K.; et al. Improved Cognitive Development among Preterm Infants Attributable to Early Supplementation of Human Milk with Docosahexaenoic Acid and Arachidonic Acid. *Pediatrics* **2008**, *121*, 1137–1145. [[CrossRef](#)]
133. Simmer, K.; Schulzke, S.M.; Patole, S. Long-Chain Polyunsaturated Fatty Acid Supplementation in Preterm Infants. *Cochrane Database Syst. Rev.* **2008**, CD000375. [[CrossRef](#)]



134. Makrides, M.; Gibson, R.A.; McPhee, A.J.; Collins, C.T.; Davis, P.G.; Doyle, L.W.; Simmer, K.; Colditz, P.B.; Morris, S.; Smithers, L.G.; et al. Neurodevelopmental Outcomes of Preterm Infants Fed High-Dose Docosahexaenoic Acid: A Randomized Controlled Trial. *JAMA* **2009**, *301*, 175–182. [[CrossRef](#)] [[PubMed](#)]
135. Gould, J.F.; Smithers, L.G.; Makrides, M. The Effect of Maternal Omega-3 (n-3) LCPUFA Supplementation during Pregnancy on Early Childhood Cognitive and Visual Development: A Systematic Review and Meta-Analysis of Randomized Controlled Trials. *Am. J. Clin. Nutr.* **2013**, *97*, 531–544. [[CrossRef](#)]
136. Innis, S.M. Essential Fatty Acids in Infant Nutrition: Lessons and Limitations from Animal Studies in Relation to Studies on Infant Fatty Acid Requirements. *Am. J. Clin. Nutr.* **2000**, *71*, 238S–244S. [[CrossRef](#)] [[PubMed](#)]
137. Gould, J.F.; Colombo, J.; Collins, C.T.; Makrides, M.; Hewawasam, E.; Smithers, L.G. Assessing Whether Early Attention of Very Preterm Infants Can Be Improved by an Omega-3 Long-Chain Polyunsaturated Fatty Acid Intervention: A Follow-up of a Randomised Controlled Trial. *BMJ Open* **2018**, *8*, e020043. [[CrossRef](#)]
138. Isaacs, E.B.; Ross, S.; Kennedy, K.; Weaver, L.T.; Lucas, A.; Fewtrell, M.S. 10-Year Cognition in Preterms after Random Assignment to Fatty Acid Supplementation in Infancy. *Pediatrics* **2011**, *128*, e890–e898. [[CrossRef](#)]
139. Westerberg, A.C.; Schei, R.; Henriksen, C.; Smith, L.; Veierød, M.B.; Drevon, C.A.; Iversen, P.O. Attention among Very Low Birth Weight Infants Following Early Supplementation with Docosahexaenoic and Arachidonic Acid. *Acta Paediatr. Oslo Nor. 1992* **2011**, *100*, 47–52. [[CrossRef](#)] [[PubMed](#)]
140. Qawasmi, A.; Landeros-Weisenberger, A.; Bloch, M.H. Meta-Analysis of LCPUFA Supplementation of Infant Formula and Visual Acuity. *Pediatrics* **2013**, *131*, e262–e272. [[CrossRef](#)] [[PubMed](#)]
141. Klevebro, S.; Juul, S.E.; Wood, T.R. A More Comprehensive Approach to the Neuroprotective Potential of Long-Chain Polyunsaturated Fatty Acids in Preterm Infants Is Needed—Should We Consider Maternal Diet and the n-6:N-3 Fatty Acid Ratio? *Front. Pediatr.* **2019**, *7*, 533. [[CrossRef](#)] [[PubMed](#)]
142. Birch, E.E.; Garfield, S.; Hoffman, D.R.; Uauy, R.; Birch, D.G. A Randomized Controlled Trial of Early Dietary Supply of Long-Chain Polyunsaturated Fatty Acids and Mental Development in Term Infants. *Dev. Med. Child Neurol.* **2000**, *42*, 174–181. [[CrossRef](#)]
143. Scott, B.L.; Bazan, N.G. Membrane Docosahexaenoate Is Supplied to the Developing Brain and Retina by the Liver. *Proc. Natl. Acad. Sci. USA* **1989**, *86*, 2903–2907. [[CrossRef](#)] [[PubMed](#)]
144. Dhopeswarkar, G.A.; Subramanian, C. Biosynthesis of Polyunsaturated Fatty Acids in the Developing Brain: I. Metabolic Transformations of Intracranially Administered 1-<sup>14</sup>C Linolenic Acid. *Lipids* **1976**, *11*, 67–71. [[CrossRef](#)]
145. Dhopeswarkar, G.A.; Subramanian, C. Intracranial Conversion of Linoleic Acid to Arachidonic Acid: Evidence for Lack of Delta8 Desaturase in the Brain. *J. Neurochem.* **1976**, *26*, 1175–1179. [[CrossRef](#)] [[PubMed](#)]
146. Sanders, T.A.; Naismith, D.J. The Metabolism of Alpha-Linolenic Acid by the Foetal Rat. *Br. J. Nutr.* **1980**, *44*, 205–208. [[CrossRef](#)] [[PubMed](#)]
147. Sanders, T.A.; Rana, S.K. Comparison of the Metabolism of Linoleic and Linolenic Acids in the Fetal Rat. *Ann. Nutr. Metab.* **1987**, *31*, 349–353. [[CrossRef](#)] [[PubMed](#)]
148. Cho, H.P.; Nakamura, M.; Clarke, S.D. Cloning, Expression, and Fatty Acid Regulation of the Human Delta-5 Desaturase. *J. Biol. Chem.* **1999**, *274*, 37335–37339. [[CrossRef](#)]
149. Aki, T.; Shimada, Y.; Inagaki, K.; Higashimoto, H.; Kawamoto, S.; Shigeta, S.; Ono, K.; Suzuki, O. Molecular Cloning and Functional Characterization of Rat Delta-6 Fatty Acid Desaturase. *Biochem. Biophys. Res. Commun.* **1999**, *255*, 575–579. [[CrossRef](#)] [[PubMed](#)]
150. Leonard, A.E.; Kelder, B.; Bobik, E.G.; Chuang, L.T.; Parker-Barnes, J.M.; Thurmond, J.M.; Kroeger, P.E.; Kopchick, J.J.; Huang, Y.S.; Mukerji, P. cDNA Cloning and Characterization of Human Delta5-Desaturase Involved in the Biosynthesis of Arachidonic Acid. *Biochem. J.* **2000**, *347 Pt 3*, 719–724. [[CrossRef](#)]
151. Al-Hilal, M.; Alsaleh, A.; Maniou, Z.; Lewis, F.J.; Hall, W.L.; Sanders, T.A.B.; O'Dell, S.D.; MARINA study team. Genetic Variation at the FADS1-FADS2 Gene Locus Influences Delta-5 Desaturase Activity and LC-PUFA Proportions after Fish Oil Supplement. *J. Lipid Res.* **2013**, *54*, 542–551. [[CrossRef](#)]
152. Lemaitre, R.N.; Tanaka, T.; Tang, W.; Manichaikul, A.; Foy, M.; Kabagambe, E.K.; Nettleton, J.A.; King, I.B.; Weng, L.-C.; Bhattacharya, S.; et al. Genetic Loci Associated with Plasma Phospholipid N-3 Fatty Acids: A Meta-Analysis of Genome-Wide Association Studies from the CHARGE Consortium. *PLoS Genet.* **2011**, *7*, e1002193. [[CrossRef](#)]
153. Deák, F.; Anderson, R.E.; Fessler, J.L.; Sherry, D.M. Novel Cellular Functions of Very Long Chain-Fatty Acids: Insight From ELOVL4 Mutations. *Front. Cell. Neurosci.* **2019**, *13*, 428. [[CrossRef](#)]
154. Monroig, O.; Rotllant, J.; Sánchez, E.; Cerdá-Reverter, J.M.; Tocher, D.R. Expression of Long-Chain Polyunsaturated Fatty Acid (LC-PUFA) Biosynthesis Genes during Zebrafish *Danio rerio* Early Embryogenesis. *Biochim. Biophys. Acta* **2009**, *1791*, 1093–1101. [[CrossRef](#)] [[PubMed](#)]
155. Tan, S.-H.; Chung, H.-H.; Shu-Chien, A.C. Distinct Developmental Expression of Two Elongase Family Members in Zebrafish. *Biochem. Biophys. Res. Commun.* **2010**, *393*, 397–403. [[CrossRef](#)] [[PubMed](#)]
156. Ritchie, S.J.; Cox, S.R.; Shen, X.; Lombardo, M.V.; Reus, L.M.; Alloza, C.; Harris, M.A.; Alderson, H.L.; Hunter, S.; Neilson, E.; et al. Sex Differences in the Adult Human Brain: Evidence from 5216 UK Biobank Participants. *Cereb. Cortex N. Y. NY* **2018**, *28*, 2959–2975. [[CrossRef](#)]

157. Baron-Cohen, S.; Lombardo, M.V.; Auyeung, B.; Ashwin, E.; Chakrabarti, B.; Knickmeyer, R. Why Are Autism Spectrum Conditions More Prevalent in Males? *PLoS Biol.* **2011**, *9*, e1001081. [[CrossRef](#)] [[PubMed](#)]
158. Gaub, M.; Carlson, C.L. Gender Differences in ADHD: A Meta-Analysis and Critical Review. *J. Am. Acad. Child Adolesc. Psychiatry* **1997**, *36*, 1036–1045. [[CrossRef](#)] [[PubMed](#)]
159. Aleman, A.; Kahn, R.S.; Selten, J.-P. Sex Differences in the Risk of Schizophrenia: Evidence from Meta-Analysis. *Arch. Gen. Psychiatry* **2003**, *60*, 565–571. [[CrossRef](#)]
160. Williamson, D.; Johnston, C. Gender Differences in Adults with Attention-Deficit/Hyperactivity Disorder: A Narrative Review. *Clin. Psychol. Rev.* **2015**, *40*, 15–27. [[CrossRef](#)] [[PubMed](#)]
161. Jäncke, L. Sex/Gender Differences in Cognition, Neurophysiology, and Neuroanatomy. *F1000Research* **2018**, *7*. [[CrossRef](#)]
162. Crowe, F.L.; Skeaff, C.M.; Green, T.J.; Gray, A.R. Serum N-3 Long-Chain PUFA Differ by Sex and Age in a Population-Based Survey of New Zealand Adolescents and Adults. *Br. J. Nutr.* **2008**, *99*, 168–174. [[CrossRef](#)]
163. Bakewell, L.; Burdge, G.C.; Calder, P.C. Polyunsaturated Fatty Acid Concentrations in Young Men and Women Consuming Their Habitual Diets. *Br. J. Nutr.* **2006**, *96*, 93–99. [[CrossRef](#)]
164. Metherel, A.H.; Armstrong, J.M.; Patterson, A.C.; Stark, K.D. Assessment of Blood Measures of N-3 Polyunsaturated Fatty Acids with Acute Fish Oil Supplementation and Washout in Men and Women. *Prostaglandins Leukot. Essent. Fatty Acids* **2009**, *81*, 23–29. [[CrossRef](#)]
165. Extier, A.; Langelier, B.; Perruchot, M.-H.; Guesnet, P.; Van Veldhoven, P.P.; Lavalie, M.; Alessandri, J.-M. Gender Affects Liver Desaturase Expression in a Rat Model of N-3 Fatty Acid Repletion. *J. Nutr. Biochem.* **2010**, *21*, 180–187. [[CrossRef](#)]
166. Kitson, A.P.; Smith, T.L.; Marks, K.A.; Stark, K.D. Tissue-Specific Sex Differences in Docosahexaenoic Acid and  $\Delta 6$ -Desaturase in Rats Fed a Standard Chow Diet. *Appl. Physiol. Nutr. Metab. Physiol. Appl. Nutr. Metab.* **2012**, *37*, 1200–1211. [[CrossRef](#)]
167. Giltay, E.J.; Gooren, L.J.G.; Toorians, A.W.F.T.; Katan, M.B.; Zock, P.L. Docosahexaenoic Acid Concentrations Are Higher in Women than in Men Because of Estrogenic Effects. *Am. J. Clin. Nutr.* **2004**, *80*, 1167–1174. [[CrossRef](#)] [[PubMed](#)]
168. Abdelmagid, S.A.; Clarke, S.E.; Roke, K.; Nielsen, D.E.; Badawi, A.; El-Soheymy, A.; Mutch, D.M.; Ma, D.W. Ethnicity, Sex, FADS Genetic Variation, and Hormonal Contraceptive Use Influence Delta-5- and Delta-6-Desaturase Indices and Plasma Docosahexaenoic Acid Concentration in Young Canadian Adults: A Cross-Sectional Study. *Nutr. Metab.* **2015**, *12*, 14. [[CrossRef](#)] [[PubMed](#)]
169. Kim, D.; Choi, J.-E.; Park, Y. Low-Linoleic Acid Diet and Oestrogen Enhance the Conversion of  $\alpha$ -Linolenic Acid into DHA through Modification of Conversion Enzymes and Transcription Factors. *Br. J. Nutr.* **2019**, *121*, 137–145. [[CrossRef](#)]
170. McNamara, R.K.; Able, J.; Jandacek, R.; Rider, T.; Tso, P. Gender Differences in Rat Erythrocyte and Brain Docosahexaenoic Acid Composition: Role of Ovarian Hormones and Dietary Omega-3 Fatty Acid Composition. *Psychoneuroendocrinology* **2009**, *34*, 532–539. [[CrossRef](#)] [[PubMed](#)]
171. Alessandri, J.-M.; Extier, A.; Al-Gubory, K.H.; Langelier, B.; Baudry, C.; LePoupon, C.; Lavalie, M.; Guesnet, P. Ovariectomy and  $17\beta$ -Estradiol Alter Transcription of Lipid Metabolism Genes and Proportions of Neo-Formed n-3 and n-6 Long-Chain Polyunsaturated Fatty Acids Differently in Brain and Liver. *J. Nutr. Biochem.* **2011**, *22*, 820–827. [[CrossRef](#)]
172. Feltham, B.A.; Balogun, K.A.; Cheema, S.K. Perinatal and Postweaning Diets High in Omega-3 Fatty Acids Have Age- and Sex-Specific Effects on the Fatty Acid Composition of the Cerebellum and Brainstem of C57BL/6 Mice. *Prostaglandins Leukot. Essent. Fatty Acids* **2019**, *148*, 16–24. [[CrossRef](#)]
173. Childs, C.E.; Romeu-Nadal, M.; Burdge, G.C.; Calder, P.C. Gender Differences in the N-3 Fatty Acid Content of Tissues. *Proc. Nutr. Soc.* **2008**, *67*, 19–27. [[CrossRef](#)] [[PubMed](#)]
174. Chen, C.T.; Haven, S.; Lecaj, L.; Borgstrom, M.; Torabi, M.; SanGiovanni, J.P.; Hibbeln, J.R. Brain PUFA Concentrations Are Differentially Affected by Interactions of Diet, Sex, Brain Regions, and Phospholipid Pools in Mice. *J. Nutr.* **2020**, *150*, 3123–3132. [[CrossRef](#)] [[PubMed](#)]
175. Dervola, K.S.; Roberg, B.A.; Weien, G.; Bogen, I.L.; Sandvik, T.H.; Sagvolden, T.; Drevon, C.A.; Johansen, E.B.; Walaas, S.I. Marine O-3 Polyunsaturated Fatty Acids Induce Sex-Specific Changes in Reinforcer-Controlled Behaviour and Neurotransmitter Metabolism in a Spontaneously Hypertensive Rat Model of ADHD. *Behav. Brain Funct. BBF* **2012**, *8*, 56. [[CrossRef](#)]
176. da Costa, A.E.M.; Gomes, N.S.; Gadelha Filho, C.V.J.; Linhares, M.G.O.E.S.; da Costa, R.O.; Chaves Filho, A.J.M.; Cordeiro, R.C.; Vasconcelos, G.S.; da Silva, F.E.R.; Araujo, T. da S.; et al. Sex Influences in the Preventive Effects of Peripubertal Supplementation with N-3 Polyunsaturated Fatty Acids in Mice Exposed to the Two-Hit Model of Schizophrenia. *Eur. J. Pharmacol.* **2021**, *897*, 173949. [[CrossRef](#)]
177. Trivers, R.L.; Willard, D.E. Natural Selection of Parental Ability to Vary the Sex Ratio of Offspring. *Science* **1973**, *179*, 90–92. [[CrossRef](#)] [[PubMed](#)]
178. Rivers, J.P.; Crawford, M.A. Maternal Nutrition and the Sex Ratio at Birth. *Nature* **1974**, *252*, 297–298. [[CrossRef](#)]
179. Austad, S.N.; Sunquist, M.E. Sex-Ratio Manipulation in the Common Opossum. *Nature* **1986**, *324*, 58–60. [[CrossRef](#)]
180. Fountain, E.D.; Mao, J.; Whyte, J.J.; Mueller, K.E.; Ellersieck, M.R.; Will, M.J.; Roberts, R.M.; Macdonald, R.; Rosenfeld, C.S. Effects of Diets Enriched in Omega-3 and Omega-6 Polyunsaturated Fatty Acids on Offspring Sex-Ratio and Maternal Behavior in Mice. *Biol. Reprod.* **2008**, *78*, 211–217. [[CrossRef](#)] [[PubMed](#)]
181. Shrestha, N.; Cuffe, J.S.M.; Holland, O.J.; Bulmer, A.C.; Hill, M.; Perkins, A.V.; Muhlhausler, B.S.; McAinch, A.J.; Hryciw, D.H. Elevated Maternal Linoleic Acid Reduces Circulating Leptin Concentrations, Cholesterol Levels and Male Fetal Survival in a Rat Model. *J. Physiol.* **2019**, *597*, 3349–3361. [[CrossRef](#)]

182. Gulliver, C.E.; Friend, M.A.; King, B.J.; Robertson, S.M.; Wilkins, J.F.; Clayton, E.H. Increased Prostaglandin Response to Oxytocin in Ewes Fed a Diet High in Omega-6 Polyunsaturated Fatty Acids. *Lipids* **2013**, *48*, 177–183. [[CrossRef](#)] [[PubMed](#)]
183. Abayasekara, D.R.; Wathes, D.C. Effects of Altering Dietary Fatty Acid Composition on Prostaglandin Synthesis and Fertility. *Prostaglandins Leukot. Essent. Fatty Acids* **1999**, *61*, 275–287. [[CrossRef](#)]
184. Pratt, N.C.; Huck, U.W.; Lisk, R.D. Offspring Sex Ratio in Hamsters Is Correlated with Vaginal PH at Certain Times of Mating. *Behav. Neural Biol.* **1987**, *48*, 310–316. [[CrossRef](#)]
185. Green, M.P.; Spate, L.D.; Parks, T.E.; Kimura, K.; Murphy, C.N.; Williams, J.E.; Kerley, M.S.; Green, J.A.; Keisler, D.H.; Roberts, R.M. Nutritional Skewing of Conceptus Sex in Sheep: Effects of a Maternal Diet Enriched in Rumen-Protected Polyunsaturated Fatty Acids (PUFA). *Reprod. Biol. Endocrinol. RBE* **2008**, *6*, 21. [[CrossRef](#)] [[PubMed](#)]
186. Marei, W.F.A.; Khalil, W.A.; Pushpakumara, A.P.G.; El-Harairy, M.A.; Abo El-Atta, A.M.A.; Wathes, D.C.; Fouladi-Nashta, A. Polyunsaturated Fatty Acids Influence Offspring Sex Ratio in Cows. *Int. J. Vet. Sci. Med.* **2018**, *6*, S36–S40. [[CrossRef](#)]
187. Lammoglia, M.A.; Willard, S.T.; Oldham, J.R.; Randel, R.D. Effects of Dietary Fat and Season on Steroid Hormonal Profiles before Parturition and on Hormonal, Cholesterol, Triglycerides, Follicular Patterns, and Postpartum Reproduction in Brahman Cows. *J. Anim. Sci.* **1996**, *74*, 2253–2262. [[CrossRef](#)] [[PubMed](#)]
188. Robinson, R.S.; Pushpakumara, P.G.A.; Cheng, Z.; Peters, A.R.; Abayasekara, D.R.E.; Wathes, D.C. Effects of Dietary Polyunsaturated Fatty Acids on Ovarian and Uterine Function in Lactating Dairy Cows. *Reprod. Camb. Engl.* **2002**, *124*, 119–131. [[CrossRef](#)]
189. Agung, B.; Otoi, T.; Wongsrikeao, P.; Taniguchi, M.; Shimizu, R.; Watari, H.; Nagai, T. Effect of Maturation Culture Period of Oocytes on the Sex Ratio of in Vitro Fertilized Bovine Embryos. *J. Reprod. Dev.* **2006**, *52*, 123–127. [[CrossRef](#)] [[PubMed](#)]
190. Gerber, A.J.; Peterson, B.S.; Giedd, J.N.; Lalonde, F.M.; Celano, M.J.; White, S.L.; Wallace, G.L.; Lee, N.R.; Lenroot, R.K. Anatomical Brain Magnetic Resonance Imaging of Typically Developing Children and Adolescents. *J. Am. Acad. Child Adolesc. Psychiatry* **2009**, *48*, 465–470. [[CrossRef](#)]
191. Dubois, J.; Dehaene-Lambertz, G.; Kulikova, S.; Poupon, C.; Hüppi, P.S.; Hertz-Pannier, L. The Early Development of Brain White Matter: A Review of Imaging Studies in Fetuses, Newborns and Infants. *Neuroscience* **2014**, *276*, 48–71. [[CrossRef](#)]
192. Coti Bertrand, P.; O’Kusky, J.R.; Innis, S.M. Maternal Dietary (n-3) Fatty Acid Deficiency Alters Neurogenesis in the Embryonic Rat Brain. *J. Nutr.* **2006**, *136*, 1570–1575. [[CrossRef](#)] [[PubMed](#)]
193. Yavin, E.; Himovichi, E.; Eilam, R. Delayed Cell Migration in the Developing Rat Brain Following Maternal Omega 3 Alpha Linolenic Acid Dietary Deficiency. *Neuroscience* **2009**, *162*, 1011–1022. [[CrossRef](#)]
194. Sakayori, N.; Kikkawa, T.; Tokuda, H.; Kiryu, E.; Yoshizaki, K.; Kawashima, H.; Yamada, T.; Arai, H.; Kang, J.X.; Katagiri, H.; et al. Maternal Dietary Imbalance between Omega-6 and Omega-3 Polyunsaturated Fatty Acids Impairs Neocortical Development via Epoxy Metabolites. *Stem Cells Dayt. Ohio* **2016**, *34*, 470–482. [[CrossRef](#)]
195. Wong, C.T.; Ussyshkin, N.; Ahmad, E.; Rai-Bhogal, R.; Li, H.; Crawford, D.A. Prostaglandin E2 Promotes Neural Proliferation and Differentiation and Regulates Wnt Target Gene Expression. *J. Neurosci. Res.* **2016**, *94*, 759–775. [[CrossRef](#)] [[PubMed](#)]
196. Joardar, A.; Sen, A.K.; Das, S. Docosahexaenoic Acid Facilitates Cell Maturation and Beta-Adrenergic Transmission in Astrocytes. *J. Lipid Res.* **2006**, *47*, 571–581. [[CrossRef](#)] [[PubMed](#)]
197. Das, M.; Das, S. Docosahexaenoic Acid (DHA) Induced Morphological Differentiation of Astrocytes Is Associated with Transcriptional Upregulation and Endocytosis of B2-AR. *Mol. Neurobiol.* **2019**, *56*, 2685–2702. [[CrossRef](#)] [[PubMed](#)]
198. Shinjyo, N.; Piscitelli, F.; Verde, R.; Di Marzo, V. Impact of Omega-6 Polyunsaturated Fatty Acid Supplementation and  $\gamma$ -Aminobutyric Acid on Astroglialogenesis through the Endocannabinoid System. *J. Neurosci. Res.* **2013**, *91*, 943–953. [[CrossRef](#)]
199. Cremona, O.; Di Paolo, G.; Wenk, M.R.; Lüthi, A.; Kim, W.T.; Takei, K.; Daniell, L.; Nemoto, Y.; Shears, S.B.; Flavell, R.A.; et al. Essential Role of Phosphoinositide Metabolism in Synaptic Vesicle Recycling. *Cell* **1999**, *99*, 179–188. [[CrossRef](#)]
200. Di Paolo, G.; Moskowitz, H.S.; Gipson, K.; Wenk, M.R.; Voronov, S.; Obayashi, M.; Flavell, R.; Fitzsimonds, R.M.; Ryan, T.A.; De Camilli, P. Impaired PtdIns(4,5)P2 Synthesis in Nerve Terminals Produces Defects in Synaptic Vesicle Trafficking. *Nature* **2004**, *431*, 415–422. [[CrossRef](#)]
201. Rohrbough, J.; Rushton, E.; Palanker, L.; Woodruff, E.; Matthies, H.J.G.; Acharya, U.; Acharya, J.K.; Broadie, K. Ceramidase Regulates Synaptic Vesicle Exocytosis and Trafficking. *J. Neurosci. Off. J. Soc. Neurosci.* **2004**, *24*, 7789–7803. [[CrossRef](#)] [[PubMed](#)]
202. Martin, R.E.; Bazan, N.G. Changing Fatty Acid Content of Growth Cone Lipids Prior to Synaptogenesis. *J. Neurochem.* **1992**, *59*, 318–325. [[CrossRef](#)]
203. Martin, R.E. Docosahexaenoic Acid Decreases Phospholipase A2 Activity in the Neurites/Nerve Growth Cones of PC12 Cells. *J. Neurosci. Res.* **1998**, *54*, 805–813. [[CrossRef](#)]
204. Auestad, N.; Innis, S.M. Dietary N-3 Fatty Acid Restriction during Gestation in Rats: Neuronal Cell Body and Growth-Cone Fatty Acids. *Am. J. Clin. Nutr.* **2000**, *71*, 312S–314S. [[CrossRef](#)] [[PubMed](#)]
205. Innis, S.M.; de La Presa Owens, S. Dietary Fatty Acid Composition in Pregnancy Alters Neurite Membrane Fatty Acids and Dopamine in Newborn Rat Brain. *J. Nutr.* **2001**, *131*, 118–122. [[CrossRef](#)] [[PubMed](#)]
206. Suzuki, H.; Manabe, S.; Wada, O.; Crawford, M.A. Rapid Incorporation of Docosahexaenoic Acid from Dietary Sources into Brain Microsomal, Synaptosomal and Mitochondrial Membranes in Adult Mice. *Int. J. Vitam. Nutr. Res. Int. Z. Vitam.-Ernährungsforschung J. Int. Vitaminol. Nutr.* **1997**, *67*, 272–278.

207. Igarashi, M.; Santos, R.A.; Cohen-Cory, S. Impact of Maternal N-3 Polyunsaturated Fatty Acid Deficiency on Dendritic Arbor Morphology and Connectivity of Developing *Xenopus Laevis* Central Neurons in Vivo. *J. Neurosci. Off. J. Soc. Neurosci.* **2015**, *35*, 6079–6092. [[CrossRef](#)] [[PubMed](#)]
208. Ziegler, A.B.; Ménagé, C.; Grégoire, S.; Garcia, T.; Ferveur, J.-F.; Bretillon, L.; Grosjean, Y. Lack of Dietary Polyunsaturated Fatty Acids Causes Synapse Dysfunction in the *Drosophila* Visual System. *PLoS ONE* **2015**, *10*, e0135353. [[CrossRef](#)]
209. Carbone, B.E.; Abouleish, M.; Watters, K.E.; Vogel, S.; Ribic, A.; Schroeder, O.H.-U.; Bader, B.M.; Biederer, T. Synaptic Connectivity and Cortical Maturation Are Promoted by the  $\omega$ -3 Fatty Acid Docosahexaenoic Acid. *Cereb. Cortex N. Y. NY* **2020**, *30*, 226–240. [[CrossRef](#)] [[PubMed](#)]
210. Fujita, S.; Ikegaya, Y.; Nishikawa, M.; Nishiyama, N.; Matsuki, N. Docosahexaenoic Acid Improves Long-Term Potentiation Attenuated by Phospholipase A(2) Inhibitor in Rat Hippocampal Slices. *Br. J. Pharmacol.* **2001**, *132*, 1417–1422. [[CrossRef](#)]
211. Mazzocchi-Jones, D. Impaired Corticostriatal LTP and Depotentiation Following IPLA2 Inhibition Is Restored Following Acute Application of DHA. *Brain Res. Bull.* **2015**, *111*, 69–75. [[CrossRef](#)]
212. Cao, H.; Li, M.-Y.; Li, G.; Li, S.-J.; Wen, B.; Lu, Y.; Yu, X. Retinoid X Receptor  $\alpha$  Regulates DHA-Dependent Spinogenesis and Functional Synapse Formation In Vivo. *Cell Rep.* **2020**, *31*, 107649. [[CrossRef](#)]
213. Kim, H.-Y.; Moon, H.-S.; Cao, D.; Lee, J.; Kevala, K.; Jun, S.B.; Lovinger, D.M.; Akbar, M.; Huang, B.X. N-Docosahexaenylethanolamide Promotes Development of Hippocampal Neurons. *Biochem. J.* **2011**, *435*, 327–336. [[CrossRef](#)]
214. Lee, J.-W.; Huang, B.X.; Kwon, H.; Rashid, M.A.; Kharebava, G.; Desai, A.; Patnaik, S.; Marugan, J.; Kim, H.-Y. Orphan GPR110 (ADGRF1) Targeted by N-Docosahexaenylethanolamine in Development of Neurons and Cognitive Function. *Nat. Commun.* **2016**, *7*. [[CrossRef](#)] [[PubMed](#)]
215. Manni, M.M.; Tiberti, M.L.; Pagnotta, S.; Barelli, H.; Gautier, R.; Antonny, B. Acyl Chain Asymmetry and Polyunsaturation of Brain Phospholipids Facilitate Membrane Vesiculation without Leakage. *eLife* **2018**, *7*. [[CrossRef](#)]
216. Hashimoto, M.; Hossain, S.; Shido, O. Docosahexaenoic Acid but Not Eicosapentaenoic Acid Withstands Dietary Cholesterol-Induced Decreases in Platelet Membrane Fluidity. *Mol. Cell. Biochem.* **2006**, *293*, 1–8. [[CrossRef](#)] [[PubMed](#)]
217. Darios, F.; Davletov, B. Omega-3 and Omega-6 Fatty Acids Stimulate Cell Membrane Expansion by Acting on Syntaxin 3. *Nature* **2006**, *440*, 813–817. [[CrossRef](#)] [[PubMed](#)]
218. Bruno, M.J.; Koeppel, R.E.; Andersen, O.S. Docosahexaenoic Acid Alters Bilayer Elastic Properties. *Proc. Natl. Acad. Sci. USA* **2007**, *104*, 9638–9643. [[CrossRef](#)]
219. Tounian, P.; Bellaïche, M.; Legrand, P. ARA or No ARA in Infant Formulae, That Is the Question. *Arch. Pediatr. Organe Off. Soc. Francaise Pediatr.* **2021**, *28*, 69–74. [[CrossRef](#)]
220. Koletzko, B.; Bergmann, K.; Brenna, J.T.; Calder, P.C.; Campoy, C.; Clandinin, M.T.; Colombo, J.; Daly, M.; Decsi, T.; Demmelmair, H.; et al. Should Formula for Infants Provide Arachidonic Acid along with DHA? A Position Paper of the European Academy of Paediatrics and the Child Health Foundation. *Am. J. Clin. Nutr.* **2020**, *111*, 10–16. [[CrossRef](#)]
221. Brenna, J.T. Long-Chain Polyunsaturated Fatty Acids and the Preterm Infant: A Case Study in Developmentally Sensitive Nutrient Needs in the United States. *Am. J. Clin. Nutr.* **2016**, *103*, 606S–615S. [[CrossRef](#)]
222. Crawford, M.A.; Wang, Y.; Forsyth, S.; Brenna, J.T. The European Food Safety Authority Recommendation for Polyunsaturated Fatty Acid Composition of Infant Formula Overrides Breast Milk, Puts Infants at Risk, and Should Be Revised. *Prostaglandins Leukot. Essent. Fatty Acids* **2015**, *102–103*, 1–3. [[CrossRef](#)]
223. Hadley, K.B.; Ryan, A.S.; Forsyth, S.; Gautier, S.; Salem, N. The Essentiality of Arachidonic Acid in Infant Development. *Nutrients* **2016**, *8*, 216. [[CrossRef](#)]
224. Harauma, A.; Yasuda, H.; Hatanaka, E.; Nakamura, M.T.; Salem, N.; Moriguchi, T. The Essentiality of Arachidonic Acid in Addition to Docosahexaenoic Acid for Brain Growth and Function. *Prostaglandins Leukot. Essent. Fatty Acids* **2017**, *116*, 9–18. [[CrossRef](#)] [[PubMed](#)]
225. Perry, V.H.; Gordon, S. Macrophages and Microglia in the Nervous System. *Trends Neurosci.* **1988**, *11*, 273–277. [[CrossRef](#)]
226. Salter, M.W.; Stevens, B. Microglia Emerge as Central Players in Brain Disease. *Nat. Med.* **2017**, *23*, 1018–1027. [[CrossRef](#)] [[PubMed](#)]
227. Greenhalgh, A.D.; David, S.; Bennett, F.C. Immune Cell Regulation of Glia during CNS Injury and Disease. *Nat. Rev. Neurosci.* **2020**, *21*, 139–152. [[CrossRef](#)] [[PubMed](#)]
228. Madore, C.; Leyrolle, Q.; Lacabanne, C.; Benmamar-Badel, A.; Joffre, C.; Nadjar, A.; Layé, S. Neuroinflammation in Autism: Plausible Role of Maternal Inflammation, Dietary Omega 3, and Microbiota. *Neural Plast.* **2016**, *2016*, 3597209. [[CrossRef](#)]
229. Thion, M.S.; Ginhoux, F.; Garel, S. Microglia and Early Brain Development: An Intimate Journey. *Science* **2018**, *362*, 185–189. [[CrossRef](#)] [[PubMed](#)]
230. Askew, K.; Gomez-Nicola, D. A Story of Birth and Death: Insights into the Formation and Dynamics of the Microglial Population. *Brain. Behav. Immun.* **2018**, *69*, 9–17. [[CrossRef](#)] [[PubMed](#)]
231. Hoeffel, G.; Ginhoux, F. Fetal Monocytes and the Origins of Tissue-Resident Macrophages. *Cell. Immunol.* **2018**, *330*, 5–15. [[CrossRef](#)]
232. Mass, E.; Ballesteros, I.; Farlik, M.; Halbritter, F.; Günther, P.; Crozet, L.; Jacome-Galarza, C.E.; Händler, K.; Klughammer, J.; Kobayashi, Y.; et al. Specification of Tissue-Resident Macrophages during Organogenesis. *Science* **2016**, *353*. [[CrossRef](#)]

233. Bennett, M.L.; Bennett, F.C.; Liddel, S.A.; Ajami, B.; Zamanian, J.L.; Fernhoff, N.B.; Mulinyawe, S.B.; Bohlen, C.J.; Adil, A.; Tucker, A.; et al. New Tools for Studying Microglia in the Mouse and Human CNS. *Proc. Natl. Acad. Sci. USA* **2016**, *113*, E1738–E1746. [[CrossRef](#)]
234. Sierra, A.; Encinas, J.M.; Deudero, J.J.P.; Chancey, J.H.; Enikolopov, G.; Overstreet-Wadiche, L.S.; Tsirka, S.E.; Maletic-Savatic, M. Microglia Shape Adult Hippocampal Neurogenesis through Apoptosis-Coupled Phagocytosis. *Cell Stem Cell* **2010**, *7*, 483–495. [[CrossRef](#)]
235. Bialas, A.R.; Stevens, B. TGF- $\beta$  Signaling Regulates Neuronal C1q Expression and Developmental Synaptic Refinement. *Nat. Neurosci.* **2013**, *16*, 1773–1782. [[CrossRef](#)] [[PubMed](#)]
236. Paolicelli, R.C.; Gross, C.T. Microglia in Development: Linking Brain Wiring to Brain Environment. *Neuron Glia Biol.* **2011**, *7*, 77–83. [[CrossRef](#)]
237. Squarzone, P.; Oller, G.; Hoeffel, G.; Pont-Lezica, L.; Rostaing, P.; Low, D.; Bessis, A.; Ginhoux, F.; Garel, S. Microglia Modulate Wiring of the Embryonic Forebrain. *Cell Rep.* **2014**, *8*, 1271–1279. [[CrossRef](#)] [[PubMed](#)]
238. Estes, M.L.; McAllister, A.K. Immune Mediators in the Brain and Peripheral Tissues in Autism Spectrum Disorder. *Nat. Rev. Neurosci.* **2015**, *16*, 469–486. [[CrossRef](#)] [[PubMed](#)]
239. Lenz, K.M.; Nelson, L.H. Microglia and Beyond: Innate Immune Cells As Regulators of Brain Development and Behavioral Function. *Front. Immunol.* **2018**, *9*, 698. [[CrossRef](#)]
240. Rey, C.; Nadjar, A.; Buaud, B.; Vaysse, C.; Aubert, A.; Pallet, V.; Layé, S.; Joffre, C. Resolvin D1 and E1 Promote Resolution of Inflammation in Microglial Cells in Vitro. *Brain. Behav. Immun.* **2016**, *55*, 249–259. [[CrossRef](#)]
241. Madore, C.; Nadjar, A.; Delpech, J.-C.; Sere, A.; Aubert, A.; Portal, C.; Joffre, C.; Layé, S. Nutritional N-3 PUFAs Deficiency during Perinatal Periods Alters Brain Innate Immune System and Neuronal Plasticity-Associated Genes. *Brain. Behav. Immun.* **2014**, *41*, 22–31. [[CrossRef](#)]
242. Labrousse, V.F.; Nadjar, A.; Joffre, C.; Costes, L.; Aubert, A.; Grégoire, S.; Bretillon, L.; Layé, S. Short-Term Long Chain Omega3 Diet Protects from Neuroinflammatory Processes and Memory Impairment in Aged Mice. *PLoS ONE* **2012**, *7*, e36861. [[CrossRef](#)] [[PubMed](#)]
243. Labrousse, V.F.; Leyrolle, Q.; Amadiou, C.; Aubert, A.; Sere, A.; Coutureau, E.; Grégoire, S.; Bretillon, L.; Pallet, V.; Gressens, P.; et al. Dietary Omega-3 Deficiency Exacerbates Inflammation and Reveals Spatial Memory Deficits in Mice Exposed to Lipopolysaccharide during Gestation. *Brain. Behav. Immun.* **2018**, *73*, 427–440. [[CrossRef](#)]
244. Delpech, J.-C.; Thomazeau, A.; Madore, C.; Bosch-Bouju, C.; Larriou, T.; Lacabanne, C.; Remus-Borel, J.; Aubert, A.; Joffre, C.; Nadjar, A.; et al. Dietary N-3 PUFAs Deficiency Increases Vulnerability to Inflammation-Induced Spatial Memory Impairment. *Neuropsychopharmacol. Off. Publ. Am. Coll. Neuropsychopharmacol.* **2015**, *40*, 2774–2787. [[CrossRef](#)]
245. Fourrier, C.; Remus-Borel, J.; Greenhalgh, A.D.; Guichardant, M.; Bernoud-Hubac, N.; Lagarde, M.; Joffre, C.; Layé, S. Docosahexaenoic Acid-Containing Choline Phospholipid Modulates LPS-Induced Neuroinflammation in Vivo and in Microglia in Vitro. *J. Neuroinflammation* **2017**, *14*, 170. [[CrossRef](#)] [[PubMed](#)]
246. Leyrolle, Q.; Decoeur, F.; Briere, G.; Amadiou, C.; Quadros, A.R.A.A.; Voytyuk, I.; Lacabanne, C.; Benmamar-Badel, A.; Bourel, J.; Aubert, A.; et al. Maternal Dietary Omega-3 Deficiency Worsens the Deleterious Effects of Prenatal Inflammation on the Gut-Brain Axis in the Offspring across Lifetime. *Neuropsychopharmacology* **2020**, *46*, 579–602. [[CrossRef](#)] [[PubMed](#)]
247. Meyer, U. Neurodevelopmental Resilience and Susceptibility to Maternal Immune Activation. *Trends Neurosci.* **2019**, *42*, 793–806. [[CrossRef](#)]
248. Chang, P.K.-Y.; Khatchadourian, A.; McKinney, R.A.; Maysinger, D. Docosahexaenoic Acid (DHA): A Modulator of Microglia Activity and Dendritic Spine Morphology. *J. Neuroinflammation* **2015**, *12*, 34. [[CrossRef](#)] [[PubMed](#)]
249. Sharon, G.; Sampson, T.R.; Geschwind, D.H.; Mazmanian, S.K. The Central Nervous System and the Gut Microbiome. *Cell* **2016**, *167*, 915–932. [[CrossRef](#)]
250. Codagnone, M.G.; Spichak, S.; O'Mahony, S.M.; O'Leary, O.F.; Clarke, G.; Stanton, C.; Dinan, T.G.; Cryan, J.F. Programming Bugs: Microbiota and the Developmental Origins of Brain Health and Disease. *Biol. Psychiatry* **2019**, *85*, 150–163. [[CrossRef](#)]
251. Li, Q.; Leung, Y.O.; Zhou, I.; Ho, L.C.; Kong, W.; Basil, P.; Wei, R.; Lam, S.; Zhang, X.; Law, A.C.K.; et al. Dietary Supplementation with N-3 Fatty Acids from Weaning Limits Brain Biochemistry and Behavioural Changes Elicited by Prenatal Exposure to Maternal Inflammation in the Mouse Model. *Transl. Psychiatry* **2015**, *5*, e641. [[CrossRef](#)] [[PubMed](#)]
252. Parenti, I.; Rabaneda, L.G.; Schoen, H.; Novarino, G. Neurodevelopmental Disorders: From Genetics to Functional Pathways. *Trends Neurosci.* **2020**. [[CrossRef](#)]
253. Barker, D.J.P. The Origins of the Developmental Origins Theory. *J. Intern. Med.* **2007**, *261*, 412–417. [[CrossRef](#)]
254. Susser, E.; Neugebauer, R.; Hoek, H.W.; Brown, A.S.; Lin, S.; Labovitz, D.; Gorman, J.M. Schizophrenia after Prenatal Famine. Further Evidence. *Arch. Gen. Psychiatry* **1996**, *53*, 25–31. [[CrossRef](#)]
255. Hsu, M.-C.; Huang, Y.-S.; Ouyang, W.-C. Beneficial Effects of Omega-3 Fatty Acid Supplementation in Schizophrenia: Possible Mechanisms. *Lipids Health Dis.* **2020**, *19*. [[CrossRef](#)] [[PubMed](#)]
256. Altshuler, G. Some Placental Considerations Related to Neurodevelopmental and Other Disorders. *J. Child Neurol.* **1993**, *8*, 78–94. [[CrossRef](#)] [[PubMed](#)]
257. Hodyl, N.A.; Aboustate, N.; Bianco-Miotto, T.; Roberts, C.T.; Clifton, V.L.; Stark, M.J. Child Neurodevelopmental Outcomes Following Preterm and Term Birth: What Can the Placenta Tell Us? *Placenta* **2017**, *57*, 79–86. [[CrossRef](#)] [[PubMed](#)]

258. Colombo, J.; Shaddy, D.J.; Kerling, E.H.; Gustafson, K.M.; Carlson, S.E. Docosahexaenoic Acid (DHA) and Arachidonic Acid (ARA) Balance in Developmental Outcomes. *Prostaglandins Leukot. Essent. Fatty Acids* **2017**, *121*, 52–56. [[CrossRef](#)]
259. Hsieh, A.T.; Anthony, J.C.; Diersen-Schade, D.A.; Rumsey, S.C.; Lawrence, P.; Li, C.; Nathanielsz, P.W.; Brenna, J.T. The Influence of Moderate and High Dietary Long Chain Polyunsaturated Fatty Acids (LCPUFA) on Baboon Neonate Tissue Fatty Acids. *Pediatr. Res.* **2007**, *61*, 537–545. [[CrossRef](#)] [[PubMed](#)]
260. Birch, E.E.; Carlson, S.E.; Hoffman, D.R.; Fitzgerald-Gustafson, K.M.; Fu, V.L.N.; Drover, J.R.; Castañeda, Y.S.; Minns, L.; Wheaton, D.K.H.; Mundy, D.; et al. The DIAMOND (DHA Intake And Measurement Of Neural Development) Study: A Double-Masked, Randomized Controlled Clinical Trial of the Maturation of Infant Visual Acuity as a Function of the Dietary Level of Docosahexaenoic Acid. *Am. J. Clin. Nutr.* **2010**, *91*, 848–859. [[CrossRef](#)]
261. Montgomery, P.; Burton, J.R.; Sewell, R.P.; Spreckelsen, T.F.; Richardson, A.J. Low Blood Long Chain Omega-3 Fatty Acids in UK Children Are Associated with Poor Cognitive Performance and Behavior: A Cross-Sectional Analysis from the DOLAB Study. *PLoS ONE* **2013**, *8*, e66697. [[CrossRef](#)]
262. Kalmijn, S.; van Boxtel, M.P.J.; Ocké, M.; Verschuren, W.M.M.; Kromhout, D.; Launer, L.J. Dietary Intake of Fatty Acids and Fish in Relation to Cognitive Performance at Middle Age. *Neurology* **2004**, *62*, 275–280. [[CrossRef](#)]
263. Middleton, P.; Gomersall, J.C.; Gould, J.F.; Shepherd, E.; Olsen, S.F.; Makrides, M. Omega-3 Fatty Acid Addition during Pregnancy. *Cochrane Database Syst. Rev.* **2018**, *11*, CD003402. [[CrossRef](#)]
264. González, F.E.; Báez, R.V. IN TIME: IMPORTANCE OF OMEGA 3 IN CHILDREN'S NUTRITION. *Rev. Paul. Pediatr.* **2017**, *35*, 3–4. [[CrossRef](#)] [[PubMed](#)]
265. Scott, D.T.; Janowsky, J.S.; Carroll, R.E.; Taylor, J.A.; Auestad, N.; Montalto, M.B. Formula Supplementation with Long-Chain Polyunsaturated Fatty Acids: Are There Developmental Benefits? *Pediatrics* **1998**, *102*, E59. [[CrossRef](#)] [[PubMed](#)]
266. Osendarp, S.J.M.; Baghurst, K.I.; Bryan, J.; Calvaresi, E.; Hughes, D.; Hussaini, M.; Karyadi, S.J.M.; van Klinken, B.J.-W.; van der Knaap, H.C.M.; Lukito, W.; et al. Effect of a 12-Mo Micronutrient Intervention on Learning and Memory in Well-Nourished and Marginally Nourished School-Aged Children: 2 Parallel, Randomized, Placebo-Controlled Studies in Australia and Indonesia. *Am. J. Clin. Nutr.* **2007**, *86*, 1082–1093. [[CrossRef](#)] [[PubMed](#)]
267. van der Merwe, L.F.; Moore, S.E.; Fulford, A.J.; Halliday, K.E.; Drammeh, S.; Young, S.; Prentice, A.M. Long-Chain PUFA Supplementation in Rural African Infants: A Randomized Controlled Trial of Effects on Gut Integrity, Growth, and Cognitive Development. *Am. J. Clin. Nutr.* **2013**, *97*, 45–57. [[CrossRef](#)] [[PubMed](#)]
268. Johnson, M.; Fransson, G.; Östlund, S.; Areskoug, B.; Gillberg, C. Omega 3/6 Fatty Acids for Reading in Children: A Randomized, Double-Blind, Placebo-Controlled Trial in 9-Year-Old Mainstream Schoolchildren in Sweden. *J. Child Psychol. Psychiatry* **2017**, *58*, 83–93. [[CrossRef](#)] [[PubMed](#)]
269. Bloch, M.H.; Qawasmi, A. Omega-3 Fatty Acid Supplementation for the Treatment of Children with Attention-Deficit/Hyperactivity Disorder Symptomatology: Systematic Review and Meta-Analysis. *J. Am. Acad. Child Adolesc. Psychiatry* **2011**, *50*, 991–1000. [[CrossRef](#)]
270. Chang, J.P.-C.; Su, K.-P.; Mondelli, V.; Satyanarayanan, S.K.; Yang, H.-T.; Chiang, Y.-J.; Chen, H.-T.; Pariante, C.M. High-Dose Eicosapentaenoic Acid (EPA) Improves Attention and Vigilance in Children and Adolescents with Attention Deficit Hyperactivity Disorder (ADHD) and Low Endogenous EPA Levels. *Transl. Psychiatry* **2019**, *9*, 303. [[CrossRef](#)]
271. Helland, I.B.; Smith, L.; Saarem, K.; Saugstad, O.D.; Drevon, C.A. Maternal Supplementation with Very-Long-Chain n-3 Fatty Acids during Pregnancy and Lactation Augments Children's IQ at 4 Years of Age. *Pediatrics* **2003**, *111*, e39–e44. [[CrossRef](#)]
272. Hoffman, D.R.; Birch, E.E.; Castañeda, Y.S.; Fawcett, S.L.; Wheaton, D.H.; Birch, D.G.; Uauy, R. Visual Function in Breast-Fed Term Infants Weaned to Formula with or without Long-Chain Polyunsaturates at 4 to 6 Months: A Randomized Clinical Trial. *J. Pediatr.* **2003**, *142*, 669–677. [[CrossRef](#)]
273. Birch, E.E.; Hoffman, D.R.; Castañeda, Y.S.; Fawcett, S.L.; Birch, D.G.; Uauy, R.D. A Randomized Controlled Trial of Long-Chain Polyunsaturated Fatty Acid Supplementation of Formula in Term Infants after Weaning at 6 Wk of Age. *Am. J. Clin. Nutr.* **2002**, *75*, 570–580. [[CrossRef](#)]
274. Voigt, R.G.; Jensen, C.L.; Fraley, J.K.; Rozelle, J.C.; Brown, F.R.; Heird, W.C. Relationship between Omega3 Long-Chain Polyunsaturated Fatty Acid Status during Early Infancy and Neurodevelopmental Status at 1 Year of Age. *J. Hum. Nutr. Diet. Off. J. Br. Diet. Assoc.* **2002**, *15*, 111–120. [[CrossRef](#)] [[PubMed](#)]
275. Fleith, M.; Clandinin, M.T. Dietary PUFA for Preterm and Term Infants: Review of Clinical Studies. *Crit. Rev. Food Sci. Nutr.* **2005**, *45*, 205–229. [[CrossRef](#)] [[PubMed](#)]
276. McCann, J.C.; Ames, B.N. Is Docosahexaenoic Acid, an n-3 Long-Chain Polyunsaturated Fatty Acid, Required for Development of Normal Brain Function? An Overview of Evidence from Cognitive and Behavioral Tests in Humans and Animals. *Am. J. Clin. Nutr.* **2005**, *82*, 281–295. [[CrossRef](#)]
277. Bongiovanni, K.D.; Depeters, E.J.; Van Eenennaam, A.L. Neonatal Growth Rate and Development of Mice Raised on Milk Transgenically Enriched with Omega-3 Fatty Acids. *Pediatr. Res.* **2007**, *62*, 412–416. [[CrossRef](#)] [[PubMed](#)]
278. Fedorova, I.; Salem, N. Omega-3 Fatty Acids and Rodent Behavior. *Prostaglandins Leukot. Essent. Fatty Acids* **2006**, *75*, 271–289. [[CrossRef](#)]
279. Lafourcade, M.; Larriou, T.; Mato, S.; Duffaud, A.; Sepers, M.; Matias, I.; De Smedt-Peyrusse, V.; Labrousse, V.F.; Bretillon, L.; Matute, C.; et al. Nutritional Omega-3 Deficiency Abolishes Endocannabinoid-Mediated Neuronal Functions. *Nat. Neurosci.* **2011**, *14*, 345–350. [[CrossRef](#)] [[PubMed](#)]

280. Moranis, A.; Delpéch, J.-C.; De Smedt-Peyrusse, V.; Aubert, A.; Guesnet, P.; Laviolle, M.; Joffre, C.; Layé, S. Long Term Adequate N-3 Polyunsaturated Fatty Acid Diet Protects from Depressive-like Behavior but Not from Working Memory Disruption and Brain Cytokine Expression in Aged Mice. *Brain. Behav. Immun.* **2012**, *26*, 721–731. [[CrossRef](#)] [[PubMed](#)]
281. Levy, S.E.; Mandell, D.S.; Schultz, R.T. Autism. *Lancet Lond. Engl.* **2009**, *374*, 1627–1638. [[CrossRef](#)]
282. Masi, A.; DeMayo, M.M.; Glozier, N.; Guastella, A.J. An Overview of Autism Spectrum Disorder, Heterogeneity and Treatment Options. *Neurosci. Bull.* **2017**, *33*, 183–193. [[CrossRef](#)] [[PubMed](#)]
283. Happé, F.; Ronald, A.; Plomin, R. Time to Give up on a Single Explanation for Autism. *Nat. Neurosci.* **2006**, *9*, 1218–1220. [[CrossRef](#)]
284. Abrahams, B.S.; Geschwind, D.H. Advances in Autism Genetics: On the Threshold of a New Neurobiology. *Nat. Rev. Genet.* **2008**, *9*, 341–355. [[CrossRef](#)] [[PubMed](#)]
285. Kinney, D.K.; Munir, K.M.; Crowley, D.J.; Miller, A.M. Prenatal Stress and Risk for Autism. *Neurosci. Biobehav. Rev.* **2008**, *32*, 1519–1532. [[CrossRef](#)] [[PubMed](#)]
286. Samsam, M.; Ahangari, R.; Naser, S.A. Pathophysiology of Autism Spectrum Disorders: Revisiting Gastrointestinal Involvement and Immune Imbalance. *World J. Gastroenterol.* **2014**, *20*, 9942–9951. [[CrossRef](#)]
287. Minshew, N.J.; Williams, D.L. The New Neurobiology of Autism: Cortex, Connectivity, and Neuronal Organization. *Arch. Neurol.* **2007**, *64*, 945–950. [[CrossRef](#)] [[PubMed](#)]
288. Minshew, N.J.; Keller, T.A. The Nature of Brain Dysfunction in Autism: Functional Brain Imaging Studies. *Curr. Opin. Neurol.* **2010**, *23*, 124–130. [[CrossRef](#)] [[PubMed](#)]
289. Hashemi, E.; Ariza, J.; Rogers, H.; Noctor, S.C.; Martínez-Cerdeño, V. The Number of Parvalbumin-Expressing Interneurons Is Decreased in the Prefrontal Cortex in Autism. *Cereb. Cortex N. Y. NY* **2017**, *27*, 1931–1943. [[CrossRef](#)]
290. Takarae, Y.; Sweeney, J. Neural Hyperexcitability in Autism Spectrum Disorders. *Brain Sci.* **2017**, *7*, 129. [[CrossRef](#)]
291. Sun, C.; Zou, M.; Wang, X.; Xia, W.; Ma, Y.; Liang, S.; Hao, Y.; Wu, L.; Fu, S. FADS1-FADS2 and ELOVL2 Gene Polymorphisms in Susceptibility to Autism Spectrum Disorders in Chinese Children. *BMC Psychiatry* **2018**, *18*, 283. [[CrossRef](#)] [[PubMed](#)]
292. Jones, K.L.; Will, M.J.; Hecht, P.M.; Parker, C.L.; Beversdorf, D.Q. Maternal Diet Rich in Omega-6 Polyunsaturated Fatty Acids during Gestation and Lactation Produces Autistic-like Sociability Deficits in Adult Offspring. *Behav. Brain Res.* **2013**, *238*, 193–199. [[CrossRef](#)]
293. El-Ansary, A.; Al-Ayadhi, L. Relative Abundance of Short Chain and Polyunsaturated Fatty Acids in Propionic Acid-Induced Autistic Features in Rat Pups as Potential Markers in Autism. *Lipids Health Dis.* **2014**, *13*, 140. [[CrossRef](#)] [[PubMed](#)]
294. Alfawaz, H.; Al-Onazi, M.; Bukhari, S.I.; Binobeid, M.; Othman, N.; Algahtani, N.; Bhat, R.S.; Moubayed, N.M.S.; Alzeer, H.S.; El-Ansary, A. The Independent and Combined Effects of Omega-3 and Vitamin B12 in Ameliorating Propionic Acid Induced Biochemical Features in Juvenile Rats as Rodent Model of Autism. *J. Mol. Neurosci. MN* **2018**, *66*, 403–413. [[CrossRef](#)] [[PubMed](#)]
295. Basil, P.; Li, Q.; Gui, H.; Hui, T.C.K.; Ling, V.H.M.; Wong, C.C.Y.; Mill, J.; McAlonan, G.M.; Sham, P.-C. Prenatal Immune Activation Alters the Adult Neural Epigenome but Can Be Partly Stabilised by a N-3 Polyunsaturated Fatty Acid Diet. *Transl. Psychiatry* **2018**, *8*, 125. [[CrossRef](#)] [[PubMed](#)]
296. Yadav, S.; Tiwari, V.; Singh, M.; Yadav, R.K.; Roy, S.; Devi, U.; Gautam, S.; Rawat, J.K.; Ansari, M.N.; Saeedan, A.S.; et al. Comparative Efficacy of Alpha-Linolenic Acid and Gamma-Linolenic Acid to Attenuate Valproic Acid-Induced Autism-like Features. *J. Physiol. Biochem.* **2017**, *73*, 187–198. [[CrossRef](#)]
297. van Elst, K.; Brouwers, J.F.; Merckens, J.E.; Broekhoven, M.H.; Birtoli, B.; Helms, J.B.; Kas, M.J.H. Chronic Dietary Changes in N-6/n-3 Polyunsaturated Fatty Acid Ratios Cause Developmental Delay and Reduce Social Interest in Mice. *Eur. Neuropsychopharmacol. J. Eur. Coll. Neuropsychopharmacol.* **2019**, *29*, 16–31. [[CrossRef](#)]
298. Pietropaolo, S.; Goubiran, M.G.; Joffre, C.; Aubert, A.; Lemaire-Mayo, V.; Crusio, W.E.; Layé, S. Dietary Supplementation of Omega-3 Fatty Acids Rescues Fragile X Phenotypes in Fmr1-Ko Mice. *Psychoneuroendocrinology* **2014**, *49*, 119–129. [[CrossRef](#)]
299. Bell, J.G.; Sargent, J.R.; Tocher, D.R.; Dick, J.R. Red Blood Cell Fatty Acid Compositions in a Patient with Autistic Spectrum Disorder: A Characteristic Abnormality in Neurodevelopmental Disorders? *Prostaglandins Leukot. Essent. Fatty Acids* **2000**, *63*, 21–25. [[CrossRef](#)]
300. Vancassel, S.; Durand, G.; Barthélémy, C.; Lejeune, B.; Martineau, J.; Guilloteau, D.; Andrés, C.; Chalon, S. Plasma Fatty Acid Levels in Autistic Children. *Prostaglandins Leukot. Essent. Fatty Acids* **2001**, *65*, 1–7. [[CrossRef](#)] [[PubMed](#)]
301. Meguid, N.A.; Atta, H.M.; Gouda, A.S.; Khalil, R.O. Role of Polyunsaturated Fatty Acids in the Management of Egyptian Children with Autism. *Clin. Biochem.* **2008**, *41*, 1044–1048. [[CrossRef](#)] [[PubMed](#)]
302. Mostafa, G.A.; Al-Ayadhi, L.Y. Reduced Levels of Plasma Polyunsaturated Fatty Acids and Serum Carnitine in Autistic Children: Relation to Gastrointestinal Manifestations. *Behav. Brain Funct. BBF* **2015**, *11*, 4. [[CrossRef](#)]
303. Jory, J. Abnormal Fatty Acids in Canadian Children with Autism. *Nutr. Burbank Los Angel. Cty. Calif* **2016**, *32*, 474–477. [[CrossRef](#)] [[PubMed](#)]
304. Yui, K.; Kawasaki, Y.; Yamada, H. Modulation of Omega-6 Polyunsaturated Fatty Acid-Dependent Signaling and Its Therapeutic Potential for the Core Symptoms in Individuals with Autism Spectrum Disorders. *Jpn. J. Biol. Psychiatry* **2016**, *27*, 41–47. [[CrossRef](#)]
305. Mazahery, H.; Stonehouse, W.; Delshad, M.; Kruger, M.C.; Conlon, C.A.; Beck, K.L.; von Hurst, P.R. Relationship between Long Chain N-3 Polyunsaturated Fatty Acids and Autism Spectrum Disorder: Systematic Review and Meta-Analysis of Case-Control and Randomised Controlled Trials. *Nutrients* **2017**, *9*, 155. [[CrossRef](#)]

306. Parletta, N.; Niyonsenga, T.; Duff, J. Omega-3 and Omega-6 Polyunsaturated Fatty Acid Levels and Correlations with Symptoms in Children with Attention Deficit Hyperactivity Disorder, Autistic Spectrum Disorder and Typically Developing Controls. *PLoS ONE* **2016**, *11*, e0156432. [[CrossRef](#)] [[PubMed](#)]
307. Sliwinski, S.; Croonenberghs, J.; Christophe, A.; Deboutte, D.; Maes, M. Polyunsaturated Fatty Acids: Do They Have a Role in the Pathophysiology of Autism? *Neuro Endocrinol. Lett.* **2006**, *27*, 465–471. [[PubMed](#)]
308. Lyall, K.; Munger, K.L.; O'Reilly, É.J.; Santangelo, S.L.; Ascherio, A. Maternal Dietary Fat Intake in Association with Autism Spectrum Disorders. *Am. J. Epidemiol.* **2013**, *178*, 209–220. [[CrossRef](#)] [[PubMed](#)]
309. Huang, Y.; Iosif, A.-M.; Hansen, R.L.; Schmidt, R.J. Maternal Polyunsaturated Fatty Acids and Risk for Autism Spectrum Disorder in the MARBLES High-Risk Study. *Autism Int. J. Res. Pract.* **2020**. [[CrossRef](#)]
310. Politi, P.; Cena, H.; Comelli, M.; Marrone, G.; Allegri, C.; Emanuele, E.; Ucelli di Nemi, S. Behavioral Effects of Omega-3 Fatty Acid Supplementation in Young Adults with Severe Autism: An Open Label Study. *Arch. Med. Res.* **2008**, *39*, 682–685. [[CrossRef](#)]
311. De Crescenzo, F.; D'Alò, G.L.; Morgano, G.P.; Minozzi, S.; Mitrova, Z.; Saulle, R.; Cruciani, F.; Fulceri, F.; Davoli, M.; Scattoni, M.L.; et al. Impact of Polyunsaturated Fatty Acids on Patient-Important Outcomes in Children and Adolescents with Autism Spectrum Disorder: A Systematic Review. *Health Qual. Life Outcomes* **2020**, *18*, 28. [[CrossRef](#)] [[PubMed](#)]
312. Infante, M.; Sears, B.; Rizzo, A.M.; Mariani Cerati, D.; Caprio, M.; Ricordi, C.; Fabbri, A. Omega-3 PUFAs and Vitamin D Co-Supplementation as a Safe-Effective Therapeutic Approach for Core Symptoms of Autism Spectrum Disorder: Case Report and Literature Review. *Nutr. Neurosci.* **2018**, *1–12*. [[CrossRef](#)] [[PubMed](#)]
313. Mazahery, H.; Conlon, C.A.; Beck, K.L.; Mugridge, O.; Kruger, M.C.; Stonehouse, W.; Camargo, C.A.; Meyer, B.J.; Jones, B.; von Hurst, P.R. A Randomised Controlled Trial of Vitamin D and Omega-3 Long Chain Polyunsaturated Fatty Acids in the Treatment of Irritability and Hyperactivity among Children with Autism Spectrum Disorder. *J. Steroid Biochem. Mol. Biol.* **2019**, *187*, 9–16. [[CrossRef](#)]
314. Cheng, Y.-S.; Tseng, P.-T.; Chen, Y.-W.; Stubbs, B.; Yang, W.-C.; Chen, T.-Y.; Wu, C.-K.; Lin, P.-Y. Supplementation of Omega 3 Fatty Acids May Improve Hyperactivity, Lethargy, and Stereotypy in Children with Autism Spectrum Disorders: A Meta-Analysis of Randomized Controlled Trials. *Neuropsychiatr. Dis. Treat.* **2017**, *13*, 2531–2543. [[CrossRef](#)] [[PubMed](#)]
315. Sheppard, K.W.; Boone, K.M.; Gracious, B.; Klebanoff, M.A.; Rogers, L.K.; Rausch, J.; Bartlett, C.; Coury, D.L.; Keim, S.A. Effect of Omega-3 and -6 Supplementation on Language in Preterm Toddlers Exhibiting Autism Spectrum Disorder Symptoms. *J. Autism Dev. Disord.* **2017**, *47*, 3358–3369. [[CrossRef](#)]
316. Keim, S.A.; Gracious, B.; Boone, K.M.; Klebanoff, M.A.; Rogers, L.K.; Rausch, J.; Coury, D.L.; Sheppard, K.W.; Husk, J.; Rhoda, D.A.  $\omega$ -3 and  $\omega$ -6 Fatty Acid Supplementation May Reduce Autism Symptoms Based on Parent Report in Preterm Toddlers. *J. Nutr.* **2018**, *148*, 227–235. [[CrossRef](#)] [[PubMed](#)]
317. Johnson, S.M.; Hollander, E. Evidence That Eicosapentaenoic Acid Is Effective in Treating Autism. *J. Clin. Psychiatry* **2003**, *64*, 848–849. [[CrossRef](#)] [[PubMed](#)]
318. Meiri, G.; Bichovsky, Y.; Belmaker, R.H. Omega 3 Fatty Acid Treatment in Autism. *J. Child Adolesc. Psychopharmacol.* **2009**, *19*, 449–451. [[CrossRef](#)] [[PubMed](#)]
319. Ooi, Y.P.; Weng, S.-J.; Jang, L.Y.; Low, L.; Seah, J.; Teo, S.; Ang, R.P.; Lim, C.G.; Liew, A.; Fung, D.S.; et al. Omega-3 Fatty Acids in the Management of Autism Spectrum Disorders: Findings from an Open-Label Pilot Study in Singapore. *Eur. J. Clin. Nutr.* **2015**, *69*, 969–971. [[CrossRef](#)]
320. Johnson, C.R.; Handen, B.L.; Zimmer, M.; Sacco, K. Polyunsaturated Fatty Acid Supplementation in Young Children with Autism. *J. Dev. Phys. Disabil.* **2010**, *22*, 1–10. [[CrossRef](#)]
321. Amminger, G.P.; Berger, G.E.; Schäfer, M.R.; Klier, C.; Friedrich, M.H.; Feucht, M. Omega-3 Fatty Acids Supplementation in Children with Autism: A Double-Blind Randomized, Placebo-Controlled Pilot Study. *Biol. Psychiatry* **2007**, *61*, 551–553. [[CrossRef](#)]
322. Bent, S.; Bertoglio, K.; Ashwood, P.; Bostrom, A.; Hendren, R.L. A Pilot Randomized Controlled Trial of Omega-3 Fatty Acids for Autism Spectrum Disorder. *J. Autism Dev. Disord.* **2011**, *41*, 545–554. [[CrossRef](#)] [[PubMed](#)]
323. Yui, K.; Koshihara, M.; Nakamura, S.; Kobayashim, Y.; Ohnishi, M. Efficacy of Adding Large Doses of Arachidonic Acid to Docosahexaenoic Acid against Restricted Repetitive Behaviors in Individuals with Autism Spectrum Disorders: A Placebo-Controlled Trial. *J. Addict. Res. Ther.* **2011**, *2–6*. [[CrossRef](#)]
324. Yui, K.; Koshihara, M.; Nakamura, S.; Kobayashi, Y. Effects of Large Doses of Arachidonic Acid Added to Docosahexaenoic Acid on Social Impairment in Individuals with Autism Spectrum Disorders: A Double-Blind, Placebo-Controlled, Randomized Trial. *J. Clin. Psychopharmacol.* **2012**, *32*, 200–206. [[CrossRef](#)]
325. Bent, S.; Hendren, R.L.; Zandi, T.; Law, K.; Choi, J.-E.; Widjaja, F.; Kalb, L.; Nestle, J.; Law, P. Internet-Based, Randomized, Controlled Trial of Omega-3 Fatty Acids for Hyperactivity in Autism. *J. Am. Acad. Child Adolesc. Psychiatry* **2014**, *53*, 658–666. [[CrossRef](#)] [[PubMed](#)]
326. Voigt, R.G.; Mellon, M.W.; Katusic, S.K.; Weaver, A.L.; Matern, D.; Mellon, B.; Jensen, C.L.; Barbaresi, W.J. Dietary Docosahexaenoic Acid Supplementation in Children with Autism. *J. Pediatr. Gastroenterol. Nutr.* **2014**, *58*, 715–722. [[CrossRef](#)] [[PubMed](#)]
327. Mankad, D.; Dupuis, A.; Smile, S.; Roberts, W.; Brian, J.; Lui, T.; Genore, L.; Zaghoul, D.; Iaboni, A.; Marcon, P.M.A.; et al. A Randomized, Placebo Controlled Trial of Omega-3 Fatty Acids in the Treatment of Young Children with Autism. *Mol. Autism* **2015**, *6*, 18. [[CrossRef](#)] [[PubMed](#)]



328. Parellada, M.; Llorente, C.; Calvo, R.; Gutierrez, S.; Lázaro, L.; Graell, M.; Guisasola, M.; Dorado, M.L.; Boada, L.; Romo, J.; et al. Randomized Trial of Omega-3 for Autism Spectrum Disorders: Effect on Cell Membrane Composition and Behavior. *Eur. Neuropsychopharmacol. J. Eur. Coll. Neuropsychopharmacol.* **2017**, *27*, 1319–1330. [[CrossRef](#)] [[PubMed](#)]
329. Boone, K.M.; Gracious, B.; Klebanoff, M.A.; Rogers, L.K.; Rausch, J.; Cury, D.L.; Keim, S.A. Omega-3 and -6 Fatty Acid Supplementation and Sensory Processing in Toddlers with ASD Symptomology Born Preterm: A Randomized Controlled Trial. *Early Hum. Dev.* **2017**, *115*, 64–70. [[CrossRef](#)]
330. Karhu, E.; Zukerman, R.; Eshraghi, R.S.; Mittal, J.; Deth, R.C.; Castejon, A.M.; Trivedi, M.; Mittal, R.; Eshraghi, A.A. Nutritional Interventions for Autism Spectrum Disorder. *Nutr. Rev.* **2019**. [[CrossRef](#)]
331. Froehlich, T.E.; Lanphear, B.P.; Epstein, J.N.; Barbaresi, W.J.; Katusic, S.K.; Kahn, R.S. Prevalence, Recognition, and Treatment of Attention-Deficit/Hyperactivity Disorder in a National Sample of US Children. *Arch. Pediatr. Adolesc. Med.* **2007**, *161*, 857–864. [[CrossRef](#)]
332. Gentile, J.P.; Atiq, R.; Gillig, P.M. Adult ADHD: Diagnosis, Differential Diagnosis, and Medication Management. *Psychiatry Edgmont Pa Townsh.* **2006**, *3*, 25–30.
333. Epstein, J.N.; Loren, R.E.A. Changes in the Definition of ADHD in DSM-5: Subtle but Important. *Neuropsychiatry* **2013**, *3*, 455–458. [[CrossRef](#)]
334. Wilens, T.E.; Biederman, J.; Faraone, S.V.; Martelon, M.; Westerberg, D.; Spencer, T.J. Presenting ADHD Symptoms, Subtypes, and Comorbid Disorders in Clinically Referred Adults with ADHD. *J. Clin. Psychiatry* **2009**, *70*, 1557–1562. [[CrossRef](#)] [[PubMed](#)]
335. Steinau, S. Diagnostic Criteria in Attention Deficit Hyperactivity Disorder—Changes in DSM 5. *Front. Psychiatry* **2013**, *4*. [[CrossRef](#)]
336. Millichap, J.G. Etiologic Classification of Attention-Deficit/Hyperactivity Disorder. *Pediatrics* **2008**, *121*, e358–e365. [[CrossRef](#)]
337. Thapar, A.; Cooper, M.; Jeffries, R.; Stergiakouli, E. What Causes Attention Deficit Hyperactivity Disorder? *Arch. Dis. Child.* **2012**, *97*, 260–265. [[CrossRef](#)] [[PubMed](#)]
338. Adams, J.; Crosbie, J.; Wigg, K.; Ickowicz, A.; Pathare, T.; Roberts, W.; Malone, M.; Schachar, R.; Tannock, R.; Kennedy, J.L.; et al. Glutamate Receptor, Ionotropic, N-Methyl D-Aspartate 2A (GRIN2A) Gene as a Positional Candidate for Attention-Deficit/Hyperactivity Disorder in the 16p13 Region. *Mol. Psychiatry* **2004**, *9*, 494–499. [[CrossRef](#)]
339. Gizer, I.R.; Ficks, C.; Waldman, I.D. Candidate Gene Studies of ADHD: A Meta-Analytic Review. *Hum. Genet.* **2009**, *126*, 51–90. [[CrossRef](#)]
340. Banaschewski, T.; Becker, K.; Scherag, S.; Franke, B.; Coghill, D. Molecular Genetics of Attention-Deficit/Hyperactivity Disorder: An Overview. *Eur. Child Adolesc. Psychiatry* **2010**, *19*, 237–257. [[CrossRef](#)]
341. Castellanos, F.X.; Lee, P.P.; Sharp, W.; Jeffries, N.O.; Greenstein, D.K.; Clasen, L.S.; Blumenthal, J.D.; James, R.S.; Ebens, C.L.; Walter, J.M.; et al. Developmental Trajectories of Brain Volume Abnormalities in Children and Adolescents with Attention-Deficit/Hyperactivity Disorder. *JAMA* **2002**, *288*, 1740–1748. [[CrossRef](#)] [[PubMed](#)]
342. Kessler, D.; Angstadt, M.; Welsh, R.C.; Sripatha, C. Modality-Spanning Deficits in Attention-Deficit/Hyperactivity Disorder in Functional Networks, Gray Matter, and White Matter. *J. Neurosci. Off. J. Soc. Neurosci.* **2014**, *34*, 16555–16566. [[CrossRef](#)]
343. Li, X.; Cao, Q.; Pu, F.; Li, D.; Fan, Y.; An, L.; Wang, P.; Wu, Z.; Sun, L.; Li, S.; et al. Abnormalities of Structural Covariance Networks in Drug-Naïve Boys with Attention Deficit Hyperactivity Disorder. *Psychiatry Res.* **2015**, *231*, 273–278. [[CrossRef](#)] [[PubMed](#)]
344. Chen, J.-R.; Hsu, S.-F.; Hsu, C.-D.; Hwang, L.-H.; Yang, S.-C. Dietary Patterns and Blood Fatty Acid Composition in Children with Attention-Deficit Hyperactivity Disorder in Taiwan. *J. Nutr. Biochem.* **2004**, *15*, 467–472. [[CrossRef](#)]
345. Young, G.S.; Maharaj, N.J.; Conquer, J.A. Blood Phospholipid Fatty Acid Analysis of Adults with and without Attention Deficit/Hyperactivity Disorder. *Lipids* **2004**, *39*, 117–123. [[CrossRef](#)] [[PubMed](#)]
346. Colter, A.L.; Cutler, C.; Meckling, K.A. Fatty Acid Status and Behavioural Symptoms of Attention Deficit Hyperactivity Disorder in Adolescents: A Case-Control Study. *Nutr. J.* **2008**, *7*, 8. [[CrossRef](#)]
347. Irmisch, G.; Richter, J.; Thome, J.; Sheldrick, A.J.; Wandschneider, R. Altered Serum Mono- and Polyunsaturated Fatty Acid Levels in Adults with ADHD. *Atten. Deficit Hyperact. Disord.* **2013**, *5*, 303–311. [[CrossRef](#)]
348. Hawkey, E.; Nigg, J.T. Omega-3 Fatty Acid and ADHD: Blood Level Analysis and Meta-Analytic Extension of Supplementation Trials. *Clin. Psychol. Rev.* **2014**, *34*, 496–505. [[CrossRef](#)] [[PubMed](#)]
349. Milte, C.M.; Sinn, N.; Buckley, J.D.; Coates, A.M.; Young, R.M.; Howe, P.R. Polyunsaturated Fatty Acids, Cognition and Literacy in Children with ADHD with and without Learning Difficulties. *J. Child Health Care Prof. Work. Child. Hosp. Community* **2011**, *15*, 299–311. [[CrossRef](#)]
350. Fuentes-Albero, M.; Martínez-Martínez, M.I.; Cauli, O. Omega-3 Long-Chain Polyunsaturated Fatty Acids Intake in Children with Attention Deficit and Hyperactivity Disorder. *Brain Sci.* **2019**, *9*, 120. [[CrossRef](#)] [[PubMed](#)]
351. Fan, X.; Bruno, K.J.; Hess, E.J. Rodent Models of ADHD. *Curr. Top. Behav. Neurosci.* **2012**, *9*, 273–300. [[CrossRef](#)]
352. Lou, H.C.; Rosa, P.; Pryds, O.; Karrebaek, H.; Lunding, J.; Cumming, P.; Gjedde, A. ADHD: Increased Dopamine Receptor Availability Linked to Attention Deficit and Low Neonatal Cerebral Blood Flow. *Dev. Med. Child Neurol.* **2004**, *46*, 179–183. [[CrossRef](#)] [[PubMed](#)]
353. Rosa-Neto, P.; Lou, H.C.; Cumming, P.; Pryds, O.; Karrebaek, H.; Lunding, J.; Gjedde, A. Methylphenidate-Evoked Changes in Striatal Dopamine Correlate with Inattention and Impulsivity in Adolescents with Attention Deficit Hyperactivity Disorder. *NeuroImage* **2005**, *25*, 868–876. [[CrossRef](#)] [[PubMed](#)]

354. Volkow, N.D.; Wang, G.-J.; Newcorn, J.; Fowler, J.S.; Telang, F.; Solanto, M.V.; Logan, J.; Wong, C.; Ma, Y.; Swanson, J.M.; et al. Brain Dopamine Transporter Levels in Treatment and Drug Naïve Adults with ADHD. *NeuroImage* **2007**, *34*, 1182–1190. [[CrossRef](#)] [[PubMed](#)]
355. Volkow, N.D.; Wang, G.-J.; Newcorn, J.; Telang, F.; Solanto, M.V.; Fowler, J.S.; Logan, J.; Ma, Y.; Schulz, K.; Pradhan, K.; et al. Depressed Dopamine Activity in Caudate and Preliminary Evidence of Limbic Involvement in Adults with Attention-Deficit/Hyperactivity Disorder. *Arch. Gen. Psychiatry* **2007**, *64*, 932–940. [[CrossRef](#)]
356. Wang, G.-X.; Ma, Y.-H.; Wang, S.-F.; Ren, G.-F.; Guo, H. Association of Dopaminergic/GABAergic Genes with Attention Deficit Hyperactivity Disorder in Children. *Mol. Med. Rep.* **2012**, *6*, 1093–1098. [[CrossRef](#)]
357. Bello, E.P.; Mateo, Y.; Gelman, D.M.; Noaín, D.; Shin, J.H.; Low, M.J.; Alvarez, V.A.; Lovinger, D.M.; Rubinstein, M. Cocaine Supersensitivity and Enhanced Motivation for Reward in Mice Lacking Dopamine D2 Autoreceptors. *Nat. Neurosci.* **2011**, *14*, 1033–1038. [[CrossRef](#)] [[PubMed](#)]
358. Linden, J.; James, A.S.; McDaniel, C.; Jentsch, J.D. Dopamine D2 Receptors in Dopaminergic Neurons Modulate Performance in a Reversal Learning Task in Mice. *eNeuro* **2018**, *5*. [[CrossRef](#)] [[PubMed](#)]
359. Volkow, N.D.; Swanson, J.M. Clinical Practice: Adult Attention Deficit-Hyperactivity Disorder. *N. Engl. J. Med.* **2013**, *369*, 1935–1944. [[CrossRef](#)] [[PubMed](#)]
360. Giros, B.; Jaber, M.; Jones, S.R.; Wightman, R.M.; Caron, M.G. Hyperlocomotion and Indifference to Cocaine and Amphetamine in Mice Lacking the Dopamine Transporter. *Nature* **1996**, *379*, 606–612. [[CrossRef](#)] [[PubMed](#)]
361. Spieglewoy, C.; Roubert, C.; Hamon, M.; Nosten-Bertrand, M.; Betancur, C.; Giros, B. Behavioural Disturbances Associated with Hyperdopaminergia in Dopamine-Transporter Knockout Mice. *Behav. Pharmacol.* **2000**, *11*, 279–290. [[CrossRef](#)]
362. Hall, F.S.; Sora, I.; Hen, R.; Uhl, G.R. Serotonin/Dopamine Interactions in a Hyperactive Mouse: Reduced Serotonin Receptor 1B Activity Reverses Effects of Dopamine Transporter Knockout. *PLoS ONE* **2014**, *9*, e115009. [[CrossRef](#)]
363. Takamatsu, Y.; Hagino, Y.; Sato, A.; Takahashi, T.; Nagasawa, S.Y.; Kubo, Y.; Mizuguchi, M.; Uhl, G.R.; Sora, I.; Ikeda, K. Improvement of Learning and Increase in Dopamine Level in the Frontal Cortex by Methylphenidate in Mice Lacking Dopamine Transporter. *Curr. Mol. Med.* **2015**, *15*, 245–252. [[CrossRef](#)]
364. Cinque, S.; Zoratto, F.; Poleggi, A.; Leo, D.; Cerniglia, L.; Cimino, S.; Tambelli, R.; Alleva, E.; Gainetdinov, R.R.; Laviola, G.; et al. Behavioral Phenotyping of Dopamine Transporter Knockout Rats: Compulsive Traits, Motor Stereotypies, and Anhedonia. *Front. Psychiatry* **2018**, *9*, 43. [[CrossRef](#)]
365. Sagvolden, T.; Metzger, M.A.; Schiørbeck, H.K.; Rugland, A.L.; Spinnangr, I.; Sagvolden, G. The Spontaneously Hypertensive Rat (SHR) as an Animal Model of Childhood Hyperactivity (ADHD): Changed Reactivity to Reinforcers and to Psychomotor Stimulants. *Behav. Neural Biol.* **1992**, *58*, 103–112. [[CrossRef](#)]
366. Vancassel, S.; Blondeau, C.; Lallemand, S.; Cador, M.; Linard, A.; Laviolle, M.; Dellu-Hagedorn, F. Hyperactivity in the Rat Is Associated with Spontaneous Low Level of N-3 Polyunsaturated Fatty Acids in the Frontal Cortex. *Behav. Brain Res.* **2007**, *180*, 119–126. [[CrossRef](#)] [[PubMed](#)]
367. Hauser, J.; Makulska-Gertruda, E.; Reissmann, A.; Sontag, T.-A.; Tucha, O.; Lange, K.W. The Effects of Nutritional Polyunsaturated Fatty Acids on Locomotor Activity in Spontaneously Hypertensive Rats. *Atten. Deficit Hyperact. Disord.* **2014**, *6*, 61–65. [[CrossRef](#)]
368. Moghaddam, M.F.; Shamekhi, M.; Rakhshani, T. Effectiveness of Methylphenidate and PUFA for the Treatment of Patients with ADHD: A Double-Blinded Randomized Clinical Trial. *Electron. Physician* **2017**, *9*, 4412–4418. [[CrossRef](#)] [[PubMed](#)]
369. Sinn, N.; Bryan, J. Effect of Supplementation with Polyunsaturated Fatty Acids and Micronutrients on Learning and Behavior Problems Associated with Child ADHD. *J. Dev. Behav. Pediatr. JDBP* **2007**, *28*, 82–91. [[CrossRef](#)] [[PubMed](#)]
370. Bélanger, S.A.; Vanasse, M.; Spahis, S.; Sylvestre, M.-P.; Lippé, S.; L'heureux, F.; Ghadirian, P.; Vanasse, C.-M.; Levy, E. Omega-3 Fatty Acid Treatment of Children with Attention-Deficit Hyperactivity Disorder: A Randomized, Double-Blind, Placebo-Controlled Study. *Paediatr. Child Health* **2009**, *14*, 89–98. [[CrossRef](#)]
371. Richardson, A.J.; Puri, B.K. A Randomized Double-Blind, Placebo-Controlled Study of the Effects of Supplementation with Highly Unsaturated Fatty Acids on ADHD-Related Symptoms in Children with Specific Learning Difficulties. *Prog. Neuropsychopharmacol. Biol. Psychiatry* **2002**, *26*, 233–239. [[CrossRef](#)]
372. Stevens, L.; Zhang, W.; Peck, L.; Kuczek, T.; Grevstad, N.; Mahon, A.; Zentall, S.S.; Arnold, L.E.; Burgess, J.R. EFA Supplementation in Children with Inattention, Hyperactivity, and Other Disruptive Behaviors. *Lipids* **2003**, *38*, 1007–1021. [[CrossRef](#)] [[PubMed](#)]
373. Assareh, M.; Davari Ashtiani, R.; Khademi, M.; Jazayeri, S.; Rai, A.; Nikoo, M. Efficacy of Polyunsaturated Fatty Acids (PUFA) in the Treatment of Attention Deficit Hyperactivity Disorder. *J. Atten. Disord.* **2017**, *21*, 78–85. [[CrossRef](#)]
374. Gillies, D.; Sinn, J.K.; Lad, S.S.; Leach, M.J.; Ross, M.J. Polyunsaturated Fatty Acids (PUFA) for Attention Deficit Hyperactivity Disorder (ADHD) in Children and Adolescents. *Cochrane Database Syst. Rev.* **2012**, CD007986. [[CrossRef](#)]
375. Checa-Ros, A.; Haro-García, A.; Seiquer, I.; Molina-Carballo, A.; Uberos-Fernández, J.; Muñoz-Hoyos, A. Early Monitoring of Fatty Acid Profile in Children with Attention Deficit and/or Hyperactivity Disorder under Treatment with Omega-3 Polyunsaturated Fatty Acids. *Minerva Pediatr.* **2019**, *71*, 313–325. [[CrossRef](#)] [[PubMed](#)]
376. Aman, M.G.; Mitchell, E.A.; Turbott, S.H. The Effects of Essential Fatty Acid Supplementation by Efamol in Hyperactive Children. *J. Abnorm. Child Psychol.* **1987**, *15*, 75–90. [[CrossRef](#)] [[PubMed](#)]
377. Voigt, R.G.; Llorente, A.M.; Jensen, C.L.; Fraley, J.K.; Berretta, M.C.; Heird, W.C. A Randomized, Double-Blind, Placebo-Controlled Trial of Docosahexaenoic Acid Supplementation in Children with Attention-Deficit/Hyperactivity Disorder. *J. Pediatr.* **2001**, *139*, 189–196. [[CrossRef](#)]

378. Hirayama, S.; Hamazaki, T.; Terasawa, K. Effect of Docosahexaenoic Acid-Containing Food Administration on Symptoms of Attention-Deficit/Hyperactivity Disorder—A Placebo-Controlled Double-Blind Study. *Eur. J. Clin. Nutr.* **2004**, *58*, 467–473. [[CrossRef](#)] [[PubMed](#)]
379. Sinn, N.; Bryan, J.; Wilson, C. Cognitive Effects of Polyunsaturated Fatty Acids in Children with Attention Deficit Hyperactivity Disorder Symptoms: A Randomised Controlled Trial. *Prostaglandins Leukot. Essent. Fatty Acids* **2008**, *78*, 311–326. [[CrossRef](#)]
380. Vaisman, N.; Kaysar, N.; Zaruk-Adasha, Y.; Pelled, D.; Brichon, G.; Zwingelstein, G.; Bodennec, J. Correlation between Changes in Blood Fatty Acid Composition and Visual Sustained Attention Performance in Children with Inattention: Effect of Dietary n-3 Fatty Acids Containing Phospholipids. *Am. J. Clin. Nutr.* **2008**, *87*, 1170–1180. [[CrossRef](#)] [[PubMed](#)]
381. Johnson, M.; Ostlund, S.; Fransson, G.; Kadesjö, B.; Gillberg, C. Omega-3/Omega-6 Fatty Acids for Attention Deficit Hyperactivity Disorder: A Randomized Placebo-Controlled Trial in Children and Adolescents. *J. Atten. Disord.* **2009**, *12*, 394–401. [[CrossRef](#)] [[PubMed](#)]
382. Raz, R.; Carasso, R.L.; Yehuda, S. The Influence of Short-Chain Essential Fatty Acids on Children with Attention-Deficit/Hyperactivity Disorder: A Double-Blind Placebo-Controlled Study. *J. Child Adolesc. Psychopharmacol.* **2009**, *19*, 167–177. [[CrossRef](#)] [[PubMed](#)]
383. Gustafsson, P.A.; Birberg-Thornberg, U.; Duchén, K.; Landgren, M.; Malmberg, K.; Pelling, H.; Strandvik, B.; Karlsson, T. EPA Supplementation Improves Teacher-Rated Behaviour and Oppositional Symptoms in Children with ADHD. *Acta Paediatr. Oslo Nor.* **1992** *2010*, *99*, 1540–1549. [[CrossRef](#)]
384. Hariri, M.; Djazayeri, A.; Djalali, M.; Saedisomeolia, A.; Rahimi, A.; Abdollahian, E. Effect of N-3 Supplementation on Hyperactivity, Oxidative Stress and Inflammatory Mediators in Children with Attention-Deficit-Hyperactivity Disorder. *Malays. J. Nutr.* **2012**, *18*, 329–335. [[PubMed](#)]
385. Manor, I.; Magen, A.; Keidar, D.; Rosen, S.; Tasker, H.; Cohen, T.; Richter, Y.; Zaaroor-Regev, D.; Manor, Y.; Weizman, A. The Effect of Phosphatidylserine Containing Omega3 Fatty-Acids on Attention-Deficit Hyperactivity Disorder Symptoms in Children: A Double-Blind Placebo-Controlled Trial, Followed by an Open-Label Extension. *Eur. Psychiatry J. Assoc. Eur. Psychiatr.* **2012**, *27*, 335–342. [[CrossRef](#)] [[PubMed](#)]
386. Milte, C.M.; Parletta, N.; Buckley, J.D.; Coates, A.M.; Young, R.M.; Howe, P.R.C. Eicosapentaenoic and Docosahexaenoic Acids, Cognition, and Behavior in Children with Attention-Deficit/Hyperactivity Disorder: A Randomized Controlled Trial. *Nutr. Burbank Los Angel. Cty. Calif* **2012**, *28*, 670–677. [[CrossRef](#)]
387. Milte, C.M.; Parletta, N.; Buckley, J.D.; Coates, A.M.; Young, R.M.; Howe, P.R.C. Increased Erythrocyte Eicosapentaenoic Acid and Docosahexaenoic Acid Are Associated With Improved Attention and Behavior in Children With ADHD in a Randomized Controlled Three-Way Crossover Trial. *J. Atten. Disord.* **2015**, *19*, 954–964. [[CrossRef](#)] [[PubMed](#)]
388. Perera, H.; Jeewandara, K.C.; Seneviratne, S.; Guruge, C. Combined  $\Omega 3$  and  $\Omega 6$  Supplementation in Children with Attention-Deficit Hyperactivity Disorder (ADHD) Refractory to Methylphenidate Treatment: A Double-Blind, Placebo-Controlled Study. *J. Child Neurol.* **2012**, *27*, 747–753. [[CrossRef](#)]
389. Behdani, F.; Hebrani, P.; Naseraee, A.; Haghighi, M.B.; Akhavanrezayat, A. Does Omega-3 Supplement Enhance the Therapeutic Results of Methylphenidate in Attention Deficit Hyperactivity Disorder Patients? *J. Res. Med. Sci. Off. J. Isfahan Univ. Med. Sci.* **2013**, *18*, 653–658.
390. Dubnov-Raz, G.; Khoury, Z.; Wright, I.; Raz, R.; Berger, I. The Effect of Alpha-Linolenic Acid Supplementation on ADHD Symptoms in Children: A Randomized Controlled Double-Blind Study. *Front. Hum. Neurosci.* **2014**, *8*, 780. [[CrossRef](#)]
391. Widenhorn-Müller, K.; Schwanda, S.; Scholz, E.; Spitzer, M.; Bode, H. Effect of Supplementation with Long-Chain  $\omega$ -3 Polyunsaturated Fatty Acids on Behavior and Cognition in Children with Attention Deficit/Hyperactivity Disorder (ADHD): A Randomized Placebo-Controlled Intervention Trial. *Prostaglandins Leukot. Essent. Fatty Acids* **2014**, *91*, 49–60. [[CrossRef](#)] [[PubMed](#)]
392. Bos, D.J.; Oranje, B.; Veerhoek, E.S.; Van Diepen, R.M.; Weusten, J.M.; Demmelmair, H.; Koletzko, B.; de Sain-van der Velden, M.G.; Eilander, A.; Hoeksma, M.; et al. Reduced Symptoms of Inattention after Dietary Omega-3 Fatty Acid Supplementation in Boys with and without Attention Deficit/Hyperactivity Disorder. *Neuropsychopharmacol. Off. Publ. Am. Coll. Neuropsychopharmacol.* **2015**, *40*, 2298–2306. [[CrossRef](#)] [[PubMed](#)]
393. Matsudaira, T.; Gow, R.V.; Kelly, J.; Murphy, C.; Potts, L.; Sumich, A.; Ghebremeskel, K.; Crawford, M.A.; Taylor, E. Biochemical and Psychological Effects of Omega-3/6 Supplements in Male Adolescents with Attention-Deficit/Hyperactivity Disorder: A Randomized, Placebo-Controlled, Clinical Trial. *J. Child Adolesc. Psychopharmacol.* **2015**, *25*, 775–782. [[CrossRef](#)]
394. Anand, P.; Sachdeva, A. Effect of Poly Unsaturated Fatty Acids Administration on Children with Attention Deficit Hyperactivity Disorder: A Randomized Controlled Trial. *J. Clin. Diagn. Res. JCDR* **2016**, *10*, OC01–OC05. [[CrossRef](#)] [[PubMed](#)]
395. Salehi, B.; Mohammadbeigi, A.; Sheykhholeslam, H.; Moshiri, E.; Dorreh, F. Omega-3 and Zinc Supplementation as Complementary Therapies in Children with Attention-Deficit/Hyperactivity Disorder. *J. Res. Pharm. Pract.* **2016**, *5*, 22–26. [[CrossRef](#)]
396. Barragán, E.; Breuer, D.; Döpfner, M. Efficacy and Safety of Omega-3/6 Fatty Acids, Methylphenidate, and a Combined Treatment in Children With ADHD. *J. Atten. Disord.* **2017**, *21*, 433–441. [[CrossRef](#)] [[PubMed](#)]
397. Kean, J.D.; Sarris, J.; Scholey, A.; Silberstein, R.; Downey, L.A.; Stough, C. Reduced Inattention and Hyperactivity and Improved Cognition after Marine Oil Extract (PCSO-524®) Supplementation in Children and Adolescents with Clinical and Subclinical Symptoms of Attention-Deficit Hyperactivity Disorder (ADHD): A Randomised, Double-Blind, Placebo-Controlled Trial. *Psychopharmacology* **2017**, *234*, 403–420. [[CrossRef](#)]

398. Dashti, N.; Hekmat, H.; Soltani, H.R.; Rahimdel, A.; Javaherchian, M. Comparison of Therapeutic Effects of Omega-3 and Methylphenidate (Ritalin®) in Treating Children with Attention Deficit Hyperactivity Disorder. *Iran. J. Psychiatry Behav. Sci.* **2014**, *8*, 7–11. [[PubMed](#)]
399. Kahn, R.S.; Sommer, I.E.; Murray, R.M.; Meyer-Lindenberg, A.; Weinberger, D.R.; Cannon, T.D.; O'Donovan, M.; Correll, C.U.; Kane, J.M.; van Os, J.; et al. Schizophrenia. *Nat. Rev. Dis. Primer* **2015**, *1*, 15067. [[CrossRef](#)]
400. Murray, R.M.; Lewis, S.W. Is Schizophrenia a Neurodevelopmental Disorder? *Br. Med. J. Clin. Res. Ed* **1987**, *295*, 681–682. [[CrossRef](#)]
401. Weinberger, D.R. Implications of Normal Brain Development for the Pathogenesis of Schizophrenia. *Arch. Gen. Psychiatry* **1987**, *44*, 660–669. [[CrossRef](#)] [[PubMed](#)]
402. McGrath, J.J.; Féron, F.P.; Burne, T.H.J.; Mackay-Sim, A.; Eyles, D.W. The Neurodevelopmental Hypothesis of Schizophrenia: A Review of Recent Developments. *Ann. Med.* **2003**, *35*, 86–93. [[CrossRef](#)] [[PubMed](#)]
403. Owen, M.J.; O'Donovan, M.C.; Thapar, A.; Craddock, N. Neurodevelopmental Hypothesis of Schizophrenia. *Br. J. Psychiatry J. Ment. Sci.* **2011**, *198*, 173–175. [[CrossRef](#)]
404. Feigenson, K.A.; Kusnecov, A.W.; Silverstein, S.M. Inflammation and the Two-Hit Hypothesis of Schizophrenia. *Neurosci. Biobehav. Rev.* **2014**, *38*, 72–93. [[CrossRef](#)] [[PubMed](#)]
405. Bechter, K. Updating the Mild Encephalitis Hypothesis of Schizophrenia. *Prog. Neuropsychopharmacol. Biol. Psychiatry* **2013**, *42*, 71–91. [[CrossRef](#)] [[PubMed](#)]
406. Cullen, A.E.; Fisher, H.L.; Roberts, R.E.; Pariante, C.M.; Laurens, K.R. Daily Stressors and Negative Life Events in Children at Elevated Risk of Developing Schizophrenia. *Br. J. Psychiatry J. Ment. Sci.* **2014**, *204*, 354–360. [[CrossRef](#)]
407. Manrique-Garcia, E.; Zammit, S.; Dalman, C.; Hemmingsson, T.; Andreasson, S.; Allebeck, P. Cannabis, Schizophrenia and Other Non-Affective Psychoses: 35 Years of Follow-up of a Population-Based Cohort. *Psychol. Med.* **2012**, *42*, 1321–1328. [[CrossRef](#)] [[PubMed](#)]
408. Xu, M.-Q.; Sun, W.-S.; Liu, B.-X.; Feng, G.-Y.; Yu, L.; Yang, L.; He, G.; Sham, P.; Susser, E.; St. Clair, D.; et al. Prenatal Malnutrition and Adult Schizophrenia: Further Evidence From the 1959-1961 Chinese Famine. *Schizophr. Bull.* **2009**, *35*, 568–576. [[CrossRef](#)] [[PubMed](#)]
409. He, P.; Chen, G.; Guo, C.; Wen, X.; Song, X.; Zheng, X. Long-Term Effect of Prenatal Exposure to Malnutrition on Risk of Schizophrenia in Adulthood: Evidence from the Chinese Famine of 1959-1961. *Eur. Psychiatry J. Assoc. Eur. Psychiatr.* **2018**, *51*, 42–47. [[CrossRef](#)]
410. Egbujo, C.N.; Sinclair, D.; Hahn, C.-G. Dysregulations of Synaptic Vesicle Trafficking in Schizophrenia. *Curr. Psychiatry Rep.* **2016**, *18*, 77. [[CrossRef](#)]
411. Grace, A.A. Dysregulation of the Dopamine System in the Pathophysiology of Schizophrenia and Depression. *Nat. Rev. Neurosci.* **2016**, *17*, 524–532. [[CrossRef](#)]
412. Weinberger, D.R.; Berman, K.F.; Daniel, D.G. Mesoprefrontal Cortical Dopaminergic Activity and Prefrontal Hypofunction in Schizophrenia. *Clin. Neuropharmacol.* **1992**, *15 Pt A (Suppl. 1)*, 568A–569A. [[CrossRef](#)]
413. Mossaheb, N.; Schloegelhofer, M.; Schaefer, M.R.; Fusar-Poli, P.; Smesny, S.; McGorry, P.; Berger, G.; Amminger, G.P. Polyunsaturated Fatty Acids in Emerging Psychosis. *Curr. Pharm. Des.* **2012**, *18*, 576–591. [[CrossRef](#)]
414. Berger, M.; Nelson, B.; Markulev, C.; Yuen, H.P.; Schäfer, M.R.; Mossaheb, N.; Schlögelhofer, M.; Smesny, S.; Hickie, I.B.; Berger, G.E.; et al. Relationship Between Polyunsaturated Fatty Acids and Psychopathology in the NEURAPRO Clinical Trial. *Front. Psychiatry* **2019**, *10*. [[CrossRef](#)] [[PubMed](#)]
415. Watanabe, A.; Toyota, T.; Owada, Y.; Hayashi, T.; Iwayama, Y.; Matsumata, M.; Ishitsuka, Y.; Nakaya, A.; Maekawa, M.; Ohnishi, T.; et al. Fabp7 Maps to a Quantitative Trait Locus for a Schizophrenia Endophenotype. *PLoS Biol.* **2007**, *5*, e297. [[CrossRef](#)] [[PubMed](#)]
416. Kim, T.; Kim, H.-J.; Park, J.K.; Kim, J.W.; Chung, J.-H. Association between Polymorphisms of Arachidonate 12-Lipoxygenase (ALOX12) and Schizophrenia in a Korean Population. *Behav. Brain Funct. BBF* **2010**, *6*, 44. [[CrossRef](#)] [[PubMed](#)]
417. Ross, B.M.; Turenne, S.; Moszczynska, A.; Warsh, J.J.; Kish, S.J. Differential Alteration of Phospholipase A2 Activities in Brain of Patients with Schizophrenia. *Brain Res.* **1999**, *821*, 407–413. [[CrossRef](#)]
418. Liu, Y.; Jandacek, R.; Rider, T.; Tso, P.; McNamara, R.K. Elevated Delta-6 Desaturase (FADS2) Expression in the Postmortem Prefrontal Cortex of Schizophrenic Patients: Relationship with Fatty Acid Composition. *Schizophr. Res.* **2009**, *109*, 113–120. [[CrossRef](#)] [[PubMed](#)]
419. Chalon, S.; Vancassel, S.; Zimmer, L.; Guilloteau, D.; Durand, G. Polyunsaturated Fatty Acids and Cerebral Function: Focus on Monoaminergic Neurotransmission. *Lipids* **2001**, *36*, 937–944. [[CrossRef](#)]
420. Healy-Stoffel, M.; Levant, B. N-3 (Omega-3) Fatty Acids: Effects on Brain Dopamine Systems and Potential Role in the Etiology and Treatment of Neuropsychiatric Disorders. *CNS Neurol. Disord. Drug Targets* **2018**, *17*, 216–232. [[CrossRef](#)]
421. Maekawa, M.; Watanabe, A.; Iwayama, Y.; Kimura, T.; Hamazaki, K.; Balan, S.; Ohba, H.; Hisano, Y.; Nozaki, Y.; Ohnishi, T.; et al. Polyunsaturated Fatty Acid Deficiency during Neurodevelopment in Mice Models the Prodromal State of Schizophrenia through Epigenetic Changes in Nuclear Receptor Genes. *Transl. Psychiatry* **2017**, *7*, e1229. [[CrossRef](#)]
422. Fedorova, I.; Alvhheim, A.R.; Hussein, N.; Salem, N. Deficit in Prepulse Inhibition in Mice Caused by Dietary N-3 Fatty Acid Deficiency. *Behav. Neurosci.* **2009**, *123*, 1218–1225. [[CrossRef](#)]

423. Kumari, V.; Soni, W.; Mathew, V.M.; Sharma, T. Prepulse Inhibition of the Startle Response in Men with Schizophrenia: Effects of Age of Onset of Illness, Symptoms, and Medication. *Arch. Gen. Psychiatry* **2000**, *57*, 609–614. [[CrossRef](#)] [[PubMed](#)]
424. Swerdlow, N.R.; Light, G.A.; Sprock, J.; Calkins, M.E.; Green, M.F.; Greenwood, T.A.; Gur, R.E.; Gur, R.C.; Lazzaroni, L.C.; Nuechterlein, K.H.; et al. Deficient Prepulse Inhibition in Schizophrenia Detected by the Multi-Site COGS. *Schizophr. Res.* **2014**, *152*, 503–512. [[CrossRef](#)]
425. Mena, A.; Ruiz-Salas, J.C.; Puentes, A.; Dorado, I.; Ruiz-Veguilla, M.; De la Casa, L.G. Reduced Prepulse Inhibition as a Biomarker of Schizophrenia. *Front. Behav. Neurosci.* **2016**, *10*. [[CrossRef](#)]
426. Shioda, N.; Yamamoto, Y.; Watanabe, M.; Binas, B.; Owada, Y.; Fukunaga, K. Heart-Type Fatty Acid Binding Protein Regulates Dopamine D2 Receptor Function in Mouse Brain. *J. Neurosci. Off. J. Soc. Neurosci.* **2010**, *30*, 3146–3155. [[CrossRef](#)] [[PubMed](#)]
427. Yamamoto, Y.; Kida, H.; Kagawa, Y.; Yasumoto, Y.; Miyazaki, H.; Islam, A.; Ogata, M.; Yanagawa, Y.; Mitsushima, D.; Fukunaga, K.; et al. FABP3 in the Anterior Cingulate Cortex Modulates the Methylation Status of the Glutamic Acid Decarboxylase67 Promoter Region. *J. Neurosci. Off. J. Soc. Neurosci.* **2018**, *38*, 10411–10423. [[CrossRef](#)]
428. Ludolph, A.G.; Kassubek, J.; Schmeck, K.; Glaser, C.; Wunderlich, A.; Buck, A.K.; Reske, S.N.; Fegert, J.M.; Mottaghy, F.M. Dopaminergic Dysfunction in Attention Deficit Hyperactivity Disorder (ADHD), Differences between Pharmacologically Treated and Never Treated Young Adults: A 3,4-Dihydroxy-6-[18F]Fluorophenyl-L-Alanine PET Study. *NeuroImage* **2008**, *41*, 718–727. [[CrossRef](#)] [[PubMed](#)]
429. Heinz, A.; Schlagenhauf, F. Dopaminergic Dysfunction in Schizophrenia: Salience Attribution Revisited. *Schizophr. Bull.* **2010**, *36*, 472–485. [[CrossRef](#)] [[PubMed](#)]
430. Ducrocq, F.; Walle, R.; Contini, A.; Oummadi, A.; Caraballo, B.; van der Veldt, S.; Boyer, M.-L.; Aby, F.; Tolentino-Cortez, T.; Helbling, J.-C.; et al. Causal Link between N-3 Polyunsaturated Fatty Acid Deficiency and Motivation Deficits. *Cell Metab.* **2020**, *31*, 755–772.e7. [[CrossRef](#)]
431. Berland, C.; Montalban, E.; Perrin, E.; Di Miceli, M.; Nakamura, Y.; Martinat, M.; Sullivan, M.; Davis, X.S.; Shenasa, M.A.; Martin, C.; et al. Circulating Triglycerides Gate Dopamine-Associated Behaviors through DRD2-Expressing Neurons. *Cell Metab.* **2020**, *31*, 773–790.e11. [[CrossRef](#)]
432. Amminger, G.P.; Schäfer, M.R.; Papageorgiou, K.; Klier, C.M.; Cotton, S.M.; Harrigan, S.M.; Mackinnon, A.; McGorry, P.D.; Berger, G.E. Long-Chain Omega-3 Fatty Acids for Indicated Prevention of Psychotic Disorders: A Randomized, Placebo-Controlled Trial. *Arch. Gen. Psychiatry* **2010**, *67*, 146–154. [[CrossRef](#)]
433. Bloemen, O.J.N.; de Koning, M.B.; Schmitz, N.; Nieman, D.H.; Becker, H.E.; de Haan, L.; Dingemans, P.; Linszen, D.H.; van Amelsvoort, T.A.M.J. White-Matter Markers for Psychosis in a Prospective Ultra-High-Risk Cohort. *Psychol. Med.* **2010**, *40*, 1297–1304. [[CrossRef](#)] [[PubMed](#)]
434. Vijayakumar, N.; Bartholomeusz, C.; Whitford, T.; Hermens, D.F.; Nelson, B.; Rice, S.; Whittle, S.; Pantelis, C.; McGorry, P.; Schäfer, M.R.; et al. White Matter Integrity in Individuals at Ultra-High Risk for Psychosis: A Systematic Review and Discussion of the Role of Polyunsaturated Fatty Acids. *BMC Psychiatry* **2016**, *16*, 287. [[CrossRef](#)]
435. Schlögelhofer, M.; Amminger, G.P.; Schaefer, M.R.; Fusar-Poli, P.; Smesny, S.; McGorry, P.; Berger, G.; Mossaheb, N. Polyunsaturated Fatty Acids in Emerging Psychosis: A Safer Alternative? *Early Interv. Psychiatry* **2014**, *8*, 199–208. [[CrossRef](#)]
436. McNamara, R.K.; Jandacek, R.; Rider, T.; Tso, P.; Hahn, C.-G.; Richtand, N.M.; Stanford, K.E. Abnormalities in the Fatty Acid Composition of the Postmortem Orbitofrontal Cortex of Schizophrenic Patients: Gender Differences and Partial Normalization with Antipsychotic Medications. *Schizophr. Res.* **2007**, *91*, 37–50. [[CrossRef](#)]
437. Khan, M.M.; Evans, D.R.; Gunna, V.; Scheffer, R.E.; Parikh, V.V.; Mahadik, S.P. Reduced Erythrocyte Membrane Essential Fatty Acids and Increased Lipid Peroxides in Schizophrenia at the Never-Medicating First-Episode of Psychosis and after Years of Treatment with Antipsychotics. *Schizophr. Res.* **2002**, *58*, 1–10. [[CrossRef](#)]
438. Arvindakshan, M.; Sitasawad, S.; Debsikdar, V.; Ghate, M.; Evans, D.; Horrobin, D.F.; Bennett, C.; Ranjekar, P.K.; Mahadik, S.P. Essential Polyunsaturated Fatty Acid and Lipid Peroxide Levels in Never-Medicating and Medicating Schizophrenia Patients. *Biol. Psychiatry* **2003**, *53*, 56–64. [[CrossRef](#)]
439. Kale, A.; Naphade, N.; Sapkale, S.; Kamaraju, M.; Pillai, A.; Joshi, S.; Mahadik, S. Reduced Folic Acid, Vitamin B12 and Docosahexaenoic Acid and Increased Homocysteine and Cortisol in Never-Medicating Schizophrenia Patients: Implications for Altered One-Carbon Metabolism. *Psychiatry Res.* **2010**, *175*, 47–53. [[CrossRef](#)]
440. Robinson, D.G.; Gallego, J.A.; John, M.; Hanna, L.A.; Zhang, J.-P.; Birnbaum, M.L.; Greenberg, J.; Naraine, M.; Peters, B.D.; McNamara, R.K.; et al. A Potential Role for Adjunctive Omega-3 Polyunsaturated Fatty Acids for Depression and Anxiety Symptoms in Recent Onset Psychosis: Results from a 16 week Randomized Placebo-Controlled Trial for Participants Concurrently Treated with Risperidone. *Schizophr. Res.* **2019**, *204*, 295–303. [[CrossRef](#)]
441. Bozzatello, P.; Brignolo, E.; De Grandi, E.; Bellino, S. Supplementation with Omega-3 Fatty Acids in Psychiatric Disorders: A Review of Literature Data. *J. Clin. Med.* **2016**, *5*, 67. [[CrossRef](#)] [[PubMed](#)]



*CHAPITRE 03 : Utilisation d'un modèle murin génétique pour modifier  
l'expression d'Elovl2 dans les astrocytes*

---

# **Intra nucleus accumbens adenovirus delivery of Cre recombinase in astrocyte of *elovl2-flox* mice alters medium spiny neurons electrophysiological properties and emotional behavior in male and female**

Martinat M <sup>1</sup>\$, Madore C <sup>1</sup>\$, Varilh M <sup>1</sup>, Rossito M <sup>1</sup>, Di Miceli M <sup>1,2</sup>, Séré A <sup>1</sup>, Grégoire S <sup>3</sup>, Acar N <sup>3</sup>\$, Bazinet R <sup>4</sup>\$, Joffre C <sup>1</sup>\$, Delpech JC <sup>1</sup>\$, Fioramonti X <sup>1</sup>, and Layé S <sup>1</sup>\*

<sup>1</sup> Univ. Bordeaux, INRAE, Bordeaux INP, NutriNeuro, UMR 1286, F-33000 Bordeaux, France

<sup>2</sup> Worcester Biomedical Research Group, School of Science and the Environment, University of Worcester, Worcester WR2 6AJ, UK

<sup>3</sup> Eye and Nutrition Research Group, Centre des Sciences du Goût et de l'Alimentation, AgroSup Dijon, CNRS, INRAE, Université Bourgogne Franche-Comté, Dijon, France

<sup>4</sup> Department of Nutritional Sciences, Faculty of Medicine, University of Toronto, Toronto, ON M5S 1A1, Canada

\$ Partners of the International Research Network Food4BrainHealth

\* Corresponding author



## **ABSTRACT**

Exposure to diets deficient in n-3 PUFAs decreases DHA throughout the cell membranes of the body. In order to determine more precisely whether a local decrease in DHA can alter synaptic plasticity, we developed an original transgenic approach that aims to decrease the bioavailability of DHA to neurons in restricted areas of the brain. For this purpose, we chose to administer a cre-mcherry adenovirus in the nucleus accumbens (NAC) of mice floxed for the gene of the enzyme ELOVL2, an elongase crucial in DHA synthesis. ELOVL2 is predominantly expressed by astrocytes which generate DHA that is then distributed to neurons. Thus, inhibition of ELOVL2 synthesis in astrocytes should be accompanied by a decrease in DHA in adjacent neurons. Patch-clamp electrophysiology measurements reveal for the first time that inhibition of astrocytic ELOVL2 alters the intrinsic properties of nearby neurons. In this case, we found a decrease in the excitability threshold of neurons and an increase in the amplitude of spontaneous activities. This suggests an alteration of the neuronal electrophysiological properties, in a context of astrocytic ELOVL2 inhibition.

## 1. INTRODUCTION

The brain contains large amounts of polyunsaturated fatty acids (PUFAs) (Bazinet and Layé, 2014), in particular docosahexaenoic acid (DHA) and arachidonic acid (AA) from the n-3 and n-6 families respectively. Several bodies of evidence collected in humans and animal models pinpoint that the alteration of brain PUFA metabolism is associated to altered emotional behavior and neuronal plasticity (Bazinet et al., 2020; Bazinet and Layé, 2014; Di Miceli et al., 2020). Although the exact mechanisms linking brain PUFAs and behavior are not completely understood, several data obtained in dietary animal model aiming at disturbing the level of n-3 and n-6 PUFAs in the brain, have revealed that the synaptic plasticity of medium spiny neurons (MSN) of the nucleus accumbens (NAc) is particularly altered when DHA and AA levels are changed at this level (Di Miceli et al., 2020; Ducrocq et al., 2020; Lafourcade et al., 2011; Lin et al., 2020; Manduca et al., 2015). In addition, altered synaptic plasticity in the NAc triggered by a chronic stress or n-3 PUFA dietary deficiency is responsible of emotional behavior alterations (Bosch-Bouju et al., 2016; Lafourcade et al., 2011; Manduca et al., 2015) and restored when mice are fed with a diet rich in DHA (Di Miceli et al., 2022; Larrieu et al., 2014). Altogether, these results strongly pinpoint the tight link between PUFA metabolism and synaptic plasticity in the NAc and emotional behavior. However, PUFA metabolism alteration was mainly triggered by dietary approaches, which impact PUFA metabolism at the level of the whole organism. In order to more precisely target PUFA metabolism in the NAc, we developed a mouse model with elongase (*elovl2*) knock-out in NAc astrocytes. DHA and AA metabolism requires successive elongation and desaturation steps of their respective precursors  $\alpha$ -linolenic acid (LNA) and linoleic acid (LA) (Jakobsson et al., 2006). In humans, *Elovl2* single nucleotide polymorphism (SNP) has been reported to alter plasmatic levels of n-6 and n-3 PUFAs (Tanaka et al., 2009). In addition, *elovl2* knock-out mice display strong impairment in DHA and AA metabolism in the brain, suggesting that this enzyme is key to PUFA homeostasis (Pauter et al., 2014; Talamonti et al., 2019). *Elovl2* is expressed in astrocytes, which are key cells in the regulation of synaptic plasticity (Human Protein Atlas) and have been shown to be crucial in the brain metabolism of DHA (Williard et al., 2001). However, whether the alteration of *elovl2* expression in astrocytes alters PUFA metabolism and neuronal activity is unknown. In addition, the differences according to sex have never been addressed.

To further gain insight in whether and how local disturbance of PUFA homeostasis in the NAc alters MSNs electrophysiological properties and/or emotional behavior, we generated a mouse model with *elovl2* genetic ablation in the NAc astrocytes. Then PUFA levels and MSNs electrophysiological properties were measured in the NAc and emotional behavior was assessed using a battery of tests in both male and female. Overall, no differences in PUFA metabolism was detected in the NAc of *elovl2* deficient astrocyte male and female mice. Alterations of some emotional parameters were detected in the KO male and female mice. In addition, electrophysiological properties of MSNs were profoundly

altered, suggesting that *elovl2* ablation in astrocytes impacts adjacent neurons in the NAc. However, the mechanisms underlying this effect remain to be understood.

## 2. MATERIAL AND METHODS

### 2.1. ANIMALS

All experiments were performed according to criteria of the European Communities Council Directive 2010/63/EU for animal experiments and were approved by the French Ministry of Research and the local ethical committee for the care and use of animals (N°APAFIS #17200 and #35867).

C56/BL6 mice *Elov12*<sup>lox/lox</sup> were obtained from C Magnan (ELOVL2 IR00005097/K5097). AAV5/2-GFAP-mcherry-Cre expressing Cre recombinase gene under astrocyte GFAP promoter and AAV-5/2-GFAP-mCherry were purchased from the ETH Zurich (Zurich, Switzerland) was injected into each male and female *Elov12*<sup>lox/lox</sup> mouse NAc.

Animals were housed in group of 6-9 animals in polycarbonate cages in an air-conditioned (22 +/- 1°C) colony room with a 12: 12 light/dark cycle according to their sex. Animals had *ad libitum* access to food and water and were weighed once a week. All mice were fed with a chow diet.

In total, 42 mice were used (20 males and 22 females). Before the virus injection, mice were genotyped using Ef/ER primers to discriminate WT, floxed homozygotes, heterozygotes and recombined as previously described (Birling et al., 2012).

The control group consisted of male and female *Elov12*<sup>lox/lox</sup> mice injected with a control virus without cre expression (ctrl males; n=10 and ctrl females; n=11); the KO *elov12* group group consisted in male and female injected with the virus expressing the cre, the synthesis of *Elov12* is knock down in the astrocytes (KO *Elov12* group) (KO *Elov12* males; n=10 and KO *Elov12* females; n=11). All virus injections were performed in male and female mice at 6 weeks old. A first cohort was used for behavioral, electrophysiological or PUFA profile assessment in the NAc or immunohistochemistry. The second cohort was used for electrophysiological and RNAscope assessment in the NAc. Experiments were performed between 6 and 8 weeks after the intra-NAc administration of the control or cre-virus.

### 2.2. VIRAL PRODUCTION

Adeno-associated virus serotype 5/2 expressing the cre (AAV-5/2-hGFAP-mCherry-iCre-WPRE-hGHp(A)) ( $6 \times 10^{12}$  genomes/mL, working dilution 1:10) was produced by the viral production facility of the ETH Zurich (Zurich, Switzerland). Control AAV-5/2-hGFAP-mCherry-WPRE-hGHp(A) ( $6 \times 10^{12}$  vg/mL) was produced by the viral production facility of the the ETH Zurich (Zurich, Switzerland).

### **2.3. STEREOTAXIC INJECTION**

Animals were anesthetized by inhalation of isoflurane (5-6% v/v ambient air) before being installed in a stereotaxic setting. The animals are maintained under isoflurane throughout the duration of the surgery (1-2% v/v) and on a heating mat to maintain body temperature at 37.5%. They received subcutaneous injection of analgesics (125µL / animal of Buprenorphine diluted at 1/100 in NaCl 0.9%, final dose at 0.05 mg/kg) 30 minutes before the induction of anesthesia. The eyes of animals are protected from desiccation by application of ophthalmic protection gel (Liposic 2mg/g).

The virus was injected into each hemisphere (0.5µL / hemisphere) with a flow rate of 0.1 µL / min using a Hamilton syringe in the nucleus accumbens (Nac) (L=1.56, AP=1.8, V=-4, in mm). The injection needle was carefully removed after 5 min waiting at the injection site and 2 min waiting half way to the top. Viscous xylocaine was applied to the wound. The animals received a subcutaneous injection of physiological saline (0.6 ml) to avoid dehydration in the first hours of his awakening as well as an injection of a nonsteroidal anti-inflammatory drug and analgesic CARPROFELICAN 50 mg/mL, diluted to 100th, 250 µL/animal). Animals were then placed in a clean cage on a heated and monitored mat for up to 6 hours after full awakening (resumption of motor activity). Animals are monitored twice daily for 3 days after surgery.

### **2.4. BEHAVIORAL TEST**

Behavioral tests were conducted in both ctrl and KO *elov12* mice 6 weeks after virus injection. Mice were weighted once a week since surgery. Mice were scored in behavioral tests performed in the light phase (between 8:00 AM and 11:00 AM). Mice were handled 5 min every day for 2 weeks before the initiation of experiments.

Anxiety-related tests were realized including Open Field test (10 min, 50 Lux), a light dark test (8 min, 300 Lux) and an EPM test (5min, 15 Lux). Between each experimental run, apparatus was cleaned to avoid olfactory disturbance. A video tracking system was used (SMART system; San Diego Instruments) to analyse the time spent in the different zone during 10 minutes of recording (Lafourcade et al., 2011; Larrieu et al., 2014).

From results obtained, an anxiety score is calculated for each animal based on normalized scores for each parameter measured on the behavioural tests (Time spent in the center of OF, total distance in the open field, time spent and number of entries in the light zone of the LD, time spent and number of entries in the open arm of the EPM, head dippings in the EPM).

### **2.5. ELECTROPHYSIOLOGY**

*Ex-vivo* patch-clamp recordings were performed on brain slices from *Elov12* mice, as previously described (Berland et al., 2020; Lafourcade et al., 2011; Zemdegs et al., 2019)

Briefly, intracardiac perfusion was done during euthanasia (exagon/lidocaine: 300/30 mg/kg, i.p) with approximately 20ml of Cold NMDG solution to evacuate the brain of all blood and cool it quickly. NMDG solution is consisting of (in mM) : 1.25 NaH<sub>2</sub>PO<sub>4</sub>, 2.5 KCl, 7 MgCl<sub>2</sub>, 20 HEPES, 0.5 CaCl<sub>2</sub>, 28 NaHCO<sub>3</sub>, 8 D-glucose, 5 L(+)-ascorbate, 3 Na-pyruvate, 2 thiourea, 93 NMDG, and 93 HCl 37%; pH: 7.3–7.4; osmolarity: 305–310 mOsm.

Sagittal striatal slices (350 µm) were prepared with a vibrating blade microtome (VT1000S, Leica Microsystems, Germany) in an ice cold oxygenated NMDG solution. Slices were placed 7 minutes in oxygenated NMDG at 32°C, then 50 minutes at room temperature in oxygenated artificial cerebrospinal fluid (ACSF) containing (in mM): 125 NaCl, 2.5 KCl, 1.25 NaH<sub>2</sub>PO<sub>4</sub>, 2.0 CaCl<sub>2</sub>, 1.0 MgCl<sub>2</sub>, 25 NaHCO<sub>3</sub>, and 25 glucose (osmolarity 308 ± 3 mOsm) and recordings were started after.

Pipette resistance was typically between 4 and 7 MΩ when filled with a potassium gluconate-based intracellular solution, consisting of (in mM): K-gluconate 128, NaCl 20, MgCl<sub>2</sub> 1, EGTA 1, CaCl<sub>2</sub> 0.3, Na<sub>2</sub>-ATP 2, Na-GTP 0.3, cAMP 0.2, and HEPES 10, pH = 7.35 (osmolarity 296 ± 3.8 mOsm). Pipette offset was zeroed before each recording.

Medium Spiny Neurons (MSN) of the NAc were visualized under direct interference contrast with a BX51WI microscope (Olympus, Tokyo, Japan), mounted on an air table (TMC, Saratoga Springs, NY, USA) and under a Faraday cage, with an upright microscope, a 40× water immersion objective combined with an infra-red filter, a monochrome CCD camera (Roper Scientific, Vianen, The Netherlands), and a PC-compatible system for analysis of images as well as contrast enhancement. Only data from MSNs near fluorescent astrocytes (mCherry) were included in the present study.

Membrane current and potential were monitored using Multiclamp700B and Digidata 1440A by Axon Instrument (Molecular Devices, San Jose, CA, USA). A concentric bipolar electrode (Phymep, Paris, France) was placed on afferent fibers to evoke EPSCs (at 0.1 Hz), recorded in MSN under voltage-clamp configuration with membrane potential clamped at –70 mV. Current over voltage (I/V) curves were acquired in I = 0 (free) current-clamp mode. All data were sampled at 20 kHz and filtered at 1 kHz. Series resistance was measured throughout the experiment with a –5 mV step lasting 50 ms. The active and passive electrophysiological properties of MSNs were calculated according to and consistent with a previous study (Di Miceli et al., 2022).

## **2.6. FATTY ACID PROFILE**

Briefly, fatty acids from the prefrontal cortex and the nucleus accumbens were analysed as previously described (Delpech et al., 2015; Labrousse et al., 2012; Madore et al., 2014). Fatty acids composition of the PFC and NAc is expressed as the percentage of total fatty acids.

## **2.7. IMMUNOHISTOCHEMISTRY**

Mice were perfused with PBS (n=2-6 animals/condition). Each brain was removed, postfixed in 4% paraformaldehyde overnight at 4°C, cryoprotected in 30% sucrose at 4°C and frozen in isopentane to be stored at -80°C. Brains were sectioned on a cryostat at 40 µm free-floating coronal sections and stored at -20°C in cryoprotectant solution. After washing off the cryoprotectant solution, slices were incubated 1h at room temperature in PBS blocking solution containing 5% Donkey serum and 0.3% Triton X-100, and immunostained with primary antibodies overnight at 4°C in PBS/5% Donkey serum/0.3% Triton X-100 (Rabbit-anti GFAP antibody (1 :1000 ; Dako Z0334), as an astrocytic marker and Goat-anti RFP antibody (1 :500 ; Rockland 200-101-379) to detect mCherry signal. Slices were then washing in PBS and incubated 2h at rt with secondary antibody in PBS/5% Donkey serum/0.3% Triton X-100 (Donkey-anti-rabbit Alexa Fluor 488 antibody (1 :1000 ; life technologies A21206) or Donkey-anti-Goat Alexa Fluor 647 antibody (1 :1000 ; life technologies A21447). Slices were then washed in PBS and mounted with UltraCruz® Hard-set Mounting Medium with Dapi (Santa Cruz Biotechnology sc-359850). Images were captured using with a Nanozoomer using a 20x objective (pixel size 0.454µm-Bordeaux Imaging Center, HAMAMATSU). Positive cells were quantified in the NAc shell (n=2-5 slices/animal ; Bregma 0.50mm-1.78mm) using Image-J ([National Institutes of Health](#)). Area of the quantified region has been measured and the data are presented as colocalisation of GFAP and mCherry staining.

## **2.8. RNASCOPE *IN SITU* HYBRIDIZATION (ISH) COMBINED WITH IMMUNOHISTOCHEMISTRY (IHC)**

Mice were deeply anesthetized and transcardially perfused with phosphate buffered saline (PBS). After the perfusion, brains were removed, post-fixed in 4% paraformaldehyde (PFA) overnight (ON) at 4°C and cryoprotected in 30% sucrose ON at 4°C. Free-floating frozen coronal cryostat slices (40 µm) were collected in a cryoprotectant solution. Before the experiment, free-floating sections were mounted on Superfrost Plus microscope slides (Fisher Scientific). Several steps of air drying (1h), baking at 60°C (1h) and fast dipping in water were necessary to ensure the adhesion of the sections to the slides. Then, tissue sections were post-fixed 1h in 4% PFA at 4°C, followed by dehydration in a ethanol series. The RNAscope mRNA-staining steps was carried out as per the manufacturer's instructions for the RNAscope Multiplex Fluorescent V2 Assay (Biotechne, #323100). Briefly, tissue sections were treated with H<sub>2</sub>O<sub>2</sub> for 10 minutes at RT and incubated in the Target Retrieval reagent 1X maintained at a boiling temperature for 5 minutes. Sections were then digested with protease III at 40°C for 30 minutes in a HybEZ hybridization oven (ACD, Hayward, CA), washed, followed by an incubation with the elovl2 probe at 40°C for 2h. Probe targeting the mRNA transcripts of ELOVL2 (target region : base pairs 1697-2808 of *Mus musculus* Elongation Of Very Long Chain Fatty Acids-Like 2, NM\_019423.2, #542711-C3) was designed by ACD (a « channel 3 » probe). The channel 3 probe Elov12 was diluted at 1:50 in the probe diluent (Biotechne, #300041) prior to application on the

tissue sections. The bacterial gene *dapB* (dihydrodipicolinate *B. subtilis* reductase) was used as negative control to assess background signals. Amplification and detection steps were performed by adding the RNAscope Multiplex FL v2 HRP-C3 revealed by a TSA reaction using Opal 690 reagent pack (1/800 ; 30 minutes at 40°C ; Akoya Biosciences ; #FP1497001KT).

After processing for fluorescent ISH, an anti-GFAP and anti-RFP immunofluorescence was carried out. Sections were post-fixed 10 minutes at RT, then washed and incubated in a blocking solution of 5% donkey serum, 0.3% Triton X-100 prepared in PBS for 30 minutes at RT. Sections were then incubated with a mix of primary antibodies overnight at 4°C : a goat polyclonal anti-RFP (1 :500, Rockland, #200-101-379) and a rabbit polyclonal anti-GFAP (1 :500, DAKO, #Z0334). After several washes, sections were placed, for 2 hours, at RT, in the dark, with a mix of secondary antibodies : donkey anti-goat Alexa Fluor 555 (1 :500, Fisher Scientific, #10246402) and donkey anti-rabbit Alexa Fluor 488 (1 :500, Fisher Scientific, #10424752). Stained slides were mounted with ultraCruz hard-set mounting medium with DAPI (Clinisciences, #sc-359850).

Microscopic imaging and statistical analysis: images were acquired using a Zeiss inverted Axio Observer fluorescent microscope (Carl Zeiss). Sections were analysed to examine the deletion of mRNA *Elov12* in the astrocytes at the level of the NAc of transfected mice. Image analyses and counting were performed in 1 section of 4 mice in each condition.

Quantification of the number of labelled dots within the tissue. Each dot represents one RNA molecule and thus, the number of dots is indicative of the number of RNA molecules present. Scoring of RNAscope/immunofluorescence staining was done manually.

## **2.9.STATISTICAL ANALYSIS**

All statistical tests were performed with GRAPHPAD PRISM 9 software. Significance was set at  $\alpha = 0.05$ . All values are reported as mean  $\pm$  standard error of the mean (SEM) and represented as histograms or with box and whiskers representation from min to max. Data analysis was performed using one-sample t-tests, two- or three-way ANOVA, followed by post hoc tests if appropriate. For the RNAscope analysis, difference between the mice injected with control virus and the one injected with KO *Elov12* virus were compared using an unpaired t-test. A P value of  $<0.05$  was considered statistically significant. Data are presented as the mean value and error bars represent SEM.

Supplemental Table S1 presents all statistical analysis results performed in the present study.

### 3. RESULTS

First, the impact of the administration of the AAV-cre specific for astrocyte in the NAc of male mice, on *elovl2* mRNA expression was assessed using RNAscope. This technic is giving us the opportunity to localize both astrocytes (GFAP) and the expression of *elovl2* RNA molecules (white dots) (**Fig. 2.A**). The hippocampus has been used as the control structure (away from the administration site). Quantitative image analysis of RNAscope data for *Elov12* and double immunofluorescence for RFP and GFAP proteins showed that expression of *Elov12* is reduced by 50 % in astrocytes targeted by the Cre+ virus (Unpaired t-test,  $t=3,995$ ,  $df=6$ ,  $p<0,01$ ) (**Fig. 2.B**).

Second, we assessed using immunohistochemistry the number of astrocytes co-labelled with mcherry, used as a proxy of the virus expression. In order to validate the injection site and to see if the virus was targeting astrocytes and in which proportion in the NAc. In male mice, no significant differences were observed (**Fig. 3**). In females, we only have preliminary datas presented in supplementary datas (**Fig. 8**).

#### **PUFA profile is not altered in the NAc of *Elov12* KO male and female mice**

Then, we evaluated if the diminution of *Elov12* expression in the astrocyte of the NAc was associated to altered PUFA profile in the NAc of control or cre AAV (*KO Elov12*) male and female mice (**Fig. 1**). The same measurements were performed in the prefrontal cortex (PFC), used as a control brain structure. No significant changes in saturated fatty acids (SFA), monounsaturated fatty acids (MUFA) and PUFA level were measured in the NAc and PFC of ctrl and *KO Elov12* (**Fig. 4 and 5**).

#### **Individual emotional behaviors are slightly altered in *Elov12* KO male and female mice, with no effect on the anxiety score**

In order to investigate whether *KO Elov12* induced changes in emotional behavior, we performed Open Field (OF), Light Dark (LD) and Elevated Plus Maze (EPM) tasks in male and female mice (**Fig. 6**). No significant differences were measured in behavioral performance of male and female mice under study in the OF test (**Fig. 6A**). Interestingly, *KO Elov12* male, but not female, mice display some anxiety-like behavior, as revealed by the significant time spent in the light area of the LD test (Unpaired t-test,  $t=2.637$ ,  $df=12$ ,  $p<0.05$ ) (**Fig. 6B**). In addition, *KO Elov12* female mice have more head dippings when placed in the EPM test (Unpaired t-test,  $t=2.260$ ,  $df=12$ ,  $p<0.05$ ) (**Fig. 6C**). The calculation of the anxiety score did not reveal significant differences between control and *KO Elov12* male and female mice (**Fig. 6D**).

#### **MSN intrinsic electrophysiological properties are altered in *Elov12* KO male and female mice**



To reach the sufficient number of animals required to perform statistical analysis, results from male and female were pooled. A significant effect of the astrocytic Elov12 KO was measured on the voltage over current relationships (Two way ANOVA, voltage effect :  $F(23,529)=167.1$ ,  $p<0.001$ , virus effect :  $F(1,23)=4.988$ ,  $p<0.05$ , interaction :  $F(23,529)=167.1$ ,  $p<0.001$ ) (**Fig. 5B**), together with altered rheobase compared to control animals (Unpaired t-test,  $t=3.442$ ,  $df=22$ ,  $p<0.01$ ) (**Fig. 5D**). In addition, the number of action potentials generated during supra-threshold current applications were altered in MSNs of KO elvol2 (Two way ANOVA, current effect :  $F(6,132)=29.03$ ,  $p<0.001$ , virus effect :  $f(1,22)=2.434$ , ns, interaction :  $F(6,132)=5.046$ ,  $p<0.001$ ) (**Fig. 7E**). However, there was no significant effect on the resting membrane potential (**Fig. 7C**). We also recorded spontaneous excitatory post synaptic current (sEPSC). MSNs from KO Elov12 display a significant decrease of the amplitude of these sEPSC (Unpaired t-test,  $t=15.03$ ,  $df=882$ ,  $p<0.001$ ) (**Fig., 7G**), but not of the interevent interval (**Fig. 7F**) or the frequency (**Fig. 7H**). Finally, the probability to trigger a spike (in %) in recorded MSNs following increasing cortical stimulations is not significantly higher in KO Elov12 animals (**Fig. 7J**).

#### 4. DISCUSSION

In this second part of our study, we focused on the local modulation of fatty acids levels. After injection of the virus into the NAc, immunohistochemical analyses of the colocalization of the GFAP and mCherry markers allowed us to confirm that cre is expressed predominantly in astrocytes. Then, using an RNAscope approach, we were able to estimate the number of astrocytic cells targeted by the virus and, among these infected cells, to quantify the expression level of elov12 transcripts. Administration of AAV-5/2-GFAP-re/mCherry in the NAc of male and female ELOVL2lox/lox mice decreases elvol2 expression by 50% at this level, but not in the hippocampus, used as a control structure. Analyses of lipid profiles in Nac and PFC show that inhibition of astrocytic elov12 synthesis did not induce differences in the level of SFAs, MUFAs or PUFAs in the NAc of males and females. This is in contrast to what has been observed in total KO models for Elov12, which show changes in PUFA levels, including increased levels of n-3 DPA and decreased DHA in the brains of KO mice (Gregory et al., 2013; Pauter et al., 2014; Talamonti et al., 2019). Our results could be explained by the fact that the changes at the astrocyte level are too small to be detected at the scale of the whole structure. But it could also be that alternative pathways take over for endogenous DHA synthesis, as is the case in zebrafish liver (Liu et al., 2020). Indeed, elov12<sup>-/-</sup> zebrafish do not show accumulation of n-3 DPA but an increase in the substrate of the delta 4 desaturase pathways, EPA, suggesting that the delta 4 pathway is an alternative for DHA synthesis (Liu et al., 2020). Furthermore, the deletion of elov12 is not complete, which may explain the absence of changes in PUFA levels in NAc. Behavioural analyses revealed alterations in emotional behaviour on parameters that differed in Elov12 knockout animals according to sex. Indeed, we were able to observe that Elov12 knockout males spend

significantly more time in the Light Dark zone than control animals. The Light Dark test confronts mice with an extremely anxiety-provoking situation that consists of exposure to a very brightly lit area. Our results suggest that male Elov12 KO mice are less anxious than control animals. Secondly, we found that female Elov12 KO mice performed less head dipping in the elevated cross maze test. This parameter consists of counting the number of times the animal engages its head and upper body above the void. Elov12 knockout females thus appear to exhibit anxiety-like behaviour compared to control animals.

Finally, we were able to observe changes in neuronal excitability. Indeed, neurons recorded in the vicinity of fluorescent astrocytes show a lower rheobase and a decrease in the number of action potentials. Analysis of the spontaneous activity of excitatory postsynaptic currents shows that the amplitude of these activities is decreased in Elov12 KO animals but not the frequency or the interval between events. To our knowledge, there are no studies that have analysed the neuronal properties under astrocytic control in the NAc. Neuronal activity in the NAc is regulated by various neurotransmitters or neuromodulators released from the afferents, notably GABAergic ones. Astrocytes are known to express glutamate transporters (GLAST and GLT-1), as well as GABA transporters (GAT1-3) (Danbolt, 2001; Gadea and López-Colomé, 2001a, 2001b). Partial inhibition of elov12 expression in the astrocyte could modify the expression of GABA and GLUT transporters at this level. To better understand how changes in elov12 expression by the astrocyte modify neuronal properties, studies of astrocytic reuptake that modulate the intensity and duration of activation of receptors located at the pre- or postsynaptic level (Tzingounis and Wadiche, 2007), limit the activation of extra-synaptic receptors (Huang and Bergles, 2004) or limit the diffusion of neurotransmitters to neighbouring synapses (Arnth-Jensen et al., 2002) are necessary.

In summary, the results obtained in the Elov12 KO model show for the first time that altering astrocytic elov12 synthesis alters emotional behaviour on gender-specific parameters and alters the electrophysiological properties of MSNs in the NAc. However, further analysis is needed to better understand the mechanisms involved in these modifications

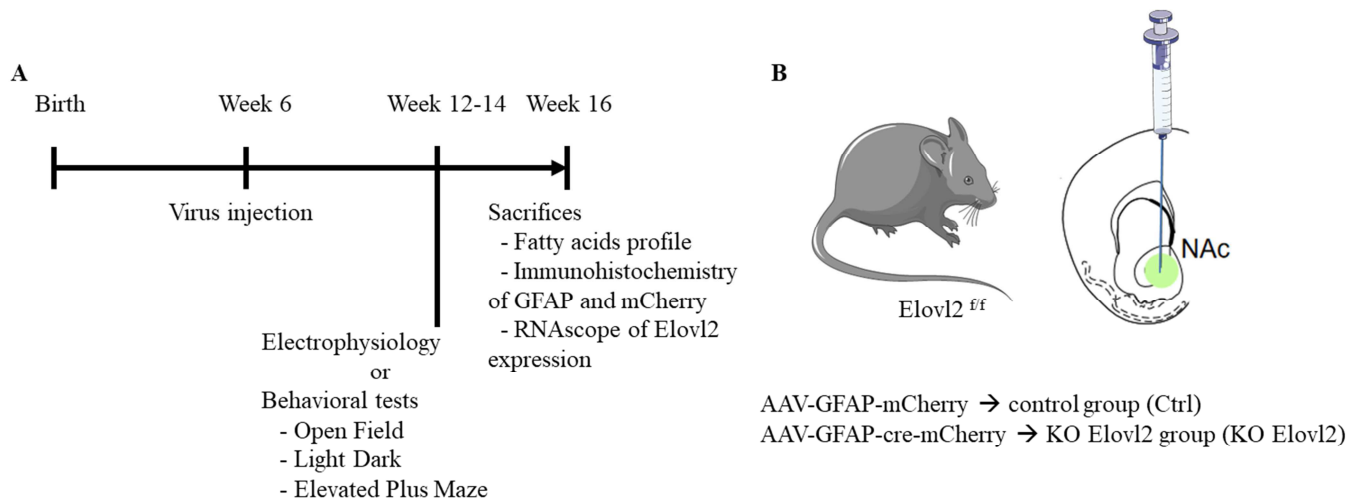


**Figure 1 :** Representation of experimental design. (A) Between 6 and 8 weeks after viral injection, behavioral tests and electrophysiological recordings are performed before biochemical analysis. (B) 6 weeks after birth, viral injection of control virus (ctrl) and cre-virus (KO Elov12) under GFAP promoter and expressing mCherry in C57Bl6j Elov12 floxed mice were done in the Nucleus Accumbens (NAc).

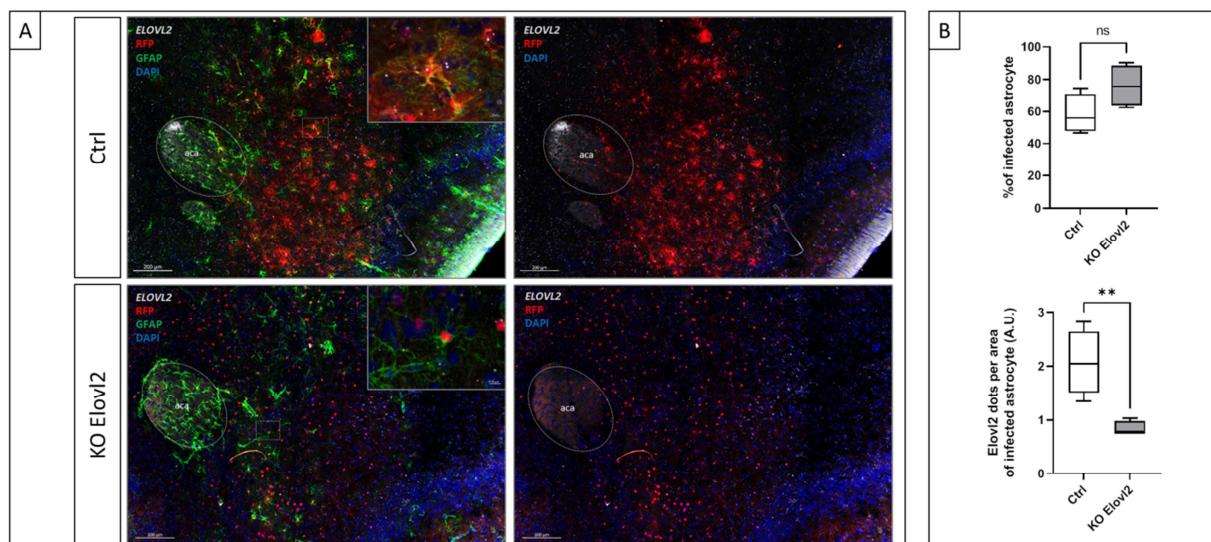


**Figure 2 :** Decrease of the expression of ELOVL2 in the astrocytes of mice injected with Cre+ virus in the Nac. (A) : Representative images of mice Elov12 lox injected with ssAAV-5/2-hGFAP-mCherry-WPRE-hGHp(A) (Cre -) or ssAAV-5/2-hGFAP-mCherry\_iCre-WPRE-hGHp(A) (Cre+) in the Nac. Simultaneous detection of one target gene *ELOVL2* (white dots) by RNAscope ISH and two proteins RFP (red) and GFAP (green) in mice injected by Cre- or Cre + virus in the Nac. Each dot (white) represents one RNA molecule of *ELOVL2*. The dotted white circle represents the anterior commissure, anterior part (aca). White dotted boxes are magnified. n=4 animals. Original magnification, x20. Scale bar = 200  $\mu$ m. (B) : Quantitative image analysis of RNAscope data for Elov12 and double immunofluorescence for RFP and GFAP proteins.

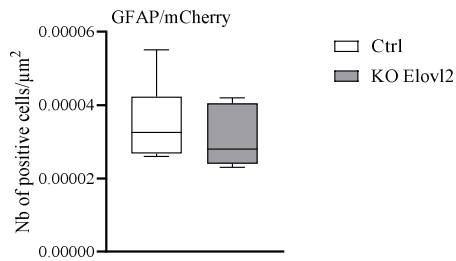
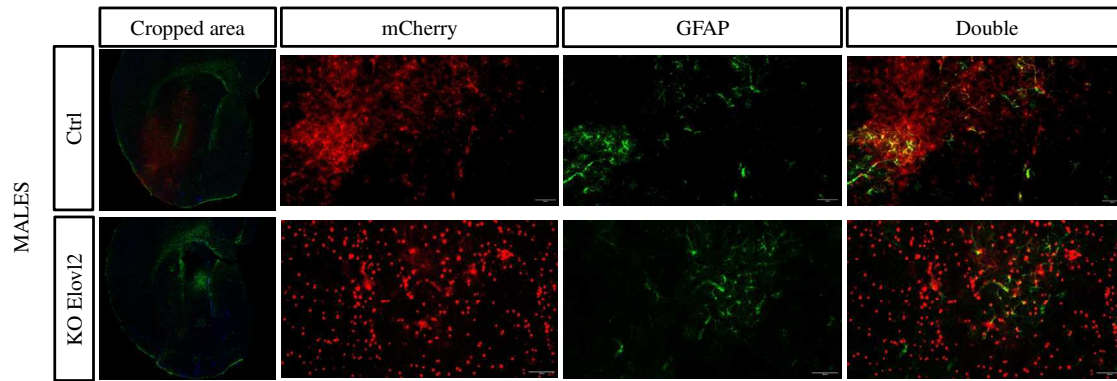


**Figure 3 :** Representative GFAP immunostaining in striatal area of mice injected with the control virus (ctrl) and the cre virus (KO Elov12). Scale bar, 100  $\mu\text{m}$ . Quantification of the colocalisation between GFAP immunostaining and mCherry fluorescence. Values (box and whiskers plots) (ctrl n=6; KO Elov12 n=7) are plotted from minimum to maximum. One-Way ANOVA followed by Bonferroni test if the ANOVA is significant. \*  $p < 0.05$ , \*\*  $p < 0.01$ , \*\*\*  $p < 0.001$  Ctrl versus KO Elov12 mice.

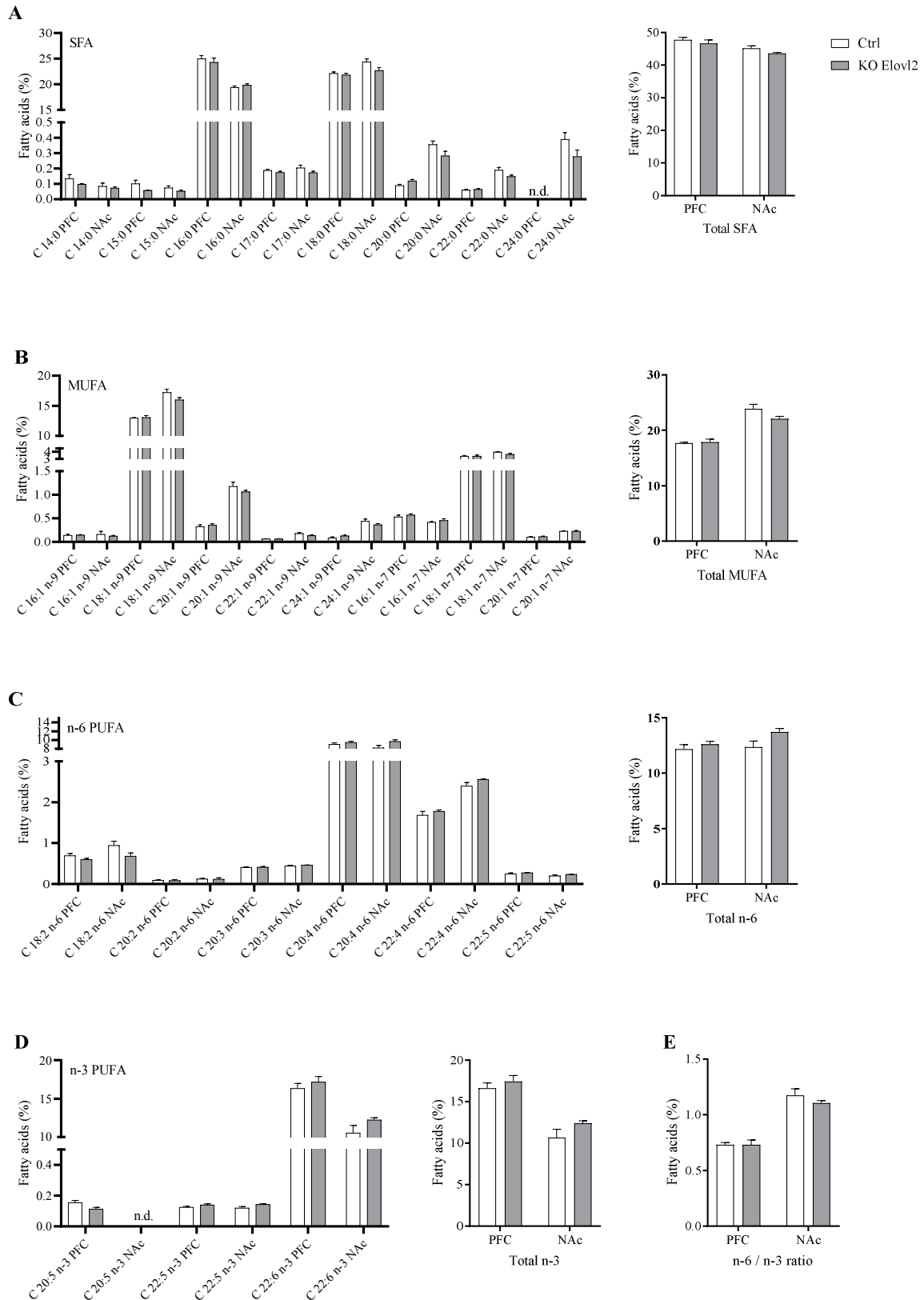


**Figure 4 :** Striatal fatty acids profiles of male mice from the control (Ctrl) virus injection or the KO for Elovl2 (KO Elovl2) condition on prefrontal (PFC) and Nucleus Accumbens (NAc) brain regions. (A) Saturated fatty acids (SFA) and total SFA. (B) Mono-unsaturated fatty acids (MUFA) and total MUFA. (C) n-6 polyunsaturated fatty acids (PUFA) and total n-6 PUFA. (D) n-3 PUFA and total n-3

PUFA. (**E**) n-6/n-3 ratio. n.d. = non detected. Results are expressed in % of total fatty acids in the hippocampus. Histograms represent mean  $\pm$  SEM (n=5/group). One-Way ANOVA followed by Bonferroni test if the ANOVA is significant. \* p<0.05, \*\* p<0.01, \*\*\* p<0.001

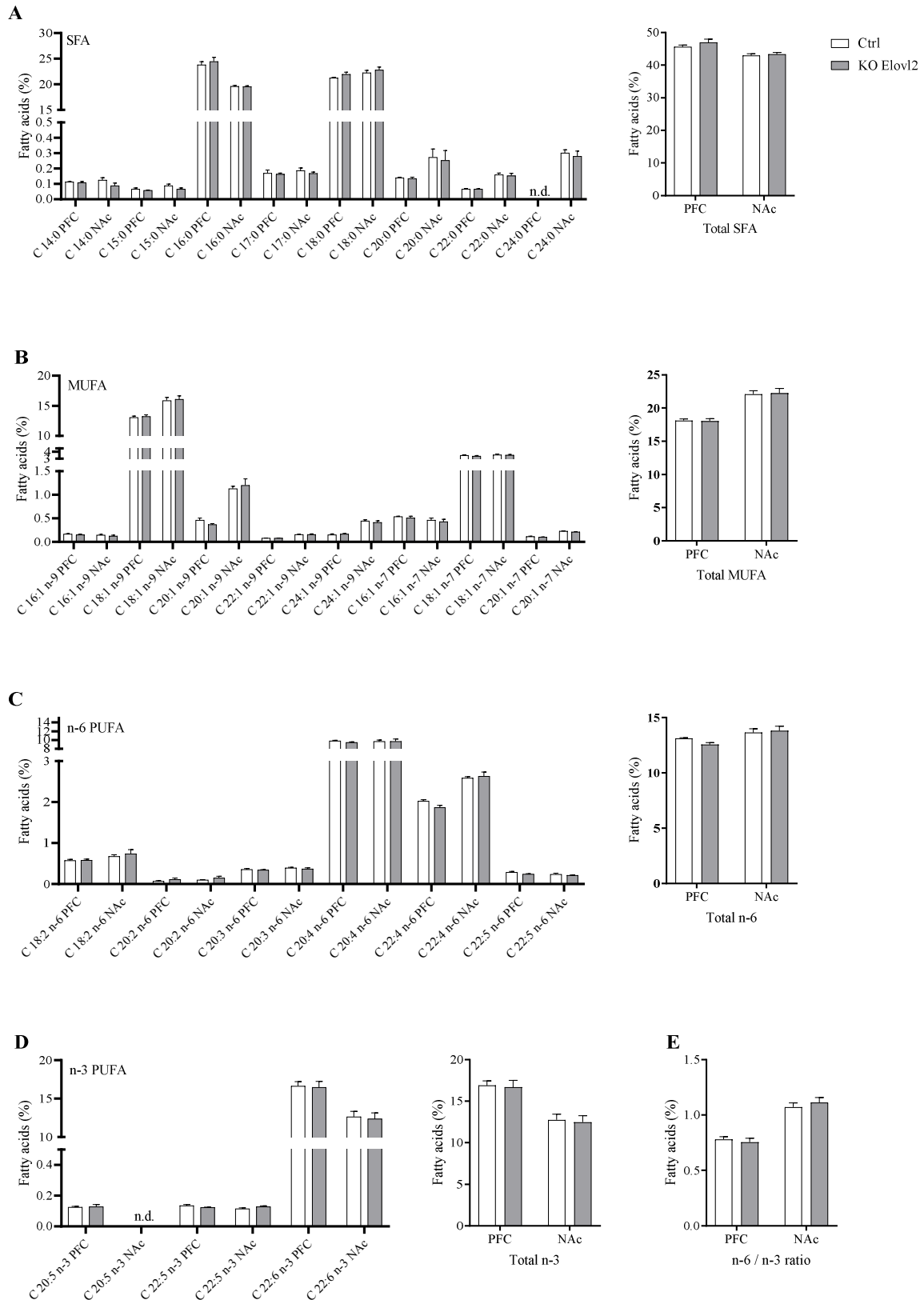


**Figure 5 :** Striatal fatty acids profiles of females mice from the control (Ctrl) virus injection or the KO for Elov12 (Elov12  $-/-$ ) condition on prefrontal (PFC) and Nucelus Accumbens (NAc) brain regions. (A) Saturated fatty acids (SFA) and total SFA. (B) Mono-unsaturated fatty acids (MUFA) and total MUFA. (C) n-6 polyunsaturated fatty acids (PUFA) and total n-6 PUFA. (D) n-3 PUFA and total n-3

PUFA. (E) n-6/n-3 ratio. n.d. = non detected. Results are expressed in % of total fatty acids in the hippocampus. Histograms represent mean  $\pm$  SEM (n=5/group). One-Way ANOVA followed by Bonferroni test if the ANOVA is significant. \* p<0.05, \*\* p<0.01, \*\*\* p<0.001

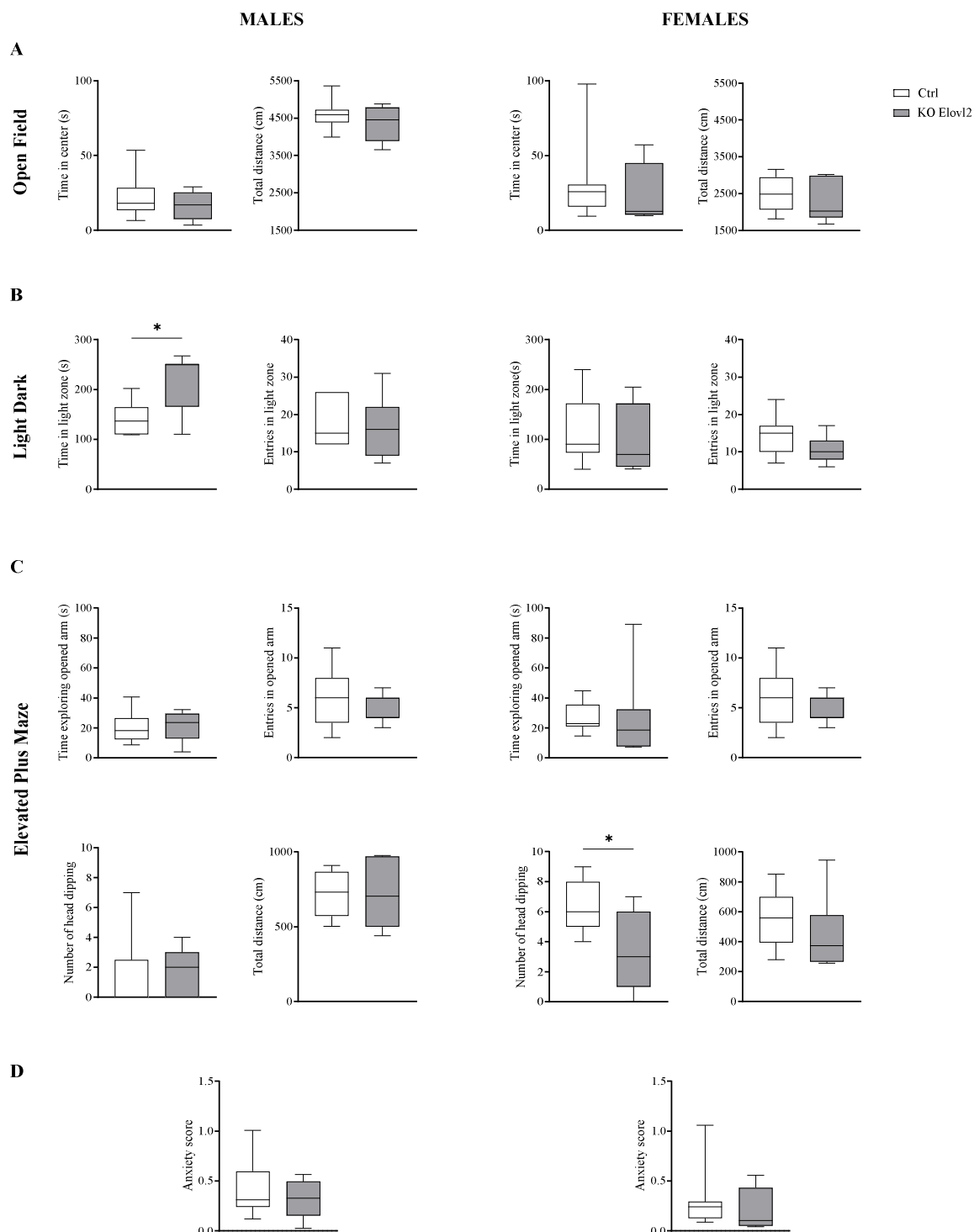


**Figure 6 :** Anxiety-like behavioral assessments in males and females control and KO Elovl2 mice. **(A)** Open Field. **(B)** Light Dark. **(C)** Elevated Plus Maze. **(D)** Anxiety scores were calculated by normalizing and balancing 6 different behavior measurements. Values (box and whiskers plots) (n=7/group) are plotted from minimum to maximum. One-Way ANOVA followed by Bonferroni test if the ANOVA is significant. \* p<0.05, \*\* p<0.01, \*\*\* p<0.001



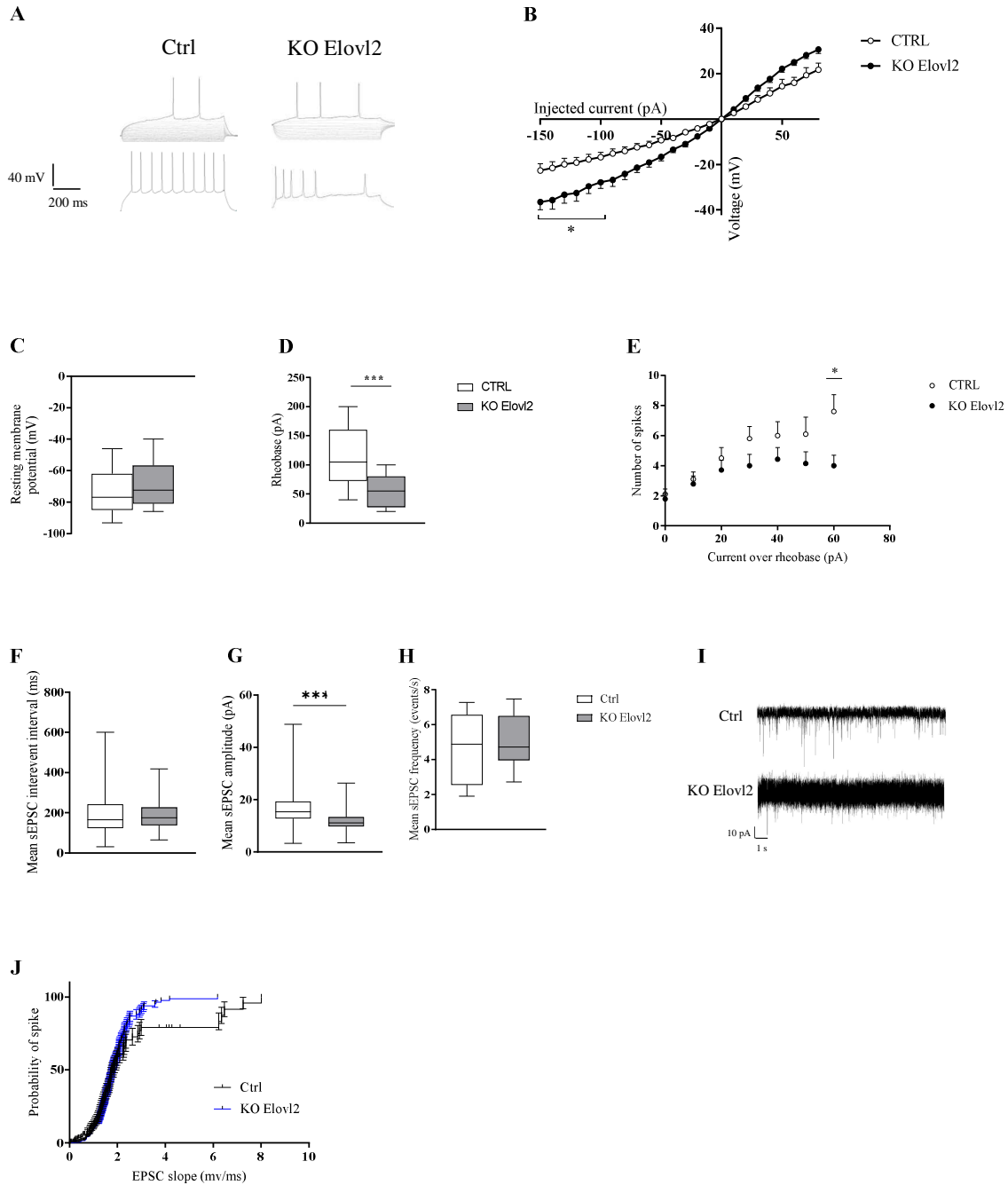


**Figure 7** : Modulation of accumbal medium spiny neurons intrinsic electrophysiological properties. **(A)** Representative firing pattern. **(B)** Voltage over current (I/V) curve. **(C)** Resting membrane potential (RMP in mV). **(D)** Rheobase (in pA). **(E)** Number of action potential (AP) generated over rheobase current (I–F) relationship. **(F–I)** Quantitative summary of interevent interval (in ms, **F**), amplitude (in pA, **G**) and frequency (in events/s, **H**) illustrated by traces (**I**). **(J)** Curves indicate the probability to trigger a spike (in %) in recorded MSNs following increasing cortical stimulations in both conditions. **(C–D–F–G–H)** Values (box and whiskers plots) are plotted from minimum to maximum. One-Way ANOVA followed by Bonferroni test if the ANOVA is significant. \*  $p < 0.05$ , \*\*  $p < 0.01$ , \*\*\*  $p < 0.001$  Statistics: \*  $p < 0.05$  and \*\*  $p < 0.01$  Ctrl versus KO Elov12 mice.

SUPPLEMENTARY DATA

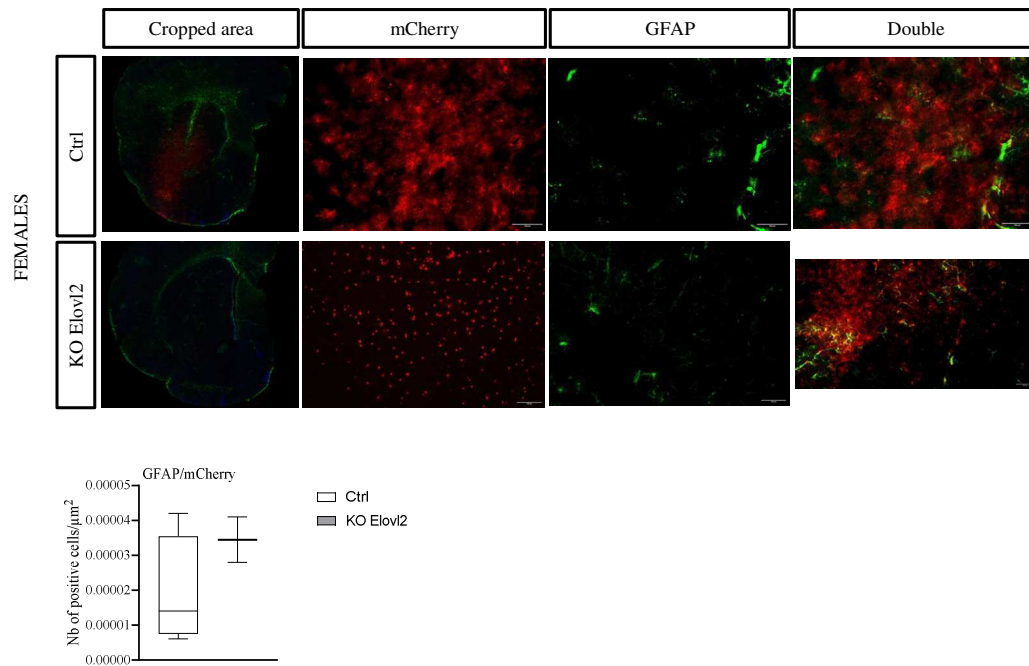


**Figure 8 :** Preliminary data of representative GFAP immunostaining in striatal area of female mice injected with the control virus (ctrl) and the cre virus (KO Elov12). Scale bar, 100 μm. Quantification of the colocalisation between GFAP immunostaining and mCherry fluorescence. Values (box and whiskers plots) (ctrl n=4; KO Elov12 n=2) are plotted from minimum to maximum.

***CHAPITRE 04 : Effet d'une supplémentation en AGPI n-3 sur le comportement émotionnel et la plasticité synaptique dans un modèle de stress***

---



Article

# Dietary Long-Chain n-3 Polyunsaturated Fatty Acid Supplementation Alters Electrophysiological Properties in the Nucleus Accumbens and Emotional Behavior in Naïve and Chronically Stressed Mice

Mathieu Di Miceli <sup>1,2,3</sup> , Maud Martinat <sup>1,3</sup> , Moira Rossitto <sup>1,3</sup>, Agnès Aubert <sup>1,3</sup>, Shoug Alashmali <sup>4,5</sup> , Clémentine Bosch-Bouju <sup>1,3</sup>, Xavier Fioramonti <sup>1,3</sup>, Corinne Joffre <sup>1,3</sup>, Richard P. Bazinet <sup>3,5</sup> and Sophie Layé <sup>1,3,\*</sup>

- <sup>1</sup> Laboratoire NutriNeuro, UMR INRAE 1286, Bordeaux INP, Université de Bordeaux, 146 Rue Léo Saignat, 33076 Bordeaux, France; m.dimiceli@worc.ac.uk (M.D.M.); maud.martinat@inrae.fr (M.M.); moira.rossitto@inrae.fr (M.R.); agnes.aubert@inrae.fr (A.A.); clementine.bosch-bouju@inrae.fr (C.B.-B.); xavier.fioramonti@inrae.fr (X.F.); corinne.joffre@inrae.fr (C.J.)
- <sup>2</sup> Worcester Biomedical Research Group, School of Science and the Environment, University of Worcester, Worcester WR2 6AJ, UK
- <sup>3</sup> International Research Network Food4BrainHealth; richard.bazinet@utoronto.ca
- <sup>4</sup> Department of Clinical Nutrition, Faculty of Applied Medical Sciences, King Abdulaziz University, Jeddah 22254, Saudi Arabia; shoug.alashmali@mail.utoronto.ca
- <sup>5</sup> Department of Nutritional Sciences, Faculty of Medicine, University of Toronto, Toronto, ON M5S 1A1, Canada
- \* Correspondence: sophie.laye@inrae.fr



**Citation:** Di Miceli, M.; Martinat, M.; Rossitto, M.; Aubert, A.; Alashmali, S.; Bosch-Bouju, C.; Fioramonti, X.; Joffre, C.; Bazinet, R.P.; Layé, S. Dietary Long-Chain n-3 Polyunsaturated Fatty Acid Supplementation Alters Electrophysiological Properties in the Nucleus Accumbens and Emotional Behavior in Naïve and Chronically Stressed Mice. *Int. J. Mol. Sci.* **2022**, *23*, 6650. <https://doi.org/10.3390/ijms23126650>

Academic Editors: Jérôme Roy and Nobuyuki Takahashi

Received: 12 May 2022

Accepted: 13 June 2022

Published: 14 June 2022

**Publisher's Note:** MDPI stays neutral with regard to jurisdictional claims in published maps and institutional affiliations.



**Copyright:** © 2022 by the authors. Licensee MDPI, Basel, Switzerland. This article is an open access article distributed under the terms and conditions of the Creative Commons Attribution (CC BY) license (<https://creativecommons.org/licenses/by/4.0/>).

**Abstract:** Long-chain (LC) n-3 polyunsaturated fatty acids (PUFAs) have drawn attention in the field of neuropsychiatric disorders, in particular depression. However, whether dietary supplementation with LC n-3 PUFA protects from the development of mood disorders is still a matter of debate. In the present study, we studied the effect of a two-month exposure to isocaloric diets containing n-3 PUFAs in the form of relatively short-chain (SC) (6% of rapeseed oil, enriched in  $\alpha$ -linolenic acid (ALA)) or LC (6% of tuna oil, enriched in eicosapentaenoic acid (EPA) and docosahexaenoic acid (DHA)) PUFAs on behavior and synaptic plasticity of mice submitted or not to a chronic social defeat stress (CSDS), previously reported to alter emotional and social behavior, as well as synaptic plasticity in the nucleus accumbens (NAc). First, fatty acid content and lipid metabolism gene expression were measured in the NAc of mice fed a SC (control) or LC n-3 (supplemented) PUFA diet. Our results indicate that LC n-3 supplementation significantly increased some n-3 PUFAs, while decreasing some n-6 PUFAs. Then, in another cohort, control and n-3 PUFA-supplemented mice were subjected to CSDS, and social and emotional behaviors were assessed, together with long-term depression plasticity in accumbal medium spiny neurons. Overall, mice fed with n-3 PUFA supplementation displayed an emotional behavior profile and electrophysiological properties of medium spiny neurons which was distinct from the ones displayed by mice fed with the control diet, and this, independently of CSDS. Using the social interaction index to discriminate resilient and susceptible mice in the CSDS groups, n-3 supplementation promoted resiliency. Altogether, our results pinpoint that exposure to a diet rich in LC n-3 PUFA, as compared to a diet rich in SC n-3 PUFA, influences the NAc fatty acid profile. In addition, electrophysiological properties and emotional behavior were altered in LC n-3 PUFA mice, independently of CSDS. Our results bring new insights about the effect of LC n-3 PUFA on emotional behavior and synaptic plasticity.

**Keywords:** DHA; EPA; ALA; chronic social defeat stress; lipid microarray; whole-cell patch-clamp electrophysiology; long-term depression; emotional behavior

## 1. Introduction

Major depressive disorder (MDD) is a leading cause of disability worldwide, with around 20% of subjects affected in the general population [1]. There are few effective treatments for depression, with current treatments leaving 10–30% of patients with no efficient response [2]. Thus, there is an urgent need to design and develop novel therapeutics to treat depression.

The long-chain (LC) n-3 polyunsaturated fatty acids (PUFAs), eicosapentaenoic acid (EPA, C20:5 n-3) and docosahexaenoic acid (DHA, C22:6 n-3), are considered promising nutritional-based therapeutic strategies for preventing and treating MDD [3–6]. The use of these fatty acids in MDD is based on the observation of an inverse association between the intake of oily fish (rich in EPA and DHA) and the prevalence of MDDs in humans, as confirmed recently [7,8]. This is also corroborated by the observation that MDD patients exhibit lower blood and brain levels of EPA and/or DHA as compared to healthy controls [9,10]. Importantly, depressive symptoms in patients were reported to be significantly reduced with a dietary supplementation containing more than 50% of EPA, but not with DHA [11]. The potent antidepressant effect of a dietary formulation with a higher amount of EPA to DHA rather than DHA alone in MDD was recently confirmed by a meta-analysis [4], although another study did not observe these effects [12]. The potential antidepressant effect of EPA was also demonstrated in animal models of depression, such as olfactory bulbectomized rats [13], chronic unpredictable mild stress [14], maternal stress [15], or chronic social defeat stress (CSDS) [16]. In particular, we previously demonstrated that a dietary intervention with a diet enriched with LC n-3 PUFA (10% EPA and 7% DHA of total fatty acids, see [17]) partially protected mice from CSDS-induced emotion behavior alteration [16,18]. Altogether, these data suggest that a dietary supplementation with EPA/DHA with a higher proportion of EPA could be efficient to improve symptoms in MDD, however the mechanisms involved are still poorly known.

Some mechanistic explanations of the antidepressant activities of EPA/DHA have been suggested [3,6]. Indeed, it has been shown that LC n-3 PUFA dietary supplementation reduces inflammatory processes, including in the brain [19,20], hypothalamic–pituitary–adrenal (HPA) axis alteration [5,21–24], apical dendritic tree alterations [16], and promotes neurogenesis [25], which are altered in depression [14]. Although there is a close link between n-3 PUFA, synaptic plasticity, and depressive-like symptoms [6,18,26,27], the effect of EPA/DHA supplementation on synaptic plasticity has been poorly studied. Furthermore, whether EPA/DHA supplementation can restore the synaptic deficit observed in animal models of depression remains to be elucidated. Indeed, we have previously reported that a diet low in n-3 PUFA, which induces a decrease of brain DHA, triggers an endocannabinoid (eCB)-dependent synaptic plasticity impairment in the nucleus accumbens (NAc) and the prefrontal cortex of mice [28,29], together with an altered apical tree of neurons [16] and eCB signaling in the brain [30]. Restoration of the eCB-dependent synaptic plasticity can be achieved through pharmacological approaches aiming at increasing eCBs at the synaptic level, thus improving depressive-like symptoms in n-3 PUFA-deficient mice [28]. These results are in accordance with the observation that accumbal activity is altered in MDD patients [31]. Importantly, eCB-dependent synaptic plasticity is altered in animal models of depression [32,33] and the pharmacological restoration of this plasticity in the NAc alleviates the deleterious effect of CSDS on emotional behavioral [33]. Altogether, these data suggest that eCB-dependent synaptic plasticity in the NAc sustains emotional behavior alterations in animal models of depression, such as CSDS.

Based on previous data, including ours, showing that dietary intervention using diets rich in LC n-3 PUFAs protects from the development of emotional behavior alteration in animal models of chronic stress [16], we analyzed whether a diet supplemented with EPA/DHA controls emotional behavior and eCB-dependent synaptic plasticity in the NAc of mice submitted or not to CSDS. For the first time, we established the PUFA and lipid metabolism molecular profiles in the NAc of mice fed a diet rich in EPA + DHA for 8 weeks, as compared to a control diet balanced in relatively short-chain (SC) n-3 PUFA

( $\alpha$ -linolenic acid, ALA), starting at weaning. Then, we examined whether such a diet rich in EPA + DHA could regulate emotional behavior and eCB-dependent plasticity in the NAc of mice submitted or not to CSDS. We identified a lipid metabolic signature in the NAc of EPA + DHA mice which parallels emotional behavior and accumbal electrophysiological properties, providing insight on the effect of diets rich in EPA + DHA on brain function and emotional behavior.

## 2. Results

### 2.1. Fatty Acids and Molecular Signature of LC n-3 PUFA Dietary Supplementation

We first characterized the fatty acid signature in the NAc of mice fed with a relatively short-chain (SC) n-3 PUFA diet (controls) or a LC n-3 PUFA (n-3 suppl) diet after 8 weeks of feeding (Figure 1).

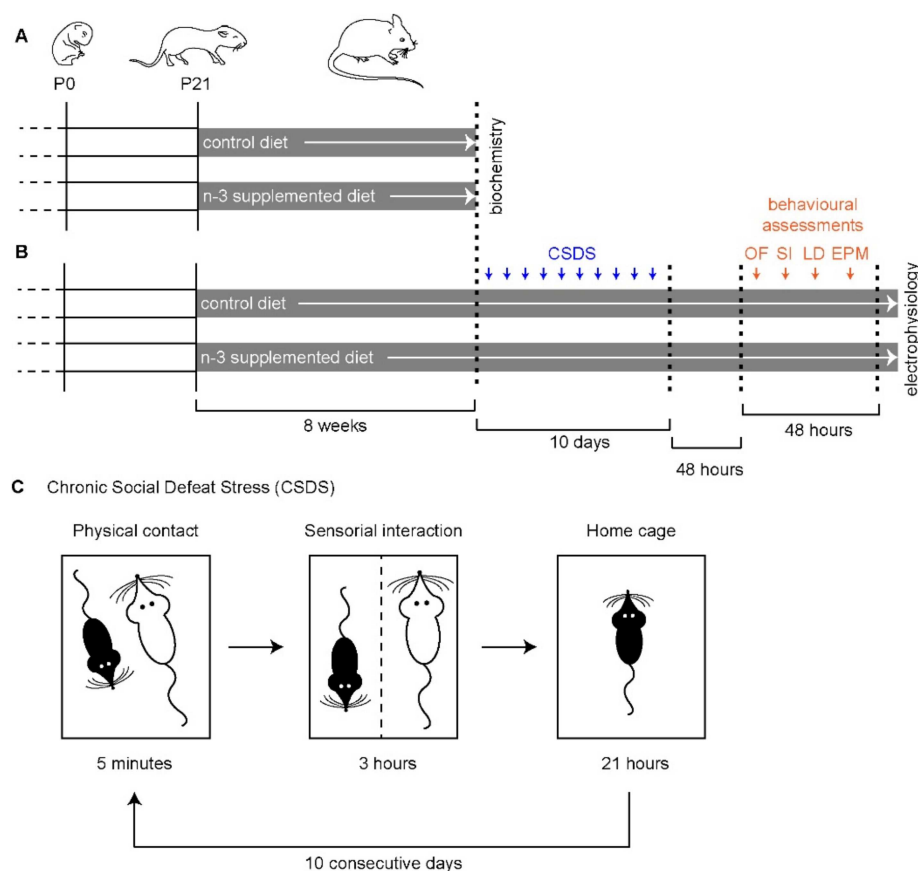


**Figure 1.** Experimental protocol used in the present study. **(A)** Control and n-3-supplemented diets were given for 8 weeks to C57Bl6/j mice, starting at weaning (P21), before performing biochemical analyses (striatal fatty acid content). **(B)** Following 8 weeks of diet, chronic social defeat stress (CSDS) was performed every day for a total of 10 consecutive days, which was followed by 48 h of behavioral testing, including the open field (OF), the social interaction (SI) test, the light–dark (LD) test, and the elevated plus maze (EPM) test. Two tests were performed per day, in the light phase. Following 48 h of rest, mice were tested for endocannabinoid-dependent plasticity (electrophysiology). **(C)** Detail of the CSDS procedure. Defeated mice are represented in black, while the Swiss CD1 aggressor is represented in white. Drawings are not to scale.

The LC n-3 PUFA diet induced significant increases in n-3 PUFA content, including DPA (n-3), DHA, and total n-3 PUFAs (Figure 2, Supplemental Table S1 (see Supplementary Materials),  $p < 0.05$ , unpaired  $t$ -tests). In line with these results, significant decreases of n-6 PUFA content were also observed, including linoleic acid (LA C18:2 n-6), arachidonic acid (ARA C20:4 n-6), docosatetraenoic acid (C22:4 n-6), DPA (n-6), and total n-6 PUFAs

(Figure 2,  $p < 0.05$ , unpaired  $t$ -tests). Interestingly, tetracosatetraenoic acid (C24:4 n-6) was increased following LC n-3 PUFA dietary supplementation ( $p < 0.05$ , unpaired  $t$ -tests). As expected, the ratio of n-3/n-6 was also significantly increased ( $p < 0.05$ , unpaired  $t$ -test) by the LC n-3 PUFA supplementation.

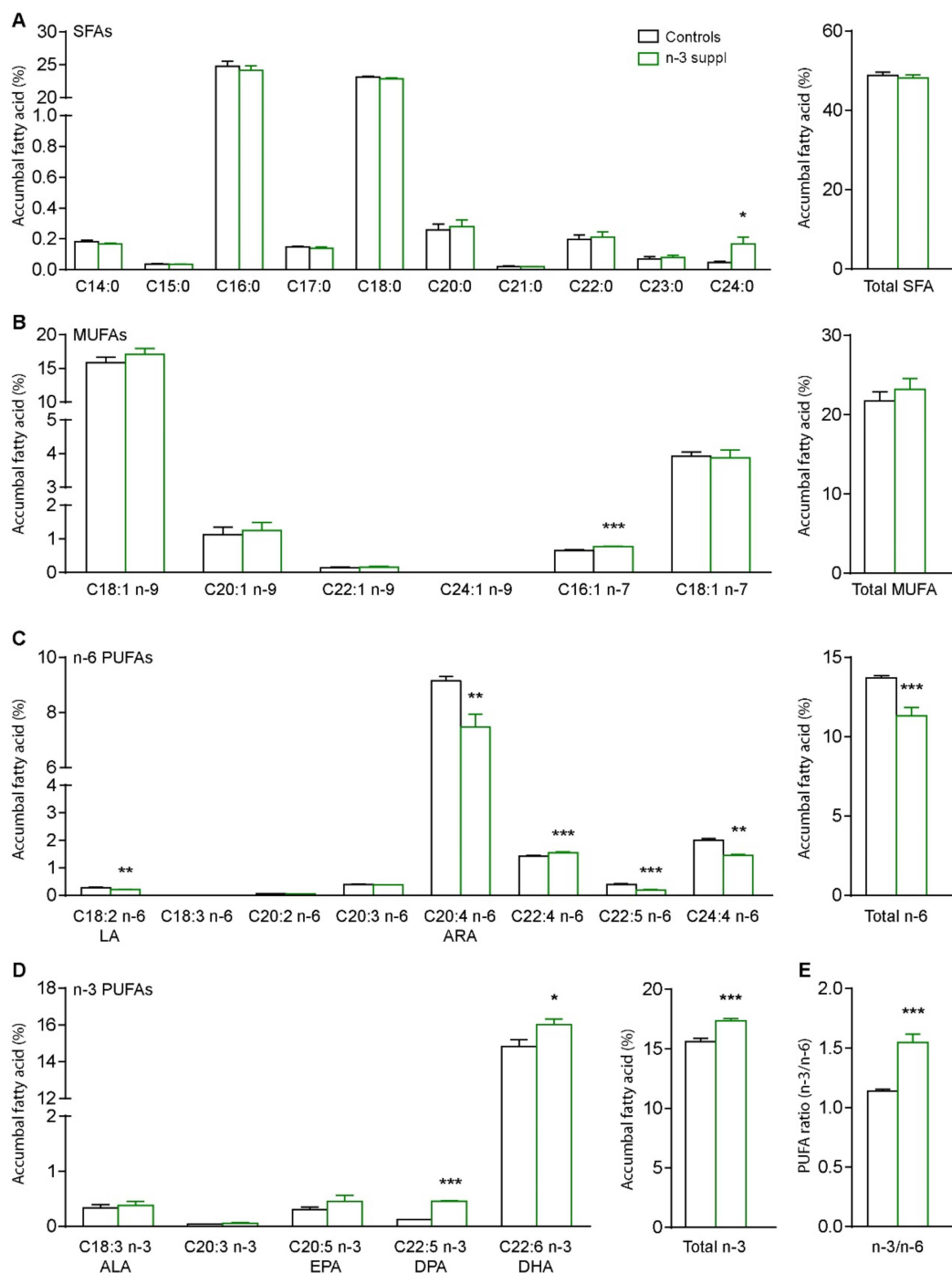


**Figure 2.** Accumbal fatty acid profiles of control and n-3-supplemented (n-3 suppl) mice. **(A)** Saturated fatty acids (SFA). **(B)** Mono-unsaturated fatty acids (MUFAs). Polyunsaturated fatty acids (PUFAs) of the n-6 **(C)** and n-3 **(D)** families. **(E)** Ratio of n-3 over n-6 PUFAs. LA: linoleic acid, ALA: alpha-linolenic acid, ARA: arachidonic acid, EPA: eicosapentaenoic acid, DPA: docosapentaenoic acid, DHA: docosahexaenoic acid. Unpaired  $t$ -tests. \*  $p < 0.05$ , \*\*  $p < 0.01$ , and \*\*\*  $p < 0.001$  vs. control. Histograms represent mean  $\pm$  SEM.

These results indicate that n-3 PUFAs dietary supplementation can alter fatty acid content in the NAc.

In agreement with the above-mentioned fatty acid modifications observed in the NAc, we observed that gene expression of lipid metabolism pathways was altered by the LC n-3 PUFA dietary exposure, as compared to the control diet. Indeed, in the NAc of mice fed with the LC n-3 PUFA diet, we observed significant increases ( $p < 0.05$ , unpaired  $t$ -tests) of gene expression in 25 out of the 89 genes tested in a lipidomic microarray (Figure 3A, Supplemental Tables S1–S3). These included genes coding for hydrolases (*Abhd4*, *Abhd6*), deshydrogenases (*Acadl*, *Acad10*, *Hadh*), elongases (*Elovl1*, *Elovl5*), synthases (*Ptgs1*, *Fasn*), transferases (*Acat1*, *Pcyt1a*, *Pcyt1b*, *Pcyt2*), as well as fatty acid receptors (*Adipor2*, *Ppard*, *Ppargc1a*, *Ptger4*, *Rxra*) and transporters (*Apoe*, *Fads2*, *Scd1*, *Slc25a20*, *Slc27a1*, *Slc27a3*, *Slc27a4*; Figure 3B). As expected, gene ontology [34] using over-representation analysis, performed with Webgestalt [35,36], identified several biological processes related to fatty acid regulation, such as fatty acid synthesis, transport, and metabolism, as well as lipid biosynthesis/metabolism and cellular lipid metabolism (Figure 3C). Furthermore, due to the design of our microarray and as expected, these gene ontology families presented redundancy (Figure 3D,E). Of note, amongst the top 50 enriched gene ontology families, *Ptger4* was associated to several families (8/50), while both *Slc25a20* and *Rxra* remained unmapped (0/50, not shown).

Altogether, these results suggest that n-3 PUFAs supplementation successfully modulates the NAc fatty acid profile, along with upregulation of genes involved in fatty acid synthesis, metabolism, and transport.

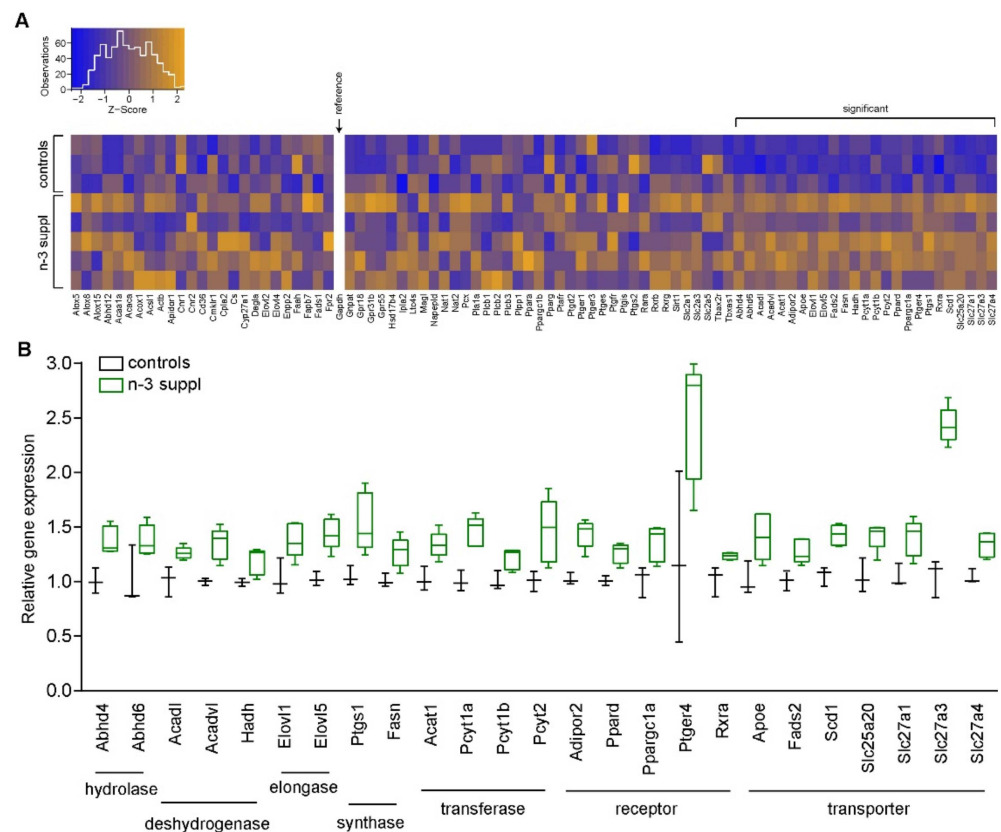
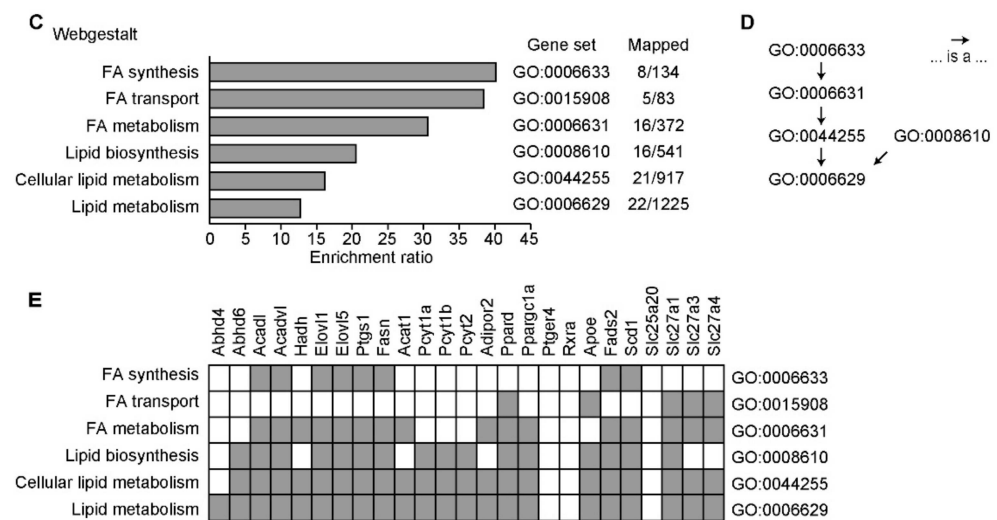


Figure 3. Cont.





**Figure 3.** n-3 supplementation increases transcription of genes involved in fatty acid processes. (A) Heatmap of transcriptional regulation of the 89 analyzed genes presenting significant or non-significant gene modifications. Gapdh is used as the housekeeping gene (reference). Insert represents Z-scores' distribution. (B) Significantly upregulated genes. Values (box and whiskers plots) are plotted from minimum to maximum. (C) Gene ontology (Webgestalt [35,36]) and enrichment ratios of the significantly upregulated genes induced by n-3 supplementation. Such an analysis yielded different gene ontology (GO) families, represented with their respective GO codes. Mapped terms within our study are indicated over the total number of genes within each GO family. (D) Redundancy of the gene ontology families. Arrows indicate inclusive relationships. (E) Detailed mapping of genes and ontology families. Genes were found to be either present (grey) or absent (white) from different gene ontology families. Ptger4 was linked to 8 families from the top 50 enriched ones, while both *Rxra* and *Slc25a20* were not mapped amongst the top 50 enriched terms.

## 2.2. Anxiolytic-like Effect of LC n-3 PUFA Dietary Supplementation

Then, in another cohort of animals, we evaluated the emotional behavior of SC (control) and LC n-3 PUFA mice submitted or not to CSDS, using a battery of tests aimed at assessing stress-related behaviors. We found that CSDS had significant effects (Supplemental Table S1) on the time spent by mice in the open field (OF), especially on variables such as time in both the central ( $F_{(1,37)} = 5.084$ ,  $p = 0.03$ ) and peripheral ( $F_{(1,37)} = 5.085$ ,  $p = 0.03$ ) zones, as well as total distance travelled ( $F_{(1,37)} = 6.824$ ,  $p = 0.013$ , Figure 4A). Similarly, mice submitted to CSDS spent significantly less time in the light zone ( $F_{(1,37)} = 4.159$ ,  $p = 0.04$ ) and significantly more time in the dark zone ( $F_{(1,37)} = 4.156$ ,  $p = 0.04$ ) during the light–dark (LD) test (Figure 4B). The number of entries in the light zone or total distance travelled by stressed mice was unchanged. In the elevated plus maze (EPM), CSDS did not induce any difference on all parameters assessed (Figure 4C). Exposure to a LC n-3 PUFA diet 8 weeks before the induction of CSDS induced anxiolytic-like effects in undefeated and defeated mice, as observed in all the variables measured in the OF test (Figure 4A) and the LD test (Figure 4B). In the EPM, LC n-3 PUFA dietary exposure had a significant effect on time spent in the center ( $F_{(1,37)} = 4.405$ ,  $p = 0.04$ ) and total distance travelled (Figure 4C,  $F_{(1,37)} = 4.832$ ,  $p = 0.03$ ). No significant interaction was observed between CSDS and LC n-3 PUFA dietary exposure, although it almost reached statistical significance in the number of head dipping in the EPM ( $p = 0.06$ , Figure 4C). Finally, mice submitted to CSDS presented significantly higher anxiety scores (Figure 4D,  $F_{(1,37)} = 5.491$ ,  $p = 0.025$ ), as observed in a previous study [33].

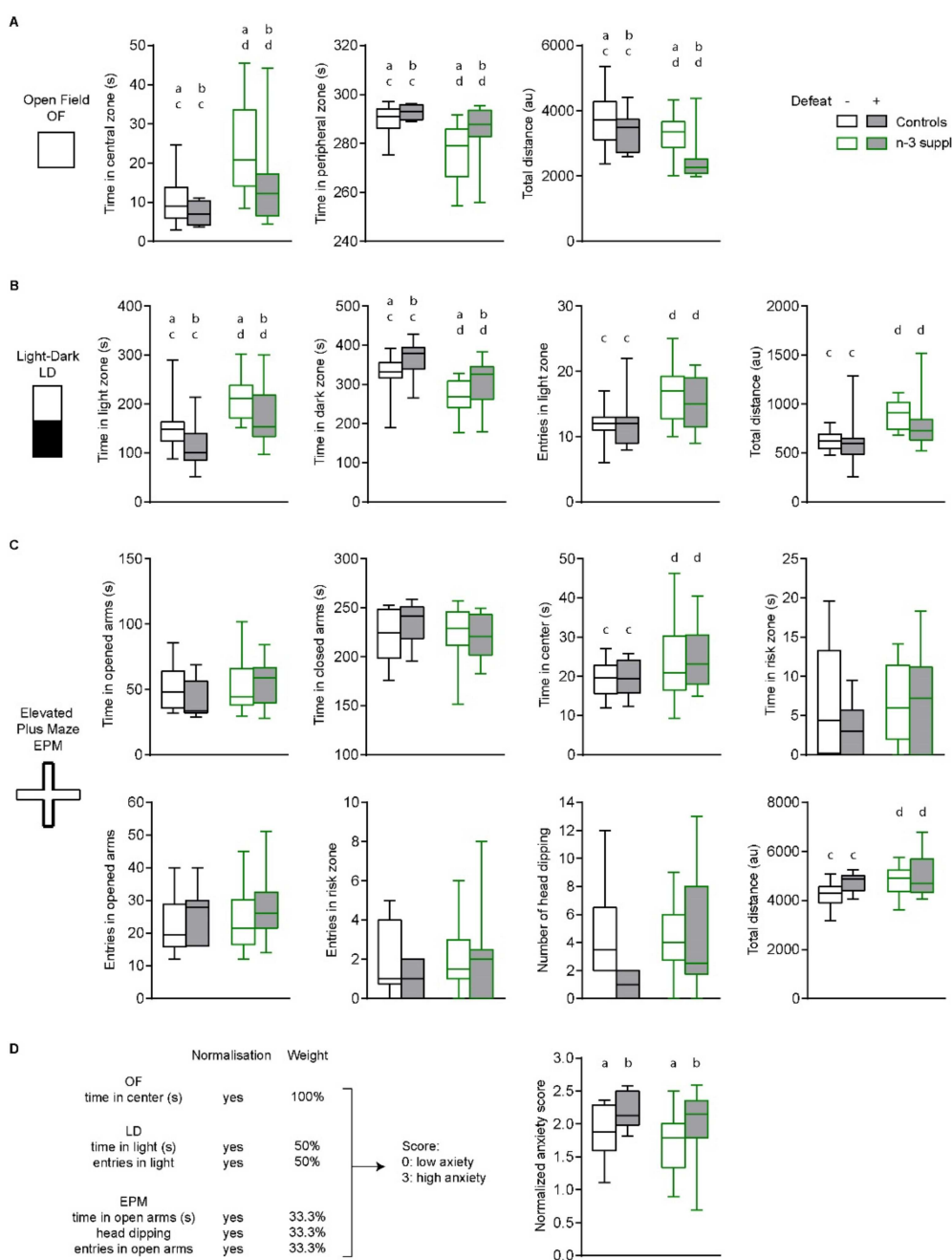


**Figure 4.** n-3 supplementation has anxiolytic effects. n-3 supplementation induces anxiolytic-like effects in the open field (OF) (A) and the light–dark (LD) tests (B) but has only minimal effects on the elevated plus maze (EPM) test (C). (D) Anxiety scores were calculated by normalizing and balancing 6 different behavior measurements. Two-way ANOVAs were performed, with ‘stress’ and ‘diet’ as factors. Statistically significant results are reported as follows: [stress] a vs. b, [diet] c vs. d. Please refer to Supplemental Table S1 for further details. Values (box and whiskers plots) are plotted from minimum to maximum.

These results indicate that n-3 PUFAs dietary supplementation can promote anxiolytic-like effects in mice, irrespective of CSDS.

### 2.3. Reversal of CSDS-Induced Social Interaction Deficits by LC n-3 PUFA Dietary Supplementation

We then measured social interaction in defeated mice fed with either SC (control) or LC n-3 PUFA-supplemented diets. Social interaction ratios were not different across groups (Figure 5A, stress:  $F_{(1,37)} = 1.337$ ,  $p = 0.25$ ; diet:  $F_{(1,37)} = 1.007$ ,  $p = 0.32$ ; interaction:  $F_{(1,37)} = 2.425$ ,  $p = 0.13$ ). In the two groups of mice exposed to CSDS, the proportion of susceptible (ratio < 1) and resilient mice (ratio > 1) [37,38] was different, although it did not reach statistical significance ( $p = 0.33$ , Fisher's exact test), likely due to the small sample size (Supplemental Table S1, Figure 5B). Resampling at 100 replicates exacerbated the differences observed in both social interaction ratios and the proportion of resilient/susceptible mice (Figure 5C), which was not due to the resampling method itself (Supplemental Figure S1, Supplemental Table S1).

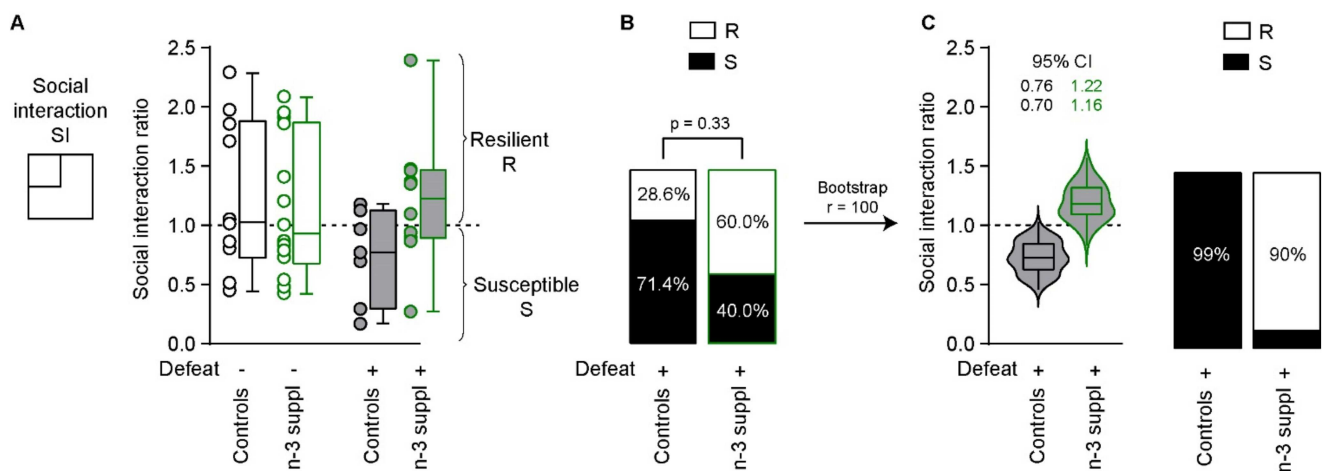


**Figure 5.** Resilience to CSDS by n-3 supplementation. (A) Stress susceptibility (S) or resilience (R) following CSDS or not in control and n-3-supplemented mice. (B) Proportions of S or R mice in the two groups. (C) Bootstrapping with 100 replicates indicates significant anxiolytic-like effects of the n-3 supplementation on social interaction scores and proportions of S vs. R mice in the different groups. Bootstrapping *per se* does not induce statistical significance when replicates are set at 100 ( $r = 100$ ) (Supplemental Figure S1). CI: confidence interval. The dotted horizontal bars in (A) and (C) indicate thresholds for susceptibility (<1) or resilience (>1) to chronic stress, according to Golden and colleagues [37]. The box and whiskers plot (A) and the violin plot (C) represent values from minimum to maximum. The box and whisker plot within the violin plot is set to represent the 2.5th to 97.5th percentiles.

These results suggest that n-3 PUFAs dietary supplementation increases social interaction following CSDS, but not under baseline conditions.

### 2.4. Alteration of Electrophysiological Properties of Accumbal Medium Spiny Neurons by LC n-3 PUFA Dietary Supplementation

We observed a significant effect of the LC n-3 PUFA supplementation on several intrinsic electrophysiological parameters of accumbal medium spiny neurons (MSN). These included significantly altered passive membrane properties, such as an increase in resting membrane potential (RMP,  $F_{(1,37)} = 5.73$ ,  $p = 0.02$ ) and capacitance ( $F_{(1,37)} = 9.92$ ,  $p = 0.003$ ), but not input resistance or rheobase (Figure 6A). CSDS and LC n-3 PUFA supplementation induced significant alterations of voltage over current relationships (stress:  $F_{(1,6)} = 11.68$ ,  $p < 0.001$ ; diet:  $F_{(1,6)} = 22.37$ ,  $p < 0.001$ ), while only n-3 supplementation had a significant effect on the number of action potentials generated during supra-threshold current applications (Figure 6B,  $F_{(1,16)} = 41.81$ ,  $p < 0.001$ ).

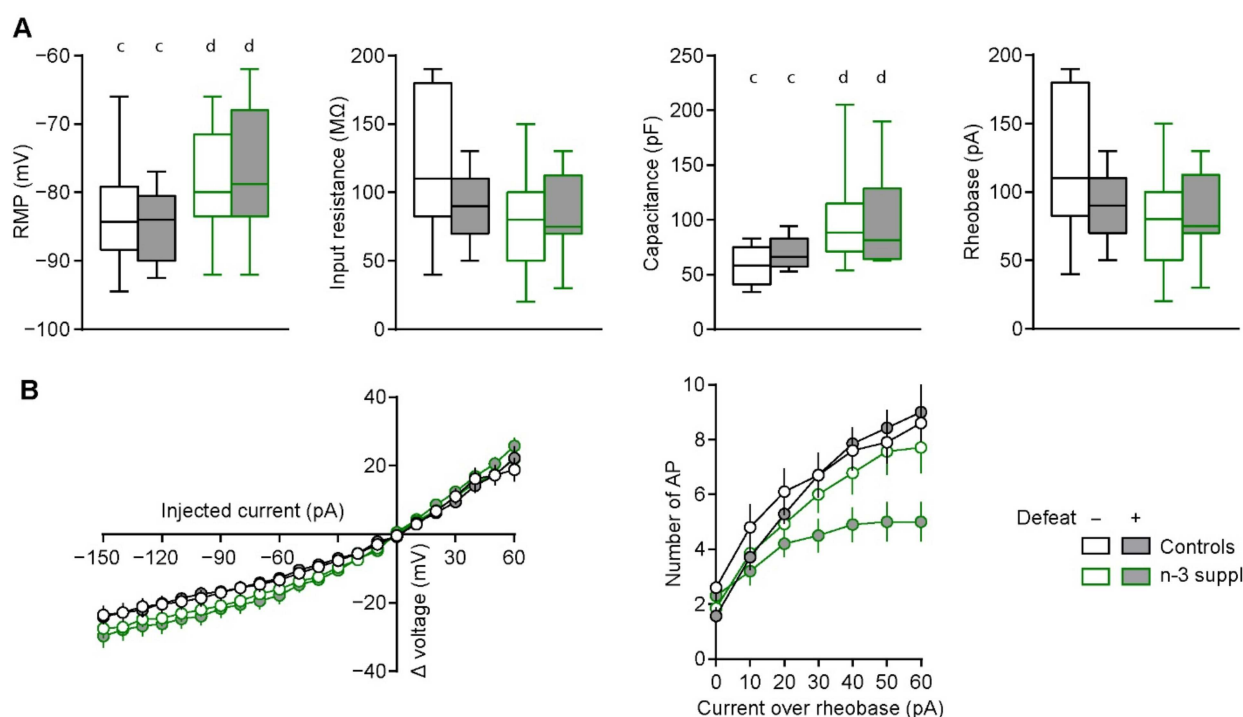


**Figure 6.** Altered intrinsic electrophysiological properties in accumbal medium spiny neurons induced by n-3 supplementation. (A) Resting membrane potential (RMP) and capacitance, but not input resistance or rheobase, were significantly increased following dietary n-3 supplementation. (B) Voltage over current (I/V) and number of action potential (AP) generated over rheobase current (I-F) relationships. Stress and n-3 supplementation induced significant effects (Supplemental Table S1). Two- and three-way ANOVAs were performed. Statistically significant results are reported as follows: [diet] c vs. d. Further statistical details are included in Supplemental Table S1. Values (box and whiskers plots) are plotted from minimum to maximum (A) or as the mean  $\pm$  SEM (B).

Furthermore, LC n-3 PUFA-supplemented mice presented a higher action potential (AP) amplitude ( $F_{(1,37)} = 9.44, p = 0.004$ ) and longer AP duration ( $F_{(1,37)} = 12.00, p = 0.001$ ), as well as a shorter delay to first spike (Table 1, Supplemental Table S1,  $F_{(1,37)} = 5.51, p = 0.02$ ). These altered spike properties suggest a potential for increased neurotransmitter release by LC n-3 PUFA supplementation.

**Table 1.** Electrophysiological spike properties in medium spiny neurons of control and n-3-supplemented (n-3 suppl) mice. Values are rounded to 1 decimal point and are represented as the mean  $\pm$  SEM. AP: action potential, CSDS: chronic social defeat stress, SEM: standard error of the mean. Refer to Supplemental Table S1 for additional details of the two-way ANOVA.

Electrophysiological Parameter	Control	Control + CSDS	n-3 Suppl	n-3 Suppl + CSDS	Significant Variable
AP threshold (mV)	$-36.8 \pm 1.9$	$-37.6 \pm 2.7$	$-40.7 \pm 0.9$	$-39.2 \pm 1.9$	-
AP amplitude (mV)	$61.0 \pm 2.9$	$62.3 \pm 3.1$	$72.0 \pm 2.1$	$69.9 \pm 3.8$	diet
AP duration (ms)	$5.6 \pm 0.5$	$5.1 \pm 0.4$	$6.5 \pm 0.5$	$7.8 \pm 0.5$	diet
Delay to first spike (ms)	$387.5 \pm 44.2$	$427.8 \pm 55.7$	$352.4 \pm 40.4$	$253.2 \pm 34.8$	diet
AP rise kinetics (mV/ms)	$34.8 \pm 3.3$	$35.0 \pm 3.9$	$31.5 \pm 2.9$	$27.0 \pm 4.3$	-
AP decay kinetics (mV/ms)	$18.3 \pm 2.2$	$21.2 \pm 3.0$	$19.4 \pm 1.3$	$15.5 \pm 1.5$	-

We then applied an electric protocol (10 Hz stimulation for 10 min) to induce long-term depression (LTD) in accumbal MSN of SC (control) and LC n-3 PUFA-supplemented mice

submitted or not to CSDS. In SC (control) (Figure 7A) and LC n-3 PUFA-supplemented (Figure 7B) mice, CSDS did not alter LTD. However, mice fed the LC n-3 PUFA-supplemented diet presented significantly decreased excitatory post-synaptic currents (EPSCs) at baseline (Figure 7C, Supplemental Table S1,  $F_{(1,34)} = 4.361, p = 0.04$ ), which were not to be attributed to differences in stimulation intensity (Figure 7D). This was also confirmed by examining input–output relationships (Supplemental Figure S2,  $F_{(1,53)} = 4.209, p = 0.04$ ). Finally, no differences were observed following the induction of LTD, where early and late EPSC amplitudes were similar across all groups (Figure 7E, Supplemental Table S1), suggesting that LC n-3 PUFA supplementation has an effect on excitatory transmission onto accumbal MSN, without altering the expression of LTD in these neurons.

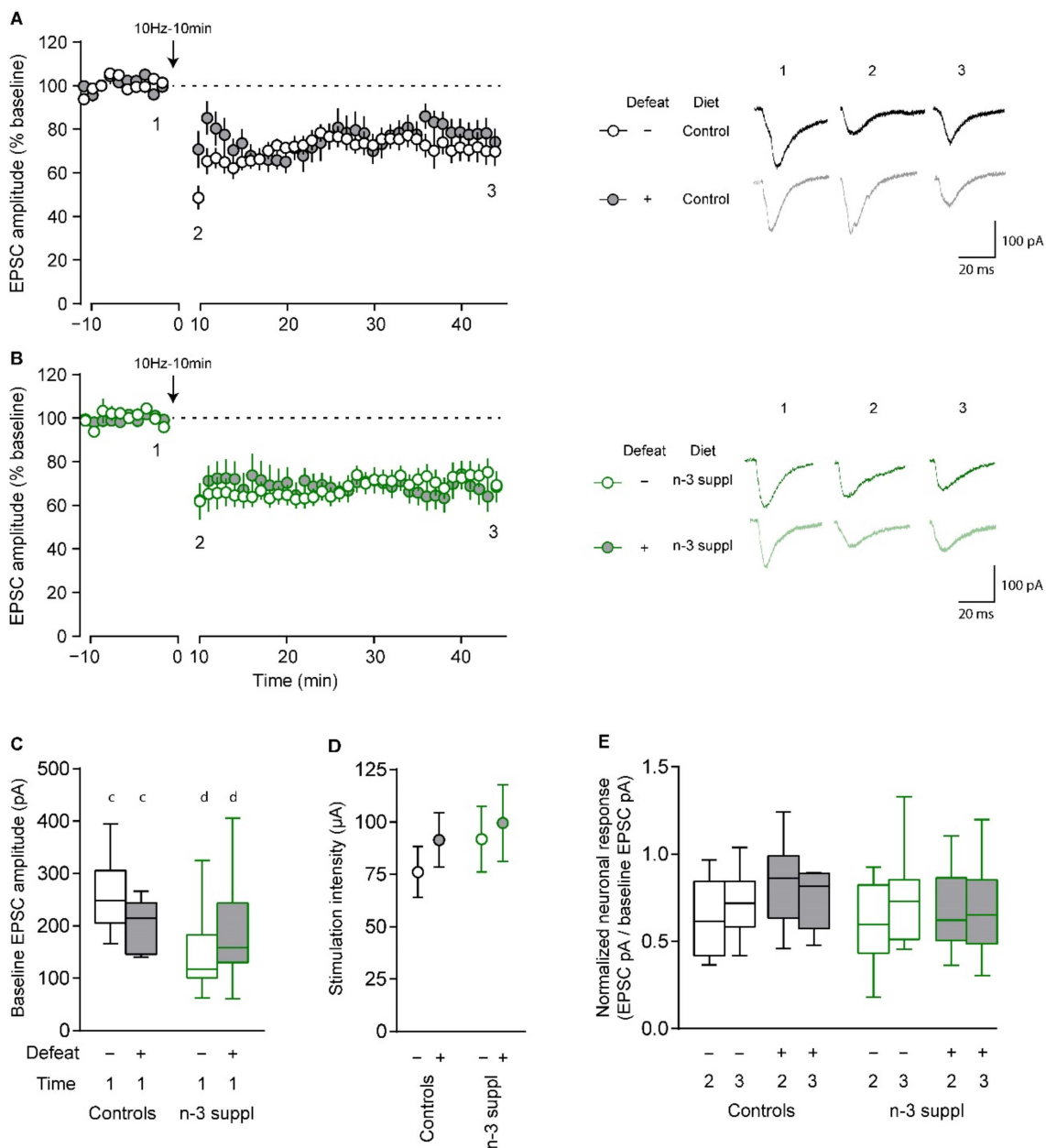


**Figure 7.** Reduced responses to electrical stimulation in accumbal medium spiny neurons. Representative recording examples of endocannabinoid-dependent plasticity induced by 10 Hz stimulations

of pre-synaptic fibers for 10 min in either control (A) or n-3-supplemented (B) animals. (C) Excitatory post-synaptic currents (EPSC) recorded at baseline of recording were significantly lower in n-3-supplemented animals. (D) Applied stimulation intensities did not vary across groups. (C,D) Two-way ANOVAs were performed, with 'stress' and 'diet' as factors. (E) Normalized neuronal responses after LTD (10 Hz, 10 min protocol). Here, normalization was achieved for each neuron by dividing EPSC responses (pA) by baseline EPSC responses (pA). Statistically significant results are reported as for diet, using *c vs. d*. Please refer to Supplemental Table S1 for further details. Values are plotted as the mean  $\pm$  SEM (A,B,D) or as minimum to maximum (C,E).

These results suggest that LC n-3 PUFA supplementation can modulate the electrophysiological properties of accumbal MSN, without altering LTD. Finally, the possible correlations between *in vivo* behavioral measurements and *ex vivo* electrophysiological properties of MSN are presented in Supplemental Figure S3.

### 3. Discussion

First, we identified for the first time the fatty acids and lipid genes signature in the NAc of adult mice fed for 2 months (starting at weaning) with a diet enriched with LC n-3 PUFA (10% EPA and 7% DHA of total lipids) as compared to a SC isocaloric diet rich in ALA (the precursor of EPA and DHA). The specific changes in this signature were accompanied by an alteration of emotional behaviors, as measured in the OF, LD, and EPM tests. Following CSDS, the number of stress-resilient mice fed with control or n-3 LC PUFA-supplemented diets was not significantly different, likely due to the low number of animals used in the test. However, using a bootstrap method aiming at modeling the repartition of stress-resilient and -prone mice suggested that the consumption of a diet enriched in LC n-3 PUFA could promote CSDS resiliency. In addition, the electrophysiological properties of accumbal MSN were altered by diets, independently of CSDS. Overall, our results pinpoint that the consumption of a diet rich in LC n-3 PUFA influences the NAc fatty acid profile, which is likely to have an effect on neurotransmission and emotional behavior.

It is well-known that n-3 PUFA dietary content influences brain fatty acid levels [39]. We and others have previously reported that PUFA levels, in particular DHA and DPA n-6, are decreased and increased, respectively, by a low level of dietary n-3 PUFA in the form of a precursor (ALA) starting at weaning/adolescence, in the NAc and prefrontal cortex (PFC) of rodents [28,40]. Decreasing DHA and increasing DPA n-6 in PFC or NAc are even more pronounced when the low n-3 PUFA diet starts at developmental stages [29,41]. In this work, we describe for the first time that a two-month-long dietary intervention starting at weaning with diets either rich in SC (ALA) or rich in LC (EPA + DHA) n-3 PUFAs had a significant effect on NAc fatty acid profiles, with a decrease of several n-6 PUFA species and an increase of several n-3 PUFA species, namely DPA n-3 and DHA, leading to strong changes in the n-3/n-6 PUFA ratio in this structure. This suggests that a short-term dietary intervention has an impact on the NAc fatty acid signature, which corroborates previous results obtained in other brain structures, such as the hippocampus [40,42]. In addition, a molecular approach allowing to measure the expression of almost 90 genes involved in fatty acid metabolism, activity, and transport revealed a specific molecular signature in the NAc of LC n-3 PUFA-supplemented mice. Among the genes for which expression was increased by the dietary exposure to LC n-3 PUFA, some are directly linked to n-3 PUFA transport, metabolism, and activity. Indeed, elongation of very-long-chain fatty acid (ELOVL) enzymes are involved in both long and very LC fatty acid metabolism, including EPA and DHA [43], and have been reported to be expressed in neurons and glial cells [44,45]. FADS2 ( $\Delta 6$  fatty acid desaturase, the rate-limiting enzyme of the LC PUFA biosynthesis) mRNA expression is also increased in the NAc of LC n-3 PUFA mice. As FADS2 is expressed in astrocytes, and not neurons, it has been suggested that, in addition to the plasma DHA pool, these cells could supply neurons with DHA [46,47]. Interestingly, in humans, some FADS genetic variation has been associated to a lower DHA bioavailability and to MDD [48]. Furthermore, FADS1 expression was shown to be reduced in the brain of patients with depression [49]. In vitro, DHA triggers a decreased expression of FADS2

in neurons and astrocytes [50]. However, in the presence of retinoic acid acting through PPAR and RXR receptors, we found that their expression increased in the NAc of LC n-3 PUFA (EPA + DHA) mice as DHA activates FADS2 expression [47]. The solute carrier 27A (SLC27A) gene family encodes fatty acid transport proteins (FATPs), some of which were found here to be upregulated in the NAc of LC n-3 PUFA-supplemented mice. SLC27A3 has been reported to be highly expressed in several organs, including the neonatal and adult brain [51]. In addition, SLC25A20, also known as carnitine acyl-carnitine carrier (CAC), is a mitochondrial carrier involved in fatty acid  $\beta$ -oxidation [52] which was highly expressed in the NAc of mice fed with LC n-3 PUFA (EPA + DHA). Fish oil supplementation has been reported to decrease CAC expression in the liver [53], but tissue expression of CAC varies in different tissue, which has been reported as very low in the brain [54]. Altogether, the increased expressions of genes belonging to LC PUFAs biosynthesis, transport, and activity are in adequation to the effects of increased LC n-3 PUFA following dietary intake.

The mRNA expression of *Ptger4*, one of the receptors of prostaglandin E2, is increased in the NAc of LC n-3 PUFA-supplemented mice. This receptor is expressed in neurons and microglia and has been previously shown to be neuroprotective in the context of brain inflammation, neurodegeneration, and lesions [55–58]. A compensatory mechanism between decreased ARA (n-6 PUFA, precursor of prostaglandin E2 [19]) and increased expression of *Ptger4* could be suspected in our experiment. Interestingly, in a non-inflammatory context, the lack of EP4 signaling is associated with increased depression-like behavior [59], suggesting that this receptor could play a role in emotional behavior, as it has been described for other prostaglandin receptors (EP2, EP3) which also mediate the prostaglandin effect on synaptic plasticity in the spinal cord [60]. However, whether *Ptger4* is involved in the effect of LC n-3 PUFA (EPA + DHA) on emotional behavior remains to be determined.

CSDS is known to induce social and emotional behavior alteration that can segregate resilient *vs.* susceptible mice [37,38,61]. Using a segregation index based on social interaction, we did not observe any significant difference in the number of susceptible and resilient mice according to the diets, which can be attributed to the low number of animals used in the present study ( $n = 7$ – $10$ ) compared to previous studies, in which between 70 to 437 animals were used [37,38,62–64]. We therefore undertook a bootstrapping strategy [65] aiming at modeling the repartition of stress-resilient and -prone mice based on the results obtained in 7–10 animals/group used in this study in accordance with local and national ethical procedures, in particular the 3R rule. Interestingly, the bootstrapping strategy suggested that LC n-3 PUFA dietary consumption could promote CSDS resiliency, as illustrated by the spread of the confidence intervals following 100 bootstrap runs (see Figure 5). Using such a strategy, we observed that LC n-3 PUFA yielded a 95% CI of the social interaction ratio strictly above 1 (1.16–1.22), indicative of stress resiliency [37,38,61] in the majority of animals. Concerning emotional behaviors, as measured by OF, LD, and EPM, we found that CSDS significantly alters several parameters which are signs of anxiety (time in the central zone (OF) or in the light zone (LD)). This suggests that anxiety-like behaviors are altered by chronic stress, as previously reported in mice fed with a regular diet [33]. In contrast, the LC n-3 PUFA dietary intervention increases the time spent in the anxious zone, as measured in OF and LD tests, suggesting that the consumption of LC n-3 PUFA promotes non-anxious behavior independently of chronic stress. However, no interactions between stress and diet were revealed. Whether the changes in PUFA levels and/or lipid metabolism in the NAc are involved in the anxiolytic effect of the consumption of a diet rich in EPA + DHA remains to be determined.

Altered emotional phenotypes are paralleled to significant electrophysiological impairments in accumbal MSN, as observed in these neurons following resilience or susceptibility to stress [33,61], likely arising from neuronal morphology remodeling [16,66]. CSDS-induced electrophysiological alterations in the NAc have been observed before [33]. However, these results were acquired on animals fed with a standard laboratory diet (A04), a diet in which the ratio of LA to ALA was 15:1, which can explain the differences observed between the current study and the previous study. In contrast to LC n-3 PUFA supple-

mentation, our laboratory has also investigated the electrophysiological consequences of n-3 deficiency. Following dietary n-3 PUFA dietary deficiency, n-3 PUFA-deficient mice presented abnormal endocannabinoid-dependent plasticity in the NAc, which could be restored via pharmacological enhancement of mGluR<sub>5</sub> or by increasing the levels of the endocannabinoid 2-arachidonoylglycerol [28]. Our previous studies have also witnessed the presence of endocannabinoid-dependent plasticity in the brain of mice fed with diets balanced in n-3 PUFAs. This was observed in different brain regions, such as the prefrontal cortex [28,29] and the hippocampus [67], which are also both impaired following dietary n-3 PUFA deficiency. The present study also identified such a plasticity in the NAc of mice fed with a balanced diet. However, we observed a decreased neuronal response following LC n-3 PUFA dietary supplementation, together with altered intrinsic properties, suggesting that n-3 PUFA content in the brain finely tunes neuronal integration [27]. Most electrophysiological properties were affected by LC n-3 PUFA dietary supplementation, while only a few were affected by chronic stress. These observations are in line with the altered emotional behavior of animals following LC n-3 PUFA dietary intake, while stress did not produce such drastic effects on emotional behavior. In the present study, we have demonstrated that dietary intake of LC n-3 PUFAs can modulate emotional behaviors and synaptic plasticity in the NAc. Whether these effects are in a direct relationship remains to be elucidated.

In the present study, only male mice were used. Indeed, we used male CD1 Swiss retired breeders as aggressors, due to the aggressive behaviors displayed by these animals. To avoid mating, female C57Bl/6j mice were not used in our paradigm. While we acknowledge that CSDS can be performed in females, using different experimental protocols [68–71], this was outside of the scope of our study. Another potential limitation resides in the fact that we did not assess the relationship between accumbal long-term potentiation (LTP), CSDS, and n-3 PUFAs dietary supplementation. On the one hand, it was previously reported that DHA can modulate hippocampal LTD [72] and that maternal n-3 PUFAs dietary intake could promote LTP in the hippocampus of rat pups [73]. On the other hand, previous studies have demonstrated that CSDS can impair LTP in the hippocampus of mice [74] and rats [75–77]. To our knowledge, there are no studies that assessed accumbal LTP in the context of n-3 PUFAs dietary supplementation and CSDS, which will be interesting topics to address in future studies.

## 4. Material and Methods

### 4.1. Ethical Approval

All experiments were performed in accordance with local Ethics policies. The study was approved by the French Ministry of Education and Research (Ministère de l'Éducation Nationale, de l'Enseignement Supérieur et de la Recherche, agreement number 20181022153 03008-V5-APAFiS-17200) following initial validation by the Ethics Committee of the University of Bordeaux (CEEA50).

### 4.2. Animals

Animals were housed under standard housing conditions in a temperature- ( $23 \pm 1$  °C) and humidity (40%)-controlled animal room facility, with a 12 h light/dark cycle (07:00–19:00 h), in polysulfone cages ( $42.5 \times 26.6 \times 18.5$  cm) with *ad libitum* access to water and experimental diet. Fifty-four C57Bl/6j (three weeks old) and fourteen (retired breeder) Swiss CD1 mice were purchased from Janvier Labs (France). All mice were male. Retired breeder Swiss CD1 mice were used as aggressors in the CSDS paradigm and were thus housed individually, while C57Bl/6j mice were housed in pairs.

### 4.3. Diets

Composition of the SC n-3- (“control”) and LC n-3-supplemented (“n-3 suppl”) diets were described previously [16,17] and were manufactured at the INRAE unit at Jouy-en-Josas, France. Diets were started at weaning (P21, Figure 1A,B), as these previous



studies have shown that a two-month supplementation with a diet enriched in tuna oil increased DHA levels in the brain [16,17]. Dietary n-3 PUFA supplementation (n-3 suppl) consisted of an isocaloric diet containing 6% of tuna oil (rich in EPA (20:5 n-3) and DHA (22:6 n-3)), while the control diet (control) consisted in 6% of rapeseed oil (rich in ALA (18:3n-3)). Proportions of EPA and DHA in the n-3-supplemented diet were 10% and 7%, respectively [17]. These diets contained similar quantities of casein, starch, cellulose, sucrose, lipids, and minerals [16,17]. Diets were maintained throughout, from P21 until the end of the experiments (biochemistry or electrophysiology, Figure 1A,B, respectively).

#### 4.4. Chronic Social Defeat Stress (CSDS)

CSDS was performed as previously described [16,33]. Briefly, SC (control) and LC (n-3 suppl) mice were placed in contact with an aggressor (Swiss CD1 mouse) for 5 min, followed by 4 h of sensorial interactions (no physical contact), every day and for 10 consecutive days (Figure 1C).

#### 4.5. Behavioral Assessments

Following the last day of CSDS, mice were scored on four different anxiety-related tests, which were performed over 48 h, as detailed previously [16,29], and during the light phase. These included an OF test (10 min, 300 lux), a social interaction test (no-target/target, 5 min each, 30 lux), a LD box test (8 min, 300 lux), and an EPM test (5 min, 15 lux). Each apparatus was cleaned between experimental runs to avoid olfactory disturbances. Run orders were randomized. Video tracking was used for *a posteriori* analyses.

Anxiety scores were calculated as previously explained [33]. Mice were assigned individual anxiety scores, calculated as the algebraic sum of normalized scores for each of the 6 analyzed anxiety-related behavior tests: (i) time spent in the center (s) of the open field, (ii) time spent (s) and (iii) number of entries in the light compartments of the light/dark box, (iv) time spent (s) and (v) number of entries in the open arms of the elevated plus maze, and (vi) number of head dipping in the risk zone of the open arms in the elevated plus maze. When more than one parameter was used for a behavioral test, we weighted each component accordingly so that each behavioral test weighted 100%. This procedure yielded scores distributed along a 0–3 scale, with 3 reflecting high anxiety. For details about normalization, please refer to Section 4.10 below (data analysis).

#### 4.6. Gene Expression Analysis

Accumbal RNA from SC (control) and LC n-3-supplemented mice were extracted using TRIzol extraction kit (Invitrogen, Life Technologies, Saint-Quentin-Fallavier, France). Purity and concentration of RNA were determined using a Nanodrop 1000 spectrophotometer (Nanodrop technologies, Wilmington, DE, USA) and a bioanalyzer (Agilent, Les Ulis, France). Gene expression profiles were performed at the GeT-TRiX facility (GenoToul, Toulouse, France) using Agilent Sureprint G3 Mouse microarrays (8 × 60 K, design 074809), as described earlier [78]. For each sample, Cyanine-3 (Cy3)-labeled cRNA was prepared from 25 ng of total RNA using the One-Color Quick Amp Labeling kit (Agilent), followed by Agencourt RNAClean XP (Agencourt Bioscience Corporation, Beverly, MA, USA). Dye incorporation and cRNA yield were checked using the Dropsense 96 UV/VIS droplet reader (Trinean, Gent, Belgium). Then, 600 ng of Cy3-labeled cRNA was hybridized on the microarray slides. Immediately after washing, slides were scanned on an Agilent G2505C Microarray Scanner using Agilent Scan Control A.8.5.1 software, and the fluorescence signal was extracted using Agilent Feature Extraction software v10.10.1.1 with default parameters. Raw data (median signal intensity) were filtered, log<sub>2</sub>-transformed, corrected for batch effects (microarray washing bath and labeling serials), and normalized using the quantile method. All genes analyzed in the present study are listed in Supplemental Table S2, together with respective forward and reverse primer sequences in Supplemental Table S3.

#### 4.7. Endogenous Fatty Acid Determination by Gas Chromatography-Flame Ion Detection

Tissue fatty acid content was determined as previously described [79]. Briefly, total lipid extracts were obtained by following the method of Folch, Lees, and Stanley [80], consisting in lipid extraction in a mixture of chloroform:methanol:potassium chloride 0.88% (2:1:0.8 by volume). After vortexing and centrifugation at  $500\times g$  (10 min), the chloroform-containing layer was pipetted into a new tube. Helium-driven gas chromatography (Varian 430, Bruker, San Jose, CA, USA) was used to determine the samples' (1  $\mu\text{L}$ ) fatty acid tissue content by comparing retention times on a DB-23 (50% cyanopropyl)-methylpolysiloxane capillary column (J&W Scientific, Agilent Technologies, Mississauga, ON, Canada) with external standard samples (GLC-674, Nu Chek Prep Inc., Elysian, MN, USA). Detection was performed using a flame ionization detector (300 °C) with air (300 mL/min) and helium (29 mL/min), with sampling rates at 20 Hz.

#### 4.8. Ex Vivo Whole-Cell Patch-Clamp Electrophysiology

Animals were deeply anaesthetized using isoflurane inhalations, followed by quick decapitation. Striatal slices, containing the NAc, were cut using a VT1000S vibratome (Leica, Germany) at a thickness of 350  $\mu\text{m}$  in ice-cold artificial cerebrospinal fluid (ACSF) containing (in mM): 125 NaCl, 2.5 KCl, 1.25  $\text{NaH}_2\text{PO}_4$ , 2.0  $\text{CaCl}_2$ , 1.0  $\text{MgCl}_2$ , 25  $\text{NaHCO}_3$ , and 25 glucose (osmolarity  $308 \pm 3$  mOsm), bubbled continuously with carbogen (95%  $\text{O}_2$  and 5%  $\text{CO}_2$ ). Slices (4–6 per animal) were then transferred to a holding chamber, incubated at 32–34 °C for 60 min, and returned to room temperature. For the slicing procedure and the resting of the slices, 10  $\mu\text{M}$  of pyruvic acid was added to the extracellular solution. During recording, slices were continuously perfused at 1.5–2.0 mL/min with oxygenated ACSF. Whole-cell patch-clamp recordings were performed at room temperature (20–22 °C) with electrodes (1.5 mm outer diameter) fabricated from filamented thick-wall fire-polished borosilicate-glass (Sutter Instruments, Novato, CA, USA), pulled using a gravity puller (Narishige, Tokyo, Japan). Pipette resistance was typically between 4 and 7 M $\Omega$  when filled with a potassium gluconate-based intracellular solution, consisting of (in mM): K-gluconate 128, NaCl 20,  $\text{MgCl}_2$  1, EGTA 1,  $\text{CaCl}_2$  0.3,  $\text{Na}_2\text{-ATP}$  2, Na-GTP 0.3, cAMP 0.2, and HEPES 10, pH = 7.35, and osmolarity  $296 \pm 3.8$  mOsm. The junction potential was +15.4 mV. Pipette offset was zeroed before each recording.

MSN of the NAc were visualized under direct interference contrast with a BX51WI microscope (Olympus, Tokyo, Japan), mounted on an air table (TMC, Saratoga Springs, NY, USA) and under a Faraday cage, with an upright microscope, a 40 $\times$  water immersion objective combined with an infra-red filter, a monochrome CCD camera (Roper Scientific, Vianen, The Netherlands), and a PC-compatible system for analysis of images as well as contrast enhancement. Recording pipettes were slowly advanced towards individual striatal MSN within the slice under positive pressure and visual control. On contact, tight gigaohm ( $\text{G}\Omega$ ) seals were achieved by applying negative pressure. The membrane patch was then ruptured by suction and both membrane current and potential were monitored using Multiclamp700B and Digidata 1440A by Axon Instrument (Molecular Devices, San Jose, CA, USA). Whole-cell access resistances, measured in voltage clamp, were in the range of 8–20 M $\Omega$ . A concentric bipolar electrode (Phymep, Paris, France) was placed on afferent fibers to evoke EPSCs (at 0.1 Hz), recorded in MSN under voltage-clamp configuration with membrane potential clamped at  $-70$  mV. Current over voltage ( $I/V$ ) curves were acquired in  $I = 0$  (free) current-clamp mode. All data were sampled at 20 kHz and filtered at 1 kHz. Series resistance was measured throughout the experiment with a  $-5$  mV step lasting 50 ms. Synaptic events were stored by using p-CLAMP 10.6 (Axon Instruments, Burlingame, CA, USA) and *a posteriori* analyzed offline on a computer with Axograph software (Axon Instruments, Burlingame, CA, USA). Only data from putative GABAergic MSN were included in the present study, identified immediately after rupture of the  $\text{G}\Omega$  seal, by evaluating responses to the injection of both hyperpolarizing and depolarizing currents, as described previously [81].

LTD was elicited by stimulating afferent fibers at 10 Hz for 10 min, as described before [82–85].

#### 4.9. Resampling

Resampling (bootstrapping) was performed in R [86] with the *boot* package, available at CRAN (Comprehensive R Archive Network; <https://cran.r-project.org>, accessed on 1 May 2022). Resampling methods, applied to biology, have been explained recently [65]. The visual inference tool (VIT), a component of iNZight [87,88], was used to track the distribution of means from resampling replicates.

#### 4.10. Data Analyses

All statistical tests were performed with R [86]. Significance was set at  $\alpha = 0.05$ . All values are reported as mean  $\pm$  standard error of the mean (SEM). Data analysis was performed using one-sample *t*-tests, two- or three-way ANOVA, followed by *post hoc* tests if appropriate. Supplemental Table S1 presents all statistical analysis results performed in the present study. Normalization of behavioral parameters was achieved by using the following formula:  $x_n = \frac{x - \min}{\max - \min}$ , where  $x_n$  is the normalized variable value, *max* is the variable maximum value, and *min* is the variable minimum value. Gene expression was calculated relative to the housekeeping gene (*Gapdh*) and normalized to control levels. Correlation matrices and heatmaps were calculated and drawn in R with the following packages: *colourvalues*, *corrplot*, *ggcorrplot*, *ggplot2*, *gplots*, *heatmap.plus*, *heatmap3*, *Hmisc*, and *RColorBrewer*. These packages are all accessible in CRAN (see above, Section 4.9).

Enrichment ratio (ER) was calculated by the formula:  $ER = \frac{\left(\frac{m}{M}\right)}{\left(\frac{n}{N}\right)} = \frac{(m \times N)}{(M \times n)}$ , where *m* is the number of mapped genes in the pathway, *N* is the total number of genes within the *mus musculus* genome (~18,985), *M* is the total number of genes in the pathway, and *n* is the number of genes found significantly upregulated in our dataset (= 25). For gene ontology (GO), Webgestalt (<http://www.webgestalt.org/>, accessed on 1 May 2022) was used [35]. All figures were optimized for color blindness. Box and whiskers and violin plots were plotted from minimum to maximum values. Please refer to Supplemental Figure S4 for body weights and food consumption. Food consumption was estimated by averaging food intake over the duration of the experimental protocol, divided by the number of animals per cage.

**Supplementary Materials:** The following supporting information can be downloaded at: <https://www.mdpi.com/article/10.3390/ijms23126650/s1>.

**Author Contributions:** Conceptualization, M.D.M. and S.L.; methodology, M.D.M., C.B.-B., X.F., R.P.B. and S.L.; investigation, M.D.M., M.M., M.R., A.A. and S.A.; microarray design, S.L., C.J. and A.A.; microarray curation, M.D.M. and A.A.; data curation, M.D.M., S.A., R.P.B. and S.L.; formal analysis, M.D.M.; writing (original draft), M.D.M. and S.L.; writing (review and editing), all authors; visualization, M.D.M., R.P.B. and S.L.; supervision, S.L.; funding acquisition, S.L. and R.P.B. All authors have read and agreed to the published version of the manuscript.

**Funding:** S.L. was supported by Fondation pour la Recherche Médicale (FRM PRINSS DEQ 20170336724), Région Nouvelle Aquitaine (00070700, 2017-1R30237-00013179, 2019-1R3M08), Chaire d'excellence Région Nouvelle Aquitaine ExoMarquAge (13059720-13062120), RRI Food4BrainHealth, INRAE.

**Institutional Review Board Statement:** Ethics Committee of the University of Bordeaux (CEEA50). French Ministry of Education and Research (Ministère de l'Éducation Nationale, de l'Enseignement Supérieur et de la Recherche), agreement number 2018102215303008-V5-APAFiS-17200.

**Informed Consent Statement:** Not applicable.

**Data Availability Statement:** The data presented in this study are available upon request from the corresponding author.

**Acknowledgments:** The authors wish to thank Grégory Artaxet, Elona Lalaj, and Eva Bruchet for animal housing. We also thank the GenoToul platform for performing the microarray experiments. The authors also thank Olivier J.J. Manzoni for invaluable discussions.

**Conflicts of Interest:** The authors declare no conflict of interest.

## References

1. Krishnan, V.; Nestler, E.J. The Molecular Neurobiology of Depression. *Nature* **2008**, *455*, 894–902. [\[CrossRef\]](#)
2. McLachlan, G. Treatment Resistant Depression: What Are the Options? *BMJ* **2018**, *363*, k5354. [\[CrossRef\]](#)
3. Bazinet, R.P.; Layé, S. Polyunsaturated Fatty Acids and Their Metabolites in Brain Function and Disease. *Nat. Rev. Neurosci.* **2014**, *15*, 771–785. [\[CrossRef\]](#) [\[PubMed\]](#)
4. Liao, Y.; Xie, B.; Zhang, H.; He, Q.; Guo, L.; Subramaniepillai, M.; Fan, B.; Lu, C.; McIntyre, R.S. Efficacy of Omega-3 PUFAs in Depression: A Meta-Analysis. *Transl. Psychiatry* **2019**, *9*, 190. [\[CrossRef\]](#)
5. Bazinet, R.P.; Metherel, A.H.; Chen, C.T.; Shaikh, S.R.; Nadjar, A.; Joffre, C.; Layé, S. Brain Eicosapentaenoic Acid Metabolism as a Lead for Novel Therapeutics in Major Depression. *Brain Behav. Immun.* **2020**, *85*, 21–28. [\[CrossRef\]](#) [\[PubMed\]](#)
6. Larrieu, T.; Layé, S. Food for Mood: Relevance of Nutritional Omega-3 Fatty Acids for Depression and Anxiety. *Front. Physiol.* **2018**, *9*, 1047. [\[CrossRef\]](#) [\[PubMed\]](#)
7. Mocking, R.J.T.; Harmsen, I.; Assies, J.; Koeter, M.W.J.; Ruhé, H.G.; Schene, A.H. Meta-Analysis and Meta-Regression of Omega-3 Polyunsaturated Fatty Acid Supplementation for Major Depressive Disorder. *Transl. Psychiatry* **2016**, *6*, e756. [\[CrossRef\]](#) [\[PubMed\]](#)
8. Luo, X.-D.; Feng, J.-S.; Yang, Z.; Huang, Q.-T.; Lin, J.; Yang, B.; Su, K.-P.; Pan, J.-Y. High-Dose Omega-3 Polyunsaturated Fatty Acid Supplementation Might Be More Superior than Low-Dose for Major Depressive Disorder in Early Therapy Period: A Network Meta-Analysis. *BMC Psychiatry* **2020**, *20*, 248. [\[CrossRef\]](#) [\[PubMed\]](#)
9. McNamara, R.K.; Rider, T.; Jandacek, R.; Tso, P. Abnormal Fatty Acid Pattern in the Superior Temporal Gyrus Distinguishes Bipolar Disorder from Major Depression and Schizophrenia and Resembles Multiple Sclerosis. *Psychiatry Res.* **2014**, *215*, 560–567. [\[CrossRef\]](#)
10. McNamara, R.K.; Strimpfel, J.; Jandacek, R.; Rider, T.; Tso, P.; Welge, J.A.; Strawn, J.R.; Delbello, M.P. Detection and Treatment of Long-Chain Omega-3 Fatty Acid Deficiency in Adolescents with SSRI-Resistant Major Depressive Disorder. *PharmaNutrition* **2014**, *2*, 38–46. [\[CrossRef\]](#)
11. Martins, J.G. EPA but Not DHA Appears to Be Responsible for the Efficacy of Omega-3 Long Chain Polyunsaturated Fatty Acid Supplementation in Depression: Evidence from a Meta-Analysis of Randomized Controlled Trials. *J. Am. Coll. Nutr.* **2009**, *28*, 525–542. [\[CrossRef\]](#)
12. Deane, K.; Jimoh, O.; O'Brien, A.; Hanson, S.; Abdelhamid, A.S.; Fox, C.; Hooper, L. Omega-3 and Polyunsaturated Fat for Prevention of Depression and Anxiety Symptoms: Systematic review and meta-analysis of randomised trials. *Br. J. Psychiatry* **2021**, *218*, 135–142. [\[CrossRef\]](#)
13. Song, C.; Zhang, X.Y.; Manku, M. Increased Phospholipase A2 Activity and Inflammatory Response but Decreased Nerve Growth Factor Expression in the Olfactory Bulbectomized Rat Model of Depression: Effects of Chronic Ethyl-Eicosapentaenoate Treatment. *J. Neurosci. Off. J. Soc. Neurosci.* **2009**, *29*, 14–22. [\[CrossRef\]](#)
14. Peng, Z.; Zhang, C.; Yan, L.; Zhang, Y.; Yang, Z.; Wang, J.; Song, C. EPA Is More Effective than DHA to Improve Depression-Like Behavior, Glia Cell Dysfunction and Hippocampal Apoptosis Signaling in a Chronic Stress-Induced Rat Model of Depression. *Int. J. Mol. Sci.* **2020**, *21*, E1769. [\[CrossRef\]](#)
15. Pusceddu, M.M.; El Aidy, S.; Crispie, F.; O'Sullivan, O.; Cotter, P.; Stanton, C.; Kelly, P.; Cryan, J.F.; Dinan, T.G. N-3 Polyunsaturated Fatty Acids (PUFAs) Reverse the Impact of Early-Life Stress on the Gut Microbiota. *PLoS ONE* **2015**, *10*, e0139721. [\[CrossRef\]](#)
16. Larrieu, T.; Hilal, M.L.; Hilal, L.M.; Fourrier, C.; De Smedt-Peyrusse, V.; Sans, N.N.S.; Capuron, L.; Layé, S. Nutritional Omega-3 Modulates Neuronal Morphology in the Prefrontal Cortex along with Depression-Related Behaviour through Corticosterone Secretion. *Transl. Psychiatry* **2014**, *4*, e437. [\[CrossRef\]](#)
17. Labrousse, V.F.; Nadjar, A.; Joffre, C.; Costes, L.; Aubert, A.; Grégoire, S.; Bretillon, L.; Layé, S. Short-Term Long Chain Omega3 Diet Protects from Neuroinflammatory Processes and Memory Impairment in Aged Mice. *PLoS ONE* **2012**, *7*, e36861. [\[CrossRef\]](#)
18. Costa, A.; Rani, B.; Bastiaanssen, T.F.S.; Bonfiglio, F.; Gunnigle, E.; Provensi, G.; Rossitto, M.; Boehme, M.; Strain, C.; Martínez, C.S.; et al. Diet Prevents Social Stress-Induced Maladaptive Neurobehavioural and Gut Microbiota Changes in a Histamine-Dependent Manner. *Int. J. Mol. Sci.* **2022**, *23*, 862. [\[CrossRef\]](#)
19. Joffre, C.; Rey, C.; Layé, S. N-3 Polyunsaturated Fatty Acids and the Resolution of Neuroinflammation. *Front. Pharmacol.* **2019**, *10*, 1022. [\[CrossRef\]](#)
20. Joffre, C.; Dinel, A.-L.; Chataigner, M.; Pallet, V.; Layé, S. N-3 Polyunsaturated Fatty Acids and Their Derivates Reduce Neuroinflammation during Aging. *Nutrients* **2020**, *12*, E647. [\[CrossRef\]](#)
21. Rapaport, M.H.; Nierenberg, A.A.; Schettler, P.J.; Kinkead, B.; Cardoos, A.; Walker, R.; Mischoulon, D. Inflammation as a Predictive Biomarker for Response to Omega-3 Fatty Acids in Major Depressive Disorder: A Proof-of-Concept Study. *Mol. Psychiatry* **2016**, *21*, 71–79. [\[CrossRef\]](#) [\[PubMed\]](#)

22. Mocking, R.J.T.; Ruhé, H.G.; Assies, J.; Lok, A.; Koeter, M.W.J.; Visser, I.; Bockting, C.L.H.; Schene, A.H. Relationship between the Hypothalamic-Pituitary-Adrenal-Axis and Fatty Acid Metabolism in Recurrent Depression. *Psychoneuroendocrinology* **2013**, *38*, 1607–1617. [[CrossRef](#)] [[PubMed](#)]
23. Rey, C.; Delpech, J.C.; Madore, C.; Nadjar, A.; Greenhalgh, A.D.; Amadiou, C.; Aubert, A.; Pallet, V.; Vaysse, C.; Layé, S.; et al. Dietary N-3 Long Chain PUFA Supplementation Promotes a pro-Resolving Oxylipin Profile in the Brain. *Brain. Behav. Immun.* **2019**, *76*, 17–27. [[CrossRef](#)] [[PubMed](#)]
24. Song, C.; Manku, M.S.; Horrobin, D.F. Long-Chain Polyunsaturated Fatty Acids Modulate Interleukin-1beta-Induced Changes in Behavior, Monoaminergic Neurotransmitters, and Brain Inflammation in Rats. *J. Nutr.* **2008**, *138*, 954–963. [[CrossRef](#)]
25. Borsini, A.; Di Benedetto, M.G.; Giacobbe, J.; Pariante, C.M. Pro- and Anti-Inflammatory Properties of Interleukin (IL6) in Vitro: Relevance for Major Depression and for Human Hippocampal Neurogenesis. *Int. J. Neuropsychopharmacol.* **2020**, *23*, pyaa055. [[CrossRef](#)]
26. Bosch-Bouju, C.; Layé, S. *Dietary Omega-6/Omega-3 and Endocannabinoids: Implications for Brain Health and Diseases*; IntechOpen: London, UK, 2016; ISBN 978-953-51-2430-6.
27. Di Miceli, M.; Bosch-Bouju, C.; Layé, S. PUFA and Their Derivatives in Neurotransmission and Synapses: A New Hallmark of Synaptopathies. *Proc. Nutr. Soc.* **2020**, *79*, 388–403. [[CrossRef](#)]
28. Manduca, A.; Bara, A.; Larrieu, T.; Lassalle, O.; Joffre, C.; Layé, S.; Manzoni, O.J. Amplification of MGlu5-Endocannabinoid Signaling Rescues Behavioral and Synaptic Deficits in a Mouse Model of Adolescent and Adult Dietary Polyunsaturated Fatty Acid Imbalance. *J. Neurosci. Off. J. Soc. Neurosci.* **2017**, *37*, 6851–6868. [[CrossRef](#)]
29. Lafourcade, M.; Larrieu, T.; Mato, S.; Duffaud, A.; Sepers, M.; Matias, I.; De Smedt-Peyrusse, V.; Labrousse, V.F.; Bretillon, L.; Matute, C.; et al. Nutritional Omega-3 Deficiency Abolishes Endocannabinoid-Mediated Neuronal Functions. *Nat. Neurosci.* **2011**, *14*, 345–350. [[CrossRef](#)]
30. Larrieu, T.; Madore, C.; Joffre, C.; Layé, S. Nutritional N-3 Polyunsaturated Fatty Acids Deficiency Alters Cannabinoid Receptor Signaling Pathway in the Brain and Associated Anxiety-like Behavior in Mice. *J. Physiol. Biochem.* **2012**, *68*, 671–681. [[CrossRef](#)]
31. Russo, S.J.; Nestler, E.J. The Brain Reward Circuitry in Mood Disorders. *Nat. Rev. Neurosci.* **2013**, *14*, 609–625. [[CrossRef](#)]
32. Chaouloff, F. Social Stress Models in Depression Research: What Do They Tell Us? *Cell Tissue Res.* **2013**, *354*, 179–190. [[CrossRef](#)]
33. Bosch-Bouju, C.; Larrieu, T.; Linders, L.; Manzoni, O.J.; Layé, S. Endocannabinoid-Mediated Plasticity in Nucleus Accumbens Controls Vulnerability to Anxiety after Social Defeat Stress. *Cell Rep.* **2016**, *16*, 1237–1242. [[CrossRef](#)]
34. Ashburner, M.; Ball, C.A.; Blake, J.A.; Botstein, D.; Butler, H.; Cherry, J.M.; Davis, A.P.; Dolinski, K.; Dwight, S.S.; Eppig, J.T.; et al. Gene Ontology: Tool for the Unification of Biology. *Nat. Genet.* **2000**, *25*, 25–29. [[CrossRef](#)]
35. Zhang, B.; Kirov, S.; Snoddy, J. WebGestalt: An Integrated System for Exploring Gene Sets in Various Biological Contexts. *Nucleic Acids Res.* **2005**, *33*, W741–W748. [[CrossRef](#)]
36. Liao, Y.; Wang, J.; Jaehnig, E.J.; Shi, Z.; Zhang, B. WebGestalt 2019: Gene Set Analysis Toolkit with Revamped UIs and APIs. *Nucleic Acids Res.* **2019**, *47*, W199–W205. [[CrossRef](#)]
37. Golden, S.A.; Covington, H.E.; Berton, O.; Russo, S.J. A Standardized Protocol for Repeated Social Defeat Stress in Mice. *Nat. Protoc.* **2011**, *6*, 1183–1191. [[CrossRef](#)]
38. Krishnan, V.; Han, M.-H.; Graham, D.L.; Berton, O.; Renthal, W.; Russo, S.J.; Laplant, Q.; Graham, A.; Lutter, M.; Lagace, D.C.; et al. Molecular Adaptations Underlying Susceptibility and Resistance to Social Defeat in Brain Reward Regions. *Cell* **2007**, *131*, 391–404. [[CrossRef](#)]
39. Joffre, C.; Grégoire, S.; De Smedt, V.; Acar, N.; Bretillon, L.; Nadjar, A.; Layé, S. Modulation of Brain PUFA Content in Different Experimental Models of Mice. *Prostaglandins Leukot. Essent. Fatty Acids* **2016**, *114*, 1–10. [[CrossRef](#)]
40. Delpech, J.-C.; Thomazeau, A.; Madore, C.; Bosch-Bouju, C.; Larrieu, T.; Lacabanne, C.; Remus-Borel, J.; Aubert, A.; Joffre, C.; Nadjar, A.; et al. Dietary N-3 PUFAs Deficiency Increases Vulnerability to Inflammation-Induced Spatial Memory Impairment. *Neuropsychopharmacol. Off. Publ. Am. Coll. Neuropsychopharmacol.* **2015**, *40*, 2774–2787. [[CrossRef](#)]
41. Kodas, E.; Vancassel, S.; Lejeune, B.; Guilloteau, D.; Chalon, S. Reversibility of N-3 Fatty Acid Deficiency-Induced Changes in Dopaminergic Neurotransmission in Rats: Critical Role of Developmental Stage. *J. Lipid Res.* **2002**, *43*, 1209–1219. [[CrossRef](#)]
42. Alashmali, S.M.; Kitson, A.P.; Lin, L.; Lacombe, R.J.S.; Bazinet, R.P. Maternal Dietary N-6 Polyunsaturated Fatty Acid Deprivation Does Not Exacerbate Post-Weaning Reductions in Arachidonic Acid and Its Mediators in the Mouse Hippocampus. *Nutr. Neurosci.* **2019**, *22*, 223–234. [[CrossRef](#)]
43. Castro, L.F.C.; Tocher, D.R.; Monroig, O. Long-Chain Polyunsaturated Fatty Acid Biosynthesis in Chordates: Insights into the Evolution of Fads and Elovl Gene Repertoire. *Prog. Lipid Res.* **2016**, *62*, 25–40. [[CrossRef](#)]
44. Balbo, I.; Montarolo, F.; Boda, E.; Tempia, F.; Hoxha, E. Elovl5 Expression in the Central Nervous System of the Adult Mouse. *Front. Neuroanat.* **2021**, *15*, 669073. [[CrossRef](#)]
45. Guttenplan, K.A.; Weigel, M.K.; Prakash, P.; Wijewardhane, P.R.; Hasel, P.; Rufen-Blanchette, U.; Münch, A.E.; Blum, J.A.; Fine, J.; Neal, M.C.; et al. Neurotoxic Reactive Astrocytes Induce Cell Death via Saturated Lipids. *Nature* **2021**, *599*, 102–107. [[CrossRef](#)]
46. Tabernero, A.; Lavado, E.M.; Granda, B.; Velasco, A.; Medina, J.M. Neuronal Differentiation Is Triggered by Oleic Acid Synthesized and Released by Astrocytes. *J. Neurochem.* **2001**, *79*, 606–616. [[CrossRef](#)] [[PubMed](#)]
47. Dziedzic, B.; Bewicz-Binkowska, D.; Zgorzynska, E.; Stulczewski, D.; Wieteska, L.; Kaza, B.; Walczewska, A. DHA Upregulates FADS2 Expression in Primary Cortical Astrocytes Exposed to Vitamin A. *Physiol. Res.* **2018**, *67*, 663–668. [[CrossRef](#)] [[PubMed](#)]

48. Cribb, L.; Murphy, J.; Froud, A.; Oliver, G.; Bousman, C.A.; Ng, C.H.; Sarris, J. Erythrocyte Polyunsaturated Fatty Acid Composition Is Associated with Depression and FADS Genotype in Caucasians. *Nutr. Neurosci.* **2018**, *21*, 589–601. [[CrossRef](#)] [[PubMed](#)]
49. McNamara, R.K.; Liu, Y. Reduced Expression of Fatty Acid Biosynthesis Genes in the Prefrontal Cortex of Patients with Major Depressive Disorder. *J. Affect. Disord.* **2011**, *129*, 359–363. [[CrossRef](#)]
50. Bewicz-Binkowska, D.; Zgorzynska, E.; Dziedzic, B.; Walczewska, A. Docosahexaenoic Acid (DHA) Inhibits FADS2 Expression in Astrocytes but Increases Survival of Neurons Co-Cultured with DHA-Enriched Astrocytes. *Int. J. Mol. Cell. Med.* **2019**, *8*, 232–240. [[CrossRef](#)]
51. Maekawa, M.; Iwayama, Y.; Ohnishi, T.; Toyoshima, M.; Shimamoto, C.; Hisano, Y.; Toyota, T.; Balan, S.; Matsuzaki, H.; Iwata, Y.; et al. Investigation of the Fatty Acid Transporter-Encoding Genes SLC27A3 and SLC27A4 in Autism. *Sci. Rep.* **2015**, *5*, 16239. [[CrossRef](#)]
52. Iacobazzi, V.; Invernizzi, F.; Baratta, S.; Pons, R.; Chung, W.; Garavaglia, B.; Dionisi-Vici, C.; Ribes, A.; Parini, R.; Huertas, M.D.; et al. Molecular and Functional Analysis of SLC25A20 Mutations Causing Carnitine-Acylcarnitine Translocase Deficiency. *Hum. Mutat.* **2004**, *24*, 312–320. [[CrossRef](#)]
53. Giudetti, A.M.; Stanca, E.; Siculella, L.; Gnoni, G.V.; Damiano, F. Nutritional and Hormonal Regulation of Citrate and Carnitine/Acylcarnitine Transporters: Two Mitochondrial Carriers Involved in Fatty Acid Metabolism. *Int. J. Mol. Sci.* **2016**, *17*, E817. [[CrossRef](#)]
54. Huizing, M.; Iacobazzi, V.; Ijlst, L.; Savelkoul, P.; Ruitenbeek, W.; van den Heuvel, L.; Indiveri, C.; Smeitink, J.; Trijbels, F.; Wanders, R.; et al. Cloning of the Human Carnitine-Acylcarnitine Carrier cDNA and Identification of the Molecular Defect in a Patient. *Am. J. Hum. Genet.* **1997**, *61*, 1239–1245. [[CrossRef](#)]
55. Woodling, N.S.; Wang, Q.; Priyam, P.G.; Larkin, P.; Shi, J.; Johansson, J.U.; Zagol-Ikapitte, I.; Boutaud, O.; Andreasson, K.I. Suppression of Alzheimer-Associated Inflammation by Microglial Prostaglandin-E2 EP4 Receptor Signaling. *J. Neurosci. Off. J. Soc. Neurosci.* **2014**, *34*, 5882–5894. [[CrossRef](#)]
56. DeMars, K.M.; McCrea, A.O.; Siwarski, D.M.; Sanz, B.D.; Yang, C.; Candelario-Jalil, E. Protective Effects of L-902,688, a Prostanoid EP4 Receptor Agonist, against Acute Blood-Brain Barrier Damage in Experimental Ischemic Stroke. *Front. Neurosci.* **2018**, *12*, 89. [[CrossRef](#)]
57. Zhang, J.; Rivest, S. A Functional Analysis of EP4 Receptor-Expressing Neurons in Mediating the Action of Prostaglandin E2 within Specific Nuclei of the Brain in Response to Circulating Interleukin-1beta. *J. Neurochem.* **2000**, *74*, 2134–2145. [[CrossRef](#)]
58. Ahmad, A.S.; Ahmad, M.; de Brum-Fernandes, A.J.; Doré, S. Prostaglandin EP4 Receptor Agonist Protects against Acute Neurotoxicity. *Brain Res.* **2005**, *1066*, 71–77. [[CrossRef](#)]
59. Fujikawa, R.; Higuchi, S.; Ikedo, T.; Nagata, M.; Hayashi, K.; Yang, T.; Miyata, T.; Yokode, M.; Minami, M. Behavioral Abnormalities and Reduced Norepinephrine in EP4 Receptor-Associated Protein (EPRAP)-Deficient Mice. *Biochem. Biophys. Res. Commun.* **2017**, *486*, 584–588. [[CrossRef](#)]
60. Li, J.; Serafin, E.; Bacceti, M.L. Prostaglandin Signaling Governs Spike Timing-Dependent Plasticity at Sensory Synapses onto Mouse Spinal Projection Neurons. *J. Neurosci. Off. J. Soc. Neurosci.* **2018**, *38*, 6628–6639. [[CrossRef](#)]
61. Francis, T.C.; Chandra, R.; Friend, D.M.; Finkel, E.; Dayrit, G.; Miranda, J.; Brooks, J.M.; Iñiguez, S.D.; O'Donnell, P.; Kravitz, A.; et al. Nucleus Accumbens Medium Spiny Neuron Subtypes Mediate Depression-Related Outcomes to Social Defeat Stress. *Biol. Psychiatry* **2015**, *77*, 212–222. [[CrossRef](#)]
62. Grossman, Y.S.; Fillinger, C.; Manganaro, A.; Voren, G.; Waldman, R.; Zou, T.; Janssen, W.G.; Kenny, P.J.; Dumitriu, D. Structure and Function Differences in the Prelimbic Cortex to Basolateral Amygdala Circuit Mediate Trait Vulnerability in a Novel Model of Acute Social Defeat Stress in Male Mice. *Neuropsychopharmacology* **2022**, *47*, 788–799. [[CrossRef](#)]
63. Li, M.-X.; Zheng, H.-L.; Luo, Y.; He, J.-G.; Wang, W.; Han, J.; Zhang, L.; Wang, X.; Ni, L.; Zhou, H.-Y.; et al. Gene Deficiency and Pharmacological Inhibition of Caspase-1 Confers Resilience to Chronic Social Defeat Stress via Regulating the Stability of Surface AMPARs. *Mol. Psychiatry* **2018**, *23*, 556–568. [[CrossRef](#)]
64. Murra, D.; Hilde, K.L.; Fitzpatrick, A.; Maras, P.M.; Watson, S.J.; Akil, H. Characterizing the Behavioral and Neuroendocrine Features of Susceptibility and Resilience to Social Stress. *Neurobiol. Stress* **2022**, *17*, 100437. [[CrossRef](#)]
65. Fieberg, J.R.; Vitense, K.; Johnson, D.H. Resampling-Based Methods for Biologists. *PeerJ* **2020**, *8*, e9089. [[CrossRef](#)]
66. Fox, M.E.; Chandra, R.; Menken, M.S.; Larkin, E.J.; Nam, H.; Engeln, M.; Francis, T.C.; Lobo, M.K. Dendritic Remodeling of D1 Neurons by RhoA/Rho-Kinase Mediates Depression-like Behavior. *Mol. Psychiatry* **2020**, *25*, 1022–1034. [[CrossRef](#)]
67. Thomazeau, A.; Bosch-Bouju, C.; Manzoni, O.; Layé, S. Nutritional N-3 PUFA Deficiency Abolishes Endocannabinoid Gating of Hippocampal Long-Term Potentiation. *Cereb. Cortex* **2017**, *27*, 2571–2579. [[CrossRef](#)]
68. Iñiguez, S.D.; Flores-Ramirez, F.J.; Riggs, L.M.; Alipio, J.B.; Garcia-Carachure, I.; Hernandez, M.A.; Sanchez, D.O.; Lobo, M.K.; Serrano, P.A.; Braren, S.H.; et al. Vicarious Social Defeat Stress Induces Depression-Related Outcomes in Female Mice. *Biol. Psychiatry* **2018**, *83*, 9–17. [[CrossRef](#)]
69. Takahashi, A.; Chung, J.-R.; Zhang, S.; Zhang, H.; Grossman, Y.; Aleyasin, H.; Flanigan, M.E.; Pfau, M.L.; Menard, C.; Dumitriu, D.; et al. Establishment of a Repeated Social Defeat Stress Model in Female Mice. *Sci. Rep.* **2017**, *7*, 12838. [[CrossRef](#)]
70. Furman, O.; Tsoory, M.; Chen, A. Differential Chronic Social Stress Models in Male and Female Mice. *Eur. J. Neurosci.* **2022**, *55*, 2777–2793. [[CrossRef](#)]

71. Harris, A.Z.; Atsak, P.; Bretton, Z.H.; Holt, E.S.; Alam, R.; Morton, M.P.; Abbas, A.I.; Leonardo, E.D.; Bolkan, S.S.; Hen, R.; et al. A Novel Method for Chronic Social Defeat Stress in Female Mice. *Neuropsychopharmacol. Off. Publ. Am. Coll. Neuropsychopharmacol.* **2018**, *43*, 1276–1283. [[CrossRef](#)]
72. Fujita, S.; Ikegaya, Y.; Nishikawa, M.; Nishiyama, N.; Matsuki, N. Docosahexaenoic Acid Improves Long-Term Potentiation Attenuated by Phospholipase A(2) Inhibitor in Rat Hippocampal Slices. *Br. J. Pharmacol.* **2001**, *132*, 1417–1422. [[CrossRef](#)] [[PubMed](#)]
73. Kavraal, S.; Oncu, S.K.; Bitiktas, S.; Artis, A.S.; Dolu, N.; Gunes, T.; Suer, C. Maternal Intake of Omega-3 Essential Fatty Acids Improves Long Term Potentiation in the Dentate Gyrus and Morris Water Maze Performance in Rats. *Brain Res.* **2012**, *1482*, 32–39. [[CrossRef](#)] [[PubMed](#)]
74. Yang, Y.; Ju, W.; Zhang, H.; Sun, L. Effect of Ketamine on LTP and NMDAR EPSC in Hippocampus of the Chronic Social Defeat Stress Mice Model of Depression. *Front. Behav. Neurosci.* **2018**, *12*, 229. [[CrossRef](#)] [[PubMed](#)]
75. Kamal, A.; Van der Harst, J.E.; Kapteijn, C.M.; Baars, A.J.M.; Spruijt, B.M.; Ramakers, G.M.J. Announced Reward Counteracts the Effects of Chronic Social Stress on Anticipatory Behavior and Hippocampal Synaptic Plasticity in Rats. *Exp. Brain Res.* **2010**, *201*, 641–651. [[CrossRef](#)]
76. Artola, A.; von Frijtag, J.C.; Fermont, P.C.J.; Gispen, W.H.; Schrama, L.H.; Kamal, A.; Spruijt, B.M. Long-Lasting Modulation of the Induction of LTD and LTP in Rat Hippocampal CA1 by Behavioural Stress and Environmental Enrichment. *Eur. J. Neurosci.* **2006**, *23*, 261–272. [[CrossRef](#)]
77. Manz, K.M.; Levine, W.A.; Seckler, J.C.; Iskander, A.N.; Reich, C.G. A Novel Adolescent Chronic Social Defeat Model: Reverse-Resident-Intruder Paradigm (RRIP) in Male Rats. *Stress Amst. Neth.* **2018**, *21*, 169–178. [[CrossRef](#)]
78. Rincel, M.; Aubert, P.; Chevalier, J.; Grohard, P.-A.; Basso, L.; Monchaux de Oliveira, C.; Helbling, J.C.; Lévy, É.; Chevalier, G.; Leboyer, M.; et al. Multi-Hit Early Life Adversity Affects Gut Microbiota, Brain and Behavior in a Sex-Dependent Manner. *Brain. Behav. Immun.* **2019**, *80*, 179–192. [[CrossRef](#)]
79. Metherel, A.H.; Domenichiello, A.F.; Kitson, A.P.; Hopperton, K.E.; Bazinet, R.P. Whole-Body DHA Synthesis-Secretion Kinetics from Plasma Eicosapentaenoic Acid and Alpha-Linolenic Acid in the Free-Living Rat. *Biochim. Biophys. Acta* **2016**, *1861*, 997–1004. [[CrossRef](#)]
80. Folch, J.; Lees, M.; Sloane Stanley, G.H. A Simple Method for the Isolation and Purification of Total Lipides from Animal Tissues. *J. Biol. Chem.* **1957**, *226*, 497–509. [[CrossRef](#)]
81. Fino, E.; Glowinski, J.; Venance, L. Effects of Acute Dopamine Depletion on the Electrophysiological Properties of Striatal Neurons. *Neurosci. Res.* **2007**, *58*, 305–316. [[CrossRef](#)]
82. Bilbao, A.; Neuhofer, D.; Sepers, M.; Wei, S.; Eisenhardt, M.; Hertle, S.; Lassalle, O.; Ramos-Uriarte, A.; Puente, N.; Lerner, R.; et al. Endocannabinoid LTD in Accumbal D1 Neurons Mediates Reward-Seeking Behavior. *iScience* **2020**, *23*, 100951. [[CrossRef](#)]
83. Scheyer, A.F.; Borsoi, M.; Pelissier-Alicot, A.-L.; Manzoni, O.J.J. Maternal Exposure to the Cannabinoid Agonist WIN 55,12,2 during Lactation Induces Lasting Behavioral and Synaptic Alterations in the Rat Adult Offspring of Both Sexes. *eNeuro* **2020**, *7*. [[CrossRef](#)]
84. Scheyer, A.F.; Borsoi, M.; Pelissier-Alicot, A.-L.; Manzoni, O.J.J. Perinatal THC Exposure via Lactation Induces Lasting Alterations to Social Behavior and Prefrontal Cortex Function in Rats at Adulthood. *Neuropsychopharmacology* **2020**, *45*, 1826–1833. [[CrossRef](#)]
85. Deroche, M.A.; Lassalle, O.; Castell, L.; Valjent, E.; Manzoni, O.J. Cell-Type- and Endocannabinoid-Specific Synapse Connectivity in the Adult Nucleus Accumbens Core. *J. Neurosci. Off. J. Soc. Neurosci.* **2020**, *40*, 1028–1041. [[CrossRef](#)]
86. R Foundation for Statistical Computing. *R Core Team R: A Language and Environment for Statistical Computing*; R Foundation for Statistical Computing: Vienna, Austria, 2013.
87. Elliott, T.; Soh, Y.H.; Barnett, D.; Anastasiadis, S. INZightPlots: Graphical Tools for Exploring Data with “INZight”. Comprehensive R Archive Network. Available online: <https://cran.r-project.org/> (accessed on 1 May 2022).
88. Wild, C.J.; Elliott, T.; Sporle, A. On Democratizing Data Science: Some INZights Into Empowering the Many. *Harv. Data Sci. Rev.* **2021**, *3*. [[CrossRef](#)]





## *DISCUSSION*

---

## 1. Synthèse des résultats obtenus

L'objectif principal de ces travaux de thèse était d'étudier comment une modification globale, par intervention par l'alimentation, ou locale, par la manipulation génétique de l'expression d'*elov2* dans le NAc, des taux d'AGPI n-3 et n-6 influencent leur métabolisme cérébral, la cognition et les comportements émotionnels et la plasticité synaptique, en tenant compte du sexe. Pour cela nous avons étudié 1) l'impact d'une diète équilibrée en AGPI n-3, sous forme d'ALA et administrée à partir du sevrage, sur les effets mnésiques et synaptiques d'une carence alimentaire maternelle en AGPI n-3 chez la descendance mâle et femelle, 2) l'impact de la manipulation génétique du gène *elov2* dans les astrocytes au niveau du NAc sur les comportements émotionnels, les taux AGPI du NAc et les propriétés électriques des MSNs de souris adultes mâles et femelles et 3) les effets neuroprotecteurs d'une diète enrichie en EPA+DHA sur les altérations comportementales et synaptiques provoquées par un stress chronique (CSDS).

Les résultats obtenus à l'issue de la complétion de **l'objectif 1** ont révélé que les souris mâles et femelles exposées depuis la vie intra-utérine à une diète carencée en AGPI n-3 développent des altérations de mémoire spatiale et de LTP hippocampique à l'âge adulte. Ces altérations neurobiologiques s'accompagnent d'altérations des taux d'AGPI n-3, notamment d'une diminution drastique de DHA, d'EPA et une augmentation d'AA dans l'hippocampe. Cependant, les profils d'oxylipines qui dérivent de ces AGPI différent entre les mâles et les femelles, et présentent des signatures distinctes sous l'effet des diètes étudiées. Le groupe de souris mâle et femelle carencées en AGPI n-3 et exposées à une diète équilibrée à partir du sevrage voient leur plasticité synaptique restaurée, alors que les profils d'AGPI, d'oxylipines et la mémoire sont différenciellement restaurés en fonction du sexe. Ainsi, si les taux de DHA, EPA et AA de l'hippocampe des souris femelles carencées-équilibrées et la mémoire sont similaires à ceux des souris nourries avec une diète équilibrée toute leur vie, l'AA reste élevé dans l'hippocampe et la mémoire altérée chez les mâles, comme chez les souris carencées (**Publication 1**, Martinat et al., pour soumission). Une revue sur l'importance des AGPI alimentaires périnataux sur le développement cérébral découle de ce thème de recherche (**Publication 2**, Martinat et al., 2021).

Les résultats obtenus à l'issue de la complétion de **l'objectif 2** indiquent que l'administration de l'AAV-5/2-GFAP-re/mCherry dans le NAc de souris ELOVL2<sup>lox/lox</sup> mâles et femelles atténue l'expression d'*elov2* de 50% à ce niveau, mais pas dans l'hippocampe, utilisé comme structure contrôle. De plus, cette inhibition d'expression touche principalement les astrocytes, qui sont ciblés par le virus. La diminution d'expression d'ELOVL2 n'est pas associée à des modifications des profils des AGPI dans le

NAc ou le cortex préfrontal, utilisé comme structure contrôle. En ce qui concerne les comportements émotionnels, des altérations significatives de temps passé dans les bras ouverts de l'EPM (mâles) ou de « head-dipping » (femelles) sont mesurées, mais pas de différences dans les autres paramètres mesurés. Enfin, de profondes modifications des propriétés intrinsèques des neurones épineux moyens du NAc, à proximité d'astrocytes *elov12* KO sont mesurées (**Publication 3**, Martinat et al., en préparation)

Les résultats obtenus à partir de l'objectif 3 montrent que les souris mâles nourries avec une diète équilibrée en ALA ou enrichie en EPA+DHA n'ont pas les mêmes profils en AGPI dans le NAc. Ces différences de composition sont associées à des différences de profils d'expression d'enzymes, récepteurs et transport des AG dans le NAc qui tracent une signature propre à la diète consommée. Les souris soumises à un stress chronique de défaite sociale (CSDS) développent des altérations de comportement social et émotionnel et de plasticité synaptique (LTD) dans le NAc qui sont moins intenses chez les souris ayant consommé une diète riche en EPA+DHA (**Publication 4**, Di Miceli M, Martinat M, et al., 2022).

## **2. Modèles animaux utilisés**

### *2.1. Modèle nutritionnel (modification globale dans le cerveau)*

D'un point de vue nutritionnel, la consommation en AGPI n-3 est inférieure aux recommandations alimentaires chez l'homme (Simopoulos, 2011). La diminution de consommation d'AGPI n-3, sous forme de précurseur ALA ou préformé DHA et EPA, se fait au profit de celle des AGPI n-6. Ceci se traduit par un ratio consommé en AGPI n-6/n-3 autour de 10 en France et supérieur à 15 aux Etats-Unis (Simopoulos, 2011; Tressou et al., 2016), alors que celui recommandé par l'ANSES est de 4. Une étude récente décrit les apports individuels en AG et leurs principales sources alimentaires au Royaume-Uni. Elle met en avant les différences d'apports en AGPI entre le Royaume-Uni et les Etats-Unis (Kelly et al., 2022). Les apports en LA des participants anglais (9,7 g/j) sont largement inférieurs à ceux des participants américains (17,4 g/j). Les apports en ALA dans cette étude (1,58 g/j) sont également inférieurs à ceux rapportés pour les adultes américains (1,82 g/j). Les graisses et huiles typiques ajoutées aux aliments pendant la cuisson et la transformation diffèrent selon les pays, ce qui peut expliquer en partie les différences d'apports en AG observées : l'huile de soja (54 g de LA pour 100 g ; 7,8 g d'ALA pour 100 g) représente ~50 % de l'huile consommée aux États-Unis. L'huile de palme (10,4 g ; 0,2 g), l'huile de colza (20 g ; 9,8 g) et l'huile de tournesol (67 g ; 0 g) représentent ensemble environ 76 % de l'huile consommée par la population générale du Royaume-Uni (Tennant and Gosling, 2015). De plus, les apports en DHA (0,18 g/j) dans la présente étude étaient plus élevés

que ceux estimés pour les américains à l'âge adulte (0,06 g/j), tandis que les apports en EPA seraient identiques (0,03 g/j). La consommation de produits de la mer, en particulier de poissons gras (Nettleton, 1995), peut expliquer une partie des différences observées entre les pays dans les apports en EPA et DHA: thon (0,01 g EPA pour 100 g ; 0,08 g DHA pour 100 g), morue (0,03 g ; 0,10 g) et le saumon (0,93 g ; 1,78 g) sont les plus consommés au Royaume-Uni. Toutes ces données sont issues des différents rapports des départements de l'agriculture des Etats-Unis et du Royaume-Unis

Ce déséquilibre est associé à un risque accru de développer des maladies cardio-vasculaires, de l'obésité ou encore de maladies neuropsychiatriques et neurologiques (Simopoulos, 2011). Afin de mieux comprendre les mécanismes neurobiologiques impliqués dans les effets de la carence alimentaire en AGPI n-3, des modèles nutritionnels chez les rongeurs ont été développés. En l'occurrence, le modèle développé au laboratoire provoque une diminution de DHA cérébral de 30 à 80 % selon les études (Delpech et al., 2015; Janssen et al., 2015; Joffre et al., 2016; Labrousse et al., 2018; Moranis et al., 2012; Moriguchi et al., 2000)

**Tableau 4** : Références utilisant différents régimes et impact sur la composition cérébrale en DHA

	Régime utilisé et composition en précurseurs (% AG totaux)	Structure	Niveaux de DHA (En % d'AG totaux)
<b>(Kodas et al., 2002)</b>	Régime équilibré (eq) (LA : 21,2% ; ALA : 3,6%) Régime déficient (def) (LA : 21,3% ; ALA : <0,1%)	Cortex préfrontal de rat	4,5 vs 1,2 (eq vs def)
<b>(Aïd et al., 2003)</b>	Régime équilibré (LA : 10,7% ; ALA : 1,6% d'AG totaux) Régime déficient (LA : 60,5% ; ALA : 0,1%)	Cortex Hippocampe	5,4 AG VS 1,3 (eq vs def) 4,0 VS 1,5 (eq vs def)
<b>(Mingam et al., 2008)</b>	Régime équilibré (LA : 10,7% ; ALA : 1,6% d'AG totaux) Régime déficient (LA : 60,5% ; ALA : 0,1%)	Cortex	3,7 vs 1,3 (eq vs def)
<b>(Lafourcade et al., 2011)</b>	Régime équilibré (LA : 10,7% ; ALA : 1,6% d'AG totaux) Régime déficient (LA : 60,5% ; ALA : 0,1%)	Cerveau entier PFC	12,15 vs 8,3 (eq vs def) 14,3 vs 8,12 (eq vs def)
<b>(Moranis et al., 2012)</b>	Régime équilibré (LA : 10,7% ; ALA : 1,6% d'AG totaux) Régime déficient (LA : 60,5% ; ALA : 0,1%)	Cortex	3,4 vs 1,4 (eq vs def)
<b>(Labrousse et al., 2012)</b>	Régime équilibré (LA : 10,7% ; ALA : 1,6%) Régime supplémenté (LA : 15,2% ; ALA : 0,9% ; DHA : 7,2%)	Cerveau adulte Cerveau âgé	9,2 vs 15,9 (eq vs supp) 8,7 vs 13,7 (eq vs supp)
<b>(Larrieu et al., 2012)</b>	Régime équilibré (LA : 10,7% ;	Cortex	16,39 vs 9,11 (eq vs def)

	ALA : 1,6% d'AG totaux) Régime déficient (LA : 60,5% ; ALA : 0,1%)		
<b>(Madore et al., 2014)</b>	Régime équilibré (LA : 10,7% ; ALA : 1,6% d'AG totaux) Régime déficient (LA : 57,4% ; ALA : 0,2%)	Cortex à P0 Cortex à P21	9,7 vs 5,1 (eq vs def) 14,1 vs 6 (eq vs def)
<b>(Delpech et al., 2015)</b>	Régime équilibré (LA : 10,7% ; ALA : 1,6% d'AG totaux) Régime déficient (LA : 57,4% ; ALA : 0,2%)	Hippocampe	15,20 vs 12,57 (eq vs def)
<b>(Joffre et al., 2016)</b>	Régime standard (std) (LA : 45,9% ; ALA : 3,3%) Régime équilibré (LA : 10,6% ; ALA : 1,6%) Régime déficient (LA : 60,5% ; ALA : 0,1%) Régime supplémenté (LA : 15,1% ; ALA : 1,1% ; DHA : 5,8%)	Cortex PFC Cervelet Hypothalamus Hippocampe	11,9 (std), 16,3 (eq), 7,4 (def) 14,3(std) 12,2 (std) 10,1 (std) 13,7 (std)
<b>(Rey et al., 2018)</b>	Régime équilibré (LA : 12,9% ; ALA : 1,6%) Régime déficient (LA : 45,3% ; ALA : 0,1%) Régime supplémenté (LA : 12,9% ; ALA : 1,1% ; DHA : 5,6%)	Cellules microgliales du cerveau	0,8 vs 0,6 vs 2,1 (eq vs def vs supp)
<b>(Labrousse et al., 2018)</b>	Régime équilibré (LA : 10,7% ; ALA : 1,6% d'AG totaux) Régime déficient (LA : 57,4% ; ALA : 0,2%)	Cerveau fœtal Placenta	6,7 vs 4,2 (eq vs def) 8,3 vs 4,61 (eq vs def)
<b>(Rey et al., 2019)</b>	Régime déficient (LA : 10,6% ; ALA : 1,6%) Régime supplémenté (LA : 12,9% ; ALA : 1,1% ; DHA : 5,6%)	Tronc cérébral Hippocampe	12,15 vs 8,13 (eq vs def) 15,20 vs 17,36 (def vs supp)

### 2.1.1 Choix du modèle de carence maternelle en AGPI n-3

Dans le cas de notre étude, nous avons choisi d'exposer les animaux à une diète carencée en AGPI n-3 dès les stades les plus précoces du développement cérébral et de façon unigénérationnelle. Les mères sont donc nourries à partir de l'accouplement soit avec un régime carencé, soit un régime équilibré en AGPI n-3 (**Tableau 4**). Il s'agit de régimes isocaloriques contenant 5 % de lipides apportés par un mélange d'huiles qui apportent les précurseurs n-6 et n-3 des AGPI-LC, à savoir le LA et l'ALA. Le régime équilibré contient majoritairement de l'huile de colza riche en ALA avec un ratio AGPI n-6/n-3 est de 6.7, proche des recommandations faites chez l'homme. Le régime carencé, obtenu à partir d'huile de tournesol riche en LA, est quant à lui plus éloigné de ce que l'on peut retrouver chez

l'homme : son ratio est proche de 300 ce qui permet de diminuer le taux cérébral de DHA chez la descendance (Joffre et al., 2016; Labrousse et al., 2018, **Tableau 5**). Des données récentes obtenues chez l'homme ont permis de déterminer les taux de d'AGPI dans le cerveau. Cependant selon les régions cérébrales ces taux peuvent varier. Par exemple, dans les travaux de Rapoport et al, les estimations des concentrations de DHA dans l'ensemble du cerveau sont basées sur les compositions régionales en acides gras - en particulier la matière grise phospholipidique dans ce cas - et utilisées pour la modélisation du métabolisme des acides gras du cerveau (Rapoport et al., 2007). Dans ces travaux, l'estimation des niveaux de DHA dans le cerveau humain entier est de 5,13g pour 1500g de cerveau, tandis que dans les travaux de Lacombe et al, la concentration de DHA observée est de 3,47g pour 1171g de cerveau humain post mortem (Lacombe et al., 2022). Il est important de noter que, chez l'homme, l'altération du métabolisme des acides gras du cerveau a été impliquée dans un certain nombre de maladies neurodégénératives, notamment les maladies d'Alzheimer et de Parkinson (Alecu and Bennett, 2019; Di Paolo and Kim, 2011), et probablement aussi la maladie de Pick (démence frontotemporale) (Bright et al., 2019).

L'utilisation d'un régime carencé uni-générationnel en AGPI n-3 est donc un bon modèle expérimental pour induire des diminutions des taux de DHA dans le cerveau de la souris et provoquer des altérations cognitives et neurobiologiques.

*Tableau 5 : composition des régimes équilibrés et carencés en AGPI n-3 utilisés*

	Régime équilibré	Régime déficient
<b>16 :0</b>	22,6	6,2
<b>18:0</b>	3,3	4,4
<b>Autre AG saturés</b>	1,8	1,6
<b>Total AGS</b>	27,7	12,2
<b>16:1 n-7</b>	0,2	0,1
<b>18:1 n-9</b>	57,9	26,0
<b>18:1 n-7</b>	1,5	0,9
<b>Autre AGMI</b>	0,4	0,2
<b>AGMI totaux</b>	60,0	27,2
<b>18:2 n-6 (LA)</b>	10,6	60,5
<b>20:4 n-6 (AA)</b>	ND	ND
<b>AGPI n-6 totaux</b>	10,7	60,5
<b>18:3 n-3 (ALA)</b>	1,6	0,1
<b>18:4 n-3</b>	ND	ND

<b>20:5 n-3</b>	ND	ND
<b>22:5 n-3</b>	ND	ND
<b>22:6 n-3 (DHA)</b>	ND	ND
<b>AGPI n-3 totaux</b>	1,6	0,2
<b>AGPI totaux</b>	12,3	60,6

*Exprimé en % du poids total en AG. Composition du régime (g/kg de régime : caséine (180) ; féculé de maïs (460); sucrose (230); cellulose (20); graisse (50); mix de minéraux (50 mix de vitamines (10). AL : acide linoléique, AA : acide arachidonique, ALA : acide  $\alpha$ -linoléique, AGMI : acide gras mono-insaturé, ND : non détecté.*

### 2.1.2 Choix de la fenêtre d'action pour restaurer un apport équilibré en AGPI n-3

Un autre élément important dans notre étude a été le choix de la fenêtre d'intervention nutritionnelle, c'est-à-dire à quel moment une partie des animaux carencés en AGPI n-3 allait être exposés à un régime équilibré en AGPI n-3. En effet, une étude en particulier a démontré qu'une exposition à un régime équilibré en AGPI n-3 au sevrage était plus efficace qu'à 7 semaines pour restaurer les taux de DHA cérébraux chez le rat (Moriguchi and Salem Jr, 2003). La durée de l'exposition est un paramètre critique, dans cette même étude un changement de régime au sevrage et durant 6 semaines permet d'induire des effets positifs à l'inverse d'une exposition au régime équilibré durant 2 semaines (Moriguchi and Salem Jr, 2003). Il est également apparu que chez les animaux plus jeunes la restauration du DHA cérébral est plus rapide que chez les animaux plus âgés carencés en AGPI n-3 (Moriguchi and Salem Jr, 2003).

De plus, nous avons fait le choix de ne pas supplémenter les animaux en DHA mais d'utiliser un régime équilibré en AGPI n-3 afin de déterminer si celui-ci est suffisant pour inverser les altérations induites par la carence. L'huile de poisson, administrée au sevrage à des animaux nourris depuis la gestation avec un régime carencé en AGPI n-3 restaure les taux de DHA dans l'hippocampe au bout de deux mois (Orr et al., 2013). D'autres études ont démontré qu'un régime déficient en AGPI n-3 (0% de DHA et EPA et <0.01% d'ALA) pendant 2 générations induit une déplétion de 75% en DHA dans le cerveau (Xiao et al., 2006). La seconde génération est ensuite supplémentée à l'âge de 5 semaines avec de l'ALA (3,5%) pendant 12 semaines (Xiao et al., 2006). Ce régime permet de restaurer les niveaux de DHA dans les régions cérébrales, sachant que l'hippocampe est la structure où la récupération du taux initial de DHA est la plus lente (Xiao et al., 2006). De plus, l'étude de Kodas et al., (Kodas et al., 2002) montre, dans le même modèle de déficience sur plusieurs générations, qu'un apport alimentaire équilibré en précurseurs des AGPI n-3 apporté soit à partir de la naissance, soit aux jours 7, 14 ou au sevrage, permet également de restaurer des taux en DHA équivalents aux

souris contrôles. Nos résultats montrent que le régime équilibré en ALA permet également une restauration des niveaux de DHA suite à une carence maternelle en ALA dès la première génération.

## 2.2. Modèle transgénique (modification locale par modification du métabolisme des AGPI au niveau astrocytaire)

Nous avons recherché si une variation locale des taux d'AGPI pouvait avoir des conséquences métaboliques et neuro-fonctionnelles. C'est pourquoi nous nous sommes dirigés vers l'expression de l'enzyme Elov12. En effet, cette enzyme catalyse la première des quatre réactions qui constituent le cycle d'élongation des AGPI-LC (C20 et C22). Ce processus enzymatique lié au réticulum endoplasmique permet l'ajout de 2 carbones à la chaîne des AGPI-LC par cycle. Elle participe également à la production d'AGPI à très longues chaînes, comme le DHA, qui sont impliqués dans de multiples processus biologiques en tant que précurseurs des lipides membranaires et médiateurs lipidiques

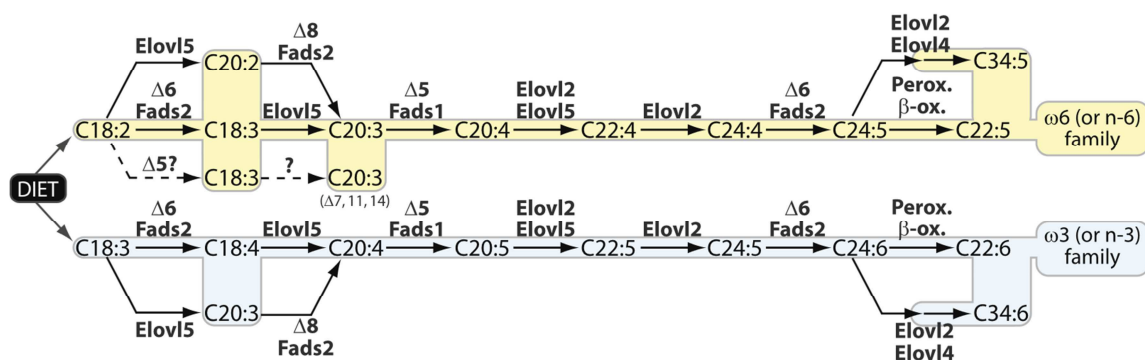


Figure 10 : Biosynthèse des Acide Gras à Longue et très Longue Chaîne chez les mammifères.

Noms des gènes de souris contribuant aux étapes d'élongation (Elov1-7) et de désaturation (Fads) des AGPI n-3 et n-6. (Extrait de Guillou et al., 2010).

Elov12 est impliquée à la fois dans les familles des AGPI n-6 et n-3 (Figure 9). En diminuant l'expression d'Elov12, nous nous attendons donc à induire des changements de niveaux d'AGPI dans le cerveau. Les travaux de Talamonti et al., ont utilisé un modèle de KO total pour Elov12 et ont ensuite mesuré les niveaux d'AGPI n-6 et n-3 dans le cerveau de souris soumise à un régime équilibré en AGPI n-3 (LA : 37,43% ; ALA : 4,24%) (Talamonti et al., 2019). Ils ont établi pour la première fois le profil de la composition en acyl-CoA de divers acides gras dans les tissus cérébraux de souris Elov12-/- (KO) et de souris de type sauvage (WT) en mesurant les métabolites par chromatographie liquide associée à la spectrométrie de masse (LC-MS/MS). Ils ont observé une accumulation significative d'EPA et de DPA n-3 dérivés du ALA associée à une diminution des niveaux de DHA dans le cerveau



des souris. Il a également été remarqué une accumulation générale, mais non significative, de LA (18:2n-6) et d'acide dihomog- $\gamma$ -linoléique (20:3n-6), et une accumulation significative de l'acide docosatétraénoïque (20:5n-6) (Talamonti et al., 2019)

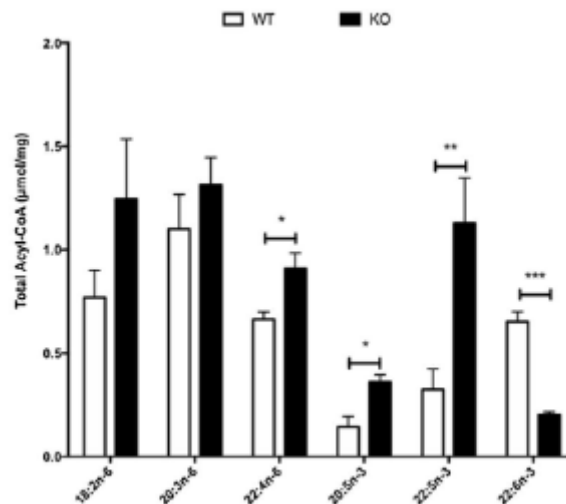


**Figure 11** : Composition en AGPI n-6 et n-3 du cerveau d'animaux WT et KO pour *Elovl2* sous régime équilibré en AGPI n-3 (extrait de Talamonti et al., 2019)

Dans le cerveau, *Elovl2* est majoritairement exprimée dans les astrocytes des différentes structures cérébrales comme le cortex, l'hippocampe ou encore le striatum, d'après The Human Protein Atlas. De plus, les astrocytes sont essentiels au développement et fonctionnement cérébral de par leurs rôles dans le contrôle du métabolisme énergétique, du renouvellement synaptique, de la neuritogenèse mais aussi de la neurotransmission (Bélanger et al., 2011; Clarke and Barres, 2013; Kucukdereli et al., 2011; Nedergaard et al., 2003; Neniskyte and Gross, 2017; Reemst et al., 2016). Nous avons donc choisi de cibler les astrocytes afin d'y induire une altération de la synthèse des AGPI-LC en bloquant l'expression de l'enzyme *Elovl2*. Grâce à une lignée de souris floxée pour *Elovl2* (*Elovl2*<sup>lox/lox</sup>) sur fond génétique C57bl6J, nous avons inhibé l'expression de *elovl2* en injectant un adénovirus-cre dans le NAc. Ce virus, dont l'expression de la cre est sous la dépendance du promoteur GFAP permet de cibler les astrocytes (Meng et al., 2015). Il existe un modèle de KO total chez la souris (*Elovl2*<sup>-/-</sup>) qui est caractérisé par une diminution des niveaux de DHA dans les testicules, le sérum, le foie, la glande mammaire et les tissus adipeux (Pauter et al., 2017; Zadavec et al., 2011). Ce modèle a également permis de démontrer que les niveaux d'acyl-CoA et la synthèse endogène de DHA médiée par *Elovl2* sont impliqués dans l'expression de plusieurs marqueurs de plasticité et d'inflammation du cerveau (Talamonti et al., 2019). Nous avons donc recherché si la diminution de l'expression d'*Elovl2* dans les astrocytes pourrait être à l'origine d'une modification structurelle des niveaux d'AGPI n-3 et n-6 associée à une modification des propriétés électrophysiologiques des

neurones environnants ainsi qu'une modification du comportement. Nos résultats ne montrent pas d'effet sur les taux d'AGPI dans le NAc mais nous avons pu observer des modifications électrophysiologiques et l'altération de certains paramètres comportementaux discutés en partie IV.

### 2.1.3 Augmentation des AGPI-LC EPA et DHA dans le cerveau par la nutrition

Dans ce travail, nous avons recherché si une diète riche en PUFA-LC n-3 est plus efficace qu'une diète équilibrée en ALA pour protéger les souris des effets neuro-délétères du CSDS. Pour cela, nous avons utilisé deux diètes isocaloriques mais différentes d'un point de vue de la composition en AGPI : une diète riche en EPA+DHA contenant un mélange d'huile de colza, d'huile de tournesol riche en acide oléique, d'huile de palme et d'huile de thon et une diète équilibrée contenant un mélange d'huile de colza (riche en ALA), d'huile de tournesol à haute teneur en acide oléique et d'huile de palme résultant en un rapport ALA/LA de ¼ (régime témoin) (Labrousse et al., 2012; Larrieu et al., 2014; Rey et al., 2019). Les animaux ont été nourris 8 semaines avec ces diètes à partir du sevrage, comme décrit précédemment (Larrieu et al., 2014; Rey et al., 2019). Cette durée d'exposition suffit à modifier drastiquement les niveaux d'AGPI dans plusieurs structures cérébrales comme l'hippocampe (Rey et al., 2019).

Tableau 6 Composition lipidiques des régimes, extrait de (Labrousse et al., 2012)

Diet	Control		LC $\omega$ 3	
	% wt of total fatty acids	g/kg diet	% wt of total fatty acids	g/kg diet
16:0	22.6	11.3	20.0	10.0
18:0	3.3	1.65	3.9	1.95
other saturated FAs	1.8	0.9	6.6	3.3
total saturated FAs	27.7	13.85	30.5	15.25
18:1 $\omega$ 9	57.9	28.95	22.6	11.3
18:1 $\omega$ 7	1.5	0.75	4.9	2.45
other monounsaturated FAs	0.6	0.3	6.7	3.35
total monounsaturated FAs	60.0	30.0	34.2	17.1
18:2 $\omega$ 6 (LA)	10.7	5.35	15.2	7.6
18:3 $\omega$ 3 (ALA)	1.6	0.8	0.9	0.45
20:5 $\omega$ 3 (EPA)	n.d.	n.d.	10.9	5.45
22:5 $\omega$ 3 (DPA)	n.d.	n.d.	1.1	0.55
22:6 $\omega$ 3 (DHA)	n.d.	n.d.	7.2	3.6
Total $\omega$ 3 PUFAs	1.6	0.8	20.1	10.05
total PUFAs	12.3	6.15	35.3	17.65
$\omega$ 6/ $\omega$ 3	6.7	6.7	0.8	0.8

FAs, fatty acids; LA, linoleic acid; ALA,  $\alpha$ -linolenic acid; EPA, eicosapentaenoic acid; DPA, docosapentaenoic acid; DHA, docosahexaenoic acid, PUFAs, polyunsaturated fatty acids.

doi:10.1371/journal.pone.0036861.t002

La consommation d'EPA et de DHA augmente non seulement les AGPI-LC n-3 dans le cerveau, mais modifient également leurs métabolites, comme les oxylipines ou les eCBs (Bosch-Bouju et al., 2016).

Ainsi, l'augmentation des niveaux d'AGPI-LC n-3 dans l'hippocampe de souris adultes est associée à l'augmentation des métabolites dérivés de l'EPA et du DHA (18-HEPE et 17-HDoHE) et la diminution des métabolites dérivés de du LA et de l'AA (TxB2, 6kPGF1a, PGE2, 15dPGJ2, 5,6-DiHETE, 14,15-EET, 15-HETE, LxA4, 13-HODE, 9-HODE) (Rey et al., 2019). Chez le rat âgé, une administration orale d'EPA et de DHA entraîne la génération de médiateurs dérivés de l'EPA et de HDoHE, -résolvines et -protectine dérivés du DHA dans le cortex (Hashimoto et al., 2015). De plus, des niveaux alimentaires élevés de DHA et d'EPA ou de faibles niveaux de LA alimentaires diminuent la production de médiateurs dérivés des AGPI n-6 (5,6-DiHETE, 14,15-EET, 15-HETE, 13-HODE, 9-HODE, TxB2 et 6kPGF1 $\alpha$ ) dans le cerveau de rongeurs (Ostermann et al., 2017; Reemst et al., 2022; Taha et al., 2018). Plusieurs études in vitro et in vivo ont également montré un lien entre la biodisponibilité d'AGPI et les eCBs et NAEs. Les porcelets qui consomment un lait supplémenté en AA ont des niveaux accrus d'AEA et de 2-AG dans le cerveau. Inversement, ceux qui consomment un régime riche en DHA ont plus de DHEA (Berger et al., 2001). Des résultats identiques ont été obtenus chez les souris (plus de DHEA, moins de 2-AG ou d'AEA) (Artmann et al., 2008; Balvers et al., 2012). Ces effets de la diète se font également ressentir sur la composition en NAEs du cerveau des petits. Ainsi, une supplémentation maternelle en AGPI n-3 augmente le DHEA et l'EPEA et diminue le 2-AG dans le cortex et l'hippocampe de la progéniture. Ces données renforcent l'idée que le profil des NAEs représente l'abondance relative des AGPI dans l'alimentation. Cependant, l'origine cellulaire des oxylipines et des NAEs dans le cerveau est peu connue. Toutes les cellules du cerveau possèdent des AGPI n-3 et n-6 dans leurs membranes (AA, DHA, EPA, LA) dont les niveaux dépendent du contenu en AGPI n-3 de la diète, notamment pour les neurones et synaptosomes (Ikemoto et al., 2000), les cellules gliales et la microglie (Destailats et al., 2010; Madore et al., 2020; Rey et al., 2018). Ces variations sont à l'origine de variations spécifiques d'oxylipines dans les cellules microgliales (Madore et al., 2020) mais cela reste à étudier plus précisément pour les autres types cellulaires. Ces données restent également à préciser pour les NAEs. Récemment, la mise en évidence que EEQ-EA (époxyecosatetraénoïque-éthanolamide) et EDP-EA (époxydocosapentaénoïque-éthanolamide), des formes époxydées d'EPEA et de DHEA par la voie CYP450, sont synthétisées par les cellules microgliales (McDougle et al., 2017), renforcent l'idée que ces cellules sont d'importants contributeurs à la production de dérivés des AGPI-LC dans le cerveau (Layé et al., 2018)

### ***3. Les effets neurobiologiques de la carence maternelle sont partiellement réversibles chez la descendance à l'âge adulte grâce à une intervention nutritionnelle : différences liées au sexe***

#### ***3.1. Les altérations du profil lipidique et dérivés sont restaurées par le régime équilibré***

Nos résultats montrent que lorsque les animaux carencés en AGPI n-3 sont exposés à un régime équilibré en AGPI n-3 au sevrage et pour une durée de 6 semaines, les taux d'AGPI n-3 sont restaurés dans l'hippocampe des femelles et des mâles. Cependant, l'AA reste élevé dans l'hippocampe des souris mâles. Pendant la période périnatale, une carence en AGPI n-3 dès la gestation induit une déplétion des taux de DHA à P0 (naissance) et P21 (sevrage) qui est compensée par une augmentation des taux de DPA n-6 dans le cortex des souris (Madore et al., 2014). Si le régime est consommé jusqu'à l'âge adulte, ces altérations persistent et sont accompagnées d'une augmentation du DPA n-6 et une diminution du DPA n-3 et du DHA dans le cerveau de souris adultes (Lafourcade et al., 2011). Notre modèle de carence maternelle en AGPI n-3 valide tous ces aspects déjà observés auparavant. À l'âge adulte, les niveaux d'AGPI n-3 et n-6 sont similaires dans l'hippocampe des mâles et des femelles nourris avec un régime déficient en AGPI n-3, avec une diminution de l'EPA et du DHA et une augmentation de l'AA et du DPA n-6 (Joffre et al., 2016). Cependant, nos travaux montrent que l'intervention avec un régime équilibré en AGPI n-3 à partir du sevrage restaure de manière différentielle le niveau d'AA, mais pas d'EPA et de DHA, dans l'hippocampe des mâles et des femelles. La restauration des niveaux de DHA et d'EPA dans l'hippocampe chez les mâles par une diète riche en AGPI n-3 a déjà été décrite chez les mâles (Xiao et al., 2006), mais pas chez les femelles. Nos résultats suggèrent qu'une intervention alimentaire à long terme modifie différenciellement le métabolisme de LA et ALA et/ou l'accrétion cérébrale des AGPI-LC n-3 et n-6 selon le genre. Le niveau de DHA dans le cortex préfrontal de patients diagnostiqués avec une dépression majeure est significativement réduit chez les femmes, mais pas chez les hommes (McNamara et al., 2007). L'hypothèse des hormones est avancée pour expliquer ces différences, et plus particulièrement les hormones ovariennes sur la biosynthèse du DHA (Childs et al., 2008; McNamara et al., 2009). La question de savoir si les changements hormonaux associés à la restauration des AGPI dans l'hippocampe des femmes, mais pas des hommes, reste à étudier. Cependant, une étude récente n'a rapporté aucune variation du niveau d'AA dans le cortex de souris femelles ovariectomisées traitées ou non à l'estradiol (Herrera et al., 2018).

Plusieurs études ont démontré que les AGPI n-3 alimentaires ont un impact sur le profil des lipides du cerveau (Carrié et al., 2000b; Joffre et al., 2016; Labrousse et al., 2012; Skorve et al., 2015). Dans notre étude, la déficience en AGPI n-3 a augmenté les niveaux de 13-HODE (dérivé lipidique de LA) et des dérivés d'AA (14,15-EET, 11,12-HETE, 8-HETE, 5-HETE, 5oxoETE, LXB4) dans le cerveau des souris femelles. Nous avons également observé une diminution chez les femelles des taux de dérivés

métaboliques de l'EPA (18-HEPE) et du DHA (17-HDoHE). Chez les mâles, la carence alimentaire en AGPI n-3 n'a induit qu'une diminution significative des taux oxylipines dérivées des AGPI n-3 DHA (14-HDoHE) et EPA (18-HEPE). En rééquilibrant le régime en AGPI n-3 à partir du sevrage, les mâles voient leurs niveaux de 13-HODE et 9-HODE significativement remonter (oxylipines dérivées de LA). Chez les femelles, l'intervention nutritionnelle à partir du sevrage a induit une diminution des dérivés de LA (13-HODE et 9-HODE) et de l'AA (14,15-EET, 11,12-EET, 5-HETE, 5oxoETE, 8 isoPGA2 et 15dPGJ2) accompagnée d'une augmentation des dérivés lipidiques du DHA (17 et 14-HDOHE) et de l'EPA (18-HEPE). L'augmentation du niveau de ces espèces dans le cerveau par une intervention alimentaire riche en AGPI n-3 a été précédemment rapportée par nous et d'autres (Rey et al., 2019; Wang et al., 2022). Les oxylipines dérivées de l'EPA et du DHA ont été signalées comme étant neuroprotectrices vis-à-vis des stimuli inflammatoires (Layé et al., 2018; Rey et al., 2019, 2018) et pourraient jouer un rôle dans la restauration de mémoire et de LTP. Cependant des études supplémentaires sont nécessaires pour déterminer cela.

Les résultats obtenus, sur les modifications des niveaux de dérivés lipidiques ou oxylipines selon le genre ont permis d'établir une signature cérébrale spécifique des oxylipines en fonction du sexe. De façon tout à fait remarquable, et en lien avec les variations observées dans les niveaux d'AGPI, les dérivés du LA et de l'EPA sont altéré par le régime dans l'hippocampe des mâles et des femelles tandis que des différences ont été observées pour les oxylipines dérivées de l'AA.

### *3.2. Récupération comportementale et de la plasticité synaptique en fonction du sexe*

Nos résultats révèlent que les performances dans les tâches spatiales sont altérées par la carence en AGPI n-3 et uniquement restaurées chez les femelles. Au vu des données obtenues chez les mâles lors du dosage des niveaux d'acides gras dans l'hippocampe, les modifications comportementales semblent étroitement liées aux niveaux d'AA cérébraux. En effet si l'on met en corrélation le paramètre « temps passé dans le bras nouveau » du test du Ymaze avec les niveaux d'AA, de DHA et d'EPA, on remarque que les résultats du groupe reversé (n-3 rev) sont inversement corrélés aux niveaux d'AA (**Figure 4.B**). Chez les femelles, aucune corrélation ne permet d'identifier un AG associé aux modifications du comportement observées (**Figure 5**).

Le fait que le maintien à des taux élevé d'AA dans l'hippocampe des souris mâles pourraient jouer un rôle dans les altérations mnésiques n'a été que peu étudié. Plusieurs études ont montré que la mémoire spatiale de travail était impactée par la déficience alimentaire en AGPI n-3 au cours du développement (Chung et al., 2008; Fedorova et al., 2009, 2007; Lim et al., 2005). Ces altérations du comportement sont restaurées par un régime équilibré ou supplémenté en AGPI n-3 (Moriguchi and

Salem Jr, 2003). Chez l'homme âgé, les concentrations plasmatiques élevées en AGPI n-6, particulièrement LA, mais pas d'AGPI n-3, sont corrélées aux altérations des fonctions exécutives. Les taux d'AGPI n-3, quant à eux, sont corrélés aux volumes des lobes frontaux et l'intégrité de la BBB (Barnes et al., 2021). Le rôle de l'AA dans la mémoire a été peu étudié. Chez le rongeur, l'ajout d'AA au régime alimentaire augmente l'AA dans le cerveau (Wainwright, 1997). La consommation d'AA chronique et le dépôt d'AA dans les tissus cortico-hippocampiques de rats âgés entraîne une hyperactivité sans amélioration de la mémoire (Inoue et al., 2019)( mais augmente la LTP dans l'hippocampe (Kotani et al., 2003). L'AA limiterait également les troubles de l'apprentissage et de la mémoire chez les rats en améliorant les dysfonctionnements cholinergiques (Li et al., 2015). L'AA et ses métabolites, notamment ceux issus de COX2 jouent un rôle dans l'homéostasie neuronale et la mémoire (López and Ballaz, 2020b). Cependant, l'augmentation chronique dans le cerveau d'AA et des eCBs associés, comme 2-AG et AEA, pourraient avoir des effets néfastes, en désensibilisant les CB1R (Lafourcade et al., 2011) ou en altérant le métabolisme du 2-AG, qui joue un rôle crucial dans la LTP et la mémoire spatiale (Schurman et al., 2019). De plus, l'injection intrahippocampique de PGE2, un produit de la cascade des AA, altère la mémoire de travail. Ainsi, l'ensemble de ces travaux indiquent un rôle de l'AA cérébral dans la cognition et la plasticité synaptique, mais son rôle exact dans les altérations de mémoire que nous avons observé restent à clarifier.

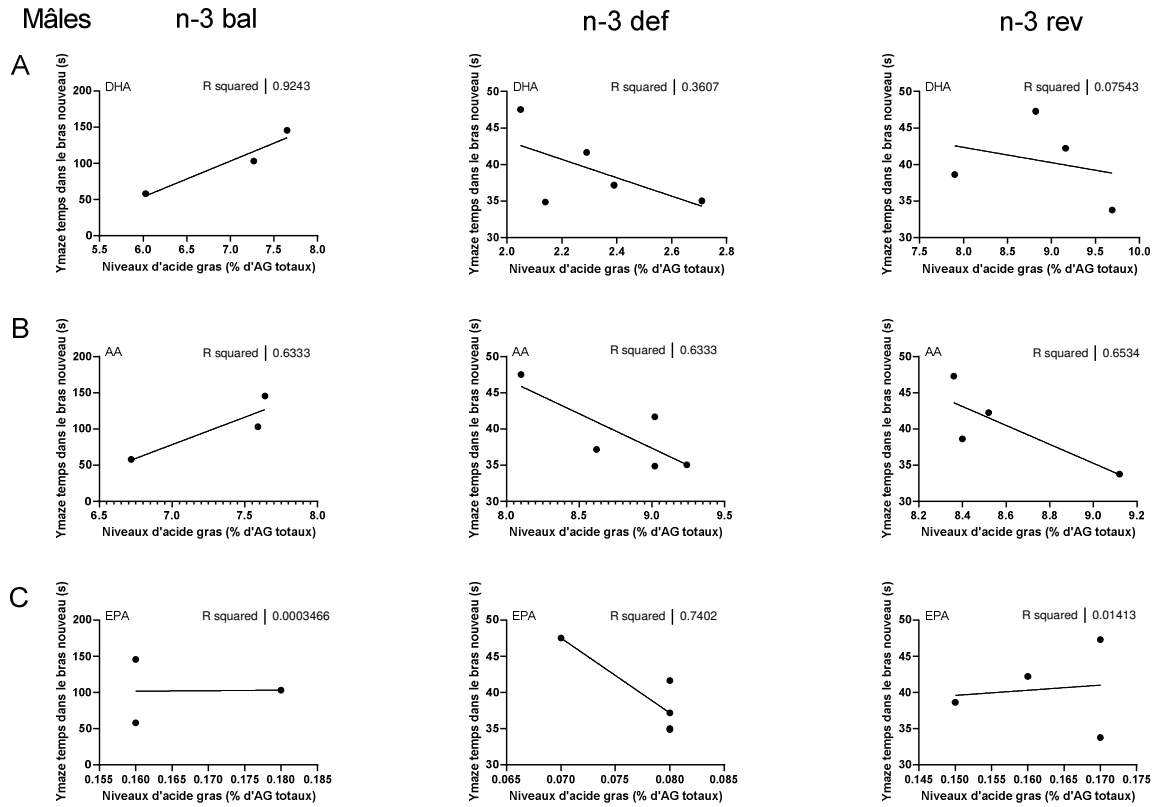


**Figure 12 :** Corrélations des taux d'AG avec le paramètre bras nouveaux du Ymaze (mâles)

par groupe du paramètre "temps passé dans le bras nouveau" du Ymaze avec les niveaux d'acide gras dans l'hippocampe (A). DHA, (B) AA, (C) EPA chez les mâles. N-3 bal = régime équilibré en AGPI n-3, n-3 def = régime déficient en AGPI n-3, n-3 rev = régime équilibré en AGPI n-3 ) partir du sevrage.

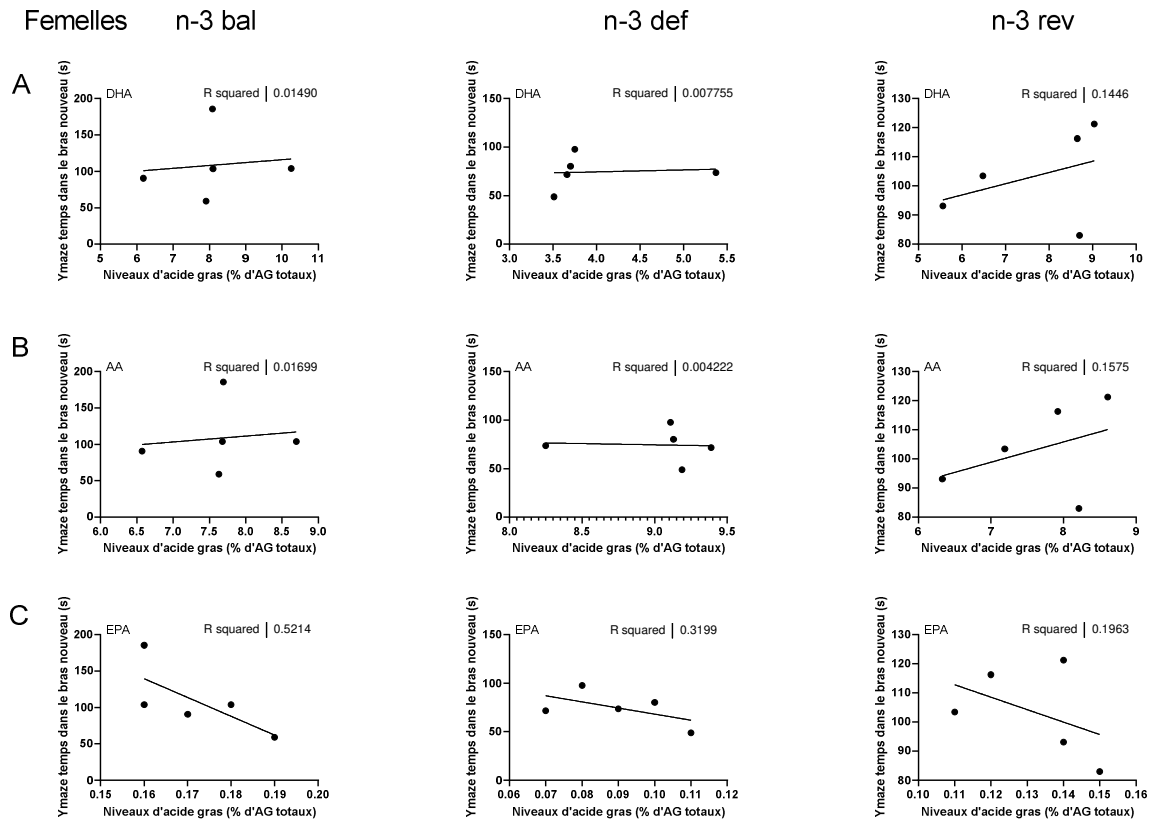


**Figure 13 :** Corrélations des taux d'AG avec le paramètre bras nouveaux du Ymaze (femelles)

Pour chaque groupe, le paramètre "temps passé dans le bras nouveau" du Ymaze est mis en corrélation avec les niveaux d'acide gras dans l'hippocampe (A). DHA, (B) AA, (C) EPA chez les mâles. N-3 bal = régime équilibré en AGPI n-3, n-3 def = régime déficient en AGPI n-3, n-3 rev = régime équilibré en AGPI n-3 à partir du sevrage.

Des études réalisées au sein du laboratoire ont montré que la carence maternelle en AGPI n-3 réduit les éléments synaptiques, ce qui entraîne un dysfonctionnement du réseau synaptique hippocampique et un déficit de la mémoire de travail spatiale (Lafourcade et al., 2011; Lozada et al., 2017; Madore et al., 2014; Thomazeau et al., 2016), mais cela n'a pas été étudié chez la femelle. Des changements de niveaux de GABA ont été montré pour affecter l'induction de la LTP de l'hippocampe (Fernandez et al., 2007). De plus la carence alimentaire en AGPI n-3 altère la plasticité et ce, dès le sevrage et ceci est dû à l'ablation de la iLTD CB1-dépendante (Thomazeau et al., 2016). Il est intéressant de noter que les mâles et les femelles récupèrent une plasticité synaptique hippocampique suite à l'intervention nutritionnelle à partir du sevrage, en revanche, les mâles ne récupèrent pas leur comportement de mémoire spatiale. Ceci peut s'expliquer par le fait que les taux d'AGPI ne sont pas restaurés de la même façon chez les mâles et les femelles, et notamment les niveaux d'AA. On peut imaginer que l'intervention nutritionnelle au sevrage est suffisante pour restaurer en partie les niveaux d'AG et la plasticité synaptique chez les mâles et les femelles mais n'est pas suffisante pour restaurer le comportement chez les mâles. L'observation de la réversibilité



des déficits comportementaux induits par la carence cérébrale en DHA a des implications sur les mécanismes cellulaires et moléculaires qui sous-tendent cet état de carence. En ce qui concerne les changements pertinents au niveau cellulaire, il a été démontré que le DHA peut protéger les neurones cultivés de l'apoptose (Kim et al., 2006) et il est possible que la mort neuronale limitée puisse expliquer les déficits comportementaux observés ici. Cependant, (Ahmad et al., 2002) ont récemment observé qu'une carence en DHA entraîne une diminution de la taille des neurones dans la région CA1 de l'hippocampe du rat, mais sans changement de la densité cellulaire. De plus, on sait que les AGPI et leurs dérivés jouent un rôle important dans la plasticité et dans le cas de la LTP, la voie des cyclooxygénases qui métabolise l'AA en dérivés lipidiques comme les prostaglandines a été étudiée. La PGE2 générée par la COX-2 régule l'excitabilité membranaire et la plasticité synaptique à long terme dans la synapse hippocampique (Chen et al., 2002). C'est également le cas pour les prostaglandines dérivées des eCBs qui constituent une nouvelle classe de médiateurs de signalisation impliqués dans la transmission et la plasticité synaptiques hippocampique (Yang et al., 2008). Les travaux de Lafourcade et al., ont également mis en évidence que la carence alimentaire en AGPI n-3 induit une augmentation des niveaux d'AA et provoque une désensibilisation des récepteurs aux cannabinoïdes (CB1) (Lafourcade et al., 2011).

Ces résultats indiquent que les altérations après une carence alimentaire en AGPI n-3 grave et prolongée le cerveau en cours de développement peuvent être partiellement corrigées par la consommation de ALA dès le sevrage. Ainsi, on peut s'attendre à ce que les jeunes enfants et les jeunes adultes qui ont été privés de sources adéquates d'acides gras n-3 au début de leur développement, récupèrent les niveaux de DHA cérébral, mais avec un délai. Cependant, une attention particulière doit être apportée à l'AA qui, s'il reste élevé est associé à un déficit cognitif. Une attention particulière doit être portée aux sources alimentaires apportées en période post-natale après une carence alimentaire, afin d'optimiser les fonctions cognitives plus tard dans la vie.

### *3.3. L'hypothèse du 18-HEPE dans la récupération synaptique*

Etant donné que les souris mâles et femelles présentent une plasticité restaurée par l'intervention nutritionnelle au sevrage, nous avons fait l'hypothèse que le mécanisme serait lié aux oxylipines qui restent communément restaurées dans l'hippocampe des souris mâles et femelles. En effet des voies métaboliques de synthèse des oxylipines comme celle de la COX-2 jouent un rôle dans la plasticité synaptique. La COX-2 participe à la transmission et à la plasticité synaptiques via son métabolite, la PGE2 (Akaneya and Tsumoto, 2006; Chen et al., 2002; Chen and Bazan, 2005; Murray and O'Connor, 2003; Sang et al., 2007).

Au vu des résultats obtenus, notamment sur les profils d'oxylipines observés, nous avons remarqué qu'une des oxylipines dont les taux dans l'hippocampe sont abolis par la carence en AGPI n-3 et restaurés par le régime équilibré en AGPI n-3 est la 18-HEPE. Cette oxylipine provient de l'EPA par l'intermédiaire de la voie des lipoxigénase et par cette même voie produit les résolvines de la série E. De plus son rôle dans la plasticité est très peu connu puisque ces dernières années les études se sont surtout concentré sur les effets du DHA dans la plasticité synaptique. Il a été montré que l'EPA présenterait au même titre que le DHA des propriétés neuroprotectrices dans la modulation de la plasticité synaptique et l'activation de la voie de la PI3-kinase, peut-être par ses effets directs sur les neurones et les cellules gliales et par sa capacité à augmenter le DHA cérébral (Kawashima et al., 2010).

J'ai conduit des travaux préliminaires pour évaluer la question suivante : l'application de 18-HEPE sur des tranches de cerveau d'animaux soumis à un régime carencé en AGPI n-3 est-elle suffisante pour pouvoir induire une LTP ? Nous avons utilisé le même protocole que celui utilisé et décrit dans le chapitre 1. A la seule différence que les tranches de cerveau ont été infusées 1h dans un bain contenant 1 $\mu$ M de 18-HEPE ou contenant 0,1% d'alcool avant enregistrement. Les résultats préliminaires obtenus montrent qu'en présence de 18-HEPE, une amplitude plus élevée des réponses après induction du protocole de stimulation à haute fréquence (HFS), symbole qu'une LTP a été induite dans l'hippocampe des mâles carencés en AGPI n-3 mais pas des femelles (**Figure 6**).

Ces premiers résultats sont encourageants mais doivent être approfondis, notamment pour identifier si les effets synaptiques du 18-HEPE se font par l'intermédiaire de récepteurs spécifiques et par quels mécanismes, notamment pour comprendre les différences d'effets liés au sexe. En l'occurrence, des expériences de dose réponse sont nécessaires. A plus long terme, il serait intéressant de tester les activités synaptiques des autres oxylipines communes restaurées par la diète enrichie en ALA et évaluer si elles agissent en synergie. Une étude récente a utilisé un mélange de médiateurs lipidiques pro-résolvants : résolvine (Rv) E1, RvD1, RvD2, marésine 1 (MaR1) et neuroprotectine D1 (NPD1) administrés par voie intranasale dans un modèle murin de maladie d'Alzheimer (Emre et al., 2021). Le traitement a amélioré les déficits de mémoire accompagnés d'une restauration des déficits d'oscillation gamma des courants post synaptiques excitateurs dans l'hippocampe, ainsi qu'une diminution de l'activation microgliale. Ces résultats ouvrent des voies potentielles pour l'exploration thérapeutique des LM pro-résolutives dans la maladie d'Alzheimer, en utilisant une voie non invasive (Emre et al., 2021). Cet article témoigne de la puissance d'une telle association et il serait tout à fait envisageable, après un screening approfondi de nos résultats des dosages d'oxylipines, d'identifier de potentiels candidats capables de restaurer à la fois le comportement et la mémoire spatiale de

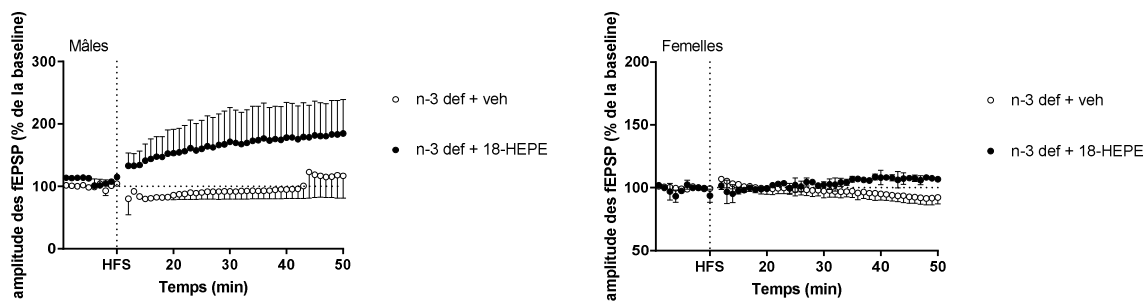


**Figure 14** : Enregistrement de la plasticité synaptique à long terme dans l'hippocampe d'animaux carencés en AGPI n-3 en présence de 18-HEPE (1µM) mâles et femelles.

#### 4. L'inhibition de la synthèse d'*elovl2* astrocytaire altère les propriétés électrophysiologiques des MSNs dans le NAc des souris mâle et femelle

Dans cette deuxième partie répondant à l'objectif n°2 de notre étude, nous nous sommes intéressés à la modulation locale des niveaux d'AG. Après injection du virus dans le NAc, des analyses immunohistochimiques de la colocalisation des marqueurs GFAP et mCherry nous ont permis de confirmer que la cre est exprimée majoritairement dans les astrocytes. Ensuite, par l'utilisation d'une approche de RNAscope, nous avons pu estimer le nombre de cellules astrocytaires ciblées par le virus et, parmi ces cellules infectées, quantifier le niveau d'expression des transcrits d'*elovl2*. L'administration de l'AAV-5/2-GFAP-re/mCherry dans le NAc de souris *ELOVL2<sup>lox/lox</sup>* mâles et femelles diminue l'expression d'*elovl2* de 50% à ce niveau, mais pas dans l'hippocampe, utilisé comme structure contrôle.

Les analyses des profils lipidiques dans le Nac et le PFC montrent que l'inhibition de la synthèse d'*elovl2* astrocytaire n'a pas induit de différences de niveau d'AGS, AGM ou AGPI dans le NAc des mâles et des femelles. Cela va à l'inverse de ce qui a été observée dans les modèle de KO total pour *Elovl2* qui mettent en évidence des modifications des niveaux d'AGPI et notamment une augmentation des niveaux de DPA n-3 et une diminution de DHA dans le cerveau des souris KO (Gregory et al., 2013; Pauter et al., 2014; Talamonti et al., 2019). Nos résultats pourraient s'expliquer par le fait que les modifications au niveau des astrocytes sont trop minimes pour être détectés à l'échelle de la structure entière. Mais il pourrait également s'agir de voies alternatives qui prennent le relai pour la synthèse endogène de DHA, comme c'est le cas dans le foie du poisson zèbre (Liu et al., 2020). En effet, le poisson zèbre *elovl2<sup>-/-</sup>* ne présente pas d'accumulation de DPA n-3 mais une augmentation du substrat de la voie delta 4 désaturase, l'EPA, suggérant que la voie delta 4 serait

une alternative pour la synthèse du DHA (Liu et al., 2020). De plus, la délétion d'elovl2 n'étant pas totale, cela peut expliquer l'absence de modifications des niveaux d'AGPI dans le NAc.

Les analyses comportementales ont mis en évidence des altérations du comportement émotionnel sur des paramètres qui diffèrent chez les animaux KO Elov12 selon le sexe. En effet, nous avons pu observer que les mâles KO Elov12 passent significativement plus de temps dans la zone éclairée du Light Dark que les animaux contrôles. Le test du Light Dark confronte les souris à une situation extrêmement anxiogène qui consiste à s'exposer à une zone très fortement éclairée. Nos résultats suggèrent donc que les souris mâles KO Elov12 seraient moins anxieuses que les animaux contrôles. Ensuite, nous avons pu remarquer que les souris femelles KO Elov12 réalisaient moins de « head dipping » dans le test du labyrinthe en croix surélevé. Ce paramètre consiste à compter le nombre de fois où l'animal engage sa tête et la partie haute de son corps au-dessus du vide. Les femelles KO Elov12 semblent donc présenter un comportement de type anxieux comparé aux animaux contrôles. A ce jour, aucune donnée de la littérature ne fait état d'un lien direct entre une diminution de la synthèse d'Elov12 et des altérations cognitives chez l'homme comme chez l'animal.

Finalement, nous avons pu observer des modifications de l'excitabilité neuronale. En effet, les neurones enregistrés à proximité d'astrocytes fluorescent présentent une rhéobase plus faible ainsi qu'une diminution du nombre de potentiels d'action. L'analyse de l'activité spontanée des courants post synaptiques excitateurs montre que l'amplitude de ces activités est diminuée chez les animaux Elov12 KO mais pas la fréquence ni l'intervalle entre événements. Il n'existe, à notre connaissance, aucune étude ayant analysé les propriétés neuronales sous contrôle astrocytaire dans le NAc. L'activité neuronale du NAc est régulée par différents neurotransmetteurs ou neuromodulateurs libérés par les afférences, notamment GABAergiques. Les astrocytes sont connus pour exprimer des transporteurs du glutamate (GLAST et GLT-1), ainsi que des transporteurs du GABA (GAT1-3) (Danbolt, 2001; Gadea and López-Colomé, 2001a, 2001b). L'inhibition partielle de l'expression d'elovl2 dans l'astrocyte pourrait modifier l'expression des transporteurs GABA et GLUT à ce niveau. Pour mieux comprendre comment les modifications d'expression d'elovl2 par l'astrocyte modifie les propriétés neuronales, des études de la recapture astrocytaire qui module l'intensité et la durée de l'activation des récepteurs situés au niveau pré- ou post-synaptique (Tzingounis and Wadiche, 2007) de limiter l'activation des récepteurs extra-synaptiques (Huang and Bergles, 2004) ou encore de limiter la diffusion des neurotransmetteurs vers les synapses voisines (Arnth-Jensen et al., 2002) sont nécessaires.

Pour compléter cette étude et déterminer plus précisément si l'inhibition partielle de l'expression d'elovl2 dans les astrocytes s'accompagne d'une altération locale de synthèse des AGPI-LC, une

analyse par immunohistochimie GFAP couplée au MALDI-IMS (spectrométrie de masse à haute résolution par microsonde à balayage atmosphérique assistée par désorption laser/ionisation à piégeage orbital) est en cours de développement en collaboration avec le Pr C Rummel (Center for Mind, Brain and Behavior, Marburg, Allemagne) (Bredehöft et al., 2019). Cette approche a permis de montrer que les phosphatidylcholines contenant de l'AA et du DHA sont distribués dans les neurones de l'hippocampe et les cellules de Purkinje du cervelet (Sugiura et al., 2009). Ainsi, cette approche devrait permettre de déterminer la résolution spatiale des lipides dans le NAc de souris KO *elovl2* et WT. Elle représente une alternative au dosage des AG dans la structure car le niveau de résolution est plus petit (15µm) et la lecture est spatiale et devrait permettre de détecter des différences régionales d'espèces moléculaires de phospholipides. Cependant la quantification reste complexe au vu de la difficulté à cibler une zone de manière reproductible entre chaque animal injecté. De plus, il est nécessaire de confirmer la diminution de l'expression d'*Elovl2* par PCR sur astrocytes isolés.

En résumé, les résultats obtenus dans le modèle de KO *Elovl2* montrent pour la première fois que la modification de la synthèse d'*elovl2* astrocytaire modifie les comportements émotionnels sur des paramètres différents selon le sexe et altère les propriétés électrophysiologiques des MSNs dans le NAc. Cependant, des analyses supplémentaires sont nécessaires pour mieux comprendre les mécanismes impliqués dans ces modifications.

### ***5. La supplémentation en AGPI n-3 à longue chaîne modifie les propriétés électrophysiologiques du NAc et le comportement émotionnel de souris naïves et stressées chroniquement***

Finalement, nous avons analysé si un régime supplémenté en EPA/DHA contrôle le comportement émotionnel et la plasticité synaptique dépendant des eCBs dans le NAc de souris soumises ou non au protocole de défaite sociale (CSDS).

Nous avons mis en évidence que les AGPI alimentaires influencent la signature moléculaire lipidique du NAc, par la détermination des AGPI et des gènes impliqués dans la synthèse, métabolisation et transport des AGPI dans le NAc de souris adultes nourries pendant 2 mois (à partir du sevrage) avec un régime supplémenté en AGPI n-3 LC (10% d'EPA et 7% de DHA des lipides totaux) par rapport à un régime isocalorique standard riche en ALA (le précurseur de l'EPA et du DHA). La modification de cette signature s'accompagne d'une altération des comportements de type émotionnel mesurés dans les tests de l'open field, du light dark et de l'EPM. La défaite sociale provoque une forte augmentation des comportements de type anxieux avec une diminution du temps passé au centre de l'OF et dans la zone éclairée du LD. Ceci corrobore avec des études précédentes réalisée sur des souris soumises à un régime équilibré et exposées au CSDS (Bosch-Bouju et al., 2016; Costa et al.,

2022; Larrieu et al., 2014). L'intervention nutritionnelle en EPA+DHA modifie le temps passé par les souris dans les zones à risque du test et les propriétés électrophysiologiques des neurones du NAc suggérant que la consommation d'AGPI-LC n-3 promeut la résilience au stress (Costa et al., 2022; Larrieu et al., 2014). Le protocole de défaite sociale provoque une altération du comportement social et émotionnel et de la plasticité synaptique du NAc chez une partie des rongeurs seulement, permettant de les ségréger en souris en résilientes ou sensibles aux effets du stress chronique (Bosch-Bouju et al., 2016; Francis et al., 2015; Golden et al., 2011; Krishnan et al., 2007). Dans notre étude, par l'utilisation de l'index de ségrégation défini par analyse des comportements sociaux (Golden et al., 2011) la normalisation des paramètres comportementaux a été réalisée en utilisant la formule suivante :  $x_n = \frac{x - \min}{\max - \min}$ , où  $x_n$  est la valeur normalisée de la variable,  $\max$  est la valeur maximale de la variable, et  $\min$  est la valeur minimale de la variable, nous n'avons pas pu discriminer de différences significatives de souris résilientes/sensibles du fait du nombre faible d'animaux. Pour nous affranchir de cette limite, nous avons donc adopté une stratégie de bootstrapping (Fieberg et al., 2020) visant à modéliser la répartition des souris résistantes et prédisposées au stress sur la base des résultats obtenus sur 7-10 animaux/groupe utilisés dans cette étude, conformément aux procédures éthiques. Cette méthode nous a permis de conclure sur l'effet protecteur du régime supplémenté en AGPI n-3 dans un contexte de stress chronique.

Chez l'homme, l'efficacité de diètes riches ou enrichies en EPA plutôt qu'en DHA vis-à-vis de la dépression a été mise en évidence dans plusieurs études cliniques et méta-analyses (Bazinet et al., 2020; Mischoulon and Fava, 2002). Les mécanismes impliqués dans l'efficacité supérieure de l'EPA par rapport à ceux du DHA vis-à-vis de la dépression ne sont pas connus. Les travaux récents montrant que les microglies sont riches en EPA et produisent des dérivés de l'EPA aux activités anti-inflammatoires apportent une piste intéressante (Bazinet et al., 2020; Layé et al., 2018) étant donné que la neuroinflammation est un facteur étiologique du stress chronique et de la dépression (Capuron and Castanon, 2014; Dantzer et al., 2008). Ainsi, dans plusieurs modèles animaux de stress chronique, l'EPA réduit la neuroinflammation (Peng et al., 2022; Song et al., 2009). Il serait intéressant de relier le profil en oxylipines et en NAEs dans le NAc des souris CSDS avec ou sans EPA+DHA, pour identifier les espèces moléculaires associées et étudier leur rôle dans la régulation de la neuroinflammation et de la plasticité synaptique au sein du NAc des souris CSDS. En effet, les eCBs sont de puissants régulateurs de la plasticité synaptique au sein du NAc (Araque et al., 2017) et régulent la neuroinflammation et l'activité des cellules microgliales (De Meij et al., 2021b) notamment au niveau du NAc. Étant donné que le CSDS altère la plasticité synaptique dans le NAc (Bosch-Bouju et al., 2016), les effets des AGPI-LC n-3 et/ou de leurs dérivés pourraient être impliqués dans la promotion de la plasticité neuronale, notamment le DHEA (Kim et al., 2022)

Pour conclure, l'ensemble des travaux de cette thèse ont montré qu'une attention particulière devrait être accordée aux AGPI n-3 en début de vie dans les populations à haut risque telles que celles représentée par les enfants prématurés. Un apport adéquat d'AGPI n-3 est nécessaire tout au long de la vie et les effets délétères de la carence en AGPI n-3 ne sont pas irréversibles chez les femelles. Ces effets sont plus nuancés chez les mâles. L'apport d'AGPI sous forme d'ALA dès le sevrage chez la souris est suffisant pour soutenir la fonction cognitive et la plasticité synaptique de l'hippocampe chez les femelles déficientes en AGPI n-3 au début de la vie, mais pas chez les mâles. Il existe donc une signature spécifique et distincte des oxylipines dans l'hippocampe des mâles et des femelles et ce profil est affecté différemment par une intervention alimentaire avec des AGPI n-3. De plus, l'AA a été identifié comme facteur de différence entre les mâles et les femelles pour les profils de lipides dans l'hippocampe.

Nos résultats montrent également au niveau structurel qu'une modification de la voie des synthèses des AGPI peut avoir des effets délétères sur la plasticité neuronale impliquée dans les comportements émotionnels. Cette diminution de l'expression d'Elovl2 peut également altérer le comportement des mâles et des femelles de façon différente tout en n'affectant pas les niveaux d'AG dans le cerveau. Pour le moment, ces résultats préliminaires nous ont permis de valider notre modèle et méritent d'être approfondis afin de mieux comprendre ce qu'il se passe en terme de profil lipidique au niveau de l'astrocyte. Des analyses électrophysiologiques plus abouties permettront également de déterminer si la libération de neurotransmetteurs est modifiée, quels récepteurs et voies de signalisation sont impliqués, etc...

De plus notre dernière étude montre que les apports en AGPI-LC n-3 modulent profondément les profils moléculaires lipidiques du NAc et signent l'activité synaptique du NAc et les comportements émotionnels en réponse au stress. Les mécanismes impliqués restent à mieux déterminer. Cependant, ces résultats apportent des éléments supplémentaires à la compréhension des effets neuroprotecteurs des AGPI n-3 issus de l'alimentation sur la santé cerveau et la protection vis-à-vis des évènements délétères pour ce dernier, comme un stress chronique.

Ces nouvelles connaissances pointent l'importance de promouvoir la consommation d'AGPI n-3 non seulement durant la période périnatale mais également au cours de la vie et la nécessité de tenir compte du sexe dans les différences de réponses du cerveau aux changements alimentaires en AGPI n-3. Ces avancées sont nécessaires à la définition d'une alimentation personnalisée pour le maintien de la santé cérébrale et la protection vis-à-vis du développement de pathologies neuropsychiatriques dans ses composantes émotionnelles et cognitives.





## ***REFERENCES***

---

- Abela, A.R., Duan, Y., Chudasama, Y., 2015. Hippocampal interplay with the nucleus accumbens is critical for decisions about time. *Eur J Neurosci* 42, 2224–2233. <https://doi.org/10.1111/ejn.13009>
- Acharyar, T.M., Li, B., Peng, W., Verghese, P.B., Shi, Y., McConnell, E., Benraiss, A., Kasper, T., Song, W., Takano, T., Holtzman, D.M., Nedergaard, M., Deane, R., 2016. Glymphatic distribution of CSF-derived apoE into brain is isoform specific and suppressed during sleep deprivation. *Molecular Neurodegeneration* 11, 74. <https://doi.org/10.1186/s13024-016-0138-8>
- Adamsky, A., Kol, A., Kreisel, T., Doron, A., Ozeri-Engelhard, N., Melcer, T., Refaeli, R., Horn, H., Regev, L., Groysman, M., London, M., Goshen, I., 2018. Astrocytic Activation Generates De Novo Neuronal Potentiation and Memory Enhancement. *Cell* 174, 59-71.e14. <https://doi.org/10.1016/j.cell.2018.05.002>
- Ahmad, A., Moriguchi, T., Salem, N., 2002. Decrease in neuron size in docosahexaenoic acid-deficient brain. *Pediatric Neurology* 26, 210–218. [https://doi.org/10.1016/S0887-8994\(01\)00383-6](https://doi.org/10.1016/S0887-8994(01)00383-6)
- Aïd, S., Vancassel, S., Poumès-Ballihaut, C., Chalon, S., Guesnet, P., Lavialle, M., 2003. Effect of a diet-induced n-3 PUFA depletion on cholinergic parameters in the rat hippocampus. *Journal of Lipid Research* 44, 1545–1551. <https://doi.org/10.1194/jlr.M300079-JLR200>
- Akaneya, Y., Tsumoto, T., 2006. Bidirectional Trafficking of Prostaglandin E2 Receptors Involved in Long-Term Potentiation in Visual Cortex. *J. Neurosci.* 26, 10209–10221. <https://doi.org/10.1523/JNEUROSCI.3028-06.2006>
- Al, M.D.M., Van Houwelingen, A.C., Kester, A.D.M., Hasaart, T.H.M., De Jong, A.E.P., Hornstra, G., 1995. Maternal essential fatty acid patterns during normal pregnancy and their relationship to the neonatal essential fatty acid status. *Br J Nutr* 74, 55–68. <https://doi.org/10.1079/BJN19950106>
- Albouery, M., Buteau, B., Grégoire, S., Cherbuy, C., Pais de Barros, J.-P., Martine, L., Chain, F., Cabaret, S., Berdeaux, O., Bron, A.M., Acar, N., Langella, P., Bringer, M.-A., 2020. Age-Related Changes in the Gut Microbiota Modify Brain Lipid Composition. *Frontiers in Cellular and Infection Microbiology* 9.
- Alecu, I., Bennett, S.A.L., 2019. Dysregulated Lipid Metabolism and Its Role in  $\alpha$ -Synucleinopathy in Parkinson's Disease. *Frontiers in Neuroscience* 13.
- Alessandri, J.-M., Guesnet, P., Vancassel, S., Astorg, P., Denis, I., Langelier, B., Aïd, S., Poumès-Ballihaut, C., Champeil-Potokar, G., Lavialle, M., 2004. Polyunsaturated fatty acids in the central nervous system: evolution of concepts and nutritional implications throughout life. *Reprod. Nutr. Dev.* 44, 509–538. <https://doi.org/10.1051/rnd:2004063>
- Al-Hilal, M., AlSaleh, A., Maniou, Z., Lewis, F.J., Hall, W.L., Sanders, T.A.B., O'Dell, S.D., 2013. Genetic variation at the FADS1-FADS2 gene locus influences delta-5 desaturase activity and LC-PUFA proportions after fish oil supplement. *Journal of Lipid Research* 54, 542–551. <https://doi.org/10.1194/jlr.P032276>
- Andreone, B.J., Chow, B.W., Tata, A., Lacoste, B., Ben-Zvi, A., Bullock, K., Deik, A.A., Ginty, D.D., Clish, C.B., Gu, C., 2017. Blood-Brain Barrier Permeability Is Regulated by Lipid Transport-Dependent Suppression of Caveolae-Mediated Transcytosis. *Neuron* 94, 581-594.e5. <https://doi.org/10.1016/j.neuron.2017.03.043>

- Araque, A., Carmignoto, G., Haydon, P.G., Oliet, S.H.R., Robitaille, R., Volterra, A., 2014. Gliotransmitters Travel in Time and Space. *Neuron* 81, 728–739. <https://doi.org/10.1016/j.neuron.2014.02.007>
- Araque, A., Castillo, P.E., Manzoni, O.J., Tonini, R., 2017. Synaptic functions of endocannabinoid signaling in health and disease. *Neuropharmacology, A New Dawn in Cannabinoid Neurobiology* 124, 13–24. <https://doi.org/10.1016/j.neuropharm.2017.06.017>
- Arendash, G.W., Jensen, M.T., Salem, N., Hussein, N., Cracchiolo, J., Dickson, A., Leighty, R., Potter, H., 2007. A diet high in omega-3 fatty acids does not improve or protect cognitive performance in Alzheimer's transgenic mice. *Neuroscience* 149, 286–302. <https://doi.org/10.1016/j.neuroscience.2007.08.018>
- Arita, M., Bianchini, F., Aliberti, J., Sher, A., Chiang, N., Hong, S., Yang, R., Petasis, N.A., Serhan, C.N., 2005. Stereochemical assignment, antiinflammatory properties, and receptor for the omega-3 lipid mediator resolvin E1. *Journal of Experimental Medicine* 201, 713–722. <https://doi.org/10.1084/jem.20042031>
- Arnardottir, H., Orr, S.K., Dalli, J., Serhan, C.N., 2016. Human milk proresolving mediators stimulate resolution of acute inflammation. *Mucosal Immunol* 9, 757–766. <https://doi.org/10.1038/mi.2015.99>
- Arnth-Jensen, N., Jabaudon, D., Scanziani, M., 2002. Cooperation between independent hippocampal synapses is controlled by glutamate uptake. *Nat Neurosci* 5, 325–331. <https://doi.org/10.1038/nn825>
- Artmann, A., Petersen, G., Hellgren, L.I., Boberg, J., Skonberg, C., Nellemann, C., Hansen, S.H., Hansen, H.S., 2008. Influence of dietary fatty acids on endocannabinoid and N-acyl ethanolamine levels in rat brain, liver and small intestine. *Biochimica et Biophysica Acta (BBA) - Molecular and Cell Biology of Lipids* 1781, 200–212. <https://doi.org/10.1016/j.bbalip.2008.01.006>
- Asatryan, A., Bazan, N.G., 2017. Molecular mechanisms of signaling via the docosanoid neuroprotectin D1 for cellular homeostasis and neuroprotection. *Journal of Biological Chemistry* 292, 12390–12397. <https://doi.org/10.1074/jbc.R117.783076>
- Ashton, J.C., Friberg, D., Darlington, C.L., Smith, P.F., 2006. Expression of the cannabinoid CB2 receptor in the rat cerebellum: An immunohistochemical study. *Neuroscience Letters* 396, 113–116. <https://doi.org/10.1016/j.neulet.2005.11.038>
- Bak, L.K., Schousboe, A., Waagepetersen, H.S., 2006. The glutamate/GABA-glutamine cycle: aspects of transport, neurotransmitter homeostasis and ammonia transfer. *Journal of Neurochemistry* 98, 641–653. <https://doi.org/10.1111/j.1471-4159.2006.03913.x>
- Balakrishnan, J., Kannan, S., Govindasamy, A., 2021. Structured form of DHA prevents neurodegenerative disorders: A better insight into the pathophysiology and the mechanism of DHA transport to the brain. *Nutrition Research* 85, 119–134. <https://doi.org/10.1016/j.nutres.2020.12.003>
- Balvers, M.G.J., Verhoeckx, K.C.M., Bijlsma, S., Rubingh, C.M., Meijerink, J., Wortelboer, H.M., Witkamp, R.F., 2012. Fish oil and inflammatory status alter the n-3 to n-6 balance of the endocannabinoid and oxylipin metabolomes in mouse plasma and tissues. *Metabolomics* 8, 1130–1147. <https://doi.org/10.1007/s11306-012-0421-9>
- Bang, S., Xie, Y.-K., Zhang, Z.-J., Wang, Z., Xu, Z.-Z., Ji, R.-R., 2018. GPR37 regulates macrophage phagocytosis and resolution of inflammatory pain. *J Clin Invest* 128, 3568–3582. <https://doi.org/10.1172/JCI99888>

- Barbour, B., Szatkowski, M., Ingledew, N., Attwell, D., 1989. Arachidonic acid induces a prolonged inhibition of glutamate uptake into glial cells. *Nature* 342, 918–920. <https://doi.org/10.1038/342918a0>
- Barnes, S., Chowdhury, S., Gatto, N.M., Fraser, G.E., Lee, G.J., 2021. Omega-3 fatty acids are associated with blood–brain barrier integrity in a healthy aging population. *Brain and Behavior* 11, e2273. <https://doi.org/10.1002/brb3.2273>
- Basak, S., Mallick, R., Duttaroy, A.K., 2020. Maternal Docosahexaenoic Acid Status during Pregnancy and Its Impact on Infant Neurodevelopment. *Nutrients* 12, 3615. <https://doi.org/10.3390/nu12123615>
- Basil, M.C., Levy, B.D., 2016. Specialized pro-resolving mediators: endogenous regulators of infection and inflammation. *Nat Rev Immunol* 16, 51–67. <https://doi.org/10.1038/nri.2015.4>
- Bauer, I., Crewther, D.P., Pipingas, A., Rowsell, R., Cockerell, R., Crewther, S.G., 2011. Omega-3 Fatty Acids Modify Human Cortical Visual Processing—A Double-Blind, Crossover Study. *PLoS ONE* 6, e28214. <https://doi.org/10.1371/journal.pone.0028214>
- Bauer, I., Hughes, M., Rowsell, R., Cockerell, R., Pipingas, A., Crewther, S., Crewther, D., 2014. Omega-3 supplementation improves cognition and modifies brain activation in young adults: EFFECTS OF OMEGA-3 FATTY ACIDS ON fMRI MEASURES. *Hum. Psychopharmacol Clin Exp* 29, 133–144. <https://doi.org/10.1002/hup.2379>
- Bazan, N.G., 2003. Synaptic lipid signaling. *Journal of Lipid Research* 44, 2221–2233. <https://doi.org/10.1194/jlr.R300013-JLR200>
- Bazinet, R.P., Layé, S., 2014. Polyunsaturated fatty acids and their metabolites in brain function and disease. *Nature Reviews Neuroscience* 15, 771–785. <https://doi.org/10.1038/nrn3820>
- Bazinet, R.P., Metherel, A.H., Chen, C.T., Shaikh, S.R., Nadjar, A., Joffre, C., Layé, S., 2020. Brain eicosapentaenoic acid metabolism as a lead for novel therapeutics in major depression. *Brain, Behavior, and Immunity, Nutrition and Immunity in Mental Health* 85, 21–28. <https://doi.org/10.1016/j.bbi.2019.07.001>
- Beauchamp, E., Rioux, V., Legrand, P., 2009. Acide myristique : nouvelles fonctions de régulation et de signalisation. *Med Sci (Paris)* 25, 57–63. <https://doi.org/10.1051/medsci/200925157>
- Bélanger, M., Allaman, I., Magistretti, P.J., 2011. Brain Energy Metabolism: Focus on Astrocyte-Neuron Metabolic Cooperation. *Cell Metabolism* 14, 724–738. <https://doi.org/10.1016/j.cmet.2011.08.016>
- Beltz, B.S., Tlusty, M.F., Benton, J.L., Sandeman, D.C., 2007. Omega-3 fatty acids upregulate adult neurogenesis. *Neuroscience Letters* 415, 154–158. <https://doi.org/10.1016/j.neulet.2007.01.010>
- Bennett, M., Gilroy, D.W., 2017. Lipid Mediators in Inflammation, in: *Myeloid Cells in Health and Disease*. John Wiley & Sons, Ltd, pp. 343–366. <https://doi.org/10.1128/9781555819194.ch19>
- Bennett, M.R., 2000. The concept of long term potentiation of transmission at synapses. *Prog Neurobiol* 60, 109–137. [https://doi.org/10.1016/s0301-0082\(99\)00006-4](https://doi.org/10.1016/s0301-0082(99)00006-4)
- Bentsen, H., 2017. Dietary polyunsaturated fatty acids, brain function and mental health. *Microbial Ecology in Health and Disease* 28, 1281916. <https://doi.org/10.1080/16512235.2017.1281916>

- Ben-Zvi, A., Lacoste, B., Kur, E., Andreone, B.J., Mayshar, Y., Yan, H., Gu, C., 2014. Mfsd2a is critical for the formation and function of the blood–brain barrier. *Nature* 509, 507–511. <https://doi.org/10.1038/nature13324>
- Berger, A., Crozier, G., Bisogno, T., Cavaliere, P., Innis, S., Di Marzo, V., 2001. Anandamide and diet: Inclusion of dietary arachidonate and docosahexaenoate leads to increased brain levels of the corresponding N-acyl ethanolamines in piglets. *Proceedings of the National Academy of Sciences* 98, 6402–6406. <https://doi.org/10.1073/pnas.101119098>
- Berland, C., Montalban, E., Perrin, E., Di Miceli, M., Nakamura, Y., Martinat, M., Sullivan, M., Davis, X.S., Shenasa, M.A., Martin, C., Tolu, S., Marti, F., Caille, S., Castel, J., Perez, S., Salinas, C.G., Morel, C., Hecksher-Sørensen, J., Cador, M., Fioramonti, X., Tschöp, M.H., Layé, S., Venance, L., Faure, P., Hnasko, T.S., Small, D.M., Gangarossa, G., Luquet, S.H., 2020. Circulating Triglycerides Gate Dopamine-Associated Behaviors through DRD2-Expressing Neurons. *Cell Metabolism* 31, 773–790.e11. <https://doi.org/10.1016/j.cmet.2020.02.010>
- Berry, C.B., Hayes, D., Murphy, A., Wießner, M., Rauen, T., McBean, G.J., 2005. Differential modulation of the glutamate transporters GLT1, GLAST and EAAC1 by docosahexaenoic acid. *Brain Research* 1037, 123–133. <https://doi.org/10.1016/j.brainres.2005.01.008>
- Best, K.P., Gibson, R.A., Makrides, M., 2022. ISSFAL Statement Number 7 – Omega-3 fatty acids during pregnancy to reduce preterm birth. *Prostaglandins, Leukotrienes and Essential Fatty Acids* 102495. <https://doi.org/10.1016/j.plefa.2022.102495>
- Bewicz-Binkowska, D., Zgorzynska, E., Dziedzic, B., Walczewska, A., 2019. Docosahexaenoic Acid (DHA) Inhibits FADS2 Expression in Astrocytes but Increases Survival of Neurons Co-cultured with DHA-enriched Astrocytes. *Int J Mol Cell Med* 8, 232–240. <https://doi.org/10.22088/IJMCM.BUMS.8.3.232>
- Bezzi, P., Volterra, A., 2011. Astrocytes: Powering Memory. *Cell* 144, 644–645. <https://doi.org/10.1016/j.cell.2011.02.027>
- Bignami, A., Eng, L.F., Dahl, D., Uyeda, C.T., 1972. Localization of the glial fibrillary acidic protein in astrocytes by immunofluorescence. *Brain Research* 43, 429–435. [https://doi.org/10.1016/0006-8993\(72\)90398-8](https://doi.org/10.1016/0006-8993(72)90398-8)
- Birling, M.-C., Dierich, A., Jacquot, S., Héroult, Y., Pavlovic, G., 2012. Highly-efficient, fluorescent, locus directed cre and FlpO deleter mice on a pure C57BL/6N genetic background. *Genesis* 50, 482–489. <https://doi.org/10.1002/dvg.20826>
- Blanco-Luquin, I., Acha, B., Urdániz-Casado, A., Sánchez-Ruiz De Gordo, J., Vicuña-Urriza, J., Roldán, M., Labarga, A., Zelaya, M.V., Cabello, C., Méndez-López, I., Mendioroz, M., 2020. Early epigenetic changes of Alzheimer’s disease in the human hippocampus. *Epigenetics* 15, 1083–1092. <https://doi.org/10.1080/15592294.2020.1748917>
- Bloch, M.H., Hannestad, J., 2012. Omega-3 fatty acids for the treatment of depression: systematic review and meta-analysis. *Mol Psychiatry* 17, 1272–1282. <https://doi.org/10.1038/mp.2011.100>
- Bornscheuer, U.T., Kazlauskas, R.J., 2004. Catalytic Promiscuity in Biocatalysis: Using Old Enzymes to Form New Bonds and Follow New Pathways. *Angewandte Chemie International Edition* 43, 6032–6040. <https://doi.org/10.1002/anie.200460416>

Borsini, A., Nicolaou, A., Camacho-Muñoz, D., Kendall, A.C., Di Benedetto, M.G., Giacobbe, J., Su, K.-P., Pariante, C.M., 2021. Omega-3 polyunsaturated fatty acids protect against inflammation through production of LOX and CYP450 lipid mediators: relevance for major depression and for human hippocampal neurogenesis. *Mol Psychiatry* 26, 6773–6788. <https://doi.org/10.1038/s41380-021-01160-8>

Borsini, A., Stangl, D., Jeffries, A.R., Pariante, C.M., Thuret, S., 2020. The role of omega-3 fatty acids in preventing glucocorticoid-induced reduction in human hippocampal neurogenesis and increase in apoptosis. *Transl Psychiatry* 10, 219. <https://doi.org/10.1038/s41398-020-00908-0>

Bosch-Bouju, C., Larrieu, T., Linders, L., Manzoni, O.J., Layé, S., 2016. Endocannabinoid-Mediated Plasticity in Nucleus Accumbens Controls Vulnerability to Anxiety after Social Defeat Stress. *Cell Reports* 16, 1237–1242. <https://doi.org/10.1016/j.celrep.2016.06.082>

Bosetti, F., 2007. Arachidonic acid metabolism in brain physiology and pathology: lessons from genetically altered mouse models. *Journal of Neurochemistry* 102, 577–586. <https://doi.org/10.1111/j.1471-4159.2007.04558.x>

Boudrault, C., Bazinet, R.P., Ma, D.W.L., 2009. Experimental models and mechanisms underlying the protective effects of n-3 polyunsaturated fatty acids in Alzheimer's disease. *The Journal of Nutritional Biochemistry* 20, 1–10. <https://doi.org/10.1016/j.jnutbio.2008.05.016>

Bourre, J.-M., Pascal, G., Durand, G., Masson, M., Dumont, O., Piciotti, M., 1984. Alterations in the Fatty Acid Composition of Rat Brain Cells (Neurons, Astrocytes, and Oligodendrocytes) and of Subcellular Fractions (Myelin and Synaptosomes) Induced by a Diet Devoid of n-3 Fatty Acids. *J Neurochem* 43, 342–348. <https://doi.org/10.1111/j.1471-4159.1984.tb00906.x>

Bourre, J.-M., Durand, G., Pascal, G., Youyou, A., 1989. Brain Cell and Tissue Recovery in Rats Made Deficient in n-3 Fatty Acids by Alteration of Dietary Fat. *The Journal of Nutrition* 119, 15–22. <https://doi.org/10.1093/jn/119.1.15>

Bourre, J.M., Piciotti, M., 1992. Delta-6 desaturation of alpha-linolenic acid in brain and liver during development and aging in the mouse. *Neuroscience Letters* 141, 65–68. [https://doi.org/10.1016/0304-3940\(92\)90335-5](https://doi.org/10.1016/0304-3940(92)90335-5)

Bowen, R.A.R., Clandinin, M.T., 2005. Maternal dietary 22: 6n-3 is more effective than 18: 3n-3 in increasing the 22: 6n-3 content in phospholipids of glial cells from neonatal rat brain. *British Journal of Nutrition* 93, 601–611. <https://doi.org/10.1079/BJN20041390>

Bowman, G.L., Dodge, H.H., Guyonnet, S., Zhou, N., Donohue, J., Bichsel, A., Schmitt, J., Hooper, C., Bartfai, T., Andrieu, S., Vellas, B., MAPT/DSA Study Group, Vellas, B., Guyonnet, S., Carrié, I., Brigitte, L., Faisant, C., Lala, F., Delrieu, J., Villars, H., Combrouze, E., Badufle, C., Zueras, A., Andrieu, S., Cantet, C., Morin, C., Van Kan, G.A., Dupuy, C., Rolland, Y., Caillaud, C., Ousset, P., Lala, F., 2019. A blood-based nutritional risk index explains cognitive enhancement and decline in the multidomain Alzheimer prevention trial. *Alzheimer's & Dementia: Translational Research & Clinical Interventions* 5, 953–963. <https://doi.org/10.1016/j.trci.2019.11.004>

Braarud, H.C., Markhus, M.W., Skotheim, S., Stormark, K.M., Frøyland, L., Graff, I.E., Kjellevoid, M., 2018. Maternal DHA Status during Pregnancy Has a Positive Impact on Infant Problem Solving: A Norwegian Prospective Observation Study. *Nutrients* 10, E529. <https://doi.org/10.3390/nu10050529>

- Brand, A., Schonfeld, E., Isharel, I., Yavin, E., 2008. Docosahexaenoic acid-dependent iron accumulation in oligodendroglia cells protects from hydrogen peroxide-induced damage. *Journal of Neurochemistry* 105, 1325–1335. <https://doi.org/10.1111/j.1471-4159.2008.05234.x>
- Brantsæter, A.L., Englund-Ögge, L., Haugen, M., Birgisdottir, B.E., Knutsen, H.K., Sengpiel, V., Myhre, R., Alexander, J., Nilsen, R.M., Jacobsson, B., Meltzer, H.M., 2017. Maternal intake of seafood and supplementary long chain n-3 poly-unsaturated fatty acids and preterm delivery. *BMC Pregnancy Childbirth* 17, 41. <https://doi.org/10.1186/s12884-017-1225-8>
- Bredenhöft, J., Bhandari, D.R., Pflieger, F.J., Schulz, S., Kang, J.X., Layé, S., Roth, J., Gerstberger, R., Mayer, K., Spengler, B., Rummel, C., 2019. Visualizing and Profiling Lipids in the OVLT of Fat-1 and Wild Type Mouse Brains during LPS-Induced Systemic Inflammation Using AP-SMALDI MSI. *ACS Chem. Neurosci.* 10, 4394–4406. <https://doi.org/10.1021/acchemneuro.9b00435>
- Breder, C.D., 1997. Cyclooxygenase Systems in the Mammalian Brain. *Annals of the New York Academy of Sciences* 813, 296–301. <https://doi.org/10.1111/j.1749-6632.1997.tb51708.x>
- Breder, C.D., Dewitt, D., Kraig, R.P., 1995. Characterization of inducible cyclooxygenase in rat brain. *Journal of Comparative Neurology* 355, 296–315. <https://doi.org/10.1002/cne.903550208>
- Brenna, J.T., 2002. Efficiency of conversion of  $\alpha$ -linolenic acid to long chain n-3 fatty acids in man. *Current Opinion in Clinical Nutrition & Metabolic Care* 5, 127–132.
- Brenna, J.T., Diau, G.-Y., 2007. The influence of dietary docosahexaenoic acid and arachidonic acid on central nervous system polyunsaturated fatty acid composition. *Prostaglandins, Leukotrienes and Essential Fatty Acids* 77, 247–250. <https://doi.org/10.1016/j.plefa.2007.10.016>
- Bright, F., Werry, E.L., Dobson-Stone, C., Piguet, O., Ittner, L.M., Halliday, G.M., Hodges, J.R., Kiernan, M.C., Loy, C.T., Kassiou, M., Kril, J.J., 2019. Neuroinflammation in frontotemporal dementia. *Nat Rev Neurol* 15, 540–555. <https://doi.org/10.1038/s41582-019-0231-z>
- Britt, J.P., Benaliouad, F., McDevitt, R.A., Stuber, G.D., Wise, R.A., Bonci, A., 2012. Synaptic and Behavioral Profile of Multiple Glutamatergic Inputs to the Nucleus Accumbens. *Neuron* 76, 790–803. <https://doi.org/10.1016/j.neuron.2012.09.040>
- Buckley, C.D., Gilroy, D.W., Serhan, C.N., 2014. Proresolving Lipid Mediators and Mechanisms in the Resolution of Acute Inflammation. *Immunity* 40, 315–327. <https://doi.org/10.1016/j.immuni.2014.02.009>
- Burckhardt, M., Herke, M., Wustmann, T., Watzke, S., Langer, G., Fink, A., 2016. Omega-3 fatty acids for the treatment of dementia. *Cochrane Database of Systematic Reviews* 2016. <https://doi.org/10.1002/14651858.CD009002.pub3>
- Burdge, G.C., Calder, P.C., 2005. Conversion of  $\alpha$ -linolenic acid to longer-chain polyunsaturated fatty acids in human adults. *Reprod. Nutr. Dev.* 45, 581–597. <https://doi.org/10.1051/rnd:2005047>
- Burdge, G.C., Slater-Jefferies, J.L., Grant, R.A., Chung, W.-S., West, A.L., Lillycrop, K.A., Hanson, M.A., Calder, P.C., 2008. Sex, but not maternal protein or folic acid intake, determines the fatty acid composition of hepatic phospholipids, but not of triacylglycerol, in adult rats. *Prostaglandins, Leukotrienes and Essential Fatty Acids* 78, 73–79. <https://doi.org/10.1016/j.plefa.2007.10.028>

- Burr, G.O., Burr, M.M., 1930. ON THE NATURE AND RÔLE OF THE FATTY ACIDS ESSENTIAL IN NUTRITION. *Journal of Biological Chemistry* 86, 587–621. [https://doi.org/10.1016/S0021-9258\(20\)78929-5](https://doi.org/10.1016/S0021-9258(20)78929-5)
- Burr, G.O., Burr, M.M., 1929. A NEW DEFICIENCY DISEASE PRODUCED BY THE RIGID EXCLUSION OF FAT FROM THE DIET. *Journal of Biological Chemistry* 82, 345–367. [https://doi.org/10.1016/S0021-9258\(20\)78281-5](https://doi.org/10.1016/S0021-9258(20)78281-5)
- Bushong, E.A., Martone, M.E., Ellisman, M.H., 2004. Maturation of astrocyte morphology and the establishment of astrocyte domains during postnatal hippocampal development. *International Journal of Developmental Neuroscience* 22, 73–86. <https://doi.org/10.1016/j.ijdevneu.2003.12.008>
- Bystrom, J., Wray, J.A., Sugden, M.C., Holness, M.J., Swales, K.E., Warner, T.D., Edin, M.L., Zeldin, D.C., Gilroy, D.W., Bishop-Bailey, D., 2011. Endogenous Epoxygenases Are Modulators of Monocyte/Macrophage Activity. *PLOS ONE* 6, e26591. <https://doi.org/10.1371/journal.pone.0026591>
- Calandria, J.M., Marcheselli, V.L., Mukherjee, P.K., Uddin, J., Winkler, J.W., Petasis, N.A., Bazan, N.G., 2009. Selective Survival Rescue in 15-Lipoxygenase-1-deficient Retinal Pigment Epithelial Cells by the Novel Docosahexaenoic Acid-derived Mediator, Neuroprotectin D1 \*. *Journal of Biological Chemistry* 284, 17877–17882. <https://doi.org/10.1074/jbc.M109.003988>
- Calder, A.J., Beaver, J.D., Winston, J.S., Dolan, R.J., Jenkins, R., Eger, E., Henson, R.N.A., 2007. Separate Coding of Different Gaze Directions in the Superior Temporal Sulcus and Inferior Parietal Lobule. *Current Biology* 17, 20–25. <https://doi.org/10.1016/j.cub.2006.10.052>
- Calder, P.C., 2001. Polyunsaturated fatty acids, inflammation, and immunity. *FATTY ACIDS* 36, 18.
- Calderon, F., Kim, H.-Y., 2004. Docosahexaenoic acid promotes neurite growth in hippocampal neurons. *J Neurochem* 90, 979–988. <https://doi.org/10.1111/j.1471-4159.2004.02520.x>
- Calon, F., Lim, G.P., Yang, F., Morihara, T., Teter, B., Ubeda, O., Rostaing, P., Triller, A., Salem, N., Ashe, K.H., Frautschy, S.A., Cole, G.M., 2004. Docosahexaenoic Acid Protects from Dendritic Pathology in an Alzheimer’s Disease Mouse Model. *Neuron* 43, 633–645. <https://doi.org/10.1016/j.neuron.2004.08.013>
- Cao, D., Kevala, K., Kim, J., Moon, H.-S., Jun, S.B., Lovinger, D., Kim, H.-Y., 2009. Docosahexaenoic acid promotes hippocampal neuronal development and synaptic function. *Journal of Neurochemistry* 111, 510–521. <https://doi.org/10.1111/j.1471-4159.2009.06335.x>
- Capuron, L., Castanon, N., 2014. La dépression, due à une inflammation ? *Cerveau et Psycho.* 63, 70.
- Carlson, G., Wang, Y., Alger, B.E., 2002. Endocannabinoids facilitate the induction of LTP in the hippocampus. *Nat Neurosci* 5, 723–724. <https://doi.org/10.1038/nn879>
- Carlson, S.E., Gajewski, B.J., Valentine, C.J., Kerling, E.H., Weiner, C.P., Cackovic, M., Buhimschi, C.S., Rogers, L.K., Sands, S.A., Brown, A.R., Mudaranthakam, D.P., Crawford, S.A., DeFranco, E.A., 2021. Higher dose docosahexaenoic acid supplementation during pregnancy and early preterm birth: A randomised, double-blind, adaptive-design superiority trial. *EclinicalMedicine* 36, 100905. <https://doi.org/10.1016/j.eclinm.2021.100905>



- Carlson, S.E., Neuringer, M., 1999. Polyunsaturated fatty acid status and neurodevelopment: A summary and critical analysis of the literature. *Lipids* 34, 171–178. <https://doi.org/10.1007/s11745-999-0351-2>
- Carrié, I., Clément, M., de Javel, D., Francès, H., Bourre, J.-M., 2000a. Specific phospholipid fatty acid composition of brain regions in mice: effects of n-3 polyunsaturated fatty acid deficiency and phospholipid supplementation. *Journal of Lipid Research* 41, 465–472. [https://doi.org/10.1016/S0022-2275\(20\)34485-0](https://doi.org/10.1016/S0022-2275(20)34485-0)
- Carrié, I., Clément, M., de Javel, D., Francès, H., Bourre, J.-M., 2000b. Phospholipid supplementation reverses behavioral and biochemical alterations induced by n-3 polyunsaturated fatty acid deficiency in mice. *Journal of Lipid Research* 41, 473–480. [https://doi.org/10.1016/S0022-2275\(20\)34486-2](https://doi.org/10.1016/S0022-2275(20)34486-2)
- Carver, C.S., 2001. Affect and the Functional Bases of Behavior: On the Dimensional Structure of Affective Experience. *Pers Soc Psychol Rev* 5, 345–356. [https://doi.org/10.1207/S15327957PSPR0504\\_4](https://doi.org/10.1207/S15327957PSPR0504_4)
- Castillo, P.E., Younts, T.J., Chávez, A.E., Hashimoto, Y., 2012. Endocannabinoid signaling and synaptic function. *Neuron* 76, 70–81. <https://doi.org/10.1016/j.neuron.2012.09.020>
- Castro, L.F.C., Tocher, D.R., Monroig, O., 2016. Long-chain polyunsaturated fatty acid biosynthesis in chordates: Insights into the evolution of Fads and Elovl gene repertoire. *Prog Lipid Res* 62, 25–40. <https://doi.org/10.1016/j.plipres.2016.01.001>
- Chai, H., Diaz-Castro, B., Shigetomi, E., Monte, E., Octeau, J.C., Yu, X., Cohn, W., Rajendran, P.S., Vondriska, T.M., Whitelegge, J.P., Coppola, G., Khakh, B.S., 2017. Neural Circuit-Specialized Astrocytes: Transcriptomic, Proteomic, Morphological, and Functional Evidence. *Neuron* 95, 531–549.e9. <https://doi.org/10.1016/j.neuron.2017.06.029>
- Chalon, S., 2006. Omega-3 fatty acids and monoamine neurotransmission. *Prostaglandins, Leukotrienes and Essential Fatty Acids, The Emerging Role of Omega-3 Fatty Acids in Psychiatry* 75, 259–269. <https://doi.org/10.1016/j.plefa.2006.07.005>
- Champeil-Potokar, G., Chaumontet, C., Guesnet, P., Lavialle, M., Denis, I., 2006. Docosahexaenoic acid (22:6n-3) enrichment of membrane phospholipids increases gap junction coupling capacity in cultured astrocytes. *European Journal of Neuroscience* 24, 3084–3090. <https://doi.org/10.1111/j.1460-9568.2006.05185.x>
- Chan, J.P., Wong, B.H., Chin, C.F., Galam, D.L.A., Foo, J.C., Wong, L.C., Ghosh, S., Wenk, M.R., Cazenave-Gassiot, A., Silver, D.L., 2018. The lysolipid transporter Mfsd2a regulates lipogenesis in the developing brain. *PLoS Biol* 16, e2006443. <https://doi.org/10.1371/journal.pbio.2006443>
- Chataigner, M., Lucas, C., Di Miceli, M., Pallet, V., Laye, S., Mehaignerie, A., Bouvret, E., Diné, A.-L., Joffre, C., 2021. Dietary Fish Hydrolysate Improves Memory Performance Through Microglial Signature Remodeling During Aging. *Frontiers in Nutrition* 8.
- Chaudhry, F.A., Reimer, R.J., Edwards, R.H., 2002. The glutamine commute. *J Cell Biol* 157, 349–355. <https://doi.org/10.1083/jcb.200201070>
- Chen, C., Bazan, N.G., 2005. Endogenous PGE2 Regulates Membrane Excitability and Synaptic Transmission in Hippocampal CA1 Pyramidal Neurons. *Journal of Neurophysiology* 93, 929–941. <https://doi.org/10.1152/jn.00696.2004>

- Chen, C., Magee, J.C., Bazan, N.G., 2002. Cyclooxygenase-2 regulates prostaglandin E2 signaling in hippocampal long-term synaptic plasticity. *J Neurophysiol* 87, 2851–2857. <https://doi.org/10.1152/jn.2002.87.6.2851>
- Chen, C.T., Bazinet, R.P., 2015.  $\beta$ -oxidation and rapid metabolism, but not uptake regulate brain eicosapentaenoic acid levels. *Prostaglandins, Leukotrienes and Essential Fatty Acids*, Special issue: Proceedings of the 11th FACS meeting 92, 33–40. <https://doi.org/10.1016/j.plefa.2014.05.007>
- Chen, C.T., Liu, Z., Ouellet, M., Calon, F., Bazinet, R.P., 2009. Rapid  $\beta$ -oxidation of eicosapentaenoic acid in mouse brain: An in situ study. *Prostaglandins, Leukotrienes and Essential Fatty Acids* 80, 157–163. <https://doi.org/10.1016/j.plefa.2009.01.005>
- Chernick, D., Ortiz-Valle, S., Jeong, A., Qu, W., Li, L., 2019. Peripheral versus central nervous system APOE in Alzheimer's disease: Interplay across the blood-brain barrier. *Neuroscience Letters* 708, 134306. <https://doi.org/10.1016/j.neulet.2019.134306>
- Chiang, N., Arita, M., Serhan, C.N., 2005. Anti-inflammatory circuitry: Lipoxin, aspirin-triggered lipoxins and their receptor ALX. *Prostaglandins, Leukotrienes and Essential Fatty Acids* 73, 163–177. <https://doi.org/10.1016/j.plefa.2005.05.003>
- Chiang, N., Dalli, J., Colas, R.A., Serhan, C.N., 2015. Identification of resolvin D2 receptor mediating resolution of infections and organ protection. *Journal of Experimental Medicine* 212, 1203–1217. <https://doi.org/10.1084/jem.20150225>
- Chiang, N., Serhan, C.N., 2017. Structural elucidation and physiologic functions of specialized pro-resolving mediators and their receptors. *Molecular Aspects of Medicine, The Physiology and Pharmacology of Specilized Pro-Resolving Mediators* 58, 114–129. <https://doi.org/10.1016/j.mam.2017.03.005>
- Childs, S., Lynch, C.O., Hennessy, A.A., Stanton, C., Wathes, D.C., Sreenan, J.M., Diskin, M.G., Kenny, D.A., 2008. Effect of dietary enrichment with either n-3 or n-6 fatty acids on systemic metabolite and hormone concentration and ovarian function in heifers. *Animal* 2, 883–893. <https://doi.org/10.1017/S1751731108002115>
- Chinnici, C.M., Yao, Y., Praticò, D., 2007. The 5-lipoxygenase enzymatic pathway in the mouse brain: Young versus old. *Neurobiology of Aging* 28, 1457–1462. <https://doi.org/10.1016/j.neurobiolaging.2006.06.007>
- Chiurchiù, V., Leuti, A., Maccarrone, M., 2018. Bioactive Lipids and Chronic Inflammation: Managing the Fire Within. *Frontiers in Immunology* 9.
- Chiurchiù, V., Leuti, A., Saracini, S., Fontana, D., Finamore, P., Giua, R., Padovini, L., Incalzi, R.A., Maccarrone, M., 2019. Resolution of inflammation is altered in chronic heart failure and entails a dysfunctional responsiveness of T lymphocytes. *The FASEB Journal* 33, 909–916. <https://doi.org/10.1096/fj.201801017R>
- Choi, S.-H., Aid, S., Bosetti, F., 2009. The distinct roles of cyclooxygenase-1 and -2 in neuroinflammation: implications for translational research. *Trends in Pharmacological Sciences* 30, 174–181. <https://doi.org/10.1016/j.tips.2009.01.002>
- Christmas, P., 2015. Chapter Six - Role of Cytochrome P450s in Inflammation, in: Hardwick, J.P. (Ed.), *Advances in Pharmacology, Cytochrome P450 Function and Pharmacological Roles in Inflammation and Cancer*. Academic Press, pp. 163–192. <https://doi.org/10.1016/bs.apha.2015.03.005>

- Chung, W.-L., Chen, J.-J., Su, H.-M., 2008. Fish Oil Supplementation of Control and (n-3) Fatty Acid-Deficient Male Rats Enhances Reference and Working Memory Performance and Increases Brain Regional Docosahexaenoic Acid Levels. *The Journal of Nutrition* 138, 1165–1171. <https://doi.org/10.1093/jn/138.6.1165>
- Chytrova, G., Ying, Z., Gomez-Pinilla, F., 2010. Exercise contributes to the effects of DHA dietary supplementation by acting on membrane-related synaptic systems. *Brain Research* 1341, 32–40. <https://doi.org/10.1016/j.brainres.2009.05.018>
- Cisbani, G., Metherel, A.H., Smith, M.E., Bazinet, R.P., 2021. Murine and human microglial cells are relatively enriched with eicosapentaenoic acid compared to the whole brain. *Neurochemistry International* 150, 105154. <https://doi.org/10.1016/j.neuint.2021.105154>
- Citri, A., Malenka, R.C., 2008. Synaptic Plasticity: Multiple Forms, Functions, and Mechanisms. *Neuropsychopharmacol* 33, 18–41. <https://doi.org/10.1038/sj.npp.1301559>
- Clandinin, M.T., Chappell, J.E., Leong, S., Heim, T., Swyer, P.R., Chance, G.W., 1980. Intrauterine fatty acid accretion rates in human brain: implications for fatty acid requirements. *Early Human Development* 4, 121–129. [https://doi.org/10.1016/0378-3782\(80\)90015-8](https://doi.org/10.1016/0378-3782(80)90015-8)
- Clarke, L.E., Barres, B.A., 2013. Emerging roles of astrocytes in neural circuit development. *Nat Rev Neurosci* 14, 311–321. <https://doi.org/10.1038/nrn3484>
- Clarke, S.E., Kang, J.X., Ma, D.W.L., 2014. The iFat1 transgene permits conditional endogenous n-3 PUFA enrichment both in vitro and in vivo. *Transgenic Res* 23, 489–501. <https://doi.org/10.1007/s11248-014-9788-x>
- Colas, R.A., Dalli, J., Chiang, N., Vlasakov, I., Sanger, J.M., Riley, I.R., Serhan, C.N., 2016. Identification and Actions of the Maresin 1 Metabolome in Infectious Inflammation. *The Journal of Immunology* 197, 4444–4452. <https://doi.org/10.4049/jimmunol.1600837>
- Coley, N., Raman, R., Donohue, M.C., Aisen, P.S., Vellas, B., Andrieu, S., 2018. Defining the Optimal Target Population for Trials of Polyunsaturated Fatty Acid Supplementation Using the Erythrocyte Omega-3 Index: A Step Towards Personalized Prevention of Cognitive Decline? *J Nutr Health Aging* 22, 982–988. <https://doi.org/10.1007/s12603-018-1052-2>
- Colucci, P., De Castro, V., Peloso, A., Splendori, M., Trezza, V., Campolongo, P., 2020. Perinatal exposure to omega-3 fatty acid imbalance leads to early behavioral alterations in rat pups. *Behavioural Brain Research* 392, 112723. <https://doi.org/10.1016/j.bbr.2020.112723>
- Compton, D., 2004. Behavior strategy learning in rat: effects of lesions of the dorsal striatum or dorsal hippocampus. *Behavioural Processes* 67, 335–342. [https://doi.org/10.1016/S0376-6357\(04\)00139-1](https://doi.org/10.1016/S0376-6357(04)00139-1)
- Corder, E.H., Saunders, A.M., Strittmatter, W.J., Schmechel, D.E., Gaskell, P.C., Small, G.W., Roses, A.D., Haines, J.L., Pericak-Vance, M.A., 1993. Gene Dose of Apolipoprotein E Type 4 Allele and the Risk of Alzheimer's Disease in Late Onset Families. *Science* 261, 921–923. <https://doi.org/10.1126/science.8346443>
- Corkrum, M., Araque, A., 2021. Astrocyte-neuron signaling in the mesolimbic dopamine system: the hidden stars of dopamine signaling. *Neuropsychopharmacology* 46, 1864–1872. <https://doi.org/10.1038/s41386-021-01090-7>

- Costa, A., Rani, B., Bastiaanssen, T.F.S., Bonfiglio, F., Gunnigle, E., Provensi, G., Rossitto, M., Boehme, M., Strain, C., Martínez, C.S., Blandina, P., Cryan, J.F., Layé, S., Corradetti, R., Passani, M.B., 2022. Diet Prevents Social Stress-Induced Maladaptive Neurobehavioural and Gut Microbiota Changes in a Histamine-Dependent Manner. *Int J Mol Sci* 23, 862. <https://doi.org/10.3390/ijms23020862>
- Covelo, A., Eraso-Pichot, A., Fernández-Moncada, I., Serrat, R., Marsicano, G., 2021. CB1R-dependent regulation of astrocyte physiology and astrocyte-neuron interactions. *Neuropharmacology* 195, 108678. <https://doi.org/10.1016/j.neuropharm.2021.108678>
- Cribb, L., Murphy, J., Froud, A., Oliver, G., Bousman, C.A., Ng, C.H., Sarris, J., 2018. Erythrocyte polyunsaturated fatty acid composition is associated with depression and FADS genotype in Caucasians. *Nutritional Neuroscience* 21, 589–601. <https://doi.org/10.1080/1028415X.2017.1327685>
- Cunnane, S.C., Francescutti, V., Brenna, J.T., Crawford, M.A., 2000. Breast-fed infants achieve a higher rate of brain and whole body docosahexaenoate accumulation than formula-fed infants not consuming dietary docosahexaenoate. *Lipids* 35, 105–111. <https://doi.org/10.1007/s11745-000-0501-6>
- Da Mesquita, S., Fu, Z., Kipnis, J., 2018. The Meningeal Lymphatic System: A New Player in Neurophysiology. *Neuron* 100, 375–388. <https://doi.org/10.1016/j.neuron.2018.09.022>
- Dalli, J., Chiang, N., Serhan, C.N., 2015. Elucidation of novel 13-series resolvins that increase with atorvastatin and clear infections. *Nat Med* 21, 1071–1075. <https://doi.org/10.1038/nm.3911>
- Dalli, J., Colas, R.A., Serhan, C.N., 2013. Novel n-3 Immunoresolvents: Structures and Actions. *Sci Rep* 3, 1940. <https://doi.org/10.1038/srep01940>
- Danbolt, N.C., 2001. Glutamate uptake. *Progress in Neurobiology* 65, 1–105. [https://doi.org/10.1016/S0301-0082\(00\)00067-8](https://doi.org/10.1016/S0301-0082(00)00067-8)
- Dantzer, R., 2001. Cytokine-Induced Sickness Behavior: Mechanisms and Implications. *Annals of the New York Academy of Sciences* 933, 222–234. <https://doi.org/10.1111/j.1749-6632.2001.tb05827.x>
- Dantzer, R., O'Connor, J.C., Freund, G.G., Johnson, R.W., Kelley, K.W., 2008. From inflammation to sickness and depression: when the immune system subjugates the brain. *Nat Rev Neurosci* 9, 46–56. <https://doi.org/10.1038/nrn2297>
- Daoudal, G., Debanne, D., 2003. Long-term plasticity of intrinsic excitability: learning rules and mechanisms. *Learn Mem* 10, 456–465. <https://doi.org/10.1101/lm.64103>
- D'Ascenzo, M., Fellin, T., Terunuma, M., Revilla-Sanchez, R., Meaney, D.F., Auberson, Y.P., Moss, S.J., Haydon, P.G., 2007. mGluR5 stimulates gliotransmission in the nucleus accumbens. *Proceedings of the National Academy of Sciences* 104, 1995–2000. <https://doi.org/10.1073/pnas.0609408104>
- Davidson, J., Abul, H., Milton, A., Rotondo, D., 2001. Cytokines and cytokine inducers stimulate prostaglandin E2 entry into the brain. *Pflügers Arch - Eur J Physiol* 442, 526–533. <https://doi.org/10.1007/s004240100572>
- Dawson, G., 2015. Measuring brain lipids. *Biochimica et Biophysica Acta (BBA) - Molecular and Cell Biology of Lipids*, Brain Lipids 1851, 1026–1039. <https://doi.org/10.1016/j.bbalip.2015.02.007>

de Groot, R.H.M., Meyer, B.J., 2020. ISSFAL Official Statement Number 6: The importance of measuring blood omega-3 long chain polyunsaturated fatty acid levels in research. *Prostaglandins, Leukotrienes and Essential Fatty Acids* 157, 102029. <https://doi.org/10.1016/j.plefa.2019.102029>

De Keyser, J., Mostert, J.P., Koch, M.W., 2008. Dysfunctional astrocytes as key players in the pathogenesis of central nervous system disorders. *Journal of the Neurological Sciences* 267, 3–16. <https://doi.org/10.1016/j.jns.2007.08.044>

De Meij, J., Alfaneq, Z., Morel, L., Decoeur, F., Leyrolle, Q., Picard, K., Carrier, M., Aubert, A., Séré, A., Lucas, C., Laforest, G., Helbling, J.-C., Tremblay, M.-E., Cota, D., Moisan, M.-P., Marsicano, G., Layé, S., Nadjar, A., 2021a. Microglial Cannabinoid Type 1 Receptor Regulates Brain Inflammation in a Sex-Specific Manner. *Cannabis Cannabinoid Res* 6, 488–507. <https://doi.org/10.1089/can.2020.0170>

De Meij, J., Alfaneq, Z., Morel, L., Decoeur, F., Leyrolle, Q., Picard, K., Carrier, M., Aubert, A., Séré, A., Lucas, C., Laforest, G., Helbling, J.-C., Tremblay, M.-E., Cota, D., Moisan, M.-P., Marsicano, G., Layé, S., Nadjar, A., 2021b. Microglial Cannabinoid Type 1 Receptor Regulates Brain Inflammation in a Sex-Specific Manner. *Cannabis and Cannabinoid Research* 6, 488–507. <https://doi.org/10.1089/can.2020.0170>

Deák, F., Anderson, R.E., Fessler, J.L., Sherry, D.M., 2019. Novel Cellular Functions of Very Long Chain-Fatty Acids: Insight From ELOVL4 Mutations. *Frontiers in Cellular Neuroscience* 13.

Delion, S., Chalon, S., Guilloteau, D., Lejeune, B., Besnard, J.C., Durand, G., 1997. Age-related changes in phospholipid fatty acid composition and monoaminergic neurotransmission in the hippocampus of rats fed a balanced or an n-3 polyunsaturated fatty acid-deficient diet. *Journal of Lipid Research* 38, 680–689. [https://doi.org/10.1016/S0022-2275\(20\)37235-7](https://doi.org/10.1016/S0022-2275(20)37235-7)

Delpech, J.-C., Thomazeau, A., Madore, C., Bosch-Bouju, C., Larrieu, T., Lacabanne, C., Remus-Borel, J., Aubert, A., Joffre, C., Nadjar, A., Layé, S., 2015. Dietary n-3 PUFAs Deficiency Increases Vulnerability to Inflammation-Induced Spatial Memory Impairment. *Neuropsychopharmacology* 40, 2774–2787. <https://doi.org/10.1038/npp.2015.127>

DeMar, J.C., Ma, K., Bell, J.M., Igarashi, M., Greenstein, D., Rapoport, S.I., 2006. One generation of n-3 polyunsaturated fatty acid deprivation increases depression and aggression test scores in rats. *Journal of Lipid Research* 47, 172–180. <https://doi.org/10.1194/jlr.M500362-JLR200>

Demers, G., Roy, J., Machuca-Parra, A.I., Dashtehei pour, Z., Bairamian, D., Daneault, C., Rosiers, C.D., Ferreira, G., Alquier, T., Fulton, S., 2020. Fish oil supplementation alleviates metabolic and anxiodepressive effects of diet-induced obesity and associated changes in brain lipid composition in mice. *Int J Obes* 44, 1936–1945. <https://doi.org/10.1038/s41366-020-0623-6>

Deng, B., Wang, C.-W., Arnardottir, H.H., Li, Y., Cheng, C.-Y.C., Dalli, J., Serhan, C.N., 2014. Maresin Biosynthesis and Identification of Maresin 2, a New Anti-Inflammatory and Pro-Resolving Mediator from Human Macrophages. *PLOS ONE* 9, e102362. <https://doi.org/10.1371/journal.pone.0102362>

Derada Troletti, C., Fontijn, R.D., Gowing, E., Charabati, M., van Het Hof, B., Didouh, I., van der Pol, S.M.A., Geerts, D., Prat, A., van Horssen, J., Kooij, G., de Vries, H.E., 2019. Inflammation-induced endothelial to mesenchymal transition promotes brain endothelial cell dysfunction and occurs during multiple sclerosis pathophysiology. *Cell Death Dis* 10, 1–13. <https://doi.org/10.1038/s41419-018-1294-2>

- Dere, E., Huston, J.P., De Souza Silva, M.A., 2007. The pharmacology, neuroanatomy and neurogenetics of one-trial object recognition in rodents. *Neuroscience & Biobehavioral Reviews* 31, 673–704. <https://doi.org/10.1016/j.neubiorev.2007.01.005>
- Destailats, F., Joffre, C., Acar, N., Joffre, F., Bezelgues, J.-B., Pasquis, B., Cruz-Hernandez, C., Rezzi, S., Montoliu, I., Dionisi, F., Bretillon, L., 2010. Differential effect of maternal diet supplementation with  $\alpha$ -Linolenic acid or n-3 long-chain polyunsaturated fatty acids on glial cell phosphatidylethanolamine and phosphatidylserine fatty acid profile in neonate rat brains. *Nutr Metab (Lond)* 7, 2. <https://doi.org/10.1186/1743-7075-7-2>
- Deyama, S., Shimoda, K., Suzuki, H., Ishikawa, Y., Ishimura, K., Fukuda, H., Hitora-Imamura, N., Ide, S., Satoh, M., Kaneda, K., Shuto, S., Minami, M., 2018. Resolvin E1/E2 ameliorate lipopolysaccharide-induced depression-like behaviors via ChemR23. *Psychopharmacology* 235, 329–336. <https://doi.org/10.1007/s00213-017-4774-7>
- Di Gregorio, E., Borroni, B., Giorgio, E., Lacerenza, D., Ferrero, M., Lo Buono, N., Ragusa, N., Mancini, C., Gaussen, M., Calcia, A., Mitro, N., Hoxha, E., Mura, I., Coviello, D.A., Moon, Y.-A., Tesson, C., Vaula, G., Couarch, P., Orsi, L., Duregon, E., Papotti, M.G., Deleuze, J.-F., Imbert, J., Costanzi, C., Padovani, A., Giunti, P., Maillat-Vioud, M., Durr, A., Brice, A., Tempia, F., Funaro, A., Boccone, L., Caruso, D., Stevanin, G., Brusco, A., 2014. ELOVL5 Mutations Cause Spinocerebellar Ataxia 38. *The American Journal of Human Genetics* 95, 209–217. <https://doi.org/10.1016/j.ajhg.2014.07.001>
- Di Marzo, V., 2020. The endocannabinoidome as a substrate for noneuphoric phytocannabinoid action and gut microbiome dysfunction in neuropsychiatric disorders. *Dialogues in Clinical Neuroscience* 22, 259–269. <https://doi.org/10.31887/DCNS.2020.22.3/vdimarzo>
- Di Miceli, M., Martinat, M., Bosch-Bouju, C., Layé, S., 2020. Régulation de l'excitabilité neuronale et de la plasticité synaptique dans le striatum ventral par le contenu alimentaire en omega-3. *Nutrition Clinique et Métabolisme* 34, 36. <https://doi.org/10.1016/j.nupar.2020.02.236>
- Di Miceli, M., Martinat, M., Rossitto, M., Aubert, A., Alashmali, S., Bosch-Bouju, C., Fioramonti, X., Joffre, C., Bazinet, R.P., Layé, S., 2022. Dietary Long-Chain n-3 Polyunsaturated Fatty Acid Supplementation Alters Electrophysiological Properties in the Nucleus Accumbens and Emotional Behavior in Naïve and Chronically Stressed Mice. *International Journal of Molecular Sciences* 23, 6650. <https://doi.org/10.3390/ijms23126650>
- Di Paolo, G., Kim, T.-W., 2011. Linking lipids to Alzheimer's disease: cholesterol and beyond. *Nat Rev Neurosci* 12, 284–296. <https://doi.org/10.1038/nrn3012>
- Dinel, A.L., Rey, C., Baudry, C., Fressange-Mazda, C., Le Ruyet, P., Nadjar, A., Pallet, P., Joffre, C., Layé, S., 2016. Enriched dairy fat matrix diet prevents early life lipopolysaccharide-induced spatial memory impairment at adulthood. *Prostaglandins, Leukotrienes and Essential Fatty Acids* 113, 9–18. <https://doi.org/10.1016/j.plefa.2016.08.013>
- DiRusso, C.C., Li, H., Darwis, D., Watkins, P.A., Berger, J., Black, P.N., 2005. Comparative Biochemical Studies of the Murine Fatty Acid Transport Proteins (FATP) Expressed in Yeast. *Journal of Biological Chemistry* 280, 16829–16837. <https://doi.org/10.1074/jbc.M409598200>
- Dong, X., Tan, P., Cai, Z., Xu, Hanlin, Li, J., Ren, W., Xu, Houguo, Zuo, R., Zhou, J., Mai, K., Ai, Q., 2017. Regulation of FADS2 transcription by SREBP-1 and PPAR- $\alpha$  influences LC-PUFA biosynthesis in fish. *Sci Rep* 7, 40024. <https://doi.org/10.1038/srep40024>

Drouin, G., Rioux, V., Legrand, P., 2019. The n-3 docosapentaenoic acid (DPA): A new player in the n-3 long chain polyunsaturated fatty acid family. *Biochimie, Fatty acids and lipopolysaccharides from health to disease* 159, 36–48. <https://doi.org/10.1016/j.biochi.2019.01.022>

Du, H., Chen, X., Zhang, J., Chen, C., 2011. Inhibition of COX-2 expression by endocannabinoid 2-arachidonoylglycerol is mediated via PPAR- $\gamma$ : PPAR $\gamma$  in 2-AG suppression of COX-2. *British Journal of Pharmacology* 163, 1533–1549. <https://doi.org/10.1111/j.1476-5381.2011.01444.x>

Duchaine, C.S., Fiocco, A.J., Carmichael, P.-H., Cunnane, S.C., Plourde, M., Lampuré, A., Allès, B., Belleville, S., Gaudreau, P., Presse, N., Ferland, G., Laurin, D., 2022. Serum  $\omega$ -3 Fatty Acids and Cognitive Domains in Community-Dwelling Older Adults from the NuAge Study: Exploring the Associations with Other Fatty Acids and Sex. *The Journal of Nutrition* 152, 2117–2124. <https://doi.org/10.1093/jn/nxac110>

Ducrocq, F., Walle, R., Contini, A., Oummadi, A., Caraballo, B., van der Veldt, S., Boyer, M.-L., Aby, F., Tolentino-Cortez, T., Helbling, J.-C., Martine, L., Grégoire, S., Cabaret, S., Vancassel, S., Layé, S., Kang, J.X., Fioramonti, X., Berdeaux, O., Barreda-Gómez, G., Masson, E., Ferreira, G., Ma, D.W.L., Bosch-Bouju, C., De Smedt-Peyrusse, V., Trifilieff, P., 2020. Causal Link between n-3 Polyunsaturated Fatty Acid Deficiency and Motivation Deficits. *Cell Metabolism* 31, 755-772.e7. <https://doi.org/10.1016/j.cmet.2020.02.012>

Dyall, S.C., Michael, G.J., Whelpton, R., Scott, A.G., Michael-Titus, A.T., 2007. Dietary enrichment with omega-3 polyunsaturated fatty acids reverses age-related decreases in the GluR2 and NR2B glutamate receptor subunits in rat forebrain. *Neurobiology of Aging* 28, 424–439. <https://doi.org/10.1016/j.neurobiolaging.2006.01.002>

Ebright, B., Assante, I., Poblete, R.A., Wang, S., Duro, M.V., Bennett, D.A., Arvanitakis, Z., Louie, S.G., Yassine, H.N., 2022. Eicosanoid lipidome activation in post-mortem brain tissues of individuals with APOE4 and Alzheimer's dementia. *Alzheimers Res Ther* 14, 152. <https://doi.org/10.1186/s13195-022-01084-7>

Emken, E.A., 1994. Metabolism of dietary stearic acid relative to other fatty acids in human subjects. *The American Journal of Clinical Nutrition* 60, 1023S-1028S. <https://doi.org/10.1093/ajcn/60.6.1023S>

Emre, C., Arroyo-García, L.E., Do, K.V., Jun, B., Ohshima, M., Alcalde, S.G., Cothorn, M.L., Maioli, S., Nilsson, P., Hjorth, E., Fisahn, A., Bazan, N.G., Schultzberg, M., 2021. Intranasal delivery of pro-resolving lipid mediators rescues memory and gamma oscillation impairment in AppNL-G-F/NL-G-F mice. *Commun Biol* 5, 245. <https://doi.org/10.1038/s42003-022-03169-3>

Emre, C., Hjorth, E., Bharani, K., Carroll, S., Granholm, A.-C., Schultzberg, M., 2020. Receptors for pro-resolving mediators are increased in Alzheimer's disease brain. *Brain Pathology* 30, 614–640. <https://doi.org/10.1111/bpa.12812>

Escartin, C., Galea, E., Lakatos, A., O'Callaghan, J.P., Petzold, G.C., Serrano-Pozo, A., Steinhäuser, C., Volterra, A., Carmignoto, G., Agarwal, A., Allen, N.J., Araque, A., Barbeito, L., Barzilai, A., Bergles, D.E., Bonvento, G., Butt, A.M., Chen, W.-T., Cohen-Salmon, M., Cunningham, C., Deneen, B., De Strooper, B., Díaz-Castro, B., Farina, C., Freeman, M., Gallo, V., Goldman, J.E., Goldman, S.A., Götz, M., Gutiérrez, A., Haydon, P.G., Heiland, D.H., Hol, E.M., Holt, M.G., Iino, M., Kastanenka, K.V., Kettenmann, H., Khakh, B.S., Koizumi, S., Lee, C.J., Liddelow, S.A., MacVicar, B.A., Magistretti, P., Messing, A., Mishra, A., Molofsky, A.V., Murai, K.K., Norris, C.M., Okada, S., Oliet, S.H.R., Oliveira, J.F., Panatier, A., Parpura, V., Pekna, M., Pekny, M., Pellerin, L., Perea, G., Pérez-Nievas, B.G., Pflieger, F.W., Poskanzer, K.E., Quintana, F.J., Ransohoff, R.M., Riquelme-Perez, M., Robel, S., Rose, C.R., Rothstein, J.D., Rouach, N., Rowitch, D.H., Semyanov, A., Sirko, S., Sontheimer, H., Swanson, R.A.,

- Vitorica, J., Wanner, I.-B., Wood, L.B., Wu, J., Zheng, B., Zimmer, E.R., Zorec, R., Sofroniew, M.V., Verkhatsky, A., 2021. Reactive astrocyte nomenclature, definitions, and future directions. *Nat Neurosci* 24, 312–325. <https://doi.org/10.1038/s41593-020-00783-4>
- Extier, A., Langelier, B., Perruchot, M.-H., Guesnet, P., Van Veldhoven, P.P., Lavielle, M., Alessandri, J.-M., 2010. Gender affects liver desaturase expression in a rat model of n-3 fatty acid repletion. *The Journal of Nutritional Biochemistry* 21, 180–187. <https://doi.org/10.1016/j.jnutbio.2008.10.008>
- Facchinetti, F., Del Giudice, E., Furegato, S., Passarotto, M., Leon, A., 2003. Cannabinoids ablate release of TNF $\alpha$  in rat microglial cells stimulated with lyopolysaccharide. *Glia* 41, 161–168. <https://doi.org/10.1002/glia.10177>
- Fairbairn, P., Tsofliou, F., Johnson, A., Dyall, S.C., 2020. Effects of a high-DHA multi-nutrient supplement and exercise on mobility and cognition in older women (MOBILE): a randomised semi-blinded placebo-controlled study. *British Journal of Nutrition* 124, 146–155. <https://doi.org/10.1017/S0007114520000719>
- Fares, S., Sethom, M.M., Hammami, M.B., Cheour, M., Feki, M., Hadj-Taieb, S., Kacem, S., 2017. Postnatal RBC arachidonic and docosahexaenoic acids deficiencies are associated with higher risk of neonatal morbidities and mortality in preterm infants. *Prostaglandins Leukot Essent Fatty Acids* 126, 112–116. <https://doi.org/10.1016/j.plefa.2017.09.015>
- Farooqui, A.A., Horrocks, L.A., Farooqui, T., 2007. Modulation of inflammation in brain: a matter of fat. *J Neurochem* 101, 577–599. <https://doi.org/10.1111/j.1471-4159.2006.04371.x>
- Farrer, L.A., Cupples, L.A., Haines, J.L., Hyman, B., Kukull, W.A., Mayeux, R., Myers, R.H., Pericak-Vance, M.A., Risch, N., van Duijn, C.M., 1997. Effects of Age, Sex, and Ethnicity on the Association Between Apolipoprotein E Genotype and Alzheimer Disease: A Meta-analysis. *JAMA* 278, 1349–1356. <https://doi.org/10.1001/jama.1997.03550160069041>
- Favé, G., Coste, T.C., Armand, M., 2004. PHYSICOCHEMICAL PROPERTIES OF LIPIDS: NEW STRATEGIES TO MANAGE FATTY ACID BIOAVAILABILITY 17.
- Favrelière, S., Perault, M.C., Huguet, F., De Javel, D., Bertrand, N., Piriou, A., Durand, G., 2003. DHA-enriched phospholipid diets modulate age-related alterations in rat hippocampus. *Neurobiology of Aging* 24, 233–243. [https://doi.org/10.1016/S0197-4580\(02\)00064-7](https://doi.org/10.1016/S0197-4580(02)00064-7)
- Fearth, C., Barberger-Gateau, P., 2015. Mediterranean Diet and Cognitive Health, in: *Diet and Nutrition in Dementia and Cognitive Decline*. Elsevier, pp. 265–283. <https://doi.org/10.1016/B978-0-12-407824-6.00025-2>
- Fedorova, I., Hussein, N., Baumann, M.H., Di Martino, C., Salem, N., 2009. An n-3 fatty acid deficiency impairs rat spatial learning in the Barnes maze. *Behavioral Neuroscience* 123, 196–205. <https://doi.org/10.1037/a0013801>
- Fedorova, I., Hussein, N., Di Martino, C., Moriguchi, T., Hoshiba, J., Majchrzak, S., Salem, N., 2007. An n-3 fatty acid deficient diet affects mouse spatial learning in the Barnes circular maze. *Prostaglandins, Leukotrienes and Essential Fatty Acids, Proceedings of the 8th Fatty Acid and Cell Signaling (FACS) Workshop held in Quebec City on June 26-28, 2007* 77, 269–277. <https://doi.org/10.1016/j.plefa.2007.10.013>
- Fedorova, I., Salem, N., 2006. Omega-3 fatty acids and rodent behavior. *Prostaglandins, Leukotrienes and Essential Fatty Acids* 75, 271–289. <https://doi.org/10.1016/j.plefa.2006.07.006>



- Fellin, T., Pascual, O., Gobbo, S., Pozzan, T., Haydon, P.G., Carmignoto, G., 2004. Neuronal Synchrony Mediated by Astrocytic Glutamate through Activation of Extrasynaptic NMDA Receptors. *Neuron* 43, 729–743. <https://doi.org/10.1016/j.neuron.2004.08.011>
- Fernandez, R.F., Kim, S.Q., Zhao, Y., Foguth, R.M., Weera, M.M., Coughlin, J.L., Nomura, D.K., Chester, J.A., Cannon, J.R., Ellis, J.M., 2018. Acyl-CoA synthetase 6 enriches the neuroprotective omega-3 fatty acid DHA in the brain. *Proceedings of the National Academy of Sciences* 115, 12525–12530. <https://doi.org/10.1073/pnas.1807958115>
- Fernandez, R.F., Pereyra, A.S., Diaz, V., Wilson, E.S., Litwa, K.A., Martínez-Gardeazabal, J., Jackson, S.N., Brenna, J.T., Hermann, B.P., Eells, J.B., Ellis, J.M., 2021. Acyl-CoA synthetase 6 is required for brain docosahexaenoic acid retention and neuroprotection during aging. *JCI Insight* 6, e144351. <https://doi.org/10.1172/jci.insight.144351>
- Fewtrell, M.S., 2006. Long-Chain Polyunsaturated Fatty Acids in Early Life: Effects on Multiple Health Outcomes, in: Lucas, A., Sampson, H.A. (Eds.), *Nestlé Nutrition Workshop Series: Pediatric Program*. KARGER, Basel, pp. 203–221. <https://doi.org/10.1159/000091073>
- Fieberg, J.R., Vitense, K., Johnson, D.H., 2020. Resampling-based methods for biologists. *PeerJ* 8, e9089. <https://doi.org/10.7717/peerj.9089>
- Flak, M.B., Koenis, D.S., Sobrino, A., Smith, J., Pistorius, K., Palmas, F., Dalli, J., 2020. GPR101 mediates the pro-resolving actions of RvD5<sub>n-3</sub> DP<sub>A</sub> in arthritis and infections. *J Clin Invest* 130, 359–373. <https://doi.org/10.1172/JCI131609>
- Fleming, I., 2011. The cytochrome P450 pathway in angiogenesis and endothelial cell biology. *Cancer Metastasis Rev* 30, 541–555. <https://doi.org/10.1007/s10555-011-9302-3>
- Flowers, S.A., Rebeck, G.W., 2020. APOE in the normal brain. *Neurobiology of Disease* 136, 104724. <https://doi.org/10.1016/j.nbd.2019.104724>
- Font-Nieves, M., Sans-Fons, M.G., Gorina, R., Bonfill-Teixidor, E., Salas-Pédomo, A., Márquez-Kisinousky, L., Santalucia, T., Planas, A.M., 2012. Induction of COX-2 Enzyme and Down-regulation of COX-1 Expression by Lipopolysaccharide (LPS) Control Prostaglandin E2 Production in Astrocytes\*. *Journal of Biological Chemistry* 287, 6454–6468. <https://doi.org/10.1074/jbc.M111.327874>
- Forsyth, S., Gautier, S., Jr, N.S., 2016. Estimated Dietary Intakes of Arachidonic Acid and Docosahexaenoic Acid in Infants and Young Children Living in Developing Countries. *ANM* 69, 64–74. <https://doi.org/10.1159/000448526>
- Fotuhi, M., Mohassel, P., Yaffe, K., 2009. Fish consumption, long-chain omega-3 fatty acids and risk of cognitive decline or Alzheimer disease: a complex association. *Nat Rev Neurol* 5, 140–152. <https://doi.org/10.1038/ncpneuro1044>
- Fourrier, C., Kropp, C., Aubert, A., Sauvart, J., Vaysse, C., Chardigny, J.-M., Layé, S., Joffre, C., Castanon, N., 2020. Rapeseed oil fortified with micronutrients improves cognitive alterations associated with metabolic syndrome. *Brain, Behavior, and Immunity* 84, 23–35. <https://doi.org/10.1016/j.bbi.2019.11.002>
- Fourrier, C., Remus-Borel, J., Greenhalgh, A.D., Guichardant, M., Bernoud-Hubac, N., Lagarde, M., Joffre, C., Layé, S., 2017. Docosahexaenoic acid-containing choline phospholipid modulates LPS-induced neuroinflammation in vivo and in microglia in vitro. *Journal of Neuroinflammation* 14, 170. <https://doi.org/10.1186/s12974-017-0939-x>

Francis, T.C., Chandra, R., Friend, D.M., Finkel, E., Dayrit, G., Miranda, J., Brooks, J.M., Iñiguez, S.D., O'Donnell, P., Kravitz, A., Lobo, M.K., 2015. Nucleus Accumbens Medium Spiny Neuron Subtypes Mediate Depression-Related Outcomes to Social Defeat Stress. *Biological Psychiatry, The Development and Progression of Depression* 77, 212–222. <https://doi.org/10.1016/j.biopsych.2014.07.021>

Fredman, G., Ozcan, L., Spolitu, S., Hellmann, J., Spite, M., Backs, J., Tabas, I., 2014. Resolvin D1 limits 5-lipoxygenase nuclear localization and leukotriene B4 synthesis by inhibiting a calcium-activated kinase pathway. *Proceedings of the National Academy of Sciences* 111, 14530–14535. <https://doi.org/10.1073/pnas.1410851111>

Fujita, S., Ikegaya, Y., Nishikawa, M., Nishiyama, N., Matsuki, N., 2001. Docosahexaenoic acid improves long-term potentiation attenuated by phospholipase A<sub>2</sub> inhibitor in rat hippocampal slices: DHA and hippocampal LTP. *British Journal of Pharmacology* 132, 1417–1422. <https://doi.org/10.1038/sj.bjp.0703970>

Futokoro, R., Hijioka, M., Arata, M., Kitamura, Y., 2022. Lipoxin A4 Receptor Stimulation Attenuates Neuroinflammation in a Mouse Model of Intracerebral Hemorrhage. *Brain Sciences* 12, 162. <https://doi.org/10.3390/brainsci12020162>

Gabbs, M., Leng, S., Devassy, J.G., Monirujjaman, M., Aukema, H.M., 2015. Advances in Our Understanding of Oxylipins Derived from Dietary PUFAs. *Advances in Nutrition* 6, 513–540. <https://doi.org/10.3945/an.114.007732>

Gadea, A., López-Colomé, A.M., 2001a. Glial transporters for glutamate, glycine and GABA I. Glutamate transporters. *Journal of Neuroscience Research* 63, 453–460. <https://doi.org/10.1002/jnr.1039>

Gadea, A., López-Colomé, A.M., 2001b. Glial transporters for glutamate, glycine, and GABA: II. GABA transporters. *Journal of Neuroscience Research* 63, 461–468. <https://doi.org/10.1002/jnr.1040>

Gan, J., Zhang, Z., Kurudimov, K., German, J.B., Taha, A.Y., 2020. Distribution of Free and Esterified Oxylipins in Cream, Cell, and Skim Fractions of Human Milk. *Lipids* 55, 661–670. <https://doi.org/10.1002/lipd.12268>

Gao, H., Yan, P., Zhang, S., Huang, H., Huang, F., Sun, T., Deng, Q., Huang, Q., Chen, S., Ye, K., Xu, J., Liu, L., 2016. Long-Term Dietary Alpha-Linolenic Acid Supplement Alleviates Cognitive Impairment Correlate with Activating Hippocampal CREB Signaling in Natural Aging Rats. *Mol Neurobiol* 53, 4772–4786. <https://doi.org/10.1007/s12035-015-9393-x>

Garagnani, P., Bacalini, M.G., Pirazzini, C., Gori, D., Giuliani, C., Mari, D., Di Blasio, A.M., Gentilini, D., Vitale, G., Collino, S., Rezzi, S., Castellani, G., Capri, M., Salvioli, S., Franceschi, C., 2012. Methylation of ELOVL2 gene as a new epigenetic marker of age. *Aging Cell* 11, 1132–1134. <https://doi.org/10.1111/accel.12005>

Gertsik, L., Poland, R.E., Bresee, C., Rapaport, M.H., 2012. Omega-3 Fatty Acid Augmentation of Citalopram Treatment for Patients with Major Depressive Disorder. *J Clin Psychopharmacol* 32, 61–64. <https://doi.org/10.1097/JCP.0b013e31823f3b5f>

Gibson, R., Makrides, M., 1998. The role of long chain polyunsaturated fatty acids (LCPUFA) in neonatal nutrition 7.

- Gilroy, D.W., Edin, M.L., De Maeyer, R.P.H., Bystrom, J., Newson, J., Lih, F.B., Stables, M., Zeldin, D.C., Bishop-Bailey, D., 2016. CYP450-derived oxylipins mediate inflammatory resolution. *Proceedings of the National Academy of Sciences* 113, E3240–E3249. <https://doi.org/10.1073/pnas.1521453113>
- Giltay, E.J., Gooren, L.J., Toorians, A.W., Katan, M.B., Zock, P.L., 2004. Docosahexaenoic acid concentrations are higher in women than in men because of estrogenic effects. *The American Journal of Clinical Nutrition* 80, 1167–1174. <https://doi.org/10.1093/ajcn/80.5.1167>
- Golden, S.A., Covington, H.E., Berton, O., Russo, S.J., 2011. A standardized protocol for repeated social defeat stress in mice. *Nature Protocols* 6, 1183–1191. <https://doi.org/10.1038/nprot.2011.361>
- Goldstein, J.L., Brown, M.S., 2009. The LDL Receptor. *Arteriosclerosis, Thrombosis, and Vascular Biology* 29, 431–438. <https://doi.org/10.1161/ATVBAHA.108.179564>
- Gómez Rodríguez, A., Talamonti, E., Naudi, A., Kalinovich, A.V., Pauter, A.M., Barja, G., Bengtsson, T., Jacobsson, A., Pamplona, R., Shabalina, I.G., 2022. Elov12-Ablation Leads to Mitochondrial Membrane Fatty Acid Remodeling and Reduced Efficiency in Mouse Liver Mitochondria. *Nutrients* 14, 559. <https://doi.org/10.3390/nu14030559>
- Gould, J.F., Makrides, M., Gibson, R.A., Sullivan, T.R., McPhee, A.J., Anderson, P.J., Best, K.P., Sharp, M., Cheong, J.L.Y., Opie, G.F., Travadi, J., Bednarz, J.M., Davis, P.G., Simmer, K., Doyle, L.W., Collins, C.T., 2022. Neonatal Docosahexaenoic Acid in Preterm Infants and Intelligence at 5 Years. *N Engl J Med* 387, 1579–1588. <https://doi.org/10.1056/NEJMoa2206868>
- Gras, C., Herzog, E., Bellenchi, G.C., Bernard, V., Ravassard, P., Pohl, M., Gasnier, B., Giros, B., Mestikawy, S.E., 2002. A Third Vesicular Glutamate Transporter Expressed by Cholinergic and Serotonergic Neurons. *J. Neurosci.* 22, 5442–5451. <https://doi.org/10.1523/JNEUROSCI.22-13-05442.2002>
- Graybiel, A.M., 1995. Building action repertoires: memory and learning functions of the basal ganglia. *Current Opinion in Neurobiology* 5, 733–741. [https://doi.org/10.1016/0959-4388\(95\)80100-6](https://doi.org/10.1016/0959-4388(95)80100-6)
- Green, J.T., Liu, Z., Bazinet, R.P., 2010. Brain phospholipid arachidonic acid half-lives are not altered following 15 weeks of N-3 polyunsaturated fatty acid adequate or deprived diet. *Journal of Lipid Research* 51, 535–543. <https://doi.org/10.1194/jlr.M000786>
- Green, J.T., Orr, S.K., Bazinet, R.P., 2008. The emerging role of group VI calcium-independent phospholipase A2 in releasing docosahexaenoic acid from brain phospholipids. *Journal of Lipid Research* 49, 939–944. <https://doi.org/10.1194/jlr.R700017-JLR200>
- Gregory, M.K., Cleland, L.G., James, M.J., 2013. Molecular basis for differential elongation of omega-3 docosapentaenoic acid by the rat Elov15 and Elov12 [S]. *Journal of Lipid Research* 54, 2851–2857. <https://doi.org/10.1194/jlr.M041368>
- Grintal, B., Champeil-Potokar, G., Lavielle, M., Vancassel, S., Breton, S., Denis, I., 2009. Inhibition of astroglial glutamate transport by polyunsaturated fatty acids: Evidence for a signalling role of docosahexaenoic acid. *Neurochemistry International* 54, 535–543. <https://doi.org/10.1016/j.neuint.2009.02.018>
- Groenewegen, H.J., Wright, C.I., Beijer, A.V. j., Voorn, P., 1999. Convergence and Segregation of Ventral Striatal Inputs and Outputs. *Annals of the New York Academy of Sciences* 877, 49–63. <https://doi.org/10.1111/j.1749-6632.1999.tb09260.x>

- Guesnet, P., Alessandri, J.-M., Astorg, P., Pifferi, F., Laviolle, M., 2005. Les rôles physiologiques majeurs exercés par les acides gras polyinsaturés (AGPI). *OCL* 12, 333–343. <https://doi.org/10.1051/ocl.2005.0333>
- Guillou, H., Zdravec, D., Martin, P.G.P., Jacobsson, A., 2010. The key roles of elongases and desaturases in mammalian fatty acid metabolism: Insights from transgenic mice. *Progress in Lipid Research* 49, 186–199. <https://doi.org/10.1016/j.plipres.2009.12.002>
- Guo, Y., Zhang, W., Giroux, C., Cai, Y., Ekambaram, P., Dilly, A., Hsu, A., Zhou, S., Maddipati, K.R., Liu, J., Joshi, S., Tucker, S.C., Lee, M.-J., Honn, K.V., 2011. Identification of the Orphan G Protein-coupled Receptor GPR31 as a Receptor for 12-(S)-Hydroxyeicosatetraenoic Acid\*. *Journal of Biological Chemistry* 286, 33832–33840. <https://doi.org/10.1074/jbc.M110.216564>
- Guttenplan, K.A., Weigel, M.K., Prakash, P., Wijewardhane, P.R., Hasel, P., Rufen-Blanchette, U., Münch, A.E., Blum, J.A., Fine, J., Neal, M.C., Bruce, K.D., Gitler, A.D., Chopra, G., Liddel, S.A., Barres, B.A., 2021. Neurotoxic reactive astrocytes induce cell death via saturated lipids. *Nature* 599, 102–107. <https://doi.org/10.1038/s41586-021-03960-y>
- Guu, T.-W., Mischoulon, D., Sarris, J., Hibbeln, J., McNamara, R.K., Hamazaki, K., Freeman, M.P., Maes, M., Matsuoka, Y.J., Belmaker, R.H., Marx, W., Pariante, C., Berk, M., Jacka, F., Su, K.-P., 2020. A multi-national, multi-disciplinary Delphi consensus study on using omega-3 polyunsaturated fatty acids (n-3 PUFAs) for the treatment of major depressive disorder. *Journal of Affective Disorders* 265, 233–238. <https://doi.org/10.1016/j.jad.2020.01.050>
- Hadley, K.B., Bauer, J., Milgram, N.W., 2017. The oil-rich alga *Schizochytrium* sp. as a dietary source of docosahexaenoic acid improves shape discrimination learning associated with visual processing in a canine model of senescence. *Prostaglandins, Leukotrienes and Essential Fatty Acids* 118, 10–18. <https://doi.org/10.1016/j.plefa.2017.01.011>
- Haggarty, P., 2010. Fatty Acid Supply to the Human Fetus. *Annu. Rev. Nutr.* 30, 237–255. <https://doi.org/10.1146/annurev.nutr.012809.104742>
- Haim, L.B., Rowitch, D.H., 2017. Functional diversity of astrocytes in neural circuit regulation. *Nat Rev Neurosci* 18, 31–41. <https://doi.org/10.1038/nrn.2016.159>
- Halassa, M.M., Fellin, T., Takano, H., Dong, J.-H., Haydon, P.G., 2007. Synaptic Islands Defined by the Territory of a Single Astrocyte. *J. Neurosci.* 27, 6473–6477. <https://doi.org/10.1523/JNEUROSCI.1419-07.2007>
- Hall, A.M., Wiczner, B.M., Herrmann, T., Stremmel, W., Bernlohr, D.A., 2005. Enzymatic Properties of Purified Murine Fatty Acid Transport Protein 4 and Analysis of Acyl-CoA Synthetase Activities in Tissues from FATP4 Null Mice\*. *Journal of Biological Chemistry* 280, 11948–11954. <https://doi.org/10.1074/jbc.M412629200>
- Hamazaki, K., Harauma, A., Otaka, Y., Moriguchi, T., Inadera, H., 2016. Serum n-3 polyunsaturated fatty acids and psychological distress in early pregnancy: Adjunct Study of Japan Environment and Children's Study. *Transl Psychiatry* 6, e737–e737. <https://doi.org/10.1038/tp.2016.2>
- Hamilton, J.A., Brunaldi, K., 2007. A Model for Fatty Acid Transport into the Brain. *J Mol Neurosci* 33, 12–17. <https://doi.org/10.1007/s12031-007-0050-3>

- Hamlett, E.D., Hjorth, E., Ledreux, A., Gilmore, A., Schultzberg, M., Granholm, A.C., 2020. RvE1 treatment prevents memory loss and neuroinflammation in the Ts65Dn mouse model of Down syndrome. *Glia* 68, 1347–1360. <https://doi.org/10.1002/glia.23779>
- Harel, M., Koven, W., Lein, I., Bar, Y., Behrens, P., Stubblefield, J., Zohar, Y., Place, A.R., 2002. Advanced DHA, EPA and ArA enrichment materials for marine aquaculture using single cell heterotrophs. *Aquaculture* 213, 347–362. [https://doi.org/10.1016/S0044-8486\(02\)00047-9](https://doi.org/10.1016/S0044-8486(02)00047-9)
- Harris, R.C., 2003. Interactions between COX-2 and the renin–angiotensin system in the kidney. *Acta Physiologica Scandinavica* 177, 423–427. <https://doi.org/10.1046/j.1365-201X.2003.01101.x>
- Harrison, D.M., Roy, S., Oh, J., Izbudak, I., Pham, D., Courtney, S., Caffo, B., Jones, C.K., van Zijl, P., Calabresi, P.A., 2015. Association of Cortical Lesion Burden on 7-T Magnetic Resonance Imaging With Cognition and Disability in Multiple Sclerosis. *JAMA Neurology* 72, 1004–1012. <https://doi.org/10.1001/jamaneurol.2015.1241>
- Harry, G.J., Kraft, A.D., 2008. Neuroinflammation and microglia: considerations and approaches for neurotoxicity assessment. *Expert Opinion on Drug Metabolism & Toxicology* 4, 1265–1277. <https://doi.org/10.1517/17425255.4.10.1265>
- Hashimoto, K., 2009. Emerging role of glutamate in the pathophysiology of major depressive disorder. *Brain Research Reviews* 61, 105–123. <https://doi.org/10.1016/j.brainresrev.2009.05.005>
- Hashimoto, K., Yoshizawa, A.C., Saito, K., Yamada, T., Kanehisa, M., 2006. The repertoire of desaturases for unsaturated fatty acid synthesis in 397 genomes. *Genome Inform* 17, 173–183.
- Hayashi, D., Mouchlis, V.D., Dennis, E.A., 2021. Omega-3 versus Omega-6 fatty acid availability is controlled by hydrophobic site geometries of phospholipase A2s. *Journal of Lipid Research* 62. <https://doi.org/10.1016/j.jlr.2021.100113>
- Hayashi, Y., Lee-Okada, H.-C., Nakamura, E., Tada, N., Yokomizo, T., Fujiwara, Y., Ichi, I., 2021. Ablation of fatty acid desaturase 2 (FADS2) exacerbates hepatic triacylglycerol and cholesterol accumulation in polyunsaturated fatty acid-depleted mice. *FEBS Letters* 595, 1920–1932. <https://doi.org/10.1002/1873-3468.14134>
- Haydon, P.G., 2001. Glia: listening and talking to the synapse. *Nat Rev Neurosci* 2, 185–193. <https://doi.org/10.1038/35058528>
- He, Y., Phan, K., Bhatia, S., Pickford, R., Fu, Y., Yang, Y., Hodges, J.R., Piguet, O., Halliday, G.M., Kim, W.S., 2021. Increased VLCFA-lipids and ELOVL4 underlie neurodegeneration in frontotemporal dementia. *Sci Rep* 11, 21348. <https://doi.org/10.1038/s41598-021-00870-x>
- Heird, W.C., 2001. The Role of Polyunsaturated Fatty Acids in Term and Preterm Infants and Breastfeeding Mothers. *Pediatric Clinics of North America* 48, 173–188. [https://doi.org/10.1016/S0031-3955\(05\)70292-3](https://doi.org/10.1016/S0031-3955(05)70292-3)
- Hennebelle, M., Morgan, R.K., Sethi, S., Zhang, Z., Chen, H., Grodzki, A.C., Lein, P.J., Taha, A.Y., 2020. Linoleic acid-derived metabolites constitute the majority of oxylipins in the rat pup brain and stimulate axonal growth in primary rat cortical neuron-glia co-cultures in a sex-dependent manner. *J Neurochem* 152, 195–207. <https://doi.org/10.1111/jnc.14818>
- Hensch, T.K., Stryker, M.P., 2004. Columnar architecture sculpted by GABA circuits in developing cat visual cortex. *Science* 303, 1678–1681. <https://doi.org/10.1126/science.1091031>

- Herrera, J.L., Ordoñez-Gutierrez, L., Fabrias, G., Casas, J., Morales, A., Hernandez, G., Acosta, N.G., Rodriguez, C., Prieto-Valiente, L., Garcia-Segura, L.M., Alonso, R., Wandosell, F.G., 2018. Ovarian Function Modulates the Effects of Long-Chain Polyunsaturated Fatty Acids on the Mouse Cerebral Cortex. *Front. Cell. Neurosci.* 12, 103. <https://doi.org/10.3389/fncel.2018.00103>
- Hewawasam, E., Collins, C.T., Muhlhausler, B.S., Yelland, L.N., Smithers, L.G., Colombo, J., Makrides, M., McPhee, A.J., Gould, J.F., 2021. DHA supplementation in infants born preterm and the effect on attention at 18 months' corrected age: follow-up of a subset of the N3RO randomised controlled trial. *Br J Nutr* 125, 420–431. <https://doi.org/10.1017/S0007114520002500>
- Hibbeln, J.R., 2002. Seafood consumption, the DHA content of mothers' milk and prevalence rates of postpartum depression: a cross-national, ecological analysis. *Journal of Affective Disorders* 69, 15–29. [https://doi.org/10.1016/S0165-0327\(01\)00374-3](https://doi.org/10.1016/S0165-0327(01)00374-3)
- Hirabayashi, T., Murayama, T., Shimizu, T., 2004. Regulatory Mechanism and Physiological Role of Cytosolic Phospholipase A<sub>2</sub>. *Biological and Pharmaceutical Bulletin* 27, 1168–1173. <https://doi.org/10.1248/bpb.27.1168>
- Holtzman, D.M., Herz, J., Bu, G., 2012. Apolipoprotein E and Apolipoprotein E Receptors: Normal Biology and Roles in Alzheimer Disease. *Cold Spring Harb Perspect Med* 2, a006312. <https://doi.org/10.1101/cshperspect.a006312>
- Hooper, C., de Souto Barreto, P., Coley, N., Cantet, C., Cesari, M., Andrieu, S., Vellas, B., 2017. Cognitive changes with omega-3 polyunsaturated fatty acids in non-demented older adults with low omega-3 index. *J Nutr Health Aging* 21, 988–993. <https://doi.org/10.1007/s12603-017-0957-5>
- Hoozemans, J.J.M., Rozemuller, A.J.M., Janssen, I., De Groot, C.J.A., Veerhuis, R., Eikelenboom, P., 2001. Cyclooxygenase expression in microglia and neurons in Alzheimer's disease and control brain. *Acta Neuropathol* 101, 2–8. <https://doi.org/10.1007/s004010000251>
- Hu, X.F., Sandhu, S.K., Harris, W.S., Chan, H.M., 2017. Conversion ratios of n-3 fatty acids between plasma and erythrocytes: a systematic review and meta-regression. *British Journal of Nutrition* 117, 1162–1173. <https://doi.org/10.1017/S0007114517001052>
- Huang, J.T., Welch, J.S., Ricote, M., Binder, C.J., Willson, T.M., Kelly, C., Witztum, J.L., Funk, C.D., Glass, C.K., 1999. Interleukin-4-dependent production of PPAR- $\alpha$  ligands in macrophages by 12/15-lipoxygenase 400, 5.
- Huang, Y., Huang, S., Lam, S.M., Liu, Z., Shui, G., Zhang, Y.Q., 2016. Acsl, the *Drosophila* ortholog of intellectual disability-related ACSL4, inhibits synaptic growth by altered lipids. *Journal of Cell Science* jcs.195032. <https://doi.org/10.1242/jcs.195032>
- Huang, Y.H., Bergles, D.E., 2004. Glutamate transporters bring competition to the synapse. *Current Opinion in Neurobiology* 14, 346–352. <https://doi.org/10.1016/j.conb.2004.05.007>
- Huang, Z.H., Reardon, C.A., Getz, G.S., Maeda, N., Mazzone, T., 2015. Selective suppression of adipose tissue apoE expression impacts systemic metabolic phenotype and adipose tissue inflammation. *Journal of Lipid Research* 56, 215–226. <https://doi.org/10.1194/jlr.M050567>
- Hunter, J.E., Fredricks, H.F., Behrendt, L., Alcolombri, U., Bent, S.M., Stocker, R., Van Mooy, B.A.S., 2021. Using High-Sensitivity Lipidomics To Assess Microscale Heterogeneity in Oceanic Sinking Particles and Single Phytoplankton Cells. *Environ. Sci. Technol.* 55, 15456–15465. <https://doi.org/10.1021/acs.est.1c02836>

- Iadecola, C., 2017. The Neurovascular Unit Coming of Age: A Journey through Neurovascular Coupling in Health and Disease. *Neuron* 96, 17–42. <https://doi.org/10.1016/j.neuron.2017.07.030>
- Ikemoto, A., Nitta, A., Furukawa, S., Ohishi, M., Nakamura, A., Fujii, Y., Okuyama, H., 2000. Dietary n-3 fatty acid deficiency decreases nerve growth factor content in rat hippocampus. *Neuroscience Letters* 285, 99–102. [https://doi.org/10.1016/S0304-3940\(00\)01035-1](https://doi.org/10.1016/S0304-3940(00)01035-1)
- Illes, P., Burnstock, G., Tang, Y., 2019. Astroglia-Derived ATP Modulates CNS Neuronal Circuits. *Trends in Neurosciences* 42, 885–898. <https://doi.org/10.1016/j.tins.2019.09.006>
- Innis, S.M., 2005. Essential fatty acid transfer and fetal development. *Placenta, Trophoblast Research. Placenta: Signaling and the Placenta* 26, S70–S75. <https://doi.org/10.1016/j.placenta.2005.01.005>
- Innis, S.M., 2004. Polyunsaturated Fatty Acids in Human Milk, in: Pickering, L.K., Morrow, A.L., Ruiz-Palacios, G.M., Schanler, R.J. (Eds.), *Protecting Infants through Human Milk, Advances in Experimental Medicine and Biology*. Springer US, Boston, MA, pp. 27–43. [https://doi.org/10.1007/978-1-4757-4242-8\\_5](https://doi.org/10.1007/978-1-4757-4242-8_5)
- Innis, S.M., 2000. The Role of Dietary n-6 and n-3 Fatty Acids in the Developing Brain. *DNE* 22, 474–480. <https://doi.org/10.1159/000017478>
- Innis, S.M., de la Presa Owens, S., 2001. Dietary Fatty Acid Composition in Pregnancy Alters Neurite Membrane Fatty Acids and Dopamine in Newborn Rat Brain. *The Journal of Nutrition* 131, 118–122. <https://doi.org/10.1093/jn/131.1.118>
- Inoue, T., Hashimoto, M., Katakura, M., Hossain, S., Matsuzaki, K., Shido, O., 2019. Effect of chronic administration of arachidonic acid on the performance of learning and memory in aged rats. *Food & Nutrition Research*. <https://doi.org/10.29219/fnr.v63.1441>
- Isaac, A.R., de Velasco, P.C., Fraga, K.Y.D., Tavares-do-Carmo, M. das G., Campos, R.M.P., Iannotti, F.A., Verde, R., Martins, D.B.G., Santos, T.A., Ferreira, B.K., de Mello, F.G., Di Marzo, V., Andrade-da-Costa, B.L. da S., de Melo Reis, R.A., 2021. Maternal omega-3 intake differentially affects the endocannabinoid system in the progeny's neocortex and hippocampus: Impact on synaptic markers. *The Journal of Nutritional Biochemistry* 96, 108782. <https://doi.org/10.1016/j.jnutbio.2021.108782>
- Isobe, Y., Arita, M., Matsueda, S., Iwamoto, R., Fujihara, T., Nakanishi, H., Taguchi, R., Masuda, K., Sasaki, K., Urabe, D., Inoue, M., Arai, H., 2012. Identification and Structure Determination of Novel Anti-inflammatory Mediator Resolvin E3, 17,18-Dihydroxyeicosapentaenoic Acid \*. *Journal of Biological Chemistry* 287, 10525–10534. <https://doi.org/10.1074/jbc.M112.340612>
- Itokazu, N., Ikegaya, Y., Nishikawa, M., Matsuki, N., 2000. Bidirectional actions of docosahexaenoic acid on hippocampal neurotransmissions in vivo. *Brain Research* 862, 211–216. [https://doi.org/10.1016/S0006-8993\(00\)02129-6](https://doi.org/10.1016/S0006-8993(00)02129-6)
- Jakobsson, A., Westerberg, R., Jakobsson, A., 2006. Fatty acid elongases in mammals: Their regulation and roles in metabolism. *Progress in Lipid Research* 45, 237–249. <https://doi.org/10.1016/j.plipres.2006.01.004>
- Janssen, C.I.F., Zerbi, V., Mutsaers, M.P.C., de Jong, B.S.W., Wiesmann, M., Arnoldussen, I.A.C., Geenen, B., Heerschap, A., Muskiet, F.A.J., Jouni, Z.E., van Tol, E.A.F., Gross, G., Homberg, J.R., Berg, B.M., Kiliaan, A.J., 2015. Impact of dietary n-3 polyunsaturated fatty acids on cognition, motor skills and hippocampal neurogenesis in developing C57BL/6J mice. *J Nutr Biochem* 26, 24–35. <https://doi.org/10.1016/j.jnutbio.2014.08.002>

- Jasani, B., Simmer, K., Patole, S.K., Rao, S.C., 2017. Long chain polyunsaturated fatty acid supplementation in infants born at term. *Cochrane Database of Systematic Reviews* 2017. <https://doi.org/10.1002/14651858.CD000376.pub4>
- Jatana, M., Giri, S., Ansari, M.A., Elango, C., Singh, A.K., Singh, I., Khan, M., 2006. Inhibition of NF- $\kappa$ B activation by 5-lipoxygenase inhibitors protects brain against injury in a rat model of focal cerebral ischemia. *J Neuroinflammation* 3, 12. <https://doi.org/10.1186/1742-2094-3-12>
- Joardar, A., Das, S., 2007. Effect of Fatty Acids Isolated from Edible Oils Like Mustard, Linseed or Coconut on Astrocytes Maturation. *Cell Mol Neurobiol* 27, 973–983. <https://doi.org/10.1007/s10571-007-9204-7>
- Joardar, A., Sen, A.K., Das, S., 2006. Docosahexaenoic acid facilitates cell maturation and  $\beta$ -adrenergic transmission in astrocytes. *Journal of Lipid Research* 47, 571–581. <https://doi.org/10.1194/jlr.M500415-JLR200>
- Joffre, C., 2019. Polyunsaturated Fatty Acid Metabolism in the Brain and Brain Cells, in: Bosch-Bouju, C., Layé, S., Pallet, V. (Eds.), *Feed Your Mind - How Does Nutrition Modulate Brain Function throughout Life?* IntechOpen. <https://doi.org/10.5772/intechopen.88232>
- Joffre, C., Dinel, A.-L., Chataigner, M., Pallet, V., Layé, S., 2020. n-3 Polyunsaturated Fatty Acids and Their Derivates Reduce Neuroinflammation during Aging. *Nutrients* 12, 647. <https://doi.org/10.3390/nu12030647>
- Joffre, C., Grégoire, S., De Smedt, V., Acar, N., Bretillon, L., Nadjar, A., Layé, S., 2016. Modulation of brain PUFA content in different experimental models of mice. *Prostaglandins, Leukotrienes and Essential Fatty Acids (PLEFA)* 114, 1–10. <https://doi.org/10.1016/j.plefa.2016.09.003>
- Joffre, C., Nadjar, A., Lebbadi, M., Calon, F., Laye, S., 2014. n-3 LCPUFA improves cognition: The young, the old and the sick. *Prostaglandins, Leukotrienes and Essential Fatty Acids* 91, 1–20. <https://doi.org/10.1016/j.plefa.2014.05.001>
- Jun, B., Mukherjee, P.K., Asatryan, A., Kautzmann, M.-A., Heap, J., Gordon, W.C., Bhattacharjee, S., Yang, R., Petasis, N.A., Bazan, N.G., 2017. Elovans are novel cell-specific lipid mediators necessary for neuroprotective signaling for photoreceptor cell integrity. *Sci Rep* 7, 5279. <https://doi.org/10.1038/s41598-017-05433-7>
- Kagawa, Y., Yasumoto, Y., Sharifi, K., Ebrahimi, M., Islam, A., Miyazaki, H., Yamamoto, Y., Sawada, T., Kishi, H., Kobayashi, S., Maekawa, M., Yoshikawa, T., Takaki, E., Nakai, A., Kogo, H., Fujimoto, T., Owada, Y., 2015. Fatty acid-binding protein 7 regulates function of caveolae in astrocytes through expression of caveolin-1. *Glia* 63, 780–794. <https://doi.org/10.1002/glia.22784>
- Kang, J.X., 2007. Fat-1 transgenic mice: A new model for omega-3 research. *Prostaglandins, Leukotrienes and Essential Fatty Acids, Proceedings of the 8th Fatty Acid and Cell Signaling (FACS) Workshop held in Quebec City on June 26-28, 2007* 77, 263–267. <https://doi.org/10.1016/j.plefa.2007.10.010>
- Kang, S.S., Ebbert, M.T.W., Baker, K.E., Cook, C., Wang, X., Sens, J.P., Kocher, J.-P., Petrucelli, L., Fryer, J.D., 2018. Microglial translational profiling reveals a convergent APOE pathway from aging, amyloid, and tau. *Journal of Experimental Medicine* 215, 2235–2245. <https://doi.org/10.1084/jem.20180653>
- Kantarci, A., Aytan, N., Palaska, I., Stephens, D., Crabtree, L., Benincasa, C., Jenkins, B.G., Carreras, I., Dedeoglu, A., 2018. Combined administration of resolvin E1 and lipoxin A4 resolves inflammation in a



- murine model of Alzheimer's disease. *Experimental Neurology* 300, 111–120. <https://doi.org/10.1016/j.expneurol.2017.11.005>
- Kaufmann, W.E., Worley, P.F., Pegg, J., Bremer, M., Isakson, P., 1996. COX-2, a synaptically induced enzyme, is expressed by excitatory neurons at postsynaptic sites in rat cerebral cortex. *Proceedings of the National Academy of Sciences* 93, 2317–2321. <https://doi.org/10.1073/pnas.93.6.2317>
- Kawaguchi, Y., Kubota, Y., 1993. Correlation of physiological subgroupings of nonpyramidal cells with parvalbumin- and calbindinD28k-immunoreactive neurons in layer V of rat frontal cortex. *Journal of Neurophysiology* 70, 387–396. <https://doi.org/10.1152/jn.1993.70.1.387>
- Kawashima, A., Harada, T., Kami, H., Yano, T., Imada, K., Mizuguchi, K., 2010. Effects of eicosapentaenoic acid on synaptic plasticity, fatty acid profile and phosphoinositide 3-kinase signaling in rat hippocampus and differentiated PC12 cells. *The Journal of Nutritional Biochemistry* 21, 268–277. <https://doi.org/10.1016/j.jnutbio.2008.12.015>
- Kelly, R.K., Pollard, Z., Young, H., Piernas, C., Lentjes, M., Mulligan, A., Huybrechts, I., Carter, J.L., Key, T.J., Perez-Cornago, A., 2022. Evaluation of the New Individual Fatty Acid Dataset for UK Biobank: Analysis of Intakes and Sources in 207,997 Participants. *Nutrients* 14, 3603. <https://doi.org/10.3390/nu14173603>
- Kharebava, G., Rashid, M.A., Lee, J.-W., Sarkar, S., Kevala, K., Kim, H.-Y., 2015. N-docosahexaenoyl ethanolamine regulates Hedgehog signaling and promotes growth of cortical axons. *Biology Open* 4, 1660–1670. <https://doi.org/10.1242/bio.013425>
- Kibret, B.G., Ishiguro, H., Horiuchi, Y., Onaivi, E.S., 2022. New Insights and Potential Therapeutic Targeting of CB2 Cannabinoid Receptors in CNS Disorders. *International Journal of Molecular Sciences* 23, 975. <https://doi.org/10.3390/ijms23020975>
- Kim, H.-K., Della-Fera, M., Lin, J., Baile, C.A., 2006. Docosahexaenoic Acid Inhibits Adipocyte Differentiation and Induces Apoptosis in 3T3-L1 Preadipocytes. *The Journal of Nutrition* 136, 2965–2969. <https://doi.org/10.1093/jn/136.12.2965>
- Kim, H.-Y., Spector, A.A., 2018. N-Docosahexaenoyl ethanolamine: A neurotrophic and neuroprotective metabolite of docosahexaenoic acid. *Molecular Aspects of Medicine, Dietary fatty acids, lipid mediators, cell function and human health* 64, 34–44. <https://doi.org/10.1016/j.mam.2018.03.004>
- Kim, M., Kim, Y., Min, S., Lee, S.-M., 2022. High Iron Exposure from the Fetal Stage to Adulthood in Mice Alters Lipid Metabolism. *Nutrients* 14, 2451. <https://doi.org/10.3390/nu14122451>
- Kita, Y., Shindou, H., Shimizu, T., 2019. Cytosolic phospholipase A2 and lysophospholipid acyltransferases. *Biochimica et Biophysica Acta (BBA) - Molecular and Cell Biology of Lipids, Novel functions of phospholipase A2* 1864, 838–845. <https://doi.org/10.1016/j.bbalip.2018.08.006>
- Koch, S., Donarski, N., Goetze, K., Kreckel, M., Stuerenburg, H.-J., Buhmann, C., Beisiegel, U., 2001. Characterization of four lipoprotein classes in human cerebrospinal fluid. *Journal of Lipid Research* 42, 1143–1151. [https://doi.org/10.1016/S0022-2275\(20\)31605-9](https://doi.org/10.1016/S0022-2275(20)31605-9)
- Kockx, M., Jessup, W., Kritharides, L., 2008. Regulation of Endogenous Apolipoprotein E Secretion by Macrophages. *Arteriosclerosis, Thrombosis, and Vascular Biology* 28, 1060–1067. <https://doi.org/10.1161/ATVBAHA.108.164350>

Kodas, E., Vancassel, S., Lejeune, B., Guilloteau, D., Chalon, S., 2002. Reversibility of n-3 fatty acid deficiency-induced changes in dopaminergic neurotransmission in rats:critical role of developmental stage. *Journal of Lipid Research* 43, 1209–1219. <https://doi.org/10.1194/jlr.M200132-JLR200>

Koletzko, B., Cetin, I., Thomas Brenna, J., for the Perinatal Lipid Intake Working Group, 2007. Dietary fat intakes for pregnant and lactating women. *Br J Nutr* 98, 873–877. <https://doi.org/10.1017/S0007114507764747>

Kotani, S., Nakazawa, H., Tokimasa, T., Akimoto, K., Kawashima, H., Toyoda-Ono, Y., Kiso, Y., Okaichi, H., Sakakibara, M., 2003. Synaptic plasticity preserved with arachidonic acid diet in aged rats. *Neuroscience Research* 46, 453–461. [https://doi.org/10.1016/S0168-0102\(03\)00123-8](https://doi.org/10.1016/S0168-0102(03)00123-8)

Kotani, S., Sakaguchi, E., Warashina, S., Matsukawa, N., Ishikura, Y., Kiso, Y., Sakakibara, M., Yoshimoto, T., Guo, J., Yamashima, T., 2006. Dietary supplementation of arachidonic and docosahexaenoic acids improves cognitive dysfunction. *Neuroscience Research* 56, 159–164. <https://doi.org/10.1016/j.neures.2006.06.010>

Kothapalli, K.S.D., Park, H.G., Guo, X., Sun, X., Zou, J., Hyon, S.S., Qin, X., Lawrence, P., Ran-Ressler, R.R., Zhang, J.Y., Gu, Z., Brenna, J.T., 2018. A novel FADS2 isoform identified in human milk fat globule suppresses FADS2 mediated  $\Delta 6$ -desaturation of omega-3 fatty acids. *Prostaglandins, Leukotrienes and Essential Fatty Acids* 138, 52–59. <https://doi.org/10.1016/j.plefa.2018.06.004>

Krashia, P., Cordella, A., Nobili, A., La Barbera, L., Federici, M., Leuti, A., Campanelli, F., Natale, G., Marino, G., Calabrese, V., Vedele, F., Ghiglieri, V., Picconi, B., Di Lazzaro, G., Schirinzi, T., Sancesario, G., Casadei, N., Riess, O., Bernardini, S., Pisani, A., Calabresi, P., Viscomi, M.T., Serhan, C.N., Chiurchiù, V., D'Amelio, M., Mercuri, N.B., 2019. Blunting neuroinflammation with resolvin D1 prevents early pathology in a rat model of Parkinson's disease. *Nat Commun* 10, 3945. <https://doi.org/10.1038/s41467-019-11928-w>

Krishnamoorthy, S., Recchiuti, A., Chiang, N., Yacoubian, S., Lee, C.-H., Yang, R., Petasis, N.A., Serhan, C.N., 2010. Resolvin D1 binds human phagocytes with evidence for proresolving receptors. *Proceedings of the National Academy of Sciences* 107, 1660–1665. <https://doi.org/10.1073/pnas.0907342107>

Krishnan, V., Han, M.-H., Graham, D.L., Berton, O., Renthal, W., Russo, S.J., LaPlant, Q., Graham, A., Lutter, M., Lagace, D.C., Ghose, S., Reister, R., Tannous, P., Green, T.A., Neve, R.L., Chakravarty, S., Kumar, A., Eisch, A.J., Self, D.W., Lee, F.S., Tamminga, C.A., Cooper, D.C., Gershenfeld, H.K., Nestler, E.J., 2007. Molecular Adaptations Underlying Susceptibility and Resistance to Social Defeat in Brain Reward Regions. *Cell* 131, 391–404. <https://doi.org/10.1016/j.cell.2007.09.018>

Kucukdereli, H., Allen, N.J., Lee, A.T., Feng, A., Ozlu, M.I., Conatser, L.M., Chakraborty, C., Workman, G., Weaver, M., Sage, E.H., Barres, B.A., Eroglu, C., 2011. Control of excitatory CNS synaptogenesis by astrocyte-secreted proteins Hevin and SPARC. *Proceedings of the National Academy of Sciences* 108, E440–E449. <https://doi.org/10.1073/pnas.1104977108>

Kutzner, L., Goloshchapova, K., Heydeck, D., Stehling, S., Kuhn, H., Schebb, N.H., 2017. Mammalian ALOX15 orthologs exhibit pronounced dual positional specificity with docosahexaenoic acid. *Biochimica et Biophysica Acta (BBA) - Molecular and Cell Biology of Lipids* 1862, 666–675. <https://doi.org/10.1016/j.bbalip.2017.04.001>

Kvamme, E., Roberg, B., Torgner, I.Aa., 2000. Phosphate-Activated Glutaminase and Mitochondrial Glutamine Transport in the Brain. *Neurochem Res* 25, 1407–1419. <https://doi.org/10.1023/A:1007668801570>

- Labrousse, V.F., Costes, L., Aubert, A., Darnaudéry, M., Ferreira, G., Amédée, T., Layé, S., 2009. Impaired Interleukin-1 $\beta$  and c-Fos Expression in the Hippocampus Is Associated with a Spatial Memory Deficit in P2X7 Receptor-Deficient Mice. *PLoS ONE* 4, e6006. <https://doi.org/10.1371/journal.pone.0006006>
- Labrousse, V.F., Leyrolle, Q., Amadieu, C., Aubert, A., Sere, A., Coutureau, E., Grégoire, S., Bretillon, L., Pallet, V., Gressens, P., Joffre, C., Nadjar, A., Layé, S., 2018. Dietary omega-3 deficiency exacerbates inflammation and reveals spatial memory deficits in mice exposed to lipopolysaccharide during gestation. *Brain, Behavior, and Immunity* 73, 427–440. <https://doi.org/10.1016/j.bbi.2018.06.004>
- Labrousse, V.F., Nadjar, A., Joffre, C., Costes, L., Aubert, A., Grégoire, S., Bretillon, L., Layé, S., 2012. Short-Term Long Chain Omega3 Diet Protects from Neuroinflammatory Processes and Memory Impairment in Aged Mice. *PLoS ONE* 7, e36861. <https://doi.org/10.1371/journal.pone.0036861>
- Lacombe, R.J.S., Chouinard-Watkins, R., Bazinet, R.P., 2018. Brain docosahexaenoic acid uptake and metabolism. *Molecular Aspects of Medicine* 64, 109–134. <https://doi.org/10.1016/j.mam.2017.12.004>
- Lacombe, R.J.S., Smith, M.E., Perlman, K., Turecki, G., Mechawar, N., Bazinet, R.P., 2022. Quantitative and carbon isotope ratio analysis of fatty acids isolated from human brain hemispheres. *Journal of Neurochemistry* n/a. <https://doi.org/10.1111/jnc.15702>
- Lafourcade, M., Elezgarai, I., Mato, S., Bakiri, Y., Grandes, P., Manzoni, O.J., 2007. Molecular Components and Functions of the Endocannabinoid System in Mouse Prefrontal Cortex. *PLoS ONE* 2, e709. <https://doi.org/10.1371/journal.pone.0000709>
- Lafourcade, M., Larrieu, T., Mato, S., Duffaud, A., Sepers, M., Matias, I., De Smedt-Peyrusse, V., Labrousse, V.F., Bretillon, L., Matute, C., Rodríguez-Puertas, R., Layé, S., Manzoni, O.J., 2011. Nutritional omega-3 deficiency abolishes endocannabinoid-mediated neuronal functions. *Nature Neuroscience* 14, 345–350. <https://doi.org/10.1038/nn.2736>
- Lamon-Fava, S., So, J., Mischoulon, D., Ziegler, T.R., Dunlop, B.W., Kinkead, B., Schettler, P.J., Nierenberg, A.A., Felger, J.C., Maddipati, K.R., Fava, M., Rapaport, M.H., 2021. Dose- and time-dependent increase in circulating anti-inflammatory and pro-resolving lipid mediators following eicosapentaenoic acid supplementation in patients with major depressive disorder and chronic inflammation. *Prostaglandins, Leukotrienes and Essential Fatty Acids* 164, 102219. <https://doi.org/10.1016/j.plefa.2020.102219>
- Languille, S., Aujard, F., Pifferi, F., 2012. Effect of dietary fish oil supplementation on the exploratory activity, emotional status and spatial memory of the aged mouse lemur, a non-human primate. *Behavioural Brain Research* 235, 280–286. <https://doi.org/10.1016/j.bbr.2012.08.014>
- Lapillonne, A., Jensen, C.L., 2009. Reevaluation of the DHA requirement for the premature infant. *Prostaglandins, Leukotrienes and Essential Fatty Acids* 81, 143–150. <https://doi.org/10.1016/j.plefa.2009.05.014>
- Larqué, E., Krauss-Etschmann, S., Campoy, C., Hartl, D., Linde, J., Klingler, M., Demmelmair, H., Caño, A., Gil, A., Bondy, B., Koletzko, B., 2006. Docosahexaenoic acid supply in pregnancy affects placental expression of fatty acid transport proteins. *The American Journal of Clinical Nutrition* 84, 853–861. <https://doi.org/10.1093/ajcn/84.4.853>

- Larrieu, T., Hilal, L.M., Fourrier, C., De Smedt-Peyrusse, V., Sans N, Capuron, L., Layé, S., 2014. Nutritional omega-3 modulates neuronal morphology in the prefrontal cortex along with depression-related behaviour through corticosterone secretion. *Translational Psychiatry* 4, e437–e437. <https://doi.org/10.1038/tp.2014.77>
- Larrieu, T., Layé, S., 2018. Food for Mood: Relevance of Nutritional Omega-3 Fatty Acids for Depression and Anxiety. *Frontiers in Physiology* 9.
- Larrieu, T., Madore, C., Joffre, C., Layé, S., 2012. Nutritional n-3 polyunsaturated fatty acids deficiency alters cannabinoid receptor signaling pathway in the brain and associated anxiety-like behavior in mice. *Journal of Physiology and Biochemistry* 68, 671–681. <https://doi.org/10.1007/s13105-012-0179-6>
- Lau, A., Tymianski, M., 2010. Glutamate receptors, neurotoxicity and neurodegeneration. *Pflugers Arch - Eur J Physiol* 460, 525–542. <https://doi.org/10.1007/s00424-010-0809-1>
- Lauritzen, L., 2001. The essentiality of long chain n-3 fatty acids in relation to development and function of the brain and retina. *Progress in Lipid Research* 40, 1–94. [https://doi.org/10.1016/S0163-7827\(00\)00017-5](https://doi.org/10.1016/S0163-7827(00)00017-5)
- Layé, S., Nadjar, A., Joffre, C., Bazinet, R.P., 2018. Anti-Inflammatory Effects of Omega-3 Fatty Acids in the Brain: Physiological Mechanisms and Relevance to Pharmacology. *Pharmacol Rev* 70, 12–38. <https://doi.org/10.1124/pr.117.014092>
- Lefèvre-Arbogast, S., Hejblum, B.P., Helmer, C., Klose, C., Manach, C., Low, D.Y., Urpi-Sarda, M., Andres-Lacueva, C., González-Domínguez, R., Aigner, L., Altendorfer, B., Lucassen, P.J., Ruigrok, S.R., De Lucia, C., Du Preez, A., Proust-Lima, C., Thuret, S., Korosi, A., Samieri, C., 2021. Early signature in the blood lipidome associated with subsequent cognitive decline in the elderly: A case-control analysis nested within the Three-City cohort study. *EBioMedicine* 64, 103216. <https://doi.org/10.1016/j.ebiom.2021.103216>
- Lei, D., Li, W., Tallman, M.J., Patino, L.R., McNamara, R.K., Strawn, J.R., Klein, C.C., Nery, F.G., Fleck, D.E., Qin, K., Ai, Y., Yang, J., Zhang, W., Lui, S., Gong, Q., Adler, C.M., Sweeney, J.A., DelBello, M.P., 2021. Changes in the brain structural connectome after a prospective randomized clinical trial of lithium and quetiapine treatment in youth with bipolar disorder. *Neuropsychopharmacol.* 46, 1315–1323. <https://doi.org/10.1038/s41386-021-00989-5>
- Lemaitre, R.N., Tanaka, T., Tang, W., Manichaikul, A., Foy, M., Kabagambe, E.K., Nettleton, J.A., King, I.B., Weng, L.-C., Bhattacharya, S., Bandinelli, S., Bis, J.C., Rich, S.S., Jr, D.R.J., Cherubini, A., McKnight, B., Liang, S., Gu, X., Rice, K., Laurie, C.C., Lumley, T., Browning, B.L., Psaty, B.M., Chen, Y.-D.I., Friedlander, Y., Djousse, L., Wu, J.H.Y., Siscovick, D.S., Uitterlinden, A.G., Arnett, D.K., Ferrucci, L., Fornage, M., Tsai, M.Y., Mozaffarian, D., Steffen, L.M., 2011. Genetic Loci Associated with Plasma Phospholipid n-3 Fatty Acids: A Meta-Analysis of Genome-Wide Association Studies from the CHARGE Consortium. *PLOS Genetics* 7, e1002193. <https://doi.org/10.1371/journal.pgen.1002193>
- Lépinay, A.L., Larrieu, T., Joffre, C., Acar, N., Gárate, I., Castanon, N., Ferreira, G., Langelier, B., Guesnet, P., Brétilon, L., Parnet, P., Layé, S., Darnaude, M., 2015. Perinatal high-fat diet increases hippocampal vulnerability to the adverse effects of subsequent high-fat feeding. *Psychoneuroendocrinology* 53, 82–93. <https://doi.org/10.1016/j.psyneuen.2014.12.008>
- Leslie, C.C., 2004. Regulation of the specific release of arachidonic acid by cytosolic phospholipase A2. *Prostaglandins, Leukotrienes and Essential Fatty Acids, Professor David F. Horrobin 1939-2003: A Tribute* 70, 373–376. <https://doi.org/10.1016/j.plefa.2003.12.012>

Leslie, C.C., Gangelhoff, T.A., Gelb, M.H., 2010. Localization and function of cytosolic phospholipase A2 $\alpha$  at the Golgi. *Biochimie, Phospholipases A2 and lipid mediators* 92, 620–626. <https://doi.org/10.1016/j.biochi.2010.03.001>

Lespérance, F., Frasare-Smith, N., St-André, E., Turecki, G., Lespérance, P., Wisniewski, S.R., 2010. The Efficacy of Omega-3 Supplementation for Major Depression: A Randomized Controlled Trial. *J Clin Psychiatry* 71, 6074. <https://doi.org/10.4088/JCP.10m05966blu>

Létondor, A., Buaud, B., Vaysse, C., Fonseca, L., Herrouin, C., Servat, B., Layé, S., Pallet, V., Alfos, S., 2014. Erythrocyte DHA level as a biomarker of DHA status in specific brain regions of n-3 long-chain PUFA-supplemented aged rats. *British Journal of Nutrition* 112, 1805–1818. <https://doi.org/10.1017/S0007114514002529>

Leyrolle, Q., Decoeur, F., Briere, G., Amadieu, C., Quadros, A.R.A.A., Voytyuk, I., Lacabanne, C., Benmamar-Badel, A., Bourel, J., Aubert, A., Sere, A., Chain, F., Schwendimann, L., Matrot, B., Bourgeois, T., Grégoire, S., Leblanc, J.G., De Moreno De Leblanc, A., Langella, P., Fernandes, G.R., Bretillon, L., Joffre, C., Uricaru, R., Thebault, P., Gressens, P., Chatel, J.M., Layé, S., Nadjar, A., 2021. Maternal dietary omega-3 deficiency worsens the deleterious effects of prenatal inflammation on the gut-brain axis in the offspring across lifetime. *Neuropsychopharmacol.* 46, 579–602. <https://doi.org/10.1038/s41386-020-00793-7>

Leyrolle, Q., Decoeur, F., Dejean, C., Brière, G., Leon, S., Bakoyiannis, I., Baroux, E., Sterley, T.-L., Bosch-Bouju, C., Morel, L., Amadieu, C., Lecours, C., St-Pierre, M.-K., Bordeleau, M., De Smedt-Peyrusse, V., Séré, A., Schwendimann, L., Grégoire, S., Bretillon, L., Acar, N., Joffre, C., Ferreira, G., Uricaru, R., Thebault, P., Gressens, P., Tremblay, M.-E., Layé, S., Nadjar, A., 2022. N-3 PUFA deficiency disrupts oligodendrocyte maturation and myelin integrity during brain development. *Glia* 70, 50–70. <https://doi.org/10.1002/glia.24088>

Leyrolle, Q., Layé, S., Nadjar, A., 2019. Direct and indirect effects of lipids on microglia function. *Neuroscience Letters* 708, 134348. <https://doi.org/10.1016/j.neulet.2019.134348>

Li, J., Serafin, E., Baccei, M.L., 2018. Prostaglandin Signaling Governs Spike Timing-Dependent Plasticity at Sensory Synapses onto Mouse Spinal Projection Neurons. *J. Neurosci.* 38, 6628–6639. <https://doi.org/10.1523/JNEUROSCI.2152-17.2018>

Li, T., Zheng, J., Wang, Z., Xu, L., Sun, D., Song, H., Wu, S., Du, M., Peng, S., Zhang, J., 2022. Maresin 1 improves cognitive decline and ameliorates inflammation and blood-brain barrier damage in rats with chronic cerebral hypoperfusion. *Brain Research* 1788, 147936. <https://doi.org/10.1016/j.brainres.2022.147936>

Li, X., Liu, R., Li, J., Chang, M., Liu, Y., Jin, Q., Wang, X., 2015. Enhanced arachidonic acid production from *Mortierella alpina* combining atmospheric and room temperature plasma (ARTP) and diethyl sulfate treatments. *Bioresource Technology* 177, 134–140. <https://doi.org/10.1016/j.biortech.2014.11.051>

Libreros, S., Shay, A.E., Nshimiyimana, R., Fichtner, D., Martin, M.J., Wourms, N., Serhan, C.N., 2021. A New E-Series Resolvin: RvE4 Stereochemistry and Function in Efferocytosis of Inflammation-Resolution. *Frontiers in Immunology* 11.

Lim, S.-Y., Doherty, J.D., McBride, K., Miller-Ihli, N.J., Carmona, G.N., Stark, K.D., Salem, N., Jr, 2005. Lead Exposure and (n-3) Fatty Acid Deficiency during Rat Neonatal Development Affect Subsequent Spatial Task Performance and Olfactory Discrimination. *The Journal of Nutrition* 135, 1019–1026. <https://doi.org/10.1093/jn/135.5.1019>

- Lin, L., Metherel, A.H., Di Miceli, M., Liu, Z., Sahin, C., Fioramonti, X., Cummins, C.L., Layé, S., Bazinet, R.P., 2020. Tetracosahexaenoylethanolamide, a novel N-acylethanolamide, is elevated in ischemia and increases neuronal output. *J Lipid Res* 61, 1480–1490. <https://doi.org/10.1194/jlr.RA120001024>
- Lin, P.-Y., Huang, S.-Y., Su, K.-P., 2010. A Meta-Analytic Review of Polyunsaturated Fatty Acid Compositions in Patients with Depression. *Biological Psychiatry, Vascular Function in Depression in Older Adults* 68, 140–147. <https://doi.org/10.1016/j.biopsych.2010.03.018>
- Lin, Y.-H., Brown, J.A., DiMartino, C., Dahms, I., Salem Jr., N., Hibbeln, J.R., 2016. Differences in long chain polyunsaturates composition and metabolism in male and female rats. *Prostaglandins, Leukotrienes and Essential Fatty Acids* 113, 19–27. <https://doi.org/10.1016/j.plefa.2016.08.008>
- Lisman, J.E., McIntyre, C.C., 2001. Synaptic plasticity: a molecular memory switch. *Curr Biol* 11, R788-791. [https://doi.org/10.1016/s0960-9822\(01\)00472-9](https://doi.org/10.1016/s0960-9822(01)00472-9)
- Liu, C., Ye, D., Wang, H., He, M., Sun, Y., 2020. Elovl2 But Not Elovl5 Is Essential for the Biosynthesis of Docosahexaenoic Acid (DHA) in Zebrafish: Insight from a Comparative Gene Knockout Study. *Mar Biotechnol* 22, 613–619. <https://doi.org/10.1007/s10126-020-09992-1>
- Liu, J.-H., Wang, Q., You, Q.-L., Li, Z.-L., Hu, N.-Y., Wang, Y., Jin, Z.-L., Li, S.-J., Li, X.-W., Yang, J.-M., Zhu, X.-H., Dai, Y.-F., Xu, J.-P., Bai, X.-C., Gao, T.-M., 2020. Acute EPA-induced learning and memory impairment in mice is prevented by DHA. *Nat Commun* 11, 5465. <https://doi.org/10.1038/s41467-020-19255-1>
- Liu, J.J., Green, P., John Mann, J., Rapoport, S.I., Sublette, M.E., 2015. Pathways of polyunsaturated fatty acid utilization: Implications for brain function in neuropsychiatric health and disease. *Brain Research* 1597, 220–246. <https://doi.org/10.1016/j.brainres.2014.11.059>
- Liu, X., Bolteus, A.J., Balkin, D.M., Henschel, O., Bordey, A., 2006. GFAP-expressing cells in the postnatal subventricular zone display a unique glial phenotype intermediate between radial glia and astrocytes. *Glia* 54, 394–410. <https://doi.org/10.1002/glia.20392>
- Liu, Y., Ren, X., Fan, C., Wu, W., Zhang, W., Wang, Y., 2022. Health Benefits, Food Applications, and Sustainability of Microalgae-Derived N-3 PUFA. *Foods* 11, 1883. <https://doi.org/10.3390/foods11131883>
- Loomans, E.M., Van den Bergh, B.R.H., Schelling, M., Vrijkotte, T.G.M., van Eijsden, M., 2014. Maternal Long-Chain Polyunsaturated Fatty Acid Status during Early Pregnancy and Children’s Risk of Problem Behavior at Age 5-6 Years. *The Journal of Pediatrics* 164, 762–768. <https://doi.org/10.1016/j.jpeds.2013.11.069>
- López, D.E., Ballaz, S.J., 2020a. The Role of Brain Cyclooxygenase-2 (Cox-2) Beyond Neuroinflammation: Neuronal Homeostasis in Memory and Anxiety. *Mol Neurobiol* 57, 5167–5176. <https://doi.org/10.1007/s12035-020-02087-x>
- López, D.E., Ballaz, S.J., 2020b. The Role of Brain Cyclooxygenase-2 (Cox-2) Beyond Neuroinflammation: Neuronal Homeostasis in Memory and Anxiety. *Mol Neurobiol* 57, 5167–5176. <https://doi.org/10.1007/s12035-020-02087-x>
- Lotrich, F.E., Albusaysi, S., Ferrell, R.E., 2013. Brain-Derived Neurotrophic Factor Serum Levels and Genotype: Association with Depression during Interferon- $\alpha$  Treatment. *Neuropsychopharmacol* 38, 985–995. <https://doi.org/10.1038/npp.2012.263>

- Lozada, L.E., Desai, A., Kevala, K., Lee, J.-W., Kim, H.-Y., 2017. Perinatal Brain Docosahexaenoic Acid Concentration Has a Lasting Impact on Cognition in Mice. *J Nutr* 147, 1624–1630. <https://doi.org/10.3945/jn.117.254607>
- Luchtman, D.W., 2013. Cognitive enhancement by omega-3 fatty acids from child-hood to old age: Findings from animal and clinical studies 16.
- Lundy, D.F., McBean, G.J., 1995. Pre-incubation of synaptosomes with arachidonic acid potentiates inhibition of [3H]D-aspartate transport. *European Journal of Pharmacology: Molecular Pharmacology* 291, 273–279. [https://doi.org/10.1016/0922-4106\(95\)90067-5](https://doi.org/10.1016/0922-4106(95)90067-5)
- Luo, Y., Kataoka, Y., Ostinelli, E.G., Cipriani, A., Furukawa, T.A., 2020. National Prescription Patterns of Antidepressants in the Treatment of Adults With Major Depression in the US Between 1996 and 2015: A Population Representative Survey Based Analysis. *Frontiers in Psychiatry* 11.
- Lynch, M.A., 2004. Long-term potentiation and memory. *Physiol Rev* 84, 87–136. <https://doi.org/10.1152/physrev.00014.2003>
- Madore, C., Leyrolle, Q., Morel, L., Rossitto, M., Greenhalgh, A.D., Delpech, J.C., Martinat, M., Bosch-Bouju, C., Bourel, J., Rani, B., Lacabanne, C., Thomazeau, A., Hopperton, K.E., Beccari, S., Sere, A., Aubert, A., De Smedt-Peyrusse, V., Lecours, C., Bisht, K., Fourgeaud, L., Gregoire, S., Bretillon, L., Acar, N., Grant, N.J., Badaut, J., Gressens, P., Sierra, A., Butovsky, O., Tremblay, M.E., Bazinet, R.P., Joffre, C., Nadjar, A., Layé, S., 2020. Essential omega-3 fatty acids tune microglial phagocytosis of synaptic elements in the mouse developing brain. *Nature Communications* 11, 6133. <https://doi.org/10.1038/s41467-020-19861-z>
- Madore, C., Nadjar, A., Delpech, J.-C., Sere, A., Aubert, A., Portal, C., Joffre, C., Layé, S., 2014. Nutritional n-3 PUFAs deficiency during perinatal periods alters brain innate immune system and neuronal plasticity-associated genes. *Brain, Behavior, and Immunity* 41, 22–31. <https://doi.org/10.1016/j.bbi.2014.03.021>
- Magnusardottir, A.R., Steingrimsdottir, L., Thorgeirsdottir, H., Gunnlaugsson, G., Skuladottir, G.V., 2009. Docosahexaenoic acid in red blood cells of women of reproductive age is positively associated with oral contraceptive use and physical activity. *Prostaglandins Leukot Essent Fatty Acids* 80, 27–32. <https://doi.org/10.1016/j.plefa.2008.10.004>
- Mahon, S., Vautrelle, N., Pezard, L., Slaght, S.J., Deniau, J.-M., Chouvet, G., Charpier, S., 2006. Distinct Patterns of Striatal Medium Spiny Neuron Activity during the Natural Sleep-Wake Cycle. *Journal of Neuroscience* 26, 12587–12595. <https://doi.org/10.1523/JNEUROSCI.3987-06.2006>
- Makrides, M., 2013. DHA supplementation during the perinatal period and neurodevelopment: Do some babies benefit more than others? *Prostaglandins, Leukotrienes and Essential Fatty Acids, The Tenth Fatty Acids and Cell Signalling Meeting (FACS-10)* 88, 87–90. <https://doi.org/10.1016/j.plefa.2012.05.004>
- Makrides, M., Best, K., Yelland, L., McPhee, A., Zhou, S., Quinlivan, J., Dodd, J., Atkinson, E., Safa, H., van Dam, J., Khot, N., Dekker, G., Skubisz, M., Anderson, A., Kean, B., Bowman, A., McCallum, C., Cashman, K., Gibson, R., 2019. A Randomized Trial of Prenatal n-3 Fatty Acid Supplementation and Preterm Delivery. *N Engl J Med* 381, 1035–1045. <https://doi.org/10.1056/NEJMoa1816832>
- Maltais, M., Lorrain, D., Léveillé, P., Viens, I., Vachon, A., Houeto, A., Presse, N., Plourde, M., 2022. Long-chain Omega-3 fatty acids supplementation and cognitive performance throughout adulthood:

A 6-month randomized controlled trial. *Prostaglandins, Leukotrienes and Essential Fatty Acids* 178, 102415. <https://doi.org/10.1016/j.plefa.2022.102415>

Manduca, A., Morena, M., Campolongo, P., Servadio, M., Palmery, M., Trabace, L., Hill, M.N., Vanderschuren, L.J.M.J., Cuomo, V., Trezza, V., 2015. Distinct roles of the endocannabinoids anandamide and 2-arachidonoylglycerol in social behavior and emotionality at different developmental ages in rats. *European Neuropsychopharmacology* 25, 1362–1374. <https://doi.org/10.1016/j.euroneuro.2015.04.005>

Mannella, F., Gurney, K., Baldassarre, G., 2013. The nucleus accumbens as a nexus between values and goals in goal-directed behavior: a review and a new hypothesis. *Front. Behav. Neurosci.* 7. <https://doi.org/10.3389/fnbeh.2013.00135>

Manual Kollareth, D.J., Deckelbaum, R.J., Liu, Z., Ramakrishnan, R., Jouvène, C., Serhan, C.N., Ten, V.S., Zirpoli, H., 2020. Acute injection of a DHA triglyceride emulsion after hypoxic-ischemic brain injury in mice increases both DHA and EPA levels in blood and brain ☆. *Prostaglandins, Leukotrienes and Essential Fatty Acids* 162, 102176. <https://doi.org/10.1016/j.plefa.2020.102176>

Manzoni, C., Mennini, T., 1997. ARACHIDONIC ACID INHIBITS 3H-GLUTAMATE UPTAKE WITH DIFFERENT POTENCIES IN RODENT CENTRAL NERVOUS SYSTEM REGIONS EXPRESSING DIFFERENT TRANSPORTER SUBTYPES. *Pharmacological Research* 35, 149–151. <https://doi.org/10.1006/phrs.1997.0129>

Marinetti, G.V., Weindl, A., Kelly, J., 1971. Lipid metabolism in the rabbit choroid plexus. *Journal of Neurochemistry* 18, 2003–2006. <https://doi.org/10.1111/j.1471-4159.1971.tb09606.x>

Marquardt, A., Stöhr, H., White, K., Weber, B.H.F., 2000. cDNA Cloning, Genomic Structure, and Chromosomal Localization of Three Members of the Human Fatty Acid Desaturase Family. *Genomics* 66, 175–183. <https://doi.org/10.1006/geno.2000.6196>

Marszalek, J.R., Kitidis, C., Dararutana, A., Lodish, H.F., 2004. Acyl-CoA Synthetase 2 Overexpression Enhances Fatty Acid Internalization and Neurite Outgrowth\*. *Journal of Biological Chemistry* 279, 23882–23891. <https://doi.org/10.1074/jbc.M313460200>

Marszalek, J.R., Kitidis, C., DiRusso, C.C., Lodish, H.F., 2005. Long-chain Acyl-CoA Synthetase 6 Preferentially Promotes DHA Metabolism\*. *Journal of Biological Chemistry* 280, 10817–10826. <https://doi.org/10.1074/jbc.M411750200>

Martin, K.C., Kosik, K.S., 2002. Synaptic tagging — who's it? *Nat Rev Neurosci* 3, 813–820. <https://doi.org/10.1038/nrn942>

Martinat, M., Rossitto, M., Di Miceli, M., Layé, S., 2021a. Perinatal Dietary Polyunsaturated Fatty Acids in Brain Development, Role in Neurodevelopmental Disorders. *Nutrients* 13, 1185. <https://doi.org/10.3390/nu13041185>

Martinat, M., Rossitto, M., Di Miceli, M., Layé, S., 2021b. Perinatal Dietary Polyunsaturated Fatty Acids in Brain Development, Role in Neurodevelopmental Disorders. *Nutrients* 13, 1185. <https://doi.org/10.3390/nu13041185>

Martinez, M., 1992. Tissue levels of polyunsaturated fatty acids during early human development. *The Journal of Pediatrics* 120, S129–S138. [https://doi.org/10.1016/S0022-3476\(05\)81247-8](https://doi.org/10.1016/S0022-3476(05)81247-8)



Martins, J.G., 2009. EPA but Not DHA Appears To Be Responsible for the Efficacy of Omega-3 Long Chain Polyunsaturated Fatty Acid Supplementation in Depression: Evidence from a Meta-Analysis of Randomized Controlled Trials. *Journal of the American College of Nutrition* 28, 525–542. <https://doi.org/10.1080/07315724.2009.10719785>

Marzo, V.D., Bifulco, M., Petrocellis, L.D., 2004. The endocannabinoid system and its therapeutic exploitation. *Nat Rev Drug Discov* 3, 771–784. <https://doi.org/10.1038/nrd1495>

Materazzi, S., Nassini, R., Andrè, E., Campi, B., Amadesi, S., Trevisani, M., Bunnett, N.W., Patacchini, R., Geppetti, P., 2008. Cox-dependent fatty acid metabolites cause pain through activation of the irritant receptor TRPA1. *Proceedings of the National Academy of Sciences* 105, 12045–12050. <https://doi.org/10.1073/pnas.0802354105>

Mazzocchi-Jones, D., 2015. Impaired corticostriatal LTP and depotentiation following iPLA2 inhibition is restored following acute application of DHA. *Brain Research Bulletin* 111, 69–75. <https://doi.org/10.1016/j.brainresbull.2014.12.010>

McDougle, D.R., Watson, J.E., Abdeen, A.A., Adili, R., Caputo, M.P., Krapf, J.E., Johnson, R.W., Kilian, K.A., Holinstat, M., Das, A., 2017. Anti-inflammatory  $\omega$ -3 endocannabinoid epoxides. *Proceedings of the National Academy of Sciences* 114, E6034–E6043. <https://doi.org/10.1073/pnas.1610325114>

McFarland, N.R., Haber, S.N., 2000. Convergent Inputs from Thalamic Motor Nuclei and Frontal Cortical Areas to the Dorsal Striatum in the Primate. *J. Neurosci.* 20, 3798–3813. <https://doi.org/10.1523/JNEUROSCI.20-10-03798.2000>

McNamara, R.K., 2016. Role of Omega-3 fatty acids in the etiology, treatment, and prevention of depression: Current status and future directions. *Journal of Nutrition & Intermediary Metabolism, Novel concepts and controversies surrounding omega-3 polyunsaturated fatty acid* 5, 96–106. <https://doi.org/10.1016/j.jnim.2016.04.004>

McNamara, R.K., Able, J., Jandacek, R., Rider, T., Tso, P., 2009. Gender differences in rat erythrocyte and brain docosahexaenoic acid composition: Role of ovarian hormones and dietary omega-3 fatty acid composition. *Psychoneuroendocrinology* 34, 532–539. <https://doi.org/10.1016/j.psyneuen.2008.10.013>

McNamara, R.K., Almeida, D.M., 2019. Omega-3 Polyunsaturated Fatty Acid Deficiency and Progressive Neuropathology in Psychiatric Disorders: A Review of Translational Evidence and Candidate Mechanisms. *Harv Rev Psychiatry* 27, 94–107. <https://doi.org/10.1097/HRP.000000000000199>

McNamara, R.K., Carlson, S.E., 2006. Role of omega-3 fatty acids in brain development and function: Potential implications for the pathogenesis and prevention of psychopathology. *Prostaglandins, Leukotrienes and Essential Fatty Acids* 75, 329–349. <https://doi.org/10.1016/j.plefa.2006.07.010>

McNamara, R.K., Hahn, C.-G., Jandacek, R., Rider, T., Tso, P., Stanford, K.E., Richtand, N.M., 2007. Selective deficits in the omega-3 fatty acid docosahexaenoic acid in the postmortem orbitofrontal cortex of patients with major depressive disorder. *Biol Psychiatry* 62, 17–24. <https://doi.org/10.1016/j.biopsych.2006.08.026>

McNamara, R.K., Liu, Y., 2011. Reduced expression of fatty acid biosynthesis genes in the prefrontal cortex of patients with major depressive disorder. *Journal of Affective Disorders* 129, 359–363. <https://doi.org/10.1016/j.jad.2010.08.021>

- Meng, X., Yang, F., Ouyang, T., Liu, B., Wu, C., Jiang, W., 2015. Specific gene expression in mouse cortical astrocytes is mediated by a 1740bp-GFAP promoter-driven combined adeno-associated virus2/5/7/8/9. *Neuroscience Letters* 593, 45–50. <https://doi.org/10.1016/j.neulet.2015.03.022>
- Merino, D.M., Johnston, H., Clarke, S., Roke, K., Nielsen, D., Badawi, A., El-Soheily, A., Ma, D.W.L., Mutch, D.M., 2011. Polymorphisms in FADS1 and FADS2 alter desaturase activity in young Caucasian and Asian adults. *Molecular Genetics and Metabolism* 103, 171–178. <https://doi.org/10.1016/j.ymgme.2011.02.012>
- Metherel, A.H., Chouinard-Watkins, R., Trépanier, M.-O., Lacombe, R.J.S., Bazinet, R.P., 2017. Retroconversion is a minor contributor to increases in eicosapentaenoic acid following docosahexaenoic acid feeding as determined by compound specific isotope analysis in rat liver. *Nutr Metab (Lond)* 14, 75. <https://doi.org/10.1186/s12986-017-0230-2>
- Meyer, R.C., Giddens, M.M., Schaefer, S.A., Hall, R.A., 2013. GPR37 and GPR37L1 are receptors for the neuroprotective and glioprotective factors prosaptide and prosaposin. *Proceedings of the National Academy of Sciences* 110, 9529–9534. <https://doi.org/10.1073/pnas.1219004110>
- Michael-Titus, A.T., Priestley, J.V., 2014. Omega-3 fatty acids and traumatic neurological injury: from neuroprotection to neuroplasticity? *Trends in Neurosciences* 37, 30–38. <https://doi.org/10.1016/j.tins.2013.10.005>
- Mingam, R., Moranis, A., Bluthé, R.-M., De Smedt-Peyrusse, V., Kelley, K.W., Guesnet, P., Lavalie, M., Dantzer, R., Layé, S., 2008. Uncoupling of interleukin-6 from its signalling pathway by dietary n-3-polyunsaturated fatty acid deprivation alters sickness behaviour in mice. *European Journal of Neuroscience* 28, 1877–1886. <https://doi.org/10.1111/j.1460-9568.2008.06470.x>
- Mirnikjoo, B., Brown, S.E., Kim, H.F.S., Marangell, L.B., Sweatt, J.D., Weeber, E.J., 2001. Protein Kinase Inhibition by  $\omega$ -3 Fatty Acids. *Journal of Biological Chemistry* 276, 10888–10896. <https://doi.org/10.1074/jbc.M008150200>
- Mischoulon, D., Dunlop, B.W., Kinkead, B., Schettler, P.J., Lamon-Fava, S., Rakofsky, J.J., Nierenberg, A.A., Clain, A.J., Crowe, T.M., Wong, A., Felger, J.C., Sangermano, L., Ziegler, T.R., Cusin, C., Fisher, L.B., Fava, M., Rapaport, M.H., 2022. Omega-3 Fatty Acids for Major Depressive Disorder With High Inflammation: A Randomized Dose-Finding Clinical Trial. *J Clin Psychiatry* 83, 42432. <https://doi.org/10.4088/JCP.21m14074>
- Mischoulon, D., Fava, M., 2002. Role of S-adenosyl-l-methionine in the treatment of depression: a review of the evidence. *The American Journal of Clinical Nutrition* 76, 1158S-1161S. <https://doi.org/10.1093/ajcn/76.5.1158S>
- Mischoulon, D., Nierenberg, A.A., Schettler, P.J., Kinkead, B.L., Fehling, K., Martinson, M.A., Rapaport, M.H., 2014. A Double-Blind, Randomized Controlled Clinical Trial Comparing Eicosapentaenoic Acid Versus Docosahexaenoic Acid for Depression. *J Clin Psychiatry* 76, 4830. <https://doi.org/10.4088/JCP.14m08986>
- Mitchell, R.W., Hatch, G.M., 2011. Fatty acid transport into the brain: Of fatty acid fables and lipid tails. *Prostaglandins, Leukotrienes and Essential Fatty Acids (PLEFA)*, Proceedings of the ISSFAL Congress 2010 85, 293–302. <https://doi.org/10.1016/j.plefa.2011.04.007>
- Mitchell, R.W., On, N.H., Del Bigio, M.R., Miller, D.W., Hatch, G.M., 2011. Fatty acid transport protein expression in human brain and potential role in fatty acid transport across human brain microvessel

endothelial cells. *Journal of Neurochemistry* 117, 735–746. <https://doi.org/10.1111/j.1471-4159.2011.07245.x>

Miyoshi, E., Wietzikoski, E.C., Bortolanza, M., Boschen, S.L., Canteras, N.S., Izquierdo, I., Da Cunha, C., 2012. Both the dorsal hippocampus and the dorsolateral striatum are needed for rat navigation in the Morris water maze. *Behavioural Brain Research* 226, 171–178. <https://doi.org/10.1016/j.bbr.2011.09.011>

Moffat, C.F., McGill, A.S., Hardy, R., Anderson, R.S., 1993. The production of fish oils enriched in polyunsaturated fatty acid-containing triglycerides. *Journal of the American Oil Chemists' Society* 70, 133–138. <https://doi.org/10.1007/BF02542615>

Moi, I.M., Leow, A.T.C., Ali, M.S.M., Rahman, R.N.Z.R.Abd., Salleh, A.B., Sabri, S., 2018. Polyunsaturated fatty acids in marine bacteria and strategies to enhance their production. *Appl Microbiol Biotechnol* 102, 5811–5826. <https://doi.org/10.1007/s00253-018-9063-9>

Monk, J.M., Liddle, D.M., Cohen, D.J.A., Tsang, D.H., Hillyer, L.M., Abdelmagid, S.A., Nakamura, M.T., Power, K.A., Ma, D.W.L., Robinson, L.E., 2016. The delta 6 desaturase knock out mouse reveals that immunomodulatory effects of essential n-6 and n-3 polyunsaturated fatty acids are both independent of and dependent upon conversion. *The Journal of Nutritional Biochemistry* 32, 29–38. <https://doi.org/10.1016/j.jnutbio.2016.01.004>

Monroig, Ó., Rotllant, J., Sánchez, E., Cerdá-Reverter, J.M., Tocher, D.R., 2009. Expression of long-chain polyunsaturated fatty acid (LC-PUFA) biosynthesis genes during zebrafish *Danio rerio* early embryogenesis. *Biochimica et Biophysica Acta (BBA) - Molecular and Cell Biology of Lipids* 1791, 1093–1101. <https://doi.org/10.1016/j.bbalip.2009.07.002>

Moranis, A., Delpech, J.-C., De Smedt-Peyrusse, V., Aubert, A., Guesnet, P., Lavielle, M., Joffre, C., Layé, S., 2012. Long term adequate n-3 polyunsaturated fatty acid diet protects from depressive-like behavior but not from working memory disruption and brain cytokine expression in aged mice. *Brain, Behavior, and Immunity* 26, 721–731. <https://doi.org/10.1016/j.bbi.2011.11.001>

Moreira, J.D., Knorr, L., Ganzella, M., Thomazi, A.P., de Souza, C.G., de Souza, D.G., Pitta, C.F., e Souza, T.M., Wofchuk, S., Elisabetsky, E., Vinadé, L., Perry, M.L.S., Souza, D.O., 2010. Omega-3 fatty acids deprivation affects ontogeny of glutamatergic synapses in rats: Relevance for behavior alterations. *Neurochemistry International* 56, 753–759. <https://doi.org/10.1016/j.neuint.2010.02.010>

Morgese, M.G., Schiavone, S., Maffione, A.B., Tucci, P., Trabace, L., 2020. Depressive-like phenotype evoked by lifelong nutritional omega-3 deficiency in female rats: Crosstalk among kynurenine, Toll-like receptors and amyloid beta oligomers. *Brain Behav Immun* 87, 444–454. <https://doi.org/10.1016/j.bbi.2020.01.015>

Moriguchi, T., Greiner, R.S., Salem Jr., N., 2000. Behavioral Deficits Associated with Dietary Induction of Decreased Brain Docosahexaenoic Acid Concentration. *Journal of Neurochemistry* 75, 2563–2573. <https://doi.org/10.1046/j.1471-4159.2000.0752563.x>

Moriguchi, T., Salem Jr, N., 2003. Recovery of brain docosahexaenoate leads to recovery of spatial task performance. *Journal of Neurochemistry* 87, 297–309. <https://doi.org/10.1046/j.1471-4159.2003.01966.x>

Morris, M.C., Evans, D.A., Bienias, J.L., Tangney, C.C., Bennett, D.A., Wilson, R.S., Aggarwal, N., Schneider, J., 2003. Consumption of Fish and n-3 Fatty Acids and Risk of Incident Alzheimer Disease. *Archives of Neurology* 60, 940–946. <https://doi.org/10.1001/archneur.60.7.940>

- Muc, M., Kreiner-Møller, E., Larsen, J.M., Birch, S., Brix, S., Bisgaard, H., Lauritzen, L., 2015. Maternal fatty acid desaturase genotype correlates with infant immune responses at 6 months. *British Journal of Nutrition* 114, 891–898. <https://doi.org/10.1017/S0007114515002561>
- Mukherjee, P., Abate, L.E., Seyfried, T.N., 2004. Antiangiogenic and Proapoptotic Effects of Dietary Restriction on Experimental Mouse and Human Brain Tumors. *Clinical Cancer Research* 10, 5622–5629. <https://doi.org/10.1158/1078-0432.CCR-04-0308>
- Murphy-Royal, C., Dupuis, J.P., Varela, J.A., Panatier, A., Pinson, B., Baufreton, J., Groc, L., Oliet, S.H.R., 2015. Surface diffusion of astrocytic glutamate transporters shapes synaptic transmission. *Nat Neurosci* 18, 219–226. <https://doi.org/10.1038/nn.3901>
- Murray, H.J., O'Connor, J.J., 2003. A role for COX-2 and p38 mitogen activated protein kinase in long-term depression in the rat dentate gyrus in vitro. *Neuropharmacology* 44, 374–380. [https://doi.org/10.1016/S0028-3908\(02\)00375-1](https://doi.org/10.1016/S0028-3908(02)00375-1)
- Musella, A., Fresegna, D., Rizzo, F.R., Gentile, A., Bullitta, S., De Vito, F., Guadalupi, L., Centonze, D., Mandolesi, G., 2017. A novel crosstalk within the endocannabinoid system controls GABA transmission in the striatum. *Sci Rep* 7, 7363. <https://doi.org/10.1038/s41598-017-07519-8>
- Naganuma, T., Sato, Y., Sassa, T., Ohno, Y., Kihara, A., 2011. Biochemical characterization of the very long-chain fatty acid elongase ELOVL7. *FEBS Letters* 585, 3337–3341. <https://doi.org/10.1016/j.febslet.2011.09.024>
- Nakamura, M.T., Nara, T.Y., 2004. Structure, Function, and Dietary Regulation of  $\Delta 6$ ,  $\Delta 5$ , and  $\Delta 9$  Desaturases. *Annual Review of Nutrition* 24, 345–376. <https://doi.org/10.1146/annurev.nutr.24.121803.063211>
- Naudí, A., Cabré, R., Jové, M., Ayala, V., Gonzalo, H., Portero-Otín, M., Ferrer, I., Pamplona, R., 2015. Chapter Five - Lipidomics of Human Brain Aging and Alzheimer's Disease Pathology, in: Hurley, M.J. (Ed.), *International Review of Neurobiology, Omic Studies of Neurodegenerative Disease: Part B*. Academic Press, pp. 133–189. <https://doi.org/10.1016/bs.irn.2015.05.008>
- Nebert, D.W., Wikvall, K., Miller, W.L., 2013. Human cytochromes P450 in health and disease. *Philosophical Transactions of the Royal Society B: Biological Sciences* 368, 20120431. <https://doi.org/10.1098/rstb.2012.0431>
- Nedergaard, M., Ransom, B., Goldman, S.A., 2003. New roles for astrocytes: Redefining the functional architecture of the brain. *Trends in Neurosciences* 26, 523–530. <https://doi.org/10.1016/j.tins.2003.08.008>
- Neniskyte, U., Gross, C.T., 2017. Errant gardeners: glial-cell-dependent synaptic pruning and neurodevelopmental disorders. *Nat Rev Neurosci* 18, 658–670. <https://doi.org/10.1038/nrn.2017.110>
- Nettleton, J.A., 1995. Omega-3 Fatty Acids and Health, in: Nettleton, J.A. (Ed.), *Omega-3 Fatty Acids and Health*. Springer US, Boston, MA, pp. 64–76. [https://doi.org/10.1007/978-1-4615-2071-9\\_2](https://doi.org/10.1007/978-1-4615-2071-9_2)
- Nguyen, L.N., Ma, D., Shui, G., Wong, P., Cazenave-Gassiot, A., Zhang, X., Wenk, M.R., Goh, E.L.K., Silver, D.L., 2014. Mfsd2a is a transporter for the essential omega-3 fatty acid docosahexaenoic acid. *Nature* 509, 503–506. <https://doi.org/10.1038/nature13241>

- Nieoullon, A., Canolle, B., Masméjean, F., Guillet, B., Pisano, P., Lortet, S., 2006. The neuronal excitatory amino acid transporter EAAC1/EAAT3: does it represent a major actor at the brain excitatory synapse? *Journal of Neurochemistry* 98, 1007–1018. <https://doi.org/10.1111/j.1471-4159.2006.03978.x>
- Nieto-Ruiz, A., García-Santos, J.A., Verdejo-Román, J., Diéguez, E., Sepúlveda-Valbuena, N., Herrmann, F., Cerdó, T., De-Castellar, R., Jiménez, J., Bermúdez, M.G., Pérez-García, M., Miranda, M.T., López-Sabater, M.C., Catena, A., Campoy, C., 2022. Infant Formula Supplemented With Milk Fat Globule Membrane, Long-Chain Polyunsaturated Fatty Acids, and Synbiotics Is Associated With Neurocognitive Function and Brain Structure of Healthy Children Aged 6 Years: The COGNIS Study. *Front. Nutr.* 9, 820224. <https://doi.org/10.3389/fnut.2022.820224>
- Okereke, O.I., Vyas, C.M., Mischoulon, D., Chang, G., Cook, N.R., Weinberg, A., Bubes, V., Copeland, T., Friedenberg, G., Lee, I.-M., Buring, J.E., Reynolds, C.F., III, Manson, J.E., 2021. Effect of Long-term Supplementation With Marine Omega-3 Fatty Acids vs Placebo on Risk of Depression or Clinically Relevant Depressive Symptoms and on Change in Mood Scores: A Randomized Clinical Trial. *JAMA* 326, 2385–2394. <https://doi.org/10.1001/jama.2021.21187>
- Oliet, S.H.R., Mothet, J.-P., 2009. Regulation of N-methyl-d-aspartate receptors by astrocytic d-serine. *Neuroscience, Protein trafficking, targeting, and interaction at the glutamate synapse* 158, 275–283. <https://doi.org/10.1016/j.neuroscience.2008.01.071>
- Oliveira, J.F., Araque, A., 2022. Astrocyte regulation of neural circuit activity and network states. *Glia* 70, 1455–1466. <https://doi.org/10.1002/glia.24178>
- Oliveira, M., Koshibu, K., Rytz, A., Giuffrida, F., Sultan, S., Patin, A., Gaudin, M., Tomezyk, A., Steiner, P., Schneider, N., 2022. Early Life to Adult Brain Lipidome Dynamic: A Temporospatial Study Investigating Dietary Polar Lipid Supplementation Efficacy. *Front. Nutr.* 9, 898655. <https://doi.org/10.3389/fnut.2022.898655>
- Omote, H., Miyaji, T., Juge, N., Moriyama, Y., 2011. Vesicular Neurotransmitter Transporter: Bioenergetics and Regulation of Glutamate Transport. *Biochemistry* 50, 5558–5565. <https://doi.org/10.1021/bi200567k>
- Orr, S.K., Palumbo, S., Bosetti, F., Mount, H.T., Kang, J.X., E, C., Greenwood, Ma, D.W., Serhan, C.N., Bazinet, R.P., 2013. Unesterified docosahexaenoic acid is protective in neuroinflammation. *J Neurochem* 127, 378–393. <https://doi.org/10.1111/jnc.12392>
- Ostermann, A.I., Waindok, P., Schmidt, M.J., Chiu, C.-Y., Smyl, C., Rohwer, N., Weylandt, K.-H., Schebb, N.H., 2017. Modulation of the endogenous omega-3 fatty acid and oxylipin profile in vivo—A comparison of the fat-1 transgenic mouse with C57BL/6 wildtype mice on an omega-3 fatty acid enriched diet. *PLOS ONE* 12, e0184470. <https://doi.org/10.1371/journal.pone.0184470>
- Ouellet, M., Emond, V., Chen, C.T., Julien, C., Bourasset, F., Oddo, S., LaFerla, F., Bazinet, R.P., Calon, F., 2009. Diffusion of docosahexaenoic and eicosapentaenoic acids through the blood–brain barrier: An in situ cerebral perfusion study. *Neurochemistry International* 55, 476–482. <https://doi.org/10.1016/j.neuint.2009.04.018>
- Owada, Y., Abdelwahab, S.A., Kitanaka, N., Sakagami, H., Takano, H., Sugitani, Y., Sugawara, M., Kawashima, H., Kiso, Y., Mobarakeh, J.I., Yanai, K., Kaneko, K., Sasaki, H., Kato, H., Saino-Saito, S., Matsumoto, N., Akaike, N., Noda, T., Kondo, H., 2006. Altered emotional behavioral responses in mice lacking brain-type fatty acid-binding protein gene. *European Journal of Neuroscience* 24, 175–187. <https://doi.org/10.1111/j.1460-9568.2006.04855.x>

- Owens, S. de la P., Innis, S.M., 1999. Docosahexaenoic and Arachidonic Acid Prevent a Decrease in Dopaminergic and Serotonergic Neurotransmitters in Frontal Cortex Caused by a Linoleic and  $\alpha$ -Linolenic Acid Deficient Diet in Formula-fed Piglets. *The Journal of Nutrition* 129, 2088–2093. <https://doi.org/10.1093/jn/129.11.2088>
- Pace-Asciak, C.R., 2015. Pathophysiology of the hepoxilins. *Biochimica et Biophysica Acta (BBA) - Molecular and Cell Biology of Lipids, Oxygenated metabolism of PUFA: analysis and biological relevance* 1851, 383–396. <https://doi.org/10.1016/j.bbalip.2014.09.007>
- Pacher, P., Bátkai, S., Kunos, G., 2006. The Endocannabinoid System as an Emerging Target of Pharmacotherapy. *Pharmacol Rev* 58, 389–462. <https://doi.org/10.1124/pr.58.3.2>
- Pamplona, F.A., Vitória, G., Sudo, F.K., Ribeiro, F.C., Isaac, A.R., Moraes, C.A., Chauvet, M.G., Ledur, P.F., Karmirian, K., Ornelas, I.M., Leo, L.M., Paulsen, B., Coutinho, G., Drummond, C., Assunção, N., Vanderborght, B., Canetti, C.A., Castro-Faria-Neto, H.C., Mattos, P., Ferreira, S.T., Rehen, S.K., Bozza, F.A., Lourenco, M.V., Tovar-Moll, F., 2022. Age-linked suppression of lipoxin A4 associates with cognitive deficits in mice and humans. *Transl Psychiatry* 12, 1–11. <https://doi.org/10.1038/s41398-022-02208-1>
- Panatier, A., Vallée, J., Haber, M., Murai, K.K., Lacaille, J.-C., Robitaille, R., 2011. Astrocytes Are Endogenous Regulators of Basal Transmission at Central Synapses. *Cell* 146, 785–798. <https://doi.org/10.1016/j.cell.2011.07.022>
- Park, H.G., Park, W.J., Kothapalli, K.S.D., Brenna, J.T., 2015. The fatty acid desaturase 2 (FADS2) gene product catalyzes A4 desaturation to yield n-3 docosahexaenoic acid and n-6 docosapentaenoic acid in human cells. *The FASEB Journal* 29, 3911–3919. <https://doi.org/10.1096/fj.15-271783>
- Patan, M.J., Kennedy, D.O., Husberg, C., Hustvedt, S.O., Calder, P.C., Khan, J., Forster, J., Jackson, P.A., 2021. Supplementation with oil rich in eicosapentaenoic acid, but not in docosahexaenoic acid, improves global cognitive function in healthy, young adults: results from randomized controlled trials. *The American Journal of Clinical Nutrition* 114, 914–924. <https://doi.org/10.1093/ajcn/nqab174>
- Pauter, A.M., Fischer, A.W., Bengtsson, T., Asadi, A., Talamonti, E., Jacobsson, A., 2019. Synergistic Effects of DHA and Sucrose on Body Weight Gain in PUFA-Deficient Elov12  $-/-$  Mice. *Nutrients* 11, 852. <https://doi.org/10.3390/nu11040852>
- Pauter, A.M., Olsson, P., Asadi, A., Herslöf, B., Csikasz, R.I., Zdravec, D., Jacobsson, A., 2014. Elov12 ablation demonstrates that systemic DHA is endogenously produced and is essential for lipid homeostasis in mice [S]. *Journal of Lipid Research* 55, 718–728. <https://doi.org/10.1194/jlr.M046151>
- Pauter, A.M., Trattner, S., Gonzalez-Bengtsson, A., Talamonti, E., Asadi, A., Dethlefsen, O., Jacobsson, A., 2017. Both maternal and offspring Elov12 genotypes determine systemic DHA levels in perinatal mice. *Journal of Lipid Research* 58, 111–123. <https://doi.org/10.1194/jlr.M070862>
- Pélerin, H., Jouin, M., Lallemand, M.-S., Alessandri, J.-M., Cunnane, S.C., Langelier, B., Guesnet, P., 2014. Gene expression of fatty acid transport and binding proteins in the blood–brain barrier and the cerebral cortex of the rat: Differences across development and with different DHA brain status. *Prostaglandins, Leukotrienes and Essential Fatty Acids* 91, 213–220. <https://doi.org/10.1016/j.plefa.2014.07.004>

- Peng, K., Lv, X., Zhao, H., Chen, B., Chen, X., Huang, W., 2022. Antioxidant and intestinal recovery function of condensed tannins in *Lateolabrax maculatus* responded to in vivo and in vitro oxidative stress. *Aquaculture* 547, 737399. <https://doi.org/10.1016/j.aquaculture.2021.737399>
- Perea, G., Navarrete, M., Araque, A., 2009. Tripartite synapses: astrocytes process and control synaptic information. *Trends in Neurosciences* 32, 421–431. <https://doi.org/10.1016/j.tins.2009.05.001>
- Pietropaolo, S., Goubran, M., Joffre, C., Aubert, A., Lemaire-Mayo, V., Crusio, W.E., Layé, S., 2014. Dietary supplementation of omega-3 fatty acids rescues fragile X phenotypes in *Fmr1-Ko* mice. *Psychoneuroendocrinology* 49, 119–129. <https://doi.org/10.1016/j.psyneuen.2014.07.002>
- Pifferi, F., Dorieux, O., Castellano, C.-A., Croteau, E., Masson, M., Guillermier, M., Van Camp, N., Guesnet, P., Alessandri, J.-M., Cunnane, S., Dhenain, M., Aujard, F., 2015. Long-chain n-3 PUFAs from fish oil enhance resting state brain glucose utilization and reduce anxiety in an adult nonhuman primate, the grey mouse lemur. *Journal of Lipid Research* 56, 1511–1518. <https://doi.org/10.1194/jlr.M058933>
- Pifferi, F., Laurent, B., Plourde, M., 2021. Lipid Transport and Metabolism at the Blood-Brain Interface: Implications in Health and Disease. *Frontiers in Physiology* 12.
- Pitino, M.A., Alashmali, S.M., Hopperton, K.E., Unger, S., Pouliot, Y., Doyen, A., O'Connor, D.L., Bazinet, R.P., 2019. Oxylipin concentration, but not fatty acid composition, is altered in human donor milk pasteurised using both thermal and non-thermal techniques. *Br J Nutr* 122, 47–55. <https://doi.org/10.1017/S0007114519000916>
- Plourde, M., Chouinard-Watkins, R., Rioux-Perreault, C., Fortier, M., Dang, M.T.M., Allard, M.-J., Tremblay-Mercier, J., Zhang, Y., Lawrence, P., Vohl, M.-C., Perron, P., Lorrain, D., Brenna, J.T., Cunnane, S.C., 2014. Kinetics of 13C-DHA before and during fish-oil supplementation in healthy older individuals. *The American Journal of Clinical Nutrition* 100, 105–112. <https://doi.org/10.3945/ajcn.113.074708>
- Plourde, M., Cunnane, S.C., 2007. Extremely limited synthesis of long chain polyunsaturates in adults: implications for their dietary essentiality and use as supplements. *Appl. Physiol. Nutr. Metab.* 32, 619–634. <https://doi.org/10.1139/H07-034>
- Pravia, C.I., Benny, M., 2020. Long-term consequences of prematurity. *Cleve Clin J Med* 87, 759–767. <https://doi.org/10.3949/ccjm.87a.19108>
- Puente, N., Elezgarai, I., Lafourcade, M., Reguero, L., Marsicano, G., Georges, F., Manzoni, O.J., Grandes, P., 2010. Localization and Function of the Cannabinoid CB1 Receptor in the Anterolateral Bed Nucleus of the Stria Terminalis. *PLOS ONE* 5, e8869. <https://doi.org/10.1371/journal.pone.0008869>
- Qi, J., Zhang, S., Wang, H.-L., Barker, D.J., Miranda-Barrientos, J., Morales, M., 2016. VTA glutamatergic inputs to nucleus accumbens drive aversion by acting on GABAergic interneurons. *Nat Neurosci* 19, 725–733. <https://doi.org/10.1038/nn.4281>
- Quinn, J.F., Raman, R., Thomas, R.G., Yurko-Mauro, K., Nelson, E.B., Van Dyck, C., Galvin, J.E., Emond, J., Jack, C.R., Weiner, M., Shinto, L., Aisen, P.S., 2010. Docosahexaenoic Acid Supplementation and Cognitive Decline in Alzheimer Disease: A Randomized Trial. *JAMA* 304, 1903–1911. <https://doi.org/10.1001/jama.2010.1510>

- Raji, C.A., Erickson, K.I., Lopez, O.L., Kuller, L.H., Gach, H.M., Thompson, P.M., Riverol, M., Becker, J.T., 2014. Regular Fish Consumption and Age-Related Brain Gray Matter Loss. *American Journal of Preventive Medicine* 47, 444–451. <https://doi.org/10.1016/j.amepre.2014.05.037>
- Ralston, J.C., Matravadia, S., Gaudio, N., Holloway, G.P., Mutch, D.M., 2015. Polyunsaturated fatty acid regulation of adipocyte FADS1 and FADS2 expression and function. *Obesity* 23, 725–728. <https://doi.org/10.1002/oby.21035>
- Rapaport, M.H., Nierenberg, A.A., Schettler, P.J., Kinkead, B., Cardoos, A., Walker, R., Mischoulon, D., 2016. Inflammation as a predictive biomarker for response to omega-3 fatty acids in major depressive disorder: a proof-of-concept study. *Mol Psychiatry* 21, 71–79. <https://doi.org/10.1038/mp.2015.22>
- Rapoport, S.I., 2003. In vivo approaches to quantifying and imaging brain arachidonic and docosahexaenoic acid metabolism. *The Journal of Pediatrics, Mechanisms of Action of LCPUFA Effects on Infant Growth and Neurodevelopment* 143, 26–34. [https://doi.org/10.1067/S0022-3476\(03\)00399-8](https://doi.org/10.1067/S0022-3476(03)00399-8)
- Rapoport, S.I., Chang, M.C.J., Spector, A.A., 2001. Delivery and turnover of plasma-derived essential PUFAs in mammalian brain. *Journal of Lipid Research* 42, 678–685. [https://doi.org/10.1016/S0022-2275\(20\)31629-1](https://doi.org/10.1016/S0022-2275(20)31629-1)
- Rapoport, S.I., Rao, J.S., Igarashi, M., 2007. Brain metabolism of nutritionally essential polyunsaturated fatty acids depends on both the diet and the liver. *Prostaglandins, Leukotrienes and Essential Fatty Acids* 77, 251–261. <https://doi.org/10.1016/j.plefa.2007.10.023>
- Recchiuti, A., Krishnamoorthy, S., Fredman, G., Chiang, N., Serhan, C.N., 2011. MicroRNAs in resolution of acute inflammation: identification of novel resolvin D1-miRNA circuits. *The FASEB Journal* 25, 544–560. <https://doi.org/10.1096/fj.10-169599>
- Reddan, J.M., Macpherson, H., White, D.J., Scholey, A., Pipingas, A., 2019. Examining the relationship between nutrition and cerebral structural integrity in older adults without dementia. *Nutr. Res. Rev.* 32, 79–98. <https://doi.org/10.1017/S0954422418000185>
- Reemst, K., Broos, J.Y., Abbink, M.R., Cimetti, C., Giera, M., Kooij, G., Korosi, A., 2022. Early-life stress and dietary fatty acids impact the brain lipid/oxyipin profile into adulthood, basally and in response to LPS (preprint). In Review. <https://doi.org/10.21203/rs.3.rs-1663016/v1>
- Reemst, K., Noctor, S.C., Lucassen, P.J., Hol, E.M., 2016. The Indispensable Roles of Microglia and Astrocytes during Brain Development. *Frontiers in Human Neuroscience* 10.
- Ren, Q., Ma, M., Ishima, T., Morisseau, C., Yang, J., Wagner, K.M., Zhang, J., Yang, C., Yao, W., Dong, C., Han, M., Hammock, B.D., Hashimoto, K., 2016. Gene deficiency and pharmacological inhibition of soluble epoxide hydrolase confers resilience to repeated social defeat stress. *Proc. Natl. Acad. Sci. U.S.A.* 113. <https://doi.org/10.1073/pnas.1601532113>
- Revilla, M., Puig-Oliveras, A., Crespo-Piazuelo, D., Criado-Mesas, L., Castelló, A., Fernández, A.I., Ballester, M., Folch, J.M., 2018. Expression analysis of candidate genes for fatty acid composition in adipose tissue and identification of regulatory regions. *Sci Rep* 8, 2045. <https://doi.org/10.1038/s41598-018-20473-3>
- Rey, C., Delpech, J.C., Madore, C., Nadjar, A., Greenhalgh, A.D., Amadiou, C., Aubert, A., Pallet, V., Vaysse, C., Layé, S., Joffre, C., 2019. Dietary n-3 long chain PUFA supplementation promotes a pro-



resolving oxylipin profile in the brain. *Brain, Behavior, and Immunity* 76, 17–27.  
<https://doi.org/10.1016/j.bbi.2018.07.025>

Rey, C., Nadjar, A., Buaud, B., Vaysse, C., Aubert, A., Pallet, V., Layé, S., Joffre, C., 2016. Resolvin D1 and E1 promote resolution of inflammation in microglial cells in vitro. *Brain, Behavior, and Immunity, Microglia, Physiology and Behavior* 55, 249–259. <https://doi.org/10.1016/j.bbi.2015.12.013>

Rey, C., Nadjar, A., Joffre, F., Amadiou, C., Aubert, A., Vaysse, C., Pallet, V., Layé, S., Joffre, C., 2018. Maternal n-3 polyunsaturated fatty acid dietary supply modulates microglia lipid content in the offspring. *Prostaglandins, Leukotrienes and Essential Fatty Acids* 133, 1–7.  
<https://doi.org/10.1016/j.plefa.2018.04.003>

Reynolds, L.M., Dutta, R., Seeds, M.C., Lake, K.N., Hallmark, B., Mathias, R.A., Howard, T.D., Chilton, F.H., 2020. FADS genetic and metabolomic analyses identify the  $\Delta 5$  desaturase (FADS1) step as a critical control point in the formation of biologically important lipids. *Sci Rep* 10, 15873.  
<https://doi.org/10.1038/s41598-020-71948-1>

Richardson, W.D., Young, K.M., Tripathi, R.B., McKenzie, I., 2011. NG2-glia as Multipotent Neural Stem Cells: Fact or Fantasy? *Neuron* 70, 661–673. <https://doi.org/10.1016/j.neuron.2011.05.013>

Riederer, M., Wallner, M., Schweighofer, N., Fuchs-Neuhold, B., Rath, A., Berghold, A., Eberhard, K., Groselj-Strele, A., Staubmann, W., Peterseil, M., Waldner, I., Mayr, J.A., Rothe, M., Holasek, S., Maunz, S., Pail, E., van der Kleyn, M., 2020. Distinct maternal amino acids and oxylipins predict infant fat mass and fat-free mass indices. *Archives of Physiology and Biochemistry* 1–12.  
<https://doi.org/10.1080/13813455.2020.1846204>

Riendeau, D., Guay, J., Weech, P.K., Laliberté, F., Yergey, J., Li, C., Desmarais, S., Perrier, H., Liu, S., Nicoll-Griffith, D., 1994. Arachidonyl trifluoromethyl ketone, a potent inhibitor of 85-kDa phospholipase A2, blocks production of arachidonate and 12-hydroxyeicosatetraenoic acid by calcium ionophore-challenged platelets. *Journal of Biological Chemistry* 269, 15619–15624.  
[https://doi.org/10.1016/S0021-9258\(17\)40726-5](https://doi.org/10.1016/S0021-9258(17)40726-5)

Robinson, D.T., Palac, H.L., Baillif, V., Van Goethem, E., Dubourdeau, M., Van Horn, L., Martin, C.R., 2017. Long chain fatty acids and related pro-inflammatory, specialized pro-resolving lipid mediators and their intermediates in preterm human milk during the first month of lactation. *Prostaglandins, Leukotrienes and Essential Fatty Acids* 121, 1–6. <https://doi.org/10.1016/j.plefa.2017.05.003>

Rogers, P.J., Appleton, K.M., Kessler, D., Peters, T.J., Gunnell, D., Hayward, R.C., Heatherley, S.V., Christian, L.M., McNaughton, S.A., Ness, A.R., 2008. No effect of n-3 long-chain polyunsaturated fatty acid (EPA and DHA) supplementation on depressed mood and cognitive function: a randomised controlled trial. *British Journal of Nutrition* 99, 421–431.  
<https://doi.org/10.1017/S0007114507801097>

Roohbakhsh, A., Etemad, L., Karimi, G., 2022. Resolvin D1: A key endogenous inhibitor of neuroinflammation. *BioFactors* 48, 1005–1026. <https://doi.org/10.1002/biof.1891>

Rothstein, J.D., Dykes-Hoberg, M., Pardo, C.A., Bristol, L.A., Jin, L., Kuncl, R.W., Kanai, Y., Hediger, M.A., Wang, Y., Schielke, J.P., Welty, D.F., 1996. Knockout of Glutamate Transporters Reveals a Major Role for Astroglial Transport in Excitotoxicity and Clearance of Glutamate. *Neuron* 16, 675–686.  
[https://doi.org/10.1016/S0896-6273\(00\)80086-0](https://doi.org/10.1016/S0896-6273(00)80086-0)

Rouch, L., Virecoulon Giudici, K., Cantet, C., Guyonnet, S., Delrieu, J., Legrand, P., Catheline, D., Andrieu, S., Weiner, M., de Souto Barreto, P., Vellas, B., for the Alzheimer's Disease Neuroimaging

- Initiative, 2022. Associations of erythrocyte omega-3 fatty acids with cognition, brain imaging and biomarkers in the Alzheimer's disease neuroimaging initiative: cross-sectional and longitudinal retrospective analyses. *The American Journal of Clinical Nutrition* nqac236. <https://doi.org/10.1093/ajcn/nqac236>
- Rustenhoven, J., Tanumihardja, C., Kipnis, J., 2021. Cerebrovascular Anomalies: Perspectives From Immunology and Cerebrospinal Fluid Flow. *Circulation Research* 129, 174–194. <https://doi.org/10.1161/CIRCRESAHA.121.318173>
- Salinas, G., Rangasetty, U.C., Uretsky, B.F., Birnbaum, Y., 2007. The Cyclooxygenase 2 (COX-2) Story: It's Time to Explain, Not Inflamm. *J Cardiovasc Pharmacol Ther* 12, 98–111. <https://doi.org/10.1177/1074248407301172>
- Samieri, C., Féart, C., Proust-Lima, C., Peuchant, E., Dartigues, J.-F., Amieva, H., Barberger-Gateau, P., 2011. Omega-3 fatty acids and cognitive decline: modulation by ApoE $\epsilon$ 4 allele and depression. *Neurobiology of Aging* 32, 2317.e13-2317.e22. <https://doi.org/10.1016/j.neurobiolaging.2010.03.020>
- Samieri, C., Okereke, O.I., E. Devore, E., Grodstein, F., 2013. Long-Term Adherence to the Mediterranean Diet Is Associated with Overall Cognitive Status, but Not Cognitive Decline, in Women. *The Journal of Nutrition* 143, 493–499. <https://doi.org/10.3945/jn.112.169896>
- Samuelsson, B., Dahlén, S.-E., Lindgren, J.Å., Rouzer, C.A., Serhan, C.N., 1987. Leukotrienes and Lipoxins: Structures, Biosynthesis, and Biological Effects. *Science* 237, 1171–1176. <https://doi.org/10.1126/science.2820055>
- Sang, N., Zhang, J., Chen, C., 2007. COX-2 oxidative metabolite of endocannabinoid 2-AG enhances excitatory glutamatergic synaptic transmission and induces neurotoxicity. *Journal of Neurochemistry* 102, 1966–1977. <https://doi.org/10.1111/j.1471-4159.2007.04668.x>
- Sastry, P.S., 1985. Lipids of nervous tissue: Composition and metabolism. *Progress in Lipid Research* 24, 69–176. [https://doi.org/10.1016/0163-7827\(85\)90011-6](https://doi.org/10.1016/0163-7827(85)90011-6)
- Sattler, R., Rothstein, J.D., 2006. Regulation and Dysregulation of Glutamate Transporters, in: Sitte, H.H., Freissmuth, M. (Eds.), *Neurotransmitter Transporters, Handbook of Experimental Pharmacology*. Springer, Berlin, Heidelberg, pp. 277–303. [https://doi.org/10.1007/3-540-29784-7\\_14](https://doi.org/10.1007/3-540-29784-7_14)
- Scheen, A., Seutin, V., Van Gaal, L.F., 2008. Le système endocannabinoïde dans le cerveau... et ailleurs. *Endocannabinoid system in the brain...and elsewhere* 63.
- Schindelin, J., Arganda-Carreras, I., Frise, E., Kaynig, V., Longair, M., Pietzsch, T., Preibisch, S., Rueden, C., Saalfeld, S., Schmid, B., Tinevez, J.-Y., White, D.J., Hartenstein, V., Eliceiri, K., Tomancak, P., Cardona, A., 2012. Fiji: an open-source platform for biological-image analysis. *Nat Methods* 9, 676–682. <https://doi.org/10.1038/nmeth.2019>
- Schurman, L.D., Carper, M.C., Moncayo, L.V., Ogasawara, D., Richardson, K., Yu, L., Liu, X., Poklis, J.L., Liu, Q.-S., Cravatt, B.F., Lichtman, A.H., 2019. Diacylglycerol Lipase-Alpha Regulates Hippocampal-Dependent Learning and Memory Processes in Mice. *J. Neurosci.* 39, 5949–5965. <https://doi.org/10.1523/JNEUROSCI.1353-18.2019>
- Schwartz, M., Cohen, I., Lazarov-Spiegler, O., Moalem, G., Yoles, E., 1999. The remedy may lie in ourselves: prospects for immune cell therapy in central nervous system protection and repair. *J Mol Med* 77, 713–717. <https://doi.org/10.1007/s001099900047>

- Serhan, C.N., 2017. Treating inflammation and infection in the 21st century: new hints from decoding resolution mediators and mechanisms. *The FASEB Journal* 31, 1273–1288. <https://doi.org/10.1096/fj.201601222R>
- Serhan, C.N., 2014. Pro-resolving lipid mediators are leads for resolution physiology. *Nature* 510, 92–101. <https://doi.org/10.1038/nature13479>
- Serhan, C.N., 2005. Lipoxins and aspirin-triggered 15-epi-lipoxins are the first lipid mediators of endogenous anti-inflammation and resolution. *Prostaglandins, Leukotrienes and Essential Fatty Acids* 73, 141–162. <https://doi.org/10.1016/j.plefa.2005.05.002>
- Serhan, C.N., Dalli, J., Colas, R.A., Winkler, J.W., Chiang, N., 2015. Protectins and maresins: New pro-resolving families of mediators in acute inflammation and resolution bioactive metabolome. *Biochimica et Biophysica Acta (BBA) - Molecular and Cell Biology of Lipids, Oxygenated metabolism of PUFA: analysis and biological relevance* 1851, 397–413. <https://doi.org/10.1016/j.bbalip.2014.08.006>
- Serhan, C.N., Gupta, S.K., Perretti, M., Godson, C., Brennan, E., Li, Y., Soehnlein, O., Shimizu, T., Werz, O., Chiurchiù, V., Azzi, A., Dubourdeau, M., Gupta, S.S., Schopohl, P., Hoch, M., Gjorgevikj, D., Khan, F.M., Brauer, D., Tripathi, A., Cesnulevicius, K., Lescheid, D., Schultz, M., Särndahl, E., Repsilber, D., Kruse, R., Sala, A., Haeggström, J.Z., Levy, B.D., Filep, J.G., Wolkenhauer, O., 2020. The Atlas of Inflammation Resolution (AIR). *Molecular Aspects of Medicine, The Atlas of Inflammation Resolution (AIR)* 74, 100894. <https://doi.org/10.1016/j.mam.2020.100894>
- Serhan, C.N., Hong, S., Gronert, K., Colgan, S.P., Devchand, P.R., Mirick, G., Moussignac, R.-L., 2002. Resolvins : A Family of Bioactive Products of Omega-3 Fatty Acid Transformation Circuits Initiated by Aspirin Treatment that Counter Proinflammation Signals. *Journal of Experimental Medicine* 196, 1025–1037. <https://doi.org/10.1084/jem.20020760>
- Serhan, C.N., Oliw, E., 2001. Unorthodox routes to prostanoid formation: new twists in cyclooxygenase-initiated pathways. *J Clin Invest* 107, 1481–1489. <https://doi.org/10.1172/JCI13375>
- Serhan, C.N., Yang, R., Martinod, K., Kasuga, K., Pillai, P.S., Porter, T.F., Oh, S.F., Spite, M., 2008. Maresins: novel macrophage mediators with potent antiinflammatory and proresolving actions. *Journal of Experimental Medicine* 206, 15–23. <https://doi.org/10.1084/jem.20081880>
- Sesack, S.R., Grace, A.A., 2010. Cortico-Basal Ganglia Reward Network: Microcircuitry. *Neuropsychopharmacol* 35, 27–47. <https://doi.org/10.1038/npp.2009.93>
- Sibbons, C.M., Thomas Brenna, J., Lawrence, P., Hoile, S.P., Clarke-Harris, R., Lillycrop, K.A., Burdge, G.C., 2014. Effect of sex hormones on n-3 polyunsaturated fatty acid biosynthesis in HepG2 cells and in human primary hepatocytes. *Prostaglandins, Leukotrienes and Essential Fatty Acids* 90, 47–54. <https://doi.org/10.1016/j.plefa.2013.12.006>
- Sidhu, V.K., Huang, B.X., Kim, H.-Y., 2011. Effects of Docosahexaenoic Acid on Mouse Brain Synaptic Plasma Membrane Proteome Analyzed by Mass Spectrometry and <sup>16</sup>O/ <sup>18</sup>O Labeling. *J. Proteome Res.* 10, 5472–5480. <https://doi.org/10.1021/pr2007285>
- Siebert, E., Paul, F., Rothe, M., Weylandt, K.H., 2017. The effect of omega-3 fatty acids on central nervous system remyelination in fat-1 mice. *BMC Neurosci* 18, 19. <https://doi.org/10.1186/s12868-016-0312-5>

- Simopoulos, Artemis P., 2011. Importance of the Omega-6/Omega-3 Balance in Health and Disease: Evolutionary Aspects of Diet, in: Simopoulos, A.P. (Ed.), *World Review of Nutrition and Dietetics*. S. Karger AG, pp. 10–21. <https://doi.org/10.1159/000327785>
- Sinclair, A.J., Begg, D., Mathai, M., Weisinger, R.S., 2007. Omega 3 fatty acids and the brain: review of studies in depression 7.
- Skorve, J., Hilvo, M., Vihervaara, T., Burri, L., Bohov, P., Tillander, V., Bjørndal, B., Suoniemi, M., Laaksonen, R., Ekroos, K., Berge, R.K., Alexson, S.E.H., 2015. Fish oil and krill oil differentially modify the liver and brain lipidome when fed to mice. *Lipids Health Dis* 14, 88. <https://doi.org/10.1186/s12944-015-0086-2>
- Smith, W.L., Murphy, R.C., 2016. The Eicosanoids, in: *Biochemistry of Lipids, Lipoproteins and Membranes*. Elsevier, pp. 259–296. <https://doi.org/10.1016/B978-0-444-63438-2.00009-2>
- Sofroniew, M.V., Vinters, H.V., 2010. Astrocytes: biology and pathology. *Acta Neuropathol* 29.
- Soleimani, F., Zaheri, F., Abdi, F., 2014. Long-Term Neurodevelopmental Outcomes After Preterm Birth. *Iran Red Crescent Med J* 16, e17965. <https://doi.org/10.5812/ircmj.17965>
- Song, B.J., Elbert, A., Rahman, T., Orr, S.K., Chen, C.T., Febbraio, M., Bazinet, R.P., 2010. Genetic Ablation of CD36 Does not Alter Mouse Brain Polyunsaturated Fatty Acid Concentrations. *Lipids* 45, 291–299. <https://doi.org/10.1007/s11745-010-3398-z>
- Song, C., Zhang, X.Y., Manku, M., 2009. Increased Phospholipase A2 Activity and Inflammatory Response But Decreased Nerve Growth Factor Expression in the Olfactory Bulbectomized Rat Model of Depression: Effects of Chronic Ethyl-Eicosapentaenoate Treatment. *J. Neurosci.* 29, 14–22. <https://doi.org/10.1523/JNEUROSCI.3569-08.2009>
- Soto-Moyano, R., Belmar, J., Perez, H., Ruiz, S., Hernandez, A., 1995. Central noradrenergic hyperactivity early in life: a hypothesis on the origin of morpho-functional brain disorders induced by malnutrition. *Biol Res* 28, 105–111.
- Sprecher, H., 2002. The roles of anabolic and catabolic reactions in the synthesis and recycling of polyunsaturated fatty acids. *Prostaglandins, Leukotrienes and Essential Fatty Acids* 67, 79–83. <https://doi.org/10.1054/plef.2002.0402>
- Stella, N., 2022. Interrogating the Impact of  $\Delta$ 9-Tetrahydrocannabinol Use During Adolescence: Microglia Lead the Way. *Biological Psychiatry* 92, 830–831. <https://doi.org/10.1016/j.biopsych.2022.09.006>
- Stoffel, W., Holz, B., Jenke, B., Binczek, E., Günter, R.H., Kiss, C., Karakesisoglou, I., Thevis, M., Weber, A.-A., Arnhold, S., Addicks, K., 2008.  $\Delta$ 6-Desaturase (FADS2) deficiency unveils the role of  $\omega$ 3- and  $\omega$ 6-polyunsaturated fatty acids. *The EMBO Journal* 27, 2281–2292. <https://doi.org/10.1038/emboj.2008.156>
- Stoffel, W., Schmidt-Soltan, I., Binczek, E., Thomas, A., Thevis, M., Wegner, I., 2020. Dietary  $\omega$ 3-and  $\omega$ 6-Polyunsaturated fatty acids reconstitute fertility of Juvenile and adult Fads2-Deficient mice. *Molecular Metabolism* 36, 100974. <https://doi.org/10.1016/j.molmet.2020.100974>
- Stonehouse, W., 2014. Does Consumption of LC Omega-3 PUFA Enhance Cognitive Performance in Healthy School-Aged Children and throughout Adulthood? Evidence from Clinical Trials. *Nutrients* 6, 2730–2758. <https://doi.org/10.3390/nu6072730>

- Stonehouse, W., Conlon, C.A., Podd, J., Hill, S.R., Minihane, A.M., Haskell, C., Kennedy, D., 2013. DHA supplementation improved both memory and reaction time in healthy young adults: a randomized controlled trial. *The American Journal of Clinical Nutrition* 97, 1134–1143. <https://doi.org/10.3945/ajcn.112.053371>
- Straus, D.S., Glass, C.K., 2001. Cyclopentenone prostaglandins: New insights on biological activities and cellular targets. *Medicinal Research Reviews* 21, 185–210. <https://doi.org/10.1002/med.1006>
- Strazielle, N., Ghersi-Egea, J.F., 2013. Physiology of Blood–Brain Interfaces in Relation to Brain Disposition of Small Compounds and Macromolecules. *Mol. Pharmaceutics* 10, 1473–1491. <https://doi.org/10.1021/mp300518e>
- Strobel, C., Jahreis, G., Kuhnt, K., 2012. Survey of n-3 and n-6 polyunsaturated fatty acids in fish and fish products. *Lipids Health Dis* 11, 144. <https://doi.org/10.1186/1476-511X-11-144>
- Strokin, M., Sergeeva, M., Reiser, G., 2007. Prostaglandin synthesis in rat brain astrocytes is under the control of the n-3 docosahexaenoic acid, released by group VIB calcium-independent phospholipase A2. *Journal of Neurochemistry* 102, 1771–1782. <https://doi.org/10.1111/j.1471-4159.2007.04663.x>
- Stroud, C.K., Nara, T.Y., Roqueta-Rivera, M., Radlowski, E.C., Lawrence, P., Zhang, Y., Cho, B.H., Segre, M., Hess, R.A., Brenna, J.T., Haschek, W.M., Nakamura, M.T., 2009. Disruption of FADS2 gene in mice impairs male reproduction and causes dermal and intestinal ulceration. *Journal of Lipid Research* 50, 1870–1880. <https://doi.org/10.1194/jlr.M900039-JLR200>
- Su, H.-M., 2010. Mechanisms of n-3 fatty acid-mediated development and maintenance of learning memory performance. *The Journal of Nutritional Biochemistry* 21, 364–373. <https://doi.org/10.1016/j.jnutbio.2009.11.003>
- Su, K.-P., Yang, H.-T., Chang, J.P.-C., Shih, Y.-H., Guu, T.-W., Kumaran, S.S., Gałeckki, P., Walczewska, A., Pariante, C.M., 2018. Eicosapentaenoic and docosahexaenoic acids have different effects on peripheral phospholipase A2 gene expressions in acute depressed patients. *Progress in Neuro-Psychopharmacology and Biological Psychiatry, Peripheral markers of inflammation, oxidative & nitrosative stress pathways and memory functions as a new target of pharmacotherapy in depression* 80, 227–233. <https://doi.org/10.1016/j.pnpbp.2017.06.020>
- Sublette, M.E., Ellis, S.P., Geant, A.L., Mann, J.J., 2011. Meta-Analysis of the Effects of Eicosapentaenoic Acid (EPA) in Clinical Trials in Depression. *J Clin Psychiatry* 72, 11703. <https://doi.org/10.4088/JCP.10m06634>
- Sugimoto, S., Mena, H.A., Sansbury, B.E., Kobayashi, S., Tsuji, T., Wang, C.-H., Yin, X., Huang, T.L., Kusuyama, J., Kodani, S.D., Darcy, J., Profeta, G., Pereira, N., Tanzi, R.E., Zhang, C., Serwold, T., Kokkotou, E., Goodyear, L.J., Cypess, A.M., Leiria, L.O., Spite, M., Tseng, Y.-H., 2022. Brown adipose tissue-derived MaR2 contributes to cold-induced resolution of inflammation. *Nat Metab* 4, 775–790. <https://doi.org/10.1038/s42255-022-00590-0>
- Sugiura, Y., Konishi, Y., Zaima, N., Kajihara, S., Nakanishi, H., Taguchi, R., Setou, M., 2009. Visualization of the cell-selective distribution of PUFA-containing phosphatidylcholines in mouse brain by imaging mass spectrometry [S]. *Journal of Lipid Research* 50, 1776–1788. <https://doi.org/10.1194/jlr.M900047-JLR200>
- Sun, B., Bang, S.-I., Jin, Y.-H., 2009. Transient receptor potential A1 increase glutamate release on brain stem neurons. *NeuroReport* 20, 1002–1006. <https://doi.org/10.1097/WNR.0b013e32832d2219>

- Sun, C., Zou, M., Wang, X., Xia, W., Ma, Y., Liang, S., Hao, Y., Wu, L., Fu, S., 2018. FADS1-FADS2 and ELOVL2 gene polymorphisms in susceptibility to autism spectrum disorders in Chinese children. *BMC Psychiatry* 18, 283. <https://doi.org/10.1186/s12888-018-1868-7>
- Sun, G.Y., Chuang, D.Y., Zong, Y., Jiang, J., Lee, J.C.M., Gu, Z., Simonyi, A., 2014. Role of Cytosolic Phospholipase A2 in Oxidative and Inflammatory Signaling Pathways in Different Cell Types in the Central Nervous System. *Mol Neurobiol* 50, 6–14. <https://doi.org/10.1007/s12035-014-8662-4>
- Sun, J., Zhang, W., 2022. Supplementation with dietary omega-3 PUFA mitigates fetal brain inflammation and mitochondrial damage caused by high doses of sodium nitrite in maternal rats. *PLOS ONE* 17, e0266084. <https://doi.org/10.1371/journal.pone.0266084>
- Sun, L., Xu, Y.-W., Han, J., Liang, H., Wang, N., Cheng, Y., 2015. 12/15-Lipoxygenase metabolites of arachidonic acid activate PPAR $\gamma$ : a possible neuroprotective effect in ischemic brain. *Journal of Lipid Research* 56, 502–514. <https://doi.org/10.1194/jlr.M053058>
- Suzumura, A., Kaneko, H., Funahashi, Y., Takayama, K., Nagaya, M., Ito, S., Okuno, T., Hirakata, T., Nonobe, N., Kataoka, K., Shimizu, H., Namba, R., Yamada, K., Ye, F., Ozawa, Y., Yokomizo, T., Terasaki, H., 2020. n-3 Fatty Acid and Its Metabolite 18-HEPE Ameliorate Retinal Neuronal Cell Dysfunction by Enhancing Müller BDNF in Diabetic Retinopathy. *Diabetes* 69, 724–735. <https://doi.org/10.2337/db19-0550>
- Tager, A.M., Bromley, S.K., Medoff, B.D., Islam, S.A., Bercury, S.D., Friedrich, E.B., Carafone, A.D., Gerszten, R.E., Luster, A.D., 2003. Leukotriene B4 receptor BLT1 mediates early effector T cell recruitment. *Nat Immunol* 4, 982–990. <https://doi.org/10.1038/ni970>
- Taha, A.Y., Hennebelle, M., Yang, J., Zamora, D., Rapoport, S.I., Hammock, B.D., Ramsden, C.E., 2018. Regulation of rat plasma and cerebral cortex oxylipin concentrations with increasing levels of dietary linoleic acid. *Prostaglandins, Leukotrienes and Essential Fatty Acids* 138, 71–80. <https://doi.org/10.1016/j.plefa.2016.05.004>
- Takeuchi, E., Yamada, D., Suzuki, S., Saitoh, A., Itoh, M., Hayashi, T., Yamada, M., Wada, K., Sekiguchi, M., 2020. Participation of the nucleus accumbens dopaminergic system in the antidepressant-like actions of a diet rich in omega-3 polyunsaturated fatty acids. *PLOS ONE* 15, e0230647. <https://doi.org/10.1371/journal.pone.0230647>
- Takeuchi, T., Iwanaga, M., Harada, E., 2003. Possible regulatory mechanism of DHA-induced anti-stress reaction in rats. *Brain Research* 964, 136–143. [https://doi.org/10.1016/S0006-8993\(02\)04113-6](https://doi.org/10.1016/S0006-8993(02)04113-6)
- Talamonti, E., Pauter, A.M., Asadi, A., Fischer, A.W., Chiurchiù, V., Jacobsson, A., 2017. Impairment of systemic DHA synthesis affects macrophage plasticity and polarization: implications for DHA supplementation during inflammation. *Cell. Mol. Life Sci.* 74, 2815–2826. <https://doi.org/10.1007/s00018-017-2498-9>
- Talamonti, E., Sasso, V., To, H., Haslam, R.P., Napier, J.A., Ulfhake, B., Pernold, K., Asadi, A., Hessa, T., Jacobsson, A., Chiurchiù, V., Viscomi, M.T., 2019. Impairment of DHA synthesis alters the expression of neuronal plasticity markers and the brain inflammatory status in mice. *FASEB j.* 34, 2024–2040. <https://doi.org/10.1096/fj.201901890RR>
- Tan, S.-H., Chung, H.-H., Shu-Chien, A.C., 2010. Distinct developmental expression of two elongase family members in zebrafish. *Biochemical and Biophysical Research Communications* 393, 397–403. <https://doi.org/10.1016/j.bbrc.2010.01.130>

- Tanaka, T., Shen, J., Abecasis, G.R., Kisiailiou, A., Ordovas, J.M., Guralnik, J.M., Singleton, A., Bandinelli, S., Cherubini, A., Arnett, D., Tsai, M.Y., Ferrucci, L., 2009. Genome-Wide Association Study of Plasma Polyunsaturated Fatty Acids in the InCHIANTI Study. *PLOS Genetics* 5, e1000338. <https://doi.org/10.1371/journal.pgen.1000338>
- Tang, M., Zhang, M., Wang, L., Li, H., Cai, H., Dang, R., Jiang, P., Liu, Y., Xue, Y., Wu, Y., 2018. Maternal dietary of n-3 polyunsaturated fatty acids affects the neurogenesis and neurochemical in female rat at weaning. *Prostaglandins, Leukotrienes and Essential Fatty Acids* 128, 11–20. <https://doi.org/10.1016/j.plefa.2017.11.001>
- Tansey, E.M., 1997. Not committing barbarisms: Sherrington and the synapse, 1897. *Brain Res Bull* 44, 211–212. [https://doi.org/10.1016/s0361-9230\(97\)00312-2](https://doi.org/10.1016/s0361-9230(97)00312-2)
- Tanskanen, A., Hibbeln, J.R., Tuomilehto, J., Uutela, A., Haukkala, A., Viinamäki, H., Lehtonen, J., Vartiainen, E., 2001. Fish Consumption and Depressive Symptoms in the General Population in Finland. *PS* 52, 529–531. <https://doi.org/10.1176/appi.ps.52.4.529>
- Taoro-González, L., Pereda, D., Valdés-Baizabal, C., González-Gómez, M., Pérez, J.A., Mesa-Herrera, F., Canerina-Amaro, A., Pérez-González, H., Rodríguez, C., Díaz, M., Marin, R., 2022. Effects of Dietary n-3 LCPUFA Supplementation on the Hippocampus of Aging Female Mice: Impact on Memory, Lipid Raft-Associated Glutamatergic Receptors and Neuroinflammation. *IJMS* 23, 7430. <https://doi.org/10.3390/ijms23137430>
- Tennant, D., Gosling, J.P., 2015. Modelling consumer intakes of vegetable oils and fats. *Food Additives & Contaminants: Part A* 32, 1397–1405. <https://doi.org/10.1080/19440049.2015.1069407>
- Terrando, N., Park, J.J., Devinney, M., Chan, C., Cooter, M., Avasarala, P., Mathew, J.P., Quinones, Q.J., Maddipati, K.R., Berger, M., 2021. Immunomodulatory lipid mediator profiling of cerebrospinal fluid following surgery in older adults. *Sci Rep* 11, 3047. <https://doi.org/10.1038/s41598-021-82606-5>
- Thomas, A., Baillet, M., Proust-Lima, C., Féart, C., Foubert-Samier, A., Helmer, C., Catheline, G., Samieri, C., 2020. Blood polyunsaturated omega-3 fatty acids, brain atrophy, cognitive decline, and dementia risk. *Alzheimers Dement*. <https://doi.org/10.1002/alz.12195>
- Thomas, A., Crivello, F., Mazoyer, B., Debette, S., Tzourio, C., Samieri, C., 2021. Fish Intake and MRI Burden of Cerebrovascular Disease in Older Adults. *Neurology* 97, e2213–e2222. <https://doi.org/10.1212/WNL.0000000000012916>
- Thomas, A., Lefèvre-Arbogast, S., Féart, C., Foubert-Samier, A., Helmer, C., Catheline, G., Samieri, C., 2022. Association of a MIND Diet with Brain Structure and Dementia in a French Population. *J Prev Alz Dis*. <https://doi.org/10.14283/jpad.2022.67>
- Thomazeau, A., Bosch-Bouju, C., Manzoni, O., Layé, S., 2016. Nutritional n-3 PUFA Deficiency Abolishes Endocannabinoid Gating of Hippocampal Long-Term Potentiation. *Cerebral Cortex* bhw052. <https://doi.org/10.1093/cercor/bhw052>
- Tjonahen, E., Oh, S.F., Siegelman, J., Elangovan, S., Percarpio, K.B., Hong, S., Arita, M., Serhan, C.N., 2006. Resolvin E2: Identification and Anti-Inflammatory Actions: Pivotal Role of Human 5-Lipoxygenase in Resolvin E Series Biosynthesis. *Chemistry & Biology* 13, 1193–1202. <https://doi.org/10.1016/j.chembiol.2006.09.011>

- Tocher, D.R., Leaver, M.J., Hodgson, P.A., 1998. Recent advances in the biochemistry and molecular biology of fatty acyl desaturases. *Prog Lipid Res* 37, 73–117. [https://doi.org/10.1016/s0163-7827\(98\)00005-8](https://doi.org/10.1016/s0163-7827(98)00005-8)
- Tomaszewski, N., He, X., Solomon, V., Lee, M., Mack, W.J., Quinn, J.F., Braskie, M.N., Yassine, H.N., 2020. Effect of APOE Genotype on Plasma Docosahexaenoic Acid (DHA), Eicosapentaenoic Acid, Arachidonic Acid, and Hippocampal Volume in the Alzheimer's Disease Cooperative Study-Sponsored DHA Clinical Trial. *JAD* 74, 975–990. <https://doi.org/10.3233/JAD-191017>
- Tressou, J., Moulin, P., Vergès, B., Guillou, C.L., Simon, N., Pasteau, S., 2016. Fatty acid dietary intake in the general French population: are the French Agency for Food, Environmental and Occupational Health & Safety (ANSES) national recommendations met? *British Journal of Nutrition* 116, 1966–1973. <https://doi.org/10.1017/S000711451600413X>
- Trivellin, G., Faucz, F.R., Daly, A.F., Beckers, A., Stratakis, C.A., 2020. HEREDITARY ENDOCRINE TUMOURS: CURRENT STATE-OF-THE-ART AND RESEARCH OPPORTUNITIES: GPR101, an orphan GPCR with roles in growth and pituitary tumorigenesis. *Endocrine-Related Cancer* 27, T87–T97. <https://doi.org/10.1530/ERC-20-0025>
- Tvrđik, P., Westerberg, R., Silve, S., Asadi, A., Jakobsson, A., Cannon, B., Loison, G., Jacobsson, A., 2000. Role of a New Mammalian Gene Family in the Biosynthesis of Very Long Chain Fatty Acids and Sphingolipids. *Journal of Cell Biology* 149, 707–718. <https://doi.org/10.1083/jcb.149.3.707>
- Tzingounis, A.V., Wadiche, J.I., 2007. Glutamate transporters: confining runaway excitation by shaping synaptic transmission. *Nat Rev Neurosci* 8, 935–947. <https://doi.org/10.1038/nrn2274>
- van de Rest, O., Geleijnse, J.M., Kok, F.J., van Staveren, W.A., Dullemeijer, C., OldeRikkert, M.G.M., Beekman, A.T.F., de Groot, C.P.G.M., 2008. Effect of fish oil on cognitive performance in older subjects: A randomized, controlled trial. *Neurology* 71, 430–438. <https://doi.org/10.1212/01.wnl.0000324268.45138.86>
- van der Lee, S.J., Teunissen, C.E., Pool, R., Shipley, M.J., Teumer, A., Chouraki, V., Melo van Lent, D., Tynkkynen, J., Fischer, K., Hernesniemi, J., Haller, T., Singh-Manoux, A., Verhoeven, A., Willemsen, G., de Leeuw, F.A., Wagner, H., van Dongen, J., Hertel, J., Budde, K., Willems van Dijk, K., Weinhold, L., Ikram, M.A., Pietzner, M., Perola, M., Wagner, M., Friedrich, N., Slagboom, P.E., Scheltens, P., Yang, Q., Gertzen, R.E., Egert, S., Li, S., Hankemeier, T., van Beijsterveldt, C.E.M., Vasan, R.S., Maier, W., Peeters, C.F.W., Jürgen Grabe, H., Ramirez, A., Seshadri, S., Metspalu, A., Kivimäki, M., Salomaa, V., Demirkan, A., Boomsma, D.I., van der Flier, W.M., Amin, N., van Duijn, C.M., 2018. Circulating metabolites and general cognitive ability and dementia: Evidence from 11 cohort studies. *Alzheimer's & Dementia* 14, 707–722. <https://doi.org/10.1016/j.jalz.2017.11.012>
- Vandal, M., Alata, W., Tremblay, C., Rioux-Perreault, C., Salem, N., Calon, F., Plourde, M., 2014. Reduction in DHA transport to the brain of mice expressing human *APOE4* compared to *APOE2*. *J. Neurochem.* 129, 516–526. <https://doi.org/10.1111/jnc.12640>
- Vasireddy, V., Uchida, Y., Salem, N., Jr, Kim, S.Y., Mandal, M.N.A., Reddy, G.B., Bodepudi, R., Alderson, N.L., Brown, J.C., Hama, H., Dlugosz, A., Elias, P.M., Holleran, W.M., Ayyagari, R., 2007. Loss of functional *ELOVL4* depletes very long-chain fatty acids ( $\geq C28$ ) and the unique  $\omega$ -O-acylceramides in skin leading to neonatal death. *Human Molecular Genetics* 16, 471–482. <https://doi.org/10.1093/hmg/ddl480>
- Vik, A., Hansen, T.V., 2021. Stereoselective syntheses and biological activities of E-series resolvins. *Org. Biomol. Chem.* 19, 705–721. <https://doi.org/10.1039/D0OB02218G>



- Virtanen, J.K., Siscovick, D.S., Longstreth, W.T., Kuller, L.H., Mozaffarian, D., 2008. Fish consumption and risk of subclinical brain abnormalities on MRI in older adults. *Neurology* 71, 439–446. <https://doi.org/10.1212/01.wnl.0000324414.12665.b0>
- Volterra, A., Trotti, D., Tromba, C., Floridi, S., Racagni, G., 1994. Glutamate uptake inhibition by oxygen free radicals in rat cortical astrocytes. *J. Neurosci.* 14, 2924–2932. <https://doi.org/10.1523/JNEUROSCI.14-05-02924.1994>
- Wainwright, P.E., 1997. Essential Fatty Acids and Behavior, in: Yehuda, S., Mostofsky, D.I. (Eds.), *Handbook of Essential Fatty Acid Biology: Biochemistry, Physiology, and Behavioral Neurobiology*. Humana Press, Totowa, NJ, pp. 299–341. [https://doi.org/10.1007/978-1-4757-2582-7\\_14](https://doi.org/10.1007/978-1-4757-2582-7_14)
- Walker, R.E., 2022. Oxylipins as Potential Regulators of Inflammatory Conditions of Human Lactation. *Metabolites* 12, 994. <https://doi.org/10.3390/metabo12100994>
- Wallis, T.P., Venkatesh, B.G., Narayana, V.K., Kvaskoff, D., Ho, A., Sullivan, R.K., Windels, F., Sah, P., Meunier, F.A., 2021. Saturated free fatty acids and association with memory formation. *Nat Commun* 12, 3443. <https://doi.org/10.1038/s41467-021-23840-3>
- Walton, H.S., Dodd, P.R., 2007. Glutamate–glutamine cycling in Alzheimer’s disease. *Neurochemistry International, Mechanisms of Neurodegeneration* 50, 1052–1066. <https://doi.org/10.1016/j.neuint.2006.10.007>
- Wang, H.-L., Zhang, Z., Hintze, M., Chen, L., 2011. Decrease in Calcium Concentration Triggers Neuronal Retinoic Acid Synthesis during Homeostatic Synaptic Plasticity. *Journal of Neuroscience* 31, 17764–17771. <https://doi.org/10.1523/JNEUROSCI.3964-11.2011>
- Wang, J., Ossemond, J., Le Gouar, Y., Boissel, F., Dupont, D., Pédrone, F., 2022. Encapsulation of Docosahexaenoic Acid Oil Substantially Improves the Oxylipin Profile of Rat Tissues. *Frontiers in Nutrition* 8.
- Wang, X., Zhu, M., Hjorth, E., Cortés-Toro, V., Eyjolfsdottir, H., Graff, C., Nennesmo, I., Palmblad, J., Eriksson, M., Sambamurti, K., Fitzgerald, J.M., Serhan, C.N., Granholm, A.-C., Schultzberg, M., 2015. Resolution of inflammation is altered in Alzheimer’s disease. *Alzheimer’s & Dementia* 11, 40–50.e2. <https://doi.org/10.1016/j.jalz.2013.12.024>
- Wang, X.-J., Zhang, S., Yan, Z.-Q., Zhao, Y.-X., Zhou, H.-Y., Wang, Y., Lu, G.-Q., Zhang, J.-D., 2011. Impaired CD200–CD200R-mediated microglia silencing enhances midbrain dopaminergic neurodegeneration: Roles of aging, superoxide, NADPH oxidase, and p38 MAPK. *Free Radical Biology and Medicine* 50, 1094–1106. <https://doi.org/10.1016/j.freeradbiomed.2011.01.032>
- Watanabe, S., Doshi, M., Hamazaki, T., 2003. n-3 Polyunsaturated fatty acid (PUFA) deficiency elevates and n-3 PUFA enrichment reduces brain 2-arachidonoylglycerol level in mice. *Prostaglandins, Leukotrienes and Essential Fatty Acids* 69, 51–59. [https://doi.org/10.1016/S0952-3278\(03\)00056-5](https://doi.org/10.1016/S0952-3278(03)00056-5)
- Watkins, J.C., 2000. l-Glutamate as a Central Neurotransmitter: Looking Back. *Biochemical Society Transactions* 28, 297–310. <https://doi.org/10.1042/bst0280297>
- Weiser, M.J., Wynalda, K., Salem, N., Butt, C.M., 2015. Dietary DHA during development affects depression-like behaviors and biomarkers that emerge after puberty in adolescent rats. *Journal of Lipid Research* 56, 151–166. <https://doi.org/10.1194/jlr.M055558>

Weiss, G.A., Troxler, H., Klinke, G., Rogler, D., Braegger, C., Hersberger, M., 2013. High levels of anti-inflammatory and pro-resolving lipid mediators lipoxins and resolvins and declining docosahexaenoic acid levels in human milk during the first month of lactation. *Lipids Health Dis* 12, 89. <https://doi.org/10.1186/1476-511X-12-89>

Werner, A., Bongers, M.E.J., Bijvelds, M.J., de Jonge, H.R., Verkade, H.J., 2004. No indications for altered essential fatty acid metabolism in two murine models for cystic fibrosis. *Journal of Lipid Research* 45, 2277–2286. <https://doi.org/10.1194/jlr.M400238-JLR200>

Westerberg, A.C., Schei, R., Henriksen, C., Smith, L., Veierød, M.B., Drevon, C.A., Iversen, P.O., 2011. Attention among very low birth weight infants following early supplementation with docosahexaenoic and arachidonic acid: Fatty acids and cognitive functions in preterm infants. *Acta Paediatrica* 100, 47–52. <https://doi.org/10.1111/j.1651-2227.2010.01946.x>

Whelan, J., 2008. (n-6) and (n-3) Polyunsaturated Fatty Acids and the Aging Brain: Food for Thought. *The Journal of Nutrition* 138, 2521–2522. <https://doi.org/10.3945/jn.108.095943>

Williard, D.E., Harmon, S.D., Kaduce, T.L., Preuss, M., Moore, S.A., Robbins, M.E.C., Spector, A.A., 2001. Docosahexaenoic acid synthesis from n-3 polyunsaturated fatty acids in differentiated rat brain astrocytes. *Journal of Lipid Research* 42, 1368–1376. [https://doi.org/10.1016/S0022-2275\(20\)30268-6](https://doi.org/10.1016/S0022-2275(20)30268-6)

Wilson, C.J., Kawaguchi, Y., 1996. The origins of two-state spontaneous membrane potential fluctuations of neostriatal spiny neurons. *J. Neurosci.* 16, 2397–2410. <https://doi.org/10.1523/JNEUROSCI.16-07-02397.1996>

Wittamer, V., Franssen, J.-D., Vulcano, M., Mirjolet, J.-F., Le Poul, E., Migeotte, I., Brézillon, S., Tyldesley, R., Blanpain, C., Detheux, M., Mantovani, A., Sozzani, S., Vassart, G., Parmentier, M., Communi, D., 2003. Specific Recruitment of Antigen-presenting Cells by Chemerin, a Novel Processed Ligand from Human Inflammatory Fluids. *Journal of Experimental Medicine* 198, 977–985. <https://doi.org/10.1084/jem.20030382>

Wu, X.Y., Ohinmaa, A., Veugelers, P.J., 2012. Diet quality, physical activity, body weight and health-related quality of life among grade 5 students in Canada. *Public Health Nutr.* 15, 75–81. <https://doi.org/10.1017/S1368980011002412>

Xiao, Y., Wang, L., Xu, R.-J., Chen, Z.-Y., 2006. DHA Depletion in Rat Brain Is Associated With Impairment on Spatial Learning and Memory 7.

Ximenes da Silva, A., Lavialle, F., Gendrot, G., Guesnet, P., Alessandri, J.-M., Lavialle, M., 2002. Glucose transport and utilization are altered in the brain of rats deficient in n-3 polyunsaturated fatty acids: Brain energy metabolism in n-3 deficient rats. *Journal of Neurochemistry* 81, 1328–1337. <https://doi.org/10.1046/j.1471-4159.2002.00932.x>

Xu, Z.-Z., Zhang, L., Liu, T., Park, J.Y., Berta, T., Yang, R., Serhan, C.N., Ji, R.-R., 2010. Resolvins RvE1 and RvD1 attenuate inflammatory pain via central and peripheral actions. *Nat Med* 16, 592–597. <https://doi.org/10.1038/nm.2123>

Yamagata, K., Andreasson, K.I., Kaufmann, W.E., Barnes, C.A., Worley, P.F., 1993. Expression of a mitogen-inducible cyclooxygenase in brain neurons: Regulation by synaptic activity and glucocorticoids. *Neuron* 11, 371–386. [https://doi.org/10.1016/0896-6273\(93\)90192-T](https://doi.org/10.1016/0896-6273(93)90192-T)

- Yamamoto, T., Yamamoto, A., Tanabe, H., Nishimura, N., 2021. Inhibited maturation of astrocytes caused by maternal n-3 PUFA intake deficiency hinders the development of brain glial cells in neonatal rats. *Br J Nutr* 1–9. <https://doi.org/10.1017/S0007114521004359>
- Yang, H., Chen, C., 2008. Cyclooxygenase-2 in Synaptic Signaling. *Current Pharmaceutical Design* 14, 1443–1451.
- Yang, H., Zhang, J., Andreasson, K., Chen, C., 2008. COX-2 oxidative metabolism of endocannabinoids augments hippocampal synaptic plasticity. *Mol Cell Neurosci* 37, 682–695. <https://doi.org/10.1016/j.mcn.2007.12.019>
- Yassine, H.N., Samieri, C., Livingston, G., Glass, K., Wagner, M., Tangney, C., Plassman, B.L., Ikram, M.A., Voigt, R.M., Gu, Y., O’Bryant, S., Minihane, A.M., Craft, S., Fink, H.A., Judd, S., Andrieu, S., Bowman, G.L., Richard, E., Albeni, B., Meyers, E., Khosravian, S., Solis, M., Carrillo, M., Snyder, H., Grodstein, F., Scarmeas, N., Schneider, L.S., 2022. Nutrition state of science and dementia prevention: recommendations of the Nutrition for Dementia Prevention Working Group. *The Lancet Healthy Longevity* 3, e501–e512. [https://doi.org/10.1016/S2666-7568\(22\)00120-9](https://doi.org/10.1016/S2666-7568(22)00120-9)
- Yeh, H.-J., He, Y.Y., Xu, J., Hsu, C.Y., Deuel, T.F., 1998. Upregulation of Pleiotrophin Gene Expression in Developing Microvasculature, Macrophages, and Astrocytes after Acute Ischemic Brain Injury. *J. Neurosci.* 18, 3699–3707. <https://doi.org/10.1523/JNEUROSCI.18-10-03699.1998>
- Yehuda, S., Rabinovitz, S., Mostofsky, D.I., 1999. Essential fatty acids are mediators of brain biochemistry and cognitive functions. *Journal of Neuroscience Research* 56, 565–570. [https://doi.org/10.1002/\(SICI\)1097-4547\(19990615\)56:6<565::AID-JNR2>3.0.CO;2-H](https://doi.org/10.1002/(SICI)1097-4547(19990615)56:6<565::AID-JNR2>3.0.CO;2-H)
- Yu, L., Boyle, P.A., Leurgans, S., Schneider, J.A., Bennett, D.A., 2014. Disentangling the effects of age and APOE on neuropathology and late life cognitive decline. *Neurobiology of Aging* 35, 819–826. <https://doi.org/10.1016/j.neurobiolaging.2013.10.074>
- Zdravec, D., Tvrdik, P., Guillou, H., Haslam, R., Kobayashi, T., Napier, J.A., Capecchi, M.R., Jacobsson, A., 2011. ELOVL2 controls the level of n-6 28:5 and 30:5 fatty acids in testis, a prerequisite for male fertility and sperm maturation in mice. *Journal of Lipid Research* 52, 245–255. <https://doi.org/10.1194/jlr.M011346>
- Zahm, D.S., Brog, J.S., 1992. On the significance of subterritories in the “accumbens” part of the rat ventral striatum. *Neuroscience* 50, 751–767. [https://doi.org/10.1016/0306-4522\(92\)90202-d](https://doi.org/10.1016/0306-4522(92)90202-d)
- Zemdegs, J., Martin, H., Pintana, H., Bullich, S., Manta, S., Marqués, M.A., Moro, C., Layé, S., Ducrocq, F., Chattipakorn, N., 2019. Metformin promotes anxiolytic and antidepressant-like responses in insulin-resistant mice by decreasing circulating branched-chain amino acids. *Journal of Neuroscience* 39, 5935–5948.
- Zerangue, N., Arriza, J.L., Amara, S.G., Kavanaugh, M.P., 1995. Differential Modulation of Human Glutamate Transporter Subtypes by Arachidonic Acid. *Journal of Biological Chemistry* 270, 6433–6435. <https://doi.org/10.1074/jbc.270.12.6433>
- Zhang, J., Qin, X., Liang, A., Kim, E., Lawrence, P., Kothapalli, K., Brenna, J., 2014. Fatty acid desaturase 3 null mouse biochemical phenotype (246.5). *The FASEB Journal* 28, 246.5. [https://doi.org/10.1096/fasebj.28.1\\_supplement.246.5](https://doi.org/10.1096/fasebj.28.1_supplement.246.5)

- Zhang, M., Ren, B., Liu, Y., Liang, G., Sun, Y., Xu, L., Zheng, J., 2017. Membrane Interactions of hIAPP Monomer and Oligomer with Lipid Membranes by Molecular Dynamics Simulations. *ACS Chem. Neurosci.* 8, 1789–1800. <https://doi.org/10.1021/acscchemneuro.7b00160>
- Zhang, T., Zuo, G., Zhang, H., 2022. GPR18 Agonist Resolvin D2 Reduces Early Brain Injury in a Rat Model of Subarachnoid Hemorrhage by Multiple Protective Mechanisms. *Cell Mol Neurobiol* 42, 2379–2392. <https://doi.org/10.1007/s10571-021-01114-2>
- Zhu, M., Wang, X., Hjorth, E., Colas, R.A., Schroeder, L., Granholm, A.-C., Serhan, C.N., Schultzberg, M., 2016. Pro-Resolving Lipid Mediators Improve Neuronal Survival and Increase A $\beta$ 42 Phagocytosis. *Mol Neurobiol* 53, 2733–2749. <https://doi.org/10.1007/s12035-015-9544-0>
- Zhu, R.-Z., Chen, M.-Q., Zhang, Z.-W., Wu, T.-Y., Zhao, W.-H., 2021. Dietary fatty acids and risk for Alzheimer’s disease, dementia, and mild cognitive impairment: A prospective cohort meta-analysis. *Nutrition* 90, 111355. <https://doi.org/10.1016/j.nut.2021.111355>
- Zussy, C., John, R., Urgin, T., Otaegui, L., Vigor, C., Acar, N., Canet, G., Vitalis, M., Morin, F., Planel, E., Oger, C., Durand, T., Rajshree, S.L., Givalois, L., Devarajan, P.V., Desrumaux, C., 2022. Intranasal Administration of Nanovectorized Docosahexaenoic Acid (DHA) Improves Cognitive Function in Two Complementary Mouse Models of Alzheimer’s Disease. *Antioxidants* 11, 838. <https://doi.org/10.3390/antiox11050838>

## LISTE DES PUBLICATIONS

---

Martin, H., Bullich, S., **MARTINAT, M.** et al. Insulin modulates emotional behavior through a serotonin-dependent mechanism. *Mol Psychiatry* (2022). <https://doi.org/10.1038/s41380-022-01812-3>

Di Miceli M, **MARTINAT M**, Rossitto M, Aubert A, Alashmali S, Bosch-Bouju C, Fioramonti X, Joffre C, Bazinet RP, Layé S. Dietary Long-Chain n-3 Polyunsaturated Fatty Acid Supplementation Alters Electrophysiological Properties in the Nucleus Accumbens and Emotional Behavior in Naïve and Chronically Stressed Mice. *International Journal of Molecular Sciences*. 2022; 23(12):6650. <https://doi.org/10.3390/ijms23126650>

**MARTINAT, M.**; Rossitto, M.; Di Miceli, M.; Layé, S. Perinatal Dietary Polyunsaturated Fatty Acids in Brain Development, Role in Neurodevelopmental Disorders. *Nutrients* 2021, 13, 1185. <https://doi.org/10.3390/nu13041185> <https://doi.org/10.3390/nu13041185>

Madore, C., Leyrolle Q., Morel L., Rossitto M., Greenhalgh A.D., Delepch J. C., **MARTINAT M.**, Bosch-Bouju C., Bourel J., Rani B., Lacabanne C., Thomazeau A., Hopperton K.E., Beccari S., Sere A., Aubert A., De Smedt-Peyrusse V., Lecours C., Bisht K., Fourgeaud L., Gregoire S., Bretillon L., Acar N., Grant N.J., Badaut J., Gressens P., Sierra A., Butovsky O., Tremblay M.E., Bazinet R.P., Joffre C., Nadjar A., Layé S., Essential omega-3 fatty acids tune microglial phagocytosis of synaptic elements in the mouse developing brain. *Nat Commun* 11, 6133 (2020). <https://doi.org/10.1038/s41467-020-19861-z>

Berland C., Montalban E., Perrin E., Di Miceli M., Nakamura Y., **MARTINAT M.**, Sullivan M., Davis X. S., Shenasa M., Martin C., Tolu S., Marti F., Caille S., Castel J., Perez S., Salinas C. G., Morel C., Hecksher-Sorensen J., Cador M., Fioramonti X., Tschop M/ H., Layé S., Venance L., Faure P., Hnasko T. S., Small Dana M., Gangarossa G., Luquet S. H., Circulating Triglycerides Gate Dopamine-Associated Behaviors Through DRD2-Expressing Neurons, *Cell Metabolism*, Volume 31, Issue 4, 2020, Pages 773-790.e11, ISSN 1550-4131. <https://doi.org/10.1016/j.cmet.2020.02.010>



***PUBLICATIONS ANNEXES***

---

## ARTICLE



# Insulin modulates emotional behavior through a serotonin-dependent mechanism

Hugo Martin<sup>1,8</sup>, Sébastien Bullich<sup>2,8</sup>, Maud Martinat<sup>1</sup>, Mathilde Chataigner<sup>1</sup>, Mathieu Di Miceli<sup>1,3</sup>, Vincent Simon<sup>4</sup>, Samantha Clark<sup>4</sup>, Jasmine Butler<sup>5</sup>, Mareike Schell<sup>6</sup>, Simran Chopra<sup>6</sup>, Francis Chaouloff<sup>4</sup>, Andre Kleinridders<sup>6</sup>, Daniela Cota<sup>4</sup>, Philippe De Deurwaerdere<sup>5</sup>, Luc Pénicaud<sup>7</sup>, Sophie Layé<sup>1</sup>, Bruno P. Guiard<sup>1,8</sup> and Xavier Fioramonti<sup>1,8</sup>✉

© The Author(s), under exclusive licence to Springer Nature Limited 2022

Type-2 Diabetes (T2D) is characterized by insulin resistance and accompanied by psychiatric comorbidities including major depressive disorders (MDD). Patients with T2D are twice more likely to suffer from MDD and clinical studies have shown that insulin resistance is positively correlated with the severity of depressive symptoms. However, the potential contribution of central insulin signaling in MDD in patients with T2D remains elusive. Here we hypothesized that insulin modulates the serotonergic (5-HT) system to control emotional behavior and that insulin resistance in 5-HT neurons contributes to the development of mood disorders in T2D. Our results show that insulin directly modulates the activity of dorsal raphe (DR) 5-HT neurons to dampen 5-HT neurotransmission through a 5-HT<sub>1A</sub> receptor-mediated inhibitory feedback. In addition, insulin-induced 5-HT neuromodulation is necessary to promote anxiolytic-like effect in response to intranasal insulin delivery. Interestingly, such an anxiolytic effect of intranasal insulin as well as the response of DR 5-HT neurons to insulin are both blunted in high-fat diet-fed T2D animals. Altogether, these findings point to a novel mechanism by which insulin directly modulates the activity of DR 5-HT neurons to dampen 5-HT neurotransmission and control emotional behaviors, and emphasize the idea that impaired insulin-sensitivity in these neurons is critical for the development of T2D-associated mood disorders.

*Molecular Psychiatry*; <https://doi.org/10.1038/s41380-022-01812-3>

## INTRODUCTION

Type 2 diabetes (T2D) is among the most prevalent chronic disease worldwide, and it is strongly associated with comorbidities including Major Depressive Disorder (MDD). Recent epidemiological studies indicate that the prevalence of MDD is at least twice as high among patients suffering from T2D [1]. Interestingly, clinical evidence suggests that impairment of insulin signaling, resulting from insulin resistance, might be one of the underlying mechanisms for the development of MDD in patients with T2D [2–4]. Preclinical studies support this hypothesis since it has been shown that insulin-resistant animal models of T2D exhibit both depressive- and anxiety-like behaviors [5–9]. Nevertheless, it remains unclear whether peripheral or brain insulin resistance plays a causal role in T2D-associated mood disorders.

The impact of impaired brain insulin signaling on mood has been investigated using transgenic animal models presenting a deletion of the insulin receptor (IR) in selective brain cells or structures [10]. For instance, Neuronal Insulin Receptor Knock-Out (NIRKO) mice, which display neuronal IR deletion, exhibit spontaneous depressive- and anxiety-like behaviors [11]. These findings support the hypothesis that brain IR signaling is crucial for the regulation of emotional behavior. The dopaminergic

system is known to modulate mood [12] and is a target of the action of insulin [13, 14]. However, the effect of insulin on the dopaminergic system does not seem to impact anxiety- or depressive-like behaviors [15]. As such, the identity of the neuronal networks underlying the effects of insulin on mood remains to be determined.

The serotonergic (5-HT) neurotransmission is a well-established monoaminergic system involved in the etiology of psychiatric disorders and more specifically in the pathophysiology of MDD and anxiety disorders [16]. This system is also the main target of antidepressant drugs such as selective serotonin reuptake inhibitors (SSRIs), which represent the most prescribed class of antidepressants. Previous studies from our group have demonstrated that 5-HT neurotransmission is impaired in animal models of T2D-associated mood disorders [6, 7, 10]. Thus, we hypothesized that insulin directly modulates the 5-HT system to control emotional behavior.

Here, we used multiple approaches to assess the role of insulin in the modulation of 5-HT neurons and associated emotional behaviors. Our data reveal that insulin directly controls the activity of 5-HT neurons in the dorsal raphe (DR). In addition, we provide evidence that the anxiolytic-like effect of insulin requires

<sup>1</sup>Univ. Bordeaux, INRAE, Bordeaux INP, NutriNeuro, UMR 1286, F-33000 Bordeaux, France. <sup>2</sup>Centre de Recherches sur la Cognition Animale (CRCA), Centre de Biologie Intégrative (CBI), CNRS UMR5169 Toulouse, France. <sup>3</sup>Worcester Biomedical Research Group, University of Worcester, WR2 6AJ Worcester, UK. <sup>4</sup>University of Bordeaux, Neurocentre Magendie, INSERM U1215 Bordeaux, France. <sup>5</sup>INCLIA, UMR CNRS, Bordeaux University, Neurocampus, Bordeaux, France. <sup>6</sup>University of Potsdam, Institute of Nutritional Science, Molecular and Experimental Nutritional Medicine, Nuthetal, Germany. <sup>7</sup>RESTORE, UMR INSERM 1301/CNRS 5070/Université Paul Sabatier/EFIS/ENVT, Toulouse, France. <sup>8</sup>These authors contributed equally: Hugo Martin, Sébastien Bullich, Bruno P. Guiard, Xavier Fioramonti. ✉email: [xavier.fioramonti@inrae.fr](mailto:xavier.fioramonti@inrae.fr)

Received: 22 December 2021 Revised: 19 September 2022 Accepted: 21 September 2022

Published online: 07 October 2022



modulation of the 5-HT system. Finally, we show that DR 5-HT neurons do not respond anymore to insulin in a model of T2D-associated mood disorders. Altogether, these findings identify a new mechanism by which insulin directly modulates the activity of DR 5-HT neurons to control emotional behaviors.

## MATERIALS AND METHODS

### Animals

Adult male mice (8–12 weeks) from different strains were collectively housed in conventional housing cages at NutriNeuro' or CRCA's animal facilities. Animals were maintained on a 12 h light-dark cycle with *ad libitum* access to food and water. All experimental procedures were conducted in accordance with the European directive 2010/63/UE and approved by the French Ministry of Research and local ethic committees (APAFIS#: 16853; 12898; 22415; 8928). C57BL/6J were purchased from Janvier laboratory (Le Genest-Saint-Isle, France). Pet1-cre-mCherry mice were obtained by crossing Pet1-cre mice (gift from Dr. P Gaspar, [17]) with B6.Cg-Gt(ROSA)26Sortm9(CAG-tdTomato)Hze/J mice (Jackson Laboratory, Bar Harbor, Maine, USA). SerRKO (Serotonin Insulin Receptor Knock-Out; cre<sup>+</sup>::IRflox<sup>+/+</sup>::mCherry<sup>+/-</sup>) mice were obtained by crossing IR<sup>flox/flox</sup> (cre<sup>+</sup>::flox<sup>+/+</sup>) mice (Jackson Laboratory) and Pet1-cre-mCherry (cre<sup>+</sup>::mCherry<sup>+/-</sup>) to specifically study insulin default of action only in 5-HT neurons. Littermates with cre<sup>+</sup>::flox<sup>-/-</sup>::mCherry<sup>+/-</sup> genotype were used as controls for the SerRKO mice. To model T2D-associated emotional disorders in rodents, a sub-group of mice was fed a high-fat diet (HFD; #D12451, Research Diet, New Brunswick, NJ, USA) or a standard diet (STD; #A04, Research Diet) for 16 weeks as previously described [6, 7].

### Drugs and treatments

**Serotonergic modulators.** To deplete 5-HT levels, mice were injected i.p. with p-chlorophenylalanine (pCPA, 150 mg/kg; Sigma, St-Quentin-Fallavier, France) twice per day (9.00 AM and 6.00 PM) for three consecutive days prior to experiments. The 5-HT<sub>1A</sub> antagonist WAY 100635 (0.5–1 mg/kg; Tocris, Bristol, UK) was injected i.p. one hour before behavioral tests.

**Intranasal delivery procedure.** Mice were handled and then habituated to intranasal delivery injections two weeks prior to testing. The day of the experiment, mice were fasted for 18 h before intranasal delivery of Human recombinant insulin (7 µg/µL insulin, diluted in NaCl 0.9%; Sigma) or vehicle (NaCl 0.9%) into mouse nares (5 µL/nare) to reach a final dose of 2 IU insulin [18]. Mice were replaced into their home cages and tested 60 min after IND injections. The dose of insulin was established based on a modified protocol [18]. Compounds (incl. insulin) injected through the intranasal route reach the brain either by crossing the epithelium of the nasal cavity or by axonal transport along the trigeminal nerve [19]. This last mechanism is the most relevant as the trigeminal nerve innervates the brain stem where the DR is located. Thus, intranasal injection of insulin lead to a rapid increase of insulin concentration in the brain stem with a  $t_{max}$  of 15 min [20].

**Intra-raphe insulin injection.** Mice were anesthetized with chloral hydrate (400 mg/kg, i.p., with additional doses when necessary) and placed in a stereotaxic apparatus. A cannula was implanted 0.5 mm posterior to the interaural line on the midline and lowered into the DR, attained at 2.5 mm depth from the brain surface. Two days after, half of the mice received 0.5 µL of artificial cerebro-spinal fluid (aCSF) (147 mM NaCl, 2.7 mM KCl, 1 mM MgCl<sub>2</sub>, 1.2 mM CaCl<sub>2</sub>, adjusted to pH 7.4 with sodium phosphate buffer 2 mM). The other half received 100 µIU of insulin in 0.5 µL aCSF. The injection flow was set to 0.1 µL/min and behavioral tests were performed 10 min after the end of the injection.

**Antidepressant add-on treatment experiment.** One hour prior to be subjected to the tail suspension test, mice were injected with an appropriate combination intranasal (insulin 2 IU or vehicle NaCl 0.9%) and intraperitoneal treatment (fluoxetine-hydrochloride 18 mg/kg; Sigma; or vehicle 0.9%).

### Behavioral tests

Animals were tested in different anxiety-like and depressive-like behavioral paradigms as previously described (Supplementary Table 1; [6, 7]). Tests were spaced by three days of recovery time and increasing in term of stress-related paradigm, starting with the less stressful test. Mouse behavior was tracked and analyzed with *Smart* (Panlab, Barcelona, Spain)

or *Bioseb* (Bioseb, Vitrolles, France) software. All behavioral experiments were subject-randomized and blind analyzed.

### FISH for IR combined with IHC for TPH2

Digoxigenin-labeled riboprobe against mouse Insr (IR-DIG, Allen Brain Atlas, #RP\_050503\_02\_H08) was prepared as previously described [4] (Supplementary Table 2).

### Tissue sampling and high-pressure liquid chromatography coupled to electrochemical detection (HPLC-ECD)

Tissue sampling and conditioning for HPLC-ECD have been performed as previously described [21, 22] (Supplementary Table 2).

### In vivo single-unit recordings of 5-HT neurons in the DR

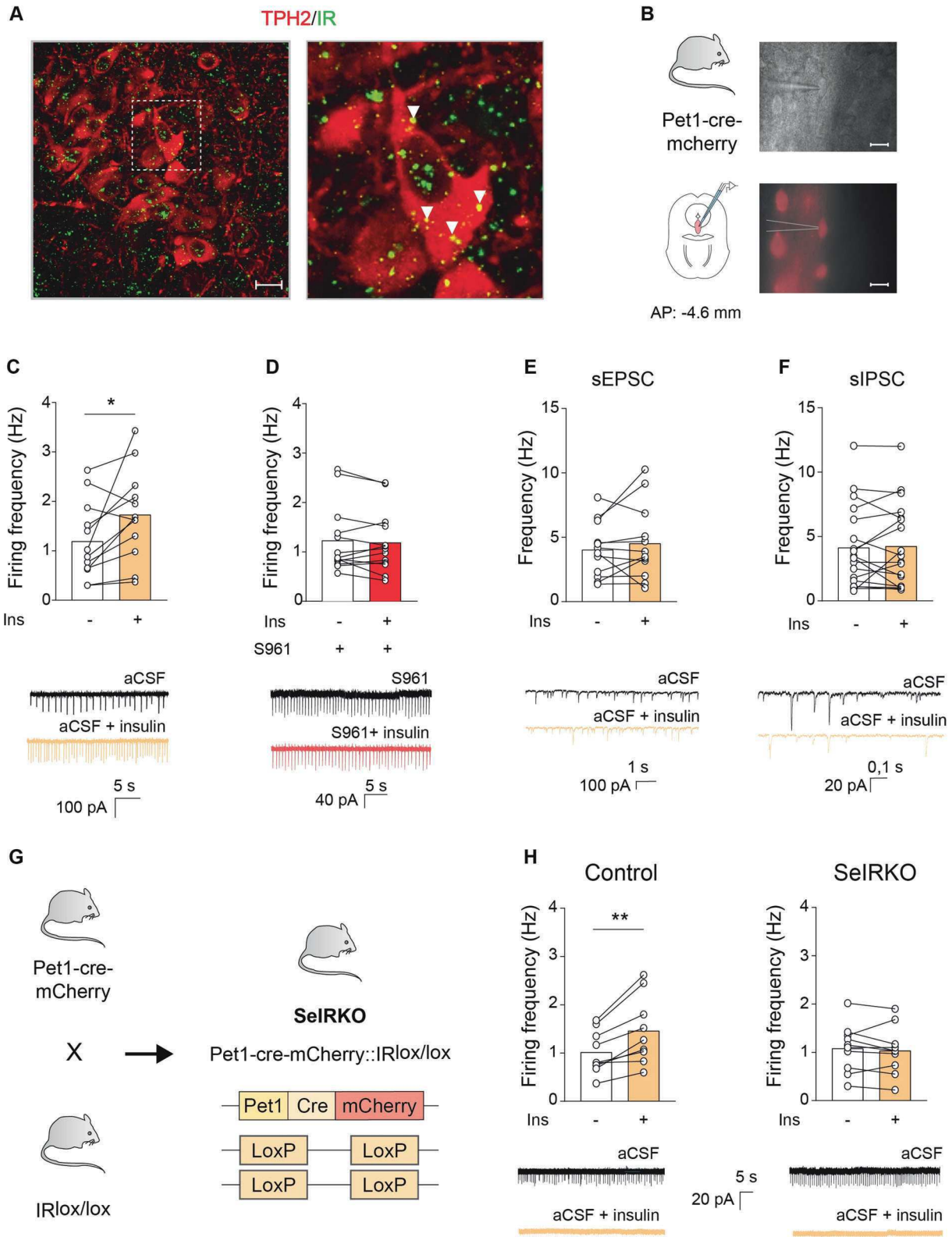
Mice were anesthetized with chloral hydrate (400 mg/kg, i.p., with additional doses when necessary) and extracellular recordings of DR 5-HT neurons were performed using single glass micropipettes (Stoelting Europe, Dublin, Ireland) pulled on a pipette puller (Narishige, Tokyo, Japan) and preloaded with a 2 M NaCl solution. Micropipettes were positioned 0.2–0.5 mm posterior to the interaural line on the midline and lowered into the DR, attained at a depth between 2.5 and 3.5 mm from the brain surface. Presumed 5-HT neurons were identified using the following criteria: a slow (0.5–2.5 Hz) and regular firing rate and a long-duration positive action potential (please see references [7, 23, 24] for additional information regarding presumed DR 5-HT neurons recordings and their pharmacological characterization). In each mouse, presumed 5-HT neurons were identified based on these criteria and their spontaneous firing rate was recorded for 2 min. Insulin was then injected i.p. at doses of 0.75 and 1.5 IU/kg either alone or in combination with WAY100635 as described in figure legend.

### Intracerebral microdialysis in the ventral Hippocampus or Dorsal Raphe of awake freely moving mice

Mice were implanted with microdialysis probes in the ventral hippocampus (vHP) or the DR. Stereotaxic coordinates from bregma were as follows (in mm): vHP: antero-posterior (AP): -2.5; lateral (L): ± 2.7; and dorso-ventral (DV): -3.0; DR: AP: -4.5; L: 0; and DV: -3.5. Twenty-four hours later, probes were connected to a microinjection pump for a continuous perfusion (flow rate: 1.5 µL/min for the vHP and 0.5 µL/min for the DR) of artificial cerebrospinal fluid (147 mM NaCl, 2.7 mM KCl, 1 mM MgCl<sub>2</sub>, and 1.2 mM CaCl<sub>2</sub>, adjusted to pH 7.4 with 2 mM sodium phosphate buffer) containing the 5-HT reuptake inhibitor escitalopram (1 µM), as previously described [25]. Samples were collected every 15 or 30 min in the vHP or DR, respectively. The four initial fractions were used to determine the basal extracellular levels of serotonin ([5-HT]<sub>ext</sub>) before injecting insulin in mice pre-treated with saline or WAY100635 (0.5 mg/kg; i.p.). The amount of 5-HT in dialysate samples post-insulin injection was expressed as percentage of the basal value. Samples were analyzed using high-performance liquid chromatography system equipped with a 2.6 µm C18 reverse-phase analytical column (50 × 3.0 mm; Accucore, Thermo Fisher Scientific, Waltham, MA, USA) coupled with electrochemical detection (Dionex Ultimate 3000, Thermo Fisher Scientific).

### Brain slice patch clamp recordings of DR 5-HT neurons

Ex-vivo patch-clamp recordings were performed on brain slices from Pet1-cre-mCherry mice, as previously described [7]. Briefly, mice were intracardially perfused during euthanasia (exagon/lidocaine: 300/30 mg/kg, i.p.) with ice-cold NMDG solution containing the following (in mM): 1.25 NaH<sub>2</sub>PO<sub>4</sub>, 2.5 KCl, 7 MgCl<sub>2</sub>, 20 HEPES, 0.5 CaCl<sub>2</sub>, 28 NaHCO<sub>3</sub>, 8 D-glucose, 5L(+)-ascorbate, 3 Na-pyruvate, 2 thiourea, 93 NMDG, and 93 HCl 37%; pH: 7.3–7.4; osmolarity: 305–310 mOsm. Brains were quickly removed and 250 µm slices containing the DR were cut with a vibroslice (Leica VT1000S, Wetzlar, Germany) and transferred at room temperature into aCSF solution (containing the following in mM: 124 NaCl, 2.5 KCl, 1.25 NaH<sub>2</sub>PO<sub>4</sub>, 2 MgCl<sub>2</sub>, 2.5 CaCl<sub>2</sub>, 2.5 D-glucose, and 25 NaHCO<sub>3</sub>; pH: 7.3–7.4; osmolarity: 305–310 mOsm) for at least 1 h. For whole cell recording, borosilicate pipette (4–6 MΩ; 1.5 mm OD, Sutter Instrument) were filled with an intracellular K-gluconate solution (containing the following (in mM): 128 K-gluconate, 20 NaCl, 1 MgCl<sub>2</sub>, 1 EGTA, 0.3 CaCl<sub>2</sub>, 2 Na<sub>2</sub>-ATP, 0.3 Na-GTP, 0.2 cAMP, and 10 HEPES; pH: 7.3–7.4; osmolarity: 280–290 mOsm), cesium chloride (containing the following (in mM): 150 CsCl, 2 MgCl<sub>2</sub>, 1 EGTA, 2 Na<sub>2</sub>-ATP, 0.2 Na-GTP, 0.2 cAMP, 10 HEPES) or filled with filtered aCSF for cell-attached recording. Recordings were made using a Multiclamp 700B



amplifier, digitized using the Digidata 1440 A interface and acquired at 2 kHz using pClamp 10.5 software (Axon Instruments, Molecular Devices, San José, CA, USA). Pipette and cell capacitances were fully compensated and junction potential was corrected off-line.

Firing frequency of DR 5-HT neurons was recorded in cell-attached mode. Because DR 5-HT neurons are silent ex vivo, phenylephrine (PHE,

5  $\mu$ M; Tocris) was perfused to stimulate basal action potential activity for 5 minutes before application of insulin (300 nM) and recorded for 10 additional minutes. Change in firing rate frequency was analyzed during the last minute of insulin application. Spontaneous excitatory (sEPSC) or inhibitory (sIPSC) postsynaptic currents were recorded in whole-cell Vclamp mode on cells held at  $-60$  mV. Gabazine (5  $\mu$ M; Tocris) was added

**Fig. 1 Insulin increases DR 5-HT neurons firing frequency by direct activation of insulin receptor expressed onto that neuronal population.** **A** Representative confocal image of TPH2-positive 5-HT neurons (red) and IR mRNA punctae (green) using fluorescence in situ hybridization. *Right panel*: magnification of the white dotted square area from the left panel. Scale: 10  $\mu$ m. White arrows show IR mRNA in 5-HT neurons. **B** Pet1-cre-mCherry mice were used for patch-clamp experiments to specifically visualize fluorescent mCherry-DR 5-HT neurons. Scale: 10  $\mu$ m. Quantification of firing rate and representative traces of cell-attached mode recording before and after insulin (300 nM) perfusion and of DR 5-HT neurons under control condition (**C**) or during bath application of the IR inhibitor S961 (100 nM, **D**). Frequency of spontaneous excitatory postsynaptic currents (EPSC, **E**) or inhibitory postsynaptic currents (IPSC, **F**) onto DR 5-HT neurons before and after insulin (300 nM) perfusion. **G** SelRKO mice were obtained by crossing Pet1-cre-mCherry mice with IR<sup>lox/lox</sup> mice allowing selective deletion of IR only in 5-HT neurons. **H** Quantification of firing rate and representative traces of cell-attached mode recording before and after insulin (300 nM) perfusion of DR 5-HT neurons in control (*Left panel*) and in SelRKO (*Right panel*) mice. The data are represented as mean  $\pm$  SEM. Statistics: Student's paired t-test: \* $p < 0.05$ ; \*\* $p < 0.01$ .

into the bath to record sEPSC while D-AP5 (10  $\mu$ M; Tocris) and CNQX (10  $\mu$ M; Tocris) were added to monitor sIPSC. Spontaneous EPSC and IPSC frequency was recorded before and after 10 min insulin (300 nM; Sigma) perfusion period and analyzed during the last minute of each period.

### Statistical analysis

Sample size has been estimated based on previous work from our group or others. No randomization was used. Investigator was not blinded to the group allocation for most experiment. Statistical analysis was performed using *Prism GraphPad 9* (San Diego, CA, USA). Data are expressed as mean  $\pm$  SEM and individual values are plotted on graph when possible. After normal Gaussian distribution was assessed using Shapiro-Wilk test, appropriate parametric (unpaired or paired Student's *t*-test) or non-parametric (Mann-Whitney or Wilcoxon matched-pairs signed rank test) tests were chosen to compare two population samples. One-way ANOVA was used when comparing one variable of several population samples and two-way ANOVA was used when analysis accounted for two distinct variables. Post-hoc analyses are mentioned in each figure legend. Outliers were identified using *Prism GraphPad 9* and discarded from the analyses. Statistics are detailed in supplementary Table 3 (Supplementary Table 3).

## RESULTS

### Insulin increases firing activity of DR 5-HT neurons

We first verified that the IR is expressed at the mRNA and protein level in the DR (Supplementary Fig. S1A, B). To determine whether the IR is expressed in DR 5-HT neurons, we used in situ fluorescence hybridization targeting IR mRNA combined with an immunodetection against the rate-limiting 5-HT synthesis enzyme Tryptophan Hydroxylase 2 (TPH2), which is selectively expressed in 5-HT neurons. This analysis shows that the IR is expressed in DR 5-HT neurons (Fig. 1A). The functional activity of the IR expressed onto DR 5-HT neurons was assessed using cell-attached patch-clamp recording on Pet1-cre-mCherry mice (Fig. 1B). Insulin (300 nM) increases action potentials frequency in 80 % of DR 5-HT neurons by  $64 \pm 21$  % (Fig. 1C: 10/12 neurons tested). The selective IR inhibitor S961 prevents the excitatory effect of insulin (Fig. 1D). In the DR, the IR is expressed in both 5-HT and non-5-HT neurons (Fig. 1A). Thus, we assessed whether the action of insulin onto 5-HT neurons is direct rather than mediated by pre-synaptic inputs. We found that insulin fails to modulate the frequency of both spontaneous excitatory (EPSC) and inhibitory (IPSC) postsynaptic currents (Fig. 1E, F). To further confirm that insulin directly activates DR 5-HT neurons, we evaluated the response of DR 5-HT neurons to insulin in mice lacking the IR selectively in 5-HT neurons (SelRKO mice; Supplementary Fig. S1D, E; Fig. 1G). Similarly, to what we have observed before, insulin increases action potentials frequency of DR 5-HT neurons in control animals but fails to activate 5-HT neurons in SelRKO mice (Fig. 1H), leading to conclude that insulin directly modulates DR 5-HT neurons through an IR-dependent mechanism.

### Insulin inhibits the serotonergic system in vivo through a 5-HT<sub>1A</sub> receptor-dependent mechanism

Extracellular recordings of DR 5-HT neurons were then performed to study the effects of insulin on this neuronal population in vivo. While we were expecting an increase in the activity of presumed

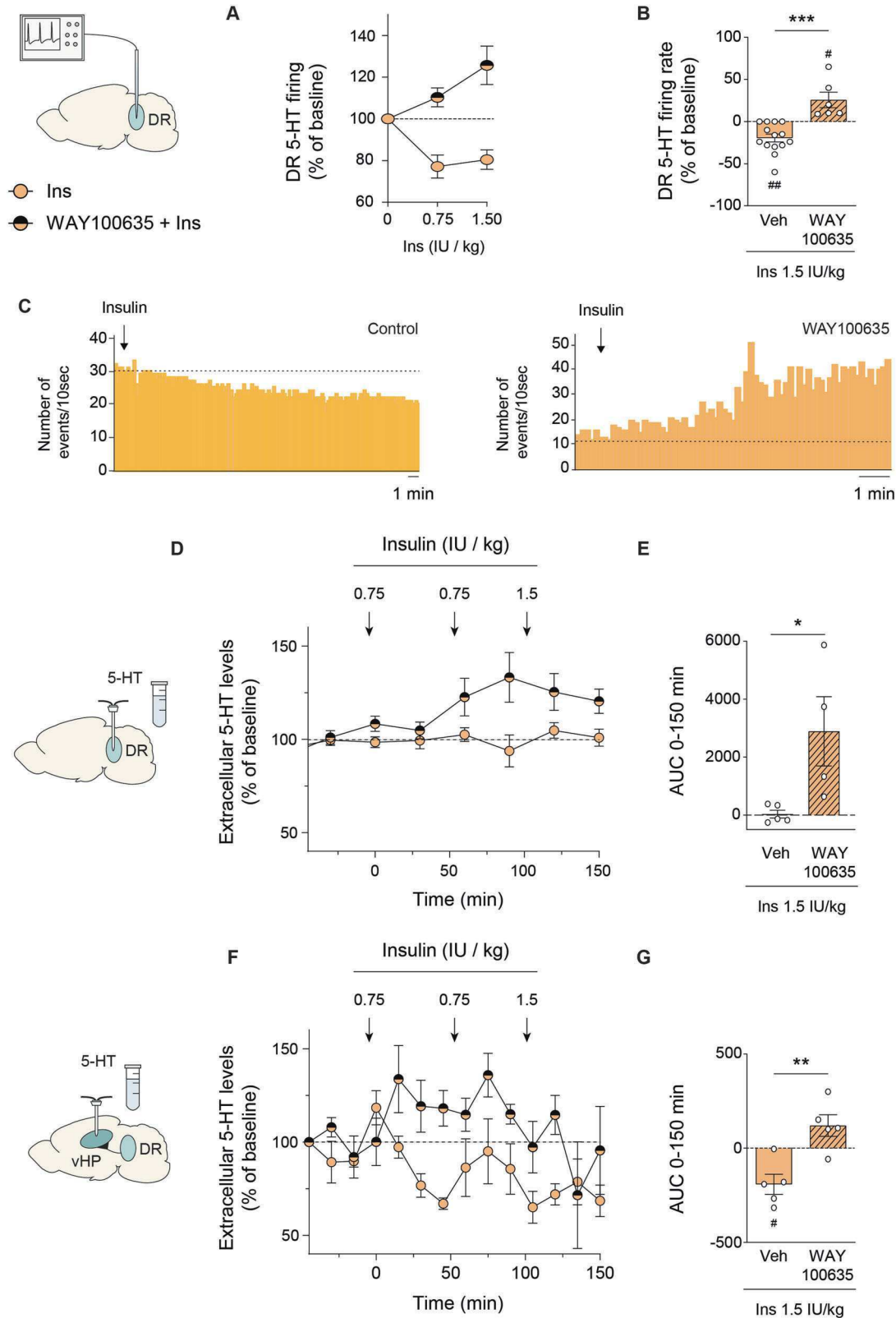
DR 5-HT neurons, we found that the intraperitoneal administration of 0.75 or 1.5 U/l insulin produces, on average, a reduction of firing by  $30 \pm 3\%$  and  $20 \pm 4\%$ , respectively, relative to baseline (Fig. 2A–C). Injecting glucose i.p. does not reverse insulin-induced decrease of presumed DR 5-HT neuronal activity suggesting that insulin, rather change in blood glucose level, impacts DR 5-HT neurons activity (Supplementary Fig. S2). This non-intuitive inhibitory response of presumed DR 5-HT neurons in vivo could be consequent to the recruitment of autoinhibitory mechanisms inherent to the raise in DR 5-HT neurons excitability induced by insulin, as observed in vitro. Interestingly, the ability of insulin to inhibit DR 5-HT neuronal activity is completely prevented by the selective 5-HT<sub>1A</sub> receptor antagonist WAY100635. Indeed, the firing rate of presumed DR 5-HT neurons in mice receiving the combination of insulin and WAY100635 is significantly higher compared to the group injected with insulin alone at both doses (Fig. 2A–C). This finding, therefore, suggests that, in vivo, insulin inhibits DR 5-HT neurons through a 5-HT<sub>1A</sub>-dependent mechanism. In support of this hypothesis, assessment of DR extracellular 5-HT levels ([5-HT]<sub>ext</sub>) by intra-DR microdialysis shows that i.p. administration of insulin increases [5-HT]<sub>ext</sub> in presence of WAY100635 whereas [5-HT]<sub>ext</sub> are not altered in absence of this pharmacological compound (Fig. 2D, E).

In addition, based on the importance of 5-HT projections in the ventral-hippocampus (vHP) in the control of mood, we then conducted intra-vHP microdialysis to determine to what extent insulin influences [5-HT]<sub>ext</sub> at the nerve terminals. Acute administration of insulin decreases [5-HT]<sub>ext</sub> in the hippocampus relative to baseline, whereas it fails to do so when combined with WAY100635 (Fig. 2F). Analysis of the area under the curves indicates that differences between the two groups are statistically significant (Fig. 2G), demonstrating that the inhibitory effect of insulin on vHP [5-HT]<sub>ext</sub> is blunted when the inhibitory feedback exerted by the 5-HT<sub>1A</sub> autoreceptor on 5-HT release is prevented.

### Anxiolytic-like effect of brain insulin requires 5-HT neurotransmission

Clinical and preclinical studies have suggested that insulin modulates emotional behaviors by acting onto the brain [26, 27]. In the present study, we determined whether the action of insulin on mood requires the 5-HT system. Intranasal insulin delivery has been widely used to assess brain insulin effect in both rodents and humans in order to avoid symptomatic insulin-induced hypoglycemia bias [28]. Accordingly, our results show that intranasal insulin delivery does not modify peripheral blood glucose (Supplementary Fig. S3A). However, it significantly decreases tissue 5-HT content in both the amygdala and nucleus accumbens (NAc), with a non-significant trend in the vHP (Supplementary Fig. S3B). Remarkably, overall, no modifications in brain noradrenaline (NA) and dopamine (DA) contents were detected, thereby highlighting the specificity of insulin action on 5-HT neurons (Supplementary Fig. S3C, D).

In the forced swim test (FST), intranasal insulin does not affect the time of immobility compared to intranasal vehicle treatment (Fig. 3A). Intranasal insulin does not modify latency to feed in the



novelty suppressed feeding (NSF) test (Fig. 3B) or the time spent in the light compartment of the Light-dark box test (Fig. 3C). However, intranasal insulin increases the time spent in the open arms in the elevated plus maze (EPM) (Fig. 3D). Consistent with the latter, intranasal insulin also elicits an anxiolytic-like effect since it

increases the time spent in the center of the open field (OF) without any changes in the locomotor activity (Fig. 3E). Interestingly, injection of insulin directly in the DR produces a similar increase in the time spent in the open arm in the EPM (Fig. 3F). To confirm the contribution of the 5-HT system in the anxiolytic

**Fig. 2 Insulin decreases DR 5-HT neurons in vivo through a 5-HT<sub>1A</sub> receptor-dependent mechanism.** **A** In vivo extracellular recordings of presumed DR 5-HT neurons. Data are mean  $\pm$  SEM of DR 5-HT firing rate (% of baseline) in response to the intraperitoneal (i.p.) administration of insulin alone (0.75 IU,  $n = 5$  and 1.5 IU,  $n = 14$ ) or in combination with the 5-HT<sub>1A</sub> receptor antagonist (WAY100635: 0.5 mg/kg,  $n = 6$ ). **B** Integrated firing histograms showing the effects of cumulative doses of insulin. **C** Representative recordings of a single presumed 5-HT neuron in response to insulin (0.75 U/kg) alone (**C**, left panel) or in presence of the 5-HT<sub>1A</sub> antagonist WAY100635 (**C**, right panel). In vivo intracerebral microdialysis in the DR (**D-E**) or the ventral hippocampus (**F-G**). Time course of the effect of cumulative doses of insulin alone ( $n = 5$ ) or in combination with WAY100635 (0.5 mg/kg; i.p,  $n = 5$ ) given at T0 on 5-HT release in the DR (**D**) or ventral hippocampus (**F**). Data are mean  $\pm$  SEM of Area Under the Curve reflecting extracellular 5-HT concentrations ([5-HT]ext) over the 0–150 min post-treatment injections in the DR (**E**) or the ventral hippocampus (**G**). Statistics: Student's unpaired t-test: \* $p < 0.05$ ; \*\* $p < 0.01$ ; \*\*\* $p < 0.001$ . One sample t-test compared to hypothetical value (0): # $p < 0.05$ ; ## $p < 0.01$ .

effects of insulin, mice were pre-treated with the Tph2 inhibitor pCPA. As expected, pCPA treatment significantly decreases tissue 5-HT levels in all brain areas analyzed, without overall change of tissue DA or NA contents (Supplementary Fig. S4). At the behavioral level, pCPA treatment prevents the anxiolytic-like response of intranasal insulin assessed in the EPM (Fig. 3G). Importantly, the anxiolytic-like effect of intranasal insulin in the EPM is also blunted in SelRKO animals as compared to their wild-type littermates (Fig. 3H). Finally, since we found that the 5-HT<sub>1A</sub> autoreceptor is involved in insulin-induced inhibition of the 5-HT tone in vivo, we sought to determine to what extent the pharmacological inactivation of this receptor influences insulin behavioral response. Our results show that the 5-HT<sub>1A</sub> receptor antagonist WAY100635 blocks the anxiolytic-like effect of intranasal insulin in the EPM (Fig. 3I).

#### Potentiated antidepressant response to fluoxetine in combination with intranasal insulin delivery

Since insulin signaling pathway has been shown to cross-talk with 5-HT signaling [29], we investigated whether intranasal insulin potentiates the response of acute fluoxetine administration. Consistent with our previous experiments assessing despair behavior in the FST, intranasal insulin treatment does not modify immobility time in the tail suspension test (TST) (Supplementary Fig. S5A) whereas fluoxetine significantly decreases the immobility time during TST (Supplementary Fig. S5A). Interestingly, the combination of intranasal insulin and fluoxetine further reduces the immobility time compared to fluoxetine treatment alone (Supplementary Fig. S5A). Acutely, fluoxetine induces anxiogenic effects [30]. Here we show that intranasal insulin does not reverse or potentiate fluoxetine-induced anxiogenic-like response in the EPM (Supplementary Fig. S5B). These data suggest that brain insulin signaling improves the antidepressant-like response of fluoxetine but does not impact its anxiogenic property.

#### DR 5-HT neurons harbor insulin-resistance in a model of T2D

Mice fed a HFD for 16 weeks develop hallmarks of T2D including basal hyperglycemia, basal hyperinsulinemia, glucose intolerance, and insulin resistance (Supplementary Fig. S6). We previously showed that HFD-fed mice display T2D-associated anxiety- and depressive-like behaviors as well as alterations in the activity of DR 5-HT neurons [6, 7]. In the present study, we aimed at determining whether such alterations in 5-HT tone are associated with impaired response to insulin in DR 5-HT neurons. We found that insulin (300 nM) fails to increase action potentials frequency of DR 5-HT neurons in Pet1-cre-mCherry mice fed an HFD for 16 weeks (Fig. 4A). Interestingly, the anxiolytic-like response to intranasal insulin is blunted in both the EPM (Fig. 4B) and the OF (Fig. 4C), raising the possibility that DR 5-HT neurons are insulin-resistant in a model of HFD-induced T2D.

#### DISCUSSION

Our study demonstrates that insulin inhibits the 5-HT system to elicits anxiolytic-like responses in mice. Such effect is mediated by direct action of insulin onto DR 5-HT neurons through the

enhancement of inhibitory somatodendritic 5-HT<sub>1A</sub>R. We also show that, in HFD-fed T2D mice, insulin fails to modulate the electrical activity of DR 5-HT neurons and to promote anxiolytic-like effects. This study provides novel mechanistic insights into how insulin modulates the serotonergic system to influence emotional behavior.

Previous studies have reported inconsistent findings on the neuronal response to insulin including increase [31] or decrease [32] in 5-HT neurotransmission. Using complementary approaches consisting in ex vivo patch-clamp electrophysiology, in vivo electrophysiology, and intracerebral microdialysis, our data suggest that the action of insulin on the 5-HT system is more complex than originally thought. Indeed, using patch-clamp, we show that insulin increases the electrical activity of DR 5-HT neurons. This effect of insulin on DR 5-HT neurons is direct since insulin does not modify the frequency of IPSC nor EPSC thereby excluding a modulation from GABAergic or glutamatergic inputs. In addition, insulin fails to increase DR 5-HT neurons firing frequency in SelRKO mice, which lack the IR selectively in 5-HT neurons. While these ex vivo experiments suggest that insulin activates the 5-HT system, in vivo studies show, on the contrary, that its systemic administration elicits inhibitory responses. Indeed, in vivo, insulin decreases both the firing rate frequency of DR 5-HT neurons and the tissue or extracellular 5-HT levels ([5-HT]ext) in different brain areas including the hippocampus. The latter data echo previous findings showing that peripheral insulin administration decreases the firing rate of 5-HT neurons in both the Raphe Pallidus and the Raphe Obscurus [33]. Going one step further, we demonstrate the involvement of a 5HT<sub>1A</sub> receptor (5-HT<sub>1A</sub>R)-dependent mechanism in the inhibitory effects of insulin in vivo. Studies have repeatedly shown that activation of 5HT<sub>1A</sub> autoreceptors located at the somatodendritic level of DR 5-HT neurons may silence these neurons and decrease [5-HT]ext in both brainstem (i.e., the DR) and forebrain projections [34, 35]. Thus, we hypothesized and demonstrated that insulin first activates DR 5-HT neurons, and consequent accumulation of endogenous [5-HT]ext in the DR ultimately inhibits DR 5-HT neurons through 5-HT<sub>1A</sub>R activation (Fig. 5A). Accordingly, our findings show that the 5-HT<sub>1A</sub>R antagonist WAY100635 prevents the inhibition of firing rate frequency of DR 5-HT neurons. At the neurochemical level, it also appears that insulin increases [5-HT]ext in both the DR and the vHP specifically in presence of WAY100635 compared to control. Thus, DR 5-HT neuronal activity is decreased in biological settings where local inhibitory feedback is preserved whereas the excitatory effects of insulin is revealed when blocking 5-HT<sub>1A</sub> autoreceptors in vivo. Nevertheless, it is important to note that there is evidence for post-synaptic 5-HT<sub>1A</sub> receptors control of DR 5-HT neurons (i.e., in the amygdala, hippocampus, or median prefrontal cortex (mPFC)) [36, 37]. In particular, data suggest that post-synaptic 5-HT<sub>1A</sub> are found on glutamatergic pyramidal neurons in the mPFC and given the fact that 5-HT<sub>1A</sub> receptors are usually inhibitory, it has been speculated that the excitation of mPFC by selective agonists involves inhibitory interneurons [38]. In such cases, one may assume that 5-HT<sub>1A</sub> receptor agonist-induced excitation of mPFC neurons would produce excitatory amino acid release in the DR, which

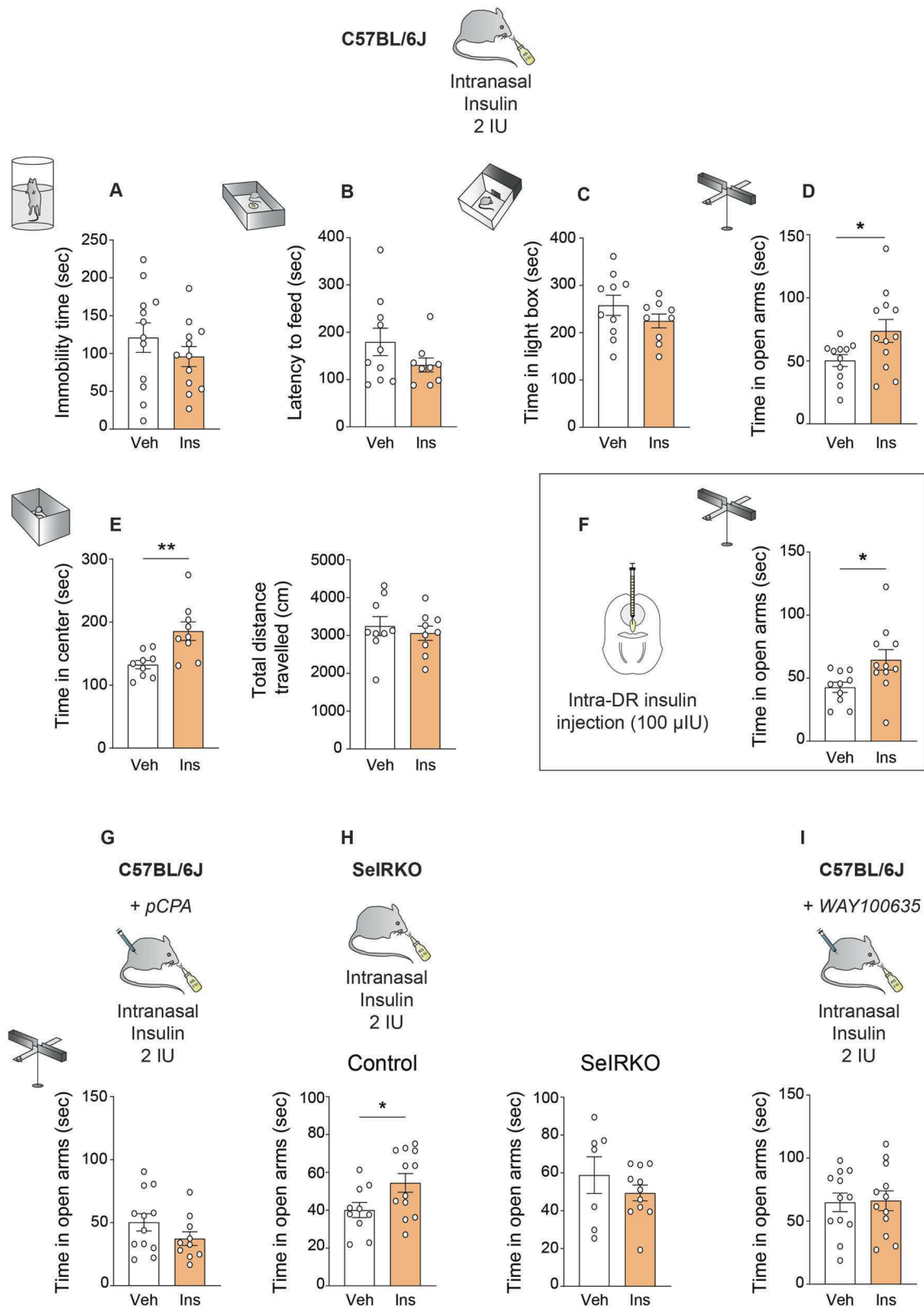


**Fig. 3** The anxiolytic like effect of intranasal insulin delivery relies on the central serotonergic system. Immobility time in the FST (A), latency to feed in the NSF (B), time spent in light box of the L/D (C), time spent in the open arms of the EPM (D) and time in the center (E, left panel) and locomotor activity in the OF (E, right panel) in response to intranasal 2 IU or vehicle delivery in naïve mice. F Time spent in the open arms of the EPM in response to intra-DR injection of insulin (100 µIU) or vehicle in naïve mice. Time spent in the open arms of the EPM in naïve mice pre-treated with pCPA (300 mg/kg/day for three consecutive days; G), in control and SeIRKO animals (H) or naïve mice pre-treated with WAY100635 (1 mg/kg; I) in response to intranasal insulin 2 IU or vehicle delivery. Data are represented as mean ± SEM. Statistics: Student's unpaired *t*-test: \**p* < 0.05; \*\**p* < 0.01.

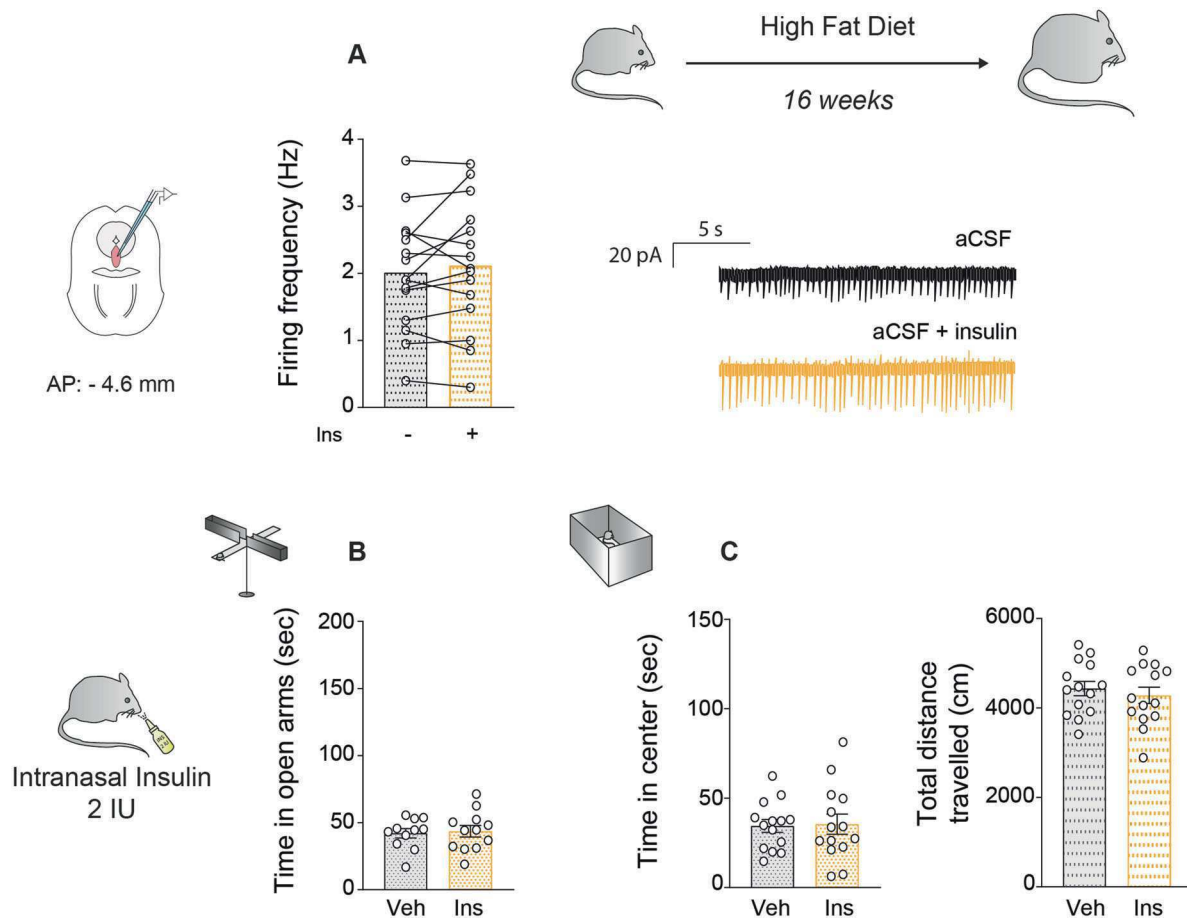


**Fig. 4** HFD feeding impairs the insulin response of the 5-HT system. **A** Pet1-cre-mCherry mice were fed a HFD for 16 weeks prior to ex-vivo electrophysiology experiments. Quantification of firing rate and representative trace of cell-attached mode recording before and after insulin (300 nM) perfusion of DR 5-HT neurons. Time spent in the open arms of the EPM (**B**), time spent in the center of the OF (**C**, left panel) and locomotor activity in the OF (**C**, right panel) of HFD-fed mice in response to intranasal insulin 2 IU or vehicle delivery. Data are represented as mean  $\pm$  SEM. Statistics: Student's unpaired *t*-test.

would activate inhibitory interneurons leading to inhibition of 5-HT neurons. Thus, such a model of regulation would support the possibility that the excitatory effects of insulin in presence of WAY100635 on DR 5-HT neuronal activity and extracellular 5-HT levels (in the DR and hippocampus) involves, at least in part, a disinhibition of this long neuronal feedback loop. From these data, one could wonder why such 5-HT<sub>1A</sub> receptors-dependent mechanism is not observed during patch-clamp recordings ex vivo. Studies have suggested that in ex-vivo patch-clamp conditions the 5HT<sub>1A</sub>-inhibition tone cannot be assessed due to the depletion of endogenous 5-HT synthesis and release [39–41].

The effect of intranasal insulin on anxiety has been previously investigated [27]. In agreement with the literature we show that insulin exerts anxiolytic effects. Yet, neuronal circuits underpinning such behavioral outcome have not been unraveled. Even if we cannot rule out the involvement of extra-DR neurons, the anxiolytic-like effect of intra-DR administration of insulin supports a role of the serotonergic system in the central effect of brain insulin. Going one step further, using pharmacological and genetic-based approaches, we confirm that anxiolysis induced by intranasal insulin relies, at least in part, on the serotonergic system. Indeed, both 5-HT depletion and selective deletion of the IR in 5-HT neurons result in a lack of anxiolytic-like effect of intranasal insulin. Interestingly, we found that intranasal insulin significantly reduces 5-HT level in the vHP, the amygdala, and the NAc. Importantly, decrease in 5-HT levels or lesion of serotonergic projections to the amygdala have been shown to mitigate anxiety-

like behavior [42, 43]. Thus, such a drop in 5-HT in response to intranasal insulin is consistent with the associated anxiolytic-like effect. In addition, we also show that blocking decreased 5-HT levels using the 5HT<sub>1A</sub>R antagonist WAY100635 prevents the anxiolytic effect of intranasal insulin administration. It is noteworthy that we cannot generalize the effect of insulin to all the behavioral tasks since our results clearly show that it produces anxiolytic effects in the EPM and in the OF while it fails to do so in the light-dark test. These paradigms rely on competition between spontaneous exploratory behavior and the innate avoidance of open or illuminated areas respectively. Since evidence suggests the existence of a high level of specialization at the level of microcircuits and cell populations involved, it is tempting to speculate that there is an overlap of the neuronal networks recruited during these tasks [44]. Nevertheless, the testing conditions are somewhat different with mice subjected to a dim lightening in the EPM/OF and a choice between a brightly-lit and dark compartment in the light-dark. A recent study demonstrates that light-dark preference behavior engages complex regulation due to the emotional valence of light [45]. Thus, even if the tests probe the same anxious behavior, the variations in experimental conditions strongly suggest that insulin could trigger a circuit specifically recruited during the EPM and the OF.

Our data show that intranasal injection of insulin promotes anxiolytic-like effects. Interestingly, we did not find any antidepressant-like effects in response to acute intranasal insulin administration in the FST or in the TST. According to the *Research*

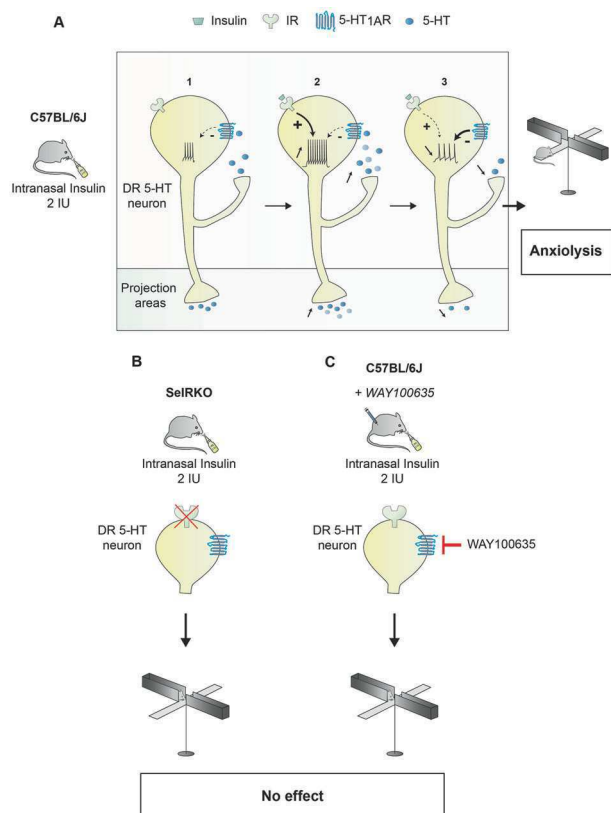


**Fig. 5 Schematic representation of the putative action of insulin onto DR 5-HT neurons and related control of emotional behaviors.** **A** At resting state, the 5-HT<sub>1A</sub> autoreceptors would exert limited effects on DR 5-HT neurons activity as previously reported [1]. Acute insulin binding to IR onto DR 5-HT neurons increases action potential firing activity and presumably extracellular 5-HT release in both projection areas and the DR through collaterals in a shorter timescale [2]. Such an accumulation of endogenous extracellular 5-HT levels around 5-HT cell bodies would, in turn, activate the autoinhibitory 5-HT<sub>1A</sub>R resulting in a decrease in firing activity and endogenous extracellular 5-HT release in an expanded timescale [3]. Reduced 5-HT levels in regions such as the amygdala might be responsible for the anxiolysis induced by intranasal insulin administration. Selective deletion of the IR in 5-HT neurons (**B**) or pre-administration of a 5-HT<sub>1A</sub>R antagonist (**C**) blocks the anxiolytic-like effect of intranasal insulin assessed in the EPM. Altogether, this study reveals that the anxiolytic-like effect of insulin relies on the 5-HT system.

*domain criteria* (RDoC) approach [46], we can assume that the acute effect of insulin might be involved in the anxiety dimension of MDD, a core symptom of the disease. However, in animal models of T2D induced by a HFD, both anxiety- and depressive-like symptoms have been reported [5–7, 47]. In these models, insulin resistance has been found in several discrete brain areas including the hippocampus, the ventral tegmental area, and or the striatum [48, 49]. Here, we provide the first evidence that such resistance also targets DR 5-HT neurons after HFD feeding and that such impairment likely explains our previous observation that 5-HT neurons display a lower electrical activity in response to a HFD [7]. Thus, we could hypothesize that insulin resistance at the level of 5-HT neurons takes a major part in the development of anxiety-like symptoms whereas decreased insulin sensitivity in other neuronal populations would rather promote depressive-like symptoms.

Clinical data show that antidepressant response efficacy is not optimal in patients with T2D as only one third presents an adequate treatment response following the first antidepressant

trial [50]. Add-on treatment strategy represents a relevant approach to improve antidepressant response [51]. Interestingly, the insulin-sensitizer agent metformin has been shown to potentiate the antidepressant effect of fluoxetine [52]. Thus, in a translational perspective, we investigated whether acute intranasal insulin could also potentiate fluoxetine antidepressant efficacy. In STD-fed animals, we observed that intranasal insulin indeed increases the antidepressant-like response of fluoxetine. However, the anxiogenic response of fluoxetine was not reversed by insulin. Although the reason of this lack of potentiating effect in the EPM remains unknown, it is possible that 1/ the fluoxetine effect is too strong to be reversed by insulin; 2/ the neuronal networks involved in the anxiogenic effect of fluoxetine are different from those mobilized by insulin. Clinical investigations are needed to support our data suggesting that enhancing insulin signaling represents an original therapeutic approach for patients with MDD presenting, or not, comorbid metabolic disorders associated to T2D.

## REFERENCES

- Anderson RJ, Freedland KE, Clouse RE, Lustman PJ. The prevalence of comorbid depression in adults with diabetes: a meta-analysis. *Diabetes Care*. 2001;24:1069–78.
- Lee JH, Park SK, Ryou JH, Oh CM, Mansur RB, Alfonsi JE, et al. The association between insulin resistance and depression in the Korean general population. *J Affect Disord*. 2017;208:553–9.
- Kan C, Silva N, Golden SH, Rajala U, Timonen M, Stahl D, et al. A systematic review and meta-analysis of the association between depression and insulin resistance. *Diabetes Care*. 2013;36:480–9.
- Phillips CM, Perry IJ. Depressive symptoms, anxiety, and well-being among metabolic health obese subtypes. *Psychoneuroendocrinology* 2015;62:47–53.
- Dutheil S, Ota KT, Wohleb ES, Rasmussen K, Duman RS. High-fat diet induced anxiety and anhedonia: impact on brain homeostasis and inflammation. *Neuropsychopharmacology* 2016;41:1874–87.
- Zemdegs J, Quesseveur G, Jarriault D, Pénicaud L, Fioramonti X, Guiard BP. High-fat diet-induced metabolic disorders impairs 5-HT function and anxiety-like behavior in mice. *Br J Pharm*. 2016;173:2095–110.
- Zemdegs J, Martin H, Pintana H, Bullich S, Manta S, Marqués MA, et al. Metformin promotes anxiolytic and antidepressant-like responses in insulin-resistant mice by decreasing circulating branched-chain amino acids. *J Neurosci*. 2019;39:5935–48.
- Hassan AM, Mancano G, Kashofer K, Fröhlich EE, Matak A, Mayerhofer R, et al. High-fat diet induces depression-like behaviour in mice associated with changes in microbiome, neuropeptide Y, and brain metabolome. *Nutr Neurosci*. 2019;22:877–93.
- Papazoglou IK, Jean A, Gertler A, Taouis M, Vacher CM. Hippocampal GSK3 $\beta$  as a molecular link between obesity and depression. *Mol Neurobiol*. 2015;52:363–74.
- Martin H, Bullich S, Guiard BP, Fioramonti X. The impact of insulin on the serotonergic system and consequences on diabetes-associated mood disorders. *J Neuroendocrinol*. 2021;33:e12928.
- Kleinridders A, Cai W, Cappellucci L, Ghazarian A, Collins WR, Vienberg SG, et al. Insulin resistance in brain alters dopamine turnover and causes behavioral disorders. *Proc Natl Acad Sci*. 2015;112:3463–8.
- Guiard BP, El Mansari M, Blier P. Prospect of a dopamine contribution in the next generation of antidepressant drugs: the triple reuptake inhibitors. *Curr Drug Targets*. 2009;10:1069–84.
- Labouèbe G, Liu S, Dias C, Zou H, Wong JCY, Karunakaran S, et al. Insulin induces long-term depression of VTA dopamine neurons via an endocannabinoid-mediated mechanism. *Nat Neurosci*. 2013;16:300–8.
- Könner AC, Hess S, Tovar S, Mesaros A, Sánchez-Lasheras C, Evers N, et al. Role for insulin signaling in catecholaminergic neurons in control of energy homeostasis. *Cell Metab*. 2011;13:720–8.
- Evans MC, Kumar NS, Inglis MA, Anderson GM. Leptin and insulin do not exert redundant control of metabolic or emotive function via dopamine neurons. *Horm Behav*. 2018;106:93–104.
- Yohn CN, Gergues MM, Samuels BA. The role of 5-HT receptors in depression. *Mol Brain*. 2017;10:28.
- Kiyasova V, Fernandez SP, Laine J, Stankovski L, Muzerelle A, Doly S, et al. A genetically defined morphologically and functionally unique subset of 5-HT neurons in the mouse raphe nuclei. *J Neurosci J Soc Neurosci*. 2011;31:2756–68.
- Hanson LR, Fine JM, Svitak AL, Faltsek KA. Intranasal administration of CNS therapeutics to awake mice. *J Vis Exp*. 2013;74:4440.



19. Dhuria SV, Hanson LR, Frey WH. Intranasal delivery to the central nervous system: mechanisms and experimental considerations. *J Pharm Sci.* 2010;99:1654–73.
20. Fan LW, Carter K, Bhatt A, Pang Y. Rapid transport of insulin to the brain following intranasal administration in rats. *Neural Regen Res.* 2019;14:1046–51.
21. Dellu-Hagedorn F, Fitoussi A, De Deurwaerdère P. Correlative analysis of dopaminergic and serotonergic metabolism across the brain to study monoaminergic function and interaction. *J Neurosci Methods.* 2017;280:54–63.
22. Puginier E, Bharatiya R, Chagraoui A, Manem J, Cho YH, Garret M, et al. Early neurochemical modifications of monoaminergic systems in the R6/1 mouse model of Huntington's disease. *Neurochem Int.* 2019;128:186–95.
23. Rainer Q, Nguyen HT, Quesseveur G, Gardier AM, David DJ, Guiard BP. Functional status of somatodendritic serotonin 1A autoreceptor after long-term treatment with fluoxetine in a mouse model of anxiety/depression based on repeated corticosterone administration. *Mol Pharm.* 2012;81:106–12.
24. Qesseveur G, Petit AC, Nguyen HT, Dahan L, Colle R, Rotenberg S, et al. Genetic dysfunction of serotonin 2A receptor hampers response to antidepressant drugs: A translational approach. *Neuropharmacology* 2016;105:142–53.
25. Guiard BP, Przybylski C, Guilloux JP, Seif I, Froger N, De Felipe C, et al. Blockade of substance P (neurokinin 1) receptors enhances extracellular serotonin when combined with a selective serotonin reuptake inhibitor: an in vivo microdialysis study in mice. *J Neurochem.* 2004;89:54–63.
26. Ferreira de Sá DS, Römer S, Brückner AH, Issler T, Hauck A, Michael T. Effects of intranasal insulin as an enhancer of fear extinction: a randomized, double-blind, placebo-controlled experimental study. *Neuropsychopharmacol Publ Am Coll Neuropsychopharmacol.* 2020;45:753–60.
27. Marks DR, Tucker K, Cavallin MA, Mast TG, Fadool DA. Awake intranasal insulin delivery modifies protein complexes and alters memory, anxiety, and olfactory behaviors. *J Neurosci.* 2009;29:6734–51.
28. Schmid V, Kullmann S, Gfrörer W, Hund V, Hallschmid M, Lipp HP, et al. Safety of intranasal human insulin: A review. *Diabetes Obes Metab.* 2018;20:1563–77.
29. Papazoglou I, Berthou F, Vicaire N, Rouch C, Markaki EM, Bailbe D, et al. Hypothalamic serotonin–insulin signaling cross-talk and alterations in a type 2 diabetic model. *Mol Cell Endocrinol.* 2012;350:136–44.
30. Portal B, Delcourte S, Rovera R, Lejards C, Bullich S, Malnou CE, et al. Genetic and pharmacological inactivation of astroglial connexin 43 differentially influences the acute response of antidepressant and anxiolytic drugs. *Acta Physiol Oxf Engl.* 2020;229:e13440.
31. MacKenzie RG, Trulsson ME. Effects of insulin and streptozotocin-induced diabetes on brain tryptophan and serotonin metabolism in rats. *J Neurochem.* 1978;30:205–11.
32. Orosco M, Nicolaidis S. Insulin and glucose-induced changes in feeding and medial hypothalamic monoamines revealed by microdialysis in rats. *Brain Res Bull.* 1994;33:289–97.
33. Martín-Cora FJ, Fornal CA, Metzler CW, Jacobs BL. Insulin-induced hypoglycemia decreases single-unit activity of serotonergic medullary raphe neurons in freely moving cats: relationship to sympathetic and motor output: Medullary 5-HT neuronal responses to glucoregulatory challenges. *Eur J Neurosci.* 2002;16:722–34.
34. Chaput Y, de Montigny C, Blier P. Effects of a selective 5-HT reuptake blocker, citalopram, on the sensitivity of 5-HT autoreceptors: electrophysiological studies in the rat brain. *Naunyn Schmiedebergs Arch Pharm.* 1986;333:342–8.
35. Czachura JF, Rasmussen K. Effects of acute and chronic administration of fluoxetine on the activity of serotonergic neurons in the dorsal raphe nucleus of the rat. *Naunyn Schmiedebergs Arch Pharm.* 2000;362:266–75.
36. Bosker FJ, Klompmakers A, Westenberg HGM. Postsynaptic 5-HT1A receptors mediate 5-hydroxytryptamine release in the amygdala through a feedback to the caudal linear raphe. *Eur J Pharm.* 1997;333:147–57.
37. Martín-Ruiz R, Ugedo L. Electrophysiological evidence for postsynaptic 5-HT(1A) receptor control of dorsal raphe 5-HT neurones. *Neuropharmacology* 2001;41:72–8.
38. Hajós M, Richards CD, Székely AD, Sharp T. An electrophysiological and neuroanatomical study of the medial prefrontal cortical projection to the midbrain raphe nuclei in the rat. *Neuroscience* 1998;87:95–108.
39. Craven R, Grahame-Smith D, Newberry N. WAY-100635 and GR127935: effects on 5-hydroxytryptamine-containing neurones. *Eur J Pharm.* 1994;271:R1–3.
40. Fletcher A, Forster EA, Bill DJ, Brown G, Cliffe IA, Hartley JE, et al. Electrophysiological, biochemical, neurohormonal and behavioural studies with WAY-100635, a potent, selective and silent 5-HT1A receptor antagonist. *Behav Brain Res.* 1996;73:337–53.
41. Johnson DA, Gartside SE, Ingram CD. 5-HT1A receptor-mediated autoinhibition does not function at physiological firing rates: evidence from in vitro electrophysiological studies in the rat dorsal raphe nucleus. *Neuropharmacology* 2002;43:959–65.
42. Deryabina IB, Andrianov VV, Muranova LN, Bogodvid TK, Gainutdinov KL. Effects of tryptophan hydroxylase blockade by P-Chlorophenylalanine on contextual memory reconsolidation after training of different intensity. *Int J Mol Sci.* 2020;21:2087.
43. Johnson PL, Molosh A, Fitz SD, Arendt D, Deehan GA, Federici LM, et al. Pharmacological depletion of serotonin in the basolateral amygdala complex reduces anxiety and disrupts fear conditioning. *Pharm Biochem Behav.* 2015;138:174–9.
44. Engin E, Smith KS, Gao Y, Nagy D, Foster RA, Tsvetkov E, et al. Modulation of anxiety and fear via distinct intrahippocampal circuits. *eLife* 2016;5:e14120.
45. Wagle M, Zarei M, Lovett-Barron M, Poston KT, Xu J, Ramey V, et al. Brain-wide perception of the emotional valence of light is regulated by distinct hypothalamic neurons. *Mol Psychiatry.* 2022;1–17. Online ahead of print.
46. Insel T, Cuthbert B, Garvey M, Heinssen R, Pine DS, Quinn K, et al. Research domain criteria (RDoC): toward a new classification framework for research on mental disorders. *Am J Psychiatry.* 2010;167:748–51.
47. Sharma S, Fulton S. Diet-induced obesity promotes depressive-like behaviour that is associated with neural adaptations in brain reward circuitry. *Int J Obes.* 2013;37:382.
48. Liu Z, Patil IY, Jiang T, Sancheti H, Walsh JP, Stiles BL, et al. High-fat diet induces hepatic insulin resistance and impairment of synaptic plasticity. *PloS One.* 2015;10:e0128274.
49. Kothari V, Luo Y, Tornabene T, O'Neill AM, Greene MW, Geetha T, et al. High-fat diet induces brain insulin resistance and cognitive impairment in mice. *Biochim Biophys Acta Mol Basis Dis.* 2017;1863:499–508.
50. Trivedi MH, Rush AJ, Wisniewski SR, Nierenberg AA, Warden D, Ritz L, et al. Evaluation of outcomes with citalopram for depression using measurement-based care in STAR\*D: Implications for clinical practice. *Am J Psychiatry.* 2006;163:28–40.
51. Blier P, Ward H. Toward optimal treatments for major depression. *CNS Spectr.* 2002;7:148–50. 153–4
52. Poggini S, Golia MT, Alboni S, Milior G, Sciarria LP, Viglione A, et al. Combined fluoxetine and metformin treatment potentiates antidepressant efficacy increasing IGF2 expression in the dorsal hippocampus. *Neural Plast.* 2019;2019:1–12.

## ACKNOWLEDGEMENTS

XF and HM thank Région Nouvelle-Aquitaine and INRAE for their support. XF has been supported by the Société Française du Diabète and the Fondation Universit  de Bordeaux. Authors are thankful to the Fondation pour la Recherche M dicale (FRM, SL) and for the RRI Food4BrainHealth (HM, SL, XF). We thank INSERM (SJ, DC), ANR-17-CE14-0007 BABrain (to DC), and ANR-18-CE14-0029 MitObesity (to DC) for their support. AK has been supported by the Deutsche Forschungsgemeinschaft grant project and by grants from the German Ministry of Education and Research (BMBF grant 031B0569) and the State of Brandenburg (DZD grant 82DZD00302). Authors are grateful to Pr. Vanessa H. Routh (Rutgers University, NJ, USA) and Pr. Thierry Alquier (University of Montreal, Canada) for their insightful comments on the manuscript.

## AUTHOR CONTRIBUTIONS

HM, and SB designed and performed experiments. MM, MC, MDM, VS, SJ, JB, MS, and SC performed experiments. FC, AK, DC, PDD, LP, and SL edited the manuscript. BG and XF designed the project and wrote the manuscript.

## COMPETING INTERESTS

The authors declare no competing interests.

## ADDITIONAL INFORMATION

**Supplementary information** The online version contains supplementary material available at <https://doi.org/10.1038/s41380-022-01812-3>.











**Correspondence** and requests for materials should be addressed to Xavier Fioramonti.

**Reprints and permission information** is available at <http://www.nature.com/reprints>

**Publisher's note** Springer Nature remains neutral with regard to jurisdictional claims in published maps and institutional affiliations.

Springer Nature or its licensor holds exclusive rights to this article under a publishing agreement with the author(s) or other rightsholder(s); author self-archiving of the accepted manuscript version of this article is solely governed by the terms of such publishing agreement and applicable law.

# Essential omega-3 fatty acids tune microglial phagocytosis of synaptic elements in the mouse developing brain

C. Madore<sup>1,2,14</sup>, Q. Leyrolle<sup>1,3,14</sup>, L. Morel<sup>1,14</sup>, M. Rossitto<sup>1,14</sup>, A. D. Greenhalgh<sup>1</sup>, J. C. Delpéch<sup>1</sup>, M. Martinat <sup>1</sup>, C. Bosch-Bouju<sup>1</sup>, J. Bourel<sup>1</sup>, B. Rani <sup>4</sup>, C. Lacabanne<sup>1</sup>, A. Thomazeau <sup>1</sup>, K. E. Hopperton<sup>5</sup>, S. Beccari <sup>6</sup>, A. Sere<sup>1</sup>, A. Aubert<sup>1</sup>, V. De Smedt-Peyrusse<sup>1</sup>, C. Lecours<sup>7</sup>, K. Bisht<sup>7</sup>, L. Fourgeaud<sup>8</sup>, S. Gregoire<sup>9</sup>, L. Bretillon <sup>9</sup>, N. Acar<sup>9</sup>, N. J. Grant<sup>10</sup>, J. Badaut <sup>11</sup>, P. Gressens<sup>3,12</sup>, A. Sierra <sup>6</sup>, O. Butovsky <sup>2,13</sup>, M. E. Tremblay <sup>7</sup>, R. P. Bazinet<sup>5</sup>, C. Joffre<sup>1</sup>, A. Nadjar <sup>1✉</sup> & S. Layé<sup>1✉</sup>

Omega-3 fatty acids (n-3 PUFAs) are essential for the functional maturation of the brain. Westernization of dietary habits in both developed and developing countries is accompanied by a progressive reduction in dietary intake of n-3 PUFAs. Low maternal intake of n-3 PUFAs has been linked to neurodevelopmental diseases in Humans. However, the n-3 PUFAs deficiency-mediated mechanisms affecting the development of the central nervous system are poorly understood. Active microglial engulfment of synapses regulates brain development. Impaired synaptic pruning is associated with several neurodevelopmental disorders. Here, we identify a molecular mechanism for detrimental effects of low maternal n-3 PUFA intake on hippocampal development in mice. Our results show that maternal dietary n-3 PUFA deficiency increases microglia-mediated phagocytosis of synaptic elements in the rodent developing hippocampus, partly through the activation of 12/15-lipoxygenase (LOX)/12-HETE signaling, altering neuronal morphology and affecting cognitive performance of the offspring. These findings provide a mechanistic insight into neurodevelopmental defects caused by maternal n-3 PUFAs dietary deficiency.

<sup>1</sup>Univ. Bordeaux, INRAE, Bordeaux INP, NutriNeuro, UMR 1286, F-33000 Bordeaux, France. <sup>2</sup>Ann Romney Center for Neurologic Diseases, Department of Neurology, Brigham and Women's Hospital, Harvard Medical School, Boston, MA, USA. <sup>3</sup>NeuroDiderot, Inserm, Université de Paris Diderot, F-75019 Paris, France. <sup>4</sup>Department of Health Sciences, University of Florence, Florence, Italy. <sup>5</sup>Department of Nutritional Sciences, University of Toronto, Toronto, ON M5S 3E2, Canada. <sup>6</sup>Achucarro Basque Center for Neuroscience, University of the Basque Country and Ikerbasque Foundation, 48940 Leioa, Spain. <sup>7</sup>Neurosciences Axis, CRCHU de Québec-Université Laval, Québec City, QC, Canada. <sup>8</sup>Molecular Neurobiology Laboratory, The Salk Institute for Biological Studies, La Jolla, CA 92037, USA. <sup>9</sup>Centre des Sciences du Goût et de l'Alimentation, AgroSup Dijon, CNRS, INRAE, Univ. Bourgogne Franche-Comté, F-21000 Dijon, France. <sup>10</sup>CNRS UPR3212, Institut des Neurosciences Cellulaires et Intégratives, Strasbourg, France. <sup>11</sup>CNRS UMR5287, University of Bordeaux, Bordeaux, France. <sup>12</sup>Centre for the Developing Brain, Department of Division of Imaging Sciences and Biomedical Engineering, King's College London, King's Health Partners, St. Thomas' Hospital, London SE1 7EH, UK. <sup>13</sup>Evergrande Center for Immunologic Diseases, Brigham and Women's Hospital, Harvard Medical School, Boston, MA, USA. <sup>14</sup>These authors contributed equally: C. Madore, Q. Leyrolle, L. Morel, M. Rossitto. ✉email: [agnes.nadjar@u-bordeaux.fr](mailto:agnes.nadjar@u-bordeaux.fr); [sophie.laye@inrae.fr](mailto:sophie.laye@inrae.fr)

Lipids are one of the main constituents of the central nervous system (CNS). Among these, arachidonic acid (AA, 20:4n-6) and docosahexaenoic acid (DHA, 22:6n-3) are the principal forms of the long chain (LC) polyunsaturated fatty acids, omega-6 and omega-3 (referred to as n-6 or n-3 PUFAs) of the grey matter. These two LC PUFAs are found predominantly in the form of phospholipids and constitute the building blocks of brain cell membranes<sup>1</sup>. AA and DHA are either biosynthesized from their respective dietary precursors, linoleic acid (LA, 18:2n-6), and  $\alpha$ -linolenic acid (ALA, 18:3n-3), or directly sourced from the diet (mainly meat and dairy products for AA, fatty fish for DHA)<sup>2</sup>. In addition, AA and DHA are crucial for cell signaling through a variety of bioactive mediators. These mediators include oxylipins derived from cyclooxygenases (COX), lipoxygenases (LOX), and cytochrome P450 (CYP) pathways<sup>1</sup> that are involved in the regulation of inflammation and phagocytic activity of immune cells<sup>3–6</sup>. An overall increase in the dietary LA/ALA ratio and a reduction in LC n-3 PUFA intake, as found in the Western diet, leads to reduced DHA and increased AA levels in the brain<sup>7</sup>.

DHA is essential for the functional maturation of brain structures<sup>8</sup>. Low n-3 PUFA consumption globally has raised concerns about its potential detrimental effects on the neurodevelopment of human infants<sup>9</sup> and the incidence of neurodevelopmental diseases, such as Autism Spectrum Disorder (ASD) and schizophrenia<sup>10</sup>.

To understand the mechanisms by which n-3/n-6 PUFA imbalance affects CNS development, we investigated the impact of maternal dietary n-3 PUFA deficiency on offspring's microglia, the resident immune cells involved in CNS development and homeostasis<sup>11</sup>. Microglia are efficient phagocytes of synaptic material and apoptotic cells, which are key processes in the developing brain<sup>12</sup>. Specifically, once neuronal circuits are established, microglia contribute to the refinement of synaptic connections by engulfing synaptic elements in early post-natal life, in a fractalkine- and complement cascade-dependent manner<sup>13–15</sup>. This refinement is important for behavioral adaptation to the environment<sup>16</sup>.

We have previously reported that a maternal dietary n-3 PUFA deficiency alters the microglial phenotype and reduces their motility in the developing hippocampus<sup>17</sup>. Therefore, we investigated the effect of maternal (i.e. gestation and lactation) n-3 PUFA deficiency on microglial function and its consequences on hippocampal development. Using multidisciplinary approaches, we reveal that maternal exposure to an n-3 PUFA deficient diet impairs offspring's microglial homeostatic signature and phagocytic activity, underpinning excessive synaptic pruning and subsequent behavioral abnormalities. N-3 PUFA deficiency drives excessive microglial phagocytosis of synaptic elements through the oxylipin 12/15-LOX/12-HETE pathway and is a key mechanism contributing to microglia-mediated synaptic remodeling in the developing brain. These results highlight the impact of bioactive fatty acid mediators on brain development and identify imbalanced nutrition as a potent environmental risk factor for neurodevelopmental disorders.

## Results

**Maternal dietary n-3 PUFA deficiency alters the morphology of hippocampal neurons and hippocampal-mediated spatial working memory.** The hippocampus plays an essential role in learning and memory, with the neurons of the CA1 region required for spatial working memory. Therefore, we assessed the effects of maternal dietary n-3 PUFA deficiency on neuronal morphology in the offspring hippocampus CA1 using Golgi-Cox staining at post-natal day (P)21. Dendritic spine density of Golgi-stained CA1 pyramidal neurons was significantly decreased in n-3 deficient mice

compared to n-3 sufficient mice (Fig. 1a, b). This was associated with a decrease in the length of dendrites, whereas the complexity of dendritic arborization was unchanged (Fig. 1a, b). Western blot analyses on whole hippocampi showed a significant decrease in the expression of the post-synaptic scaffold proteins PSD-95 and Cofilin, but not of SAP102, in n-3 deficient vs. n-3 sufficient mice (Fig. 1c, d). AMPA and NMDA subunit expression levels were unaffected (Supplementary Fig. 1A, B). In the Y-maze task, a hippocampus-dependent test assessing spatial working memory, P21 n-3 deficient mice were unable to discriminate between the novel and familiar arms of the maze, unlike the n-3 sufficient mice (Fig. 1e). These data show that maternal n-3 PUFA deficiency disrupts early-life (P21) spine density, neuronal morphology and alters spatial working memory.

## Maternal dietary n-3 PUFA deficiency increases microglia-mediated synaptic loss.

As microglia phagocytose pre- and post-synaptic elements to shape neural networks<sup>13,14</sup>, we used electron microscopy (EM) to analyze, at high spatial resolution, microglia–synapse interactions in the hippocampal CA1 region of n-3 deficient vs. n-3 sufficient mice (Fig. 2a, b). At P21, i.e. at the peak of hippocampal synaptic pruning<sup>18</sup>, we found significantly more contacts between Iba1-positive microglial processes and the synaptic cleft and more dendritic spine inclusions within those processes in n-3 deficient mice (Fig. 2b). Microglial processes from n-3 deficient mice contained more inclusions within endosomes such as spines and other cellular elements, along with a reduced accumulation of debris in the extracellular space, thus suggesting an increase in phagocytic activity<sup>16</sup> (Fig. 2a, b). This was not due to changes in microglial process size, as diet did not affect process morphology (Supplementary Fig. 2A). In addition, confocal imaging and 3D reconstruction of microglia showed that PSD95-immunoreactive puncta within Iba1-positive microglia were more abundant in the hippocampus of n-3 deficient mice, corroborating the EM data (Fig. 2c, d). To provide further support to this increase in microglial phagocytosis, we stimulated *ex vivo* hippocampal microglia from n-3 deficient vs. n-3 sufficient P21 mice with pHrodo *E. coli* bioparticles. The pHrodo dye-labelled *E. coli* becomes fluorescent upon entering acidic phagosomes, enabling the assessment of phagocytic activity of microglia. The results revealed that the percentage of phagocytic microglia is significantly higher in n-3 deficient mice across the time points studied (Fig. 2e, f and Supplementary Fig. 2B). Increased microglial phagocytosis in the hippocampus was not a compensation to a decrease in microglial density, as there were no differences in microglial density assessed by stereological counting in the different hippocampal sub-regions, including the CA1 (Supplementary Fig. 2C, D).

Enhanced microglial phagocytic activity was also not linked to an increase in cell death, as the volume of the hippocampus, number of neurons and astrocytes, number of apoptotic cells and expression of pro-apoptotic protein Bax and anti-apoptotic protein Bcl-2 were not different between diets (Supplementary Fig. 3A–F). Furthermore, it is unlikely that n-3 PUFA deficiency-induced increase in phagocytosis resulted from brain infiltration of peripherally-derived macrophages. This is consistent with the observation that maternal n-3 PUFA deficiency did not modulate the number of CD11b-high/CD45-high cells within the whole brain (Supplementary Fig. 3G) and that the blood-brain barrier was intact in both diet groups as revealed by the expression of Claudin-5 and GFAP as well as IgG extravasation (Supplementary Fig. 3H–M).

**Maternal dietary n-3 PUFA deficiency dysregulates microglial homeostasis.** During brain development, microglia display a unique transcriptomic signature that supports their physiological

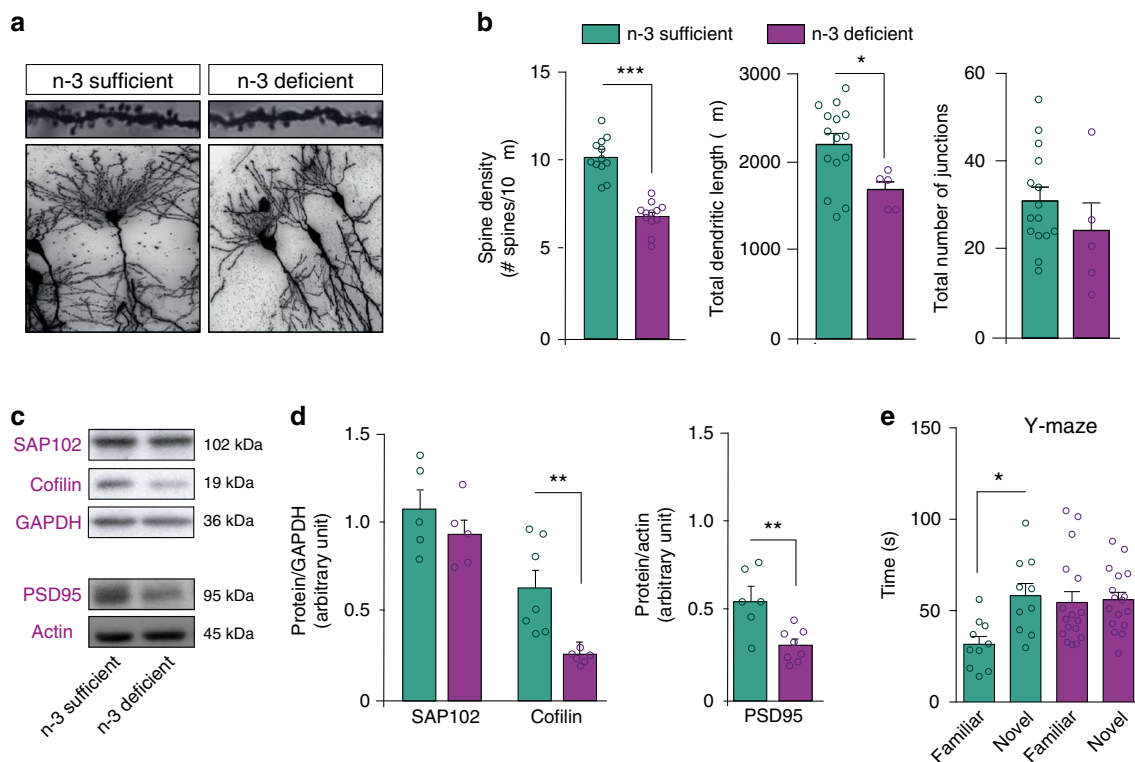
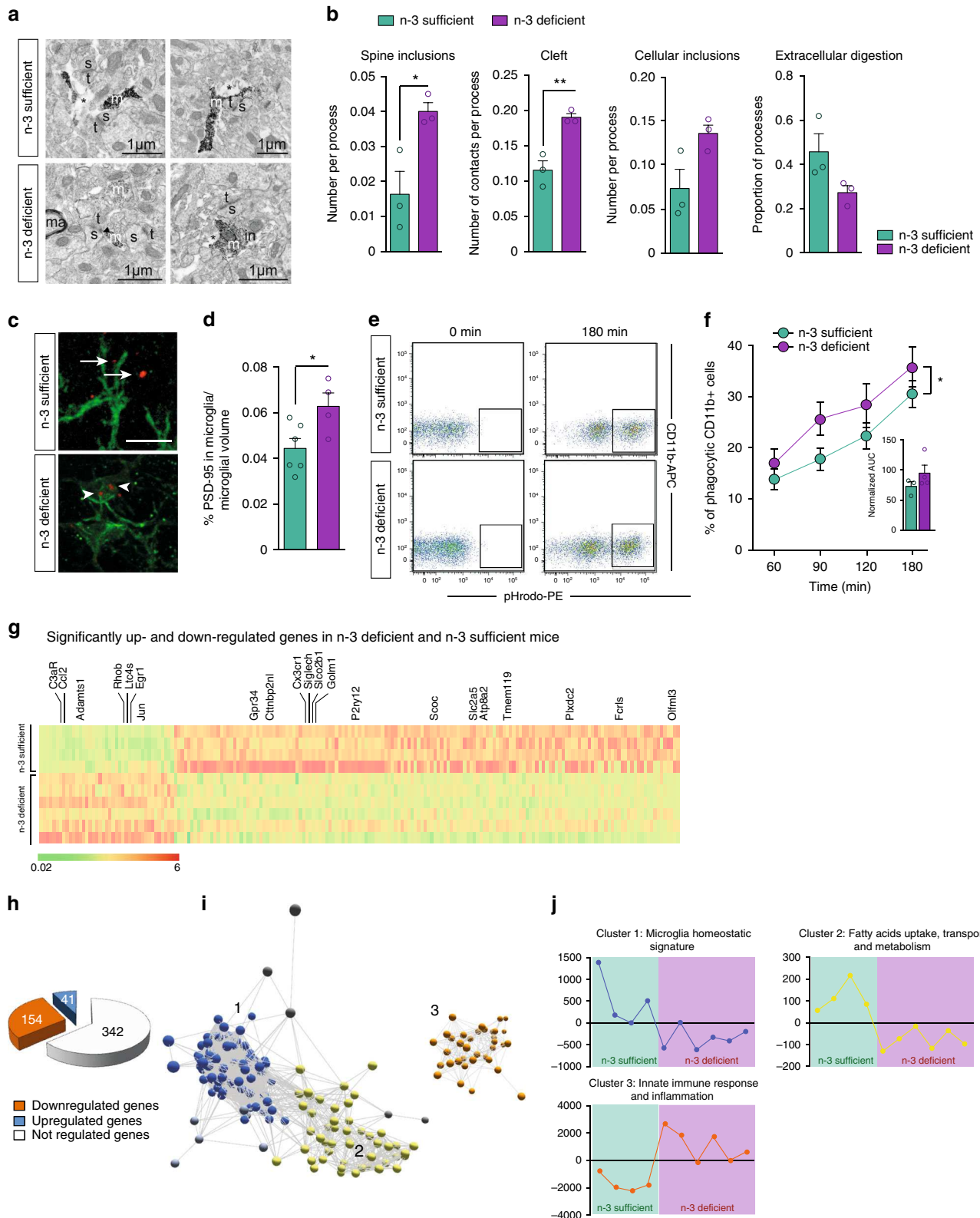


**Fig. 1** Maternal n-3 PUFA deficiency alters neuronal morphology and function. **a** Representative images of tertiary apical dendrites (upper panel) and dendritic arborization (lower panel) of hippocampal CA1 pyramidal neurons from n-3 sufficient and n-3 deficient mice at P21 (Golgi staining). **b** Quantification of spine density, total dendritic length and total number of junctions in n-3 deficient and n-3 sufficient animals. For spine counting,  $n = 12$  CA1 pyramidal neurons of the hippocampus, 15–45 segments per animal, 3 mice per group. Means  $\pm$  SEM. Two-tailed unpaired Student's  $t$ -test,  $t = 6.396$ ,  $***p < 0.0001$ . For dendritic arborization and total dendritic length,  $n = 5$  neurons from 3 mice for n-3 deficient mice and  $n = 15$  neurons from 4 mice for n-3 sufficient mice. Two-tailed unpaired Student's  $t$ -test; Dendritic length,  $t = 2.501$ ,  $*p = 0.0223$ ; number of junctions:  $t = 1.118$ ,  $p = 0.28$ . **c** Representative western blots. **d** Expression of scaffolding proteins in n-3 deficient mice relative to n-3 sufficient mice. Means  $\pm$  SEM;  $n = 5$ –8 mice per group. Two-tailed unpaired Student's  $t$ -test,  $t = 0.9986$ ,  $p = 0.35$ , SAP102;  $t = 3.572$ ,  $**p = 0.0044$ , cofilin;  $t = 3.529$ ,  $**p = 0.0042$ , PSD95. **e** Time spent in novel vs familiar arm in the Y maze task. Means  $\pm$  SEM;  $n = 10$ –17 mice per group. Two-way ANOVA followed by Bonferroni post hoc test: diet effect,  $F(1,50) = 5.47$ ,  $p = 0.071$ ; arm effect,  $F(1,50) = 10.08$ ,  $p = 0.015$ ; interaction,  $F(1,50) = 8.08$ ,  $p = 0.029$ ; familiar vs novel arm for n-3 diet mice:  $*p < 0.05$ . Source data are provided as a Source data file.

functions, including in synaptic refinement<sup>19</sup>. Therefore, we investigated whether and how n-3 PUFA deficiency modulates the homeostatic molecular signature of microglia isolated from n-3 deficient vs. n-3 sufficient mouse brains. Using a Nanostring-based mRNA chip containing 550 microglia-enriched genes<sup>20</sup>, 154 of these genes were found to be significantly down-regulated and 41 genes up-regulated in microglia from n-3 deficient mice whole brains (Fig. 2g, j and Table 1). Among the 40 genes reported to be unique to homeostatic microglia by<sup>20</sup>, 20 were significantly dysregulated, indicating that maternal n-3 PUFA deficiency alters homeostatic functions of microglia (Fig. 2g). We next sought to define the diet-specific microglial phenotype by assessing patterns of gene co-expression using unbiased network analysis software, Miru<sup>21</sup>. The utility of identifying gene expression patterns and transcriptional networks underpinning common functional pathways in microglia has been previously described<sup>22</sup>. Using a Markov clustering algorithm to non-subjectively subdivide our data into discrete sets of co-expressed genes, we found three major clusters of genes that were differentially regulated in n-3 deficient mice (Fig. 2i, j). The mean expression profiles of these three clusters showed that clusters 1 (microglial homeostatic signature) and 2 (fatty acid uptake, transport and metabolism) contained genes whose expression was relatively lower in the n-3 deficient group as compared to n-3 sufficient group. In contrast, cluster 3 (innate immune response and inflammation) contained genes with relatively greater

expression in n-3 deficient mice (Fig. 2j). These results show that an n-3 PUFA deficient diet dysregulates microglial homeostasis and increases microglial immune and inflammatory pathways during development.

**Fatty acid changes in microglia, not in synaptic elements, exacerbate phagocytosis after maternal dietary n-3 PUFA deficiency.** N-3 PUFA deficient diets cause fatty acid alterations in whole brain tissue<sup>23</sup>, yet it is unclear to what extent individual cell types or cell compartments incorporate these changes. To assess this, we profiled the fatty acid composition of microglia and synaptosomes isolated from n-3 sufficient and n-3 deficient mice (Fig. 3a, b). We observed that maternal n-3 PUFA deficiency significantly altered the fatty acid profile of both microglia and synaptosomes, with an increase in n-6 fatty acids and a decrease in n-3 fatty acids (Fig. 3a, b). In particular, DHA was decreased in microglia from n-3 deficient mice (Fig. 3a), while C22:5n-6 (or DPA n-6), the n-6-derived structural equivalent of DHA, was increased as a marker of n-3 PUFA deficiency<sup>24</sup> (Fig. 3a). Total AA was not significantly modified by the diet in microglia (Fig. 3a), unlike total AA levels in the whole hippocampus (Supplementary Fig. 4). In synaptosomes, total AA and DPA n-6 levels were significantly increased while total DHA level was significantly decreased and DPA n-6 inversely increased, as observed in microglia (Fig. 3b). In synaptosomes, more fatty acids



were significantly modified by the diet, such as the saturated fatty acid (SFA) stearic acid (18:0) and docosanoic acid (C22:0), and the monounsaturated fatty acids (MUFA) C16:1 n-7, C16:1 n-9, C18:1 n-9, and C20:1 n-9. Overall, our results show that n-3 and n-6 PUFA profiles of both microglia and synaptosomes are altered by low maternal n-3 PUFA intake, displaying similarities and discrepancies (Fig. 3a, b).

To directly evaluate the effect of microglial and synaptosome fatty acid alterations on microglial phagocytic activity, we developed an ex vivo assay in which we exposed freshly isolated n-3 sufficient or n-3 deficient microglia to n-3 sufficient or n-3 deficient pHrodo-labelled synaptosomes (Fig. 3c). We measured microglial phagocytic activity based on the level of cellular accumulation of pHrodo fluorescence (Fig. 3c). Phagocytosis was

**Fig. 2 Maternal n-3 PUFA deficiency increases microglial phagocytosis and gene expression profile.** **a, b** Representative images (**a**) and quantification (**b**) of EM data from the CA1 region of n-3 sufficient and n-3 deficient mice. s spine, m microglial processes, t terminals, \* extracellular debris, ma myelinated axons. Arrowheads point to synaptic clefts. Scale bars = 1  $\mu$ m. Two-tailed unpaired Student's *t*-test; *t* = 5.24, \*\**p* = 0.0063, cleft; *t* = 3.366, \**p* = 0.0282, spine inclusions; *t* = 2.601, *p* = 0.06, cellular inclusions; *t* = 2.119, *p* = 0.1015, extracellular digestion. **c** Three-dimensional reconstructions of PSD95-immunoreactivity (red) outside (arrowheads) or colocalized with (arrows) microglial cells (green). **d** Quantification of PSD95 and Iba1 immunoreactivity colocalization in the CA1 region of n-3 deficient and n-3 sufficient group. Means  $\pm$  SEM; *n* = 4–6 mice per group. Two-tailed unpaired Student's *t*-test; *t* = 2.583, \**p* = 0.032. **e** Representative bivariate dot plots of isolated microglial cells gated on CD11b<sup>+</sup>/CD45<sup>low</sup> expression from n-3 sufficient and n-3 deficient mice. **f** FACS analysis of phagocytic uptake of pHrodo-labeled *E. Coli* bioparticles by CD11b<sup>+</sup> microglial cells from both dietary groups after 180 min of incubation (expressed as the percent of cells that are CD11b<sup>+</sup> and PE positive). Means  $\pm$  SEM; *n* = 3–4 per condition. Two-way ANOVA; diet effect: *F*(1, 20) = 5.628, \**p* = 0.028; time effect, *F*(3,20) = 10.04, *p* = 0.0003; Interaction, *F*(3,20) = 0.1771, *p* = 0.91. The area under the curve is presented as an independent graph in **c**. Two-tailed unpaired Student's *t*-test, *t* = 1.289, *p* = 0.25. **g** Heatmap of significantly up or downregulated genes in each dietary group. Each lane represents one animal (*n* = 4 or 6 per group). The 20 homeostatic microglia unique genes that were significantly affected by the diet are labelled. **h** Number of microglial genes that are up-regulated, down-regulated or not regulated by the diet. **i** A transcript-to-transcript correlation network graph of transcripts significantly differentially expressed by diet groups was generated in Miru (Pearson correlation threshold *r*  $\geq$  0.85). Nodes represent transcripts (probe sets), and edges represent the degree of correlation in expression between them. The network graph was clustered using a Markov clustering algorithm, and transcripts were assigned a color according to cluster membership. **j** Mean expression profile of all transcripts within clusters 1, 2, and 3 where each point represents an animal and the average gene expression of all genes within that cluster for that animal. Source data are provided as a Source data file.

**Table 1 Composition of the diets (g/kg diet).**

Ingredient	Amount
Casein	180
Cornstarch	460
Sucrose	230
Cellulose	20
Fat <sup>a</sup>	50
Mineral mix <sup>b</sup>	50
Vitamin mix <sup>c</sup>	10

<sup>a</sup>For detailed composition, see Table 2.

<sup>b</sup>Composition (g/kg): sucrose, 110.7; CaCO<sub>3</sub>, 240; K<sub>2</sub>HPO<sub>4</sub>, 215; CaHPO<sub>4</sub>, 215; MgSO<sub>4</sub>·7H<sub>2</sub>O, 100; NaCl, 60; MgO, 40; FeSO<sub>4</sub>·7H<sub>2</sub>O, 8; ZnSO<sub>4</sub>·7H<sub>2</sub>O, 7; MnSO<sub>4</sub>·H<sub>2</sub>O, 2; CuSO<sub>4</sub>·5H<sub>2</sub>O, 1; Na<sub>2</sub>SiO<sub>3</sub>·3H<sub>2</sub>O, 0.5; AlK(SO<sub>4</sub>)<sub>2</sub>·12H<sub>2</sub>O, 0.2; K<sub>2</sub>CrO<sub>4</sub>, 0.15; NaF, 0.1; NiSO<sub>4</sub>·6H<sub>2</sub>O, 0.1; H<sub>2</sub>BO<sub>3</sub>, 0.1; CoSO<sub>4</sub>·7H<sub>2</sub>O, 0.05; KIO<sub>3</sub>, 0.04; (NH<sub>4</sub>)<sub>6</sub>Mo<sub>7</sub>O<sub>24</sub>·4H<sub>2</sub>O, 0.02; LiCl, 0.015; Na<sub>2</sub>SeO<sub>3</sub>, 0.015; NH<sub>4</sub>VO<sub>3</sub>, 0.01.

<sup>c</sup>Composition (g/kg): sucrose, 549.45; retinyl acetate, 1; cholecalciferol, 0.25; DL- $\alpha$ -tocopheryl acetate, 20; phylloquinone, 0.1; thiamin HCl, 1; riboflavin, 1; nicotinic acid, 5; calcium pantothenate, 2.5; pyridoxine HCl, 1; biotin, 1; folic acid, 0.2; cyanobalamin, 2.5; choline HCl, 200; DL-methionin, 200; p-aminobenzoic acid, 5; inositol, 10.

significantly increased in microglia from n-3 deficient mice, independent of the fatty acid profile of the synaptosome (Fig. 3c). These data show that both microglial and synaptosome fatty acid profiles are modified by maternal n-3 PUFA deficiency, but changes in microglial fatty acid composition drive the exacerbation of microglia-mediated synaptic loss.

### Maternal n-3 PUFA deficiency alters neuronal morphology and working spatial memory in a complement-dependent manner.

Recently, the classical complement cascade has been described as a key mediator of microglia synaptic refinement in the developing brain<sup>25</sup>. Moreover, our EM data revealed more spine inclusions within microglia and more contacts between these cells and the synaptic cleft (Fig. 2a, b). Thus, we explored the implication of the complement cascade in the exacerbation of microglia-mediated synaptic refinement observed in n-3 deficient mice.

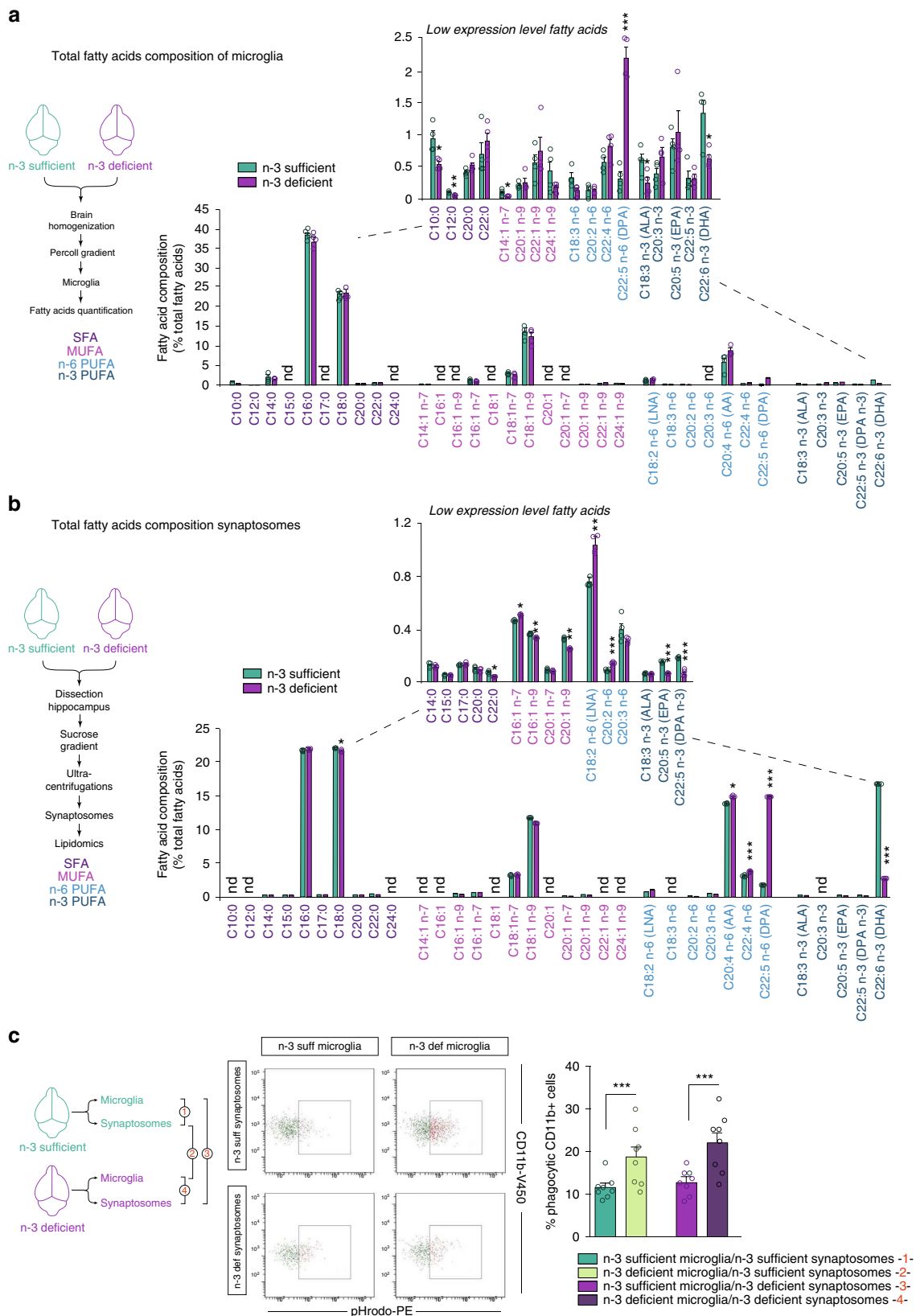
The complement system acts as a recognition mechanism by which C1q, the initiating protein of the cascade, tags synapses to be removed. C1q-tagging leads to the cleavage of C3 and subsequent deposition of C3a and C3b, which activates CD11b and C3aR respectively on microglia and triggers synaptic elimination by microglial phagocytosis<sup>25,26</sup>. C1q immunostaining was significantly increased in both the hippocampus CA1 and DG

in n-3 deficient mice (Fig. 4a). Protein expression levels of CD11b (a subunit of CR3) was slightly, yet significantly increased in the DG in n-3 deficient mice (Fig. 4b). CD11b gene expression was also enhanced in the whole hippocampus in these mice (Supplementary Fig. 5). Our analyses also revealed a robust increase of C3aR immunostaining in the whole hippocampus of n-3 deficient mice, corroborating microglia transcriptomic data (Figs. 4c and 2g and Table 1). The C3aR-positive cells were uniformly distributed throughout the hippocampus, including the CA1. Expression levels of *Cx3cr1*, *Cx3cl1* and *Tgfb*, all involved in microglia-mediated synaptic pruning<sup>13,27</sup>, were found to be increased in the whole hippocampus of n-3 deficient mice (Supplementary Fig. 5). Finally, we quantified the C3 protein on freshly extracted hippocampus synaptosomes from n-3 deficient and n-3 sufficient mice using an ELISA assay. We found higher amounts of C3 under n-3 PUFA deficiency (Fig. 4D). These findings indicate that low n-3 PUFA intake alters the developmental expression of complement cascade proteins both in microglia and at the synapse.

To test whether proper neuronal function could be restored by acting on the complement pathway in vivo, we antagonized CR3 activation in n-3 deficient mice. We first confirmed that a CR3 antagonist XVA-143, blocked n-6 PUFA (AA) induced increases in phagocytosis in vitro (Supplementary Fig. 6A–D). We then administered the CR3 antagonist, XVA-143<sup>28</sup> in vivo in the hippocampus four days before assessing the expression of the post-synaptic protein PSD95 at P21. Antagonizing CR3 prevented PSD-95 expression decrease in the hippocampus of n-3 deficient mice (Fig. 4e). Injection of XVA-143 also restored optimal memory abilities in n-3 deficient mice in the Y-maze task (Fig. 4f). These results show that complement activation increases microglia-mediated synaptic refinement when dietary n-3 PUFAs are low. Thus, a global increase in C3/CR3 interaction may account for the altered neuronal function observed in the hippocampus of n-3 deficient mice.

### Enhancement of microglia-mediated synaptic refinement by maternal PUFA deficiency is phosphatidyl serine recognition-independent.

Microglia possess a number of phagocytic receptors to eliminate neuronal elements, notably by binding to externalized phosphatidyl serine (PS) at the surface of neurons<sup>29</sup>. Since PUFAs are the main constituents of membrane phospholipids, we assessed whether microglial phagocytic activity was enhanced through PS recognition (Supplementary Fig. 7). First, we showed that cell-surface PS, stained with



annexin-V, was unchanged between diets in the hippocampus (Supplementary Fig. 7A). We also quantified the expression levels of the microglial PS-binding protein milk fat globule EGF factor 8 (MFG-E8), which binds and activates a vitronectin receptor (VNR), TAM receptor tyrosine kinases (MER

and Axl), triggering receptor expressed on myeloid cells-2 (TREM2) and CD33<sup>29,30</sup>. Only MFG-E8 expression level was significantly increased by maternal n-3 PUFA dietary deficiency (Supplementary Fig. 7B–G). We administered a blocking peptide cRGD which inhibits the interaction between

**Fig. 3 Maternal dietary n-3 PUFA deficiency exacerbates microglial phagocytosis of synaptic elements by predominantly impacting microglia.** **a** Fatty acid composition of microglial cells sorted from n-3 sufficient and n-3 deficient mice. Means  $\pm$  SEM;  $n = 4$  mice per group. Insert: higher magnification of low expressed fatty acids. Two-tailed unpaired Student's  $t$ -test;  $t = 3.37$ ,  $*p = 0.015$ , C10:0;  $t = 4.852$ ,  $**p = 0.0028$ , C12:0;  $t = 2.473$ ,  $*p = 0.0482$ , C14:1 n-7;  $t = 9.646$ ,  $***p < 0.0001$ , DPA n-6;  $t = 2.558$ ,  $*p = 0.043$ , ALA;  $t = 2.972$ ,  $*p = 0.0249$ , DHA; nd not detected. **b** Fatty acid composition of synaptosomes sorted from n-3 sufficient and n-3 deficient mice. Means  $\pm$  SEM;  $n = 4$  mice per group. Insert: higher magnification of low expressed fatty acids. Two-tailed unpaired Student's  $t$ -test;  $t = 2.82$ ,  $*p = 0.047$ , C17:0;  $t = 3.05$ ,  $*p = 0.038$ , C18:0;  $t = 5.05$ ,  $**p = 0.0072$ , C18:1 n-9;  $t = 2.99$ ,  $*p = 0.04$ , C18:2 n-6;  $t = 26$ ,  $***p < 0.0001$ , C20:2 n-6;  $t = 3.57$ ,  $*p = 0.023$ , C22:4 n-6;  $t = 12.68$ ,  $***p = 0.0002$ , DPA n-6;  $t = 4.49$ ,  $*p = 0.011$ , C20:5 n-3;  $t = 7.12$ ,  $**p = 0.0021$ , DHA; nd not detected. **c** FACS analysis of phagocytic uptake of pHrodo-labeled synaptosomes (sorted from n-3 sufficient or n-3 deficient mice) by CD11b<sup>+</sup> microglial cells (sorted from n-3 sufficient or n-3 deficient mice). Analyses were performed 2 h post-synaptosomes application. On FACS plots: x-axis = (pHrodo intensity (PE intensity), y-axis = SSC. Means  $\pm$  SEM;  $n = 8$  per condition. Two-way ANOVA: microglial fatty acid status effect,  $F(1,28) = 19.77$ ,  $***p = 0.0001$ ; synaptosomes fatty acid status effect,  $F(1,28) = 1.63$ ,  $p = 0.2123$ ; interaction,  $F(1,28) = 0.2826$ ,  $p = 0.599$ . Source data are provided as a Source data file.

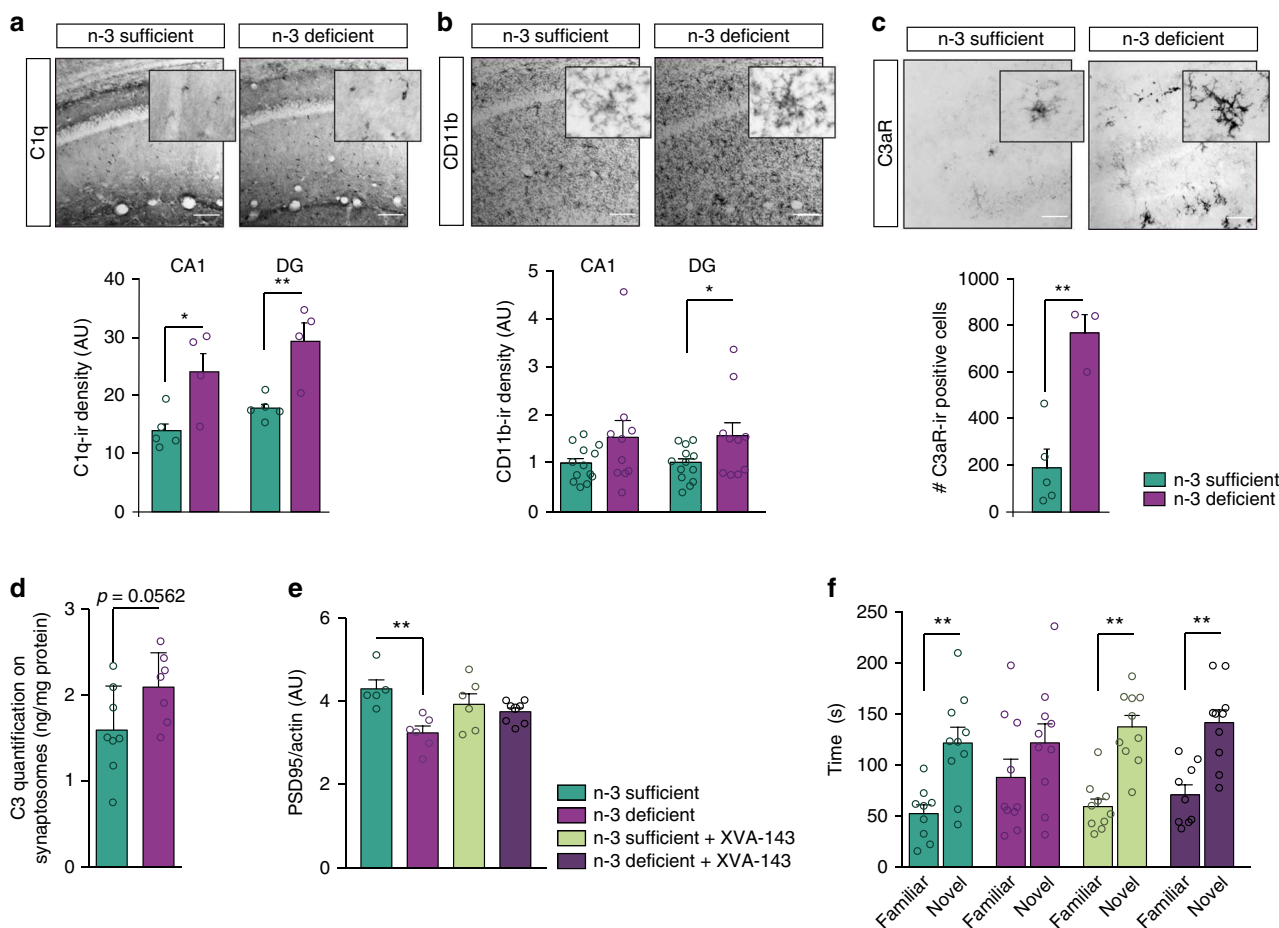


**Fig. 4 Maternal n-3 PUFA deficiency exacerbates microglia-mediated shaping of neuronal networks in a complement-dependent manner.** **a-c** Representative images and quantification of C1q, CD11b, and C3aR immunostaining in coronal sections of n-3 deficient and n-3 sufficient mice hippocampus. Scale bar = 100  $\mu$ m. Means  $\pm$  SEM;  $n = 3-13$  mice per group. Two-tailed unpaired Student's  $t$ -test;  $t = 1.553$ ,  $p = 0.135$ , CD11b CA1;  $t = 2.114$ ,  $*p = 0.466$ , CD11b DG;  $t = 0.5495$ ,  $*p = 0.0223$ , C1q CA1;  $t = 3.938$ ,  $**p = 0.0056$ , C1q DG;  $t = 4.91$ ,  $**p = 0.0027$ , C3aR, total hippocampus. **d** Protein quantification (ELISA) reveals that synaptosomes from n-3 deficient mice express more C3 than n-3 sufficient animals. Means  $\pm$  SEM;  $n = 7-8$  mice per group; Two-tailed unpaired Student's  $t$ -test;  $t = 2.097$ ,  $p = 0.0562$ . **e** Quantification of PSD95 protein expression in n-3 sufficient vs n-3 deficient mice treated with XVA-143 or its vehicle. Means  $\pm$  SEM;  $n = 5-8$ . Two-way ANOVA followed by Bonferroni post hoc test: diet effect,  $F(1,21) = 11.89$ ,  $p = 0.0024$ ; treatment effect,  $F(1,21) = 0.1436$ ,  $p = 0.708$ ; interaction,  $F(1,21) = 5.977$ ,  $p = 0.0234$ ; n-3 sufficient vs n-3 deficient,  $**p < 0.01$ . **f** Time spent in novel vs familiar arm in the Y maze task in n-3 sufficient vs n-3 deficient mice treated with XVA-143 or its vehicle. Means  $\pm$  SEM;  $n = 9-10$  mice per group. Paired  $t$ -test: n-3 sufficient group,  $**p = 0.0019$ ; n-3 deficient group,  $p = 0.357$ ; n-3 sufficient + XVA-143 group,  $**p = 0.0013$ ; n-3 deficient + XVA-143 group,  $**p = 0.0099$ . Source data are provided as a Source data file.

MFG-E8 and VNR vs a scrambled control (sc-cRGD), to n-3 deficient vs n-3 sufficient mice animals and quantified the expression of the post-synaptic protein PSD-95. Blocking MFG-E8 action on microglia did not prevent the reduction in

PSD-95 expression in the hippocampus of n-3 deficient mice (Supplementary Fig. 7H). These results indicate that modulation of the microglial phagocytic capacity by early-life PUFAs is PS recognition-independent.



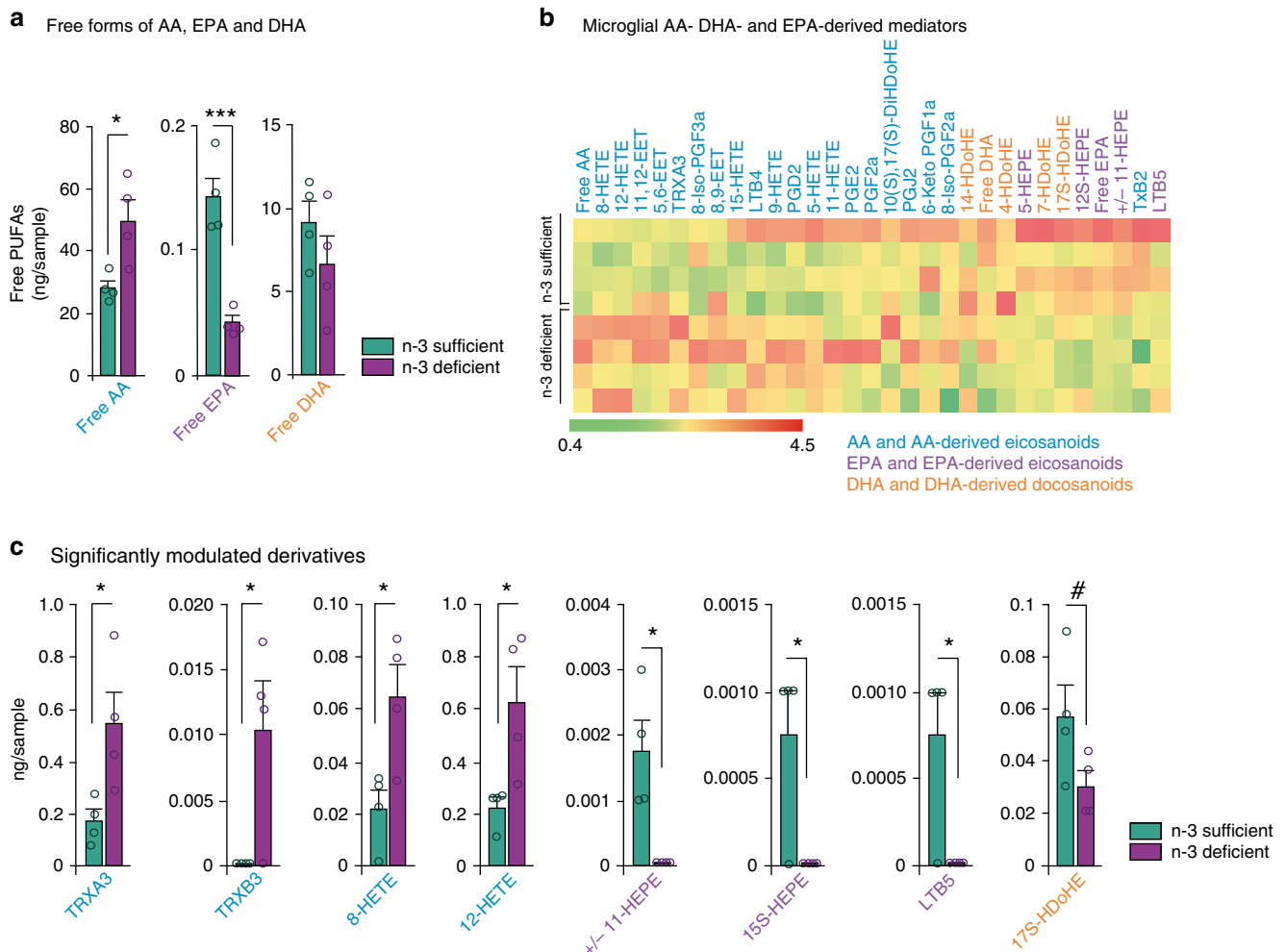
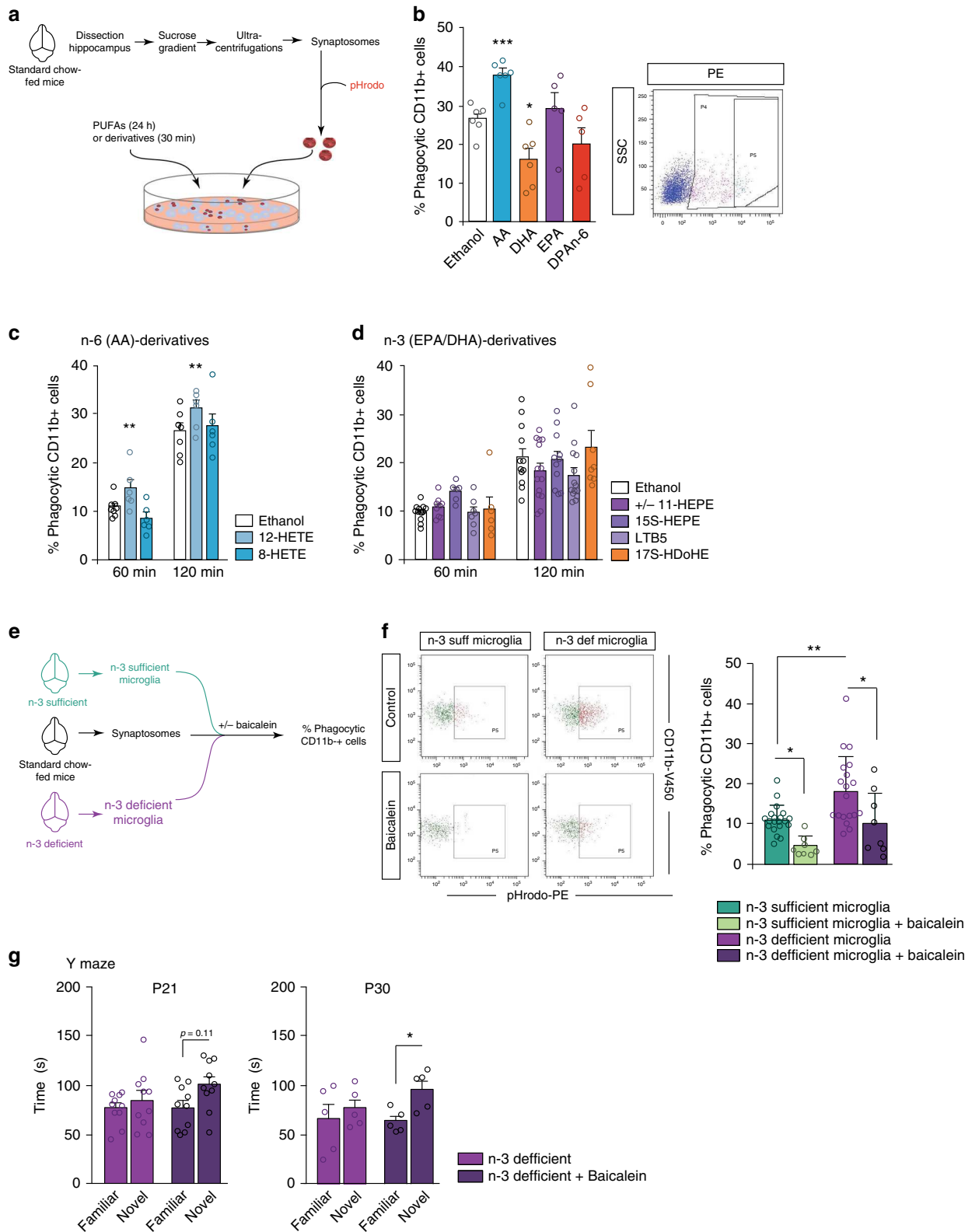


**Fig. 5** Maternal n-3 PUFA deficiency alters fatty acid profile in microglia. **a** Quantification of free (unesterified) forms of AA, EPA, and DHA levels in microglia. Means  $\pm$  SEM;  $n = 4$  mice per group. Two-tailed unpaired Student's  $t$ -test;  $t = 3$ ,  $*p = 0.024$ , free AA;  $t = 6.12$ ,  $***p = 0.0009$ , free EPA;  $t = 1.149$ ,  $p = 0.2942$ , free DHA. **b** Heat map of all AA-, EPA-, and DHA-derived intracellular mediators expressed by microglia. **c** AA- EPA- and DHA-derived mediators that are significantly modulated by early-life n-3 PUFA deficient diet. Means  $\pm$  SEM;  $n = 4$  mice per group. Two-tailed unpaired Student's  $t$ -test;  $t = 2.693$ ,  $*p = 0.0359$ , TRXA3;  $t = 2.867$ ,  $*p = 0.0286$ , TRXB3;  $t = 3.028$ ,  $*p = 0.0231$ , 8-HETE;  $t = 2.886$ ,  $*p = 0.0278$ , 12-HETE;  $t = 3.656$ ,  $*p = 0.0106$ , +/-11-HEPE;  $t = 3$ ,  $*p = 0.024$ , 15S-HEPE;  $t = 3$ ,  $*p = 0.024$ , LTB5;  $t = 1.975$ ,  $p = 0.0957$ , 17S-HDoHE. Source data are provided as a Source data file.

**Maternal n-3 PUFA deficiency alters microglial PUFA metabolism in the offspring.** Our data suggest that n-3 PUFA deficiency specifically drives exacerbated microglial phagocytosis (Fig. 3). We, therefore, assessed the mechanisms by which microglial PUFA metabolism was driving their phagocytic activity. Microglia isolated from n-3 deficient mice had higher levels of free, unesterified, AA, and lower quantities of free EPA, as determined by high-performance liquid chromatography with tandem mass spectrometry (LC-MS-MS) (Fig. 5a). When unesterified from the cellular membrane, free PUFAs are rapidly converted to bioactive mediators (or oxylipins) with potential effects on microglial cells<sup>1,31,32</sup>. Interestingly, microglia from n-3 deficient animals presented greater levels of AA-derived bioactive mediators and lower amounts of DHA- and EPA-derived mediators (Fig. 5b). Four AA-derived oxylipins were significantly increased by maternal n-3 PUFA deficiency: trioxilins TRXA3 and TRXB3, 8-HETE, 12-HETE, while three EPA-derived species were significantly decreased: +/-11-HEPE, 15S-HEPE, and LTB5. The DHA-derived 17SHDoHE was also reduced ( $p = 0.0957$ ) (Fig. 5c). Hence, we show the post-natal microglia oxylipin signature in the

context of low maternal n-3 PUFA intake and how it is modified by the dietary content in n-3 PUFAs.

**Activation of a 12/15-LOX/12-HETE signaling pathway increases microglial phagocytic activity under maternal n-3 PUFA deficiency.** Using pharmacological approaches, we continued to dissect the molecular mechanisms linking n-3 PUFA deficiency and microglial phagocytosis of dendritic spines by assessing the oxylipins identified above. We first tested the potential role of AA, EPA, and DHA free forms and their bioactive metabolites identified in Fig. 5 (except trioxilins TRXA3 and TRXB3, which are not commercially available) on microglial phagocytosis in vitro. We applied synaptosomes that were conjugated to a pH-sensitive dye (pHrodo), as a surrogate of synaptic refinement processes on cultured microglia (Fig. 6a). Twenty-four-hour application of AA on microglial cells significantly increased their phagocytic activity towards synaptosomes (Fig. 6b). These observations confirmed our data showing that AA increased phagocytosis of latex beads by primary microglial cells (Supplementary Fig. 6A, B). Conversely, incubation with



DHA significantly decreased phagocytosis (Fig. 6b), while EPA and DPA n-6 had no effect when compared to controls (Fig. 6b). Then, we applied PUFA bioactive mediators for 30 min before applying pHrodo synaptosomes and studied the kinetics of phagocytosis over the following 120 min. We show that the AA-derived 12-HETE significantly increased microglia phagocytosis of synaptosomes while 8-HETE had no effect (Fig. 6c). None of

the EPA- and DHA-derived bioactive mediators affected primary microglia phagocytic activity (Fig. 6d). For all conditions, the percentage of phagocytic cells is significantly higher at 120 min post-treatment (Fig. 6c, d).

AA is metabolized into 12-HETE via the 12/15-LOX enzyme and its activity is blocked by baicalein, which reduces 12-HETE production<sup>33,34</sup>. We then tested whether inhibiting 12/15-LOX

**Fig. 6 Maternal n-3 PUFA deficiency exacerbates microglial phagocytic activity towards synapses by activating the 12/15-LOX/12-HETE signaling pathway.** **a** Experimental setup. **b** FACS analysis of phagocytic uptake of pHrodo-labeled synaptosomes by CD11b<sup>+</sup> microglial cells in primary culture exposed to PUFAs. Means  $\pm$  SEM;  $n = 5-6$  per condition. Two-tailed unpaired Student's *t*-test; \*\*\* $p = 0.0005$ , AA; \* $p = 0.0118$ , DHA;  $p = 0.55$ , EPA;  $p = 0.153$ , DPA n-6. **c, d** FACS analysis of phagocytic uptake of pHrodo-labeled synaptosomes by CD11b<sup>+</sup> microglial cells in primary culture exposed to n-6 AA-derived (**c**) or n-3 EPA- and DHA-derived (**d**) lipids. Means  $\pm$  SEM;  $n = 6-14$  per condition. AA derivatives: Two-way ANOVA: time effect,  $F(1,33) = 171.8$ , \*\*\* $p < 0.0001$ ; treatment effect,  $F(2,33) = 5.538$ , \*\* $p = 0.0084$ ; interaction,  $F(2,33) = 0.686$ ,  $p = 0.51$ . EPA and DHA derivatives: Two-way ANOVA: time effect,  $F(1,64) = 57.25$ , \*\*\* $p < 0.0001$ ; treatment effect,  $F(2,64) = 1.462$ ,  $p = 0.239$ ; interaction,  $F(2,64) = 1.904$ ,  $p = 0.157$ . **e** Experimental setup. **f** FACS analysis of phagocytic uptake of pHrodo-labeled synaptosomes by freshly sorted n-3 deficient and n-3 sufficient CD11b<sup>+</sup> microglial cells, exposed to baicalein or its solvent. Analyses were performed 2 h post-synaptosomes application. Two-way ANOVA: microglia fatty acid status effect,  $F(1,51) = 12.6$ , \*\*\* $p = 0.0008$ ; treatment effect,  $F(1,51) = 16.06$ ,  $p = 0.0002$ ; interaction,  $F(1,51) = 0.1912$ ,  $p = 0.6638$ . **g** Time spent in novel vs familiar arm in the Y maze task in P21 and P30 n-3 deficient mice treated with baicalein or its vehicle. Means  $\pm$  SEM;  $n = 10$  (P21) or 5 (P30) mice per group. Paired *t*-test: P21: n-3 deficient group,  $p = 0.5$ ; n-3 deficient + baicalein group,  $p = 0.11$ ; P30: n-3 deficient group,  $p = 0.57$ ; n-3 deficient + baicalein group, \* $p = 0.029$ . Source data are provided as a Source data file.

activity was able to restore normal phagocytic activity in n-3 PUFA deficient microglial cells. We used an ex vivo assay in which we exposed freshly sorted n-3 sufficient or n-3 deficient microglia to pHrodo synaptosomes with or without the 12/15-LOX inhibitor baicalein (Fig. 6e). We show that baicalein significantly reduced synaptosome phagocytosis by n-3 deficient microglia (Fig. 6f). Injection of baicalein persistently restored optimal memory abilities in n-3 deficient mice in the Y-maze task (Fig. 6g), without altering anxiety level (Supplementary Fig. 8A). Baicalein had no effect in n-3 sufficient mice (Supplementary Fig. 8B). These results confirm that the 12/15-LOX/12-HETE pathway is active in n-3 deficient microglia to increase their phagocytic activity towards synaptic elements. In addition, baicalein improves memory deficits in n-3 PUFA deficient mice.

**The 12/15-LOX/12-HETE signaling pathway acts upstream of the complement cascade.** We finally assessed the relationship between 12/15-LOX/12-HETE signaling pathway and the expression of genes from the complement cascade under n-3 PUFA deficiency. We exposed freshly sorted n-3 sufficient or n-3 deficient microglia to the 12/15-LOX inhibitor baicalein or its vehicle and quantified the expression level of CD11b and C3aR mRNAs, 2 h later (Fig. 7a). We show that *c3ar* gene expression was increased in n-3 deficient microglia while the expression of *cd11b* was not significantly modulated by the diet. This is in line with our immunostaining experiments in which CD11b was moderately increased under n-3 PUFA deficiency, only in the DG, while C3aR was robustly increased in the whole hippocampus (Fig. 4b). Baicalein significantly reduced C3aR expression in n-3 deficient microglia, while it had no effect on CD11b (Fig. 7b, c). These results suggest that in non-stimulated n-3 deficient microglia, the 12/15-LOX/12-HETE signaling pathway is implicated in the maintenance of a high C3aR tone, while the activity of CD11b (as shown in Fig. 4e, f) is likely to depend on other mechanisms.

Once activated, the expression of most immune receptors is dampened as part of a global regulatory mechanism<sup>35</sup>. We thus examined the relationship between the 12/15-LOX/12-HETE signaling pathway and the complement cascade in the condition of stimulation of microglia with synaptosomes. We exposed freshly sorted cells to pHrodo synaptosomes in the presence of baicalein or its vehicle and quantified the expression level of *cd11b* and *c3ar* (Fig. 7d). The expression level of CD11b was significantly increased by baicalein in n-3 deficient microglia, whereas inhibiting the 12/15 LOX enzyme did not affect C3aR mRNA expression (Fig. 7e, f). This suggests that once microglia phagocytose synaptosomes, the 12/15-LOX/12-HETE signaling pathway inhibits CD11b expression while allowing phagocytosis of neuronal material (Fig. 6f). We finally studied the expression levels of BLT2 and GPR31, the two principal 12-HETE receptors

(Supplementary Fig. 9A). While GPR31 was expressed by the cells, BLT2 gene expression was almost not measurable in microglia in vitro. Hence, we then focused on the expression of GPR31 in vivo, on freshly isolated n-3 deficient and n-3 sufficient microglia, treated with vehicle or baicalein, in the absence or presence of synaptosomes. We could not find any significant modification of GPR31 mRNA expression level in any of the conditions tested (Supplementary Fig. 9B, C). Further experiments are needed to decipher whether 12 HETE effect on phagocytosis is mediated by GPR31.

Altogether, our data suggest that the 12/15-LOX/12-HETE signaling pathway modulates microglial phagocytosis under n-3 PUFA deficiency, partly by regulating the expression of the C3a and C3b receptors.

## Discussion

The phagocytic activity of microglia during development is crucial in shaping neuronal networks, and dysfunction of this activity contributes to neurodevelopmental disorders<sup>15</sup>. Here we show that low maternal n-3 PUFA intake-induced modification of microglia fatty acid composition is a potent driver leading to exacerbation of spine phagocytosis in the offspring. This process is complement-dependent, a mechanism that has been repeatedly reported to be the molecular bridge of microglia phagocytosis of spines<sup>14,27,36</sup>. Our data also reveal that n-3 PUFA deficiency alters the shaping of hippocampal neurons and spatial working memory in pups. Finally, we identified a previously unknown function of 12-HETE, a LOX metabolite of AA, in the regulation of microglial phagocytosis. This microglial 12/15-LOX/12-HETE pathway is also likely to contribute to alterations in spine density and connectivity observed in synaptopathies and neurodevelopmental disorders<sup>37</sup>. Considering that n-3 PUFAs also determine the offspring's microglia homeostatic molecular signature and fatty acid profile, our study suggests that the maternal nutritional environment is essential for proper microglial activity in the developing brain. These findings further support the importance of dietary n-3 PUFAs in the neurodevelopmental trajectory, pointing to their role in microglia-spine interactions.

Previous clinical and epidemiological studies revealed a relationship between dietary n-3 PUFA content, brain development, and the prevalence of neurodevelopmental disorders<sup>38</sup>. The n-3 PUFA index, which reports the level of n-3 PUFAs (EPA + DHA) in erythrocytes and that is used as a biomarker for cardiovascular diseases, is now also considered a biomarker for several neurodevelopmental diseases such as ASD<sup>39</sup>, attention deficit hyperactivity disorder (ADHD)<sup>40</sup> and schizophrenia<sup>41</sup>. The lack of n-3 PUFA during pregnancy and early post-natal life could participate in the etiology of these diseases. Since these essential fatty acids are necessary for healthy brain development, low dietary supply or impairment of their metabolism is suggested to be

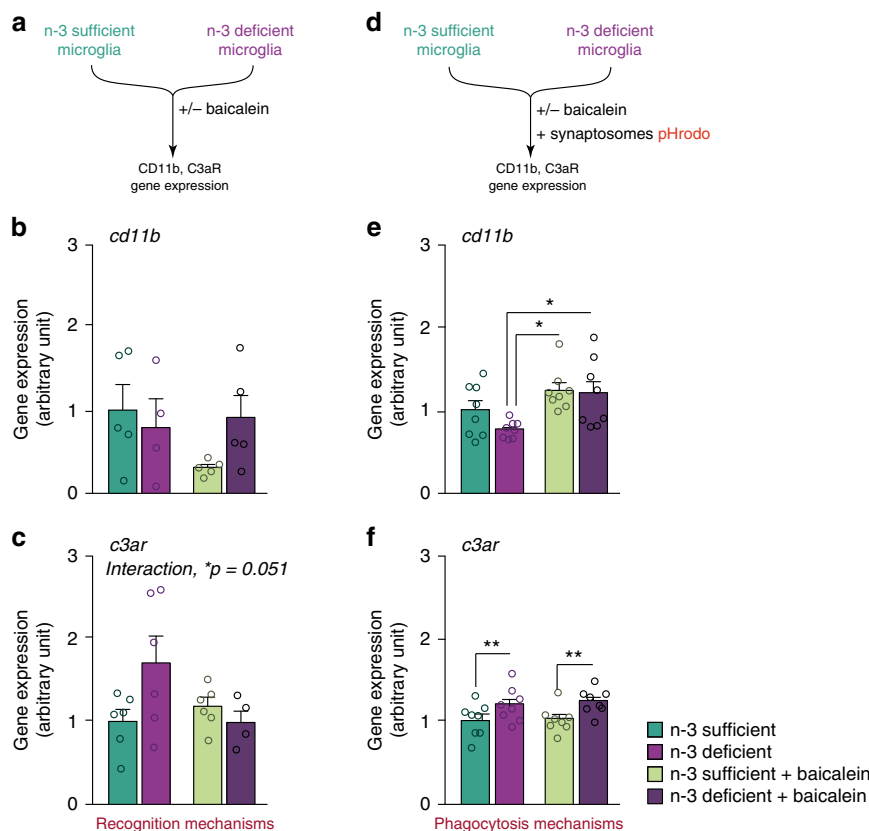


**Fig. 7** The 12/15-LOX/12-HETE signaling pathway controls gene expression of the complement pathway. **a** Experimental setup. **b, c** Quantification of *cd11b* and *c3ar* mRNA expression in freshly sorted n-3 deficient and n-3 sufficient microglia, treated with baicalein or its vehicle. Means  $\pm$  SEM;  $n = 4$ –6 per group. Two-way ANOVA: *cd11b*: diet effect,  $F(1,15) = 0.57$ ,  $p = 0.46$ ; treatment effect,  $F(1,15) = 1.37$ ,  $p = 0.26$ ; interaction,  $F(1,15) = 2.48$ ,  $p = 0.14$ ; *c3ar*: diet effect,  $F(1,18) = 1.36$ ,  $p = 0.26$ ; treatment effect,  $F(1,18) = 1.52$ ,  $p = 0.23$ ; interaction,  $F(1,18) = 4.36$ ,  $*p = 0.051$ . **d** Experimental setup. **e, f** Quantification of *cd11b* and *c3ar* mRNA expression in freshly sorted n-3 deficient and n-3 sufficient microglia, exposed to synaptosomes for 2 h and treated with baicalein or its vehicle. Means  $\pm$  SEM;  $n = 8$  per group. Two-way ANOVA followed by Bonferroni post hoc test: *cd11b*: diet effect,  $F(1,28) = 0.16$ ,  $p = 0.19$ ; treatment effect,  $F(1,28) = 0.92$ ,  $**p = 0.0028$ ; interaction,  $F(1,28) = 0.072$ ,  $p = 0.36$ ; n-3 deficient + vehicle vs n-3 deficient + baicalein,  $*p = 0.014$ ; n-3 deficient + vehicle vs n-3 deficient + baicalein,  $*p = 0.029$ ; *c3ar*: diet effect,  $F(1,28) = 0.35$ ,  $**p = 0.0034$ ; treatment effect,  $F(1,28) = 0.0043$ ,  $p = 0.72$ ; interaction,  $F(1,28) = 0.0019$ ,  $p = 0.81$ . Source data are provided as a Source data file.

involved in the etiology of several psychiatric diseases, including neurodevelopmental disorders<sup>1</sup>. Indeed, decreased DHA levels have been reported in several brain regions of patients diagnosed with such disorders<sup>42</sup>. Low n-3 PUFA index is also associated with reduced brain size or connectivity, as well as to reduced cortical functional connectivity during an attentional task<sup>43</sup>. Of special interest is the limbic system as the hippocampus activity in Humans has been reported to be altered in subjects with low n-3 PUFA status and consistently altered in animal models of n-3 PUFA deficiency<sup>44,45</sup>. Hippocampal alterations are reported in several neurodevelopmental disorders, including ASD, that could account for a neurodevelopmental compensatory mechanism to preserve cognitive domains<sup>46</sup>. Preterm infants display lower brain DHA concentrations as compared to term infants on the same ALA fortified diet<sup>47</sup>. Very low birth weight is a high-risk factor for both n-3 PUFA deficiency and neurodevelopmental disorders/cognitive impairments<sup>48</sup>. These children display improved recognition memory at 6-months of age when supplemented with LC n-3 PUFA<sup>49</sup> while the brain structure was unchanged later in life (8 years old)<sup>50</sup>. Whether the pathophysiology of cognitive alterations, a common feature of neurodevelopmental disorders, may be linked to inadequate bioavailability of n-3 PUFA in the hippocampus is of high interest in part due to the increasing knowledge on the role of nutrition in psychiatric disorders and in particular ASD, ADHD and schizophrenia.

Overall, this knowledge suggests the use of specific dietary supplementation with n-3 PUFA as an environmental modifiable factor. Indeed, dietary supplementation or increase intake of food rich in n-3 PUFA could counteract the adverse effect of low n-3 PUFA intake. Our data shed light on an oxylipin-dependent mechanism underlying these clinical observations.

Our data are in line with previous studies showing that the 12/15-LOX/12-HETE pathway is altered in several pathological conditions in macrophage/microglia and especially in inflammatory conditions. Human macrophages incubated with 12-HETE showed induced gene expression after lipopolysaccharide (LPS) application<sup>51</sup>. Indeed, 12-HETE in macrophages was shown to activate extracellular signal-regulated kinase 1/2 (ERK1/2) and nuclear factor kappa-light-chain-enhancer of activated B cells (NF $\kappa$ B) via GPR31<sup>52</sup>. In humans, it was found that the expression of 12/15-LOX was increased in CD68-positive activated microglia<sup>53</sup>. Moreover, 12/15-LOX and Gpr31 receptor gene expression is increased in microglia along with aging<sup>22</sup> and in DAM/MGnD<sup>54</sup>. Here, no change in *gpr31* gene expression was observed in microglia treated with 12-HETE in vitro or exposed to a n-3 PUFA deficient diet in vivo. However, downstream analysis of GPR31 activation after 12-HETE application or expression should be tested.

Previous studies conducted in rodents and primates showed that early-life dietary n-3 PUFA deficiency impairs learning and

memory in adulthood<sup>55,56</sup>. Here, we show that perinatal n-3 PUFA deficiency-induced memory deficits occur as soon as weaning. This corroborates observations in humans that prenatal and cord blood n-3 PUFA levels are positively correlated with later-life cognitive abilities in infants<sup>57</sup>. In our study, cognitive alterations were associated with a decrease in dendritic length, whereas the complexity of dendritic arborization was unchanged, supporting the previous reports<sup>58</sup>. A significant decrease of post-synaptic scaffold proteins PSD-95 and Cofilin in the hippocampus of n-3 deficient mice at weaning, suggests an early alteration of synaptic plasticity (Madore et al., 2014). This is in line with a previous study showing that loss of PSD-95 is inversely correlated with DHA dietary supply in a mouse model of Alzheimer's disease<sup>59</sup> suggesting that PSD-95 expression depends on DHA levels in a broader context than just neurodevelopment. N-3 PUFA deficiency-mediated dendritic arborization alteration has been associated with functional defects of neuronal networks in the adult hippocampus and cortex<sup>60,61</sup> and atypical whole-brain functional community structure<sup>62</sup>, a surrogate of cognitive deficits<sup>63</sup>. Finally, our finding of abnormal hippocampal neuronal spine density in n-3 PUFA deficient mice at weaning corroborates data previously found<sup>58</sup>.

Lipid changes driving metabolic alterations in microglia and their impact on phagocytosis in the developing brain are understudied. Knowing that microglia are now regarded as key controllers of synaptic architecture due to their phagocytic activity<sup>13,14,16</sup>, we show that specific fatty acid mediators drive microglia phagocytic activity toward synapses. Our findings of a decrease in n-3 PUFAs and increase in n-6 PUFAs in the whole hippocampus, microglia, and synaptosomes of n-3 deficient mice is consistent with a large body of literature<sup>24,64</sup>. It is well established that in response to n-3 PUFA deficiency, brain DHA decreases and is replaced by DPA n-6<sup>24,64</sup>. We have previously shown that microglia from n-3 deficient dams have higher levels of DPA n-6<sup>65</sup>. While the mechanisms of this replacement at the level of the microglia are not clear, in whole brain, the uptake of DPA n-6 from the plasma free pool increases dramatically<sup>66</sup>.

Oxylipins are involved in the regulation of inflammation and phagocytic activity of immune cells<sup>1</sup>. Their production is largely influenced by n-3 PUFA dietary supply, including in the brain<sup>32</sup>. Using LC-MS-MS, we examined their role in microglial phagocytic activity during development. We show that n-3 PUFA deficient microglia have a unique oxylipin profile, linked to altered free forms of AA, EPA, and DHA. AA and its LOX-derived mediator 12-HETE promote microglia phagocytosis of synaptosomes. While there is no data available in the literature on microglia, this pathway has already been described as essential in the clearance of apoptotic cells by peripheral macrophages during inflammation<sup>67</sup>. Therefore, we predict that the 12/15-LOX enzyme is involved in AA-mediated increase in microglia phagocytosis in vitro. Conversely, DHA (but not its LOX derivative, 17S-HDOHE) decreased microglial phagocytosis in vitro. Previous work reported that DHA inhibits microglia phagocytic activity of myelin both in vivo and in vitro<sup>68</sup> and normalizes inflammation-induced microglial phagocytic activity of spines in vitro<sup>69</sup>. Hence, it is likely that DHA dampens microglial phagocytosis via a repressive effect on synaptosome phagocytosis and/or a decrease in pro-inflammatory factors expression, in accordance with previous work showing its anti-inflammatory activity both in vitro and in vivo<sup>70–73</sup>. Additionally, recent work found that DHA decreases microglia phagocytic activity of myelin debris in the spinal cord after injury through mir-124<sup>68</sup>, a non-coding nucleotide involved in synaptic plasticity. In macrophages, mir-124 has been shown to regulate actin-related protein 2/3 (ARP2/3), which is involved in the formation of the phagocytic cup<sup>74</sup>. This is in line with results showing that DHA reduced LPS-

induced phagocytic activity of microglia, through a reduction of filopodia<sup>75</sup>.

12-HETE is produced by the 12/15 LOX enzyme and conversion of AA by 12-HETE is enhanced in n-3 PUFA deficient microglia in the context of brain injury, autoimmune and neurodegenerative diseases<sup>53</sup>. 12/15 LOX is also expressed in the developing human brain by CD68-positive microglia and oligodendrocytes<sup>53</sup>. We show that blocking activity of 12/15-LOX by baicalein<sup>34</sup> attenuates the excessive n-3 PUFA deficient microglia phagocytic activity, which is coherent with the role of this enzyme in mediating phagocytic activity of apoptotic cells by macrophages<sup>67</sup>. Hence, we describe a cell-specific fatty acid profile of microglia and provide a comprehensive description of the processes involved in n-3 PUFA deficiency-induced microglial alterations, including 12/15-LOX/12-HETE pathway as the molecular trigger enhancing the phagocytic activity of microglia toward spines.

We further deciphered the relationship between the 12/15-LOX/12-HETE pathway and the complement system. Our data reveal that the phagocytic capacity of microglia is increased only when the cells are n-3 deficient, even though C3 is overexpressed on n-3 deficient synaptosomes. These data suggest that both opsonization of synapses and recognition of C3 by its microglial receptors are required to trigger phagocytosis. This confirms a plethora of reports on the complement-dependent phagocytosis in the immune system. It is already well described that there is little to no ingestion of opsonized elements without phagocyte activation<sup>76</sup>. Conversely, CR3-mediated phagocytosis is dependent on receptor conformational changes, lateral diffusion, and clustering, processes that require activating stimuli<sup>77</sup>). Hence, binding of C3 to the complement receptors can be considered as the recognition (“find-me”) mechanism of spines to be removed by microglia, as previously shown in other experimental contexts<sup>14,78</sup>, while activation of the 12/15-LOX/12-HETE pathway is the triggering signal for phagocytosis by microglia. This is coherent with the observation that the complement cascade classically interacts with inflammatory pathways to control the activity of phagocytes<sup>79</sup>.

Interestingly, C3a, that binds to microglial C3aR, is usually considered as a chemoattractant signal, attracting immune cells including microglia toward the structures to be cleared, while C3b, that binds to CR3 (CD11b + CD18) opsonizes the target to be removed<sup>79</sup>. Our data show that the 12/15-LOX/12-HETE pathway controls the basal expression of C3aR in n-3 deficient microglia, suggesting that it may control the capacity of microglia to reach the target. However, the 12/15-LOX/12-HETE pathway does not regulate the gene expression of CD11b, which is in line with the observations that CD11b activation is more dependent on conformational changes and redistribution in the cellular membrane rather than on transcriptional regulation<sup>77</sup>. As for CD11b activity, our data suggest that the 12/15-LOX/12-HETE pathway is involved in the homeostatic down-regulation of CD11b expression once the opsonized elements have been recognized by microglia. Overall, our data suggest that the 12/15-LOX/12-HETE pathway is activated upstream of the complement cascade, controlling the gene expression level and activity of this latter. We also found that 12/15-LOX/12-HETE pathway modulates microglial phagocytic activity as baicalein reduces synaptosomes engulfment. More experiments should be conducted to decipher the interplay of 12/15-LOX/12-HETE and the complement pathways in the phagocytic activity of n-3 deficient microglia.

Deficits in microglia-mediated synaptic refinement lead to dysfunctional neuronal networks and behavioral abnormalities resembling some aspects of neurodevelopmental disorders<sup>15,80,81</sup>. Here, we show that n-3 PUFA deficient microglia display an

altered homeostatic molecular profile at weaning with features similar to neurodegenerative microglia, previously reported as more phagocytic<sup>54</sup>. We further identified the complement system, and not PS exposure, as the molecular mechanism driving spine phagocytic activity upon n-3 PUFA deficiency. This is consistent with previous work showing that in the hippocampus, PS-dependent and complement-independent trogocytosis of pre-synaptic elements remodels neuronal network during normal brain development<sup>82,83</sup> while complement-dependent phagocytosis of synapses is promoted in models of brain diseases presenting neuronal network abnormalities, including neurodevelopmental disorders<sup>13,14,38</sup>. Of note, neither PS recognition nor the complement cascade seem to be involved in synaptic refinement in n-3 sufficient mice. This suggests that (1) other mechanisms of microglia-mediated synaptic refinement are in place in the hippocampus of these animals or (2) microglia-mediated synaptic refinement is not prominent in the hippocampus of these animals. Microglia use a plethora of recognition mechanisms for phagocytosis of neuronal elements/dead bodies<sup>33,84</sup> but few studies have addressed the microglia-spine interaction in the developing hippocampus. On the other hand, several mechanisms, including microglia-independent processes such as neuronal macroautophagy or phagocytosis by astrocytes, control synaptic pruning in the developing brain, though the proportion of synaptic pruning relying on microglia in the developing hippocampus is not known<sup>85</sup>. Our data suggest that synaptic pruning mechanisms in the developing hippocampus of n-3 sufficient mice may favor microglia-independent processes.

Overall, our data also describe a role for the 12/15-LOX/12-HETE oxylipin pathway as a crucial metabolic signaling axis in the regulation of n-3 PUFA deficient microglia activity. We also delineate that maternal dietary n-3 PUFA deficiency drives microglia in the offspring into a complement-dependent phagocytic phenotype, aberrantly reducing synaptic elements, which drive hippocampal synaptic network dysfunction and spatial working memory deficit. Our findings not only support the necessity of adequate n-3 PUFA status during brain development<sup>86</sup>, but also reveal that maternal lipid nutrition, by modulating microglial fatty acid metabolism and sensing, can be an important determinant of neurodevelopmental synaptopathies such as ASD. Regarding the clinical implications, these data highlight the relevance of diagnosing DHA/EPA deficits in expectant mothers and in early-life. We provide knowledge on highly targetable cellular and molecular pathways linking maternal nutrition and neurodevelopmental disorders. Indeed, specific dietary strategies can enhance PUFA status in microglia<sup>65</sup>, being promising avenues for the prevention and treatment of neurodevelopmental disorders.

## Methods

Animal experiments were carried out according to the Quality Reference System of INRA and approved by the local ethical committee for care and use of animals (#APAFIS 4198 and 15533). Male and female CD1 mice 8-week old were purchased from Janvier Labs (Le Gesnest St Isle, France) and were SPF-housed in temperature and humidity-controlled cages on a 12 h light/dark cycle with food and water ad libitum. The use of CD1 mice, an outbred strain, implies intrinsic inter-individual differences which we consider as an asset, considering the translational perspective of our research.

**Diet.** After mating, CD1 females were single housed and randomly assigned to either a n-3 deficient or a n-3 sufficient diet, both containing 5% fat, in the form of sunflower oil (rich in LA, the “n-3 deficient diet”) or a mixture of different oils of which rapeseed oil (rich in ALA, the “n-3 sufficient diet”) throughout gestation and lactation<sup>20</sup> (Tables 2 and 3). The composition of the standard chow diet is closer to the n-3 deficient diet in terms of LA, total n-6 PUFA, total PUFAs, while it is more similar to the n-3 sufficient diet in terms of LA/ALA ratio and ALA. Hence, we used the n-3 sufficient diet as our control as it more consistently contains higher levels of n-3 PUFAs and lower levels of n-6 PUFAs than the n-3 deficient diet. The content of proteins, carbohydrates, and lipids varies as well (3.1% of lipids in the

**Table 2 Fatty acid composition of the diets (% wt of total fatty acids).**

Diets	Deficient	Sufficient	Standard chow (A04)
16:0	7.3	22.6	20.3
18:0	4.1	3.3	2.2
Other saturated FAs	1.6	1.8	1.8
Total saturated FAs	13.0	27.7	24.3
18:1n-9	28.1	57.9	19.3
18:1n-7	0.9	1.5	1.5
Other monounsaturated FAs	0.2	0.4	3.9
Total monounsaturated FAs	29.4	60.0	24.7
18:2n-6 (LA)	57.4	10.6	45.9
Other n-6 PUFAs	n.d.	n.d.	0.3
Total n-6 PUFAs	57.4	10.7	46.2
18:3n-3 (ALA)	0.2	1.6	3.3
20:5 n-3	n.d.	n.d.	0.6
22:5 n-3	n.d.	n.d.	0.1
22:6 n-3	n.d.	n.d.	0.8
Total n-3 PUFAs	0.2	1.6	4.8
Total PUFAs	57.6	12.3	51.0
LA/ALA	287	6.6	13.9

FAs fatty acids, PUFAs polyunsaturated fatty acids, LA linoleic acid, ALA  $\alpha$ -linolenic acid, n.d. not detected (under the limit for the detection by gas chromatography, <0.05%).

standard chow vs 5% in the n-3 sufficient diet). All experiments were performed on the offspring from n-3 deficient and n-3 sufficient dams at post-natal day (P) 21. Pups from different dams were used for each measurement to avoid any cage effect. Each mother had 2–3 litters and was put back on a standard diet for a minimum of one month between each litter.

**Drugs.** Cyclo(Arg-Gly-Asp-D-Phe-Val) (cRGD; Bachem, H-2574) and its control, scrambled, peptide c(RADfV) (or sc-cRGD; Bachem, H-4088) were dissolved in acetic acid (1N) and further diluted into aCSF to a final concentration of 1 mM. A volume of 1  $\mu$ l of cRGD or sc-cRGD was injected in the CA1 region of the hippocampus, bilaterally, at P14. Animals were euthanized at P21 and processed for Western blot analysis.

XVA-143 (kindly provided by Hoffmann-La Roche) was dissolved in aCSF at 5 mM. In all, 1  $\mu$ l was injected bilaterally in the CA1 region of the hippocampus at P17. Animals were used at P21 for behavioral and biochemical analyses. For primary microglial cell cultures, XVA-143 was applied 30 min before beads incubation at a final concentration of 1  $\mu$ M.

Baicalin (Sigma-Aldrich, #465119) was applied at a final concentration of 20  $\mu$ M in 0.2% DMSO for ex vivo experiments. For behavioral assessment, baicalin was injected intraperitoneally at a concentration of 20 mg/kg.

**Cortex fatty acid composition.** Fatty acid composition was studied in the cortex (not hippocampus) of animals as: (1) cortex and hippocampus fatty acid composition vary similarly under the diets used in this study; (2) to reduce the number of animals. Cortical fatty acids were extracted according to the method of Folch, fatty acids were transmethylated according to the method of Morrison and Smith and fatty acid methyl esters (FAMES) were analyzed on a FOCUS GC chromatograph (Thermo Electron Corporation) equipped with a split injector and a flame ionization detector.

**Microglia isolation and sorting.** Brains were homogenized in Hanks' Balanced Salt Solution (HBSS), pH 7.4 passing through a 70  $\mu$ m nylon cell strainer. Homogenates were centrifuged at 600 g for 6 min. Supernatants were removed and cell pellets were re-suspended in 70% isotonic Percoll (GE Healthcare, Aulnay sous Bois, France). Single cell suspensions were prepared and centrifuged over a 37%/70% discontinuous Percoll gradient (GE Healthcare) at 2000g for 20 min, mononuclear cells were isolated from the interface. For each brain extraction  $\sim 3 \times 10^5$  cells were isolated. Cells were washed and in order to sort resident microglia from recruited myeloid cells, we used a monoclonal antibody that recognizes FCRLS, which is expressed on microglia, but not on infiltrating myeloid cells (Butovsky et al.<sup>20</sup>). Isolated cells were stained with rat anti-FCRLS [clone 4G11, 3 mg ml<sup>-1</sup>, validated in Butovsky et al.<sup>20</sup>] and then followed by a secondary detection using an anti-rat IgG PE (Biolegend).

Cells were sorted using a FACS Aria 5-Blue 2-Violet 2-Red laser configuration (BD Biosciences).

**Table 3 List of all genes that are significantly modulated by maternal n-3 PUFA deficiency.**

Up-regulated genes	Ratio n-3 deficient/ n-3 sufficient				
Ccl3	50,2	Slco2b1	0,55	Ttr	0,35
Ccl4	18,9	Golm1	0,55	BMP6	0,35
Rasgef1b	9,5	A430107D22Rik	0,55	NOX1	0,34
Cd83	5,4	D830030K20Rik	0,54	Nav2	0,34
Atf3	5,3	Vat1l	0,54	Mmp12	0,34
Ccrl2	4,7	LOC100038847	0,54	Hist1h2ac	0,34
C3ar1	4,4	Ifi202b	0,54	Siglec1	0,33
Ccl2	4,1	Rgmb	0,54	Plxna1	0,32
Ppp1r15a	3,5	Ccr5	0,54	Fcrls	0,32
Nlrp3	3,0	ADAM17	0,54	Slco4a1	0,31
Apoe	3,0	Ppp1r9a	0,53	Cbr3	0,31
Rgs1	2,9	Rnf180	0,53	Slc46a1	0,31
Trim47	2,8	Fcgr1lla (CD16a)	0,53	Upk1b	0,29
Adamts1	2,8	P2ry12	0,53	Khdrbs3	0,29
Dab2	2,7	CD200R	0,52	Tnfrsf17	0,29
Klhl38	2,6	Gpr165	0,52	TREM1	0,28
1810011010Rik	2,6	Fgd2	0,52	Il7r	0,28
CEBPB	2,5	Trem2	0,51	Ak1	0,28
Myc	2,4	P4ha1	0,51	BMP7	0,28
Cd14	2,4	Gtf2h2	0,51	WNT5A	0,27
Fos	2,3	Zfp691	0,51	Kitl	0,24
Il1a	2,3	Tmem144	0,51	Chi3l1	0,22
Rgl1	2,2	Plxna4	0,51	Cfb	0,21
Fosb	2,2	Itgax	0,51	Arg1	0,20
Manba	2,2	Bend6	0,51	Olfml3	0,18
Npl	2,1	Csf3r	0,51	Gal3st4	0,17
cathepsin	2,0	SEMA3C	0,50		
Rhob	2,0	Bco2	0,50		
Ltc4s	2,0	MPO (myeloperoxidase)	0,50		
Egr1	2,0	ENSMUSG00000079376	0,50		
Fth1	1,9	Erf	0,50		
Abca1	1,9	Tmc7	0,49		
Jun	1,9	4933406P04Rik	0,49		
Socs3	1,8	Mmp2	0,48		
Junb	1,7	Tmem204	0,48		
SREBP1	1,7	Tlr3	0,48		
Tlr2	1,6	Spnb4	0,47		
Il1r12	1,5	Scoc	0,47		
Ctsl	1,5	B930046C15Rik	0,47		
9030625A04Rik	1,4	Asph	0,47		
SRA1	1,4	WNT7A	0,47		
		Pycard	0,46		
Down-regulated genes		Sall1	0,46		
Icam1	0,82	Pros1	0,46		
HIST1H2AB	0,76	Garnl3	0,46		
Ryk	0,75	Fabp5	0,45		
Grm1	0,75	MR	0,45		
Rtn1	0,75	Camk2n1	0,44		
Tfeb	0,74	B4galt4	0,44		
Map3k7	0,72	Slc2a5	0,44		
Slc24a3	0,71	Il21r	0,43		
Qdpr	0,70	IL34	0,43		
ADAM10	0,68	Atp8a2	0,43		
Cxxc5	0,67	Jam2	0,43		
Ckb	0,67	Myo1b	0,42		
Ttc28	0,66	Gpr56	0,42		
Tmem100	0,66	Ebf3	0,42		
Nfia	0,65	Olfml2b	0,42		
Tm9sf4	0,65	Fgfr1	0,42		
Snn	0,64	Tmem119	0,42		
Abi3	0,64	Scamp5	0,42		
Epn2	0,64	Fads1	0,41		
Sema4d	0,63	Psd	0,41		
Map2k1	0,62	Tmeff1	0,41		

**Table 3 (continued)**

Up-regulated genes	Ratio n-3 deficient/ n-3 sufficient		
Zfp1	0,62	Ptprm	0,41
Rbbp9	0,62	Tlr5	0,40
Adora3	0,62	Adamts16	0,40
Ang	0,61	Eng	0,40
Gpr34	0,61	CD36	0,39
Rtn4r1	0,61	Itga9	0,39
Bin1	0,60	Gpr40	0,39
Acp2	0,60	Tspan18	0,39
Epb4.112	0,60	Escr	0,39
Cttnbp2nl	0,60	Cntn1	0,39
Itgb5	0,59	WNT2	0,39
Sgce	0,58	Gp9	0,38
D18Erttd653e	0,58	Arhgap22	0,37
Gm10790	0,57	Pon3	0,37
Tjp1	0,57	Plxdc2	0,37
Spsb1	0,57	Tanc2	0,37
C3	0,57	Rab6b	0,36
Lair1	0,57	Kcnd1	0,36
Tppp	0,57	Csm3	0,36
IL6ST	0,56	NRG1	0,36
Cx3cr1	0,56	Capn3	0,35
Siglech	0,56		

Only genes with  $P < 0.05$  are considered significant.

**Cell culture and treatments.** For in vitro phagocytic assays, primary mixed glial cell cultures were prepared from the cortices of P0–1 CD1 mice. After dissection in 0.1 M PBS with 6% glucose and 2% penicillin–streptomycin (Gibco, Cergy Pontoise, France) and removal of the meninges, the cortices were chopped and subsequently mechanically dissociated. The suspension was diluted in low glucose DMEM (31885, Gibco) supplemented with 10% fetal bovine serum (Gibco) and 1% penicillin–streptomycin. Microglia were isolated from primary mixed glial cultures on DIV14 using a reciprocating shaker (45 min at RT) and repeated rinsing with their medium using a 10 mL pipette. Media was subsequently removed, microglia pelleted via centrifugation ( $504 g \times 10$  min) and following resuspension maintained in DMEM at a concentration of  $4 \times 10^5$  cells/mL in six-well culture plates. Cells were then treated for 24 h in serum-free medium containing 50  $\mu$ mol/L fatty acid-free bovine serum albumin (BSA) added either with DHA, AA, DPA-n-6 or EPA 30  $\mu$ mol/L in 0.1% ethanol or 0.1% ethanol. For oxylipins, 30 min prior to the phagocytosis assay, culture medium was replaced by serum-free DMEM containing 100 nM of the given lipid in 0.03% ethanol, or 0.03% ethanol.

**Phagocytic assay.** Ex vivo assays: the phagocytic capacity of microglia was determined by the level of pHrodo™ Red fluorescence accumulated in the cells. First, we used pHrodo-conjugated *E. Coli* bioparticles. A suspension of  $2.5 \times 10^5$  sorted microglia cells in 100  $\mu$ L of RPMI/1% BSA was incubated with bioparticles in an incubator at 37 °C and 5% of CO<sub>2</sub> for each time point. Cells were then pelleted by centrifugation at 1000 $\times g$  for 10 min at 4 °C, resuspended in 200  $\mu$ L of RPMI/1% BSA and stained with CD11b-APC [clone M1/70, eBioscience] and rat CD45-PerCP-Cy™5.5 [clone 30-F11, BDBiosciences] antibodies for quantification by flow cytometry. We also developed a model using pHrodo-conjugated synaptosomes as a substrate for the phagocytosis. Synaptosomes were prepared from P21 mice hippocampus, and labeled with pHrodo Red, succinimidyl ester (Thermo Fisher Scientific, P36600) according to manufacturer instructions. Synaptosomes were resuspended at a concentration of 10 mg/ml in DMEM. Microglia were plated at a density of  $5.10^5$  cells/well in 24-well plates and received 150  $\mu$ g of synaptosomes for 120 min in an incubator at 37 °C and 5% CO<sub>2</sub>. When needed, baicalein was applied at a final concentration of 20  $\mu$ M in 0.2% DMSO 90 min prior to the beginning of the assay (i.e. the addition of synaptosomes). Cells were collected by gentle trypsin treatment, rinsed and resuspended in PBS/1%BSA buffer to be stained with CD11b-V450 [clone M1/70, BDBiosciences], CD45 PerCP Cy5.5 [Clone 30-F11, BDBiosciences], Ly6G-APC [clone 1A8, BDBiosciences] and Ly6C-APC-Cy™7 [clone AL-21, BDBiosciences] both for negative exclusion and analysis by cytometry. After selection of the CD11b+/CD45low, cells were gated on PE channel for quantification of pHrodo fluorescence.

Experiments in Figs. 3c and 6f have been performed on the same batches in order to spare animals. Hence, data used for Fig. 3c control groups are a randomly chosen subset of Fig. 6f's data.

In vitro, two different substrates were used: FCS-coated Yelloworange fluorescent carboxylated microspheres (Fluoresbrite® YO Carboxylate Microspheres 3.00  $\mu$ m, Polysciences Europe GmbH, #19393-5) or the pHrodo-conjugated synaptosomes as described above. To quantify their phagocytic index, primary microglial cell cultures were incubated with a suspension of microspheres at a concentration of  $1.1 \times 10^7$  microspheres/ml for 30 min at 37 °C, intensively washed, and finally fixed with 4% paraformaldehyde. Cells were stained with anti-Iba1 antibodies. A blinded experimenter counted beads per cell using NIS Elements AR 3.26 software. To measure phagocytic activity by cytometry, cells were incubated for 60 or 120 min with 150  $\mu$ g of synaptosomes per well. Medium was removed and cell collected following trypsin treatment, pelleted, rinsed in PBS/1% BSA, and stained with CD11b-FITC [clone M1/70, BDBiosciences] antibody for cytometry analysis.

FACS data were acquired using an LSR Fortessa 2-Blue 6-Violet 3-Red 5-YelGr laser configuration (BD Biosciences). Diva 8.0 (BD Biosciences) and FlowJo 10.5 (FlowJo, LLC) were used for data analyses.

**Microglia fatty acid analysis.** Fatty acid analyses requiring lots of material, we pooled microglia from 4 brains for  $n = 1$ . Based on our experience, we sort 400,000 cells out of the brain of P21 mice, hence measurements were made on around 1.6 million microglia. It is noted in ng/sample in the legend.

**Fatty acids:** Extraction and quantification of total fatty acids by GC-FID: Microglia from 3 to 4 brains per sample were lysed in 100% methanol and extracted via from the Folch method (2:1:0.8 chloroform: methanol: 0.88% KCl) and analyzed by a Varian-430 gas chromatograph (Varian, Lake Forest CA).

**Lipid mediators:** Isolation and quantification of brain eicosanoids and docosanoids by LC-MS-MS: Pooled microglia extracted from 3 to 4 brains per sample were lysed in 15% methanol and stored at  $-80$  °C prior to analysis. One ng of internal standard mixture was added to each sample, and lipid mediators were extracted, analyzed by LC-MS-MS and quantified as previously described<sup>87</sup>.

**Synaptosomes preparation and fatty acid quantification.** Synaptosomes were prepared from P21 mice hippocampus<sup>88</sup>. The two hippocampi of each animal were dissected and placed in 1 mL of ice-cold iso-osmolar buffer. The tissues were homogenized with 2 cm<sup>3</sup> rotating potter with 12 strokes at 900 rpm. The homogenate was centrifuged at 1000 $\times g$  for 5 min at 4 °C, the supernatant was collected in a new tube and centrifuged at 12,500 $\times g$  for 8 min at 4 °C. The supernatant was removed and the pellet resuspended with 1 mL of ice-cold iso-osmolar buffer. The discontinuous sucrose gradients were prepared in ultracentrifuge tubes with ice-cold 1.2 M sucrose solution and 0.8 M sucrose solution. The resuspended pellet was placed on top of the sucrose gradient. The centrifugation at 50,000 $\times g$  for 1 h at 4 °C provided a visible layer at the interface of sucrose gradients. This fraction



(synaptosomes) was collected with a syringe. Synaptosomes were then rinsed with 100 mM pH 8.5 sodium bicarbonate buffer and stored for further experiments.

Fatty acid quantification was run as already explained for the cortex fatty acid composition (see above).

**RNA isolation and Nanostring RNA counting.** Total RNA was extracted from isolated microglia using mirVana™ miRNA isolation kit (Ambion) according to the manufacturer's protocol. We performed nCounter multiplexed target profiling of 542 microglial transcripts (MG550). MG550 encompasses 400 unique and enriched microglial genes we have identified previously<sup>20</sup> and additional 150 inflammation-, inflammasome- and phagocytosis-related genes. In all, 100 ng of total RNA per sample were used in all described nCounter analyses according to the manufacturer's protocol<sup>20</sup>.

**Network analysis.** To investigate gene coexpression relationships between groups, a pairwise transcript-to-transcript matrix was calculated in the software tool Miru (Kajeka, UK) from the set of differentially expressed transcripts using a Pearson correlation threshold  $r = 0.85$ . A network graph was generated where nodes represent individual probe sets (transcripts/genes), and edges between them correlation of expression pattern with Pearson correlation coefficients above the selected threshold. The graph was clustered into discrete 6 groups of transcripts sharing similar expression profiles using the Markov clustering algorithm (inflation 2.2).

**Electron microscopy.** Mice were anesthetized with sodium pentobarbital (80 mg/kg, i.p.) and perfused with 0.2% glutaraldehyde in 4% PFA. Transverse sections of the brain (50  $\mu$ m thick) were cut in PBS (50 mM at pH 7.4) using a vibratome and stored at  $-20^{\circ}\text{C}$  in cryoprotectant solution (30% glycerol and 30% ethylene glycol in PBS).

Sections were washed in PBS and quenched with 0.3%  $\text{H}_2\text{O}_2$  in PBS for 5 min and then with 0.1%  $\text{NaBH}_4$  for 30 min at room temperature (RT), washed in Tris-buffered saline (TBS; 50 mM at pH 7.4) and processed freely-floating for immunoperoxidase staining. Sections were pre-incubated for 1 h at RT in a blocking solution of TBS containing 10% fetal bovine serum, 3% bovine serum albumin, and 0.01% Triton X100, before overnight incubation at  $4^{\circ}\text{C}$  in rabbit anti-Iba1 antibody (1:1000; Wako Pure Chemical Industries) and rinsed in TBS. After incubation for 1.5 h at RT in goat anti-rabbit IgGs conjugated to biotin (1:200 in blocking solution; Jackson ImmunoResearch) and for 1 h with ABC Vectastain mix (1:100 in TBS; Vector Laboratories), the labeling was revealed using diaminobenzidine (DAB; 0.05%) and hydrogen peroxide (0.015%) in TBS. After immunostaining, sections were post-fixed flat in 1% osmium tetroxide and dehydrated in ascending concentrations of ethanol. They were treated with propylene oxide, impregnated in Durcupan (EMS) overnight at RT, mounted between ACLAR embedding films (EMS), and cured at  $55^{\circ}\text{C}$  for 72 h. Areas of CA1 stratum radiatum were excised from the embedding films and re-embedded at the tip of resin blocks. Ultrathin (65–80 nm) sections were cut with an ultramicrotome (Leica Ultracut UC7), collected on bare square-mesh grids, and examined at 80 kV with a FEI Tecnai Spirit G2 transmission electron microscope.

Pictures were randomly taken at 9300X in the CA1 stratum radiatum of each animal, for a total surface of  $\sim 2000\ \mu\text{m}^2$  of neuropil captured per animal, using an ORCA-HR digital camera (10 MP; Hamamatsu). Cellular profiles were identified according to criteria previously defined<sup>89</sup>. For quantitative analysis, each captured Iba1-positive microglial process was analyzed. A phagocytic index was compiled by summing up the vacuoles and endosomes containing cellular materials such as membranes, axon terminals with 40-nm synaptic vesicles and dendritic spines with a postsynaptic density, on a microglial process basis<sup>16</sup>. Images were analyzed using the AMT Image Capture Engine Software 601.384.

**Immunohistochemistry.** Mice were deeply anesthetized with isoflurane and transcardially perfused with PBS followed by 4% PFA. Brain was removed, post-fixed in PFA overnight at  $4^{\circ}\text{C}$  and cryoprotected in 30% sucrose at  $4^{\circ}\text{C}$ . Immunohistochemistry experiments were performed on free-floating coronal 30  $\mu$ m cryostat slices. The following antibodies were used: 1:1000 rabbit anti-Iba1 (Wako, #019-19741), 1:100 mouse anti-PSD95 ([www.anticorps-en-ligne.fr](http://www.anticorps-en-ligne.fr), ABIN1304920), 1:500 rat anti-CD11b (AbD Serotec, #MCA711), 1:500 rabbit anti-C1q (Abcam, #ab182451), 1:20 mouse anti-C3aR (Hycult biotech, #HM1123), 1:1000 rabbit anti-GFAP (Dako, Z03334), 1:1000 mouse anti-NeuN (Millipore, #MAB377), 1:200 rabbit anti-Annexin V (Abcam, #ab14196), 1:500 mouse anti-claudin 5 (Life Technologies: Invitrogen), 1:500 IRDye 800 conjugated affinity purified goat-anti-mouse IgG (Rockland, Gilbertsville, PA). Primary antibodies were visualized with appropriate secondary antibodies conjugated with Alexa fluorophores (Invitrogen) and counterstained with DAPI or with biotin. When biotinylated, secondary antibodies were revealed using the streptavidin-biotin-immunoperoxidase technique, giving a black precipitate.

**Image analysis.** Densitometry: Individual images were analyzed with Fiji or Image J software (Image J, open source), using the following procedure: (1) user-defined thresholding value applied to each image, (2) calculation of area of staining from background for each protein of interest. Final values are represented as a surface

area in pixel values. Control sections for all studies in which primary or secondary antibodies were omitted resulted in negative staining (not shown).

Stereological analysis: Iba1- and GFAP-immunoreactive cell numbers and volume of the hippocampus were thoroughly determined in the hippocampus with the unbiased stereological sampling method based on optical disector stereological probe.

Apoptotic cells counting: The number of apoptotic cells (cells with pycnotic/karyorrhectic morphology) was estimated using unbiased stereology methods, and is reported as cells/mm<sup>3</sup>.

**Quantitative real-time PCR.** Total RNA was extracted from hippocampi using TRIzol (Invitrogen, Life Technologies™). RNA purity and concentration were determined using a Nanodrop spectrophotometer (Nanodrop technologies, Wilmington, DE). In all, 2  $\mu$ g of RNA was reverse transcribed to synthesize cDNA using Superscript III (Invitrogen, Life Technologies™) and random primer according to the manufacturer's protocol. Quantitative PCR were performed on 384-well plates using epMotion 5070 (Eppendorf). 10  $\mu$ l of cDNA diluted 1:5 (20 ng/ $\mu$ l) were amplified by real-time PCR. Primer references: C1qa Mm00432142\_m1; C3 Mm00437838\_m1; TREM2 Mm00451744\_m1; CD11b Mm01271262\_m1 (for in vitro experiments); CD33 Mm00491152\_m1; CX3CR1 Mm00438354\_m1; CX3CL1 Mm00436454\_m1; TGFb Mm03024053\_m1; beta-2 microglobulin Mm00437762\_m1 (housekeeping gene) (Life Technologie). For in vivo quantification of CD11b mRNA expression, we used SYBR Green technology. Ten  $\mu$ l of cDNA diluted 1/60 (1.66 ng/ $\mu$ l) were amplified by real-time PCR. Primers sequences: CD11b Forward AATGATGCTACCTGGGTTAT GCT/Reverse TGA TAC CGA GGT GTCCTAAAAC; Housekeeping gene beta-2 microglobulin: Forward CTGATACATACGCTGCAGAGTAA/Reverse GATC ACATGTCTCGATCCCAGTAG. For all experiments, the difference between target and housekeeping gene Ct values ( $\Delta$ Ct) was calculated to normalize for differences in the amount of total nucleic acid added to each reaction and in the efficiency of the RT step. The expression of target gene (linear value) normalized to the housekeeping gene was determined by  $2^{-\Delta\text{Ct}}$ .

**Droplet digital (dd)PCR.** Total RNA was extracted using the RNeasy® micro Kit (Qiagen, Germany) according to the manufacturer's protocol. The integrity of the RNA was checked by capillary electrophoresis using the RNA 6000 Pico Labchip kit and the Bioanalyser 2100 (Agilent Technologies, Massy, France), and quantity was estimated using a DS.11 (DeNovix, USA). The RNA integrity number (RIN) was above 7.5. cDNA was synthesized from 6 ng of total RNA using QScript XLT cDNA supermix (QuantaBio). Quantitative PCR was used for the choice of the reference gene and performed using a LightCycler® 480 Real-Time PCR System (Roche, Meylan, France). Quantitative PCR reactions were done using transcript-specific primers, cDNA, and LightCycler 480 SYBR Green I Master (Roche) in a final volume of 10  $\mu$ l. For the determination of the reference gene, the Genorm method was used. The elongation factor 1-alpha 1 (Eef1a1) and peptidylprolyl isomerase A (Ppia) genes were used as reference genes.

ddPCR was used for the quantification of the interest genes. PCRs were prepared with cDNA and the required QX200 ddPCR EvaGreen Supermix (Bio-Rad) with a final concentration of 150 nM for each transcript-specific primer to a final volume of 20  $\mu$ l. Each reaction was loaded into a sample well of an 8-well disposable cartridge (Bio-Rad) followed by 70  $\mu$ l of droplet generator oil (Bio-Rad), which was added to the oil wells of the cartridge. Droplets were formed in the QX200 droplet generator (Bio-Rad). Droplets were then transferred to a 96-well PCR plate, heatsealed with foil in a Pxi PCR Plate Sealer Bio-Rad and amplified with an Eppendorf Nexus Gradient master cycler ( $95^{\circ}\text{C}$  primary denaturation/activation for 5 min, followed by 45 cycles of  $95^{\circ}\text{C}$  for 30 sec and  $61^{\circ}\text{C}$  for 1 min, followed by  $4^{\circ}\text{C}$  5 min and a final  $90^{\circ}\text{C}$  heat treatment for 5 min). PCRs were analyzed with the QX200 droplet reader (Bio-Rad) and data analysis was performed with QuantaSoft software (version 1.7; Bio-Rad). qPCR primer sequences: Eef1a1 (GenBank NM\_010106): Forward TGAACCATCCAGGCCAAATC, Reverse: GCATGCTATGTGGCTGTGT; Ppia (GenBank NM\_008907): Forward CAAATGCTGGACCAAAACACAA, Reverse: GCCATCCAGCCATTCAGTCT; C3ar1 (GenBank NM\_009779): Forward TCCCATCTCTCCCTACTTTGCA, Reverse: TGTTTTAGGCACACCATGGTAAA; Itgam (GenBank NM\_001082960): Forward CTCATCACTGGCCCTATACAA, Reverse: GCAGTTCATTCATCATGTCTCT; Gpr31b (GenBank NM\_001013832): Forward GCTGCAGTGTCCAGCAAGC, Reverse: TGTACTGTGCAGGCAGGTGAG.

**Golgi staining.** Brains were processed for Golgi-Cox staining using the FD Rapid Golgi Staining kit (FD Neurotechnologies, Inc). Brains were left in the staining solution for 12 days, frozen in isopentane solution and kept at  $-80^{\circ}\text{C}$  until sectioning and coloration. The brains were cryostat-cut at a thickness of 100  $\mu$ m. Sections were mounted on gelatin-coated slides and analyzed using a motorized Leica DM5000 microscope at  $\times 63$  magnification. The images were acquired using a CCD Coolsnap camera and Metamorph software. For analysis, we randomly selected pyramidal neurons from the CA1 region of the dorsal hippocampus that were fully penetrated by the Golgi coloration and distinguishable from other neurons (n-3 deficient mice had less usable neurons than n-3 sufficient mice). Spine density in these neurons was determined by counting the number of spines on at least 3 basal and 3 apical dendritic segments of 10  $\mu$ m in length. Segments

from dendrites situated as far from the cell body as possible, with no overlap with other dendrites were randomly selected. Primary dendrites were never used for analysis as their thickness hampers detection of spines. Spine density was calculated per 10  $\mu\text{m}$  and averaged across the different segments in the same neuron. Images were processed with Mercator Pro 7.9.11.

**Western blotting.** Brains were carefully placed on a glass plate over dry ice to collect hippocampi that were immediately frozen and stored at  $-80^\circ\text{C}$  until use. Samples were homogenized in lysis buffer plus anti-phosphatase solution (Tris/HCl 20 mM pH 7.4 with EDTA 1 mM, MgCl<sub>2</sub> 5 mM, dithiothreitol 1 mM, Na orthovanadate 2 mM, protease inhibitors cocktail 1X and Na fluoride 1 mM). Homogenates were centrifuged 10 min at 2200  $\times g$  to remove nuclei. Supernatants were stored at  $-80^\circ\text{C}$ . Protein contents were determined by Bio-Rad protein assay according to the manufacturer's protocol (Bio-Rad) and then heated to  $100^\circ\text{C}$  for 5 min in Laemmli sample buffer (2% sodium dodecyl sulfate and 5% dithiothreitol).

Equal quantities of proteins (20  $\mu\text{g}$ /well) were electrophoresed onto an 8% or 12% polyacrylamide gel with a 4% stacking gel. Proteins were blotted on PVDF membranes (Immobilon, Millipore, Paris, France). Membranes were saturated by incubation with 5% milk in TBS and Tween 0.1% for 1 h. Blots were probed overnight at  $4^\circ\text{C}$  with 1:1,000 rabbit anti-PSD95 (Cell signaling Technology, 3450 S), 1:500 rabbit anti-Bax (Santa Cruz, SC-493), 1:500 rabbit anti-Bcl2 (Santa Cruz Biotechnology, SC-492), 1:1,000 mouse anti-Mer (R&D systems, AF591), 1:1,000 mouse anti-Axl (R&D systems, AF854), 1:1,000 rabbit anti-ERK1/2 (Cell Signaling Technology, 137F5), 1:500 goat anti-MFG-E8 (R&D systems, AF2805), 1:1000 rabbit anti-GluA1 (Santa Cruz Biotechnology, SC-28799), 1:1000 rabbit anti-GluA2 (Santa Cruz Biotechnology, SC-7611), 1:1000 goat anti-GluN2A (Santa Cruz Biotechnology, SC-1468), 1:1000 goat anti-GluN2B (Santa Cruz Biotechnology, SC-1469), 1:1000 rabbit anti-GluN1 (Santa Cruz Biotechnology, SC-31556), 1:5000 rabbit anti-SAP102 (Synaptic System, 124213), 1:300 mouse anti-cofilin (Abcam, Ab-54532), 1:5000 rabbit anti-actin (Cell Signaling Technology, 4967), 1:5000 rabbit anti-GAPDH (Cell Signaling Technology, 2118S). After washing in TBS-Tween, membranes were incubated with the secondary antibody coupled to Horse Radish Peroxidase (HRP, Southern Biotechnology Associates, Birmingham, AL, USA) diluted in TBS-Tween supplemented with 3% milk, for 2 h at room temperature. Membranes were washed and the complex was detected with an ECL kit (ElectroChemoLuminescence, Amersham, Orsay, France). Optical density capture of the signal obtained was performed with the Syngene Chemigenius2 apparatus (Synoptics, Cambridge, UK). Intensity of the signal was quantified using GeneTools software (Synoptics, Cambridge, UK).

**C3 ELISA assay.** The level of C3 protein located on synaptosomes was measured using the Mouse C3 (Complement Factor 3) ELISA Kit (Genway Biotech GWB-7555C7). Synaptosomes were prepared using the hippocampi of 2 mice per sample. After extraction, synaptosomes were lysed using sonication in TB. Quantifications were performed according to manufacturer instructions, in duplicates and by loading 5  $\mu\text{g}$  of proteins extract per well, and using the following software Wallac 1420 instrument Workout 2.5 (PerkinElmer).

**Y maze task.** P21-old mice were handled daily and weighed before and during behavioral experiments. Sessions were recorded with a ceiling-mounted video camera and analyzed using Smart software (Panlab, Barcelona, Spain). The Y-maze was used to assess spatial working memory<sup>90</sup>. Each arm was 34 cm long, 8 cm wide, and 14 cm high. The floor of the maze was covered with corn cob litter, which was mixed between each trial to remove olfactory cues. Visual cues were placed in the testing room and kept constant during the whole test. In the first trial, one arm was closed with a guillotine door and mice were allowed to visit two arms of the maze for 5 min. After a 30-min to 3 h inter-trial interval (ITI), mice were placed back in the start arm and allowed free access to the three arms for 5 min. Start and closed arms were randomly assigned for each mouse. When required, baicalin was injected intraperitoneally at a concentration of 20 mg/kg, at P14, P17, and 30 min prior the first trial (at P21 or P30 depending on the experiments). Data are presented as the time spent exploring the novel and the familiar arms during the second trial.

**Statistical analyses.** For most experiments, experimental groups were compared using Student *t*-test or non-parametric Mann-Whitney test (when equality of variance or normality failed). We used the Grubbs' test, also called the ESD method (extreme studentized deviate), to determine whether the most extreme value in the list is a significant outlier from the rest. Paired *t*-tests were used for Y-maze experiments (familiar vs novel arm for each experimental group). A two-way ANOVA was used for XVA-143, cRGD, and baicalin experiments (except Y-maze), ex vivo and in vitro phagocytic activity. All data were expressed as means  $\pm$  standard error of the mean (SEM). A  $p < 0.05$  was considered as statistically significant. Statistics were performed using GraphPad Prism 7.0.

**Reporting summary.** Further information on research design is available in the Nature Research Reporting Summary linked to this article.

## Data availability

Source data are provided with this paper. All data supporting the findings are provided within this paper and its supplementary information. Fatty acids derivatives data are available on Metabolights. Our study is identified as [MTBLS1952](https://www.ebi.ac.uk/metabolights/study/MTBLS1952). Transcriptomic data are available in the GEO database. Accession number: [GSE158181](https://www.ncbi.nlm.nih.gov/geo/query/acc.cgi?acc=GSE158181).

Received: 24 July 2019; Accepted: 3 November 2020;

Published online: 30 November 2020

## References

- Bazinet, R. P. & Layé, S. Polyunsaturated fatty acids and their metabolites in brain function and disease. *Nat. Rev. Neurosci.* **15**, 771–785 (2014).
- Abedi, E. & Sahari, M. A. Long-chain polyunsaturated fatty acid sources and evaluation of their nutritional and functional properties. *Food Sci. Nutr.* **2**, 443–463 (2014).
- Serhan, C. N. & Petasis, N. A. Resolvins and protectins in inflammation resolution. *Chem. Rev.* **111**, 5922–5943 (2011).
- Calder, P. C. The relationship between the fatty acid composition of immune cells and their function. *Prostaglandins Leukot. Essent. Fat. Acids* **79**, 101–108 (2008).
- Layé, S., Nadjar, A., Joffre, C. & Bazinet, R. P. Anti-inflammatory effects of Omega-3 fatty acids in the brain: physiological mechanisms and relevance to pharmacology. *Pharmacol. Rev.* **70**, 12–38 (2018).
- Bazan, N. G. The metabolism of omega-3 polyunsaturated fatty acids in the eye: the possible role of docosahexaenoic acid and docosanoids in retinal physiology and ocular pathology. *Prog. Clin. Biol. Res.* **312**, 95–112 (1989).
- Lands, W. E., Morris, A. & Libelt, B. Quantitative effects of dietary polyunsaturated fats on the composition of fatty acids in rat tissues. *Lipids* **25**, 505–516 (1990).
- Innis, S. M. Fatty acids and early human development. *Early Hum. Dev.* **83**, 761–766 (2007).
- Koletzko, B. et al. The roles of long-chain polyunsaturated fatty acids in pregnancy, lactation and infancy: review of current knowledge and consensus recommendations. *J. Perinat. Med.* **36**, 5–14 (2008).
- McNamara, R. K., Vannest, J. J. & Valentine, C. J. Role of perinatal long-chain omega-3 fatty acids in cortical circuit maturation: Mechanisms and implications for psychopathology. *World J. Psychiatry* **5**, 15–34 (2015).
- Ransohoff, R. M. & Perry, V. H. Microglial physiology: unique stimuli, specialized responses. *Annu. Rev. Immunol.* **27**, 119–145 (2009).
- Tay, T. L. et al. Microglia gene: impacts on psychiatric disorders across the lifespan. *Front Mol. Neurosci.* **10**, 421 (2017).
- Paolicelli, R. C. et al. Synaptic pruning by microglia is necessary for normal brain development. *Science* **333**, 1456–1458 (2011).
- Schafer, D. P. et al. Microglia sculpt postnatal neural circuits in an activity and complement-dependent manner. *Neuron* **74**, 691–705 (2012).
- Tay, T. L., Savage, J. C., Hui, C. W., Bisht, K. & Tremblay, M.-È. Microglia across the lifespan: from origin to function in brain development, plasticity and cognition. *J. Physiol.* **595**, 1929–1945 (2017).
- Tremblay, M.-È., Lowery, R. L. & Majewska, A. K. Microglial interactions with synapses are modulated by visual experience. *PLoS Biol.* **8**, e1000527 (2010).
- Madore et al. Nutritional n-3 PUFAs deficiency during perinatal periods alters brain innate immune system and neuronal plasticity-associated genes. *Brain Behav. Immun.* **41**, 22–31 (2014).
- Semple, B. D., Blomgren, K., Gimlin, K., Ferriero, D. M. & Noble-Haueslein, L. J. Brain development in rodents and humans: Identifying benchmarks of maturation and vulnerability to injury across species. *Prog. Neurobiol.* **106–107**, 1–16 (2013).
- Butovsky, O. & Weiner, H. L. Microglial signatures and their role in health and disease. *Nat. Rev. Neurosci.* **19**, 622–635 (2018).
- Butovsky, O. et al. Identification of a unique TGF- $\beta$ -dependent molecular and functional signature in microglia. *Nat. Neurosci.* **17**, 131–143 (2014).
- Freeman, T. C. et al. Construction, visualisation, and clustering of transcription networks from microarray expression data. *PLoS Comput. Biol.* **3**, 2032–2042 (2007).
- Grabert, K. et al. Microglial brain region-dependent diversity and selective regional sensitivities to aging. *Nat. Neurosci.* **19**, 504–516 (2016).
- Joffre, C. et al. Modulation of brain PUFA content in different experimental models of mice. *Prostaglandins Leukot. Essent. Fat. Acids* **114**, 1–10 (2016).
- Kim, H.-Y., Akbar, M. & Lau, A. Effects of docosapentaenoic acid on neuronal apoptosis. *Lipids* **38**, 453–457 (2003).
- Schafer, D. P. & Stevens, B. Phagocytic glial cells: sculpting synaptic circuits in the developing nervous system. *Curr. Opin. Neurobiol.* **23**, 1034–1040 (2013).

26. Lian, H. et al. Astrocyte-microglia cross talk through complement activation modulates amyloid pathology in mouse models of Alzheimer's disease. *J. Neurosci.* **36**, 577–589 (2016).
27. Bialas, A. R. & Stevens, B. TGF- $\beta$  signaling regulates neuronal C1q expression and developmental synaptic refinement. *Nat. Neurosci.* **16**, 1773–1782 (2013).
28. Hajishengallis, G., Shakhatreh, M.-A. K., Wang, M. & Liang, S. Complement receptor 3 blockade promotes IL-12-mediated clearance of *Porphyromonas gingivalis* and negates its virulence in vivo. *J. Immunol.* **179**, 2359–2367 (2007).
29. Brown, G. C. & Neher, J. J. Microglial phagocytosis of live neurons. *Nat. Rev. Neurosci.* **15**, 209–216 (2014).
30. Fourgeaud, L. et al. TAM receptors regulate multiple features of microglial physiology. *Nature* **532**, 240–244 (2016).
31. Serhan, C. N., Chiang, N. & Dalli, J. The resolution code of acute inflammation: Novel pro-resolving lipid mediators in resolution. *Semin. Immunol.* **27**, 200–215 (2015).
32. Rey, C. et al. Dietary n-3 long chain PUFA supplementation promotes a pro-resolving oxylipin profile in the brain. *Brain Behav. Immun.* **76**, 17–27 (2019).
33. Xu, J. et al. Inhibition of 12/15-lipoxygenase by baicalein induces microglia PPAR $\beta/\delta$ : a potential therapeutic role for CNS autoimmune disease. *Cell Death Dis.* **4**, e569 (2013).
34. Deschamps, J. D., Kenyon, V. A. & Holman, T. R. Baicalein is a potent in vitro inhibitor against both reticulocyte 15-human and platelet 12-human lipoxygenases. *Bioorg. Med. Chem.* **14**, 4295–4301 (2006).
35. Zanon, I. et al. CD14 controls the LPS-induced endocytosis of Toll-like receptor 4. *Cell* **147**, 868–880 (2011).
36. Vasek, M. J. et al. A complement-microglial axis drives synapse loss during virus-induced memory impairment. *Nature* **534**, 538–543 (2016).
37. Lepeta, K. et al. Synaptopathies: synaptic dysfunction in neurological disorders - A review from students to students. *J. Neurochem.* **138**, 785–805 (2016).
38. Madore et al. Neuroinflammation in autism: plausible role of maternal inflammation, dietary Omega 3, and microbiota. *Neural Plast.* **2016**, 3597209 (2016).
39. Parellada, M. et al. Randomized trial of omega-3 for autism spectrum disorders: effect on cell membrane composition and behavior. *Eur. Neuropsychopharmacol.* **27**, 1319–1330 (2017).
40. Hawkey, E. & Nigg, J. T. Omega-3 fatty acid and ADHD: blood level analysis and meta-analytic extension of supplementation trials. *Clin. Psychol. Rev.* **34**, 496–505 (2014).
41. Hoer, W. P. et al. Red blood cell polyunsaturated fatty acids measured in red blood cells and schizophrenia: a meta-analysis. *Psychiatry Res.* **207**, 1–12 (2013).
42. Brown, C. M. & Austin, D. W. Autistic disorder and phospholipids: a review. *Prostaglandins Leukot. Essent. Fat. Acids* **84**, 25–30 (2011).
43. Almeida, D. M., Jandacek, R. J., Weber, W. A. & McNamara, R. K. Docosahexaenoic acid biostatus is associated with event-related functional connectivity in cortical attention networks of typically developing children. *Nutr. Neurosci.* **20**, 246–254 (2017).
44. Delpech, J.-C. et al. Dietary n-3 PUFAs deficiency increases vulnerability to inflammation-induced spatial memory impairment. *Neuropsychopharmacology* **40**, 2774–2787 (2015).
45. McNamara, R. K. & Almeida, D. M. Omega-3 polyunsaturated fatty acid deficiency and progressive neuropathology in psychiatric disorders: a review of translational evidence and candidate mechanisms. *Harv. Rev. Psychiatry* **27**, 94–107 (2019).
46. Richards, R. et al. Increased hippocampal shape asymmetry and volumetric ventricular asymmetry in autism spectrum disorder. *Neuroimage Clin.* **26**, 102207 (2020).
47. Farquharson, J. et al. Effect of diet on the fatty acid composition of the major phospholipids of infant cerebral cortex. *Arch. Dis. Child.* **72**, 198–203 (1995).
48. Johnson, S. et al. Psychiatric disorders in extremely preterm children: longitudinal finding at age 11 years in the EPICure study. *J. Am. Acad. Child Adolesc. Psychiatry* **49**, 453–463 (2010). e1.
49. Henriksen, C. et al. Improved cognitive development among preterm infants attributable to early supplementation of human milk with docosahexaenoic acid and arachidonic acid. *Pediatrics* **121**, 1137–1145 (2008).
50. Almaas, A. N. et al. Diffusion tensor imaging and behavior in premature infants at 8 years of age, a randomized controlled trial with long-chain polyunsaturated fatty acids. *Early Hum. Dev.* **95**, 41–46 (2016).
51. Namgaladze, D. et al. AMP-activated protein kinase suppresses arachidonate 15-lipoxygenase expression in interleukin 4-polarized human macrophages. *J. Biol. Chem.* **290**, 24484–24494 (2015).
52. Guo, Y. et al. Identification of the orphan G protein-coupled receptor GPR31 as a receptor for 12-(S)-hydroxyicosatetraenoic acid. *J. Biol. Chem.* **286**, 33832–33840 (2011).
53. Haynes, R. L. & van Leyen, K. 12/15-lipoxygenase expression is increased in oligodendrocytes and microglia of periventricular leukomalacia. *Dev. Neurosci.* **35**, 140–154 (2013).
54. Krasemann, S. et al. The TREM2-APOE pathway drives the transcriptional phenotype of dysfunctional microglia in neurodegenerative diseases. *Immunity* **47**, 566–581 (2017). e9.
55. Wainwright, P. E. Dietary essential fatty acids and brain function: a developmental perspective on mechanisms. *Proc. Nutr. Soc.* **61**, 61–69 (2002).
56. Moriguchi, T., Greiner, R. S. & Salem, N. Behavioral deficits associated with dietary induction of decreased brain docosahexaenoic acid concentration. *J. Neurochem.* **75**, 2563–2573 (2000).
57. Kohlboeck, G. et al. Effect of fatty acid status in cord blood serum on children's behavioral difficulties at 10 y of age: results from the LISAPlus Study. *Am. J. Clin. Nutr.* **94**, 1592–1599 (2011).
58. Calderon, F. & Kim, H.-Y. Docosahexaenoic acid promotes neurite growth in hippocampal neurons. *J. Neurochem.* **90**, 979–988 (2004).
59. Calon, F. et al. Docosahexaenoic acid protects from dendritic pathology in an Alzheimer's disease mouse model. *Neuron* **43**, 633–645 (2004).
60. Larrieu, T., Hilal, M. L., De Smedt-Peyrusse, V., Sans, N. & Layé, S. Nutritional Omega-3 deficiency alters glucocorticoid receptor-signaling pathway and neuronal morphology in regionally distinct brain structures associated with emotional deficits. *Neural Plast.* **2016**, 8574830 (2016).
61. Thomazeau, A., Bosch-Bouju, C., Manzoni, O. & Layé, S. Nutritional n-3 PUFA deficiency abolishes endocannabinoid gating of hippocampal long-term potentiation. *Cereb. Cortex* **27**, 2571–2579 (2017).
62. Grayson, D. S., Kroenke, C. D., Neuringer, M. & Fair, D. A. Dietary omega-3 fatty acids modulate large-scale systems organization in the rhesus macaque brain. *J. Neurosci.* **34**, 2065–2074 (2014).
63. Rosenberg, M. D. et al. A neuromarker of sustained attention from whole-brain functional connectivity. *Nat. Neurosci.* **19**, 165–171 (2016).
64. Stark, K. D., Lim, S.-Y. & Salem, N. Artificial rearing with docosahexaenoic acid and n-6 docosapentaenoic acid alters rat tissue fatty acid composition. *J. Lipid Res.* **48**, 2471–2477 (2007).
65. Rey, C. et al. Maternal n-3 polyunsaturated fatty acid dietary supply modulates microglia lipid content in the offspring. *Prostaglandins Leukot. Essent. Fat. Acids* **133**, 1–7 (2018).
66. Igarashi, M. et al. Fifteen weeks of dietary n-3 polyunsaturated fatty acid deprivation increase turnover of n-6 docosapentaenoic acid in rat-brain phospholipids. *Biochim. Biophys. Acta* **1821**, 1235–1243 (2012).
67. Uderhardt, S. et al. 12/15-lipoxygenase orchestrates the clearance of apoptotic cells and maintains immunologic tolerance. *Immunity* **36**, 834–846 (2012).
68. Yip, P. K. et al. Docosahexaenoic acid reduces microglia phagocytic activity via miR-124 and induces neuroprotection in rodent models of spinal cord contusion injury. *Hum. Mol. Genet.* **28**, 2427–2448 (2019).
69. Chang, P. K.-Y., Khatchadourian, A., McKinney, R. A. & Maysinger, D. Docosahexaenoic acid (DHA): a modulator of microglia activity and dendritic spine morphology. *J. Neuroinflammation* **12**, 34 (2015).
70. De Smedt-Peyrusse, V. et al. Docosahexaenoic acid prevents lipopolysaccharide-induced cytokine production in microglial cells by inhibiting lipopolysaccharide receptor presentation but not its membrane subdomain localization. *J. Neurochem.* **105**, 296–307 (2008).
71. Hjorth, E. et al. Omega-3 fatty acids enhance phagocytosis of Alzheimer's disease-related amyloid- $\beta$ 42 by human microglia and decrease inflammatory markers. *J. Alzheimers Dis.* **35**, 697–713 (2013).
72. Zendedel, A. et al. Omega-3 polyunsaturated fatty acids ameliorate neuroinflammation and mitigate ischemic stroke damage through interactions with astrocytes and microglia. *J. Neuroimmunol.* **278**, 200–211 (2015).
73. Hopperton, K. E., Trépanier, M.-O., Giuliano, V. & Bazinet, R. P. Brain omega-3 polyunsaturated fatty acids modulate microglia cell number and morphology in response to intracerebroventricular amyloid- $\beta$  1-40 in mice. *J. Neuroinflammation.* **13**, 257 (2016).
74. Herdoiza Padilla, E. et al. mir-124-5p regulates phagocytosis of human macrophages by targeting the actin cytoskeleton via the ARP2/3 complex. *Front Immunol.* **10**, 2210 (2019).
75. Tremblay, M.-E. et al. Remodeling of lipid bodies by docosahexaenoic acid in activated microglial cells. *J. Neuroinflammation* **13**, 116 (2016).
76. Brown, E. J. Complement receptors and phagocytosis. *Curr. Opin. Immunol.* **3**, 76–82 (1991).
77. Gorgani, N. N. et al. Complement receptor of the Ig superfamily enhances complement-mediated phagocytosis in a subpopulation of tissue resident macrophages. *J. Immunol.* **181**, 7902–7908 (2008).
78. Hong, S. et al. Complement and microglia mediate early synapse loss in Alzheimer mouse models. *Science* **352**, 712–716 (2016).
79. Boackle, S. A. & Holers, V. M. Role of complement in the development of autoimmunity. *Curr. Dir. Autoimmun.* **6**, 154–168 (2003).
80. Zhan, Y. et al. Deficient neuron-microglia signaling results in impaired functional brain connectivity and social behavior. *Nat. Neurosci.* **17**, 400–406 (2014).
81. Bar, E. & Barak, B. Microglia roles in synaptic plasticity and myelination in homeostatic conditions and neurodevelopmental disorders. *Glia*. <https://doi.org/10.1002/glia.23637>. (2019)

82. Filipello, F. et al. The microglial innate immune receptor TREM2 Is required for synapse elimination and normal brain connectivity. *Immunity* **48**, 979–991 (2018). e8.
83. Weinhard, L. et al. Microglia remodel synapses by presynaptic trogocytosis and spine head filopodia induction. *Nat. Commun.* **9**, 1228 (2018).
84. Diaz-Aparicio, I., Beccari, S., Abiega, O. & Sierra, A. Clearing the corpses: regulatory mechanisms, novel tools, and therapeutic potential of harnessing microglial phagocytosis in the diseased brain. *Neural Regen. Res.* **11**, 1533–1539 (2016).
85. Lieberman, O. J., McGuirt, A. F., Tang, G. & Sulzer, D. Roles for neuronal and microglial autophagy in synaptic pruning during development. *Neurobiol. Dis.* **122**, 49–63 (2019).
86. Gould, J. F., Smithers, L. G. & Makrides, M. The effect of maternal omega-3 (n-3) LCPUFA supplementation during pregnancy on early childhood cognitive and visual development: a systematic review and meta-analysis of randomized controlled trials. *Am. J. Clin. Nutr.* **97**, 531–544 (2013).
87. Lin, L. E. et al. Chronic dietary n-6 PUFA deprivation leads to conservation of arachidonic acid and more rapid loss of DHA in rat brain phospholipids. *J. Lipid Res.* **56**, 390–402 (2015).
88. De-Smedt-Peyrusse, V., Darriet, L., Trifilieff, P., Herzog, E. & Angelo, M. F. Subcellular Fractionation of Brain Tissue from Small Tissue Explants. in *Synaptosomes* (ed. Murphy, K. M.), 75–84. (Springer New York, 2018). [https://doi.org/10.1007/978-1-4939-8739-9\\_5](https://doi.org/10.1007/978-1-4939-8739-9_5).
89. Tremblay, M.-E., Riad, M. & Majewska, A. Preparation of mouse brain tissue for immunoelectron microscopy. *J. Vis. Exp.* <https://doi.org/10.3791/2021>. (2010)
90. Moranis, A. et al. Long term adequate n-3 polyunsaturated fatty acid diet protects from depressive-like behavior but not from working memory disruption and brain cytokine expression in aged mice. *Brain Behav. Immun.* **26**, 721–731 (2012).

## Acknowledgements

Funding for this research was provided by the Institut National pour la Recherche Agronomique (INRAE), the Bordeaux Univ, the Foundation for Medical Research (FRM, DEQ20170336724 to S.L.), the French Foundation (FDF, #00070700) and the Fédération pour la Recherche sur le Cerveau (FRC Connect). C.M. was funded by the French Ministry for Research and by the Fondation pour la Recherche Medicale (ARF201909009101). C.B.B. was supported by the French National Agency for Research (ANR-12-BSV4-0025-04, to S.L.) and Agreenskills (MSCA cofund-INRAE), J.C.D. was supported by the Region Nouvelle Aquitaine (2011.1303003, to S.L.), Q.L. was supported by the Region Ile de France (PICRI, the Cerebral Palsy Foundation #13020605, to A.N.) and the FRM, AT was supported by the French National Agency for Research (ANR-2010-BLAN-141403, to S.L.), ADG was supported by Agreenskills (MSCA cofund-INRAE) and Marie-Curie European Grant, C.L. was supported by IDEX grant, M.M. was funded by FRM (DEQ20170336724, to S.L.) and M.R. was supported by the Region Nouvelle-Aquitaine (2017-1R30237-00013179, to S.L.). A.S. was supported by grants from the Spanish Ministry of Economy and Competitiveness with FEDER funds to AS (BFU2015-66689, RYC-2013-12817), a BBVA Foundation Grant for Researchers and Cultural Creators to A.S., and a Basque Government grant (PI\_2016\_1\_0011) to AS. PG was supported by Inserm, Université de Paris, ERA-NET Neuron (Micromet). This work was partly funded by NeurATRIS ANR-11-INBS-0011 of the French Investissements d'Avenir Program run by the ANR. MET, C.L., and K.B. were supported by grants from NARSAD and the CIHR awarded to MET. We would like to thank C. Tridon, S. Delbary and B. Péré for taking care of the mice, Rémi Van der Vynck for his assistance in the Western blot experiment, and Celine Lucas for technical assistance. This work benefited from the facilities and expertise of the imaging platform Imag'In ([www.incia.u-bordeaux1.fr](http://www.incia.u-bordeaux1.fr)), which is supported by CNRS and Region Aquitaine and from the

Bordeaux Imaging Center. We thank Atika Zouine and Vincent Pitard for their technical assistance at the Flow cytometry facility, CNRS UMS 3427, INSERM US 005, Univ. Bordeaux, F-33000 Bordeaux, France. Analysis of eicosanoids and docosanoids was performed at the Analytical Facility for Bioactive Molecules (AFBM) of the Centre for the Study of Complex Childhood Diseases (CSCCD) at the Hospital for Sick Children, Toronto, Ontario. CSCCD was supported by the Canadian Foundation for Innovation (CFI). We thank the Biochemistry and Biophysics Platform of the Bordeaux Neuro-campus at the Bordeaux University funded by the LABEX BRAIN (ANR-10-LABX-43) and Yann Rufin for the Western Blot analysis.

## Author contributions

The data reported in this study can be found in the supplementary materials. C.M., Q.L., L.M., M.R., M.M., B.R., C.L., C.B.B., J.B., A.T., J.C.D., A.Sere., A.A., and V.D.P. performed most experiments. K.E.H. performed and R.P.B. oversaw the fatty acid analyses of microglia. S.B. and A.Sierra. performed and A.S. oversaw the apoptosis experiments. C.L., K.B., and M.E.T. performed and M.E.T. oversaw the E.M. experiments. S.G., N.A., and L.B. performed and analyzed fatty acid experiments on whole hippocampus. J.B. performed and analyzed BBB experiments. C.M. performed and O.B. oversaw transcriptomic analyses. A.D.G. analyzed transcriptomic data. N.J.G. performed FACS phagocytosis experiments. L.F. performed and analyzed TAM receptors Western blots. P.G. contributed to the design of the experiments. C.J. performed whole structure fatty acid composition experiments and conducted the data analyses. S.L. and A.N. equally supervised the entire project and wrote the paper. All authors proof-read the manuscript.

## Competing interests

The authors declare no competing interests.

## Additional information

**Supplementary information** is available for this paper at <https://doi.org/10.1038/s41467-020-19861-z>.

**Correspondence** and requests for materials should be addressed to A.N. or S.L.

**Peer review information** *Nature Communications* thanks the anonymous reviewer(s) for their contribution to the peer review of this work. Peer reviewer reports are available.

**Reprints and permission information** is available at <http://www.nature.com/reprints>

**Publisher's note** Springer Nature remains neutral with regard to jurisdictional claims in published maps and institutional affiliations.



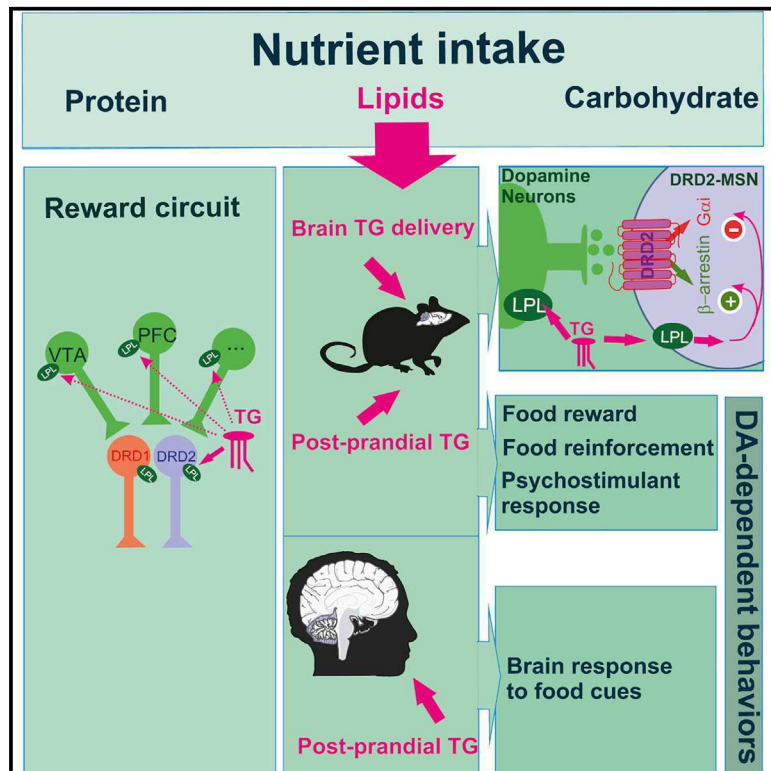
**Open Access** This article is licensed under a Creative Commons Attribution 4.0 International License, which permits use, sharing, adaptation, distribution and reproduction in any medium or format, as long as you give appropriate credit to the original author(s) and the source, provide a link to the Creative Commons license, and indicate if changes were made. The images or other third party material in this article are included in the article's Creative Commons license, unless indicated otherwise in a credit line to the material. If material is not included in the article's Creative Commons license and your intended use is not permitted by statutory regulation or exceeds the permitted use, you will need to obtain permission directly from the copyright holder. To view a copy of this license, visit <http://creativecommons.org/licenses/by/4.0/>.

© The Author(s) 2020

# Cell Metabolism

## Circulating Triglycerides Gate Dopamine-Associated Behaviors through DRD2-Expressing Neurons

### Graphical Abstract



### Authors

Chloé Berland, Enrica Montalban, Elodie Perrin, ..., Dana M. Small, Giuseppe Gangarossa, Serge H. Luquet

### Correspondence

giuseppe.gangarossa@u-paris.fr (G.G.), serge.luquet@univ-paris-diderot.fr (S.H.L.)

### In Brief

Dietary triglycerides (TGs) can gate dopamine receptor type 2 (DRD2)-expressing neurons' activity and dopamine-dependent behaviors. These results highlight a new physiological mechanism by which nutritional inputs can directly tune reward-associated behaviors and provide a new basis by which energy-rich diets may lead to (mal) adaptations in brain circuits that underlie compulsive behavior.

### Highlights

- Dopamine receptor type 2 (DRD2)-expressing neurons respond to dietary triglycerides (TGs)
- Dietary TGs modulate dopamine-dependent behaviors
- Lipoprotein lipase participates in the action of TGs on the reward circuit
- In humans, plasma TGs influence brain responses to food



# Circulating Triglycerides Gate Dopamine-Associated Behaviors through DRD2-Expressing Neurons

Chloé Berland,<sup>1,2</sup> Enrica Montalban,<sup>1</sup> Elodie Perrin,<sup>3,15</sup> Mathieu Di Miceli,<sup>4,15</sup> Yuko Nakamura,<sup>5,6,15</sup> Maud Martinat,<sup>4,15</sup> Mary Sullivan,<sup>5,6</sup> Xue S. Davis,<sup>5,6</sup> Mohammad Ali Shenasa,<sup>7</sup> Claire Martin,<sup>1</sup> Stefania Tolu,<sup>9</sup> Fabio Marti,<sup>9</sup> Stephanie Caille,<sup>8</sup> Julien Castel,<sup>1</sup> Sylvie Perez,<sup>3</sup> Casper Gravesen Salinas,<sup>11</sup> Chloé Morel,<sup>1</sup> Jacob Hecksher-Sørensen,<sup>10,11</sup> Martine Cadot,<sup>8</sup> Xavier Fioramonti,<sup>4</sup> Matthias H. Tschöp,<sup>2,12,13</sup> Sophie Layé,<sup>4</sup> Laurent Venance,<sup>3</sup> Philippe Faure,<sup>9</sup> Thomas S. Hnasko,<sup>7,14</sup> Dana M. Small,<sup>5,6</sup> Giuseppe Gangarossa,<sup>1,16,\*</sup> and Serge H. Luquet<sup>1,5,16,17,\*</sup>

<sup>1</sup>Université de Paris, BFA, UMR 8251, CNRS, F-75014 Paris, France

<sup>2</sup>Helmholtz Diabetes Center, Helmholtz Zentrum München, German Research Center for Environmental Health, München, Neuherberg, Germany

<sup>3</sup>Center for Interdisciplinary Research in Biology, College de France, INSERM U1050, CNRS UMR 7241, Labex Memolife, 75005 Paris, France

<sup>4</sup>Université Bordeaux, INRA, Bordeaux INP, NutriNeuro, UMR 1286, F-33000 Bordeaux, France

<sup>5</sup>The Modern Diet and Physiology Research Center, New Haven, CT, USA

<sup>6</sup>Department of Psychiatry, Yale University School of Medicine, New Haven, CT, USA

<sup>7</sup>Department of Neurosciences, University of California, San Diego, La Jolla, CA, USA

<sup>8</sup>Université Bordeaux, Institut de Neurosciences Cognitives et Intégratives d'Aquitaine, CNRS, UMR5287, 33076 Bordeaux, France

<sup>9</sup>Sorbonne Université, CNRS UMR 8246, INSERM, Neurosciences Paris Seine, Institut de Biologie Paris-Seine, Paris, France

<sup>10</sup>Global Research, Novo Nordisk A/S, Måløv, Denmark

<sup>11</sup>Gubra ApS, Hørsholm Kongevej 11B, 2970 Hørsholm, Denmark

<sup>12</sup>Division of Metabolic Diseases, TUM, Munich, Germany

<sup>13</sup>Institute for Advanced Study, TUM, Munich, Germany

<sup>14</sup>Research Service VA San Diego Healthcare System, San Diego, CA 92161, USA

<sup>15</sup>These authors contributed equally

<sup>16</sup>Senior author

<sup>17</sup>Lead Contact

\*Correspondence: [giuseppe.gangarossa@u-paris.fr](mailto:giuseppe.gangarossa@u-paris.fr) (G.G.), [serge.luquet@univ-paris-diderot.fr](mailto:serge.luquet@univ-paris-diderot.fr) (S.H.L.)

<https://doi.org/10.1016/j.cmet.2020.02.010>

## SUMMARY

Energy-dense food alters dopaminergic (DA) transmission in the mesocorticolimbic (MCL) system and can promote reward dysfunctions, compulsive feeding, and weight gain. Yet the mechanisms by which nutrients influence the MCL circuitry remain elusive. Here, we show that nutritional triglycerides (TGs), a conserved post-prandial metabolic signature among mammals, can be metabolized within the MCL system and modulate DA-associated behaviors by gating the activity of dopamine receptor subtype 2 (DRD2)-expressing neurons through a mechanism that involves the action of the lipoprotein lipase (LPL). Further, we show that in humans, post-prandial TG excursions modulate brain responses to

food cues in individuals carrying a genetic risk for reduced DRD2 signaling. Collectively, these findings unveil a novel mechanism by which dietary TGs directly alter signaling in the reward circuit to regulate behavior, thereby providing a new mechanistic basis by which energy-rich diets may lead to (mal)adaptations in DA signaling that underlie reward deficit and compulsive behavior.

## INTRODUCTION

Feeding results from a complex and dynamic integration of signals reflecting metabolic needs, but also cognitive, appetitive, and emotional drives, which collectively contribute to adaptive strategies to maintain caloric intake and body weight. The

### Context and Significance

The release of dopamine in the reward circuit is involved in the hedonic and motivational aspects of feeding. In susceptible individuals, the hedonic drive to consume palatable food can contribute to the obesity epidemic by promoting compulsive eating beyond metabolic needs. However, the physiological basis linking nutritional inputs to reward deficits is still unclear. In this work, we show that dietary triglycerides (TGs) can alter cell-type-specific processes within the reward circuit, thereby regulating food reward-related behaviors. This finding allows to directly bridge plasma lipids with the activity of dopamine-sensitive neurons in the reward circuit, hence providing new insights in the understanding of why and how lipid-rich food or chronically elevated plasma lipids may promote reward deficits and compulsive behaviors.



mesocorticolimbic dopamine (MCL-DA) circuitry encodes the reinforcing and motivational properties of food (Dallman et al., 2005; Di Chiara and Imperato, 1988; Volkow et al., 2012). DA neurons in the ventral tegmental area (VTA) and substantia nigra pars compacta represent a major source of DA in the dorsal and ventral striatum, where DA binds to receptors located on striatal medium-sized spiny neurons (MSNs). The DA receptors are G-coupled receptors associated with the  $G_{s\alpha/off}$  protein for the D1 family (DRD1), or with the  $G_i$  protein for the D2 family (DRD2), thus forming two distinct populations, notably the DRD1- and DRD2-MSNs (Baik, 2013; Gerfen et al., 1990; Jackson and Westlind-Danielsson, 1994), which also dynamically integrate inputs from prefrontal cortex, thalamus, and limbic structures. DA release and signaling within the MCL system plays a pivotal role in reward prediction errors (Schultz, 2016), associative learning (Frank and Fossella, 2011), motor-planning, decision-making, and the attribution of incentive salience to reward-related stimuli (Berridge, 2009).

Converging lines of evidence have now clearly established that both overconsumption of palatable food and metabolic syndrome (obesity) drive maladaptive modifications within the MCL system. These dysfunctions lead to impulsivity (Adams et al., 2015; Babbs et al., 2013; Guo et al., 2014), altered hedonic and motivational drive, uncontrolled craving, and, ultimately, compulsive and addictive-like feeding (Johnson and Kenny, 2010; Michaelides et al., 2012; Vucetic and Reyes, 2010; Wang et al., 2001). For instance, high-fat-diet-induced impulsivity in rodents correlates with the magnitude of reduction in DRD2 but not DRD1 signaling (Adams et al., 2015), and genetic downregulation of striatal DRD2 leads to a reward-deficit state and compulsive eating in rats exposed to high-fat food (Johnson and Kenny, 2010). In humans, body mass index (BMI) is associated with striatal DRD2 redistribution and opportunistic eating behavior (Guo et al., 2014). Additionally, the inheritable genetic polymorphism TaqIA A1, which correlates in humans with a ~30%–40% decrease of striatal DRD2 abundance, creates a favorable substrate for uncontrolled feeding and obesity (Ritchie and Noble, 2003; Stice et al., 2015; Stice et al., 2008). Several observations suggest that nutritional fat might directly alter DA transmission independently of adiposity and BMI. Indeed, high-fat diet was shown to reduce DRD2 expression and DA turn-over, leading to decreased reward-seeking behaviors (Davis et al., 2008; Hryhorczuk et al., 2016; South and Huang, 2008), reduced cognitive function (Farr et al., 2008), and increased impulsivity (Adams et al., 2015). Triglycerides (TGs) represent a major source of available lipid substrates, and the transient increase of TG-rich particles after a meal is a naturally occurring physiological phenomenon. However, TGs are chronically high in obesity (Ruge et al., 2009). Post-prandial plasma TG levels predict body weight gain and uncontrolled feeding in rodents (Karatayev et al., 2009) and promote cognitive impairments in obese mice (Farr et al., 2008). In humans, brain imaging studies have highlighted a correlation between circulating TGs and neuronal response to food reward (Sun et al., 2014). Several experiments using radio-labeled FFAs (free fatty acids) or TGs confirmed that both TGs and TG-rich particles cross the blood-brain barrier, being transported and locally metabolized in the brain (Banks et al., 2018; Cansell

et al., 2014). Collectively, these observations suggest that plasma TGs potentially act on DA signaling substrates to modulate reward. Finally, the rate-limiting enzyme of TG metabolism, the lipoprotein lipase (LPL), is expressed in rodents' brains (Ben-Zeev et al., 1990; Bessesen et al., 1993; Eckel and Robbins, 1984; Goldberg et al., 1989; Paradis et al., 2004). The activity of central LPL has been associated with body weight control and reward-drive behavior (Cansell et al., 2014; Picard et al., 2013; Wang et al., 2011). These observations raise the possibility that post-prandial LPL-mediated hydrolysis of TG-rich particles in the MCL could play a role in high-fat-diet-induced adaptations within the reward circuitry (Berland et al., 2016).

Here, we provide evidence supporting a key role of dietary TG-induced adaptations in DRD2-expressing neurons. First, in both human and mouse brains, *Lpl* mRNA is present in the mesocorticolimbic structures, including in VTA DA neurons and striatal MSNs. Second, using *in vivo* brain-specific TG delivery and *ex vivo* whole-cell patch-clamp recordings, we provide multiple lines of evidence indicating that circulating TGs act within the reward system to gate the excitability and cellular responses of DRD2-expressing neurons. Third, central TGs can act as a direct reinforcer and regulate reward-seeking and other dopamine-dependent behaviors. Fourth, we use functional magnetic resonance imaging (fMRI) to show that TG levels are associated with altered region-specific brain activity to food-related cues. Importantly, and in line with our mouse data, these associations are sensitive to genetic variations affecting DRD2-dependent signaling. Collectively, these findings reveal a previously unappreciated mechanism by which dietary TGs can act directly in the MCL system to regulate DRD2-expressing neurons' activity and reward-seeking behaviors.

## RESULTS

### The TG-Processing Enzyme Lipoprotein Lipase Is Expressed in Both Mouse and Human Mesocorticolimbic Structures

Pioneering studies have shown that *Lpl* mRNA is expressed in rodent brains (Ben-Zeev et al., 1990; Bessesen et al., 1993; Goldberg et al., 1989; Paradis et al., 2004). Here, we wondered whether *Lpl* mRNA was present in reward-related structures, namely the dorsal striatum (DS), the nucleus accumbens (NAc), and the VTA. Using fluorescent *in situ* hybridization we observed that *Lpl* mRNA co-localizes with a large portion of *Drd1*- and *Drd2*-expressing MSNs in the DS (Figure 1A) and the NAc, as well as in VTA *Th*-neurons (Figure S1B). *Lpl* mRNA expression data from available single-cell RNA sequencing atlas (Zeisel et al., 2018) or cell-type transcriptomic characterization of striatal neurons (Doyle et al., 2008) revealed that, in midbrain and striatal structures, *Lpl* mRNA was enriched in VTA DA neurons compared to local inhibitory neurons (Figure S1C), and in striatal DRD1- and DRD2-MSNs compared to striatal cholinergic interneurons (Figure 1B). In addition, expression data from the rodent and human Allen Brain Atlas (Hawrylycz et al., 2012; Lein et al., 2007) revealed that *Lpl* mRNA is expressed in the MCL of both species (Figures S1A and S1D).

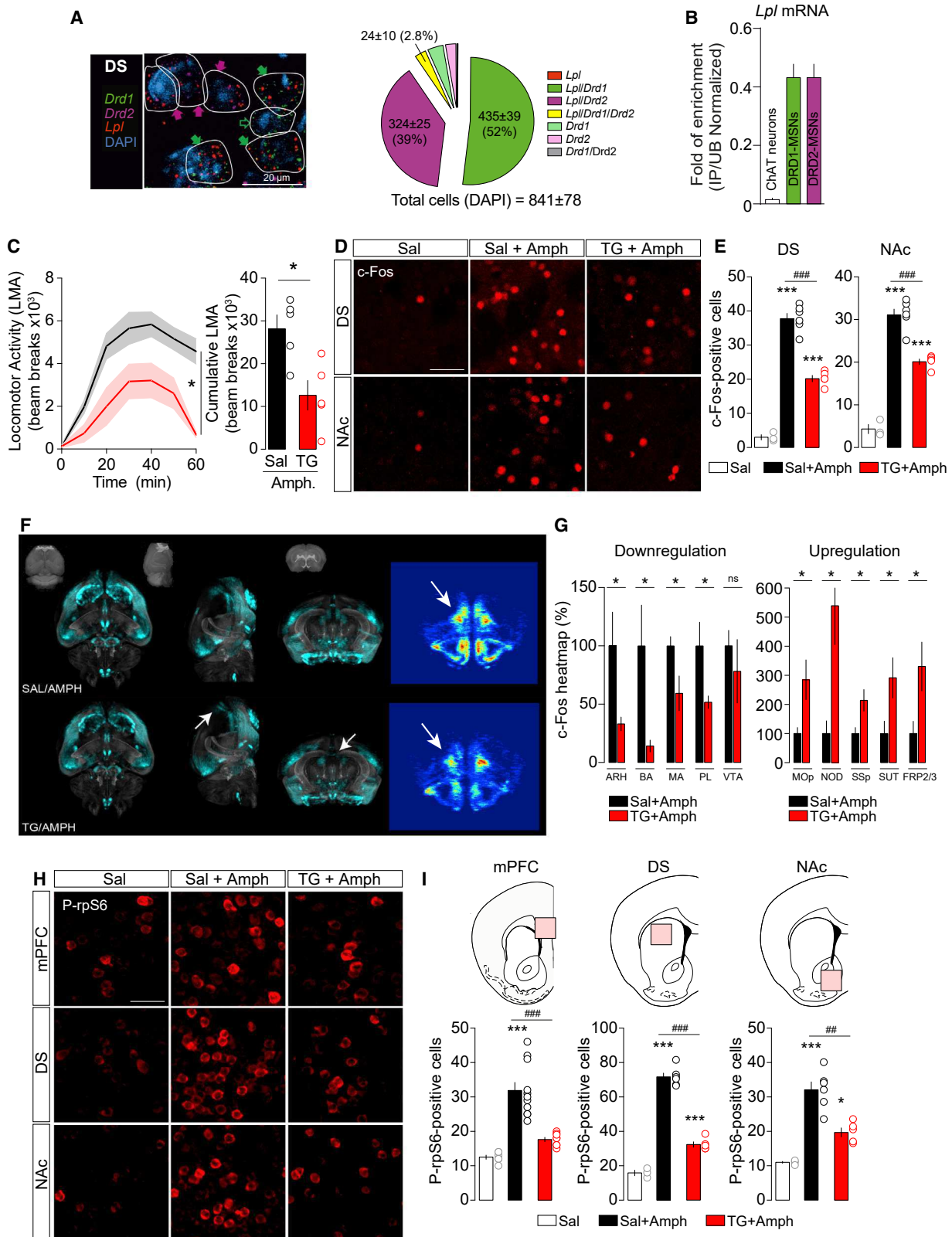


**Figure 1. Striatal TG Metabolism Decreases Amphetamine-Induced Behavioral and Molecular Adaptations**

(A) Representative photomicrographs and semiquantitative analysis of RNAscope fluorescence *in situ* hybridization (FISH) signal for Lipoprotein lipase (*Lpl*, red), dopamine receptor 1 and 2 (*Drd1* green, *Drd2* violet) in the dorsal striatum (DS). DAPI (blue) was used to identify cells. Scale bars: 20  $\mu$ m. The white lines represent

(legend continued on next page)



### Striatal TG Metabolism Decreases Amphetamine-Induced Behavioral and Molecular Adaptations

To decipher the central action of TGs respecting the physiological route by which nutrients access the brain, mice were perfused with TGs through an indwelling catheter into the carotid artery in the direction of the brain (Cansell et al., 2014). Here, we investigated whether TGs, or any derived metabolites, could be detected in the mouse striatum. C57Bl6/J mice received a 6 h saline or TG perfusion (0.1  $\mu$ l/min, Figure S2A), after which striata were dissected out for lipidomic analysis. Brain TG delivery significantly increased striatal content of TGs and metabolites (Figure S2B, Table S1, striatal FFAs and glycolipids content in Data S1 and S2), hence confirming that our experimental setting efficiently reproduces blood-to-brain TG entry and access to MCL structures.

Next, we investigated whether TG modulate the molecular activations induced by amphetamine (3 mg/kg). As we previously described (Cansell et al., 2014), TGs blunted the hyperlocomotor effects of amphetamine (Figure 1C), but also reduced the cellular c-Fos response evoked by amphetamine in both dorsal striatum and NAc (Figures 1D and 1E). In order to have a more global view of central TG-responsive structures, we also performed whole-brain c-Fos immunostaining using the iDISCO method (immunolabeling-enabled 3D imaging of solvent-cleared organs) coupled with light sheet microscopy (Figure 1F). Whole-brain heatmaps of c-Fos signal revealed a modulatory action of brain TG delivery on neural responses to amphetamine in anatomically distinct structures. In particular, whereas brain TG delivery enhanced neural responses to amphetamine in fronto-cortical regions, a blunted c-Fos induction was observed in several subcortical areas (Figure 1G). In line with the pattern of c-Fos activation, amphetamine-induced activation of the ribosomal protein S6 (rpS6 phosphorylation, Ser<sup>235/236</sup>), a marker of translational activity, was also dramatically decreased in the prefrontal cortex (mPFC), dorsal striatum, and the NAc (Figures 1H and 1I). Altogether, these results show that brain TG delivery inhibits amphetamine-induced neuronal activation and protein translation in reward-related structures.

### TGs Exert Modulatory Actions onto Dopamine Signaling and Behaviors

The above-mentioned results reveal that TGs may alter the ability of MSNs to integrate DA-dependent signals. We thus explored

whether central TG sensing was accompanied by alterations of key molecular pathways known to shape MSNs activity and be strongly modulated by DA (Beaulieu and Gainetdinov, 2011). Western blot analysis of striatal tissues revealed that brain TG delivery decreased p70S6K and rpS6 phosphorylation, at both mitogen-activated protein kinases (MAPK)-dependent (Ser<sup>235/236</sup>) and mammalian target of rapamycin (mTOR)-dependent (Ser<sup>240/244</sup>) sites, as well as extracellular signal-regulated kinase (ERK1/2) phosphorylation (Figures 2A and 2B). In addition, we found a reduction of phosphorylated DARPP-32<sup>Thr34</sup>, a direct protein kinase A (PKA)-dependent target. Interestingly, we also observed reduced levels of tyrosine hydroxylase (TH) phosphorylation, indicating a reduction in TH activity in the DA terminals that innervate the striatum (Lew et al., 1999; Salvatore et al., 2016) (Figures 2A and 2B).

Because DA signaling in MSNs can also trigger the PKB/Akt-GSK3 pathway, we explored Akt/GSK-3 $\beta$  signaling phosphorylation as a proxy for  $\beta$ -arrestin recruitment (Figures 2C and 2D). Akt phosphorylation remained unchanged at Thr<sup>308</sup>, but was significantly decreased at Ser<sup>473</sup>, while GSK-3 $\beta$  phosphorylation at Ser<sup>9</sup> was reduced (Figures 2E and 2F), indicating that this signaling pathway is activated following TG delivery (Beaulieu et al., 2004, 2005; Peterson et al., 2015). Indeed, a significant modulation of key phospho-proteins (p-rpS6, p-ERK1/2, p-DARPP-32, p-TH, and p-GSK-3 $\beta$ ) was also observed following multiple comparison corrections (see Table S5). Altogether, these results reveal that striatal TG sensing modulates MSNs signaling by decreasing canonical PKA-, MAPK-, and mTOR-dependent signaling while promoting  $\beta$ -arrestin-dependent Akt/GSK-3 $\beta$  signaling.

Next, to explore whether brain TG delivery exhibits an action on either DRD2- or DRD1-dependent behaviors, we assessed the consequences of brain TG delivery on behavioral and cellular responses triggered by pharmacological manipulation of DRD1 and DRD2 receptors. The hyperlocomotion triggered by a first or second injection of the DRD1 agonist SKF38393 (10 mg/kg) was similar between saline- or TG-perfused mice (Figure 2G). However, brain TG delivery was still fully efficient in reducing amphetamine-induced hyperlocomotion assessed on the same animals after the 2 consecutive days of SKF38393 treatment (Day 3, Figure 2H). Consistently, DRD1-dependent increase in striatal c-Fos remained unaffected by

the cellular limits. Filled and empty arrows within representative photomicrographs indicate co-expression or absence, respectively, of *Lpl* according to the presence of *Drd1* (green arrows) and *Drd2* (violet arrows) transcripts.

(B) Translating ribosome affinity purification (TRAP) technique (Doyle et al., 2008) reveals a specific enrichment of *Lpl* mRNA in medium spiny neurons (MSNs) as compared to cholinergic neurons in the striatum. Each immunoprecipitation (IP) is compared to the average of unbound (UB) samples from the same tissue to calculate a ratio of IP/UB as a measure of enrichment. IP/UB are represented for cholinergic, DRD1-, and DRD2-expressing MSNs.

(C) Amphetamine (Amph)-induced locomotor activity (LMA) and cumulative LMA after a 6-h saline (Sal, n = 5) or TG (TG, n = 5) central perfusion followed by amphetamine administration (3 mg/kg). Statistics: \*p < 0.05 Sal versus TG.

(D and E) Representative confocal photomicrographs and quantification of c-Fos-positive cells in the dorsal striatum (DS) and the nucleus accumbens (NAc) of animals infused with saline and injected with saline (Sal, n = 3) or amphetamine (Sal+Amph, n = 6) and animals infused with TG and injected with amphetamine (TG+Amph, n = 5). Scale bars: 50  $\mu$ m. Statistics: \*\*\*p < 0.001 Sal versus Sal+Amph or Sal versus TG+Amph; ###p < 0.001 Sal+Amph versus TG+Amph).

(F and G) Representative pictures showing whole-brain c-Fos-based signal and heatmaps quantification of brain structures in which central TG perfusion (TG/AMPH, n = 5) negatively or positively affect amphetamine-induced c-Fos response compared to controls (Sal/AMPH, n = 5). ARH: Arcuate hypothalamic nucleus, BA: Bed nucleus of the accessory olfactory tract, MA: Magnocellular nucleus, PL: Prelimbic area, VTA: Ventral tegmental area, Mop: Primary motor area, NOD: Nodulus (X), SSP: Primary somatosensory area, SUT: supratrigeminal nucleus, FRP2/3: Frontal pole, layer 2/3. Statistics: \*p < 0.05 TG+Amph versus Sal+Amph.

(H and I) Representative confocal photomicrographs and quantification of phosphorylated ribosomal protein S6 (Ser<sup>235/236</sup>)-positive cells in the medial prefrontal cortex (mPFC), dorsal striatum (DS), and nucleus accumbens (NAc) of animals infused with saline (Sal, n = 3) or amphetamine (Sal+Amph, n = 6) and animals infused with TG and injected with amphetamine (TG+Amph, n = 5). Statistics: \*\*\*p < 0.001 Sal versus Sal+Amph; ###p < 0.001 TG+Amph versus Sal+Amph, ##p < 0.01 TG+Amph versus Sal+Amph). For statistical details, see Table S5.

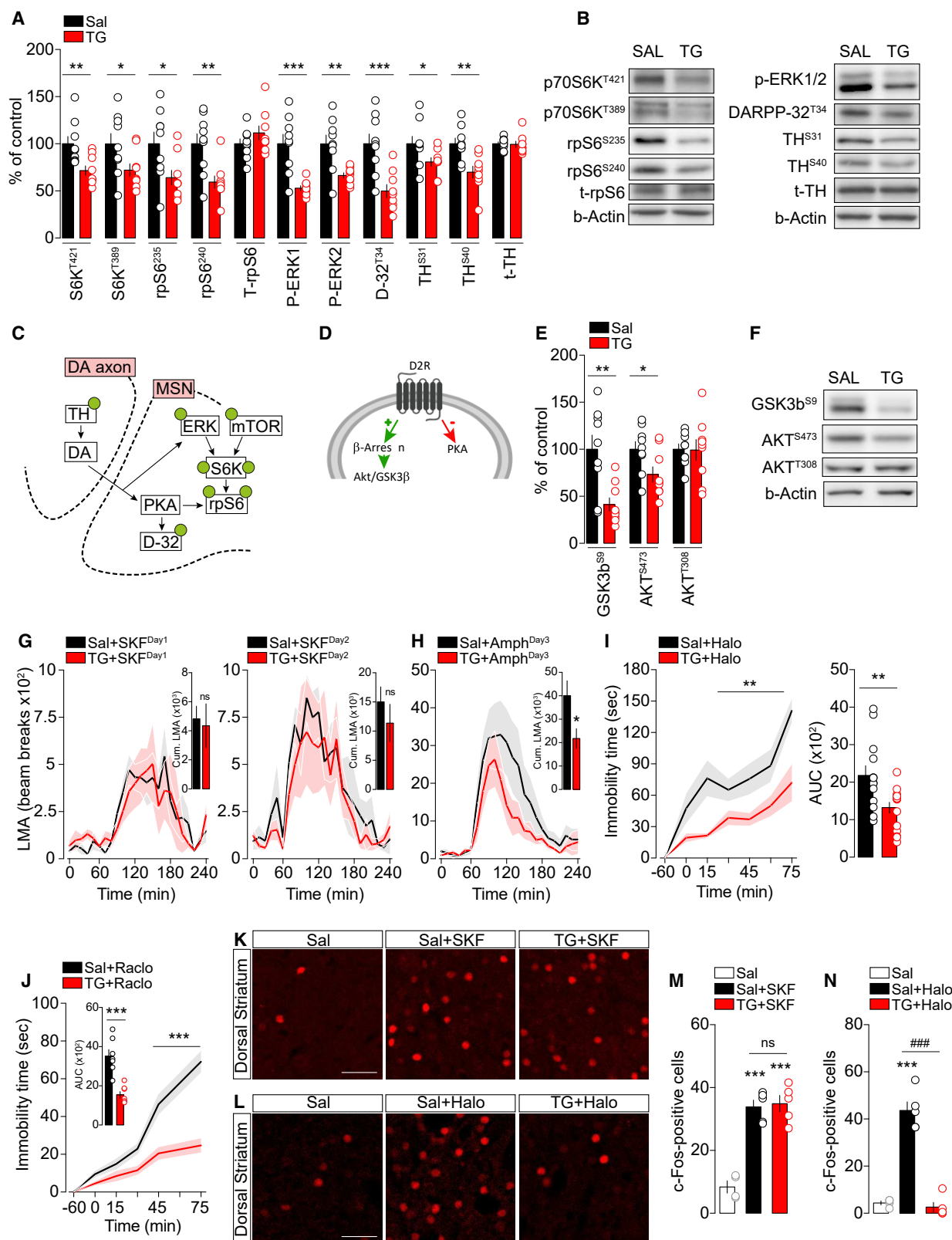


**Figure 2. Central TG Delivery Blunts DRD2-Dependent Striatal Signaling Pathways**

(A and B) Protein quantifications (A) and representative western blots (B) of signaling cascades classically downstream to dopamine receptors in the striatum after a 6-h central delivery of triglycerides (TG,  $n = 9$ ) or saline (Sal,  $n = 9$ ). Nomenclature: p70S6K (p70 ribosomal S6 kinase), rpS6 (ribosomal protein S6), t-rpS6 (total-

(legend continued on next page)

central TG delivery on a separate cohort of mice (Figures 2K and 2M).

In sharp contrast, brain TG delivery drastically reduced the cataleptic response triggered by two well-characterized DRD2 antagonists: haloperidol (0.5 mg/kg) or raclopride (0.6 mg/kg) (Figures 2I and 2J). As previously described (Bertran-Gonzalez et al., 2008), pharmacological blockade of DRD2 robustly increased the number of c-Fos- and rpS6-Ser<sup>235/236</sup>-positive neurons (putative DRD2-MSNs) in saline-treated animals, while this molecular response was dramatically reduced in mice receiving brain TG delivery (Figures 2L, 2N, S3A, and S3B). These results demonstrate that within the striatum, TGs preferentially impact DRD2-neuronal responses, possibly by reducing DRD2 signaling and/or DRD2-neurons excitability.

### Triglycerides Alter Excitability of DRD2-MSNs

The behavioral and cellular pharmacological responses mentioned above point to a particular role for DRD2-expressing neurons in sensing and/or responding to circulating TGs. To explicitly test this hypothesis, we used whole-cell patch-clamp recordings to determine active and passive membrane properties of both DRD1-MSNs (in *Drd1a*-tdTomato transgenic mice) and DRD2-MSNs (in *Drd2*-eGFP transgenic mice) in response to bath application of vehicle or triglyceride triolein at a concentration (4  $\mu$ M, 0.35 mg/dl) within the physiological range of cerebrospinal TGs (0.65  $\pm$  0.06 mg/dl, Banks et al., 2018). We assessed neuronal excitability in both the dorsal striatum and the NAc, and MSNs were recognized according to (1) fluorescence (tdTomato or eGFP, Figure 3A), (2) hyperpolarized resting membrane potentials, and (3) characteristic spiking profiles in response to current injections such as a marked inward rectification of the I/V relationship (Figure 3B).

Strikingly, in both striatal and accumbal structures, bath-applied triolein (~15–20 min, 4  $\mu$ M) further hyperpolarized the resting membrane potential (RMP) (Figures 3C and 3E) and increased the action potential rise time in DRD2-MSNs without significant influence in DRD1-MSNs (Figures 3D and 3F). Other parameters (for full list, see Tables S2 and S3) such as the membrane time constant and the action potential half width were modulated by triolein in striatal DRD2-MSNs (Figure S4, Table S2). Altogether, these results demonstrate that TGs selectively reduce the excitability of DRD2-MSNs.

To test whether DRD2-MSNs show reduced activity *in vivo*, we used fiber photometry to record real-time calcium transients in DRD2 neurons of behaving mice. Prior work has demonstrated

that DRD2-MSNs are transiently activated during action initiation (Cui et al., 2013). We thus used Cre-dependent expression of GCaMP6f in *Drd2*-Cre mice together with brain TG delivery in mice placed into a novel environment (new cage) (Figures 3G and 3H). We first used separate groups of C57BL/6 mice to assess the exact time window at which brain TG delivery started to inhibit spontaneous locomotor activity following exposure to a new cage. We found that the increase in exploratory drive to a new cage was similar between saline- or TG-perfused animals within the first ~10 min, becoming significantly reduced over the following 60 min (Figure S5). Therefore, in order to fully dissociate the action of TGs onto spontaneous locomotor activity from their effects on DRD2-MSNs calcium activity to novelty-induced exploration, we chose a 3-min window of exploration, which corresponds to the most intense period of activity in both experimental groups (Figure S5). Since DRD2-MSNs are transiently activated during action initiation (Cui et al., 2013), GCaMP-encoded calcium fluorescence was measured during the first 50 s of exploration. Transfer to a new cage was associated with a rapid and significant increase in DRD2-neurons calcium activity in saline-perfused mice (Figure 3I). Such increase was not significant in TG-perfused animals (Figure 3J). We then decided to analyze the dynamics of calcium transients during different temporal intervals (10 s/bin) of exploration (Figure 3K) and observed that the initial increase in exploration-evoked calcium signal in DRD2 neurons (B2 versus B1, TG-mice) decayed more rapidly in TG-perfused animals compared to control mice (Figure 3L). These *in vivo* results agree with the reduced excitability of DRD2-MSNs following *ex vivo* TG application, and further indicate that central TG delivery gates striatal DRD2-MSNs responses during behavior.

### Triglycerides Dynamically Influence Dopamine Neuron Activity

The above-mentioned results reveal that TGs rapidly influence DRD2-MSNs by modulating their activity and associated behavioral outputs. However, *Lpl* is also expressed in VTA DA neurons (Figure S1), thereby raising the question whether TGs may also modulate DA neurons. To test this hypothesis, we performed single-unit recordings of VTA DA neurons in anaesthetized mice during acute (<30 min) and long-term (6 h) brain TG delivery. We found that 10 min (Figure 4A) acute brain TG delivery did not affect the *in vivo* electrical activity of VTA DA neurons (Figure 4A). However, prolonged TG perfusion (5–6 h) led to a significant decrease in DA-neurons firing rate and burst activity

ribosomal protein S6), ERK (Extracellular-signal Regulated Kinase), DARPP-32 (32 kDa dopamine and cAMP regulated phosphoprotein), TH (tyrosine hydroxylase), t-TH (total-Tyrosine hydroxylase). Statistics: \* $p < 0.05$ , \*\* $p < 0.01$  and \*\*\* $p < 0.001$  TG versus Sal.

(C and D) Post-synaptic molecular signaling induced by DA in MSNs (C) and DRD2-specific signaling (D).

(E and F) Protein quantification (E) and representative western blots (F) of the Akt/GSK-3 $\beta$  pathway in the striatum. Nomenclature: GSK-3 $\beta$  (glycogen synthase kinase 3 $\beta$ ). Statistics: \* $p < 0.05$  and \*\* $p < 0.01$  TG versus Sal.

(G and H) Locomotor activity (LMA) induced by the DRD1 agonist SKF38393 (10 mg/kg) (G) and by amphetamine (3 mg/kg) (H) on 3 consecutive days after 6 h of central delivery of saline (Sal,  $n = 6$ ) or triglycerides (TG,  $n = 6$ ). Statistics: \* $p < 0.05$  TG+Amph<sup>Day3</sup> versus Sal+Amph<sup>Day3</sup>.

(I and J) Quantification of immobility time and area under the curve (AUC) induced by administration of haloperidol (0.5 mg/kg) (I) or raclopride (0.6 mg/kg) (J) after 6 h of central delivery of saline (Sal,  $n = 13$  for haloperidol,  $n = 7$  for raclopride) or triglycerides (TG,  $n = 15$  for haloperidol,  $n = 7$  for raclopride). Statistics: haloperidol (\*\* $p < 0.01$  TG+Halo versus Sal+Halo), raclopride (\*\*\* $p < 0.001$  TG+Raclo versus Sal+Raclo).

(K–N) Representative confocal photomicrographs in the dorsal striatum (K and L) and quantification of c-Fos-positive cells (M and N) 1 h after administration of the DRD1 agonist SKF38393 (K and M) or the DRD2 antagonist haloperidol (L and N) in saline- (Sal/SKF,  $n = 6$ , Sal/Halo,  $n = 5$ ) and TG-perfused mice (TG/SKF,  $n = 5$ , TG/Halo,  $n = 5$ ) compared to saline-treated animals (Sal/Sal,  $n = 3$ ). Scale bars: 50  $\mu$ m. Statistics: SKF38393 (\*\*\* $p < 0.001$  Sal+SKF or TG+SKF versus Sal), haloperidol (\*\*\* $p < 0.001$  Sal+Halo versus Sal, ### $p < 0.001$  TG+Halo versus Sal+Halo). For statistical details, see Table S5.

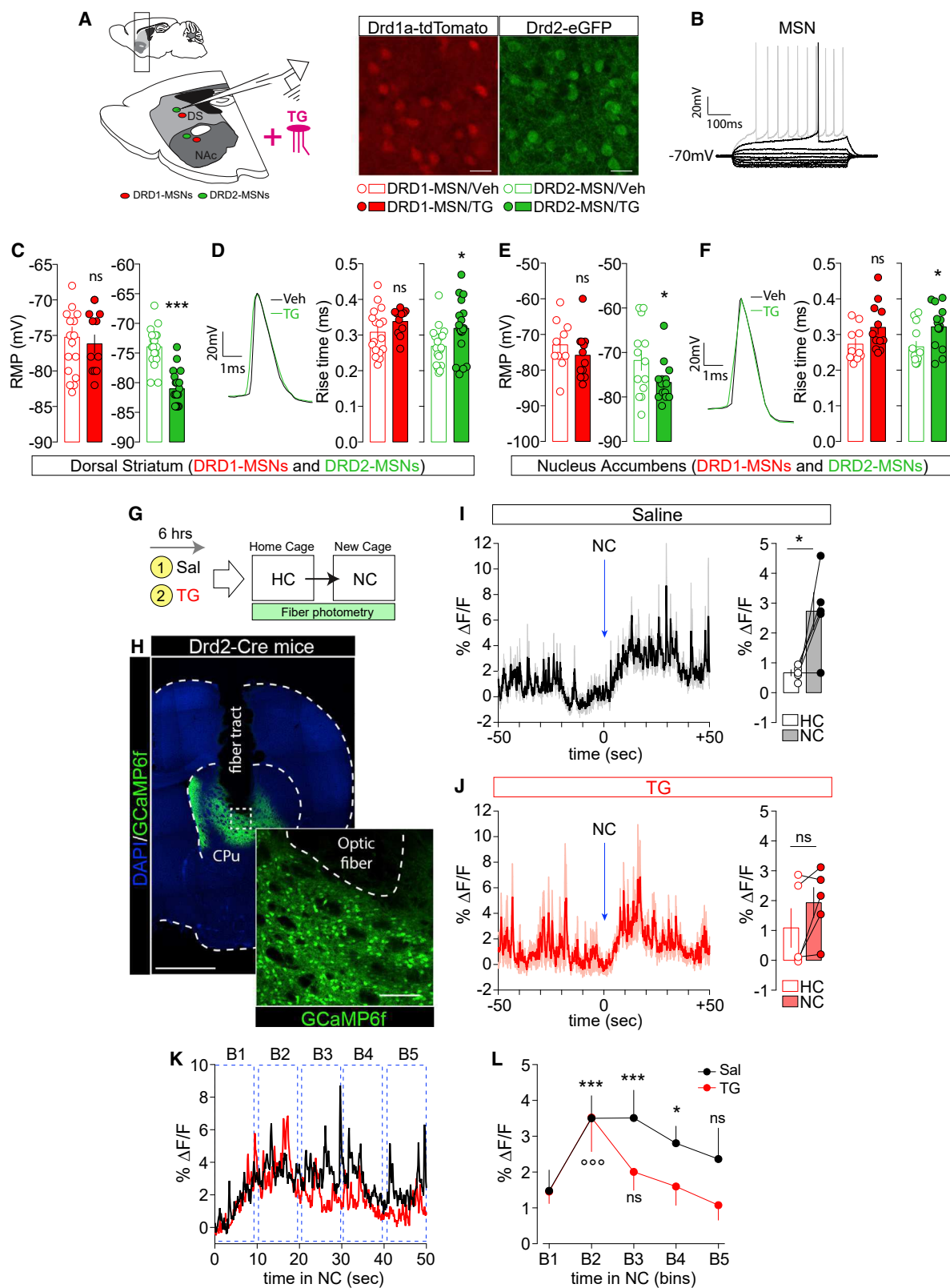


**Figure 3. Nutritional TGs Gate D2R-MSNs Activity *In Vitro* and *In Vivo***

(A) Drawing indicates the sagittal slice used for whole-cell patch-clamp recording in *Drd1a*-tdTomato and *Drd2*-eGFP transgenic mice. Confocal images show DRD1-MSNs (red) and DRD2-MSNs (green) in the dorsal striatum (DS). Scale bars: 50  $\mu$ m.

(legend continued on next page)

(Figure 4B). This decrease in DA-neurons activity is consistent with the decreased phosphorylation of TH (Lindgren et al., 2001) observed in the striatum of TG-perfused mice (Figures 2A and 2B). These data show that sustained increase in TGs can reduce VTA DA-neurons activity in anaesthetized mice.

Next, we compared the consequences of acute and long-term (6 h) brain TG delivery on amphetamine-induced hyperlocomotion. Our results reveal that acute brain TG delivery decreased amphetamine-induced hyperlocomotion to a similar extent as observed following long-term brain TG delivery (Figures 4C and 4D). This result supports a mechanism by which central actions of TGs occur first in striatal structures, with later impacts on midbrain DA neurons.

### Central Triglycerides Can Act as Reinforcer and Modulate Food-Seeking Behavior

Given the time-dependent modulatory action of TGs onto pre- and post-synaptic components of the reward system, we next explored the rewarding properties of short- and long-term brain TG delivery. We first used the conditioned-place preference test (CPP) to assess whether short-term brain TG delivery could be reinforcing. We used an unbiased apparatus-biased protocol in which animals were first allowed to explore two defined compartments (pre-test) before enduring 8 days of conditioning sessions. The least-preferred compartment (pre-test) was associated with a 1-h brain TG delivery or saline control (Figure 5A). Following conditioning, animals were allowed to explore the two compartments during the post-test session. Importantly, the pre- and post-test sessions were performed without any central TG administration, so that exploration of the complete apparatus was not affected by the treatment. Animals conditioned with 1-h brain TG delivery displayed a significant preference for the compartment associated with TGs (Figure 5B). This result shows that central detection of TGs can serve as a direct positive reinforcer.

In order to further establish the reinforcing properties of centrally delivered TGs, we next used a self-administration paradigm for intracarotid TG delivery. Since self-administration paradigms generally require rapid perception of the reinforcer, we used a faster delivery of central TGs (each active nose-poke led to delivery of 10  $\mu$ l intracarotid TG bolus over 60 s compared to 0.1–0.3  $\mu$ l/min prior). We first verified that the increased rate of TG perfusion did not perturb general brain hemodynamics. Using photoacoustic imaging, we found no

major modifications in oxygenated hemoglobin and cerebral blood flow at rates of 1 or 10  $\mu$ l/min (data not shown). Thus, animals were placed in operant chambers equipped with two nose-poke holes, the active hole being paired with central infusion of TGs or saline, and the inactive hole without consequence (Figure 5C). While TG and saline groups exhibited equivalent discrimination scores, mice receiving TG infusions performed more active nose-poke visits in both food-sated and 24-h-deprived conditions compared to control animals (Figure 5D). These similar results observed in both sated and food-deprived conditions support the idea that the positive reinforcement of centrally detected TGs is not solely contingent on caloric demands.

Overall, both the CPP and self-administration data support the hypothesis that short-term TGs can act in the brain to support positive reinforcement.

Because plasma TGs typically rise during the post-prandial period, TGs acting on the mesocorticolimbic circuit may modify food perception and/or reward properties; for example, serving as a satiating or reward signal. Therefore, we next explored whether brain TG delivery could modulate the reinforcing properties of high-fat high-sucrose diet (HFHS). We used a CPP paradigm similar to that described above, but each conditioning chamber was now paired to either regular or HFHS food. Before food-conditioning sessions, mice received long-term brain TG delivery or saline (6 h) (Figure 5E). Compared to controls, TG-mice spent significantly more time in the HFHS-paired compartment during the post-test session (Figure 5F). Notably, in this experiment, mice were not food-restricted in order to maximize reward-driven food preference over metabolic demands, perhaps explaining why HFHS pairing was not sufficient to drive a strong place preference in saline-perfused mice. Interestingly, cumulative HFHS consumption during the conditioning session was significantly greater in saline group compared to TG group (5.51 kcal  $\pm$  0.34 versus 4.30  $\pm$  0.34 in saline versus TG group respectively,  $p = 0.0039$ ), thereby indicating that the TG group required less palatable food to produce a CPP. These results reveal that central TG sensing potentiates the reinforcing aspects of palatable food and, since a stronger preference was achieved with less HFHS consumption, brain TG delivery may enhance reward sensitivity by lowering the threshold at which reward and/or satiety is achieved.

(B–F) Characteristic voltage response of a striatal MSN to a series of 500-ms current pulses with current steps increasing by 10 pA (B). Resting membrane potential (RMP) in dorso-striatal (C) and accumbal (E) DRD1- (red) and DRD2-MSNs (green) with (TG) and without (Veh) bath-applied triolein (4  $\mu$ M). Statistics: \* $p < 0.05$  and \*\*\* $p < 0.001$  TG versus Veh. Traces indicate one action potential in striatal (D) and accumbal (F) DRD2-MSNs with (TG, green trace) and without (Veh, black trace) bath-applied triolein. Histograms indicate the action potential rise time (in ms) in dorso-striatal (D) and accumbal (F) DRD1- (red) and DRD2-MSNs (green). Statistics: \* $p < 0.05$  TG versus Veh.

(G) Drawing indicates the behavioral protocol used to elicit environmental stimuli-evoked calcium transients. HC = homecage, NC = new cage.

(H) Confocal image of cell-type-specific expression of GCaMP6f in the dorsal striatum of Drd2-Cre mice. Scale bars: 1 mm (mosaic, DAPI/GCaMP6f) and 150  $\mu$ m (inset, GCaMP6f).

(I and J) Dynamics of averaged calcium traces in saline- (I) and TG-perfused mice (J) over a period of 100 s (50 s in the home cage and 50 s in the new cage). Time 0 corresponds to the moment when the animal is placed in the new cage (NC). Data are represented as the percent change in fluorescence over the mean fluorescence (%  $\Delta F/F$ ). Histograms (I and J) indicate the overall %  $\Delta F/F$  in both home cage (HC) and new cage (NC) in saline- and TG-perfused mice. Statistics: \* $p < 0.05$  NC versus HC in saline-perfused mice.

(K) Temporal dynamics of evoked calcium events (%  $\Delta F/F$ ) during exploration of the new cage (0 to 50 s) with temporal subdivision in bins (B1 to B5, each bin is 10 s).

(L) Curves show averaged calcium signals (saline in black and TG in red) during each temporal bin. Statistics: \*\*\* $p < 0.001$  (B2 and B3 versus B1 for saline-mice), \* $p < 0.05$  (B4 versus B1 for saline-mice) and °°° $p < 0.001$  (B2 versus B1 for TG-mice). For statistical details, see Table S5.

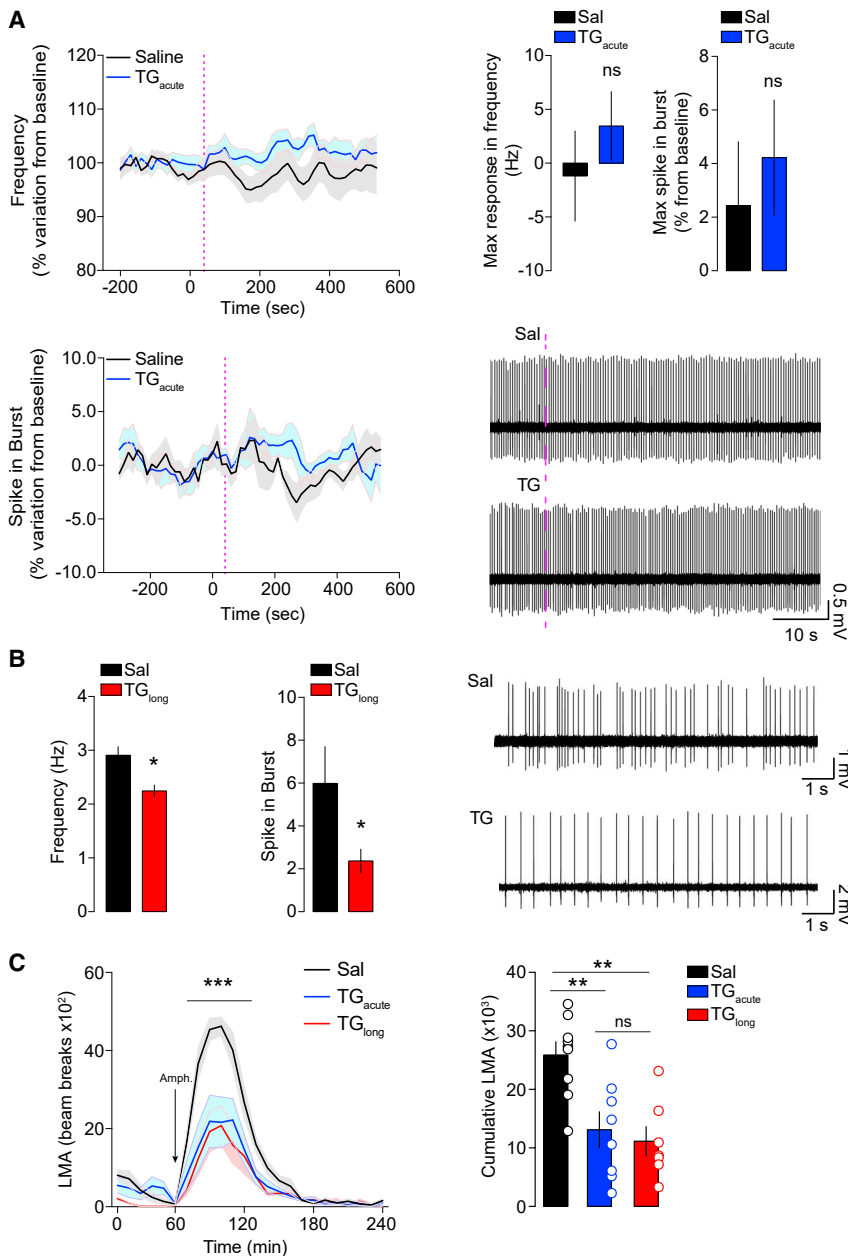


### Figure 4. Centrally Delivered TGs Exert a Time- and Dose-Dependent Action on Pre-Synaptic Dopaminergic Neurons

(A) Data show single-cell extracellular electrophysiological recordings of dopaminergic neurons in the VTA of anaesthetized animals receiving Sal or TG injections through the carotid artery, with a follow-up of neuronal frequency and firing for 10 min. Histograms display the maximum frequency recorded for each neuron and the maximal spike in burst.

(B) Animals were centrally infused for 6 h with Sal or TG then anaesthetized, and dopaminergic neurons of the VTA were recorded. Data show representative traces of DA-neurons recordings as well as average frequencies and spikes observed during the recordings. Statistics: \* $p < 0.05$  TG<sub>long</sub> versus Sal for each independent comparison.

(C) Locomotor activity (LMA) profile and cumulative LMA following amphetamine (3 mg/kg) administration in animals receiving brain delivery of acute TG ( $n = 8$ ), long-term TG ( $n = 7$ ), or saline ( $n = 9$ ). Statistics: C \*\*\* $p < 0.001$  (TG<sub>acute</sub> or TG<sub>long</sub> versus Sal groups), D \*\* $p < 0.01$  (TG<sub>acute</sub> or TG<sub>long</sub> versus Sal groups). For statistical details, see Table S5.

received a 6-h brain TG delivery or saline prior to access to the palatable drink (Figure 5H). TG-perfused mice reduced binge consumption by ~50% (Figure 5H). This result shows that central TGs can oppose compulsive eating in line with a putative role for TG sensing in enhancing reward sensitivity such that animals require less palatable food. It is also possible that increased TGs may counterbalance the decreased *Lpl* expression in NAC.

### Lpl Gates DRD2-MSN Excitability and Reward-Associated Behavior

Using complementary approaches, we next explored neuronal TG sensing by directly manipulating LPL in the reward system. Using virally Cre-delivered strategy, we deleted *Lpl* in the ventral striatum (NAC) and the midbrain (VTA) of *Lpl*<sup>lox/lox</sup>

Finally, we explored how brain TG delivery modulates food consumption in a context of altered reward sensitivity in a compulsive binge-eating behavioral model (Kessler et al., 2016; Valdivia et al., 2015). *Ad libitum*-fed mice were exposed to intermittent, restricted access (1 h/day) to fat and sugar mixture (10% sucrose and 20% lipids from Intralipid) for 10 days. In that setting, mice rapidly maximized their intake during the first 5 days (Figure 5H). We first observed that a 9-day binge regimen led to a significant decrease in *Lpl* mRNA expression in the NAC but not in the dorsal striatum (Figure 5G), while no major modifications in *Drd1* or *Drd2* mRNA expressions were detected in either region. We then tested whether centrally delivered TGs were able to modulate binge-like behavior. On day 10 of our binge protocol, mice

mice (Figures 5I and 5M). Disruption of *Lpl* in the nucleus accumbens (NAC-*Lpl*<sup>Δ/Δ</sup>; or control mice referred to as NAC-*Lpl*<sup>lox/lox</sup>) led to increased operant responding for food rewards (Figures 5J–5L), as previously reported (Cansell et al., 2014). Strikingly, disruption of *Lpl* in the midbrain (VTA-*Lpl*<sup>Δ/Δ</sup>, Figure 5M) had the opposite consequence and decreased operant performance for food-pellet rewards (Figures 5N–5P). These results suggest that TG sensing may play opposite roles at pre- and post-synaptic sides of the dopamine circuit, underscoring the complexity of bimodal actions of TGs on the reward system.

Since our data point toward DRD2 neurons as privileged targets for TG sensing, and since TGs reduce DRD2-MSNs excitability, we investigated the functional role of LPL as a regulatory component of DRD2-expressing neurons activity. We

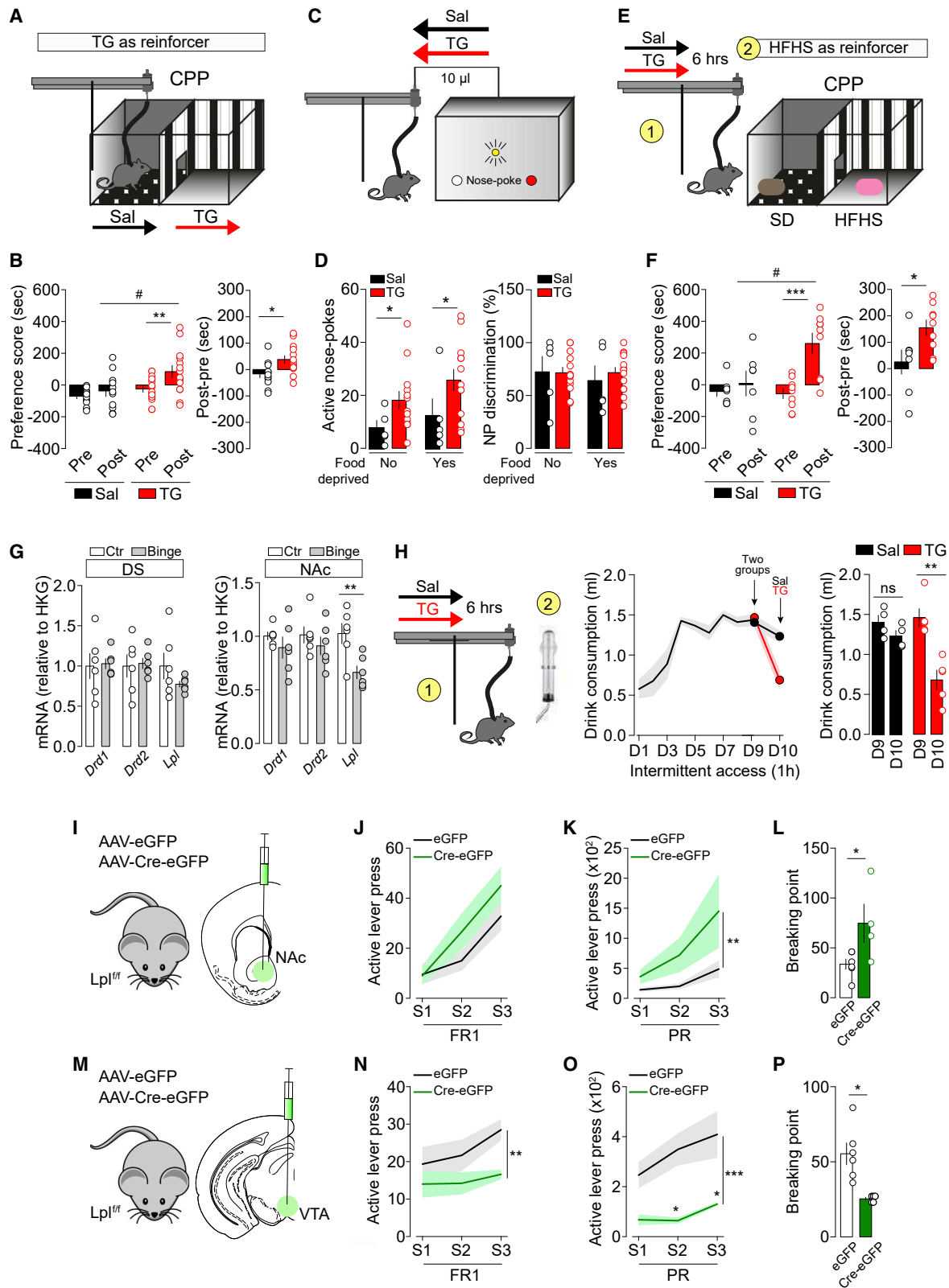


**Figure 5. Central TG Sensing Is Reinforcing and Modulates Food Reward**

(A) Experimental design of the conditioned place preference (CPP) using central TG delivery as reinforcer. On day 1, animals are put in the middle of the cage and explore freely the two compartments of the apparatus for 15 min. The following days of conditioning sessions (1 h each session), the animals learn to associate

(legend continued on next page)

generated mice lacking the *Lpl* gene in DRD2 neurons by crossing *Drd2<sup>Cre/+</sup>* and *Lpl<sup>lox/lox</sup>* mice (*Drd2<sup>Cre/+</sup>::Lpl<sup>+/+</sup>* and *Drd2<sup>Cre/+</sup>::Lpl<sup>fl/fl</sup>*) (Figure 6A). These mice then received intra-NAc injections of AAV-hSyn-DIO-mCherry to allow Cre-dependent expression of mCherry in DRD2-expressing neurons. *Ex vivo* patch-clamp recordings were then performed on NAc mCherry-positive DRD2-MSNs to measure neuronal modifications triggered by the cell-type-specific deletion of *Lpl* in DRD2 neurons (Figures 6B and 6C). Analysis of active and passive membrane properties (for complete list, see Table S4) revealed that *Lpl* deletion in DRD2-MSNs did not significantly affect resting membrane potential (Figure 6D) or rheobase (Figure 6E), but was associated with a slight increase in membrane resistance (Figure 6F) and a close-to-significant ( $p = 0.051$ ) increase in the delay to first spike (Figure 6G). These results point toward an increased excitability of DRD2-MSNs in *Drd2<sup>Cre/+</sup>::Lpl<sup>fl/fl</sup>* animals.

Given the critical role of the excitatory glutamatergic cortico-accumbal transmission in controlling the activity of MSNs, we also recorded the occurrence of spiking activity of DRD2-MSNs following stimulation of mPFC fibers (Figure 6B). We found that deletion of *Lpl* in DRD2 neurons was associated with an increased probability to spike in response to cortical stimulation (Figure 6H), further revealing that if their ability to sense TGs is impaired, these neurons become more excitable.

We next explored the behavioral consequences of *Lpl* deletion in DRD2 neurons. Conditional knockout (KO) mice (*Drd2<sup>Cre/+</sup>::Lpl<sup>fl/fl</sup>*, cKO) displayed enhanced reward-seeking behavior and increased breaking-point values in operant conditioning (Figures 6I and 6J), altered amphetamine-induced locomotor activity (Figure 6K), and decreased cataleptic response to haloperidol (Figure 6L) compared to control mice. Overall, these results clearly establish a key role for LPL onto DRD2-expressing cells as a modulator of DRD2-MSNs excitability and DA-dependent behaviors.

Finally, we tested the integrity of TG sensing in *Drd2<sup>Cre/+</sup>::Lpl<sup>fl/fl</sup>* mice. Control (*Drd2<sup>Cre/+</sup>::Lpl<sup>+/+</sup>*) and cKO (*Drd2<sup>Cre/+</sup>::Lpl<sup>fl/fl</sup>*) mice were equipped with intracarotid catheter and perfused with saline or TGs. We found that the decreased locomotor response

caused by brain TG delivery was absent in cKO mice (Figure 6M), thereby further strengthening the close association between LPL in DRD2 neurons and the ability to detect TGs.

Importantly, genetic deletion of *Lpl* in DRD2 neurons did not alter spontaneous locomotor activity, body composition, or basal metabolic efficiency (Figure S6), thus indicating that the above-mentioned behaviors are not the confounding consequence of altered homeostatic functions. Altogether, these data establish a key role for LPL in DRD2-expressing cells in gating DRD2-MSNs excitability and DRD2/DA-dependent behaviors.

### In Humans, Post-Prandial Change in Tryglycerides Are Associated with Brain Responses to Food Cues and Depends on DRD2-Associated Genotype

We reasoned that since *Lpl* mRNA share overlapping expression in common territories of the rodent and human brain (Figure S1), post-prandial TGs might influence brain responses to food cues in these regions in a DRD2-dependent manner. We used fMRI to measure BOLD responses to food and non-food aromas in fasted versus fed nutritional states and tested whether differential responses were associated with post-prandial TGs (Figure 7A) in participants carrying a copy of the A1 allele of the Taq1A polymorphism (Festled et al., 2010; Stice et al., 2008), a mutation known to robustly affect DRD2 signaling (Barnard et al., 2009; Jönsson et al., 1999; Ritchie and Noble, 2003).

We first tested whether internal states or perceptual ratings of the odors differed depending on odorant (food versus non-food), nutritional conditions (hungry, fixed meal, or *ad libitum* meal), or genotype (A1+ versus A1-). Effects are summarized in Figure S7. Next, the effect of time, nutritional condition, genotype, and the interaction among these factors on the concentrations of TGs were tested using a mixed-design ANOVA. There was a significant effect of condition ( $F_{(2,54)} = 8.00$ ,  $p = 0.001$ ) and an interaction between nutritional condition and time ( $F_{(2,54)} = 10.15$ ,  $p < 0.001$ ) on TG levels, but no three-way interactions. *Post hoc* analysis revealed that TG levels significantly increased following the meal in the fixed meal condition

one or another compartment to central delivery of saline (Sal) or triglycerides (TG). After 8 days of conditioning (four sessions in each compartment), animals freely explore the two compartments for 15 min. The analysis considers the time spent in the brain TG delivery- or saline-associated compartments before and after conditioning.

(B) Preference score of CPP and difference of time spent in the conditioned sites between post-test and pre-test between reinforced and non-reinforced compartments. Statistics: \*\* $p < 0.01$  TG-Post versus TG-Pre, # $p < 0.05$  TG-Post versus Sal-Post, post-pre (\* $p < 0.05$  TG<sub>Post-Pre</sub> versus Sal<sub>Post-Pre</sub>).

(C) Experimental design of nose-poke-associated self-administration of saline (Sal,  $n = 5$ ) or triglycerides (TG,  $n = 13$ ).

(D) Active nose-pokes and nose-pokes discrimination (distinction between active and inactive nose-pokes, %) are shown in *ad libitum* and food-deprived conditions. Statistics: \* $p < 0.05$  TG versus Sal.

(E) Experimental design of CPP using palatable food as reinforcer in mice that received a 6-h central perfusion of saline (Sal,  $n = 8$ ) or triglycerides (TG,  $n = 9$ ) prior to conditioning sessions. Conditioning consisted in 8 alternated sessions with standard diet (SD) or high-fat high-sucrose (HFHS) diet access for 30 min.

(F) Preference score of CPP and difference of time spent in the palatable food-associated compartment between post-test and pre-test between reinforced and non-reinforced compartment. Statistics: preference score (\*\*\* $p < 0.001$  TG-Post versus TG-Pre, # $p < 0.05$  TG-Post versus Sal-Post), post-pre (\* $p < 0.05$  TG<sub>Post-Pre</sub> versus Sal<sub>Post-Pre</sub>).

(G) Quantitative real-time PCR quantifications of *Lpl*, *Drd1*, *Drd2* mRNA abundance relative to HKG in dorsal striatum and NAc of mice after a binge-eating protocol consisting of 9 days of intermittent access to palatable fat and sugar beverage. Statistics: NAc *Lpl* \*\* $p < 0.01$  binge versus control mice.

(H) When animal reached a maximum intake (day 9, D9), on D10 they were centrally infused (6 h) with saline (Sal,  $n = 4$ ) or triglycerides (TG,  $n = 5$ ) before the intermittent access to the palatable drink. The graph shows palatable drink consumption on D9 and D10, prior or after central infusions respectively. Statistics: \*\* $p < 0.01$  D10 versus D9 for TG-group.

(I-P) Viral delivery of eGFP or Cre-eGFP in the NAc (I, NAc-*Lpl<sup>lox/lox</sup>*,  $n = 6$ ; NAc-*Lpl<sup>Δ/Δ</sup>*,  $n = 4$ ) or the VTA (M, VTA-*Lpl<sup>lox/lox</sup>*,  $n = 6$ ; VTA-*Lpl<sup>Δ/Δ</sup>*,  $n = 5$ ) of *Lpl<sup>lox/lox</sup>* mice. Operant behavior performances in fixed ratio sessions (J and N, FR1: fixed ratio 1), progressive ratio (K and O, PR: progressive ratio), and breaking point (L and P). Statistics: \*\*\* $p < 0.001$ , \*\* $p < 0.01$  and \* $p < 0.05$ . For statistical details, see Table S5.



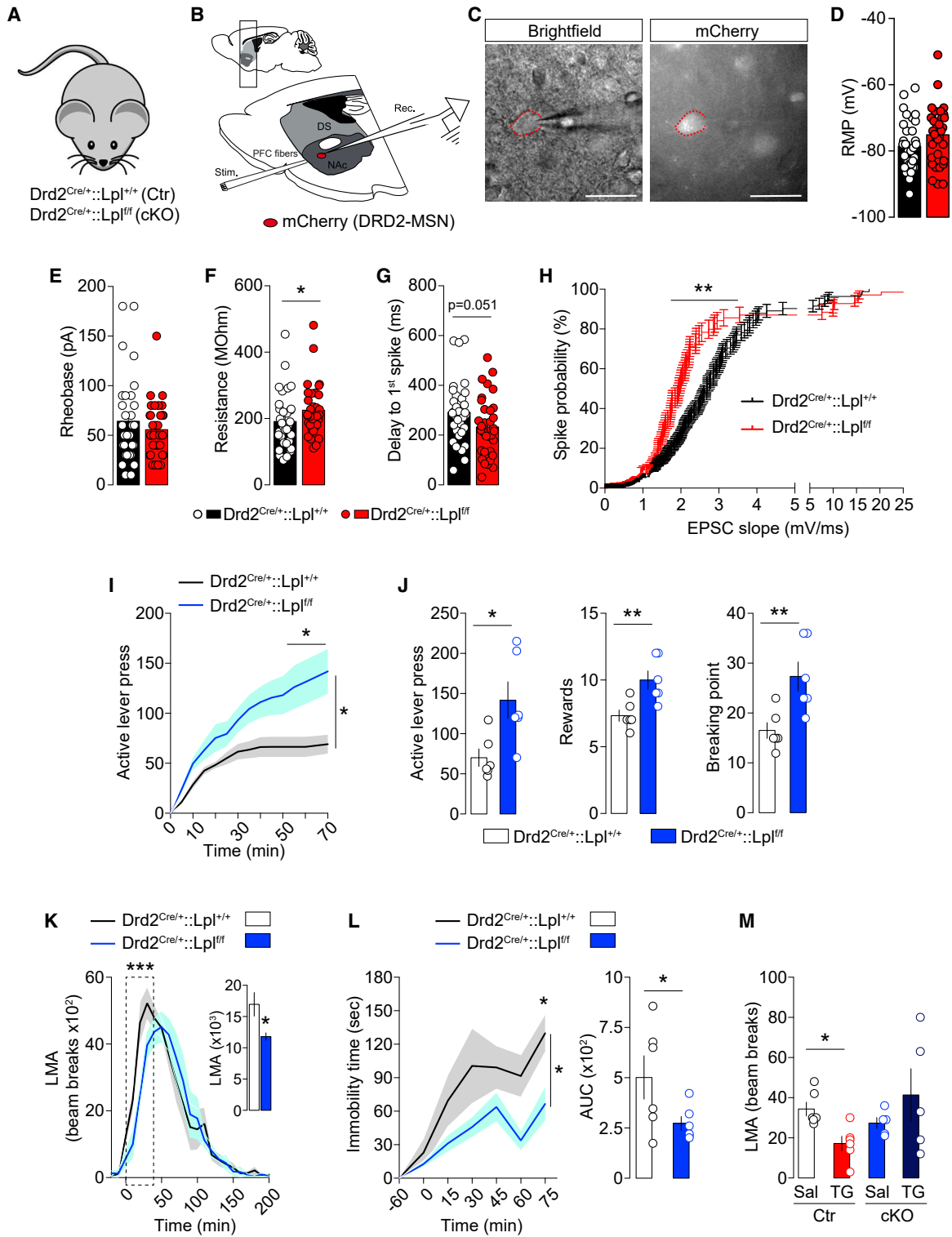


**Figure 6. Lpl in DRD2 Neurons Controls Excitability and Behavioral Responses to DA-Associated Behaviors**

(A) Genetic strategy to delete Lpl from DRD2 neurons:  $Drd2^{Cre/+};Lpl^{+/+}$  mice (control, Ctr) and  $Drd2^{Cre/+};Lpl^{fl/fl}$  mice (cKO).

(B) Drawing illustrates the sagittal slice used for cortical stimulation and patch-clamp recordings in  $Drd2^{Cre/+};Lpl^{+/+}$  and  $Drd2^{Cre/+};Lpl^{fl/fl}$  transgenic mice, all injected with an AAV-hSyn-DIO-mCherry in the nucleus accumbens (NAc).

(legend continued on next page)

( $p = 0.009$ ), but not in the *ad libitum* meal condition ( $p = 0.08$ ), and that TG levels decreased over the course of the hungry session ( $p = 0.001$ ) (Figure S7). Since plasma TG excursion was only significant in the fixed meal condition, we focused our imaging analysis on the data from the fixed neuroimaging scan.

TG excursion was unrelated to BOLD responses to food versus non-food odors in hungry versus fixed scans in the regions of interest (ROIs) or at the whole-brain level for the group considered as a whole (i.e., collapsing across genotype). However, when genotype (A1+ versus A1-) was included in the model, a significant effect emerged in the vmPFC at 3, 56, and -5 ( $p = 0.04$  following family-wise error [FWE] correction for multiple comparisons across the number of voxels in the ROI and Bonferroni correction for the number of ROI tests performed) (Figure 7B). Importantly, this analysis included FFAs, glucose and insulin excursions, as well as fullness, hunger, and liking ratings as covariates, indicating that post-prandial TGs are unique modulators of vmPFC activity in this experimental setting. Further analysis of independent effects in the A1- and A1+ groups revealed that this interaction arose from a significant positive association in A1+ at 0, 56, and -5 ( $p = 0.02$ ) and a weak non-significant negative association in A1- (Figure 7C). Note also that since the extent of TG excursions did not differ in A1+ versus A1-, this differential effect cannot be attributed to indirect effects of genotype on TG excursions, but rather should result from the effect of this gene variant on DRD2. Collectively, these data strongly support our hypothesis that in humans, circulating TGs are associated with brain response to food cues in the vmPFC in a DRD2-dependent manner.

## DISCUSSION

Excessive consumption of energy-dense food increases the vulnerability to develop uncontrolled craving, compulsive feeding, and ultimately excessive body weight gain (Kenny et al., 2013; Rothmund et al., 2007; Stice et al., 2008; Volkow et al., 2013). However, the possibility of a direct action of circulating TGs on key reward-encoding brain structures has been largely unappreciated. In this work, we demonstrate that circulating post-prandial TGs exert an integrative and multimodal regulatory action onto pre- and post-synaptic neurons of the reward system through an LPL-dependent mechanism.

### Bridging Dietary Inputs to Reward Circuit through Triglyceride Sensing

The presence of TG lipases, including LPL, is required to allow cellular FFA entry upon TG hydrolysis. Here, we provide evidence that in the MCL, *Lpl* mRNA expressions exhibit a certain degree of enrichment in midbrain VTA DA neurons and

striatal DRD1- and DRD2-MSNs (Figures 1A, 1B, and S1), which confer upon these cells the ability to detect and metabolize TGs.

Using brain-specific intracarotid TG delivery, we discovered that nutritional TGs exert time- and dose-dependent actions on VTA DA neurons (long-term exposure) and post-synaptic striatal neurons (short- and long-term exposures). Central TG delivery preferentially dampened DRD2- but not DRD1-related cellular and behavioral responses. This privileged sensitivity of DRD2-expressing neurons to TGs was further supported by (1) *ex vivo*-patch clamp recordings revealing that bath-applied TGs reduced the excitability of DRD2- but not DRD1-MSNs (Figures 3 and S4), and genetic deletion of *Lpl* in DRD2-expressing cells resulted in increased neuronal excitability (Figures 6A–6H); and by (2) *in vivo* recordings where brain TG delivery decreased striatal DRD2-neurons calcium events to environmental cues (Figures 3G–3L).

Consistent with a role for TG sensing in the reward circuit, central TG delivery produced reinforcement on its own (Figures 5A–5D) and modulated the reinforcing aspects of palatable food (Figures 5E–5H). Using loss of function approaches we determined that the action of centrally detected TG relies, at least in part, on the integrity of the LPL in the DA reward circuit and onto DRD2-expressing cells (Figures 5 and 6). Altogether, these results unravel a functional role of LPL-mediated TG sensing onto DRD2 neurons (pre- and post-synaptic neurons) in the control of DA-associated behaviors.

Interestingly, the fact that brain TG delivery could produce positive reinforcement (CPP paradigm) while decreasing motivational drive to lever press for food rewards may appear contradictory at first glance. However, several studies have reported a similar degree of dichotomy between appetitive learning and motivational drive following manipulation of DRD2-MSNs. Indeed, pharmacological inhibition of DRD2-MSNs by activation of DRD2-coupled Gi signaling was sufficient to promote place preference (White et al., 1991). On the other hand, inhibition of DRD2-MSNs in striatal and accumbal regions was reported to decrease motivation to work for food rewards (Soares-Cunha et al., 2016, 2018) while increasing reward reinforcement (Carvalho Poyraz et al., 2016; Durieux et al., 2009; O'Neal et al., 2019).

Hence, the ability of TGs to directly decrease DRD2-MSNs excitability in both dorsal striatum and NAc (Figures 3 and S4) would be predicted to similarly produce two opposite outputs of increased reinforcement and decreased motivation. Whether this mechanism might be instrumental in establishing a set-point of “reward-like sensitivity” is indeed a matter of debate, although it is tempting to speculate that acute and/or chronic brain exposure to circulating TGs could be a fundamental mechanism by which excessive high-fat food intake or

(C–G) Representative picture of a recorded mCherry-positive accumbal DRD2-MSN (C). Histograms indicate the resting membrane potential (RMP in mV, D), the rheobase (in pA, E), the membrane resistance (in MOhm, F) and the delay to first spike (in ms, G) of mCherry-positive accumbal MSNs in both genotypes, *Drd2<sup>Cre/+</sup>::Lpl<sup>+/+</sup>* (black) versus *Drd2<sup>Cre/+</sup>::Lpl<sup>fl/fl</sup>* (red) transgenic mice.

(H) Curves indicate the probability to trigger a spike (in %) in recorded mCherry-positive MSNs following increasing cortical stimulations in both genotypes. Statistics: \* $p < 0.05$  and \*\* $p < 0.01$  *Drd2<sup>Cre/+</sup>::Lpl<sup>fl/fl</sup>* versus *Drd2<sup>Cre/+</sup>::Lpl<sup>+/+</sup>* mice.

(I and J) Operant conditioning performances of *Drd2<sup>Cre/+</sup>::Lpl<sup>+/+</sup>* and *Drd2<sup>Cre/+</sup>::Lpl<sup>fl/fl</sup>* transgenic mice during the active lever press (I). Cumulative active lever press, rewards, and breaking point (J). Statistics: \* $p < 0.05$  *Drd2<sup>Cre/+</sup>::Lpl<sup>fl/fl</sup>* versus *Drd2<sup>Cre/+</sup>::Lpl<sup>+/+</sup>* mice.

(K–M) Locomotor activity (LMA) to amphetamine (3 mg/kg) (K), immobility response to the DRD2 antagonist haloperidol (0.5 mg/kg) during the catalepsy test (L), and spontaneous 6-h locomotor activity (LMA) following central saline or TG delivery (M). Statistics: \*\*\* $p < 0.001$ , \* $p < 0.05$ . For statistical details, see Table S5.

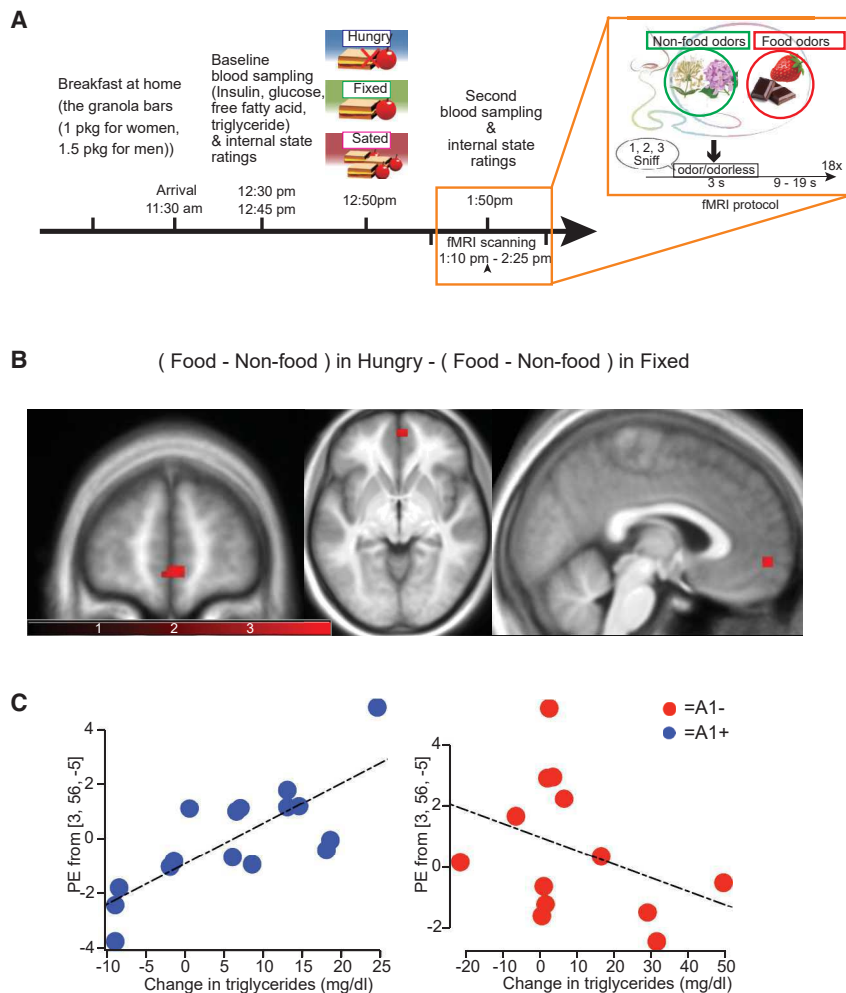


**Figure 7. Post-Prandial TGs Control Human Brain Responses to Food Cues in a DRD2-Dependent Manner (TaqIA Polymorphism Carriers)**

(A) Experimental protocol for fMRI studies and odor stimulation.

(B) Blood oxygen level dependent (BOLD) responses to food versus non-food odors in Hungry versus Fixed conditions correlates with meal-induced changes in TG differentially as a function of genotype in the ventromedial prefrontal cortex (vmPFC) at 3, 56, and -5 ( $p = 0.04$  following FWE correction for comparison across the voxels in the vmPFC ROI and subsequent Bonferroni correction for the number of ROIs tested. Note that this analysis includes all covariates (changes in plasma glucose, insulin and FFA, and changes in internal state and odor perception ratings).

(C) Scatterplots showing the correlation with plasma TG and A1/A2 genotype in the vmPFC. For statistical details, see Table S5.

like system that may drive to a stop signal. This is in line with our results which show (1) reduced cellular excitability of D2R-MSNs following brief application of TG, (2) no *in vivo* impairment in DA-neurons firing following acute delivery of TGs, and (3) reduced *in vivo* firing of DA neurons following long-term delivery of TG.

It is worth mentioning that our current data cannot clearly and univoqually discriminate between a time- and dose-dependent action of TG directly onto VTA neurons and the hypothetical inhibition of midbrain DA neurons as the consequence of inhibited DRD2-projecting neurons to

the VP. Further studies are required to fully depict the exact sequences of such dynamically orchestrated mechanisms.

### Molecular Mechanisms and Physiological Implication of Trygliceride-Mediated Modulation of DRD2 Neurons

We found that central administration of TGs dampens key striatal molecular pathways, notably the MAPK-, mTOR-, and PKA-dependent pathways, indicative of reduced DA-coupled signaling (Figures 2A and 2B). These molecular events are supported by our patch-clamp recordings, which reveal cell-type-specific TG-induced alterations of active and passive membrane properties exclusively in DRD2-MSNs (Figures 3 and S4). In fact, since these signaling pathways play a strong modulatory role on glutamate receptors, voltage-dependent ion channels and transcription factors (for review, see Nagai et al., 2016 and Surmeier et al., 2007), it is formally possible that their modifications, as observed following TG delivery, will alter DRD2-MSNs excitability and neuronal responses. Another non-mutually exclusive hypothesis—by which TGs could modulate DRD2-neurons activity—could involve  $\beta$ -arrestin, mediating DRD2 internalization, and activation of the protein kinase B/Akt,  $\beta$ -arrestin 2, and protein phosphatase 2 (PP2A) complex (Beaulieu et al., 2005). This complex has been shown to operate in striatal DRD2-MSNs

obesity-associated hypertriglyceridemia would ultimately lower reward sensitivity and drive compulsive feeding. Another non-mutually exclusive possibility would be that, as observed in our experiments, sustained TG exposure, by decreasing midbrain DA-neurons firing, would consequentially decrease motivational drive and reward sensitivity. Hence, a common general mechanism would be that, by binding to DRD1 (Gs-coupled receptors) and DRD2 (Gi-coupled receptors) receptors, dopamine would lead to activation of DRD1-MSNs and inhibition of DRD2-MSNs, in virtue of their segregated cellular location. By inhibiting DRD2-MSNs, TGs may then result in promoting positive reinforcement, thus bypassing a direct dopamine action onto DRD2-MSNs. These dopamine- and TG-dependent mechanisms may occur on the same cell-types (DRD2-MSNs for instance), but through potentially distinct molecular and metabolic paths, which at the moment remain unknown.

The inhibition of DA-neurons firing within the VTA following long-term TG perfusion agrees with this scenario. For instance, disinhibition of GABAergic ventral pallidal (VP) neurons by TG-inhibited GABAergic DRD2-MSNs would ultimately drive to inhibition of VTA DA neurons as previously described in the literature (Soares-Cunha et al., 2016, 2018). As a consequence, this anatomic-functional interconnectivity would then lead to a backup-

independently of cAMP pathway through the Akt/GSK-3 $\beta$  cascade (Beaulieu et al., 2004, 2005). In our hands, brain TG delivery activated  $\beta$ -arrestin signaling pathway as indicated by the phosphorylation status of both Akt<sup>Ser473</sup> and GSK3 $\beta$ <sup>Ser9</sup> (Figures 2E and 2F) while decreasing canonical DRD2 signaling. Hence, centrally detected TGs could exert a biased action onto DRD2 neurons by decreasing canonical GPCR-coupled cascades while enhancing DRD2- $\beta$ -arrestin signaling.

Of note, synthetic  $\beta$ -arrestin-biased DRD2 ligands (Allen et al., 2011) were shown to oppose amphetamine-induced hyperlocomotion to a similar extent to what we observed with brain TG delivery (Allen et al., 2011).

Altogether, these molecular and cellular adaptations, beside supporting the reduced cellular excitability of DRD2 neurons, also provide a mechanistic explanation for the altered behavioral responses to amphetamine and other dopaminergic agents (raclopride and haloperidol) in the presence of increased circulating TGs.

Importantly, the action of TGs onto DRD2-MSNs activity will inevitably mitigate DRD2-MSNs responsiveness to various inputs including those mediated by DA through its DRD2 receptors.

This is specifically enlightening given that defective DRD2 abundance and signaling has been repeatedly associated with conditions of hypertriglyceridemia such as high-fat feeding or obesity (Adams et al., 2015; Alsiö et al., 2010; Guo et al., 2014; Kenny et al., 2013; Volkow et al., 2008). Interestingly, while these studies provide focal attention onto DRD2, none of them preclude the possibility that DRD2-cells activity would be impaired in pathophysiological conditions associated with overfeeding. In that view, it remains formally possible that the consequence onto DRD2 signaling (i.e., internalization or recycling) might ultimately be the result of altered DRD2-MSNs neural activity.

Finally, we also describe that, in humans, the effect of the meal on brain responses to food versus non-food aromas in the vmPFC was directly proportional to post-prandial TG excursions and that this effect was genotype-dependent, with A1+ carriers showing a strong positive association between changes in BOLD responses and changes in TGs. On the contrary, non-carriers (A1-) exhibited a weak non-significant negative correlation (Figure 7). We did not observe effects in the ventral striatum. However, BOLD responses reflect the activity evoked by inputs into a region, which is consistent with the intimate connection of the vmPFC with the reward system. Importantly, our model co-varied out the potential confounding effects of meal-induced changes in FFAs, glucose, and insulin, as well as changes in ratings of internal state or odor perception. We can therefore conclude that in humans, as we report in mice, post-prandial TGs regulate brain responses to food cues in a DRD2-dependent manner.

In conclusion, this study reveals that dietary TGs can directly alter MCL circuit functions and influence reward reinforcement and food-seeking behaviors by gating DRD2-MSNs activity and associated DA-encoded behaviors. Although we do not fully decipher the precise causal molecular events underlying how dietary lipids gate DRD2-neurons activity, this work provides, for the first time, converging evidence at the behavioral, cellular, molecular, and translational level to directly bridge dietary TG inputs to DRD2 neurons as well as DA-encoded reward events.

These integrative and orchestrated events might provide new avenues for therapeutic innovations in compulsive feeding and obesity-associated pathologies.

### Limitations of Study

Although our study reveals a novel cell-type-specific action of nutritional TGs on the reward system, the molecular underpinnings by which TGs gate the activity of DRD2-expressing neurons remain to be depicted. Indeed, such mechanisms could encompass intracellular lipids metabolism or byproducts signaling, direct membrane G-coupled fatty acid receptors or generation of bioactive lipids. Another functional limitation is the use of DRD2-Cre-mediated Lpl knockdown, which does not fully allow us to specify the involvement of midbrain or striatal DRD2-expressing neuron in TG sensing, as Lpl deletion will occur in both structures. In addition, when trying to isolate the role of post-prandial lipids, we did not consider other energy-related signals that could potentially participate in the overall response. For lipidomic analysis, we chose not to perform multiple comparison analysis, but all raw lipidomic data are available in the Supplemental Information. In our translational approach, the study carried out in humans shows a correlation between brain responses to food cues and plasma TG levels; however, we could not directly test for other reward-driven behaviors nor assess for the isolated action of TGs following intravenous perfusion.

### STAR★METHODS

Detailed methods are provided in the online version of this paper and include the following:

- KEY RESOURCES TABLE
- LEAD CONTACT AND MATERIALS AVAILABILITY
- EXPERIMENTAL MODEL AND SUBJECT DETAILS
  - Animals Studies
  - Human Studies
- METHOD DETAILS
  - Catheter Implantation and Infusion Procedures
  - Viral Production
  - Stereotaxic Procedures
  - Ex Vivo Whole-Cell Patch-Clamp Electrophysiology
  - Measurement of Locomotor Activity
  - Pharmacological Manipulations
  - Catalepsy Test
  - Operant Conditioning System
  - Nose-Poke Operandum for TG Self-administration
  - Conditioned Place Preference (CPP)
  - Binge Feeding Experiment
  - Fiber Photometry and Data Analysis
  - Fluorescent *In Situ* Hybridization
  - Lipidomics
  - In Vivo Electrophysiological Recordings
  - Tissue Preparation and Immunofluorescence
  - Western Blotting
  - Doppler Imaging
  - Whole-Brain c-Fos Immunostaining
  - Isolation of Total RNA and Quantitative RT-PCR
  - Metabolic Efficiency Analysis

- Human Methods and Analysis
- Participant Recruitment
- Genotyping for TaqI A1 Polymorphism
- Food and Non-food Odor Stimuli
- Stimulus Delivery
- Experimental Procedures
- Training Session
- fMRI Scanning Sessions
- fMRI Data Acquisition
- Data Analysis (Human Studies)
- **QUANTIFICATION AND STATISTICAL ANALYSIS**
  - Statistical Analysis
- **DATA AND CODE AVAILABILITY**

#### SUPPLEMENTAL INFORMATION

Supplemental Information can be found online at <https://doi.org/10.1016/j.cmet.2020.02.010>.

#### ACKNOWLEDGMENTS

We acknowledge funding support from the Centre National de la Recherche Scientifique (CNRS), the Université de Paris, the Bayerische Forschungsstiftung, the Allen Foundation Inc., the Nutricia Research Foundation, the Groupe Lipides et Nutrition (GLN), the Modern Diet and Physiology Research Center (MDPRC), the National Research Agency ANR SVSE 1 2011: "Lipobrain" and ANR-16-CE14-0026 "Fat4Brain," and the Fondation pour la Recherche Médicale (FRM). T.S.H. was supported from NIH-NIDA R01DA036612, VA I01BX003759, and a pilot project through P30DK063491. S.L., M.M., M.D.M., E.M., and C.B. received support from the FRM. We thank Rim Hassouna, Ewout Foppen, Anne Sophie Delbes, Raphaël GP Denis, Florence Darlot, Fabien Ducrocq, and Ossie Quehenberger for valuable technical and conceptual help. We thank Dr. Emmanuel Valjent for sharing *Drd2-Cre* mice for the initial experiment. We thank Olja Kacanski for administrative support, Isabelle Le Parco, Ludovic Maingault, Angélique Dauvin, Aurélie Djemat, Florianne Michel, Maggy Boa, and Daniel Quintas for animals' care and Sabria Allithi for genotyping. We acknowledge the technical platform Functional and Physiological Exploration (FPE) of the Université de Paris, BFA, UMR 8251, CNRS, Paris, France; the viral production facility of the UMR INSERM 1089; and the animal core facility "Buffon" of the Université de Paris/Institut Jacques Monod.

#### AUTHOR CONTRIBUTIONS

C.B. designed, performed, and analyzed most of the experiments. E.M. performed transcriptomic meta-analyses and behavioral and molecular studies. E.P., M.D.M., M.M., S.P., S.L., X.F., and L.V. performed and analyzed *ex vivo* patch-clamp electrophysiology. D.M.S., Y.N., M.S., and X.S.D. performed human studies and data analysis. S.T., F.M., and P.F. performed and analyzed *in vivo* electrophysiology recordings. M.A.S. performed the RNA-seq and lipidomics studies. J.C. helped with surgery and behavioral procedures. C. Morel helped perform western blots and dissections. C. Martin designed and performed doppler imaging and fiber photometry experiments. M.C. and S.C. designed and performed self-administration experiments. J.H.-S. and C.C.S. performed the iDISCO analysis. M.H.T., G.G., T.S.H., and S.H.L. secured funding. T.S.H. and D.M.S. provided scientific guidance and experimental design. S.H.L. and G.G. supervised the whole project, interpreted the data, and wrote the manuscript with contribution from all coauthors.

#### DECLARATION OF INTERESTS

The authors declare no competing interests.

Received: April 23, 2019

Revised: December 16, 2019

Accepted: February 13, 2020

Published: March 5, 2020

#### REFERENCES

- Adams, W.K., Sussman, J.L., Kaur, S., D'souza, A.M., Kieffer, T.J., and Winstanley, C.A. (2015). Long-term, calorie-restricted intake of a high-fat diet in rats reduces impulse control and ventral striatal D2 receptor signalling - two markers of addiction vulnerability. *Eur. J. Neurosci.* **42**, 3095–3104.
- Allen, J.A., Yost, J.M., Setola, V., Chen, X., Sassano, M.F., Chen, M., Peterson, S., Yadav, P.N., Huang, X.P., Feng, B., et al. (2011). Discovery of  $\beta$ -arrestin-biased dopamine D2 ligands for probing signal transduction pathways essential for antipsychotic efficacy. *Proc. Natl. Acad. Sci. USA* **108**, 18488–18493.
- Alsö, J., Olszewski, P.K., Norbäck, A.H., Gunnarsson, Z.E., Levine, A.S., Pickering, C., and Schiöth, H.B. (2010). Dopamine D1 receptor gene expression decreases in the nucleus accumbens upon long-term exposure to palatable food and differs depending on diet-induced obesity phenotype in rats. *Neuroscience* **171**, 779–787.
- Arch, J.R., Hislop, D., Wang, S.J., and Speakman, J.R. (2006). Some mathematical and technical issues in the measurement and interpretation of open-circuit indirect calorimetry in small animals. *Int. J. Obes.* **30**, 1322–1331.
- Babbs, R.K., Sun, X., Felsted, J., Chouinard-Decorte, F., Veldhuizen, M.G., and Small, D.M. (2013). Decreased caudate response to milkshake is associated with higher body mass index and greater impulsivity. *Physiol. Behav.* **121**, 103–111.
- Baik, J.H. (2013). Dopamine signaling in reward-related behaviors. *Front. Neural Circuits* **7**, 152.
- Banks, W.A., Farr, S.A., Salameh, T.S., Niehoff, M.L., Rhea, E.M., Morley, J.E., Hanson, A.J., Hansen, K.M., and Craft, S. (2018). Triglycerides cross the blood-brain barrier and induce central leptin and insulin receptor resistance. *Int. J. Obes.* **42**, 391–397.
- Barnard, N.D., Noble, E.P., Ritchie, T., Cohen, J., Jenkins, D.J., Turner-McGrievy, G., Gloede, L., Green, A.A., and Ferdowsian, H. (2009). D2 dopamine receptor Taq1A polymorphism, body weight, and dietary intake in type 2 diabetes. *Nutrition* **25**, 58–65.
- Beaulieu, J.M., Sotnikova, T.D., Yao, W.D., Kockeritz, L., Woodgett, J.R., Gainetdinov, R.R., and Caron, M.G. (2004). Lithium antagonizes dopamine-dependent behaviors mediated by an AKT/glycogen synthase kinase 3 signaling cascade. *Proc. Natl. Acad. Sci. USA* **101**, 5099–5104.
- Bartoshuk, L.M., Duffy, V.B., Green, B.G., Hoffman, H.J., Ko, C.W., Lucchina, L.A., Marks, L.E., Snyder, D.J., and Weiffenbach, J.M. (2004). Valid across-group comparisons with labeled scales: the gLMS versus magnitude matching. *Physiol. Behav.* **82**, 109–114.
- Beaulieu, J.M., and Gainetdinov, R.R. (2011). The physiology, signaling, and pharmacology of dopamine receptors. *Pharmacol. Rev.* **63**, 182–217.
- Beaulieu, J.M., Sotnikova, T.D., Marion, S., Lefkowitz, R.J., Gainetdinov, R.R., and Caron, M.G. (2005). An Akt/beta-arrestin 2/PP2A signaling complex mediates dopaminergic neurotransmission and behavior. *Cell* **122**, 261–273.
- Ben-Zeev, O., Doolittle, M.H., Singh, N., Chang, C.H., and Schotz, M.C. (1990). Synthesis and regulation of lipoprotein lipase in the hippocampus. *J. Lipid Res.* **31**, 1307–1313.
- Berland, C., Cansell, C., Hnasko, T.S., Magnan, C., and Luquet, S. (2016). Dietary triglycerides as signaling molecules that influence reward and motivation. *Curr. Opin. Behav. Sci.* **9**, 126–135.
- Berridge, K.C. (2009). 'Liking' and 'wanting' food rewards: brain substrates and roles in eating disorders. *Physiol. Behav.* **97**, 537–550.
- Bertran-Gonzalez, J., Bosch, C., Maroteaux, M., Matamalas, M., Hervé, D., Valjent, E., and Girault, J.A. (2008). Opposing patterns of signaling activation in dopamine D1 and D2 receptor-expressing striatal neurons in response to cocaine and haloperidol. *J. Neurosci.* **28**, 5671–5685.
- Bessesen, D.H., Richards, C.L., Etienne, J., Goers, J.W., and Eckel, R.H. (1993). Spinal cord of the rat contains more lipoprotein lipase than other brain regions. *J. Lipid Res.* **34**, 229–238.
- Cansell, C., Castel, J., Denis, R.G., Rouch, C., Delbes, A.S., Martinez, S., Mestivier, D., Finan, B., Maldonado-Aviles, J.G., Rijnsburger, M., et al. (2014). Dietary triglycerides act on mesolimbic structures to regulate the

- rewarding and motivational aspects of feeding. *Mol. Psychiatry* 19, 1095–1105.
- Carvalho Poyraz, F., Holzner, E., Bailey, M.R., Meszaros, J., Kenney, L., Kheirbek, M.A., Balsam, P.D., and Kellendonk, C. (2016). Decreasing Striatopallidal Pathway Function Enhances Motivation by Energizing the Initiation of Goal-Directed Action. *J. Neurosci.* 36, 5988–6001.
- Cui, G., Jun, S.B., Jin, X., Pham, M.D., Vogel, S.S., Lovinger, D.M., and Costa, R.M. (2013). Concurrent activation of striatal direct and indirect pathways during action initiation. *Nature* 494, 238–242.
- Dallman, M.F., Pecoraro, N.C., and la Fleur, S.E. (2005). Chronic stress and comfort foods: self-medication and abdominal obesity. *Brain Behav. Immun.* 19, 275–280.
- Davis, J.F., Tracy, A.L., Schurdak, J.D., Tschop, M.H., Lipton, J.W., Clegg, D.J., and Benoit, S.C. (2008). Exposure to elevated levels of dietary fat attenuates psychostimulant reward and mesolimbic dopamine turnover in the rat. *Behav. neurosci.* 122, 1257–1263.
- Di Chiara, G., and Imperato, A. (1988). Drugs abused by humans preferentially increase synaptic dopamine concentrations in the mesolimbic system of freely moving rats. *Proc. Natl. Acad. Sci. USA* 85, 5274–5278.
- Doyle, J.P., Dougherty, J.D., Heiman, M., Schmidt, E.F., Stevens, T.R., Ma, G., Bupp, S., Shrestha, P., Shah, R.D., Doughy, M.L., et al. (2008). Application of a translational profiling approach for the comparative analysis of CNS cell types. *Cell* 135, 749–762.
- Durieux, P.F., Bearzatto, B., Guiducci, S., Buch, T., Waisman, A., Zoli, M., Schiffmann, S.N., and de Kerchove d'Exaerde, A. (2009). D2R striatopallidal neurons inhibit both locomotor and drug reward processes. *Nat. Neurosci.* 12, 393–395.
- Eckel, R.H., and Robbins, R.J. (1984). Lipoprotein lipase is produced, regulated, and functional in rat brain. *Proc. Natl. Acad. Sci. USA* 81, 7604–7607.
- Epstein, L.H., Temple, J.L., Neaderhiser, B.J., Salis, R.J., Erbe, R.W., and Leddy, J.J. (2007). Food reinforcement, the dopamine D-2 receptor genotype, and energy intake in obese and nonobese humans. *Behav. Neurosci.* 121, 877–886.
- Even, P.C., and Nadkarni, N.A. (2012). Indirect calorimetry in laboratory mice and rats: principles, practical considerations, interpretation and perspectives. *Am. J. Physiol. Regul. Integr. Comp. Physiol.* 303, R459–R476.
- Farr, S.A., Yamada, K.A., Butterfield, D.A., Abdul, H.M., Xu, L., Miller, N.E., Banks, W.A., and Morley, J.E. (2008). Obesity and hypertriglyceridemia produce cognitive impairment. *Endocrinology* 149, 2628–2636.
- Felsted, J.A., Ren, X., Chouinard-Decorte, F., and Small, D.M. (2010). Genetically determined differences in brain response to a primary food reward. *J. Neurosci.* 30, 2428–2432.
- Fino, E., Glowinski, J., and Venance, L. (2007). Effects of acute dopamine depletion on the electrophysiological properties of striatal neurons. *Neurosci. Res.* 58, 305–316.
- Frank, M.J., and Fossella, J.A. (2011). Neurogenetics and pharmacology of learning, motivation, and cognition. *Neuropsychopharmacology* 36, 133–152.
- Gerfen, C.R., Engber, T.M., Mahan, L.C., Susel, Z., Chase, T.N., Monsma, F.J., Jr., and Sibley, D.R. (1990). D1 and D2 dopamine receptor-regulated gene expression of striatonigral and striatopallidal neurons. *Science* 250, 1429–1432.
- Goldberg, I.J., Soprano, D.R., Wyatt, M.L., Vanni, T.M., Kirchgessner, T.G., and Schotz, M.C. (1989). Localization of lipoprotein lipase mRNA in selected rat tissues. *J. Lipid Res.* 30, 1569–1577.
- Green, B.G., Dalton, P., Cowart, B., Shaffer, G., Rankin, K., and Higgins, J. (1996). Evaluating the 'Labeled Magnitude Scale' for measuring sensations of taste and smell. *Chem Senses* 21, 323–334.
- Guo, J., Simmons, W.K., Herscovitch, P., Martin, A., and Hall, K.D. (2014). Striatal dopamine D2-like receptor correlation patterns with human obesity and opportunistic eating behavior. *Mol. Psychiatry* 19, 1078–1084.
- Hawrylycz, M.J., Lein, E.S., Guillozet-Bongaarts, A.L., Shen, E.H., Ng, L., Miller, J.A., van de Lagemaat, L.N., Smith, K.A., Ebbert, A., Riley, Z.L., et al. (2012). An anatomically comprehensive atlas of the adult human brain transcriptome. *Nature* 489, 391–399.
- Hryhorczuk, C., Florea, M., Rodaros, D., Poirier, I., Daneault, C., Des Rosiers, C., Arvanitogiannis, A., Alquier, T., and Fulton, S. (2016). Dampened Mesolimbic Dopamine Function and Signaling by Saturated but not Monounsaturated Dietary Lipids. *Neuropsychopharmacology* 41, 811–821.
- Jackson, D.M., and Westlind-Danielsson, A. (1994). Dopamine receptors: molecular biology, biochemistry and behavioural aspects. *Pharmacol. Ther.* 64, 291–370.
- Johnson, P.M., and Kenny, P.J. (2010). Dopamine D2 receptors in addiction-like reward dysfunction and compulsive eating in obese rats. *Nat. Neurosci.* 13, 635–641.
- Johnson, B.N., and Sobel, N. (2007). Methods for building an olfactometer with known concentration outcomes. *J. Neurosci. Methods* 160, 231–245.
- Jönsson, E.G., Nöthen, M.M., Grünhage, F., Farde, L., Nakashima, Y., Propping, P., and Sedvall, G.C. (1999). Polymorphisms in the dopamine D2 receptor gene and their relationships to striatal dopamine receptor density of healthy volunteers. *Mol. Psychiatry* 4, 290–296.
- Karatayev, O., Gaysinskaya, V., Chang, G.Q., and Leibowitz, S.F. (2009). Circulating triglycerides after a high-fat meal: predictor of increased caloric intake, orexigenic peptide expression, and dietary obesity. *Brain Res.* 1298, 111–122.
- Kenny, P.J., Voren, G., and Johnson, P.M. (2013). Dopamine D2 receptors and striatopallidal transmission in addiction and obesity. *Curr. Opin. Neurobiol.* 23, 535–538.
- Kessler, R.M., Hutson, P.H., Herman, B.K., and Potenza, M.N. (2016). The neurobiological basis of binge-eating disorder. *Neurosci. Biobehav. Rev.* 63, 223–238.
- Lein, E.S., Hawrylycz, M.J., Ao, N., Ayres, M., Bensinger, A., Bernard, A., Boe, A.F., Boguski, M.S., Brockway, K.S., Byrnes, E.J., et al. (2007). Genome-wide atlas of gene expression in the adult mouse brain. *Nature* 445, 168–176.
- Lerner, T.N., Shilyansky, C., Davidson, T.J., Evans, K.E., Beier, K.T., Zalocusky, K.A., Crow, A.K., Malenka, R.C., Luo, L., Tomer, R., and Deisseroth, K. (2015). Intact-Brain Analyses Reveal Distinct Information Carried by SNc Dopamine Subcircuits. *Cell* 162, 635–647.
- Lew, J.Y., Garcia-Espana, A., Lee, K.Y., Carr, K.D., Goldstein, M., Haycock, J.W., and Meller, E. (1999). Increased site-specific phosphorylation of tyrosine hydroxylase accompanies stimulation of enzymatic activity induced by cessation of dopamine neuronal activity. *Mol. Pharmacol.* 55, 202–209.
- Lim, J., Wood, A., and Green, B.G. (2009). Derivation and evaluation of a labeled hedonic scale. *Chem Senses* 34, 739–751.
- Lindgren, N., Xu, Z.Q., Herrera-Marschitz, M., Haycock, J., Hökfelt, T., and Fisone, G. (2001). Dopamine D(2) receptors regulate tyrosine hydroxylase activity and phosphorylation at Ser40 in rat striatum. *Eur. J. Neurosci.* 13, 773–780.
- Michaelides, M., Thanos, P.K., Volkow, N.D., and Wang, G.J. (2012). Dopamine-related frontostriatal abnormalities in obesity and binge-eating disorder: emerging evidence for developmental psychopathology. *Int. Rev. Psychiatry* 24, 211–218.
- Nagai, T., Yoshimoto, J., Kannon, T., Kuroda, K., and Kaibuchi, K. (2016). Phosphorylation Signals in Striatal Medium Spiny Neurons. *Trends Pharmacol. Sci.* 37, 858–871.
- O'Neal, T.J., Nooney, M.N., Thien, K., and Ferguson, S.M. (2019). Chemo-genetic modulation of accumbens direct or indirect pathways bidirectionally alters reinstatement of heroin-seeking in high- but not low-risk rats. *Neuropsychopharmacology*. <https://doi.org/10.1038/s41386-019-0571-9>.
- Paradis, E., Clavel, S., Julien, P., Murthy, M.R., de Bilbao, F., Arsenijevic, D., Giannakopoulos, P., Vallet, P., and Richard, D. (2004). Lipoprotein lipase and endothelial lipase expression in mouse brain: regional distribution and selective induction following kainic acid-induced lesion and focal cerebral ischemia. *Neurobiol. Dis.* 15, 312–325.
- G. Paxinos, and K. Franklin, eds. (2003). *The Mouse Brain in Stereotaxic Coordinates: Compact, Second Edition* (Gulf Professional Publishing).
- Peterson, S.M., Pack, T.F., Wilkins, A.D., Urs, N.M., Urban, D.J., Bass, C.E., Lichtarge, O., and Caron, M.G. (2015). Elucidation of G-protein and  $\beta$ -arrestin

- functional selectivity at the dopamine D2 receptor. *Proc. Natl. Acad. Sci. USA* **112**, 7097–7102.
- Picard, A., Rouch, C., Kassis, N., Moullé, V.S., Croizier, S., Denis, R.G., Castel, J., Coant, N., Davis, K., Clegg, D.J., et al. (2013). Hippocampal lipoprotein lipase regulates energy balance in rodents. *Mol. Metab.* **3**, 167–176.
- Renier, N., Wu, Z., Simon, D.J., Yang, J., Ariel, P., and Tessier-Lavigne, M. (2014). iDISCO: a simple, rapid method to immunolabel large tissue samples for volume imaging. *Cell* **159**, 896–910.
- Ritchie, T., and Noble, E.P. (2003). Association of seven polymorphisms of the D2 dopamine receptor gene with brain receptor-binding characteristics. *Neurochem. Res.* **28**, 73–82.
- Rothmund, Y., Preuschhof, C., Bohner, G., Bauknecht, H.C., Klingebiel, R., Flor, H., and Klapp, B.F. (2007). Differential activation of the dorsal striatum by high-calorie visual food stimuli in obese individuals. *Neuroimage* **37**, 410–421.
- Ruge, T., Hodson, L., Cheeseman, J., Dennis, A.L., Fielding, B.A., Humphreys, S.M., Frayn, K.N., and Karpe, F. (2009). Fasted to fed trafficking of Fatty acids in human adipose tissue reveals a novel regulatory step for enhanced fat storage. *J. Clin. Endocrinol. Metab.* **94**, 1781–1788.
- Salinas, C.B.G., Lu, T.T., Gabery, S., Marstal, K., Alanentalo, T., Mercer, A.J., Cornea, A., Conradsen, K., Hecksher-Sørensen, J., Dahl, A.B., et al. (2018). Integrated Brain Atlas for Unbiased Mapping of Nervous System Effects Following Liraglutide Treatment. *Sci. Rep.* **8**, 10310.
- Salvatore, M.F., Calipari, E.S., and Jones, S.R. (2016). Regulation of Tyrosine Hydroxylase Expression and Phosphorylation in Dopamine Transporter-Deficient Mice. *ACS Chem. Neurosci.* **7**, 941–951.
- Schultz, W. (2016). Dopamine reward prediction-error signalling: a two-component response. *Nat. Rev. Neurosci.* **17**, 183–195.
- Soares-Cunha, C., Coimbra, B., David-Pereira, A., Borges, S., Pinto, L., Costa, P., Sousa, N., and Rodrigues, A.J. (2016). Activation of D2 dopamine receptor-expressing neurons in the nucleus accumbens increases motivation. *Nat. Commun.* **7**, 11829.
- Soares-Cunha, C., Coimbra, B., Domingues, A.V., Vasconcelos, N., Sousa, N., and Rodrigues, A.J. (2018). Nucleus Accumbens Microcircuit Underlying D2-MSN-Driven Increase in Motivation. *eNeuro* **5**, <https://doi.org/10.1523/ENEURO.0386-18.2018>.
- South, T., and Huang, X.F. (2008). High-fat diet exposure increases dopamine D2 receptor and decreases dopamine transporter receptor binding density in the nucleus accumbens and caudate putamen of mice. *Neurochem. Res.* **33**, 598–605.
- Stice, E., Burger, K.S., and Yokum, S. (2015). Reward Region Responsivity Predicts Future Weight Gain and Moderating Effects of the Taq1A Allele. *J. Neurosci.* **35**, 10316–10324.
- Stice, E., Spoor, S., Bohon, C., and Small, D.M. (2008). Relation between obesity and blunted striatal response to food is moderated by Taq1A A1 allele. *Science* **322**, 449–452.
- Stice, E., Spoor, S., Bohon, C., Veldhuizen, M.G., and Small, D.M. (2008). Relation of reward from food intake and anticipated food intake to obesity: a functional magnetic resonance imaging study. *J. Abnorm. Psychol.* **117**, 924–935.
- Sun, X., Veldhuizen, M.G., Wray, A.E., de Araujo, I.E., Sherwin, R.S., Sinha, R., and Small, D.M. (2014). The neural signature of satiation is associated with ghrelin response and triglyceride metabolism. *Physiol. Behav.* **136**, 63–73.
- Sun, X., Kroemer, N.B., Veldhuizen, M.G., Babbs, A.E., de Araujo, I.E., Gitelman, D.R., Sherwin, R.S., Sinha, R., and Small, D.M. (2015). Basolateral amygdala response to food cues in the absence of hunger is associated with weight gain susceptibility. *J. Neurosci.* **35**, 7964–7976.
- Surmeier, D.J., Ding, J., Day, M., Wang, Z., and Shen, W. (2007). D1 and D2 dopamine-receptor modulation of striatal glutamatergic signaling in striatal medium spiny neurons. *Trends Neurosci.* **30**, 228–235.
- Valdivia, S., Cornejo, M.P., Reynaldo, M., De Francesco, P.N., and Perello, M. (2015). Escalation in high fat intake in a binge eating model differentially engages dopamine neurons of the ventral tegmental area and requires ghrelin signaling. *Psychoneuroendocrinology* **60**, 206–216.
- Volkow, N.D., Wang, G.J., Telang, F., Fowler, J.S., Thanos, P.K., Logan, J., Alexoff, D., Ding, Y.S., Wong, C., Ma, Y., and Pradhan, K. (2008). Low dopamine striatal D2 receptors are associated with prefrontal metabolism in obese subjects: possible contributing factors. *Neuroimage* **42**, 1537–1543.
- Volkow, N.D., Wang, G.J., Fowler, J.S., Tomasi, D., and Baler, R. (2012). Food and drug reward: overlapping circuits in human obesity and addiction. *Curr. Top. Behav. Neurosci.* **11**, 1–24.
- Volkow, N.D., Wang, G.J., Tomasi, D., and Baler, R.D. (2013). Obesity and addiction: neurobiological overlaps. *Obes. Rev.* **14**, 2–18.
- Vucetic, Z., and Reyes, T.M. (2010). Central dopaminergic circuitry controlling food intake and reward: implications for the regulation of obesity. *Wiley Interdiscip. Rev. Syst. Biol. Med.* **2**, 577–593.
- Wang, G.J., Volkow, N.D., Logan, J., Pappas, N.R., Wong, C.T., Zhu, W., Netusil, N., and Fowler, J.S. (2001). Brain dopamine and obesity. *Lancet* **357**, 354–357.
- Wang, H., Astarita, G., Taussig, M.D., Bharadwaj, K.G., DiPatrizio, N.V., Nave, K.A., Piomelli, D., Goldberg, I.J., and Eckel, R.H. (2011). Deficiency of lipoprotein lipase in neurons modifies the regulation of energy balance and leads to obesity. *Cell Metab.* **13**, 105–113.
- White, N.M., Packard, M.G., and Hiroi, N. (1991). Place conditioning with dopamine D1 and D2 agonists injected peripherally or into nucleus accumbens. *Psychopharmacology (Berl.)* **103**, 271–276.
- Wu, Q., and Palmiter, R.D. (2011). GABAergic signaling by AgRP neurons prevents anorexia via a melanocortin-independent mechanism. *Eur. J. Pharmacol.* **660**, 21–27.
- Zeisel, A., Hochgerner, H., Lonnerberg, P., Johnsson, A., Memic, F., van der Zwan, J., Haring, M., Braun, E., Borm, L.E., La Manno, G., et al. (2018). Molecular Architecture of the Mouse Nervous System. *Cell* **174**, 999–1014.e22.

## STAR★METHODS

## KEY RESOURCES TABLE

REAGENT or RESOURCE	SOURCE	IDENTIFIER
<b>Antibodies</b>		
rabbit anti-phospho-rpS6 Ser <sup>235/236</sup>	Cell Signaling Technology	RRID: AB_331679
rabbit anti-phospho-rpS6 Ser <sup>240/244</sup>	Cell Signaling Technology	RRID: AB_331682
Total rpS6	Cell Signaling Technology	RRID: AB_2238583
rabbit anti-phospho-p70S6K Thr <sup>421</sup> /Ser <sup>424</sup>	Cell Signaling Technology	RRID: AB_2265913
rabbit anti-phospho-p70S6KThr <sup>389</sup>	Cell Signaling Technology	RRID: AB_2269803
rabbit anti-phospho-ERK1/2	Cell Signaling Technology	RRID: AB_331646
rabbit anti-phospho-DARPP-32 Thr <sup>34</sup>	Cell Signaling Technology	RRID: AB_2797914
rabbit anti-phospho-TH Ser <sup>31</sup>	Millipore	RRID: AB_177464
rabbit anti-phospho-TH Ser <sup>40</sup>	Cell Signaling Technology	RRID: AB_2201522
mouse anti-TH	Millipore	RRID: AB_2313764
mouse $\beta$ -actin	Sigma	RRID: AB_476692
rabbit anti-phospho-Akt Ser <sup>473</sup>	Cell Signaling Technology	RRID: AB_2315049
rabbit anti-phospho-Akt Thr <sup>308</sup>	Cell Signaling Technology	RRID: AB_2629447
rabbit anti-phospho-GSK3 $\beta$ Ser <sup>9</sup>	Cell Signaling Technology	RRID: AB_2115201
goat anti-cFos	Santa Cruz Biotechnology	RRID: AB_2106783
rabbit anti-cFos	Synaptic Systems	RRID: AB_2231974
anti-rabbit Cy3 AffiniPure	Jackson ImmunoResearch	RRID: AB_2307443
anti-goat Dylight488	Vector labs	RRID: AB_2336400
IgG-HRP anti-mouse	Dako	RRID: AB_2636929
HRP anti-rabbit	Cell Signaling Technology	RRID: AB_2099233
Rabbit pAb anti c-Fos (Ab-5) (4-17)	Calbiochem	RRID: AB_2106755
anti-rabbit Cy5 AffiniPure	Jackson ImmunoResearch	RRID: AB_2338013
<b>Bacterial and Virus Strains</b>		
AAV 2/9 CBA.nls myc Cre.eGFP	The backbone was kindly provided by Richard Palmiter (Univ. of Washington, Seattle, USA).	N/A
AAV2/9.CMV.GFP	viral production facility of the UMR INSERM 1089 (Nantes, France)	N/A
pAAV.hSyn.eGFP.WPRE.bGH	gift from James M. Wilson	Addgene viral prep #105539-AAV9
pAAV.CMV.HI.eGFP-Cre.WPRE.SV40	a gift from James M. Wilson	Addgene viral prep #105545-AAV9
pAAV-hSyn-DIO-mCherry	a gift from Bryan Roth	Addgene viral prep #50459-AAV8
pAAV.Syn.Flex.GCaMP6f.WPRE.SV40	was a gift from Douglas Kim	Addgene viral prep #100833-AAV9
<b>Diets, food cues</b>		
Chow Diet	Safe diets	A03
High-Fat high-Sucrose	Brogaarden	31797 D12451 Research Diet
Sucrose pellets	TestDiet, Richmond, USA	N/A
Food odour 'chocolate cookie'	Bell Labs Flavors and Fragrances	6002335
Food odour 'strawberry and cream'	Bell Labs Flavors and Fragrances	6106524
Food odour 'honeysuckle'	Chey N-3 from Firmenich, Inc	039831
Food odour 'lilac'	Bell Labs Flavors and Fragrances	31731066
<b>Chemicals</b>		
Haloperidol hypochloride	Tocris	931
SKF38393 hydrobromide	Tocris	0922
Raclopride	Tocris	1810/10

(Continued on next page)



<b>Continued</b>		
REAGENT or RESOURCE	SOURCE	IDENTIFIER
Intralipid 20%	Fresenius Kabi France	N/A
Amphetamine	Sigma Aldrich	A5880
<b>Deposited Data</b>		
Lpl expression in the mouse human & brain was extracted from Brain Allen Institute <i>in situ</i> -hybridization and microarray data (Hawrylycz et al., 2012)	<a href="http://mouse.brain-map.org/">http://mouse.brain-map.org/</a>	N/A
Single Cell RNA seq analysis of Lpl enrichment was extracted from Zeisel et al., 2018	<a href="http://mousebrain.org/genesearch.html">http://mousebrain.org/genesearch.html</a>	N/A
RNA seq database for Lpl expression was extracted and reanalyzed from Doyle et al. (2008)	<a href="https://www.ncbi.nlm.nih.gov/pubmed/19013282">https://www.ncbi.nlm.nih.gov/pubmed/19013282</a> <a href="https://www.ncbi.nlm.nih.gov/geo/geo2r/?acc=GSE13379">https://www.ncbi.nlm.nih.gov/geo/geo2r/?acc=GSE13379</a>	N/A
<b>Experimental Models: Organisms/Strains</b>		
C57BL/6J mice	Janvier	N/A
B6.129S4-Lpltm1ljj/J (Lpl lox/lox mice)	Jackson Labs	<a href="https://www.jax.org/strain/006503">https://www.jax.org/strain/006503</a>
Tg(Drd2-cre)ER44Gsat/Mmucd mice	Gensat	<a href="http://www.informatics.jax.org/allele/MGI:3836635">http://www.informatics.jax.org/allele/MGI:3836635</a>
Tg(Drd2-EGFP)S118Gsat mice	Gensat	<a href="http://www.informatics.jax.org/allele/MGI:3843608">http://www.informatics.jax.org/allele/MGI:3843608</a>
Drd1a-Cre (Tg(Drd1-cre) EY262Gsat (to generate Drd1a-tdTomato)	Gensat	<a href="http://www.informatics.jax.org/allele/MGI:3836631">http://www.informatics.jax.org/allele/MGI:3836631</a>
Ai14(RCL-tdT)-D mice (to generate Drd1a-tdTomato)	Jackson Labs	<a href="https://www.jax.org/strain/007908">https://www.jax.org/strain/007908</a>
<b>Oligonucleotides</b>		
<i>Drd1</i> probe for RNA scope	RNAscope® Probe - form Advanced Cell Diagnostic	Mm-Drd1-C2 461901-C2
<i>Drd2</i> probe for RNA scope	RNAscope® Probe - Cell Diagnostic	Mm-Drd2-C3 406501-C3
<i>Lpl</i> for RNA scope	RNAscope® Probe - Cell Diagnostic	Mm-Lpl 402791
<i>Th</i> for RNA scope	RNAscope® Probe - Cell Diagnostic	Mm-Th-C3 317621-C3
TaqIA A1 forward 5'-CCCTTCCTGAGTGTCATCA-3')	Invitrogen	N/A
TaqIA A1 reverse 5'-CGGCTGGCCAAGTTGTCT-3')	Invitrogen	N/A
<i>Drd1</i> for RT-PCR quantification forward primer 5'-tctggttacctgatccctca-3'		N/A
<i>Drd1</i> for RT-PCR quantification reverse primer 5'-gcctcctccctcttcagg-3'		N/A
<i>Drd2</i> for RT-PCR quantification forward primer 5'-tgaacagcgagagaatgg-3'		N/A
<i>Drd2</i> for RT-PCR quantification reverse primer 5'-ctggtgctgacagcatctc-3'		N/A
<i>Lpl</i> RT-PCR quantification forward primer 5'-CACAGTGGCCGAGAGCGAGAA-3'		N/A
<i>Lpl</i> RT-PCR quantification reverse primer 5'-gctGAGTCCTTCCCTTCTGCAG-3'		N/A
Rpl19 HKG RT-PCR quantification forward primer 5'-GGCAGGCATATGGGCATA-3'		N/A
Rpl19 HKG RT-PCR quantification reverse primer 5'-GGCGGTCAATCTTCTGGATT-3'		N/A
<b>Software and Algorithms</b>		
Phenomaster TSE Systems GmbH		N/A
TSE system for operant behavior	TSE Systems GmbH	N/A

(Continued on next page)

**Continued**

REAGENT or RESOURCE	SOURCE	IDENTIFIER
Intellimaze	TSE Systems GmbH	N/A
GraphPad Prism 6	GraphPad Software	RRID:SCR_002798
R software	<a href="https://www.r-project.org">https://www.r-project.org</a>	N/A
ImageJ	NIH	RRID:SCR_003070
Imaris 7.6.5	Bitplane, Zurich, Switzerland	N/A
SPM8 software (Statistical Parametric Mapping, Wellcome Department of Imaging Neuroscience)	Wellcome Trust Centre for Neuroimaging	N/A
TDT Synapse Essentials Software	Tucker-Davis Technologies	N/A
MATLAB R2010b 7.11.0	The MathWorks, Inc.	N/A
NeuroSynth	<a href="http://www.neurosynth.org">www.neurosynth.org</a>	N/A
Other		
Mono Fiberoptic Cannula		MFC_400/460-0.48_5mm_ MF1.25_FLT

**LEAD CONTACT AND MATERIALS AVAILABILITY**

Further information and requests for resources and reagents should be directed to and will be fulfilled by the Lead Contact, Serge Luquet ([serge.luquet@univ-paris-diderot.fr](mailto:serge.luquet@univ-paris-diderot.fr))

This study did not generate new unique reagents.

**EXPERIMENTAL MODEL AND SUBJECT DETAILS****Animals Studies**

All animal experiments were performed with approval of the Animal Care Committee of the University Paris Diderot-Paris 7 (CEB-25-2016) or the University Bordeaux Committee (CEEA 50, number Apafis #3265-2015121811059640v6). Ten-week-old male mice C57BL/6J (25-30 g, Janvier, Le Genest St Isle, France) were individually housed in a room maintained at  $22 \pm 1^\circ\text{C}$  with light from 07:00 to 19:00 h. Regular chow diet (3 438 kcal/kg, protein 19%, lipid 5%, carbohydrates 55%, reference #U8959 version 63 Safe, Augy, France) and water were provided *ad libitum*, unless stated otherwise. All the behavioral experiments were performed during the light cycle, unless stated otherwise. All transgenic mouse lines were obtained from Jackson laboratory or Gensat/MMRRC: Lipoprotein lipase  $Lpl^{lox/lox}$  mice (strain B6.129S4-Lpltm11jg/J, n° 006503), *Drd2-Cre* mice (STOCK Tg(*Drd2-cre*)ER44Gsat/Mmucd), *Drd2-eGFP* mice (Tg(*Drd2-EGFP*)S118Gsat), *Drd1a-tdTomato* mice were generated by crossing *Drd1a-Cre* animals (Tg(*Drd1-cre*)EY262Gsat, Gensat/MMRRC) with Ai14(RCL-tdT)-D mice (B6;129S6-Gt(ROSA)26Sortm14(CAG-tdTomato)Hze/J, Jackson laboratory).

**Human Studies****Participant Recruitment**

Twenty-nine right-handed participants (age range 18 – 39, M = 26.80, SD = 5.49; BMI range 19.5 – 33.6, M = 23.94, SD = 3.86; male = 16, female = 13) were recruited from the greater New Haven area through the Yale University Interdisciplinary Research Consortium on Stress, Self-Control and Addiction (IRCSSA) P30 Subject's core as well as via flyer advertisement. Participants were screened over the phone to be less than 40 years of age, free of psychiatric disorders, eating disorders, current dieting behavior, alcoholism, use of tobacco or drugs other than alcohol, history of head injury with loss of consciousness, use of daily medication other than monophasic birth control, chemosensory impairments, lactose intolerance or food allergies. We did not impose a BMI upper-limit. Individuals were included so long as they felt comfortable while inserted in the scanner bore. Females provided the date of their last period to ensure that they were not scanned during menstruation or ovulation. All participants provided written informed consent at their first lab visit and the study was approved by the Yale Human Investigations Committee.

**METHOD DETAILS****Catheter Implantation and Infusion Procedures**

Surgery and central infusion were carried out as previously described (Cansell et al., 2014). Mice were anesthetized with isoflurane and received 10 mg/kg intraperitoneal injection (i.p.) of Buprécare® (Buprenorphine 0.3 mg) diluted 1/100 in NaCl 0.9% and 10 mg/kg of Ketofen® (Ketoprofen 100 mg) diluted 1/100 in NaCl 0.9%. Home-made catheters were inserted in the left carotid artery toward the brain. Importantly, no heparin was used during the study to prevent LPL activity changes. Catheters clotting was prevented through regular flushing with small volumes of NaCl 0.9%. Infusions started after a recovery period of 7–10 days by connecting

catheters to a swiveling infusion device allowing animals to move freely and access water and food. After 2 days of habituation to the infusion device, mice received NaCl 0.9% (Sal mice) or TG emulsion (TG mice) (Intralipid 20%) at a rate of 0.1–0.3  $\mu\text{L}/\text{min}$  for 6 h. At the end of the behavioral experiments, catheters viability was assessed with Etomidate injections.

### Viral Production

The plasmid CBA.nls myc Cre.eGFP expressing the myc-nls-Cre-GFP fusion protein (Wu and Palmiter, 2011) was kindly provided by Richard Palmiter (Univ. of Washington, Seattle, USA). Adeno-associated virus serotype 2/9 (AAV2/9) ( $6 \times 10^{11}$  genomes/mL and  $1.7 \times 10^8$  infectious units/ $\mu\text{L}$ ) was produced by the viral production facility of the UMR INSERM 1089 (Nantes, France). Control AAV2/9.CMV.GFP (titer  $\geq 1 \times 10^{11}$  vg/mL) was produced by the viral production facility of the UMR INSERM 1089 (Nantes, France). pAAV.CMV.HI.eGFP-Cre.WPRE.SV40 (titer  $\geq 1 \times 10^{12}$  vg/mL) was a gift from James M. Wilson (Addgene viral prep #105545-AAV9; <https://www.addgene.org/105545/>; RRID:Addgene\_105545). pAAV-hSyn-DIO-mCherry (titer  $\geq 1 \times 10^{13}$  vg/mL, working dilution 1:10) was a gift from Bryan Roth (Addgene plasmid #50459-AAV8; <http://www.addgene.org/50459/>; RRID:Addgene\_50459).

pAAV.Syn.Flex.GCaMP6f.WPRE.SV40 (titer  $\geq 1 \times 10^{13}$  vg/mL, working dilution 1:5) was a gift from Douglas Kim (Addgene viral prep #100833-AAV9; <https://www.addgene.org/100833/>; RRID:Addgene\_100833).

### Stereotaxic Procedures

Mice were anaesthetized with isoflurane and received 10  $\text{mg}\cdot\text{kg}^{-1}$  intraperitoneal injection (i.p.) of Buprécare® (Buprenorphine 0.3 mg) diluted 1/100 in NaCl 0.9% and 10 mg/kg of Ketofen® (Ketoprofen 100 mg) diluted 1/100 in NaCl 0.9%, and placed on a stereotaxic frame (Model 940, David Kopf Instruments, California). Viruses (0.5  $\mu\text{L}$ ) were injected either bilaterally or unilaterally (fiber photometry) into the ventral tegmental area (VTA) ( $L = \pm 0.5$ ;  $AP = -3.4$ ;  $V = -4.4$ , mm), the nucleus accumbens (NAc) ( $L = \pm 1$ ;  $AP = +1$ ;  $V = -4.2$ , in mm) or the dorsal striatum ( $L = +1.5$ ;  $AP = +0.86$ ;  $V = -3.25$ , in mm) at a rate of 0.1  $\mu\text{L}/\text{min}$ . The injection needle was carefully removed after 5 min waiting at the injection site and 2 min waiting half way to the top. Optical fiber for calcium imaging into the striatum was implanted 100  $\mu\text{m}$  above the viral injection site.

### Ex Vivo Whole-Cell Patch-Clamp Electrophysiology

Animals (8–12 weeks old) were terminally anaesthetized using isoflurane. Sagittal striatal slices (350  $\mu\text{m}$ -thick), containing the dorsal striatum and the nucleus accumbens, were cut using a VT1000S vibratome (VT1000S, Leica Microsystems, Nussloch, Germany) in ice-cold oxygenated solution (ACSF: 125 mM NaCl, 2.5 mM KCl, 25 mM glucose, 25 mM  $\text{NaHCO}_3$ , 1.25 mM  $\text{NaH}_2\text{PO}_4$ , 2 mM  $\text{CaCl}_2$ , 1 mM  $\text{MgCl}_2$ , 1 mM pyruvic acid). Slices were then incubated at 32–34°C for 60 min before returning to room temperature in holding ACSF. For whole-cell recordings, borosilicate glass pipettes of 6–8 M $\Omega$  resistance were filled with a potassium gluconate-based internal solution consisting of (in mM): 122 K-gluconate, 13 KCl, 10 HEPES, 10 phosphocreatine, 4 Mg-ATP, 0.3 Na-GTP, 0.3 EGTA (adjusted to pH 7.35 with KOH, osmolarity  $296 \pm 3.8$  mOsm). Signals were amplified using with EPC10-2 amplifiers (HEKA Elektronik, Lambrecht, Germany). All recordings were performed at 32–34°C, using a temperature control system (Bath-controller V, Luigs&Neumann, Ratingen, Germany) and slices were continuously superfused with extracellular solution at a rate of 2 mL/min. Recordings were sampled at 10 kHz, using the Patchmaster v2x32 program (HEKA Elektronik). DRD1-MSNs (Drd1-tdTomato mice), DRD2-MSNs (Drd2-eGFP) and mCherry-expressing MSNs (Drd2<sup>Cre/+</sup>::Lpl<sup>+/+</sup> and Drd2<sup>Cre/+</sup>::Lpl<sup>fl/fl</sup> mice) were visualized under direct interference contrast with an upright BX51WI microscope (Olympus, Japan), with a 40x water immersion objective combined with an infra-red filter, a monochrome CCD camera (Roper Scientific, the Netherlands) and a compatible system for analysis of images as well as contrast enhancement. Current over voltage (I/V) curves were acquired in current-clamp mode with membrane potentials maintained at  $-70$  mV.

For the bath-applied TG experiments, triolein (4  $\mu\text{M}$ ) was prepared just before use and applied 15–20 min before recording. 20  $\mu\text{L}$  of freshly thawed glyceryl trioleate (T7140 Sigma) was emulsified in 1 mL of gum Arabic solution (5% in ACSF) by a 4 min probe sonication on ice, leading to a milky white emulsion (20.3 mM glyceryl trioleate) which was stable for several h on ice and readily dispersible in ACSF (final concentration of 4  $\mu\text{M}$ ) for recording. The vehicle solution was obtained by omitting glyceryl trioleate.

For experiments related to synaptic transmission, a concentric bipolar electrode (Phymep, France) was placed on the mPFC afferent glutamatergic fibers to evoke EPSCs at 0.2 Hz, recorded in MSNs under current-clamp configuration with membrane potentials maintained at  $-60$  mV. Only data from fluorescent (mCherry, tdTomato and eGFP) MSNs were included in the present study. The active and passive electrophysiological properties of MSNs were calculated according to and consistent with a previous study (Fino et al., 2007).

### Measurement of Locomotor Activity

Locomotor activity was recorded in an automated online measurement system using an infrared beam-based activity monitoring system (Phenomaster, TSE Systems GmbH, Bad Homburg, Germany).

### Pharmacological Manipulations

During two consecutive days before any procedure (habituation phase) mice were injected in their home-cage with NaCl 0.9% (i.p.). On the test day, animals were perfused for 6 h with NaCl 0.9% or TG and received injections (i.p.) of d-Amphetamine sulfate (3 mg/kg, A5880, Sigma-Aldrich, L'Isle d'Abeau, France), haloperidol hydrochloride (0.5 mg/kg, #0931, Tocris Biosciences, Bristol, United

Kingdom), raclopride (0.6 mg/kg, #1810, Tocris Biosciences, Bristol, United Kingdom) or SKF38393 (10 mg/kg, #0922, Tocris Biosciences, Bristol, United Kingdom). All drugs were dissolved in NaCl 0.9%.

### Catalepsy Test

Animals were centrally infused with saline or TG for 6 h and then injected with haloperidol (0.5 mg/kg) or raclopride (0.6 mg/kg) one h before the catalepsy test. At  $t = 0, 15, 30, 45, 60, 75, 90$  min, animals were taken out of their home cage and placed in front of a 4 cm elevated steel bar, with the forelegs placed upon the bar while the hind legs remained on the ground surface. The time during which animals remained still was measured. Animals that failed to remain on the bar for at least 30 s during the whole test were excluded. A behavioral threshold of 180 s was set so the animals remaining in the cataleptic position for this duration were put back in their cage until the next time point.

### Operant Conditioning System

#### Lever Operandum for Pellets

Mice were food-restricted and maintained at 90% of their initial body weight to facilitate initial learning and performance during the whole operant conditioning. Computer-controlled operant conditioning was conducted in 12 identical conditioning chambers (Phenomaster, TSE Systems GmbH, Bad Homburg, Germany) during the light phase, at the same h every day until the end of the procedure. The mice had intermittent access to an operant wall in their home cages. Each operant wall had two levers located 3 cm lateral to a central pellet dispenser, with the left lever arbitrarily designated as the active lever. The reinforcer was a single 20-mg peanut butter flavored sucrose tablet (TestDiet, Richmond, USA). Operant training was carried out daily with no interruption for 2 h under a fixed-ratio 1 (FR1). When the discrimination score between active and inactive lever press (active lever presses/inactive lever presses) exceeded 2, mice were shifted for 4 consecutive days to 1.5 h sessions under a progressive ratio (PR) [3 lever press more for each subsequent reinforcer ( $r = 3N+3$ ;  $N =$  reinforcer number)].

#### Nose-Poke Operandum for TG Self-administration

##### Nose-Poke (NP) Operandum

Mice were single housed on a 12 h reverse light/dark cycle (lights off 08:00 h) with water and food *ad libitum*. Operant conditioning chambers (Imetronic, Pessac, France) consisted in sound-attenuated boxes equipped with two nose-pokes counterbalanced as active or inactive across left and right. Illumination of a dim house-light signaled the start and the end of each session. 10 days after catheter implantation, mice were first trained to explore the cages with 50  $\mu$ l saccharine 0.1% delivery being contingently presented in a liquid dipper after each active hole visits on a Fixed Ratio 1 (FR-1) reinforcement schedule, then increased to FR-2 until mice reached criterion ( $> 10$  reinforcements in 30 min and  $> 50\%$  discrimination between NP). After saccharine pretraining, mice were moved to TG self-administration sessions of 60 min under a fixed-ratio 2 (FR-2) schedule of reinforcement. Active NP visits delivered 10  $\mu$ l of intracarotid TG accompanied by a 60 s presentation of a cue light above the active NP and followed by a 20 s time out during which nose-poke visits had no consequences. Mice were randomly assigned to self-administer saline ( $n = 5$ ) or TG ( $n = 13$ ). In order to test the role of internal states on TG self-administration, animals were tested under two conditions: food satiated or 24 h deprived.

#### Conditioned Place Preference (CPP)

The CPP experiments were performed at the onset of the dark period on an unbiased apparatus. All the compartments were completely cleaned before each session of conditioning. Locomotor activity was recorded with infrared beam-based activity monitoring system and analyzed with the provided software (Phenomaster, TSE Systems GmbH, Bad Homburg, Germany). The least preferred compartment during the exploration phase was designated as the reward-baited compartment (biased protocol). Animals with more than 65% of preference for a compartment on the pre-test day were removed. On day 1, animals were carefully put in the middle of the cage and freely explored the two-compartments apparatus for 15 min. The subsequent days included conditioning sessions of one-h brain TG delivery conditioning alternated with one-h brain saline delivery conditioning. After 8 days of conditioning (4 sessions in each compartment), animals freely explored the two compartments for 15 min. The time spent in the reward-paired compartment before versus after conditioning was the primary outcome variable.

For the high-fat high-sugar (HFHS) conditioning, animals were centrally infused for 6 h in their home cages prior to conditioning sessions, for 10 consecutive days.

#### Binge Feeding Experiment

Animal were implanted with intracarotid catheter and single-housed one week prior to any experiments. Food intake and body weight were measured daily at 10 AM. Intracarotid saline or Intralipid perfusion were performed 6 h prior to intermittent access to drinking solution of high-fat high-sugar solution (Intralipid 20% enriched with sucrose 10%) daily at 10:30 AM during 10 consecutive days for one h.

#### Fiber Photometry and Data Analysis

A chronically implantable cannula (Doric Lenses, Québec, Canada) composed of a bare optical fiber (400  $\mu$ m core, 0.48 N.A.) and a fiber ferrule was implanted 100  $\mu$ m above the location of the viral injection site in the dorsal striatum (DS: L = +1.5; AP = +0.86; V = -3.25, in mm). The fiber was fixed onto the skull using dental cement (Super-Bond C&B, Sun Medical). Real time fluorescence

emitted from the calcium sensor GCaMP6f expressed by neurons with the DRD2 receptor was recorded using fiber photometry as described previously in the literature (Lerner et al., 2015). Fluorescence was collected in the dorsal striatum using a single optical fiber for both delivery of excitation light streams and collection of emitted fluorescence.

The fiber photometry setup used 2 light emitting LEDs: 405 nm LED sinusoidally modulated at 330 Hz and a 465 nm LED sinusoidally modulated at 533 Hz (Doric Lenses) merged in a FMC4 MiniCube (Doric Lenses) that combines the 2 wavelengths excitation light streams and separate them from the emission light. The MiniCube was connected to a Fiberoptic rotary joint (Doric Lenses) connected to the cannula. A RZ5P lock-in digital processor controlled by the Synapse software (Tucker-Davis Technologies, TDT, USA), commanded the voltage signal sent to the emitting LEDs via the LED driver (Doric Lenses). The light power before entering the implanted cannula was measured with a power meter (PM100USB, Thorlabs) before the beginning of each recording session. The irradiance was  $\sim 9$  mW/cm<sup>2</sup>. The fluorescence emitted by the GCaMP6f activation in response to light excitation was collected by a femtowatt photoreceiver module (Doric Lenses) through the same fiber patch cord. The signal was then received by the RZ5P processor (TDT). On-line real time demodulation of the fluorescence due to the 405nm and the 465 nm excitations was performed by the Synapse software (TDT). A camera was synchronized with the recording using the Synapse software.

Signals were exported to MATLAB R2016b (Mathworks) and analyzed offline. After careful visual examination of all trials, they were clean of artifacts in these time intervals. The timing of events was extracted from the video. For each session, signal analysis was performed on two-time intervals: one extending from  $-50$  to  $0$  s (home cage, HC) and the other from  $0$  to  $+50$  s (new cage, NC).

From a reference window (from  $-180$  to  $-60$  s), a least-squares linear fit was applied to the 405 nm signal to align it to the 465 nm signal, producing a fitted 405 nm signal. This was then used to calculate the  $\Delta F/F$  that was used to normalize the 465 nm signal during the test window as follows:  $\Delta F/F = (465 \text{ nm signal}_{\text{test}} - \text{fitted } 405 \text{ nm signal}_{\text{ref}}) / \text{fitted } 405 \text{ nm signal}_{\text{ref}}$ . To compare signal variations between the two conditions (HC versus NC), for each mouse, the value corresponding to the entry point of the animal in the new cage was set at zero.

### Fluorescent *In Situ* Hybridization

In order to delineate the expression patterns of *Lpl*, *Th*, *Drd1* and *Drd2* transcripts within the mesolimbic circuitry of the brain, the RNAscope, a commercialized *in situ* hybridization assay was used. Adult male mice ( $n = 3$ ) were euthanized and their brains were immediately extracted and flash frozen in isopentane. Brains were sectioned at  $20 \mu\text{m}$  with a Leica cryostat, and coronal sections were probed for gene expression according to the protocols provided by Advanced Cell Diagnostics. *Th* and *Lpl* expressions were assayed in the VTA; *Drd1*, *Drd2* and *Lpl* expressions were assayed in the both the dorsal striatum (DS) and NAc. Z stacked images were captured with a Zeiss AxioObserver fluorescent microscope, Zeiss Apotome 2.0 and through a 63x objective lens. Three different rostro-caudal coronal sections for each structure (VTA, DS and NAc) were used. 3 images/section were taken from the lateral VTA, whereas 4 images/section were taken for both DS and NAc. Counts were added per section level (according to bregma) and per structure so as to have a representative sample. Cells that exhibited at least 4 puncta (RNA molecules) in addition to DAPI were counted as expressing the respective gene. All error bars represent  $\pm$  SEM.

### Lipidomics

Seven pairs of mice were infused at  $0.2 \mu\text{l}/\text{min}$  for 4 h with either saline or triglycerides. Immediately following infusion, mice were euthanized, and had their striatal (dorsal striatum and NAc) brain tissues rapidly extracted and frozen on dry ice. Lipid and protein analyses were performed at the UCSD Lipidomics Core. Relative abundances of individual species per sample were normalized to protein concentration per sample.

### *In Vivo* Electrophysiological Recordings

Adult male mice (10 weeks) perfused for 6 h with TG or saline were anesthetized with chloral hydrate (8%), 400 mg/kg i.p. supplemented as required to maintain optimal anesthesia throughout the experiment and positioned in a stereotaxic frame. A hole was drilled in the skull above midbrain DA nuclei (coordinates:  $3 \pm 0.3$  mm posterior to bregma,  $0.5 \pm 0.1$  mm [VTA] lateral to the midline (Paxinos and Franklin, 2003). Recording electrodes were pulled from borosilicate glass capillaries (with outer and inner diameters of 1.50 and 1.17 mm, respectively) with a Narishige electrode puller. The tips were broken under microscope control and filled with 0.5% sodium acetate. Electrodes had tip diameters of 1–2  $\mu\text{m}$  and impedances of 20–50 M $\Omega$ . A reference electrode was placed in the subcutaneous tissue. The recording electrodes were lowered vertically through the hole with a micro drive. Electrical signals were amplified by a high-impedance amplifier and monitored with an oscilloscope and an audio monitor. The unit activity was digitized at 25 kHz and stored in Spike2 program. The electrophysiological characteristics of DA neurons were analyzed in the active cells encountered when systematically passing the microelectrode in a stereotaxically defined block of brain tissue including the VTA. Its margins ranged from  $-2.9$  to  $-3.3$  mm posterior to bregma (AP),  $0.4$  to  $0.6$  mm mediolateral (ML) and  $4$  to  $5$  mm ventral (DV). Sampling was initiated on the right side and then on the left side. Extracellular identification of DA neurons was based on their location as well as on the set of unique electrophysiological properties that distinguish DA from non-DA neurons *in vivo*: (i) a typical triphasic action potential with a marked negative deflection; (ii) a long duration ( $> 2.0$  ms); (iii) an action potential width from start to negative trough  $> 1.1$  ms; (iv) a slow firing rate ( $< 10$  Hz and  $> 1$  Hz). Electrophysiological recordings were analyzed using the R software (<https://www.r-project.org>). DA cell firing was analyzed with respect to the average firing rate and the percentage of spikes within bursts (%SWB, number of spikes within burst divided by total number of spikes). Bursts were identified as discrete events consisting of a sequence of spikes such that: their onset is defined by two consecutive spikes within an interval  $< 80$  ms

whenever and they terminate with an inter-spike interval > 160 ms. Firing rate and %SWB were measured on successive windows of 60 s, with a 45 s overlapping period on a total period of 300 s. Responses to TG or Saline acute injections are presented as the Mean of percentage of firing frequency variation from the baseline  $\pm$  SEM. For statistical analysis, maximum of firing variation induced by TG occurring 180 s after the injection are compared to the maximum of firing rate variation induced by saline occurring 180 s after the injection by non-parametric Mann-Whitney paired test.

### Tissue Preparation and Immunofluorescence

Mice were rapidly anaesthetized with pentobarbital (500 mg/kg, i.p., Sanofi-Aventis, France) and transcardially perfused with 4% (weight/vol.) paraformaldehyde in 0.1 M sodium phosphate buffer (pH 7.5). Brains were post-fixed overnight in the same solution and stored at 4°C. 30  $\mu$ m-thick sections were cut with a vibratome (Leica VT1000S, France), stored at  $-20^{\circ}$ C in a solution containing 30% ethylene glycol, 30% glycerol and 0.1 M sodium phosphate buffer. Sections were processed as follows: Day 1: free-floating sections were rinsed in Tris-buffered saline (TBS; 0.25 M Tris and 0.5 M NaCl, pH 7.5), incubated for 5 min in TBS containing 3% H<sub>2</sub>O<sub>2</sub> and 10% methanol, and then rinsed three times for 10 min each in TBS. After 15 min incubation in 0.2% Triton X-100 in TBS, sections were rinsed three times in TBS again. Slices were then incubated overnight or 72 h at 4°C with the following primary antibodies: rabbit anti-phospho-rpS6<sup>Ser235/236</sup> overnight (1:500, Cell Signaling Technology), goat anti-c-Fos (1:250, Santa Cruz Biotechnology) or rabbit anti-c-Fos (1:500, Synaptic Systems) for 72 h. Sections were rinsed three times for 10 min in TBS and incubated for 60 min with secondary antibodies anti-rabbit Cy3 AffiniPure (1:1000, Jackson ImmunoResearch) and anti-goat Dylight488 (1:1000, Vector labs). Sections were rinsed twice for 10 min in TBS and once in TB (0.25 M Tris) before mounting.

Acquisitions were performed with a confocal microscope (Zeiss LSM 510) with a color digital camera and AxioVision 3.0 imaging software. Images used for quantification were all single confocal sections. Photomicrographs were obtained with the following band-pass and long-pass filter settings: A488 (band pass filter: 505–530) and Cy3 (band pass filter: 560–615). The objectives and the pinhole setting (1 airy unit, au) remained unchanged during the acquisition of a series for all images. Quantification of immunopositive cells was performed using the cell counter plugin of the ImageJ software taking as standard reference a fixed threshold of fluorescence.

### Western Blotting

Mouse head was cut and immediately immersed in liquid nitrogen for 4 s. The brain was then removed and dissected on ice-cold surface, sonicated in 200  $\mu$ l of 1% SDS supplemented with 0.2% phosphatase inhibitors and 0.1% protease inhibitors, and boiled for 10 min. Aliquots (2.5  $\mu$ l) of the homogenates were used for protein quantification using a BCA kit (BC Assay Protein Quantitation Kit, Interchim Uptima, Montluçon, France). Equal amounts of proteins (15  $\mu$ g) for each sample were loaded onto 10%–12% polyacrylamide gels. Proteins were separated by SDS-PAGE and transferred to PVDF membranes (Millipore). The membranes were immunoblotted with the following antibodies: rabbit anti-phospho-rpS6<sup>Ser235/236</sup> (1:1000, Cell Signaling Technology), rabbit anti-phospho-rpS6<sup>Ser240/244</sup> (1:1000, Cell Signaling Technology), rabbit anti-phospho-p70S6K<sup>Thr421/Ser424</sup> (1:1000, Cell Signaling Technology), rabbit anti-phospho-p70S6K<sup>Thr389</sup> (1:1000, Cell Signaling Technology), mouse  $\beta$ -actin (1:5000, Sigma), rabbit anti-phospho-ERK1/2 (1:2000, Cell Signaling Technology), rabbit anti-phospho-DARPP-32<sup>Thr34</sup> (1:750, Cell Signaling Technology), rabbit anti-phospho-TH<sup>Ser31</sup> (1:1000, Cell Signaling Technology), rabbit anti-phospho-TH<sup>Ser40</sup> (1:1000, Cell Signaling Technology), mouse anti-TH (1:2000, Millipore), rabbit anti-phospho-Akt<sup>Ser473</sup> (1:1000, Cell Signaling Technology), rabbit anti-phospho-Akt<sup>Thr308</sup> (1:1000, Cell Signaling Technology), rabbit anti-phospho-GSK3 $\beta$ <sup>S9</sup> (1:1000, Cell Signaling Technology). Detection was based on HRP-coupled secondary antibody binding detected using ECL as detection system. The secondary antibodies were anti-mouse (1:5000, Dako) and anti-rabbit (1:10000, Cell Signaling Technology). Quantification was performed using the ImageJ software.

### Doppler Imaging

Color Doppler scans of the brain were performed with a Vevo LAZR system (FujiFilm VisualSonics, Toronto, ON, Canada) using the LZ201 transducer (9–18 MHz bandwidth). Mice equipped with a carotid artery catheter were maintained anesthetized with isoflurane. Hair was removed on the head with depilatory cream and mice were positioned prone for imaging. The transducer was positioned to scan a coronal section of the whole head centered on the posterior cerebral artery. Images were acquired continuously. Catheter was connected to an infusion device that delivered NaCl 0.9% or TG emulsion (Intralipid 20%) at rates of 0.1  $\mu$ l/min; 1  $\mu$ l/min or 10  $\mu$ l/min. Images were exported and analyzed using ImageJ software.

### Whole-Brain c-Fos Immunostaining

C57BL/6J male mice received a 6 h saline or Intralipid perfusion and were sacrificed 1 h after amphetamine injection (3 mg/kg). Brains were excised and post fixed in 4% paraformaldehyde overnight at room temperature and transferred stepwise to 100% methanol using the following protocol. 20% methanol (in ddH<sub>2</sub>O) for 1 h, 40% methanol for 1 h, 60% methanol for 1 h, 80% methanol for 1 h, and 100% methanol for 1 h twice. iDISCO staining was performed as described in Renier et al. (Renier et al., 2014) with one exception. All the washing steps after incubation with primary and secondary antibody were extended from one to three days. Incubation time for primary and secondary antibody was 4 days each. The primary antibody was Rabbit pAb anti c-Fos (Ab-5) (4-17) from Calbiochem (1:10,000 dilution), and the secondary antibody was Cy5-anti rabbit from Jackson ImmunoResearch (1:1000 dilution). Brain samples were scanned using an UltraMicroscope II LSFM system (Lavisision Biotec, Bielefeld, Germany) in 4.06  $\mu$ m for the c-Fos activation study. Auto-fluorescence was recorded at 545 nm for anatomy information, while the c-Fos signal was acquired

with a 620 nm emission filter. Images were registered to a digital brain atlas using the Elastix software library<sup>11</sup>. A source image  $I_S(x)$  was registered to a target image  $I_T(x)$  by finding a coordinate transformation  $T(x)$  that made  $I_S(T(x))$  spatially aligned with  $I_T(x)$ . We used an affine coordinate transformation for initialization followed by non-rigid b-spline coordinate transformation which was iteratively optimized with respect to the mutual information between the source and the target. Registration parameters for mapping of LSM data were similar to those used in Renier et al. (Renier et al., 2014). Imaris (Release 7.6.5, Bitplane, Zurich, Switzerland) was used to generate Figure 2F. ROI based analysis of the total fluorescence signal for c-Fos heatmap intensities were computed using multiple t tests assuming unequal variance. The heatmaps were generated as described in (Salinas et al., 2018). The statistical analysis was performed using GraphPad Prism (Release 6, GraphPad Software, Inc., United States).

### Isolation of Total RNA and Quantitative RT-PCR

Each sample consisted of the tissue deriving from one mouse brain. Mice were sacrificed by cervical dislocation. The dorsal striatum (DS) and the NAc were quickly dissected out and placed on ice. Each tissue sample was homogenized in TRIzol with 3 mm tungsten carbide beads (QIAGEN cat.No. 69997). Total RNA was extracted with TRIzol Reagent (Life Technologies) according to manufacturer's instructions. The RNA was quantified by using the NanoDrop 1000 spectrophotometer. Between 85 and 500 ng of mRNA from each sample were used for retro-transcription, performed with the Reverse Transcriptase M-MLV (Life Technologies) following the manufacturer's instructions. Quantitative real time PCRs, were performed in a LightCycler 1.5 detection system (Roche, Meylan France) using the LightCycler FastStart DNA Master plus SYBR Green I kit (Roche) in 384-well plates according to the manufacturer's instruction. All reactions were carried out in duplicate (Striatum) or triplicate (Hypothalamus). Results are presented as normalized to the house-keeping gene and the delta-CT method was used to obtain a FC.

### Metabolic Efficiency Analysis

Mice were monitored for whole energy expenditure (EE) or Heat (H), oxygen consumption and carbon dioxide production, respiratory exchange rate ( $RER = VCO_2/VO_2$ , where V is a volume), and locomotor activity using calorimetric cages with bedding, food and water (Labmaster, TSE Systems GmbH, Bad Homburg, Germany).

Ratio of gases was determined through an indirect open circuit calorimeter (for review (Arch et al., 2006; Even and Nadkarni, 2012)). This system monitors  $O_2$  and  $CO_2$  concentration by volume at the inlet ports of a tide cage through which a known flow of air is being ventilated (0.4 L/min) and compared regularly to a reference empty cage. For optimum analysis, the flow rate was adjusted according to the animal body weights to set the differential in the composition of the expired gases between 0.4 and 0.9% (Labmaster, TSE Systems GmbH, Bad Homburg, Germany).

The flow was previously calibrated with  $O_2$  and  $CO_2$  mixture of known concentrations (Air Liquide, S.A. France). Oxygen consumption, carbon dioxide production and energy expenditure were recorded every 15 min for each animal during the entire experiment. Whole energy expenditure was calculated using the Weir equation respiratory gas exchange measurements. Food consumption was measured as the instrument combines a set of highly sensitive feeding and drinking sensors for automated online measurements. Mice had free access to food and water *ad libitum*. To allow measurement of every ambulatory movement, each cage was embedded in a frame with an infrared light beam-based activity monitoring system with online measurement at 100 Hz. The sensors for gases and detection of movement operated efficiently in both light and dark phases, allowing continuous recording.

Mice were monitored for body weight and composition at the entry and the exit of the experiment. Body mass composition (lean tissue mass, fat mass, free water and total water content) was analyzed using an Echo Medical systems' EchoMRI (Whole Body Composition Analyzers, EchoMRI, Houston, USA), according to manufacturer's instructions. Briefly, mice were weighed before they were put in a mouse holder and inserted in MRI analyzer. Readings of body composition were given within 1 min.

Data analysis was performed on Excel XP using extracted raw value of  $VO_2$  consumed,  $VCO_2$  production (express in mL/h), and energy expenditure (kcal/h). Subsequently, each value was expressed by total body weight extracted from the EchoMRI analysis.

### Human Methods and Analysis

The procedures for the human fMRI experiment are described in detail in the Supplemental Information. In brief, 29 participants underwent three days of scanning during which they were instructed to sniff pulses of food and non-food (floral) aromas while their blood oxygen level dependent (BOLD) signal was measured. This comparison isolates BOLD responses to calorie-predictive food cues that are independent from general experiences of pleasantness, and therefore reflect a specific measure of food cue reactivity. Internal state was manipulated across days so that scanning occurred when subjects were fasted (HUNGRY) or fed a standard or *ad libitum* meal (FIXED versus SATIED). Internal state ratings and perceptual ratings of odor stimuli were assessed throughout the sessions and blood samples were acquired at baseline and 30, 60, and 90 min from the start of the meal or equivalent time point on the hungry day. Imaging data were acquired on a Siemens 3.0 Tesla TIM Trio Scanner at the Yale University Magnetic Resonance Research Center using our standard procedures for acquisition and analysis (Sun et al., 2015; Sun et al., 2014). Responses were considered significant corrected for multiple comparisons using family wise error (FWE) correction across the whole brain or across the number of voxels in the NAc or its prefrontal projection region, the ventromedial prefrontal cortex (vmPFC). These regions of interest (ROI) were selected based on the animal findings and were created by searching the Neurosynth database for NAc and vmPFC responses to food cues, followed by extraction of the centroids from the resultant peak responses. 10 mm spheres were then drawn around the centroids to perform small volume correction.

### Participant Recruitment

Twenty-nine right-handed participants (age range 18–39,  $M = 26.80$ ,  $SD = 5.49$ ; BMI range 19.5–33.6,  $M = 23.94$ ,  $SD = 3.86$ ; male = 16, female = 13) were recruited from the greater New Haven area through the Yale University Interdisciplinary Research Consortium on Stress, Self-Control and Addiction (IRCSSA) P30 Subject's core as well as via flyer advertisement. Participants were screened over the phone to be less than 40 years of age, free of psychiatric disorders, eating disorders, current dieting behavior, alcoholism, use of tobacco or drugs other than alcohol, history of head injury with loss of consciousness, use of daily medication other than monophasic birth control, chemosensory impairments, lactose intolerance or food allergies. We did not impose a BMI upper-limit. Individuals were included so long as they felt comfortable while inserted in the scanner bore. Females provided the date of their last period to ensure that they were not scanned during menstruation or ovulation. All participants provided written informed consent at their first lab visit and the study was approved by the Yale Human Investigations Committee.

### Genotyping for TaqI A1 Polymorphism

Saliva samples were obtained from the participants using Oragene Discover collection kits and DNA extraction was performed as directed by the manufacturer (DNA Genotek). TaqIA A1 allele status was determined by amplifying a 304 bp region with PCR using forward (5'-CCCTTCCTGAGTGTTCATCA-3') and reverse (5'-CGGCTGGCCAA GTTGCT-3') primers as described by [Epstein et al., \(2007\)](#). The products of the amplification were digested overnight with the restriction enzyme TaqIA. The resulting DNA fragments were tagged with ethidium bromide and separated via gel electrophoresis. The appearance of a 304 bp band indicated the presence of the TaqI A1 allele. Sixteen participants were carriers of the A1 allele of the dopamine D2 receptor (DRD2) gene region (A1+; age range 19–37,  $M = 27.38$ ,  $SD = 5.28$ ; BMI range 19.5–33.6,  $M = 25.04$ ,  $SD = 4.66$ ; male = 9, female = 7), and 13 were non-carriers (A1-; age range 18–39,  $M = 26.08$ ,  $SD = 5.87$ ; BMI range 19.9–25.68,  $M = 22.59$ ,  $SD = 2.00$ ; male = 7, female = 6).

### Food and Non-food Odor Stimuli

Food odors were “chocolate cookie” and “strawberry and cream” odors (6002335, 6106524 from Bell Labs Flavors and Fragrances, Inc.). Non-food odors were “honeysuckle” and “lilac” odors (039831 Chey N-3 from Firmenich, Inc.; 31731066 Lilac 71 from International Flavors and Fragrances, Inc.).

### Stimulus Delivery

Odors were presented by a custom built, MRI compatible olfactometer programmed in Labview (National Instruments). A detailed description of the olfactory stimulation system can be found in a previous publication ([Stice et al., 2008](#)). In brief, mass flow controllers (MKS Instruments) adjust the flow of humidified and temperature-controlled air over stainless steel wells containing an odorant, allowing the air to pick up vaporized odor molecules. The independent odor channels converge into a mixing manifold and exit through 1 of 2 Teflon tubes where the first is dedicated to odors and the second is dedicated to clean air. The trunk terminates in a Teflon manifold (Teqcom) resting on the participant's chest. A vacuum line connected to this manifold creates a closed loop to evacuate odorized as well as odorless (OL) air, preventing head space contamination. The participants receive OL and odor stimuli embedded in a continuous stream of clean, OL air from the manifold through a nasal mask (Philips Respironics). As air exits the mask, it is drawn out through a final Teflon tube by another vacuum line. The mask is also coupled to a pneumotachograph to measure airflow in the nose ([Johnson and Sobel, 2007](#)), which is in turn connected to a spirometer (AD Instruments). The signal from the spirometer is fed into an amplifier (AD Instruments, PowerLab 4SP) and digitally recorded at 100 Hz using Chart 5.5.6 (AD Instruments).

### Experimental Procedures

All participants underwent a training session, and three fMRI scanning sessions (Hungry, Fixed and Sated conditions). All sessions were conducted on separate days and scan order was counterbalanced.

### Training Session

Participants were instructed to refrain from eating or drinking anything other than water for at least an h before the session. Anthropometric measurements were taken at the beginning of the session. Body weight and height were measured using a Detecto 439 balance beam scale with stadiometer at The John B. Pierce Laboratory. BMI was calculated as weight (in kilograms) divided by the squared height (in meters) of the participant ( $BMI = \text{kg}/\text{m}^2$ ).

Participants were trained to make computerized ratings of their internal state as well as the perceptual qualities of our stimuli on computerized scales. Participants rated the intensity of their feelings of hunger and fullness using adapted cross modal general Labeled Magnitude Scales (gLMS) consisting of a 100 mm vertical line scale with the labels “no sensation” at the lower anchor point and “strongest imaginable sensation” at the upper anchor point ([Bartoshuk et al., 2004](#); [Green et al., 1996](#)). Stimulus ratings consisted of ratings of each stimulus's intensity, liking, wanting to eat, edibility and familiarity. Intensity was measured by adapted cross modal gLMS. Liking was measured using a labeled hedonic scale (LHS) consisting of a 100 mm vertical line scale with the labels “most disliked sensation imaginable” at the lower anchor point, “most liked sensation imaginable” at the upper anchor point, and “neutral” in the middle ([Lim et al., 2009](#)). Wanting to eat, edibility, and familiarity were measured using a 20 mm cross-modal visual analog scale. Wanting to eat labels were “I would never want to consume this” (–10), “neutral” (0) and “I would want to consume this more than anything” (+10). Edibility labels were “not edible at all” at (–10), neutral at (0) and “very edible” at (+10). Familiarity labels were “not familiar at all” (–10), “neutral” (0) and “very familiar” (+10).



After training to make computerized ratings, participants participated in mock scanner training to become familiarized with the task, and to determine whether it would be uncomfortable to be in the scanner with the nasal mask. During mock scanning, the odor stimuli or OL were delivered using the olfactometer. First, each odor was delivered one at a time and participants verbally rated the intensity of each presentation by telling the experimenter approximately where on the gLMS the odor's intensity fell in relation to the scale's labels (e.g., "Very Strong," "A little less than Weak," "Halfway between Moderate and Strong"). An experimenter then manually adjusted the odorant concentration settings on the olfactometer so that each odor was rated moderate in intensity. This resulted in the creation of a personalized dilution profile for each odor and each participant, allowing us to control for individual differences in sensory acuity. Next, participants made internal state ratings as well as perceptual ratings of each of the stimuli using a mouse on a computer monitor viewed via back projection on a headcoil-mounted mirror and then underwent a simulated fMRI run. After completing the ratings, participants underwent odor runs in the mock scanner. At the end of this training session, participants were then given commercially available pre-packaged granola bars (190 kcal per package) for breakfast on the day of fMRI scanning session.

### fMRI Scanning Sessions

All participants were instructed to eat the breakfast bars (1 package for women, 1.5 packages for men) in the morning at home, and then refrain from eating or drinking, with the exception of water, until their session. Participants arrived at the scanning center at 11:45 AM. Starting at 12:15 PM, a Teflon catheter was inserted into an antecubital vein for blood sampling. Baseline blood samples were obtained at 12:30 and 12:45 PM. Five minutes after the baseline blood sampling, participants ate a fixed-portion lunch (1 sandwich and 1 serving of apple slices for women, 1.5 sandwiches and 1 serving of apple slices for men) for the Fixed condition, or an *ad libitum* lunch (3 sandwiches and 4 servings of apple slices for both women and men and instructed to eat as much as they'd like) for the Sated condition, or nothing for the Hungry condition. For a fixed-portion lunch or an *ad libitum* lunch, participants received apple slices (approximately 25 kcal of apple per bag) and their choice of sandwich from the options of tuna, ham, turkey, or avocado served on white bread with cheese, tomato, and mayonnaise. Each sandwich was designed to contain approximately 400 kcal and was cut into quarters before serving to discourage participants from interpreting each entire sandwich as one large "portion." The amount and type of foods consumed at *ad libitum* lunch were recorded without the participants' knowledge.

After eating lunch, participants were escorted to the scanner at approximately 1 PM. The second blood samples were collected at 60 min from time of meal (or no meal) onset. Internal state ratings were obtained concomitant to the baseline and second blood samples were obtained (at 12:45 PM and 1:50 PM). Temporal variability of onset of each blood sampling between each condition was minimized.

Once inside the fMRI scanner, participants underwent four odor runs. Each odor run was 5 min 54 s long. Participants were instructed to breathe in through their nose after receiving the verbal cue "3, 2, 1, sniff" through headphones. Odor or OL delivery always occurred immediately following the auditory cue so that delivery was time-locked to sniff onset. Olfactory stimulation lasted for 3 s followed by a 9–19 s rest period before the next trial. There were 6 repetitions each of food odors, non-food odors, and OL stimuli. Participants were asked to keep their eyes closed during the functional runs, and no behavioral task was required other than to experience the stimuli. Before and after the fMRI scan, participants provided their stimulus ratings in the MRI scanner. At 60 min from meal (or no meal), participants provided internal state ratings for hunger and fullness. The odor runs were interspersed with additional anatomical and functional scans using taste stimuli that are reported in a separate manuscript (Sun et al., 2014).

### fMRI Data Acquisition

Imaging data were acquired on a Siemens 3.0 Tesla TIM Trio Scanner at the Yale University Magnetic Resonance Research Center. High-resolution T1-weighted structural scans were acquired for each participant with the following parameters: TR = 2230 ms, TE = 1.73 ms, flip angle = 9°, matrix = 256 × 256, 1 mm thick slices, FOV = 250 × 250, 176 slices. For fMRI runs, a susceptibility-weighted single-shot echo-planar sequence was used to image regional distribution of the BOLD signal. At the beginning of each functional run, the MR signal was allowed to equilibrate over 6 scans for a total of 12 s, which were subsequently excluded from the analyses. Acquisition parameters were: TR = 2000 ms, TE = 20 ms, flip angle = 80°, FOV = 220, matrix = 64 × 64, slice thickness = 3 mm. Forty contiguous slices were acquired in an interleaved method to reduce the cross-talk of the slice selection pulse.

### Data Analysis (Human Studies)

#### Ratings for Internal State and Stimuli

All statistics were performed in SPSS Version 21.0 (SPSS Inc., Chicago, IL, USA). Internal state ratings for each participant were log transformed. One participant's stimulus ratings from the Hungry, Fixed, and Sated conditions and another's from the Sated condition were omitted due to technical malfunction of equipment during collection. One participant's internal state ratings from the Hungry condition and another's from the Sated condition were also omitted due to technical malfunction. Those missing values were completed by inserting mean values. A mixed-design analysis of variance (ANOVA) was performed to assess the effects of condition, time, and group, as well as interactions between the above, on internal state and stimulus ratings.

#### Food Intake

An unpaired t test was performed to test whether caloric intake from lunch of the Sated condition would differ between groups.

### **Blood Collection and Analysis**

Samples were centrifuged immediately and kept on ice for the duration of each condition, then frozen at either  $-80^{\circ}\text{C}$  [free fatty acid (FFA) and insulin] or  $-20^{\circ}\text{C}$  (glucose, triglycerides). Plasma levels of insulin were measured with radioimmunoassay kits that utilize the double antibody technique with  $^{125}\text{I}$ -labeled hormone and hormone antiserum (Cat. # HI-14K, EMD Millipore Corporation, Billerica MA). Glucose, FFA and triglyceride concentrations were measured using enzymatic colorimetric techniques (FFA: Cat. # 999-34691, 991034891, 993-35191, Wako Pure Chemical Industries, Ltd., Osaka, Japan. Triglycerides: Cat. # SA1023, RX1023; Glucose: Cat. # SA1014, RX1014, Alfa Wassermann Diagnostic Techniques, West Caldwell NJ).

The effects of time, condition, and group, as well as interactions between the above, on the concentration of triglycerides were tested using a mixed-design ANOVA. We then tested the association between caloric intake and baseline triglyceride concentrations at the Sated session in each group by Pearson's correlation analysis.

### **Neuroimaging Data**

Neuroimaging data were analyzed using SPM8 software (Statistical Parametric Mapping, Wellcome Department of Imaging Neuroscience) in MATLAB R2010b 7.11.0 (Mathworks, Inc.). Functional images were time-acquisition corrected to the slice obtained at 50% of the TR and realigned to the mean image. Anatomical and functional images were normalized to the standard MNI template brain implemented in SPM8, resulting in voxel sizes of 3 and 1  $\text{mm}^3$ , respectively. Functional time-series data were detrended and then smoothed using a 6 mm FWHM isotropic Gaussian kernel. Motion parameters were included as regressors in the design matrix at the single participant level.

A design matrix was created for each participant for odor runs across all scan days that produced 2 events of interest: 1) Odors (Food + Non-food odors) and 2) OL. Event onsets were defined as the beginning of odor onset and event durations were defined as the 3 s of odor delivery. A 270 s high pass filter was applied to the time series data to remove low frequency noise and slow signal drifts. The general linear model was employed to estimate condition-specific effects at each model. A canonical hemodynamic response function was used to model neural response to events of interest.

To investigate the effect of genotype on the association between postprandial serum triglyceride change (60 min after lunch - baseline) and difference in brain response to food odors (food odor - non-food odor) between conditions [(Hungry - Fixed) and (Hungry - Sated)], individual contrast maps of [(food odor - non-food odor) Hungry - (food odor - non-food odor) Fixed/Sated] were entered into regression models with postprandial serum triglyceride changes as a covariate. The T-map threshold was set at  $p$  uncorrected  $< 0.005$  and a 5-voxel cluster size. Peak voxels of the unpredicted cluster were considered significant at  $p < 0.05$  family wise error (FWE) corrected across the entire brain for multiple comparisons. Next, region-of-interest (ROI) searches were performed using anatomical ROIs. Peaks within these regions were considered significant at  $p < 0.05$  FWE corrected across the individual ROI. All ROI masks (ventral striatum and vmPFC) were selected by searching the Neurosynth database for NAc and vmPFC responses to food cues, followed by extraction of the centroids from the resultant peak responses. 10mm spheres were then drawn around the centroids for small volume correction.

## **QUANTIFICATION AND STATISTICAL ANALYSIS**

### **Statistical Analysis**

Except for human study, all statistical comparisons were performed with Prism 6 (GraphPad Software, La Jolla, CA, USA). The statistical tests used are listed along with the statistical values in the Supplemental Tables. In condition of intracarotid catheter implantation, outliers were discarded based on evidence of lost tubing patent and failed perfusion. All the data were analyzed using either Student t test (paired or unpaired) with equal variances or One-way ANOVA or Two-way ANOVA. Lipidomic results were analyzed by simple comparisons (unpaired t test). Levels of phospho-proteins were analyzed by both simple comparisons (unpaired t test) and multiple comparisons (Two-way ANOVA). In all cases, significance threshold was automatically set at  $p < 0.05$ . ANOVA analyses were followed by Bonferroni post hoc test for specific comparisons only when overall ANOVA revealed a significant difference (at least  $p < 0.05$ ). All details related to statistical analyses are summarized in [Table S5](#).

## **DATA AND CODE AVAILABILITY**

This study did not generate/analyze [datasets/code].